METABOLIC ADJUSTMENTS AND GENE EXPRESSION REPROGRAMMING FOR SYMBIOTIC NITROGEN FIXATION IN LEGUME NODULES

EDITED BY: Brett James Ferguson, Kiwamu Minamisawa, Nacira Belen Muñoz and Hon-Ming Lam

PUBLISHED IN: Frontiers in Plant Science and Frontiers in Microbiology

frontiers Research Topics

frontiers

ISSN 1664-8714
ISBN 978-2-88963-027-1
DOI 10.3389/978-2-88963-027-1

About Frontiers

Frontiers is more than just an open-access publisher of scholarly articles: it is a pioneering approach to the world of academia, radically improving the way scholarly research is managed. The grand vision of Frontiers is a world where all people have an equal opportunity to seek, share and generate knowledge. Frontiers provides immediate and permanent online open access to all its publications, but this alone is not enough to realize our grand goals.

Frontiers Journal Series

The Frontiers Journal Series is a multi-tier and interdisciplinary set of open-access, online journals, promising a paradigm shift from the current review, selection and dissemination processes in academic publishing. All Frontiers journals are driven by researchers for researchers; therefore, they constitute a service to the scholarly community. At the same time, the Frontiers Journal Series operates on a revolutionary invention, the tiered publishing system, initially addressing specific communities of scholars, and gradually climbing up to broader public understanding, thus serving the interests of the lay society, too.

Dedication to Quality

Each Frontiers article is a landmark of the highest quality, thanks to genuinely collaborative interactions between authors and review editors, who include some of the world's best academicians. Research must be certified by peers before entering a stream of knowledge that may eventually reach the public - and shape society; therefore, Frontiers only applies the most rigorous and unbiased reviews.
Frontiers revolutionizes research publishing by freely delivering the most outstanding research, evaluated with no bias from both the academic and social point of view. By applying the most advanced information technologies, Frontiers is catapulting scholarly publishing into a new generation.

What are Frontiers Research Topics?

Frontiers Research Topics are very popular trademarks of the Frontiers Journals Series: they are collections of at least ten articles, all centered on a particular subject. With their unique mix of varied contributions from Original Research to Review Articles, Frontiers Research Topics unify the most influential researchers, the latest key findings and historical advances in a hot research area! Find out more on how to host your own Frontiers Research Topic or contribute to one as an author by contacting the Frontiers Editorial Office: researchtopics@frontiersin.org

METABOLIC ADJUSTMENTS AND GENE EXPRESSION REPROGRAMMING FOR SYMBIOTIC NITROGEN FIXATION IN LEGUME NODULES

Topic Editors:
Brett James Ferguson, The University of Queensland, Australia
Kiwamu Minamisawa, Tohoku University, Japan
Nacira Belen Muñoz, National Institute of Agricultural Technology, Argentina
Hon-Ming Lam, The Chinese University of Hong Kong, Hong Kong

Citation: Ferguson, B. J., Minamisawa, K., Muñoz, N. B., Lam, H.-M., eds. (2019). Metabolic Adjustments and Gene Expression Reprogramming for Symbiotic Nitrogen Fixation in Legume Nodules. Lausanne: Frontiers Media SA.
doi: 10.3389/978-2-88963-027-1

Table of Contents

frontiers in Plant Science

EDITORIAL
published: 09 July 2019
doi: 10.3389/fpls.2019.00898

Editorial: Metabolic Adjustments and Gene Expression Reprogramming for Symbiotic Nitrogen Fixation in Legume Nodules

Brett James Ferguson[1]*, *Kiwamu Minamisawa*[2], *Nacira Belen Muñoz*[3] and *Hon-Ming Lam*[4]*

[1] School of Agriculture and Food Sciences, The University of Queensland, Brisbane, QLD, Australia, [2] Graduate School of Life Sciences, Tohoku University, Sendai, Japan, [3] National Institute of Agricultural Technology, Córdoba, Argentina, [4] Center for Soybean Research of The State Key Laboratory of Agrobiotechnology, School of Life Sciences, The Chinese University of Hong Kong, Shatin, Hong Kong

Keywords: nitrogen fixation, nodules, metabolic adjustment, gene expression reprogramming, long-range signals, legume, rhizobia

Editorial on the Research Topic

Metabolic Adjustments and Gene Expression Reprogramming for Symbiotic Nitrogen Fixation in Legume Nodules

OPEN ACCESS

Edited and reviewed by:
Benjamin Gourion, UMR2594 Laboratoire Interactions Plantes-Microorganismes (LIPM), France

***Correspondence:**
Brett James Ferguson
b.ferguson1@uq.edu.au
Hon-Ming Lam
honming@cuhk.edu.hk

Specialty section:
This article was submitted to Plant Microbe Interactions, a section of the journal Frontiers in Plant Science

Received: *04 May 2019*
Accepted: *24 June 2019*
Published: *09 July 2019*

Citation:
Ferguson BJ, Minamisawa K, Muñoz NB and Lam H-M (2019) Editorial: Metabolic Adjustments and Gene Expression Reprogramming for Symbiotic Nitrogen Fixation in Legume Nodules. Front. Plant Sci. 10:898. doi: 10.3389/fpls.2019.00898

Legumes are important sources of food, feed, and biofuel. Their ability to enter into a symbiotic relationship with nitrogen-fixing rhizobia has a strong impact on environment and agriculture. Maximizing the use of legumes and improving the nodulation and nitrogen fixation processes are seen as pivotal steps toward enhancing agricultural sustainability, where nitrogen fixation has a key role in soil functions, nutrient cycling, soil biodiversity, ecosystem services, and even food security (Foyer et al., 2016; El Mujtar et al., 2019).

The symbiosis involves compatible legume-rhizobia species to recognize one another in the rhizosphere, followed by the bacteria infecting the host and initiating the formation of nodules that would eventually house the bacteria (Ferguson et al., 2010). The environment inside the nodule is ideal for rhizobia to convert atmospheric di-nitrogen gas into alternative nitrogenous compounds that can be used by the host plant. The number of nodules is tightly controlled by the host, based on the balance between its need to acquire nitrogen and its ability to expend resources and energy forming and maintaining these resource-demanding structures (Ferguson et al., 2019). The interaction between legumes and rhizobia is a typical example of co-evolution. For example, in soybean, improvement in nitrogen fixation capacity could be part of the result of the domestication process (Muñoz et al., 2016), whereas adaptive transcription profiles were observed when rhizobia were inoculated into different soybean accessions (Jiao et al., 2018).

Xu et al. demonstrated that humic acids could regulate the quorum sensing capacity of *Sinorhizobium meliloti*, suggesting that water-soluble humic materials could potentially be used to improve rhizobial growth and their symbiotic nitrogen fixation efficiency. This was partially demonstrated using water-soluble humic materials to repress the expression of the quorum sensing gene *expR* by augmenting its interaction with the novel regulator *QsrR*. Hara et al. identified functional nitrogen-fixing bacteria associated with the non-legume *Sorghum bicolor*, showing that the major functional nitrogen-fixing bacteria associating with sorghum roots are unique *Bradyrhizobium* species that resemble photosynthetic and non-nodulating *Bradyrhizobium* strains. Based on these findings, they discussed the nitrogen-fixing potential of the rhizobia-sorghum interaction, and investigated the overall *Bradyrhizobium* diversity. Nguyen et al. worked with *Bradyrhizobium* species and demonstrated that the *innB* gene encodes a novel type III effector that

controls symbiosis with *Vigna radiata* (mung bean). Expression of *innB* was shown to be dependent on plant flavonoids and the transcriptional regulator, TtsI. Other effector proteins like innB in the type III secretion system could positively or negatively influence the nodulation and/or nitrogen fixation processes during the co-evolution of rhizobial mutualists with host legume genotypes (Okazaki et al., 2013; Sugawara et al., 2018).

A number of approaches using molecular and functional characterization techniques were used to investigate the roles of various legume signals in nodule development. Rípodas et al. investigated transcription factors of the Nuclear Factor Y (NF-Y) family in *Phaseolus vulgaris*, indicating that both PvNF-YA1 and PvNF-YB7 are part of a network enabling *P. vulgaris* plants to discriminate and select for bacterial strains that perform better at nodule formation, possibly by forming a heterotrimeric complex with PvNF-YC1. This could have wide-ranging implications in the selection of superior varieties for legume nodulation. Sogawa et al. studied the role of SNARE proteins that mediate membrane trafficking in eukaryotic cells, showing that both LjVAMP72a and LjVAMP72b facilitate the legume-rhizobia symbioses and root hair development by affecting the secretory pathway in the host plant. Fernandez-Göbel et al. characterized the rapid systemic redox changes induced during the interactions between soybean and *Bradyrhizobium japonicum*. In addition to molecular genetic studies, they used non-nodulating and super-nodulating soybean mutants to establish that early systemic redox signaling during nodule development depends on Nod factor perception and the induced tolerance response depends on the autoregulation of the nodulation mechanism. In addition, the mini review by Libault highlights current advances in legume nodulation at the level of single cell-types, providing perspectives on the single cell and single cell-type approaches when applied to legume nodulation and how they can be used to enhance the understanding of the complex signaling interactions during rhizobia infection of legume root cells.

The metabolic pathways of carbon, nitrogen, and phosphorus are tightly regulated by the host plant during nodulation and nitrogen fixation. Liu et al. reviewed how host plants balance their needs for these critical resources with those of their microsymbiont partners. They highlighted the network of transporters that traffic these essential metabolites between the two partners through the symbiosome membrane, and how they are regulated by transcription factors that control the expressions of these transporters under different environmental conditions. Conversely, nitrate has been reported to rapidly and reversibly inhibit nodule growth and nitrogen fixation of soybean. Yamashita et al. compared the effects of nitrate to those of ammonium, urea, and glutamine on nodule growth and nitrogen fixation. Interestingly, the long-term supply of nitrate, urea, or glutamine promoted the growth of lateral roots and leaves, which were suppressed by ammonium.

Wongdee et al. and Yang et al. looked at improving nitrogen fixation from different angles. Wongdee et al. investigated *Bradyrhizobium* sp. DOA9, which has the unusual ability to fix nitrogen during both free-living and symbiotic growth. Their findings enhance the understanding of the complex mechanisms that regulate the nitrogenase genes in the DOA9 strain, including the key genes for enabling nitrogen fixation. Yang et al. on the other hand, examined the genetic mechanisms underlying nitrogen fixation in soybean. These authors identified two quantitative trait loci (QTLs) that might be valuable markers for breeding soybean varieties having high biological nitrogen fixation.

This Research Topic aims to highlight current findings in the areas of nodule development and nitrogen fixation, with a focus on the regulation of the molecular factors involved in these processes. The contributing articles are reflections of the highly active research community and the breadth of study in these areas. Collectively, they provide a detailed understanding of the molecular components involved in these processes and point to future directions in the field of legume-rhizobia research.

AUTHOR CONTRIBUTIONS

H-ML coordinated the preparation and completed the final version of this editorial. BF wrote the first draft. KM and NM contributed to the writing.

ACKNOWLEDGMENTS

Research in the laboratories of the Topic Editors is supported by ARC Discovery Project Grants DP130102266, DP130103084, and DP190102995 (BF), by JSPS KAKENHI Grant Number 18H02112 (KM), and the Hong Kong Research Grants Council General Research Fund 14108014 and Area of Excellence Scheme AoE/M-403/16 (H-ML).

REFERENCES

El Mujtar, V., Muñoz, N., Prack Mc Cormick, B., Pulleman, M., and Tittonell, P. (2019). Role and management of soil biodiversity for food security and nutrition; where do we stand? *Glob. Food Sec.* 20, 132–144. doi: 10.1016/j.gfs.2019.01.007

Ferguson, B. J., Indrasumunar, A., Hayashi, S., Lin, M.-H., Lin, Y.-H., Reid, D. E., et al. (2010). Molecular analysis of legume nodule development and autoregulation. *J. Integr. Plant Biol.* 52, 61–76. doi: 10.1111/j.1744-7909.2010.00899.x

Ferguson, B. J., Mens, C., Hastwell, A. H., Zhang, M., Su, H., Jones, C. H., et al. (2019). Legume nodulation: The host controls the party. *Plant Cell Environ.* 42:41–51. doi: 10.1111/pce.13348

Foyer, C. H., Lam, H.-M., Nguyen, H. T., Siddique, K. H., Varshney, R. K., Colmer, T. D., et al. (2016). Neglecting legumes has compromised human health and sustainable food production. *Nat. Plants* 2:16112. doi: 10.1038/NPLANTS.2016.112

Jiao, J., Ni, M., Zhang, B., Zhang, Z., Young, J. P. W., Chan, T.-F., et al. (2018). Coordinated regulation of core and accessory genes in the multipartite genome of *Sinorhizobium fredii*. *PLoS Genet.* 14:e1007428. doi: 10.1371/journal.pgen.1007428

Muñoz, N., Qi, X., Li, M.-W., Xie, M., Gao, Y., Cheung, M.-Y., et al. (2016). Improvement in nitrogen fixation capacity could be part of the

domestication process in soybean. *Heredity* 117, 84–93. doi: 10.1038/hdy.2016.27

Okazaki, S., Kaneko, T., Sato, S., and Saeki, K. (2013). Hijacking of leguminous nodulation signaling by the rhizobial type III secretion system. *Proc. Natl. Acad. Sci. U.S.A.* 110, 17131–17136. doi: 10.1073/pnas.1302360110

Sugawara, M., Takahashi, S., Umehara, Y., Iwano, H., Tsurumaru, H., Odake, H., et al. (2018). Variation in bradyrhizobial NopP effector determines symbiotic incompatibility with *Rj2*-soybeans via effector-triggered immunity. *Nat. Commun.* 9:3139. doi: 10.1038/s41467-018-05663-x

Conflict of Interest Statement: The authors declare that the research was conducted in the absence of any commercial or financial relationships that could be construed as a potential conflict of interest.

frontiers in Microbiology

ORIGINAL RESEARCH
published: 24 July 2018
doi: 10.3389/fmicb.2018.01644

Regulation of Nitrogen Fixation in *Bradyrhizobium* sp. Strain DOA9 Involves Two Distinct NifA Regulatory Proteins That Are Functionally Redundant During Symbiosis but Not During Free-Living Growth

Jenjira Wongdee[1], Nantakorn Boonkerd[1], Neung Teaumroong[1], Panlada Tittabutr[1]† and Eric Giraud[2]*†*

[1] School of Biotechnology, Institute of Agricultural Technology, Suranaree University of Technology, Nakhon Ratchasima, Thailand, [2] Laboratoire des Symbioses Tropicales et Méditerranéennes, Institut de Recherche Pour le Développement (IRD), UMR IRD, SupAgro, INRA, CIRAD, Université de Montpellier, Montpellier, France

OPEN ACCESS

Edited by:
Kiwamu Minamisawa,
Tohoku University, Japan

Reviewed by:
Christian Staehelin,
Sun Yat-sen University, China
Takashi Okubo,
Japan Agency for Marine-Earth Science and Technology, Japan

***Correspondence:**
Panlada Tittabutr
panlada@sut.ac.th
Eric Giraud
eric.giraud@ird.fr

† These authors have contributed equally to this work.

Specialty section:
This article was submitted to Plant Microbe Interactions, a section of the journal Frontiers in Microbiology

Received: 18 May 2018
Accepted: 02 July 2018
Published: 24 July 2018

Citation:
Wongdee J, Boonkerd N, Teaumroong N, Tittabutr P and Giraud E (2018) Regulation of Nitrogen Fixation in Bradyrhizobium sp. Strain DOA9 Involves Two Distinct NifA Regulatory Proteins That Are Functionally Redundant During Symbiosis but Not During Free-Living Growth. Front. Microbiol. 9:1644. doi: 10.3389/fmicb.2018.01644

The *Bradyrhizobium* sp. DOA9 strain displays the unusual properties to have a symbiotic plasmid and to fix nitrogen during both free-living and symbiotic growth. Sequence genome analysis shows that this strain contains the structural genes of dinitrogenase (*nifDK*) and the *nifA* regulatory gene on both the plasmid and chromosome. It was previously shown that both *nifDK* clusters are differentially expressed depending on growth conditions, suggesting different mechanisms of regulation. In this study, we examined the functional regulatory role of the two *nifA* genes found on the plasmid (*nifAp*) and chromosome (*nifAc*) that encode proteins with a moderate level of identity (55%) and different structural architectures. Using *gusA* (β-glucuronidase) reporter strains, we showed that both *nifA* genes were expressed during both the free-living and symbiotic growth stages. During symbiosis with *Aeschynomene americana*, mutants in only one *nifA* gene were not altered in their symbiotic properties, while a double *nifA* mutant was drastically impaired in nitrogen fixation, indicating that the two NifA proteins are functionally redundant during this culture condition. In contrast, under *in vitro* conditions, the *nifAc* mutant was unable to fix nitrogen, and no effect of the *nifAp* mutation was detected, indicating that NifAc is essential to activate *nif* genes during free-living growth. In accordance, the nitrogenase fixation deficiency of this mutant could be restored by the introduction of *nifAc* but not by *nifAp* or by two chimeric *nifA* genes encoding hybrid proteins with the N-terminus part of NifAc and the C-terminus of NifAp. Furthermore, transcriptional analysis by RT-qPCR of the WT and two *nifA* mutant backgrounds showed that NifAc and NifAp activated the expression of both chromosome and plasmid structural *nifDK* genes during symbiosis, while only NifAc activated the expression of *nifDKc* during free-living conditions. In summary, this study provides a better overview of the complex mechanisms of regulation of the nitrogenase genes in the DOA9 strain that involve two distinct NifA proteins, which are exchangeable during symbiosis for the activation of *nif* genes but not during free-living growth where NifAc is essential for the activation of *nifDKc*.

Keywords: NifA, *Bradyrhizobium*, symbiosis, legume, nitrogen, nitrogenase, Rhizobium

INTRODUCTION

Rhizobium-legume symbiosis is considered as the major contributor of biologically fixed nitrogen to terrestrial ecosystems. The reduction of atmospheric N_2 is catalyzed by the nitrogenase enzyme complex, which requires high-energy input in the form of ATP and electrons to break the triple bond. In addition, this enzymatic complex is highly sensitive to molecular oxygen, which irreversibly inactivates the enzyme. Diazotrophic bacteria have evolved sophisticated regulatory circuits of their nitrogen fixation (*nif*) genes in response to oxygen and nitrogen availability to prevent unnecessary energy consumption and permit the synthesis of the nitrogenase complex only during the proper environmental conditions (Burris and Roberts, 1993; Fischer, 1994).

A master regulator of nitrogen fixation is the NifA protein, which acts in association with the RNA polymerase sigma factor RpoN (σ^{54}) to activate the expression of *nif* genes by binding to an upstream activating sequence (UAS; 5′-TGT-N_{10}-ACA-3′). The NifA proteins show a typical three-domain structure. The N-terminal GAF domain is a ubiquitous signaling motif found in signaling and sensory proteins from all three kingdoms of life (Ho et al., 2000). The central domain interacts with the σ^{54}-RNA polymerase and possesses ATPase activity, while the C-terminal domain shows a helix-turn-helix (HTH) motif involved in DNA-binding. The activity of NifA is directly sensitive to molecular oxygen, and in some cases, is also directly affected by combined nitrogen (Kullik et al., 1989; Souza et al., 1999; Steenhoudt and Vanderleyden, 2000). In addition, the *nifA* gene is subjected to transcriptional regulation, although the mechanisms vary depending on the rhizobial strain. For example, in *Sinorhizobium meliloti*, *nifA* expression is activated by the FixLJ two-component regulatory system in response to low oxygen tension, while in *Bradyrhizobium japonicum*, the *fixR-nifA* operon is controlled by the redox-responsive two-component system RegSR (Bauer et al., 1998).

The rhizobia generally display only one *nifA* copy, but one exception has been described for *Mesorhizobium loti*, which contains two *nifA* genes, *nifA1* and *nifA2*, both located on the symbiotic island (Nukui et al., 2006). The *nifA1* gene is most similar to the *nifA* of *Rhizobium etli*, *R. leguminosarum*, and *S. meliloti*, and it is found in an identical genomic context associated with other *nif* genes, while *nifA2* is most similar to *nifA* from *B. japonicum* and is not found in the vicinity of known *nif* genes (Sullivan et al., 2013). Interestingly, the two *nifA* genes are not functionally redundant, since the *M. loti nifA2* mutant form nodules that do not fix nitrogen, while the *nifA1* mutant is not affected symbiotically (Nukui et al., 2006).

Another example of the presence of two *nifA* genes has recently emerged with the analysis of the genome sequence of the non-photosynthetic *Bradyrhizobium* sp. DOA9 strain (Okazaki et al., 2015). This bacterium, isolated from rice paddy fields using *Aeschynomene americana* as a trap legume (Noisangiam et al., 2012), displays several unusual properties. First, unlike all described bradyrhizobia, this strain contains a symbiotic megaplasmid (pDOA9) that harbors *nod* and *nif* genes (Okazaki et al., 2015). Second, on both the chromosome and the plasmid, it can be distinguished the nitrogenase *nifHDK* genes that encode the subunits of the nitrogenase complex. In both cases, the *nifHDK* genes are split into two clusters, *nifH* and *nifDK* (Okazaki et al., 2015). Third, as described for photosynthetic bradyrhizobia, the bacteria that do contain a chromosomal *nifV* gene can fix nitrogen in both the free living and symbiotic states (Wongdee et al., 2016). Data from previous research indicated that both *nifDK* clusters contribute to nitrogenase activity during symbiosis with *A. americana*, while the *nifDK* cluster found on the chromosome is the major contributor to the nitrogenase activity of the bacteria under free-living conditions (Wongdee et al., 2016). These data indicate that the two *nifDK* clusters identified in the DOA9 strain should be differentially regulated. This is supported by the fact that the DOA9 display two *nifA* genes but also two *rpoN* homologous genes, both located on each replicon. The simple explanation is that the *nifA* found on the chromosome (*nifAc*) and the *nifA* found on the plasmid (*nifAp*) specifically regulated the *nifDK* cluster found on the replicon where *nifA* is present. However, crosstalk between these two regulatory circuits would also be expected, given that NifDKp proteins require the expression of the accessory *nif* genes to form a functional nitrogenase. In particular, the *nifENX* genes whose products are needed for synthesis of the iron-molybdenum cofactor of nitrogenase, exist as a unique copy and are found downstream of the *nifDKc* cluster.

Thus, in the present work, we aimed to investigate in more detail the regulatory functions of the two *nifA* genes identified for the *Bradyrhizobium* sp. DOA9. In a first approach, we analyzed the expression levels of both *nifA* genes under different culture conditions using translational fusions to *gusA* (β-glucuronidase). We then analyzed the contribution of each regulatory protein to the control of bacterial nitrogenase activity under free-living and symbiotic states by constructing single and double *nifA* mutants. Finally, the expression level of several *nif* genes in three different backgrounds, the DOA9 wild-type (WT), Δ*nifAc*, and Δ*nifAp* mutant strains, were analyzed to identify which genes are activated by NifAc and NifAp.

MATERIALS AND METHODS

Bacterial Strains and Culture Media

The *Bradyrhizobium* sp. DOA9 WT was obtained from the School of Biotechnology, Suranaree University of Technology, Thailand, while all mutants were constructed in the Laboratoire des Symbioses Tropicales et Méditerranéennes (LSTM), France. These bacterial strains were grown at 28°C for 4 days in Yeast extract-mannitol (YM) medium (Vincent, 1970) or a BNM-B minimal medium (Renier et al., 2011). *Escherichia coli* strains were grown in LB medium at 37°C. When required, the media were supplemented with the appropriate antibiotics at the following concentrations: 100 μg/ml kanamycin, 200 μg/ml streptomycin, 20 μg/ml nalidixic acid, and 20 μg/ml cefotaxime.

Construction of the Reporter and Mutant Strains

All DNA fragments were amplified using the primers listed in **Supplementary Table S1**. To construct the reporter strains, DOA9-*Pm-fixRnifAc* and DOA9-*Pm-nifAp*, the 500-bp upstream region of *fixR* and the *nifAp* operon were amplified by PCR and cloned into the plasmid pVO155-*npt2-cefo-npt2-gfp*. This plasmid, which is a derivative of the pVO155 plasmid (Oke and Long, 1999), could not replicate in the *Bradyrhizobium* strains. The plasmid carries the promoterless *gusA*, *gfp*, kanamycin, and cefotaxime genes under the constitutive promoter *npt2* (Okazaki et al., 2016). To construct the two DOA9Ω*nifA* (insertion) mutants, 300 to 400 base pairs (bp) of the internal sequence of each *nifA* gene were amplified by PCR and cloned into the plasmid pVO155-*npt2-cefo-npt2-gfp*. To construct the DOA9Δ*nifA* deletion mutants, the upstream and downstream regions (between 700 and 1000-bp) of each *nifA* gene were amplified and merged using overlap extension PCR. Then, the fragment was cloned into the plasmid pK18 mob-*cefo-sacB*. This plasmid carries the *sacB* gene, which induces bacterial death in the presence of sucrose and the kanamycin-resistance gene (Tsai and Alley, 2000) as well as the cefotaxime gene under the *npt2* promoter that was added to the *KpnI* site. The various constructed plasmids were transferred into the DOA9 strain by mating, followed by the insertion or deletion of the selected mutants as previously described (Wongdee et al., 2016).

Complementation of the DOA9Δ*nifAc* Mutant

For the DOA9Δ*nifAc* mutant, the complete *nifAc*, *nifAp*, or hybrid of *nifAc* and *nifAp* genes were amplified and cloned downstream of the *npt2* promoter into the pMG103-*npt2-cefo* plasmid that harbored a cefotaxime resistance gene (Wongdee et al., 2016). This plasmid is stable and replicative in the DOA9 strain. To construct the hybrid *nifA* genes, the 5′-region of *nifAc* and the 3′-region of *nifAp* were amplified and merged using overlap extension PCR. The constructed plasmids were introduced into the competent cells of the DOA9Δ*nifAc* mutant by electroporation. The complemented strains were selected on YM plates supplemented with 20 μg/ml cefotaxime and 20 μg/ml nalidixic acid.

Plant Cultivation and Analysis Under Symbiotic Condition

The symbiosis efficiency of the *Bradyrhizobium* DOA9 strain and its derivatives were tested with *A. americana* No. 281 collected from the LSTM greenhouse. The seeds were surface sterilized by immersion in sulfuric acid under shaking for 45 min. Seeds were thoroughly washed with sterile distilled water and incubated overnight in sterile water. Seeds were transferred for 1 day at 37°C in the darkness on 0.8% agar plates for germination. Plantlets were transferred onto the top of the test tubes and covered by aluminum paper for hydroponic culture in buffered nodulation medium (BNM) (Ehrhardt et al., 1992). Plants were grown in a 28°C growth chamber with a 16-h light and 8-h dark regime and 70% humidity. Seven days after transfer, each seedling was inoculated with 1 ml of cell suspension resulting from a 5-day-old bacterial culture washed in BNM and adjusted to an optical density of one at 600 nm. For nodulation and the nitrogen fixation assay, 10 to 20 plants per condition were taken at 20 days post-inoculation (dpi) and analyzed for the number of nodules and nitrogenase activity as previously described (Bonaldi et al., 2010). The experiments were performed in duplicate.

Cytological Analysis

To follow the GUS activity in the nodules elicited by the reporter strains, 30- to 40-μm-thick sections from fresh nodule samples were prepared using a vibratome (VT1000S; Leica, Nanterre, France) and incubated at 37°C in the dark in GUS assay buffer for 1 h, as described in Bonaldi et al. (2010). After staining, the sections were mounted and observed under bright-field illumination with a macroscope (Nikon AZ100; Champigny-sur-Marne, France).

Determination of Nitrogenase Activity Under Free-Living Conditions

To determine the nitrogenase enzyme activity under free-living conditions, the *Bradyrhizobium* sp. strain DOA9 and derivatives were grown in 10-ml test tubes hermetically closed (BD Vacutainer, Franklin Lakes, NJ, United States) containing 2 ml of semisolid BNM-B medium (agar 0.8% w/v). The BNM-B medium is a synthetic plant growth medium (Ehrhardt et al., 1992) supplemented with a carbon (10 mM succinate) and a cocktail of vitamins (riboflavin at 0.2 μg/ml, biotin at 0.12 μg/ml, thiamine-HCl at 0.8 μg/ml, myo-inositol at 0.5 μg/ml, p-aminobenzoic acid at 0.1 μg/ml, nicotinic acid at 0.5 μg/ml, calcium pantothenate at 0.8 μg/ml, and cyanocobalamin at 1 ng/ml) to support growth of *Bradyrhizobium* strains (Renier et al., 2011). It is to note that the BNM-B medium was not supplemented with a nitrogenous source but the bacteria growth is possible thanks to the dinitrogen and oxygen present in the air constituting the initial headspace of the test tube. Just after closing hermitically the tubes, acetylene gas (1 ml) was injected to a final concentration of 10%. The cultures were then incubated at 28°C without shaking, and the gas samples were analyzed at 7 dpi for ethylene production by gas chromatography, as previously described (Renier et al., 2011).

Determination of β-Glucuronidase (GUS) Activity Under Free-Living Conditions

The two DOA9 reporter strains were grown for 4 days in YM medium, collected, and washed with BNM-B medium as described above. Bottles of 150-ml sealed with rubber stoppers and containing 55-ml of BNM-B medium and 95-ml of air were then inoculated with DOA9 reporter strains to an initial OD_{600} of 0.05. The cultures were then incubated at 28°C without shaking. After 7 days, the bacterial culture was removed from the bottle, and GUS activity was measured using the substrate *p*-nitrophenyl glucuronide (PNPG) as described by Jefferson (1987). β-glucuronidase units were calculated according to Miller (1972).

RNA Purification, cDNA Synthesis, and qRT-PCR

The expression of genes involved in nitrogen fixation of strain DOA9 was determined from cells grown under free-living conditions and bacteroids obtained from nodules of *A. americana* under symbiotic conditions. For free-living conditions, the bacterial cells were grown in 150-ml bottles as described just above. For harvesting, cultures were added to a 1:10 volume of "stop solution" [10% Tris-HCl-buffered phenol (pH 8) in ethanol], and cells removed from the liquid medium by centrifugation for 10 min (10,000 rpm, 4°C). The cell pellets were frozen in liquid nitrogen and stored at −80°C. Analysis under symbiotic conditions and RNA isolation from bacteroids were processed from approximately 1 g of frozen nodules by homogenization with a tungsten carbide bead (3 mm; Qiagen, Hilden, Germany) in 2-ml microcentrifuge tubes. Total RNA was isolated from the free-living bacterial cells, and the nodules were disrupted with a hot (65°C) phenol-extraction procedure that was previously described (Babst et al., 1996). RNA was purified and treated with DNase using mini-prep kits (Qiagen, Valencia, CA, United States). Then, the cDNA was synthesized with iScript TM Reverse transcription Supermix for RT-qPCR (Bio-Rad, Hercules, CA, United States). Then, 10–50 ng of each cDNA sample was added to PowerUP^{TM} SYBRTM Green master mixed buffer (Applied Biosystems, United States, Canada), and the appropriate amount of specific primers (listed in **Supplementary Table S2**) were used in the qRT-PCR analyses using an annealing temperature at 55°C for all reactions. The expression of target genes was relatively compared with the expression of the housekeeping gene, *dnaK*, using QuantStudio Design & Analysis Software from Applied Biosystems.

RESULTS

Bradyrhizobium sp. Strain DOA9 Displays Two Distinct *nifA* Genes Located on Both Chromosome and Mega-Plasmid (pDOA9)

Two *nifA* homologous genes can be identified in the *Bradyrhizobium* DOA9 strain. One copy found on the chromosome, termed *nifAc*, is located approximately 6 kb from the *nifDKENX* operon and found just downstream of the *fixR* gene (**Figure 1A**). In *B. japonicum*, *nifA* is also found downstream of *fixR*. It has been shown that the two genes are part of the same transcript (Thöny et al., 1987), suggesting that *fixR nifAc* also forms an operon in the DOA9 strain. Downstream of this operon, a gene (*fer*) encoding a 4Fe-4S ferredoxin and a *suf* operon composed of four genes (*sufB*, *sufC*, *sufD*, and *sufS*) were identified and have been shown to function in the assembly of iron-sulfur clusters (Takahashi and Tokumoto, 2002). The other copy found on the plasmid, known as *nifAp,* is surrounded by genes of unknown function, and no known *nif* or *fix* genes are found in the vicinity. The two corresponding NifA proteins are clearly distinct and are of different lengths; NifAc (579 aa) and NifAp (503 aa) display only 52% identity. A Pfam analysis to identify functional domains showed that NifAc displays a classical NifA architecture with a N-terminal GAFdomain, a central sigma 54 interaction domain and a C-terminal HTHdomain. NifAp shows a less classical structure with only the presence of the central and HTH domains (**Figure 1B**). The divergence of NifAp is not limited to the absence of the N-terminal GAF domain, since phylogenetic analysis showed that this protein formed an outgroup that was well separated from the NifA proteins identified in *Bradyrhizobium* strains (**Figure 1D**).

Interestingly, in both cases, a close examination of the promoter regions of the *fixRnifAc* operon and *nifAp* permitted the identification by manual analysis of a putative NifA and a RpoN binding sites, suggesting that both NifA proteins could autoregulate their own expression level and that of their homolog (**Figure 1C**).

Two *nifA* Genes Identified in DOA9 Strain Are Both Expressed During Symbiosis and Free-Living Growth

To analyze the expression of the two *nifA* genes identified in the *Bradyrhizobium* DOA9 strain, we constructed two reported strains (DOA9-*Pm-fixRnifAc* and DOA9-*Pm-nifAp*) by integrating the nonreplicative plasmid pVO155-*npt2-cefo-npt2-gfp*, which carries a promoterless *gusA* gene (Okazaki et al., 2016) downstream of the promoter region of the *fixRnifAc* operon and *nifAp* gene. Since the DOA9 strain was isolated using *A. americana* as a trap, we analyzed these two reporter strains in this host plant. Observations at 14 dpi showed that both reporter strains were able to nodulate and fix nitrogen similar to the WT-strain, indicating that the integration of the pVO155 plasmid in these two promoter regions did not alter the symbiotic performance of the strain (**Figures 2A–G**). Cytological analysis revealed a β-glucuronidase activity in the nodules, which was elicited by the two reporter strains, in contrast to the WT-nodules for which no activity could be detected (**Figures 2E–G**). Although X-gluc (5-Bromo-4-chloro-3-indolyl-β-D-glucuronide cyclohexylamine salt) staining is a qualitative measurement of gene expression, the naked eye could observe that the nodules elicited by DOA9-*Pm-nifAp* displayed a more intense blue color than those elicited by the DOA9-*Pm-fixRnifAc* reporter strain (**Figures 2F,G**), which indicates slight differences in the expression of the two *nifA* genes.

Similar observations were also made during free-living growth under microaerobic conditions and the absence of a combined nitrogen source. Indeed, after 7 days of culture in these conditions, the β-glucuronidase activity measured for DOA9-*Pm-nifAp* (30 Miller unit) was higher than that detected for the DOA9-*Pm-fixRnifAc* reporter strain (22 Miller Unit) (**Figure 2H**). Taken together, these data indicate that the two *nifA* genes identified in the DOA9 strain are expressed during symbiotic and free-living conditions and that in both conditions, the level of expression of *nifAp* is slightly higher than that of *nifAc*.

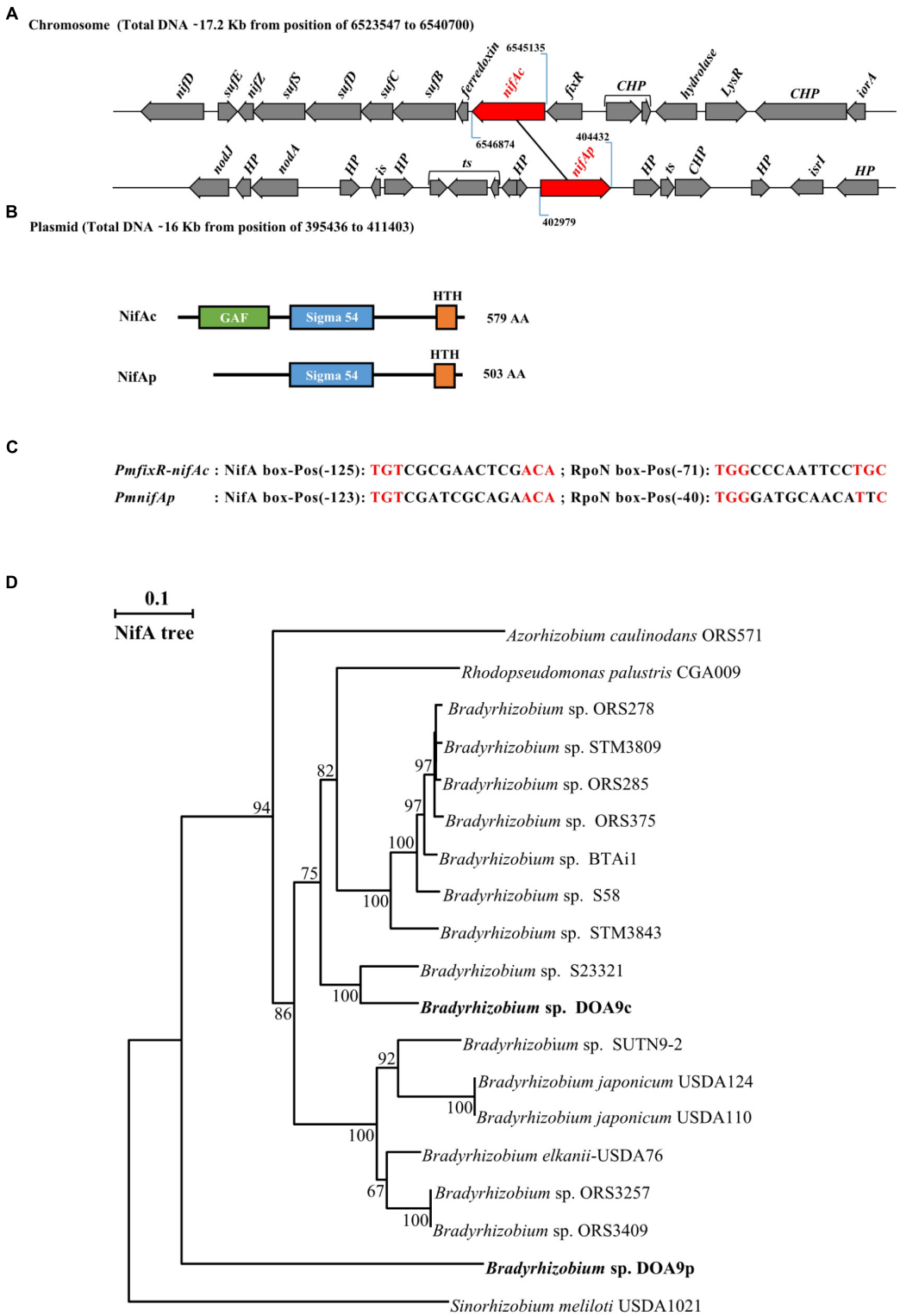

FIGURE 1 | *Bradyrhizobium* sp. strain DOA9 strain displays two distinct *nifA* genes. **(A)** Genetic organization of the two *nifA* genes (in red) located on both the chromosome and plasmid of the DOA9 strain. *nifAc, nifA* located on the chromosome; *nifAp, nifA* located on the plasmid; CHP: Conserved Hypothetical protein, HP: Hypothetical protein, *is*: intregrase and *ts*: transposase. **(B)** Predicted domain structure of both NifA proteins. **(C)** Putative NifA and RpoN boxes identified in promoter region of *fixR-nifAc* operon and *nifAp*. Pos: position of 5′ end nucleotide of motif relative to annotated start codon. **(D)** NifA phylogenetic tree showing relationship between NifA of bradyrhizobia. Sequences were aligned by CLUSTALX, and the tree was generated using the neighbor-joining method (Saitou and Nei, 1987) and displayed using NJPLOT (Perrière and Gouy, 1996). Bootstrap values, expressed as percentages of 1000 replications, are shown at branching points.

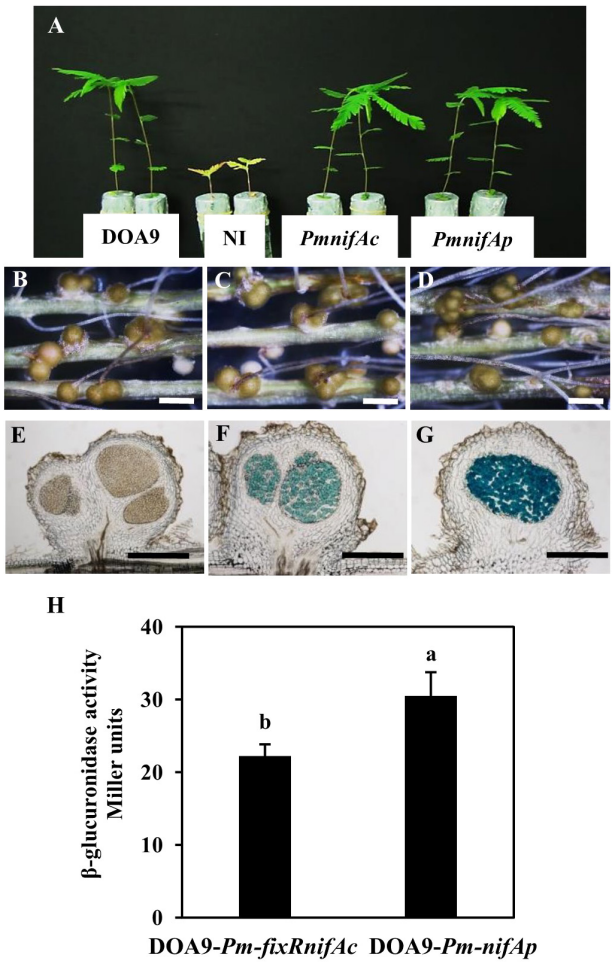

FIGURE 2 | The two *nifA* genes of *Bradyrhizobium* sp. DOA9 strain are expressed during symbiosis with *Aeschynomene americana*. **(A)** Comparison of growth of plants (aerial part) non-inoculated (NI) or inoculated with WT and reporter strains DOA9-*Pm-fixRnifAc* and DOA9-*Pm-nifAp* (at 14 dpi). **(B–D)** Root nodules observed with a stereomicroscope stereomicroscope. **(B)** Nodules elicited by WT; **(C)** Nodules elicited by DOA9-*Pm-fixRnifAc*; **(D)** Nodules elicited by DOA9-*Pm-nifAp*. **(E–G)** Expression of *gusA* reporter gene revealed on 40 μm nodule sections stained with X-Gluc. Nodules elicited by WT **(E)**, DOA9-*Pm-fixRnifAc* **(F)** and DOA9-*Pm-nifAp* **(G)**. Scale bars are 1 mm for **(B–D)** and 250 μm **(E–G)**. **(H)**, β-glucuronidase activity of DOA9-*Pm-fixRnifAc* and DOA9-*Pm-nifAp* reporter strains grown after 7 days of culture under free-living conditions (microaerobiosis and not combined nitrogen source). Different letters above error bars indicate significant differences at $P < 0.05$ (Tukey's HSD test).

nifAc and *nifAp* Genes in *Bradyrhizobium* sp. DOA9 Strain Are Functionally Redundant During Symbiosis

The NifA protein has been shown to be essential for symbiotic nitrogen fixation in several rhizobia (Szeto et al., 1984; Schetgens et al., 1985; Fischer et al., 1986; Iismaa and Watson, 1989). To appreciate the relative importance of each *nifA* gene identified in DOA9 during symbiosis, we constructed various *nifA* mutants, single *nifA* mutants, either by insertion (DOA9Ω*nifAc* and DOA9Ω*nifAp*) or deletion (DOA9Δ*nifAc* and DOA9Δ*nifAp*), and a double *nifA* mutant (DOA9Δ*nifAp*::Ω*nifAc*). As shown in **Figures 3A–C** and **Supplementary Figure S1**, the plants inoculated with the different single mutants displayed no significant difference from those inoculated with the WT strain in terms of their growth, the number of nodules formed or the measured nitrogenase activity indicating that the single mutation of the *nifAc* or *nifAp* gene had no impact on the symbiotic performance of the strain. In contrast, the plants inoculated with the double *nifA* mutant (Δ*nifAp*::Ω*nifAc*) displayed a strict fix minus phenotype (**Figure 3B**), and the growth of the plants was similar to that of the non-inoculated plants. Notably, the double *nifA* mutant induced nodules that were smaller and displayed symptoms of senescence (they were white instead of pink, indicating the absence of leghemoglobin and the central tissue was digested) (**Figures 3D–G**). Taken together these data suggest that the two NifA proteins identified in the DOA9 strain are functionally redundant during symbiosis and that at least one functional NifA protein is absolutely required for symbiotic nitrogenase activity, as observed in other rhizobia.

TABLE 1 | Nitrogenase activity in *Bradyrhizobium* sp. DOA9 (WT) and *nifA* mutant strains grown under free-living conditions as described in Material and Methods.

Treatments*	Acetylene reduction (nmol/h/culture)	SD
Non-inoculation	ND	ND
WT	3,643.55	±18.01
Ω*nifAc*	ND	ND
Δ*nifAc*	ND	ND
Ω*nifAp*	3,588.72	±74.99
Δ*nifAp*	3,547.54	±35.54
Δ*nifAp::*Ω*nifAc*	ND	ND
Δ*nifAc*::pMG103:*nifAc*	3,535.37	±137.4
Δ*nifAc*::pMG103:*nifAp*	ND	ND
Δ*nifAc*::pMG103:*nifAp hybrid1*	ND	ND
Δ*nifAc*::pMG103:*nifAp hybrid2*	ND	ND

**Nitrogen-starved cells were inoculated into glass vials containing 2 mL of medium and 10 mL of gas headspace and incubated at 30°C for 7 days in semisolid culture. SD, standard deviation determined from three replicates; ND, non detected.*

NifAc Is Essential for Nitrogen Fixation Under Free-Living Conditions

To determine whether the two *nifA* genes were also exchangeable during free-living conditions, we analyzed the nitrogenase activity of the different constructed *nifA* mutants after 7 days of culture in semisolid BNM medium. The *nifAc* mutants including DOA9Ω*nifAc* and DOA9Δ*nifAc* were obviously unable to fix nitrogen in their free-living state (**Table 1**). In contrast, DOA9Ω*nifAp* and DOA9Δ*nifAp* mutants displayed nitrogenase activity similar to the WT strain. These data indicate that NifAc is essential for nitrogenase activity during the free-living condition, while NifAp does not play a significant role in this condition. As expected, it was found that the double *nifA* mutant was not able to fix nitrogen in the free-living state (**Table 1**).

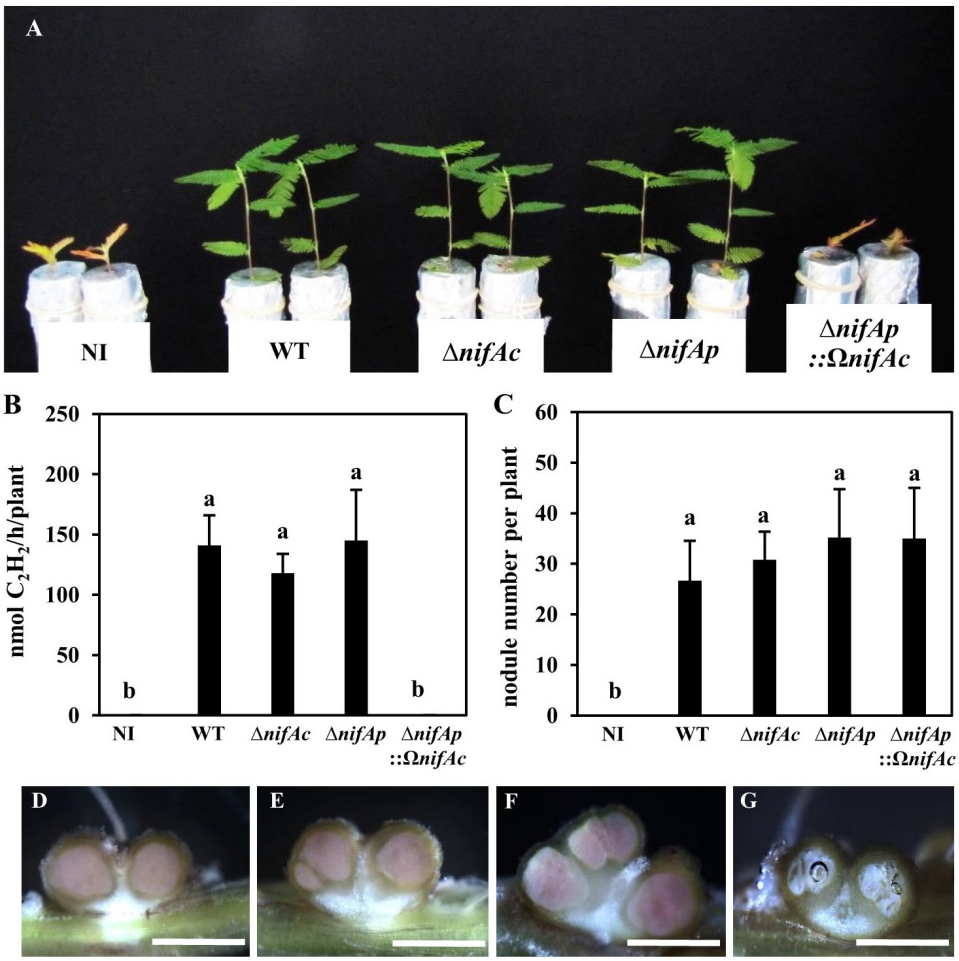

FIGURE 3 | The two *nifA* genes in *Bradyrhizobium* sp. DOA9 strain are functionally redundant during symbiosis with *Aeschynomene americana.* **(A)** Comparison of plant growth (aerial part) non-inoculated (NI) or inoculated with WT and mutant strains DOA9Δ*nifAc*, DOA9Δ*nifAp* and DOA9Δ*nifAp*::Ω*nifAc*DOA9 (at 20 dpi). **(B)** Amount of acetylene-reducing activity (ARA) in *A. americana* plants inoculated with WT and mutant strains. **(C)** Number of nodules per plant inoculated by WT and *nifA* mutant strains **(D–F)** Transversal sections of nodules elicited by WT **(D)**, DOA9Δ*nifAc* **(E)**, DOA9Δ*nifAp* **(F)**, and DOA9Δ*nifAp*::Ω*nifAc* **(G)** mutants. Scale bars are 1 mm for **(D–G)**. In **(B,C)**, error bars represent standard error (n = 10). Different letters above error bars indicate significant differences at $P < 0.05$ (Tukey's HSD test).

Because NifAp lacks the N-terminal GAF domain, a simple hypothesis would be to postulate that NifAp protein is not active under free-living conditions, due to the absence of this functional domain. To check this hypothesis, we constructed two chimeric NifA hybrid proteins, one corresponding to the almost complete NifAp, to which has been added the first 70 AA of NifAc, the second corresponding to the sigma 54 interaction domain and HTH domain of NifAp (from the AA 150 to 503), to which was added the complete GAF domain of NifAc (the first 220 AA). These constructs were cloned into the pMG103 plasmid under the constitutive *npt2* promoter and reintroduced into the DOA9Δ*nifAc* mutant (**Supplementary Figure S2**). As controls, we also reintroduced the complete *nifAc* or *nifAp* gene using the same plasmid and *npt2* promoter. As shown in **Table 1**, only the reintroduction of the complete *nifAc* gene completely restored the nitrogenase activity of the DOA9Δ*nifAc* mutant. No gain of function was observed for all other constructs. This suggests that simple addition of the GAF domain is not sufficient to rebuild functional activity in NifAp protein under free-living conditions.

NifAc and NifAp Activate Differently the Expression of Chromosome and Plasmid *nifHdk* Genes According to the Culture Conditions

The analysis of *nifA* mutants on plants suggested that the two NifA proteins are functionally redundant, but considering that a functional redundancy of the *nifHDK* genes found on the chromosome and the plasmid was also reported (Wongdee et al., 2016), we cannot completely exclude the possibility that the absence of phenotype observed for the single *nifA* mutants results in fact to this last redundancy. In other words, we can ask whether

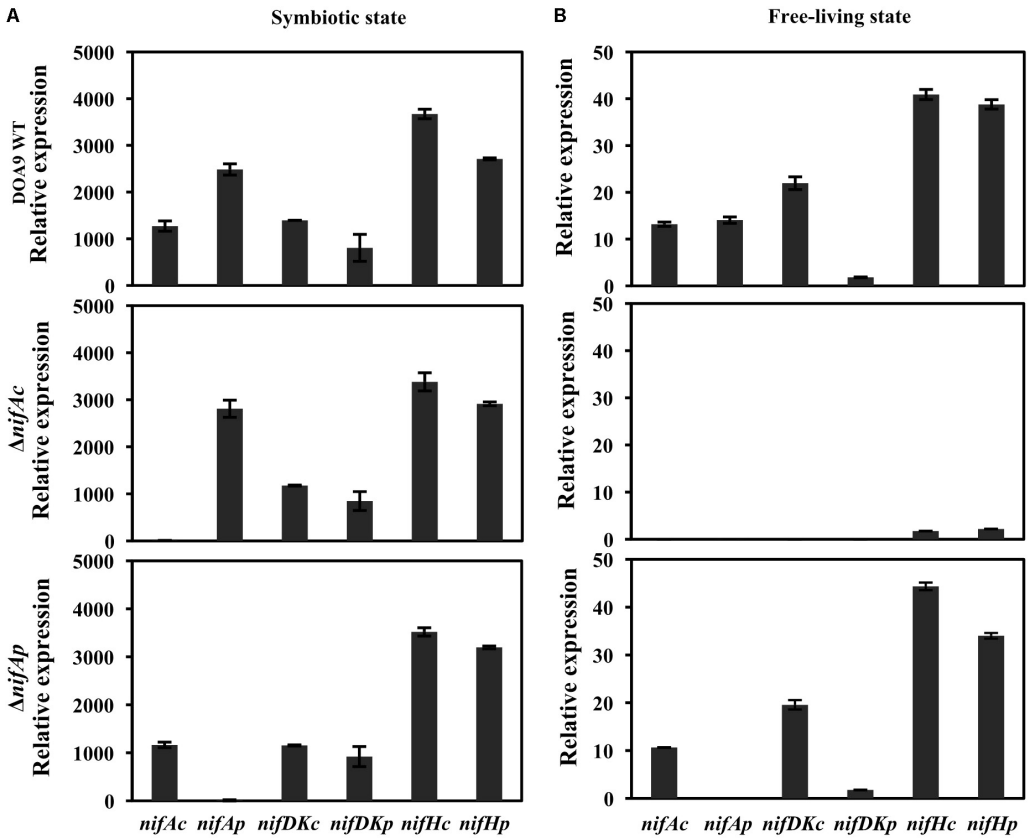

FIGURE 4 | Expression of nitrogen-fixing genes (*nifDKc*, *nifDKp*, *nifHc*, and *nifHp*) and *nifAc*, *nifAp* genes in *Bradyrhizobium* sp. DOA9 (WT) and *nifA* mutant strains grown under symbiosis **(A)** or free-living conditions **(B)**. Bacteroid cells were obtained from *A. americana* nodules at 20 days post-inoculation **(A)**, and bacterial cells grown under free-living conditions were obtained after 7 days of culture in BNM-B medium without glutamate **(B)**. Total RNA was extracted and subjected to quantitative reverse transcription-PCR (qRT-PCR) with an internal standard of *dnaK*. All data were from one representative experiment that was repeated three times. Error bars indicate standard deviation.

each NifA protein activates only one specific set of *nifHDK* genes, or both sets found on the chromosome and the plasmid.

To answer this question, we used quantitative reverse transcription PCR (qRT-PCR) to analyze the level of expression of the structural *nif* genes (*nifDKc*, *nifHc*, *nifDKp*, *nifHp*) as well as controls, namely, the two regulatory *nifA* genes (*nifAc*, *nifAp*) in both the WT and the two Δ*nifAc* and Δ*nifAp* mutants. As shown in **Figure 4A**, during symbiosis, the expression profiles of all structural *nif* genes is well conserved in the WT and the two *nifA* mutants. This clearly demonstrates that in this condition, the two NifA proteins can activate the expression of the two *nifHDK* sets, definitively confirming their functional redundancy in this condition. In contrast, during free-living growth, we observed that the Δ*nifAc* mutant differed drastically from the WT and the Δ*nifAp* mutant (**Figure 4B**). Indeed, in the Δ*nifAc* mutant, no expression of *nifDKc* and *p* was detected and the expression levels of *nifHc* and *p* were also extremely low. These data, which were in concordance with the absence of nitrogenase activity detected in this mutant, confirms the essential role of NifAc protein in the activation of *nif* genes under free-living conditions. In addition, for this mutant, no expression of *nifAp* could be detected, indicating that NifAc also activates the expression of *nifAp* which is in accordance with the presence of putative NifA and RpoN binding sites found in the *nifAp* promoter region.

In contrast, the pattern of expression of the *nif* genes remains very similar between the WT strain and the Δ*nifAp* mutant during free-living conditions, confirming that NifAp is dispensable during this condition. Interestingly, in these culture conditions, *nifDKc* was expressed at a far higher level than *nifDKp*. These data are in agreement with our previous study, which showed that NifDKc was the major contributor to the bacterial nitrogenase activity under free-living conditions (Wongdee et al., 2016).

Taken together, these data confirm that the two NifA proteins are exchangeable in the activation of *nif* genes during symbiosis, but not during free-living conditions, where NifAc is essential.

DISCUSSION

In this study, we showed that the two *nifA* genes present in the *Bradyrhizobium* sp. DOA9 strain are expressed during both symbiotic and free-living growth and encoded functional proteins. In particular, we observed that these two NifA are

perfectly exchangeable for the regulation of nitrogen fixation during symbiosis. These data were unexpected, given the moderate level of identity between these two proteins and the difference observed in their architectural organization (see Discussion below). Furthermore, in the only other example rhizobial strain reported to contain two *nifA* genes, *Mesorhizobium loti*, there was no functional redundancy observed between these two NifA proteins since the Δ*nifA2* mutant gave a Fix$^-$ phenotype, while no symbiotic defect was observed for the Δ*nifA1* mutant (Sullivan et al., 2001; Nukui et al., 2006). In fact, the regulatory role of NifA1 in this last bacterium is unclear, since the expression of NifA-regulated genes, i.e., those containing NifA and RpoN binding sites boxes in their promoter, were drastically impacted in the Δ*nifA2* mutant but not in the Δ*nifA1* background (Sullivan et al., 2013).

The origin of these two *nifA* genes in the DOA9 strain is puzzling. Their localization on different replicons and their moderate level of identity suggest that they were separately acquired, rather than via duplication of a single gene. In both cases, a Blast search using the amino acid sequence of NifAp or NifAc returned as best hits *Bradyrhizobium* NifA homologs, suggesting that both *nifA* genes derived from a common ancestor. However, while the percentage of identity of NifAc with the other bradyrhizobial NifA ranges between 91 to 76 %, this percentage drops to 55-50% for NifAp. In accordance, a phylogenetic analysis (**Figure 1D**) clearly showed that NifAp forms an outgroup from the bradyrhizobial NifA proteins. Furthermore, *nifAp* is found in an unusual genomic context, as no known *nif* or *fix* genes are found in the vicinity, in contrast to the other rhizobial *nifA* genes that were always found associated with genes involved in nitrogen fixation (Fischer, 1994). The presence of insertion sequence elements belonging to the IS3 family surrounding *nifAp* suggests the possibility that *nifAp* could have been separated from *nif* genes by a transposition event (**Supplementary Text S1**).

In all of the rhizobia in which *nifA* has been studied, it has been shown that NifA is absolutely required to activate nitrogen fixation during symbiosis (Szeto et al., 1984; Schetgens et al., 1985; Fischer et al., 1986; Iismaa and Watson, 1989). If the plant perceives that the nodules are ineffective, a sanctioning program is rapidly triggered (Westhoek et al., 2017), such as observed in this study for the double *nifA* mutant for which the nodules were senescing. Therefore, we can assume that NifA is essential for the symbiotic life of rhizobia and that there is a high selective pressure to maintain its functionality. DOA9 contains two *nifA* genes, and this likely relaxed this selective pressure and permitted a higher evolution rate of one homologous gene, i.e., *nifAp*. On the other hand, although *nifAp* has strongly diverged from the other *nifA*, NifAp remains functional, as it can activate both *nifHDKc* and *p* during symbiosis in the absence of NifAc. This suggests that maintaining two functional NifA proteins in DOA9 strain may be selectively advantageous even if there is an overlap in their regulatory function.

The major striking difference between NifAp and NifAc or the other bradyrhizobial NifA is the lack of an N-terminal GAF domain. There are several reports in various diazotrophic bacteria indicating that the GAF domain plays a key role in the modulation of NifA activity. For example, in *Azotobacter vinelandii*, the GAF domain binds 2-oxoglutarate, a key metabolic signal of carbon status, the presence of which influences the interaction with the antiactivator protein NifL (Martinez-Argudo et al., 2004). In the same vein, in *Herbaspirillum seropedicae,* NifA regulation by ammonium involves its N-terminal GAF domain and the signal transduction protein GlnK (Aquino et al., 2015). In contrast, to our knowledge, no functional role has been attributed to the N-terminal GAF domain of the rhizobial NifA proteins. It does not play an obvious role, since its deletion in the NifA of *S. meliloti* or *B. diazoefficiens* does not impair the ability of the protein to activate *nif* genes (Beynon et al., 1988; Fischer et al., 1988). Furthermore, it exists among rhizobia, one example (*R. leguminosarum)*, for which NifA naturally lacks this GAF domain and which, despite this, maintains its essential role in the activation of *nif* genes during symbiosis indicating that this domain is dispensable, at least under this culture condition (Iismaa and Watson, 1989). Therefore, it is not so surprising that NifAp maintains a regulatory role during symbiosis, despite the lack of a N-terminal GAF domain. It is more surprising that NifAp is not functional during free-living growth. Our RT-qPCR analysis clearly showed that in free-living conditions, *nifAp* was expressed, which excludes the possibility that the lack of complementation of the Δ*nifAc* mutant is due to the absence of NifAp synthesis. It is possible that the GAF domain, which is dispensable during symbiosis, plays a more prominent role in NifA activity under *in vitro* conditions. We tested this hypothesis by constructing two chimeric NifA hybrid proteins containing the N-terminal part of NifAc and the C-terminal part of NifAp, but these constructs did not restore the free-living nitrogen fixing deficiency of the Δ*nifAc* mutant. Nevertheless, we cannot completely reject this hypothesis because it is possible that these hybrid NifA proteins did not have the correct conformation. Further studies at the protein level remain necessary to better understand the function and mode of action of both NifA homologs under free-living conditions.

The mechanism of regulations involving NifA in the DOA9 strain are certainly more complex than expected, considering that this strain also contains two *rpoN* homologous genes found on both the plasmid and chromosome. NifA activates *nif* gene expression and other genes by forming a complex with RpoN (Gong et al., 2007; Hauser et al., 2007). We can ask whether each NifA protein can form a complex with both RpoN proteins and depending on the NifA and RpoN composition, whether the activity of this complex and its affinity for a DNA binding motif differs. Intriguingly, while the promoter regions of *nifDKc* and *nifHc* contain a perfectly conserved NifA binding site (5′-TGT-N_{10}-ACA-3′), only a nonconventional site differing by one nucleotide has been identified in the upstream regions of *nifDKp*, *nifHp* (Wongdee et al., 2016). Analysis of the expression of these *nif* genes suggests that these slight variations do not impact the ability of the two NifA proteins to activate the *nifDK* and *nifH* genes on both the chromosome and plasmid during symbiosis, since a similar level of expression of these different *nif* genes was observed for the 3 bacterial backgrounds tested (WT and the two *nifA* mutants). However, at the same time,

under free-living growth, *nifDKc* was more highly expressed than *nifDKp*. Therefore, we cannot exclude the hypothesis that these slight variations in the upstream activating sequence differentially impact the affinity of NifA (at least for NifAc) according to the environmental conditions. Behind the control of *nif* genes, the NifA protein influences various cellular processes in rhizobia (Fischer et al., 1986; Gong et al., 2007; Hauser et al., 2007). Thus, it is attractive to speculate that the presence of multiple NifA and RpoN proteins in the DOA9 strain facilitates the switch from a free-living to a symbiotic lifestyle and vice-versa, allowing better control of the expression of various sets of genes.

AUTHOR CONTRIBUTIONS

JW, NT, NB, PT, and EG conceived the experiments. JW, NT, PT, and EG conducted the experiments. JW, NT, PT, and EG analyzed the results and wrote the paper. All authors reviewed the manuscript.

FUNDING

This work was supported by the ARTS and BEST programs from IRD-France (Fellowship respectively to JW and PT) and the Franco-Thai PHC Siam program (project SIAM N°29589XA). This work was also supported by Suranaree University of Technology and the Office of the Higher Education Commission under the NRU project of Thailand.

SUPPLEMENTARY MATERIAL

The Supplementary Material for this article can be found online at: https://www.frontiersin.org/articles/10.3389/fmicb.2018.01644/full#supplementary-material

FIGURE S1 | The two *nifA* genes in *Bradyrhizobium* sp. DOA9 strain are functionally redundant during symbiosis with *Aeschynomene americana*. **(A)** Comparison of plant growth (aerial part) non-inoculated (NI) or inoculated with WT and insertion mutant strains DOA9Ω*nifAc* and DOA9Ω*nifAp* (at 20 dpi). **(B–D)** Root nodules observed with a fluorescent stereomicroscope equipped with a green fluorescent protein (GFP) filter. **(B)** Nodules elicited by WT; **(C)** Nodules elicited by DOA9Ω*nifAc*; **(D)** Nodules elicited by DOA9Ω*nifAp*. **(E)** Acetylene-reducing activity (ARA) in *A. americana* plants inoculated with WT and insertion mutant strains DOA9Ω*nifAc* and DOA9Ω*nifAp*. **(F)** Number of nodules per plant elicited by WT and DOA9Ω*nifAc* and DOA9Ω*nifAp*. **(G-I)** Cross section of nodule elicited by WT **(G)** and mutants DOA9Ω*nifAc* **(H)** and DOA9Ω*nifAp* **(I)**. Scale bars are 250 μm for **(D–G)**. In **(E,F)**, error bars represent standard error (n = 10). Different letters above error bars indicate significant differences at $P < 0.05$ (Tukey's HSD test).

FIGURE S2 | *Bradyrhizobium* sp. strain DOA9 strain displays two distinct *nifA* genes. **(A)** Sequence alignment of NifAc and NifAp. Arrows and boxes indicate different portions of NifAp and NifAc used to form chimeric NifA proteins **(B)**. The color boxes indicate NifAc protein domains including GAF (blue), sigma factor 54 (δ^{54}) interaction (purple), and HTH (green) domains. **(B)** Schematic representation of different versions of *nifA* introduced into plasmid pMG103-*npt2-cefo* under control of the constitutive *nptII* promoter. Each constructed plasmid was transferred into DOA9Δ*nifAc* cells for complementation experiments (see **Table 1**).

TABLE S1 | Primers used in this study.

TABLE S2 | Primers used in the qRT-PCR experiment.

TEXT S1 | Analysis of Insertion sequences in the *nifAp* surrounding region.

REFERENCES

Aquino, B., Stefanello, A. A., Oliveira, M. A., Pedrosa, F. O., Souza, E. M., Monteiro, R. A., et al. (2015). Effect of point mutations on *Herbaspirillum seropedicae* NifA activity. *Braz. J. Med. Biol. Res.* 48, 683–690. doi: 10.1590/1414-431X20154522

Babst, M., Hennecke, H., and Fischer, H. M. (1996). Two different mechanisms are involved in the heat-shock regulation of chaperonin gene expression in *Bradyrhizobium japonicum*. *Mol. Microbiol.* 19, 827–839. doi: 10.1046/j.1365-2958.1996.438968.x

Bauer, E., Kaspar, T., Fischer, H. M., and Hennecke, H. (1998). Expression of the *fixR-nifA* operon in *Bradyrhizobium japonicum* depends on a new response regulator, RegR. *J. Bacteriol.* 180, 3853–3863.

Beynon, J. L., Williams, M. K., and Cannon, F. C. (1988). Expression and functional analysis of the *Rhizobium meliloti nifA* gene. *EMBO J.* 7, 7–14. doi: 10.1002/j.1460-2075.1988.tb02777.x

Bonaldi, K., Gherbi, H., Franche, C., Bastien, G., Fardoux, J., Barker, D., et al. (2010). The Nod factor-independent symbiotic signaling pathway: development of *Agrobacterium rhizogenes*-mediated transformation for the legume *Aeschynomene indica*. *Mol. Plant Microbe Interact.* 23, 1537–1544. doi: 10.1094/MPMI-06-10-0137

Burris, R. H., and Roberts, G. P. (1993). Biological nitrogen fixation. *Annu. Rev. Nutr.* 1993, 17–35. doi: 10.1146/annurev.nu.13.070193.001533

Ehrhardt, D. W., Atkinson, E. M., and Long, S. R. (1992). Depolarization of alfalfa root hair membrane potential by *Rhizobium meliloti* Nod factors. *Science* 256, 998–1000. doi: 10.1126/science.10744524

Fischer, H. M. (1994). Genetic regulation of nitrogen fixation in rhizobia. *Microbiol. Rev.* 58, 352–386. s

Fischer, H. M., Alvarez-Morales, A., and Hennecke, H. (1986). The pleiotropic nature of symbiotic regulatory mutants: *Bradyrhizobium japonicum nifA* gene is involved in control of *nif* gene expression and formation of determinate symbiosis. *EMBO J.* 5, 1165–1173. doi: 10.1002/j.1460-2075.1986.tb04342.x

Fischer, H. M., Bruderer, T., and Hennecke, H. (1988). Essential and non-essential domains in the *Bradyrhizobium japonicum* NifA protein: identification of indispensible cysteine residues potentially involved in redox reactivity and/or metal binding. *Nucleic Acids Res.* 16, 2207–2224. doi: 10.1093/nar/16.5.2207

Gong, Z., Zhu, J., Yu, G., and Zou, H. (2007). Disruption of *nifA* gene influences multiple cellular processes in *Sinorhizobium meliloti*. *J. Genet. Genomics* 34, 783–789. doi: 1016/S1673-8527(07)60089-7

Hauser, F., Pessi, G., Friberg, M., Weber, C., Rusca, N., Lindemann, A., et al. (2007). Dissection of the *Bradyrhizobium japonicum* NifA-RpoN regulon, and identification of a ferredoxin gene (*fdxN*) for symbiotic nitrogen fixation. *Mol. Genet. Genomics* 278, 255–271. doi: 10.1007/s00438-007-0246-9

Ho, Y. S., Burden, L. M., and Hurley, J. H. (2000). Structure of the GAF domain, a ubiquitous signaling motif and a new class of cyclic GMP receptor. *EMBO J.* 19, 5288–5299. doi: 10.1093/emboj/20.6.1483

Iismaa, S. E., and Watson, J. M. (1989). The *nifA* gene product from *Rhizobium leguminosarum* biovar *trifolii* lacks the N-terminal domain found in other NifA proteins. *Mol. Microbiol.* 3, 943–955. doi: 10.1111/j.1365-2958.1989.tb00244.x

Jefferson, R. A. (1987). Assaying chimeric genes in plants: the GUS fusion system. *Plant Mol. Biol. Rep.* 5, 387–405. doi: 10.1007/BF02667740

Kullik, I., Hennecke, H., and Fischer, H. M. (1989). Inhibition of *Bradyrhizobium japonicum nifA*-dependent *nif* gene activation by oxygen occurs at the NifA protein level and is irreversible. *Arch. Microbiol.* 151, 191–197. doi: 10.1007/BF00413129

Martinez-Argudo, I., Little, R., and Dixon, R. (2004). Role of the amino-terminal GAF domain of the NifA activator in controlling the response to the antiactivator protein NifL. *Mol. Microbiol.* 52, 1731–1744. doi: 10.1111/j.1365-2958.2004.04089.x

Miller, J. (1972). *Experiments in Molecular Genetics*. Cold Spring Harbor, NY: Cold Spring Harbor Laboratory

Noisangiam, R., Teamtisong, K., Tittabutr, P., Boonkerd, N., Toshiki, U., Minamisawa, K., et al. (2012). Genetic diversity, symbiotic evolution, and

proposed infection process of *Bradyrhizobium* strains isolated from root nodules of *Aeschynomene americana* L. in Thailand. *Appl. Environ. Microbiol.* 78, 6236–6250. doi: 10.1128/AEM.00897-12

Nukui, N., Minamisawa, K., Ayabe, S., and Aoki, T. (2006). Expression of the 1-aminocyclopropane- 1-carboxylic acid deaminase gene requires symbiotic nitrogen-fixing regulator gene *nifA2* in *Mesorhizobium loti* MAFF303099. *Appl. Environ. Microbiol.* 72, 4964–4969. doi: 10.1128/AEM.02745-05

Okazaki, S., Noisangiam, R., Okubo, T., Kaneko, T., Oshima, K., Hattori, M., et al. (2015). Genome analysis of a novel *Bradyrhizobium* sp. DOA9 carrying a symbiotic plasmid. *PLoS One.* 10:e0117392. doi: 10.1371/journal.pone.0117392

Okazaki, S., Tittabutr, P., Teulet, A., Thouin, J., Fardoux, J., Chaintreuil, C., et al. (2016). *Rhizobium-legume* symbiosis in the absence of Nod factors: two possible scenarios with or without the T3SS. *ISME J.* 10, 64–74. doi: 10.1038/ismej.2015.103

Oke, V., and Long, S. R. (1999). Bacterial genes induced within the nodule during the *Rhizobium-legume* symbiosis. *Mol. Microbiol.* 32, 837–849. doi: 10.1046/j.1365-2958.1999.01402.x

Perrière, G., and Gouy, M. (1996). WWW-query: an on-line retrieval system for biological sequence banks. *Biochimie* 78, 364–369. doi: 10.1016/0300-9084(96)84768-7

Renier, A., Maillet, F., Fardoux, J., Poinsot, V., Giraud, E., and Nouwen, N. (2011). Photosynthetic *Bradyrhizobium* sp. strain ORS285 synthesizes 2-O-methyl-fucosylated lipochitooligo-saccharides for *nod* gene-dependent interaction with *Aeschynomene* plants. *Mol. Plant Microbe Interact.* 24, 1440–1447. doi: 10.1094/MPMI-05-11-0104

Saitou, N., and Nei, M. (1987). The neighbor-joining method: a new method for reconstructing phylogenetic trees. *Mol. Biol. Evol.* 4, 406–425. doi: 10.1093/oxfordjournals.molbev.a040454

Schetgens, R. M. P., Hontely, J. G. J., van den Bos, R. C., and van Kammen, A. (1985). Identification and phenotypical characterization of a cluster of *fix* genes, including a *nif* regulatory gene, from *Rhizobium leguminosarum* PRE. *Mol. Gen. Genet.* 200, 368–374. doi: 10.1007/BF00425719

Souza, E. M., Pedrosa, F. O., Drummond, M., Rigo, L. U., and Yates, M. G. (1999). Control of *Herbaspirillum seropedicae* NifA activity by ammonium ions and oxygen. *J. Bacteriol.* 181, 681–684.

Steenhoudt, O., and Vanderleyden, J. (2000). *Azospirillum*, a free-living nitrogen-fixing bacterium closely associated with grasses: genetic, biochemical and ecological aspects. *FEMS Microbiol. Rev.* 24, 487–506. doi: 10.1111/j.1574-6976.2000.tb00552.x

Sullivan, J. T., Brown, S. D., and Ronson, C. W. (2013). The NifA-RpoN regulon of *Mesorhizobium loti* strain R7A and its symbiotic activation by a novel LacI/GalR-family regulator. *PLoS One* 8:e53762. doi: 10.1371/journal.pone.0053762

Sullivan, J. T., Brown, S. D., Yocum, R. R., and Ronson, C. W. (2001). The *bio* operon on the acquired symbiosis island of *Mesorhizobium* sp. strain R7A includes a novel gene involved in pimeloyl-CoA synthesis. *Microbiol.* 147, 1315–1322. doi: 10.1099/00221287-147-5-1315

Szeto, W. W., Zimmerman, J. L., Sundaresan, V., and Ausubel, F. M. (1984). A *Rhizobium meliloti* symbiotic regulatory gene. *Cell* 36, 1035–1043. doi: 10.1016/0092-8674(84)90053-9

Takahashi, Y., and Tokumoto, U. (2002). A third bacterial system for the assembly of iron-sulfurclusters with homologs in archaea and plastids. *J. Biol. Chem.* 277, 28380–28383. doi: 10.1074/jbc.C200365200

Thöny, B., Fischer, H. M., Anthamatten, D., Bruderer, T., and Hennecke, H. (1987). The symbiotic nitrogen fixation regulatory operon (*fixRnifA*) of *Bradyrhizobium japonicum* is expressed aerobically and is subject to a novel, *nifA*-independent type of activation. *Nucleic Acids Res.* 15, 8479–8499. doi: 10.1093/nar/15.20.8479

Tsai, J. W., and Alley, M. R. (2000). Proteolysis of the McpA chemoreceptor does not require the *Caulobacter* major chemotaxis operon. *J. Bacteriol.* 182, 504–507. doi: 10.1128/JB.182.2.504-507.2000

Vincent, J. M. (1970). *A manual for the practical study of root-nodule bacteria. Handbook No. 15*. Hoboken, NJ: Blackwell Scientific Publications.

Westhoek, A., Field, E., Rehling, F., Mulley, G., Webb, I., Poole, P. S., et al. (2017). Policing the legume-Rhizobium symbiosis: a critical test of partner choice. *Sci. Rep.* 7:1419. doi: 10.1038/s41598-017-01634-2

Wongdee, J., Songwattana, P., Nouwen, N., Noisangiam, R., Fardoux, J., Chaintreuil, C., et al. (2016). *nifDK* clusters located on the chromosome and megaplasmid of *Bradyrhizobium* sp. strain DOA9 contribute differently to nitrogenase activity during symbiosis and free-living growth. *Mol. Plant Microbe Interact.* 29, 767–773. doi: 10.1094/MPMI-07-16-0140-R

Conflict of Interest Statement: The authors declare that the research was conducted in the absence of any commercial or financial relationships that could be construed as a potential conflict of interest.

frontiers in Plant Science

MINI REVIEW
published: 08 November 2018
doi: 10.3389/fpls.2018.01600

Transcriptional Reprogramming of Legume Genomes: Perspective and Challenges Associated With Single-Cell and Single Cell-Type Approaches During Nodule Development

Marc Libault[1,2,3]*

[1] Department of Agronomy and Horticulture, University of Nebraska-Lincoln, Lincoln, NE, United States, [2] Centre for Plant Science Innovation, University of Nebraska-Lincoln, Lincoln, NE, United States, [3] Center for Root and Rhizobiome Innovation, University of Nebraska-Lincoln, Lincoln, NE, United States

OPEN ACCESS

Edited by:
Brett James Ferguson, The University of Queensland, Australia

Reviewed by:
Christian Staehelin, Sun Yat-sen University, China
Stefanie Wienkoop, Universität Wien, Austria

***Correspondence:**
Marc Libault
marc.libault@unl.edu

Specialty section:
This article was submitted to Plant Microbe Interactions, a section of the journal Frontiers in Plant Science

Received: *17 August 2018*
Accepted: *17 October 2018*
Published: *08 November 2018*

Citation:
Libault M (2018) Transcriptional Reprogramming of Legume Genomes: Perspective and Challenges Associated With Single-Cell and Single Cell-Type Approaches During Nodule Development. Front. Plant Sci. 9:1600. doi: 10.3389/fpls.2018.01600

Transcriptomic approaches revealed thousands of genes differentially or specifically expressed during nodulation, a biological process resulting from the symbiosis between leguminous plant roots and rhizobia, atmospheric nitrogen-fixing symbiotic bacteria. Ultimately, nodulation will lead to the development of a new root organ, the nodule. Through functional genomic studies, plant transcriptomes have been used by scientists to reveal plant genes potentially controlling nodulation. However, it is important to acknowledge that the physiology, transcriptomic programs, and biochemical properties of the plant cells involved in nodulation are continuously regulated. They also differ between the different cell-types composing the nodules. To generate a more accurate picture of the transcriptome, epigenome, proteome, and metabolome of the cells infected by rhizobia and cells composing the nodule, there is a need to implement plant single-cell and single cell-types strategies and methods. Accessing such information would allow a better understanding of the infection of plant cells by rhizobia and will help understanding the complex interactions existing between rhizobia and the plant cells. In this mini-review, we are reporting the current knowledge on legume nodulation gained by plant scientists at the level of single cell-types, and provide perspectives on single cell/single cell-type approaches when applied to legume nodulation.

Keywords: legume, nodulation, root hair, single cell-type single-cell, transcriptome

INTRODUCTION

Nodulation is a complex biological process which occurs between the root system of plants (i.e., legumes and the genus Parasponia of the *Ulmaceae* family) and rhizobia, soil bacteria capable to fix and assimilate the atmospheric dinitrogen. The establishment of nitrogen-fixing nodules requires two developmental programs, one leading to the formation of infection threads

(plant-made structures through which rhizobia grow to reach the developing nodule) and one leading to nodule morphogenesis. Several molecular, physiological and cellular aspects of this biological interaction were characterized during the past two decades. For instance, the root and bacterial exudates used to initiate the recognition between the two partners are now well-characterized [e.g., plants flavonoids and iso-flavonoids (Phillips et al., 1994), bacterial nodulation factor (Nod factor) (Lerouge et al., 1990), and polysaccharides (Fraysse et al., 2003)]. More specifically, Nod factors are lipo-chitooligosaccharides whose synthesis is stimulated upon recognition of plant flavonoids by rhizobial NodD proteins (Oldroyd and Downie, 2008). Several functional genomic studies revealed the role of plant genes in controlling the perception then infection of the legume root hair cells and nodule cells by rhizobia (Oldroyd, 2013). Notably, the nodulation signaling pathway, a conserved gene regulatory pathway between legume species which is induced upon recognition of the Nod factor by Nod factor receptors, was characterized across several legume species (Oldroyd, 2013). In addition to these functional genomic studies, the development of microarrays followed by the emergence of high-throughput sequencing technologies led researchers to better characterize the overall response of the legume transcriptome to rhizobia inoculation and infection. For instance, these transcriptomic analyses were conducted to reveal the early responses of the legume root hair cells to rhizobia inoculation as well as the transcriptomic changes occurring during nodule development [see below for a more detailed description of these studies (Colebatch et al., 2002, 2004; Barnett et al., 2004; El Yahyaoui et al., 2004; Kouchi et al., 2004; Lee et al., 2004; Asamizu et al., 2005; Starker et al., 2006; Benedito et al., 2008; Brechenmacher et al., 2008; Hogslund et al., 2009; Libault et al., 2009; Afonso-Grunz et al., 2014; Roux et al., 2014; Kant et al., 2016; Peng et al., 2017; Yuan et al., 2017)].

While these studies allowed the identification of numerous differentially expressed genes, opening avenues for new functional analyses, the cellular complexity of the samples used to establish these transcriptomic resources remains a difficulty to accurately understand the response of plant cells to rhizobia inoculation and infection. For instance, only root hair cells localized in one specific zone of the root, the "susceptible zone" of the root system, are potentially infected. Similarly, only a subset of the nodule cells is infected by rhizobia upon endocytosis and formation of the symbiosome, a plant cell compartment containing the symbiotic bacteria. To overcome the problem associated with sample heterogeneity, researchers implemented strategies to isolate specific cell-types before applying the collection of high-throughput sequencing methodologies such as microarray hybridization and RNA-sequencing technology. Such strategy successfully revealed the activation and repression of transcriptomic programs in response to rhizobia inoculation and infection. In this mini-review, we are discussing the outcome of these analyses, their limitation, and opportunities to develop new strategies to better capture the dynamic changes of the legume transcriptome during the various stages of the nodulation process.

ROOT HAIR INFECTION BY RHIZOBIA

The infection of the plant root hair cell by rhizobia is a continuous process which is initiated by the chemical recognition between plant and rhizobia [i.e., plants flavonoids and iso-flavonoids are recognized by the bacteria leading to the activation of the transcriptional regulators NodD (Fisher and Long, 1993), and bacterial Nod factors as well as exopolysaccharides are recognized by Lysin motif-receptor-like kinases of host plants (Limpens et al., 2003; Madsen et al., 2003; Radutoiu et al., 2003; Kawaharada et al., 2015)]. This recognition between the two partners is required to insure the specificity of the interaction and the success of the symbiosis. Upon recognition, the plant root hair cell will adopt molecular and morphological changes in order to enhance its infection by rhizobia. For instance, a gradual and constant reorientation of the direction of root hair growth will lead to the curling of the root hair cell. This curling is needed in order to trap rhizobia into an infection pocket to enhance the infection rate of the root hair cells. The reallocation of plasma membrane proteins in response to rhizobia is also one of the earliest responses of the plant to rhizobia inoculation. Specifically, several proteins of the microdomain fraction of the plasma membrane are reallocated at the tip of the root hair cells only several hours after bacterial inoculation (Haney and Long, 2010; Qiao et al., 2017). Functional analysis of the *Medicago truncatula* flotillin proteins suggest that this reallocation is needed before the formation of the pre-infection thread, then during the initiation and elongation of the infection thread and the progression of rhizobia in the root hair cells in this tubular structure (Haney and Long, 2010).

As described above, the initiation of the nodulation process results from sequential and progressive changes in root hair cell physiological, morphological, and molecular responses. While the morphological responses of the root hair cells consecutively to rhizobia inoculation (e.g., root hair cell branching and curling) are well-documented based on their ease to be monitored under the microscope, the molecular response of the root hair cells remains poorly described, especially when considering the specific programs required at each step of the infection of the root hair cell (El Yahyaoui et al., 2004; Kouchi et al., 2004; Lohar et al., 2006; Hogslund et al., 2009; Libault et al., 2010b; Breakspear et al., 2014; Damiani et al., 2016; Jardinaud et al., 2016; **Figure 1**). Having the objective to carefully decipher the transcriptomic programs and the time-course of gene activity consecutively to rhizobia inoculation, single cell-type strategies were implemented. For instance, researchers isolated root sections enriched in rhizobia-susceptible root hair cells (Lohar et al., 2006; Hogslund et al., 2009; **Figure 1**). This strategy was useful since it led to the identification of hundreds of genes differentially expressed in response to bacteria inoculation. To reach a higher level of resolution of these responses, populations of root hair cells were isolated from the root system at different time after bacterial inoculation (Libault et al., 2010b; Breakspear et al., 2014; **Figure 1**). Such approach highlighted the regulation of thousands of genes including many genes of the Nodulation Signaling Pathway, the differential expression of genes at different time of the infection, and the transient activation of the plant defense system (Libault et al., 2010b). The rapid inhibition of

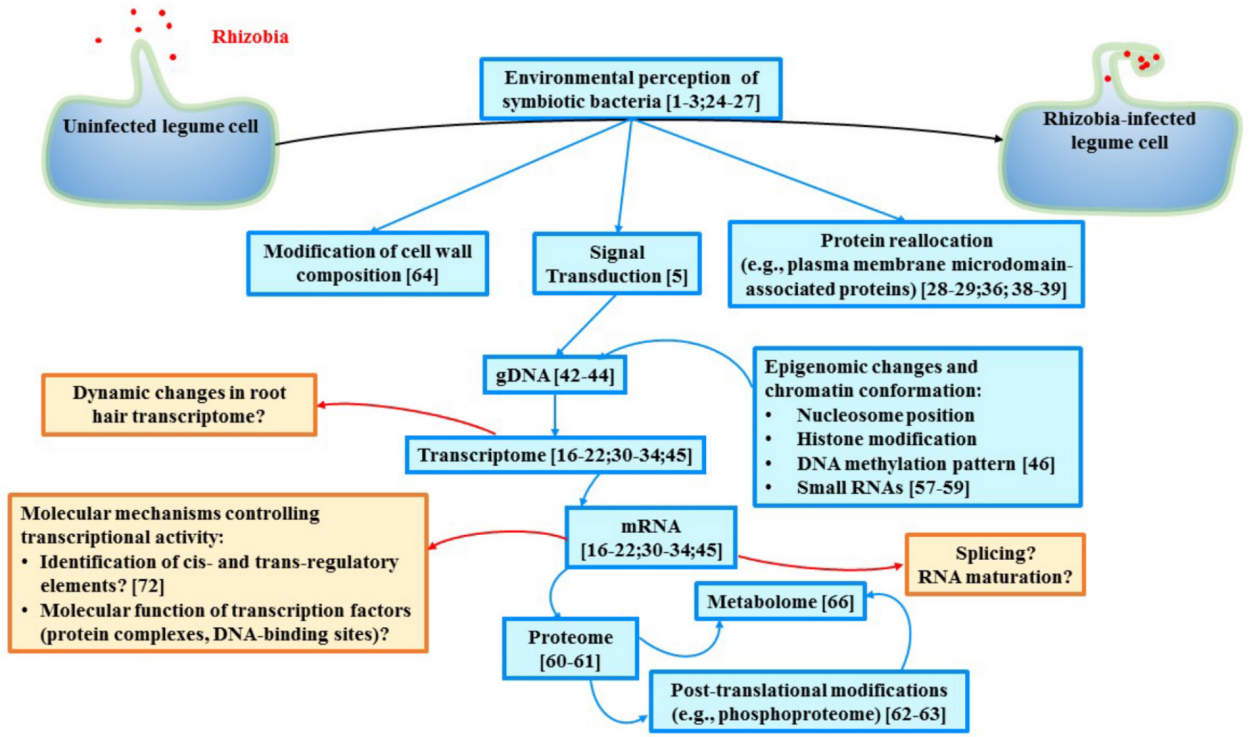

FIGURE 1 | Schematic representation of the current biological knowledge gained during the past years in legume symbiosis at the level of single cell-types (blue boxes) and some of the major remaining gaps existing in our understanding of legume nodulation (red boxes). Relevant studies are mentioned in each box. In addition to gain more knowledge in various aspects of legume nodulation, data integration must be conducted. Ideally, multi-omic analyses at the level of single cell relevant to study the nodulation process (e.g., infected root hair cells and cells composing the nodule) should be conducted. Another challenge is related to the dynamic molecular changes occurring in those cells during the recognition, interaction, infection then symbiosis between plant cells and rhizobia. Taking in consideration the permanent adaptation of each cell involved in nodulation will clearly enhance our understanding of legume nodulation.

the plant defense system in root hair cells is likely required to promote the infection of the plant by rhizobia (El Yahyaoui et al., 2004; Kouchi et al., 2004; Libault et al., 2010b).

Despite this effort, the temporal regulation of the expression of the legume genes upon rhizobia inoculation was difficult to highlight. This is inherent to the nodulation process itself since new root hair cells are continuously infected and each infection is independently progressing from another. Hence, the lack of synchronization of the infection of the root hairs by rhizobia logically leads to the isolation of a heterogeneous plant material: a mixture of unresponsive root hair cells (those located outside of the susceptible zone of the root system), responsive but uninfected root hairs, and responsive and infected root hairs. The latter category could also be divided in unique populations of cells according to their stage of infection by rhizobia.

THE LEGUME NODULE, A COMPLEX ROOT ORGAN

Concomitantly to root hair cell infection, the cortical cells of the root are actively dividing leading to the formation of the nodule primordia. The location of these divisions differ between legume species. For instance, in *M. truncatula*, the inner cortex and pericycle actively divide upon rhizobia inoculation whereas, in *Lotus japonicus*, the outer cortex cells divide (Szczyglowski et al., 1998; Timmers et al., 1999; Xiao et al., 2014). Alongside, the infection thread progresses in and between plant cells until it reaches those dividing cells. There, the bacteria which are differentiated in bacteroids, are released in the symbiosome, an organelle-like structure where the bacteroids are surrounded by the host plasma membrane. The presence of microdomain-associated proteins in the symbiosome membrane suggests a role of these membrane proteins in regulating the communication existing between the symbionts and the infected plant cells of the nodule (Haney and Long, 2010; Lefebvre et al., 2010; Qiao and Libault, 2017; Qiao et al., 2017).

Nodule organogenesis differs between legume species. For instance, indeterminate nodule development requires the maintenance of the primordia even upon formation of a mature indeterminate nodule (e.g., *M. truncatula* and *Pisum sativum*). Oppositely, in determinate nodules (e.g., *Glycine max*, *L. japonicus*, and *Phaseolus vulgaris*), the initially active nodule meristem will degenerate in mature nodules. As a consequence, the cellular organization differ between determinate and indeterminate nodules (Brewin, 1991; Ferguson et al., 2010). In indeterminate nodule four major zones can be distinguished. These zones are biologically different one from

another. Zone #1 which is located at the tip of the nodule is the site of the permanent nodule meristem. Zone #2 corresponds to the infection zone where the bacteria infect the plant cells. Zone #3 is the nitrogen fixation zone where the bacteroids fix and assimilate for the plant the atmospheric dinitrogen. Zone #4 is located on the basal side of the nodule zone and is the location of the senescence of the nodule cells. Oppositely to indeterminate nodules, determinate nodules are not organized in zones. However, these nodules remain structurally organized: the plant cells colonized by rhizobia are exclusively located in the center of the globular nodules and are surrounded by uninfected epidermal, cortex, and vascular cells. In addition to their complex cellular composition, the nodules are also characterized by the level of endoreduplication of their cells, a duplication of the genomic DNA without cell division (Foucher and Kondorosi, 2000; Vinardell et al., 2003; Kondorosi and Kondorosi, 2004). While most plant cells contain 2C of genomic DNA, the infected cells of the nodules can reach 4, 8, 16, 32, 64C, etc., of genomic DNA content where C is the haploid DNA content. As a consequence, the zone #3 of indeterminate nodules is characterized by its massive endoreduplication.

To date, most transcriptomic analyses conducted on legume nodules focused on their developmental stages rather than their cellular complexity [e.g., *L. japonicus* (Colebatch et al., 2002, 2004; Kouchi et al., 2004; Asamizu et al., 2005; Hogslund et al., 2009), *M. truncatula* (Barnett et al., 2004; El Yahyaoui et al., 2004; Starker et al., 2006; Benedito et al., 2008), *G. max* (Lee et al., 2004; Brechenmacher et al., 2008; Libault et al., 2009; Yuan et al., 2017), *Cicer arietinum* (Afonso-Grunz et al., 2014; Kant et al., 2016), and *Arachis hypogaea* (Peng et al., 2017; **Figure 1**]. In indeterminate nodules, Roux et al. (2014) collected different zones of the *M. truncatula* nodules validating the use of laser microdissection in order to better depict the unique transcriptional properties of each zone. This method helps validating the used of laser microdissection to enhance the purity of the biological samples used from nodules (Roux et al., 2018). More recently, the same group revealed the role of Mt*DME* (*DEMETER*) as a major regulator of the transcriptional activity of nodule genes and transposable elements (Satge et al., 2016). However, additional biological information is needed to reveal the complexity of the transcriptional regulation, especially in determinate nodules.

APPLYING SINGLE-CELL/SINGLE CELL-TYPE APPROACHES TO BETTER UNDERSTAND LEGUME NODULATION

In order to better understand the role of legume genes during the nodulation process, it is important to reveal the dynamic changes of their expression during nodulation (**Figure 1**). Such study should be conducted on infected root hair cells and nodule cells in order to capture the complexity of the molecular regulation at different stages of the infection of plant cells by the symbiotic bacteria. Accordingly, there is a need to isolate and separate each legume cell or cell-types (i.e., population of plant cells sharing the same biological function) infected by rhizobia or contributing to nodulation such as the root hairs preferentially located in the susceptible zone of the root and the different nodule cell-types (e.g., epidermal cells, vascular cells, and infected and uninfected cortex cells of the nodule).

Various methodologies were established to isolate plant cell-types (see Libault et al., 2017 for review). These methods consist in isolating transgenic plant cell protoplasts (i.e., living plant cells devoid in cell walls upon digestion of the cell wall by a cocktail of cellulases, hemicellulases, and pectinases) expressing the green fluorescent protein (GFP) in a cell-type dependent manner using fluorescent-activated cell sorting (FACS) (Birnbaum et al., 2003; Brady et al., 2007; Dinneny et al., 2008; Iyer-Pascuzzi et al., 2011; Petersson et al., 2015; Marx, 2016). Another approach consists in sequencing the transcriptome of cell nuclei upon their isolation (e.g., isolation of biotinylated nuclei) expecting that the cellular and nuclear transcriptomes are similar (Deal and Henikoff, 2011). A more sophisticated approach allowing the sequencing of transcripts interacting with ribosomes consists in the isolation of mRNA using a cell type-preferential tagged ribosomal protein (Zanetti et al., 2005). Applying those methods, genes preferentially expressed in specific root cell-types were characterized validating the idea of root cell-type-preferential transcriptomes. More recently, the gDNA methylation profiles from 6 different root cell-types from Arabidopsis were established (Kawakatsu et al., 2016). Another strategy successfully applied when analyzing the transcriptomic, epigenomic (Yan et al., 2013, 2015, 2016), proteomic (Larrainzar et al., 2007; Thal et al., 2018), phosphoproteomic (Nguyen et al., 2012; Rose et al., 2012), metabolomics (Brechenmacher et al., 2010), and glycomic (Muszynski et al., 2015) responses of legume plants during the nodulation process consist in to the massive isolation of root hairs inoculated with rhizobia (Brechenmacher et al., 2009, 2012; Libault et al., 2010a,c).

However, single cell-type approaches have several limitations when considering the nodulation process. For instance, while the isolation of a population of legume root hairs enhances plant sample homogeneity leading to a more accurate depiction of the molecular mechanisms controlling root hair infection by rhizobia, it is important to acknowledge the heterogeneity of this cellular population according to their unique stages of differentiation, unique responses to their environment, different stages in their infection by rhizobia, and the stochastic variations existing between cells. Also, other strategies need to be established to properly investigate the unique transcriptomic signature of the cells composing the nodule. To overcome these limitations, single-cell approaches (i.e., individual analysis of the transcriptome of each cell composing a complex organ) coupled with droplet-based microfluidic systems (Kolodziejczyk et al., 2015) are emerging. These systems [e.g., Chromium Single Cell Gene Expression Solution (10× Genomics), ddSEq (Bio-Rad), C1 (Fluidigm)] allow the separation and isolation of each single-cell preliminary to their molecular analysis. However, there are several technical limitations to consider when using these droplet-based microfluidic systems. For instance, the use of plant protoplasts in droplet-based microfluidic systems remains challenging due to the cell size discrimination of these systems (e.g., the 10× Genomics gel beads and C1 Fluidigm chips cannot

incorporate cells/nuclei larger than 52 and 25 μm of diameter, respectively). This size exclusion might lead to the absence or relative depletion of the transcriptome of large plant cells. Also, protoplast bursting remains a major concern leading to a decrease in RNA-seq library construction efficiency and a marginal representation of low-represented cell types (Shulse et al., 2018). Consequently, isolated plant nuclei represent an interesting alternative but it presupposes that the cell and nuclear transcriptomes are similar. Previous studies concluded that working on isolated nuclei is an acceptable way to overcome the problem of fragile cells (Deal and Henikoff, 2011). There is a need to validate this results on plant cells before to fully consider isolated nuclei as an alternative to single-cell biology. Consequently, the application of droplet technology on plant cells will require the combination of unique expertise in plant cell biology, molecular biology, and bioinformatics in order to generate viable biological samples compatible with droplet-based microfluidic systems. Being capable to overcome these limitations will open new avenues not only to understand legume nodulation but also to reveal the dynamic changes of the plant cell molecular responses during the infection process (**Figure 1**).

CONCLUSION AND PERSPECTIVES

Accessing single-cell transcriptomes is only a first step to fully understand legume nodulation. Additional avenues must be considered in order to develop a system-level understanding of legume nodulation including the integration of transcriptomic, epigenomic, proteomic, and metabolomics datasets. In addition, gene regulatory networks including the characterization of the binding sites of transcription factors controlling the nodulation process (Andriankaja et al., 2007) should also be more systematically characterized. As mentioned above, such experiments should be conducted at the level of single cells or, at least, at the level of single cell-types. In order to reach this goal, new strategies and technologies has been recently applied on plants or should be adapted to plant single cell biology (**Figure 1**). For instance, recent improvements of the sensitivity of mass-spectrometers and the development of new biochemical tools allow the characterization of plant single-cell proteomes (Misra et al., 2014; Zhu et al., 2016), and the three-dimensional spatial distributions of plant metabolites including from soybean nodules (Stopka et al., 2017; Velickovic et al., 2018). The establishment of single cell ATAC-seq methodology [Assay for Transposase-Accessible Chromatin using sequencing (Cusanovich et al., 2015)] to reveal the folding of the chromatin fiber of eukaryotic cells at the level of single cell also represents an interesting approach to better understand the impact of the epigenome on gene expression. However, the future access to such methodology will need to be adapted and applied to plant single cells.

AUTHOR CONTRIBUTIONS

ML designed, wrote, and edited this mini-review.

FUNDING

This work was funded by a grant from the National Science Foundation-Plant Genome Research Program (#IOS-1339194), by a grant from the National Science Foundation-CAREER Program (#IOS-1453613), and with the support of the University of Nebraska–Lincoln, The Center for Plant Science Innovation at the University of Nebraska–Lincoln, and The Center for Root and Rhizobiome Innovation at the University of Nebraska–Lincoln.

REFERENCES

Afonso-Grunz, F., Molina, C., Hoffmeier, K., Rycak, L., Kudapa, H., Varshney, R. K., et al. (2014). Genome-based analysis of the transcriptome from mature chickpea root nodules. *Front. Plant Sci.* 5:325. doi: 10.3389/fpls.2014.00325

Andriankaja, A., Boisson-Dernier, A., Frances, L., Sauviac, L., Jauneau, A., Barker, D. G., et al. (2007). AP2-ERF transcription factors mediate Nod factor dependent Mt ENOD11 activation in root hairs via a novel cis-regulatory motif. *Plant Cell* 19, 2866–2885. doi: 10.1105/tpc.107.052944

Asamizu, E., Nakamura, Y., Sato, S., and Tabata, S. (2005). Comparison of the transcript profiles from the root and the nodulating root of the model legume *Lotus japonicus* by serial analysis of gene expression. *Mol. Plant Microbe Interact.* 18, 487–498. doi: 10.1094/MPMI-18-0487

Barnett, M. J., Toman, C. J., Fisher, R. F., and Long, S. R. (2004). A dual-genome symbiosis chip for coordinate study of signal exchange and development in a prokaryote-host interaction. *Proc. Natl. Acad. Sci. U.S.A.* 101, 16636–16641. doi: 10.1073/pnas.0407269101

Benedito, V. A., Torres-Jerez, I., Murray, J. D., Andriankaja, A., Allen, S., Kakar, K., et al. (2008). A gene expression atlas of the model legume *Medicago truncatula*. *Plant J.* 55, 504–513. doi: 10.1111/j.1365-313X.2008.03519.x

Birnbaum, K., Shasha, D. E., Wang, J. Y., Jung, J. W., Lambert, G. M., Galbraith, D. W., et al. (2003). A gene expression map of the Arabidopsis root. *Science* 302, 1956–1960. doi: 10.1126/science.1090022

Brady, S. M., Orlando, D. A., Lee, J. Y., Wang, J. Y., Koch, J., Dinneny, J. R., et al. (2007). A high-resolution root spatiotemporal map reveals dominant expression patterns. *Science* 318, 801–806. doi: 10.1126/science.1146265

Breakspear, A., Liu, C., Roy, S., Stacey, N., Rogers, C., Trick, M., et al. (2014). The root hair "infectome" of *Medicago truncatula* uncovers changes in cell cycle genes and reveals a requirement for Auxin signaling in rhizobial infection. *Plant Cell* 26, 4680–4701. doi: 10.1105/tpc.114.133496

Brechenmacher, L., Kim, M. Y., Benitez, M., Li, M., Joshi, T., Calla, B., et al. (2008). Transcription profiling of soybean nodulation by *Bradyrhizobium japonicum*. *Mol. Plant Microbe Interact.* 21, 631–645. doi: 10.1094/MPMI-21-5-0631

Brechenmacher, L., Lee, J., Sachdev, S., Song, Z., Nguyen, T. H., Joshi, T., et al. (2009). Establishment of a protein reference map for soybean root hair cells. *Plant Physiol.* 149, 670–682. doi: 10.1104/pp.108.131649

Brechenmacher, L., Lei, Z., Libault, M., Findley, S., Sugawara, M., Sadowsky, M. J., et al. (2010). Soybean metabolites regulated in root hairs in response to the symbiotic bacterium *Bradyrhizobium japonicum*. *Plant Physiol.* 153, 1808–1822. doi: 10.1104/pp.110.157800

Brechenmacher, L., Nguyen, T. H., Hixson, K., Libault, M., Aldrich, J., Pasa-Tolic, L., et al. (2012). Identification of soybean proteins from a single cell type: the root hair. *Proteomics* 12, 3365–3373. doi: 10.1002/pmic.201200160

Brewin, N. J. (1991). Development of the legume root nodule. *Annu. Rev. Cell Biol.* 7, 191–226. doi: 10.1146/annurev.cb.07.110191.001203

Colebatch, G., Desbrosses, G., Ott, T., Krusell, L., Montanari, O., Kloska, S., et al. (2004). Global changes in transcription orchestrate metabolic differentiation

during symbiotic nitrogen fixation in *Lotus japonicus*. *Plant J.* 39, 487–512. doi: 10.1111/j.1365-313X.2004.02150.x

Colebatch, G., Kloska, S., Trevaskis, B., Freund, S., Altmann, T., and Udvardi, M. K. (2002). Novel aspects of symbiotic nitrogen fixation uncovered by transcript profiling with cDNA arrays. *Mol. Plant Microbe Interact.* 15, 411–420. doi: 10.1094/MPMI.2002.15.5.411

Cusanovich, D. A., Daza, R., Adey, A., Pliner, H. A., Christiansen, L., Gunderson, K. L., et al. (2015). Multiplex single cell profiling of chromatin accessibility by combinatorial cellular indexing. *Science* 348, 910–914. doi: 10.1126/science.aab1601

Damiani, I., Drain, A., Guichard, M., Balzergue, S., Boscari, A., Boyer, J. C., et al. (2016). Nod factor effects on root hair-specific transcriptome of *Medicago truncatula*: focus on plasma membrane transport systems and reactive oxygen species networks. *Front. Plant Sci.* 7:794. doi: 10.3389/fpls.2016.00794

Deal, R. B., and Henikoff, S. (2011). The INTACT method for cell type-specific gene expression and chromatin profiling in *Arabidopsis thaliana*. *Nat. Protoc.* 6, 56–68. doi: 10.1038/nprot.2010.175

Dinneny, J. R., Long, T. A., Wang, J. Y., Jung, J. W., Mace, D., Pointer, S., et al. (2008). Cell identity mediates the response of Arabidopsis roots to abiotic stress. *Science* 320, 942–945. doi: 10.1126/science.1153795

El Yahyaoui, F., Kuster, H., Ben Amor, B., Hohnjec, N., Puhler, A., Becker, A., et al. (2004). Expression profiling in *Medicago truncatula* identifies more than 750 genes differentially expressed during nodulation, including many potential regulators of the symbiotic program. *Plant Physiol.* 136, 3159–3176. doi: 10.1104/pp.104.043612

Ferguson, B. J., Indrasumunar, A., Hayashi, S., Lin, M. H., Lin, Y. H., Reid, D. E., et al. (2010). Molecular analysis of legume nodule development and autoregulation. *J. Integr. Plant Biol.* 52, 61–76. doi: 10.1111/j.1744-7909.2010.00899.x

Fisher, R. F., and Long, S. R. (1993). Interactions of Nodd at the Nod box - Nodd binds to 2 distinct sites on the same face of the helix and induces a bend in the DNA. *J. Mol. Biol.* 233, 336–348. doi: 10.1006/jmbi.1993.1515

Foucher, F., and Kondorosi, E. (2000). Cell cycle regulation in the course of nodule organogenesis in *Medicago*. *Plant Mol. Biol.* 43, 773–786. doi: 10.1023/A:1006405029600

Fraysse, N., Couderc, F., and Poinsot, V. (2003). Surface polysaccharide involvement in establishing the rhizobium-legume symbiosis. *Eur. J. Biochem.* 270, 1365–1380. doi: 10.1046/j.1432-1033.2003.03492.x

Haney, C. H., and Long, S. R. (2010). Plant flotillins are required for infection by nitrogen-fixing bacteria. *Proc. Natl. Acad. Sci. U.S.A.* 107, 478–483. doi: 10.1073/pnas.0910081107

Hogslund, N., Radutoiu, S., Krusell, L., Voroshilova, V., Hannah, M. A., Goffard, N., et al. (2009). Dissection of symbiosis and organ development by integrated transcriptome analysis of *Lotus japonicus* mutant and wild-type plants. *PLoS One* 4:e6556. doi: 10.1371/journal.pone.0006556

Iyer-Pascuzzi, A. S., Jackson, T., Cui, H., Petricka, J. J., Busch, W., Tsukagoshi, H., et al. (2011). Cell identity regulators link development and stress responses in the Arabidopsis root. *Dev. Cell* 21, 770–782. doi: 10.1016/j.devcel.2011.09.009

Jardinaud, M. F., Boivin, S., Rodde, N., Catrice, O., Kisiala, A., Lepage, A., et al. (2016). A laser dissection-RNAseq analysis highlights the activation of cytokinin pathways by Nod factors in the *Medicago truncatula* root epidermis. *Plant Physiol.* 171, 2256–2276. doi: 10.1104/pp.16.00711

Kant, C., Pradhan, S., and Bhatia, S. (2016). Dissecting the root nodule transcriptome of chickpea (*Cicer arietinum* L.). *PLoS One* 11:e0157908. doi: 10.1371/journal.pone.0157908

Kawaharada, Y., Kelly, S., Nielsen, M. W., Hjuler, C. T., Gysel, K., Muszynski, A., et al. (2015). Receptor-mediated exopolysaccharide perception controls bacterial infection. *Nature* 523, 308–312. doi: 10.1038/nature14611

Kawakatsu, T., Stuart, T., Valdes, M., Breakfield, N., Schmitz, R. J., Nery, J. R., et al. (2016). Unique cell-type-specific patterns of DNA methylation in the root meristem. *Nat. Plants* 2:16058. doi: 10.1038/nplants.2016.58

Kolodziejczyk, A. A., Kim, J. K., Svensson, V., Marioni, J. C., and Teichmann, S. A. (2015). The technology and biology of single-cell RNA sequencing. *Mol. Cell* 58, 610–620. doi: 10.1016/j.molcel.2015.04.005

Kondorosi, E., and Kondorosi, A. (2004). Endoreduplication and activation of the anaphase-promoting complex during symbiotic cell development. *FEBS Lett.* 567, 152–157. doi: 10.1016/j.febslet.2004.04.075

Kouchi, H., Shimomura, K., Hata, S., Hirota, A., Wu, G. J., Kumagai, H., et al. (2004). Large-scale analysis of gene expression profiles during early stages of root nodule formation in a model legume, *Lotus japonicus*. *DNA Res.* 11, 263–274. doi: 10.1093/dnares/11.4.263

Larrainzar, E., Wienkoop, S., Weckwerth, W., Ladrera, R., Arrese-Igor, C., and Gonzalez, E. M. (2007). *Medicago truncatula* root nodule proteome analysis reveals differential plant and bacteroid responses to drought stress. *Plant Physiol.* 144, 1495–1507. doi: 10.1104/pp.107.101618

Lee, H., Hur, C. G., Oh, C. J., Kim, H. B., Pakr, S. Y., and An, C. S. (2004). Analysis of the root nodule-enhanced transcriptome in soybean. *Mol. Cells* 18, 53–62.

Lefebvre, B., Timmers, T., Mbengue, M., Moreau, S., Herve, C., Toth, K., et al. (2010). A remorin protein interacts with symbiotic receptors and regulates bacterial infection. *Proc. Natl. Acad. Sci. U.S.A.* 107, 2343–2348. doi: 10.1073/pnas.0913320107

Lerouge, P., Roche, P., Faucher, C., Maillet, F., Truchet, G., Prome, J. C., et al. (1990). Symbiotic host-specificity of *Rhizobium meliloti* is determined by a sulphated and acylated glucosamine oligosaccharide signal. *Nature* 344, 781–784. doi: 10.1038/344781a0

Libault, M., Brechenmacher, L., Cheng, J., Xu, D., and Stacey, G. (2010a). Root hair systems biology. *Trends Plant Sci.* 15, 641–650. doi: 10.1016/j.tplants.2010.08.010

Libault, M., Farmer, A., Brechenmacher, L., Drnevich, J., Langley, R. J., Bilgin, D. D., et al. (2010b). Complete transcriptome of the soybean root hair cell, a single-cell model, and its alteration in response to *Bradyrhizobium japonicum* infection. *Plant Physiol.* 152, 541–552. doi: 10.1104/pp.109.148379

Libault, M., Farmer, A., Brechenmacher, L., May, G. D., and Stacey, G. (2010c). Soybean root hairs: a valuable system to investigate plant biology at the cellular level. *Plant Signal. Behav.* 5, 419–421.

Libault, M., Joshi, T., Takahashi, K., Hurley-Sommer, A., Puricelli, K., Blake, S., et al. (2009). Large-scale analysis of putative soybean regulatory gene expression identifies a Myb gene involved in soybean nodule development. *Plant Physiol.* 151, 1207–1220. doi: 10.1104/pp.109.144030

Libault, M., Pingault, L., Zogli, P., and Schiefelbein, J. (2017). Plant systems biology at the single-cell level. *Trends Plant Sci.* 22, 949–960. doi: 10.1016/j.tplants.2017.08.006

Limpens, E., Franken, C., Smit, P., Willemse, J., Bisseling, T., and Geurts, R. (2003). LysM domain receptor kinases regulating rhizobial Nod factor-induced infection. *Science* 302, 630–633. doi: 10.1126/science.1090074

Lohar, D. P., Sharopova, N., Endre, G., Penuela, S., Samac, D., Town, C., et al. (2006). Transcript analysis of early nodulation events in *Medicago truncatula*. *Plant Physiol.* 140, 221–234. doi: 10.1104/pp.105.070326

Madsen, E. B., Madsen, L. H., Radutoiu, S., Olbryt, M., Rakwalska, M., Szczyglowski, K., et al. (2003). A receptor kinase gene of the LysM type is involved in legume perception of rhizobial signals. *Nature* 425, 637–640. doi: 10.1038/nature02045

Marx, V. (2016). Plants: a tool box of cell-based assays. *Nat. Methods* 13, 551–554. doi: 10.1038/nmeth.3900

Misra, B. B., Assmann, S. M., and Chen, S. (2014). Plant single-cell and single-cell-type metabolomics. *Trends Plant Sci.* 19, 637–646. doi: 10.1016/j.tplants.2014.05.005

Muszynski, A., O'Neill, M. A., Ramasamy, E., Pattathil, S., Avci, U., Pena, M. J., et al. (2015). Xyloglucan, galactomannan, glucuronoxylan, and rhamnogalacturonan I do not have identical structures in soybean root and root hair cell walls. *Planta* 242, 1123–1138. doi: 10.1007/s00425-015-2344-y

Nguyen, T. H., Brechenmacher, L., Aldrich, J. T., Clauss, T. R., Gritsenko, M. A., Hixson, K. K., et al. (2012). Quantitative phosphoproteomic analysis of soybean root hairs inoculated with *Bradyrhizobium japonicum*. *Mol. Cell. Proteomics* 11, 1140–1155. doi: 10.1074/mcp.M112.018028

Oldroyd, G. E. (2013). Speak, friend, and enter: signalling systems that promote beneficial symbiotic associations in plants. *Nat. Rev. Microbiol.* 11, 252–263. doi: 10.1038/nrmicro2990

Oldroyd, G. E., and Downie, J. A. (2008). Coordinating nodule morphogenesis with rhizobial infection in legumes. *Annu. Rev. Plant Biol.* 59, 519–546. doi: 10.1146/annurev.arplant.59.032607.092839

Peng, Z., Liu, F., Wang, L., Zhou, H., Paudel, D., Tan, L., et al. (2017). Transcriptome profiles reveal gene regulation of peanut (*Arachis hypogaea* L.) nodulation. *Sci. Rep.* 7:40066. doi: 10.1038/srep40066

Petersson, S. V., Linden, P., Moritz, T., and Ljung, K. (2015). Cell-type specific metabolic profiling of *Arabidopsis thaliana* protoplasts as a tool for plant systems biology. *Metabolomics* 11, 1679–1689. doi: 10.1007/s11306-015-0814-7

Phillips, D. A., Dakora, F. D., Sande, E., Joseph, C. M., and Zon, J. (1994). Synthesis, release, and transmission of alfalfa signals to rhizobial symbionts. *Plant Soil* 161, 69–80. doi: 10.1007/BF02183086

Qiao, Z., Brechenmacher, L., Smith, B., Strout, G. W., Mangin, W., Taylor, C., et al. (2017). The GmFWL1 (FW2-2-like) nodulation gene encodes a plasma membrane microdomain-associated protein. *Plant Cell Environ.* 40, 1442–1455. doi: 10.1111/pce.12941

Qiao, Z., and Libault, M. (2017). Function of plasma membrane microdomain-associated proteins during legume nodulation. *Plant Signal. Behav.* 12, e1365215. doi: 10.1080/15592324.2017.1365215

Radutoiu, S., Madsen, L. H., Madsen, E. B., Felle, H. H., Umehara, Y., Gronlund, M., et al. (2003). Plant recognition of symbiotic bacteria requires two LysM receptor-like kinases. *Nature* 425, 585–592. doi: 10.1038/nature02039

Rose, C. M., Venkateshwaran, M., Volkening, J. D., Grimsrud, P. A., Maeda, J., Bailey, D. J., et al. (2012). Rapid phosphoproteomic and transcriptomic changes in the rhizobia-legume symbiosis. *Mol. Cell. Proteomics* 11, 724–744. doi: 10.1074/mcp.M112.019208

Roux, B., Rodde, N., Jardinaud, M. F., Timmers, T., Sauviac, L., Cottret, L., et al. (2014). An integrated analysis of plant and bacterial gene expression in symbiotic root nodules using laser-capture microdissection coupled to RNA sequencing. *Plant J.* 77, 817–837. doi: 10.1111/tpj.12442

Roux, B., Rodde, N., Moreau, S., Jardinaud, M. F., and Gamas, P. (2018). Laser capture micro-dissection coupled to RNA sequencing: a powerful approach applied to the model legume *Medicago truncatula* in interaction with *Sinorhizobium meliloti*. *Methods Mol. Biol.* 1830, 191–224. doi: 10.1007/978-1-4939-8657-6_12

Satge, C., Moreau, S., Sallet, E., Lefort, G., Auriac, M. C., Rembliere, C., et al. (2016). Reprogramming of DNA methylation is critical for nodule development in *Medicago truncatula*. *Nat. Plants* 2:16166. doi: 10.1038/nplants.2016.166

Shulse, C. C. B., Turco, G., Zhu, Y., Brady, S., and Dickel, D. (2018). High-throughput single-cell transcriptome profiling of plant cell types. *bioRxiv* [Preprint]. doi: 10.1101/402966

Starker, C. G., Parra-Colmenares, A. L., Smith, L., Mitra, R. M., and Long, S. R. (2006). Nitrogen fixation mutants of *Medicago truncatula* fail to support plant and bacterial symbiotic gene expression. *Plant Physiol.* 140, 671–680. doi: 10.1104/pp.105.072132

Stopka, S. A., Agtuca, B. J., Koppenaal, D. W., Pasa-Tolic, L., Stacey, G., Vertes, A., et al. (2017). Laser-ablation electrospray ionization mass spectrometry with ion mobility separation reveals metabolites in the symbiotic interactions of soybean roots and rhizobia. *Plant J.* 91, 340–354. doi: 10.1111/tpj.13569

Szczyglowski, K., Shaw, R. S., Wopereis, J., Copeland, S., Hamburger, D., Kasiborski, B., et al. (1998). Nodule organogenesis and symbiotic mutants of the model legume *Lotus japonicus*. *Mol. Plant Microbe Interact.* 11, 684–697. doi: 10.1094/MPMI.1998.11.7.684

Thal, B., Braun, H. P., and Eubel, H. (2018). Proteomic analysis dissects the impact of nodulation and biological nitrogen fixation on Vicia faba root nodule physiology. *Plant Mol. Biol.* 97, 233–251. doi: 10.1007/s11103-018-0736-7

Timmers, A. C. J., Auriac, M. C., and Truchet, G. (1999). Refined analysis of early symbiotic steps of the *Rhizobium-Medicago* interaction in relationship with microtubular cytoskeleton rearrangements. *Development* 126, 3617–3628.

Velickovic, D., Agtuca, B. J., Stopka, S. A., Vertes, A., Koppenaal, D. W., Pasa-Tolic, L., et al. (2018). Observed metabolic asymmetry within soybean root nodules reflects unexpected complexity in rhizobacteria-legume metabolite exchange. *ISME J.* 12, 2335–2338. doi: 10.1038/s41396-018-0188-8

Vinardell, J. M., Fedorova, E., Cebolla, A., Kevei, Z., Horvath, G., Kelemen, Z., et al. (2003). Endoreduplication mediated by the anaphase-promoting complex activator CCS52A is required for symbiotic cell differentiation in *Medicago truncatula* nodules. *Plant Cell* 15, 2093–2105. doi: 10.1105/tpc.014373

Xiao, T. T., Schilderink, S., Moling, S., Deinum, E. E., Kondorosi, E., Franssen, H., et al. (2014). Fate map of *Medicago truncatula* root nodules. *Development* 141, 3517–3528. doi: 10.1242/dev.110775

Yan, Z., Hossain, M. S., Arikit, S., Valdes-Lopez, O., Zhai, J., Wang, J., et al. (2015). Identification of microRNAs and their mRNA targets during soybean nodule development: functional analysis of the role of miR393j-3p in soybean nodulation. *New Phytol.* 207, 748–759. doi: 10.1111/nph.13365

Yan, Z., Hossain, M. S., Valdes-Lopez, O., Hoang, N. T., Zhai, J., Wang, J., et al. (2016). Identification and functional characterization of soybean root hair microRNAs expressed in response to *Bradyrhizobium japonicum* infection. *Plant Biotechnol. J.* 14, 332–341. doi: 10.1111/pbi.12387

Yan, Z., Hossain, M. S., Wang, J., Valdes-Lopez, O., Liang, Y., Libault, M., et al. (2013). miR172 regulates soybean nodulation. *Mol. Plant Microbe Interact.* 26, 1371–1377. doi: 10.1094/MPMI-04-13-0111-R

Yuan, S. L., Li, R., Chen, H. F., Zhang, C. J., Chen, L. M., Hao, Q. N., et al. (2017). RNA-Seq analysis of nodule development at five different developmental stages of soybean (Glycine max) inoculated with *Bradyrhizobium japonicum* strain 113-2. *Sci. Rep.* 7:42248. doi: 10.1038/srep42248

Zanetti, M. E., Chang, I. F., Gong, F., Galbraith, D. W., and Bailey-Serres, J. (2005). Immunopurification of polyribosomal complexes of Arabidopsis for global analysis of gene expression. *Plant Physiol.* 138, 624–635. doi: 10.1104/pp.105.059477

Zhu, Y., Li, H., Bhatti, S., Zhou, S., Yang, Y., Fish, T., et al. (2016). Development of a laser capture microscope-based single-cell-type proteomics tool for studying proteomes of individual cell layers of plant roots. *Hortic. Res.* 3:16026. doi: 10.1038/hortres.2016.26

Conflict of Interest Statement: The author declares that the research was conducted in the absence of any commercial or financial relationships that could be construed as a potential conflict of interest.

frontiers in Microbiology

ORIGINAL RESEARCH
published: 18 December 2018
doi: 10.3389/fmicb.2018.03155

InnB, a Novel Type III Effector of *Bradyrhizobium elkanii* USDA61, Controls Symbiosis With *Vigna* Species

*Hien P. Nguyen[1], Safirah T. N. Ratu[2], Michiko Yasuda[2], Michael Göttfert[3] and Shin Okazaki[1,2]**

[1] United Graduate School of Agricultural Science, Tokyo University of Agriculture and Technology, Tokyo, Japan, [2] Graduate School of Agriculture, Tokyo University of Agriculture and Technology, Tokyo, Japan, [3] Institute of Genetics, Technische Universität Dresden, Dresden, Germany

Bradyrhizobium elkanii USDA61 is incompatible with mung bean (*Vigna radiata* cv. KPS1) and soybean (*Glycine max* cv. BARC2) and unable to nodulate either plant. This incompatibility is due to the presence of a functional type III secretion system (T3SS) that translocates effector protein into host cells. We previously identified five genes in *B. elkanii* that are responsible for its incompatibility with KPS1 plants. Among them, a novel gene designated as *innB* exhibited some characteristics associated with the T3SS and was found to be responsible for the restriction of nodulation on KPS1. In the present study, we further characterized *innB* by analysis of gene expression, protein secretion, and symbiotic phenotypes. The *innB* gene was found to encode a hypothetical protein that is highly conserved among T3SS-harboring rhizobia. Similar to other rhizobial T3SS-associated genes, the expression of *innB* was dependent on plant flavonoids and a transcriptional regulator TtsI. The InnB protein was secreted via the T3SS and was not essential for secretion of other nodulation outer proteins. In addition, T3SS-dependent translocation of InnB into nodule cells was confirmed by an adenylate cyclase assay. According to inoculation tests using several *Vigna* species, InnB promoted nodulation of at least one *V. mungo* cultivar. These results indicate that *innB* encodes a novel type III effector controlling symbiosis with *Vigna* species.

Keywords: symbiosis, type III secretion system, effector, *Bradyrhizobium elkanii*, *Vigna* species

OPEN ACCESS

Edited by:
Kiwamu Minamisawa, Tohoku University, Japan

Reviewed by:
Christian Staehelin, Sun Yat-sen University, China
Francisco Javier López-Baena, Universidad de Sevilla, Spain

***Correspondence:**
Shin Okazaki
sokazaki@cc.tuat.ac.jp

Specialty section:
This article was submitted to Plant Microbe Interactions, a section of the journal Frontiers in Microbiology

Received: *15 September 2018*
Accepted: *05 December 2018*
Published: *18 December 2018*

Citation:
Nguyen HP, Ratu STN, Yasuda M, Göttfert M and Okazaki S (2018) InnB, a Novel Type III Effector of Bradyrhizobium elkanii USDA61, Controls Symbiosis With Vigna Species. Front. Microbiol. 9:3155. doi: 10.3389/fmicb.2018.03155

INTRODUCTION

Symbiotic relationships between legumes and soil bacteria, collectively called rhizobia, substantially contribute to agricultural production and the nitrogen cycle on the Earth (Broughton et al., 2000; Perret et al., 2000). Rhizobia induce the formation of specialized organs, known as root nodules, and are accommodated within them. The rhizobia in these nodules terminally differentiate into bacteroids, which are capable of reducing atmospheric nitrogen to ammonium assimilated by plants. In exchange, the host plants supply carbon sources and provide an appropriate environment for rhizobia (Oldroyd et al., 2011).

The nodulation process involves a complex exchange of molecular signals between rhizobia and plants that enables the hosts to distinguish compatible rhizobia from potential pathogens. Certain flavonoids exuded by host legume roots interact specifically with the rhizobial protein NodD, which binds to specific promoter sequences (called *nod* boxes) and activates the transcription of *nodulation* (*nod*) genes (Cullimore et al., 2001; Radutoiu et al., 2007). The products of *nod* genes synthesize rhizobial signal molecules called nodulation factors (NFs). NFs are recognized by host receptors (NF receptors, NFRs) that activate the host-signaling pathway, resulting in rhizobial infection and nodule organogenesis (Cullimore et al., 2001; Radutoiu et al., 2007; Madsen et al., 2010; Miwa and Okazaki, 2017).

Flavonoids from host legumes also induce secretion of specific proteins via the bacterial type III protein secretion system (T3SS). The T3SS was originally identified as a translocation system of effector proteins that function as virulence or avirulence proteins (Hueck, 1998). A similar system has been identified in numerous rhizobia (Viprey et al., 1998; Göttfert et al., 2001; Krause et al., 2002; Krishnan et al., 2003; López-Baena et al., 2008; Okazaki et al., 2009, 2010; Sánchez et al., 2009; Pérez-Montaño et al., 2016). The gene cluster for the rhizobial T3SS (*tts*) consists of genes encoding a secretion apparatus, secreted proteins and a transcriptional activator TtsI that induces the expression of *tts* genes by binding to conserved *cis*-elements termed *tts* boxes. Rhizobial type III secreted proteins are designated as nodulation outer proteins (Nops) (Krause et al., 2002; Marie et al., 2004; López-Baena et al., 2008; Wassem et al., 2008; Okazaki et al., 2009). Rhizobial T3SSs and secreted effectors, called T3 effectors, are involved in host-range determination and nodulation efficiency (Marie et al., 2003; Deakin and Broughton, 2009). Depending on the host plant, T3 effectors can have a positive, negative or neutral effect on symbiosis (Staehelin and Krishnan, 2015; Miwa and Okazaki, 2017).

Bradyrhizobium elkanii establishes symbiosis with a wide range of legumes, including soybean (*Glycine max*), mung bean (*Vigna radiata*), groundnut (*Arachis hypogaea*) and *Aeschynomene* spp. We previously reported that the T3SS of *B. elkanii* promotes nodule formation on soybean cultivar Enrei and *Aeschynomene* spp. but restricts nodulation on soybean cultivars carrying the *Rj4* allele (Faruque et al., 2015) and *V. radiata* cv. KPS1 (Okazaki et al., 2009). We identified five genes of USDA61 responsible for the incompatibility with *V. radiata* cv. KPS1 (Nguyen et al., 2017), one of which, designated as *innB* (***in****compatible* ***n****odulation B*), is preceded by a *tts* box and thus predicted to possess a T3SS-related function. Inoculation assays showed that *innB* is specifically responsible for the incompatibility with KPS1 but not for *Rj4* soybeans (Nguyen et al., 2017). In the present study, we further characterized the *innB* gene by transcriptional and protein analyses. We also observed infection properties and evaluated its symbiotic roles by inoculating several *Vigna* species. Our results reveal that *innB* encodes a novel type III effector that controls symbiosis with *Vigna* species.

MATERIALS AND METHODS

Microbiological and Molecular Techniques

The bacterial strains used in this study are listed in **Supplementary Table S1**. *B. elkanii* USDA61 and mutant strains were grown at 28°C on arabinose–gluconate (AG) medium (Sadowsky et al., 1987) or peptone salts yeast extract (PSY) medium (Regensburger and Hennecke, 1983) and *Escherichia coli* strains were grown at 37°C on LB medium (Green and Sambrook, 2012). Antibiotics were added to the media at the following concentrations: for *B. elkanii*, polymyxin at 50 μg ml^{-1}, kanamycin and streptomycin at 200 μg ml^{-1}; for *E. coli*, kanamycin and streptomycin at 50 μg ml^{-1}, tetracycline at 10 μg ml^{-1}.

For the construction of InnB-3xFLAG translational fusion, the oligonucleotides 3FLAPstI and 3FLASphI (**Supplementary Table S2**) were annealed and cloned into the *Pst*I-*Sph*I site of the plasmid pK18mob (Schäfer et al., 1994), generating the plasmid pK18mob3xFLAG. The partial *innB* fragment was amplified by PCR using primers innB-PstI-fullF and innB-BamHI-fullR and then cloned into pK18mob3xFLAG to generate pInnB7593xFLAG. For the construction of InnB-Cya fusions, the streptomycin-resistance gene (*aadA*) was amplified by PCR using primers aadAfor and aadArev and then cloned into the DraI sites of the pSLC5 plasmid (Wenzel et al., 2010), generating pSLC5Sm. The *innB* fragment was amplified by PCR using primers innB-PstI-fullF and innB-BamHI-fullR and cloned into the *Eco*RI and *Xba*I sites of pSLC5Sm, generating pInnB759Cya. For complementation, *innB* and its promoteor region (Accession No. KX499541, **Supplementary Data S1**) was amplified by PCR using primers BeinnBSacI-InfuF and BeinnBKpnI-InfuR and cloned into the *Sac*I and *Kpn*I sites of the plasmid pBjGroEL4::DsRed2, generating pBjGroEL4::proinnB. The resulting plasmid was mobilized into the *innB*-deficient mutant BE53 (Nguyen et al., 2017) by conjugation (Krause et al., 2002) using the helper plasmid pRK2013. Integration of the plasmids into the chromosome of *B. elkanii* strains was confirmed by antibiotic resistance, PCR and sequencing. DsRed- and GusA-tagged *B. elkanii* strains were obtained by integration of the plasmids pBjGroEL4::DsRed2 (Hayashi et al., 2014) and pCAM120 (Wilson et al., 1995), respectively.

Plant Assays

Seeds of mung bean (*V. radiata* cv. KPS1), black gram [*Vigna mungo* (L.) Hepper cv. PI173934] and soybean (*G. max* cv. Enrei) were surface sterilized and germinated as described previously (Nguyen et al., 2017). One day after transplantation, seedlings were inoculated with *B. elkanii* strains (1 ml of 10^7 cells ml^{-1} per seedling). The plants were grown in a plant growth cabinet (LPH-410SP; NK Systems, Co. Ltd., Osaka, Japan) at 25°C and 70% humidity under a day/night regimen of 16/8 h. The symbiotic phenotypes including nodule number, nodule fresh weight and

whole plant fresh weight were examined 8, 15, 30, or 35 days post-inoculation depending on the experiment.

Microscopy

For microscopic analysis, nodules were fixed with 0.1 M cacodylate buffer containing 2.5% (vol/vol) glutaraldehyde in phosphate saline buffer at 4°C overnight. The fixed nodules were embedded in 5% agar and sectioned using a microtome (VT1000s; Leica Biosystems, Germany) and then observed under the microscope (SZX9; Olympus, Japan). GUS staining was performed as described previously (Okazaki et al., 2007).

RNA Extraction and Real-Time RT-PCR

RNAs were extracted from *B. elkanii* cells as described by Babst et al. (1996). Briefly, *B. elkanii* strains were grown at 28°C on PSY medium on a rotary shaker at 180 rpm. When OD_{600} values of the culture reached 0.4, 10 μM of genistein was added and the cultures were sampled at 4 and 24 h, respectively. cDNA synthesis and real-time RT-PCR were performed as described by Yasuda et al. (2016). The RNA isolations and real-time RT-PCR analyses were performed at least twice in triplicate. Transcript levels were normalized to the expression of the housekeeping gene *atpD*, measured in the same samples (Wen et al., 2016).

Purification and Analysis of Extracellular Proteins

For isolation of extracellular proteins, AG medium was inoculated with 1 : 100 dilution from a *B. elkanii* preculture and incubated at 28°C for 48 h. Supernatants were recovered from 500 ml of the bacterial cultures by two rounds of centrifugation (4000 × *g* at 4°C for 1 h and 8000 × *g* at 4°C for 30 min). The supernatants were then lyophilized, and extracellular proteins were extracted as described previously (Okazaki et al., 2009, 2010). Extracellular proteins were separated by 15% SDS-PAGE and stained with Coomassie brilliant blue (CBB) as described previously (Okazaki et al., 2010). For western blot analysis, protein samples were separated on a 4–15 or 4–20% SDS polyacrylamide gel, and identification of the target proteins was carried out as described by Hempel et al. (2009) using an antibody raised against FLAG and NopA. Briefly, the protein samples were transferred to polyvinylidene difluoride (PVDF) membranes (Bio-Rad, United States) and blocked with Western Blot Blocking Buffer (Fish Gelatin) (Takara, Japan). The immunoreaction was detected using an ECL Prime Kit (GE Healthcare, United Kingdom) and a LAS-3000 Luminescent Image Analyzer (Fujifilm, Japan).

Adenylate Cyclase (Cya) Assay

To quantify cAMP levels, root nodules were collected at 18 dpi, immediately frozen in liquid nitrogen and ground to a fine powder. The nodule powder was suspended in a 5× volume of 0.1 M HCl (per nodule weight) and centrifuged. The supernatant was diluted to quantify cAMP concentrations in the detection range and subjected directly to cAMP measurement using a cyclic AMP (direct) enzyme immunoassay (EIA) kit (Cayman Chemical Company, Ann Arbor, MI, United States) according to the manufacturer's instructions.

Bioinformatic and Statistical Analysis

Amino acid sequences were aligned using MUSCLE or CLUSTAL W algorithms. A phylogenetic tree was constructed by the neighbor-joining method in MEGA 7.0 (Kumar et al., 2016). For statistical analysis, the data were subjected to analysis of variance (ANOVA), and a *post hoc* test (Fisher's test at $p \leq 0.05$) was done using Minitab statistical software version 16.0.

RESULTS

InnB Is Exclusively Conserved Among Rhizobia

We previously demonstrated that *innB* of *B. elkanii* USDA61 was responsible for host-specific nodulation restriction on *V. radiata* cv. KPS1 (Nguyen et al., 2017). The presence of a conserved *tts* box motif in the promoter region of *innB* suggested its T3SS-related function (**Supplementary Data S1**). In addition, the N-terminal region of InnB exhibits characteristics of T3-secreted proteins: as detailed by Guttman et al. (2002) and Petnicki-Ocwieja et al. (2002), a high percentage of serines and the aliphatic amino acids proline and valine as the third or fourth residues (**Supplementary Figure S1**).

A BLASTP search revealed that homologs of InnB are present in T3SS-harboring rhizobia, but not in T3SS-harboring pathogens (**Figure 1**). Because the InnB homologs were highly diverse in length, we divided the selected homologs into high- and low-query-coverage groups and analyzed their phylogenetic relationships separately. Phylogenetic analysis of the high-query-coverage homologs uncovered three clearly distinct branches. InnB and its homologs in *B. elkanii* USDA76 (WP_018270178, 100% identity) and *Bradyrhizobium* sp. R5 (SDD80475, 74% identity) were separate from the two groups comprising *Mesorhizobium* and other *Bradyrhizobium* strains (**Figure 1A**). We also discovered three *Mesorhizobium* species containing InnB homologs, but their similarity to InnB was low. InnB homologs with a low query coverage were split into four different groups: *Mesorhizobium* strains, *B. elkanii* USDA61, *B. diazoefficiens* USDA110 and *B. japonicum* USDA6, *B. diazoefficiens* USDA122 and *B. japonicum* Is-34 (**Figure 1B**).

An amino acid alignment was conducted using selected homologs, namely, those in *B. yuanmingense* CCBAU10071 (SCB50985, 72% identity), *B. yuanmingense* BR3267 (KRP85897, 73% identity, not annotated), *B. japonicum* USDA6 (BAL13100, 71% identity), *B. diazoefficiens* USDA110 (BAC47263, 70% identity), *B. diazoefficiens* USDA122 (APO50625, 70% identity) and *B. japonicum* Is-34 (KGT81182, 70% identity) (**Figure 1C** and **Supplementary Figure S1**). The homologs in two strains, *B. yuanmingense* CCBAU10071 (SCB50985, query coverage 98%) and BR3267 (KRP85897, query coverage 89%), had many highly conserved amino acids that could be aligned with the InnB amino acid sequence. In contrast, the homologs in *B. diazoefficiens* and *B. japonicum* strains with a query coverage lower than 80% aligned with different parts of

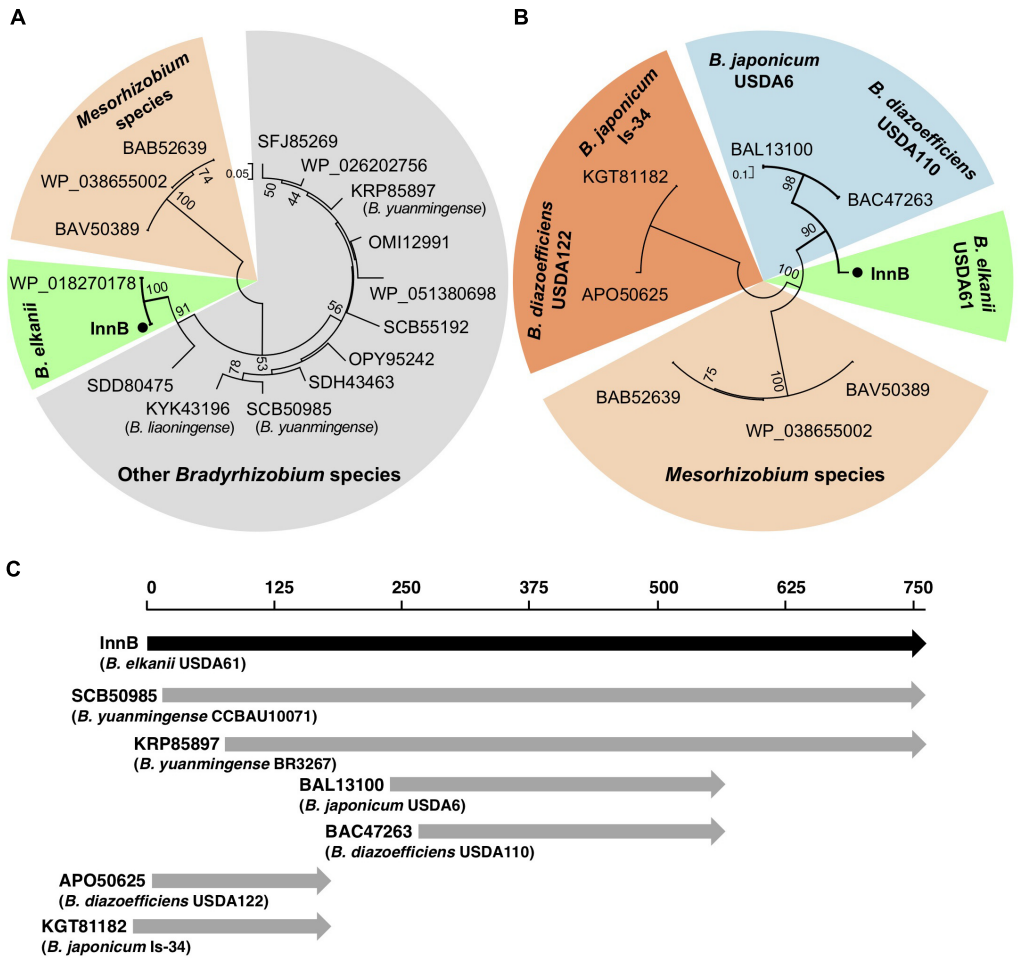

FIGURE 1 | Phylogenetic trees and comparative alignment of InnB and its homologs. **(A,B)** Phylogenetic trees of homologs having a query coverage of at least 80% **(A)** and less than 80% **(B)**. **(C)** Alignment of InnB and its homologs in several rhizobial strains.

InnB (**Figure 1C** and **Supplementary Figure S1**). Interestingly, the homologs BAL13100 (in USDA6) and BAC47263 (in USDA110) were highly similar to the internal part of InnB, while those in USDA122 (APO50625) and Is-34 (KGT81182) aligned well with the N-terminus of InnB. All four of these homologs lacked amino acids that aligned with the amino acid residues 569 to 759 of InnB (**Supplementary Figure S1**).

Expression of *innB* Is Dependent on Genistein and the Transcriptional Regulator TtsI

The presence of a conserved *tts* box motif in the promoter region of *innB* suggests that its expression is controlled by TtsI and host-derived flavonoids. We therefore analyzed the expression of *innB* in the wild-type USDA61 and the *ttsI*-deficient mutant BEttsI (Okazaki et al., 2013) in the presence and absence of genistein by real-time RT-PCR. Transcriptional levels of *innB*, *nopA*, and *nodC* genes in the wild-type background were increased upon induction with genistein (**Figure 2**). The *innB* and *nopA* showed a very similar expression and induction pattern with significantly higher expression after 24 h (**Figure 2** and **Supplementary Figure S2**). In BEttsI, the expression of *innB* was completely abolished along with that of *nopA*, which suggests that *innB* expression was controlled by genistein and TtsI. Intriguingly, the expression of *nodC* was slightly reduced in the *ttsI* mutant background. However, it is unknown how TtsI might affect *nodC* expression.

InnB Is Not Essential for the Secretion of Other Nops

To confirm that InnB is a T3 effector and that mutation of *innB* does not alter secretion of other Nops, we analyzed the extracellular protein profiles of strains USDA61 and BErhcJ, a mutant defective for T3 protein secretion (Okazaki et al., 2009), and the *innB*-deficient mutant BE53 in the absence or presence of genistein (10 μM). The proteins from bacterial culture supernatants were extracted and separated by SDS-PAGE (**Figure 3**). The protein profile of the BErhcJ mutant differed from that of USDA61, with several predicted T3SS-secreted proteins,

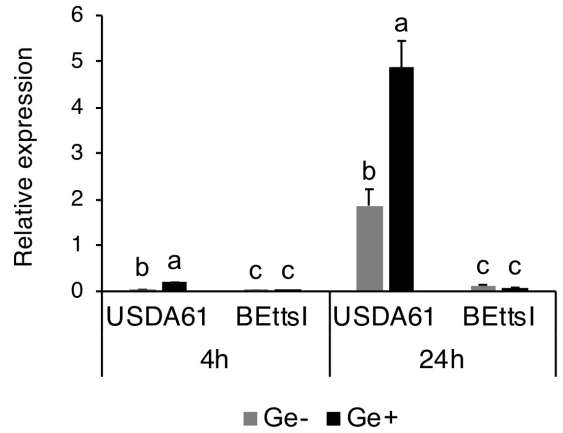

FIGURE 2 | Expression of *innB* in wild-type and mutant *Bradyrhizobium elkanii* strains. Real-time RT-PCR was performed using total RNAs isolated from USDA61 and the *ttsI*-deficient mutant BEttsI grown in the absence (Ge–) or presence (Ge+) of the inducer flavonoid genistein (10 μM) after 4 and 24 h. The expression level of each gene was normalized relative to the *atpD* gene (ATP synthase) using the ΔΔCt method. The expression data are the mean of triplicates, and the error bars indicate standard deviations. Statistical analysis by Fisher's method was performed to compare the relative expression levels of *innB* in USDA61 and BEttsI in the absence/presence of genistein at each timepoint, respectively. Means followed by different letters at the same timepoint are significantly different at the 5% level.

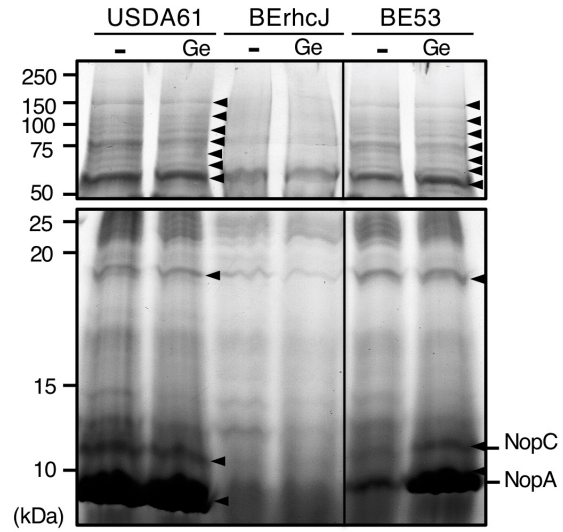

FIGURE 3 | Extracellular protein profiles of *B. elkanii* strains. USDA61, BErhcJ, and *innB*-deficient mutant BE53 were cultured in the absence (–) or presence (Ge) of 10 μM genistein. The extracellular proteins were stained with Coomassie brilliant blue (CBB). Proteins were separated by 15% SDS-PAGE. Size-marker molecular masses (kDa) are shown on the left. Arrowheads indicate protein bands that were visible in cultures of USDA61 and BE53 but not BErhcJ.

such as NopA and NopC being absent. In contrast, the protein pattern of BE53 was similar to that of the wild-type USDA61 and secretions of NopA and NopC were detected. These results suggest that the mutation in *innB* was not essential for the secretion of other Nops. We also examined the secretion of InnB using the FLAG-tagged construct, however, we could not detect the FLAG-tagged InnB in culture supernatants of USDA61 (**Supplementary Figure S3**).

InnB Is a T3 Effector Translocated Inside Plant Cells

To confirm whether InnB is a T3 effector that functions in host cells, its translocation was analyzed using adenylate cyclase (Cya) as a reporter. In the presence of ATP and a calmodulin-like protein, cAMP production is catalyzed by the Cya enzyme only within eukaryotic cells (Sory and Cornelis, 1994). Once the Cya-fused effector is delivered to the host cell, cAMP production will be detected. In this study, Cya fused to the carboxy terminus of InnB was integrated into the *B. elkanii* strains USDA61 and BErhcJ, resulting in the mutants BEinnBC and BErhcJinnBC, respectively. The translocation of InnB was confirmed using fresh nodules of the USDA61-compatible cultivar *G. max* cv. Enrei harvested at 18 dpi. A low level of cAMP was detected in nodules induced by the wild-type USDA61 and the BErhcJinnBC mutant expressing the InnB-Cya fusion (**Figure 4**). However, the cAMP level was significantly higher in nodules formed by USDA61 containing the InnB-Cya fusion, which suggests that InnB was translocated into the host cell.

InnB Negatively Affects Nodulation of *V. radiata*

We previously reported that the insertion of a transposon in *innB* abolishes nodulation incompatibility between USDA61 and

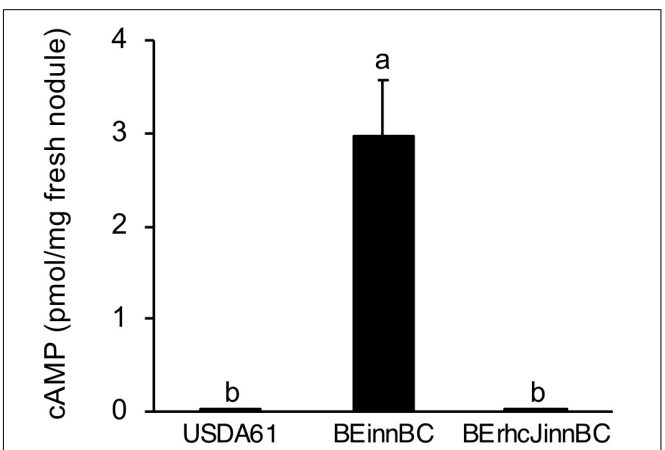

FIGURE 4 | cAMP levels measured in nodules harvested at 18 dpi from the USDA61-compatible plant *Glycine max* cv. Enrei. Plants were inoculated with the rhizobial strains BEinnBC and BErhcJinnBC, which carry an *innB-cya* fusion in the USDA61 and BErhcJ background, respectively. The wild-type USDA61 contained no *cya* reporter. Nodules were randomly collected from at least four plants individually inoculated with each strain. The data are means of triplicates, and the error bars indicate standard deviations. Statistical analysis by Fisher's method was performed to compare cAMP levels. Means followed by the different letters are significantly different at the 5% level.

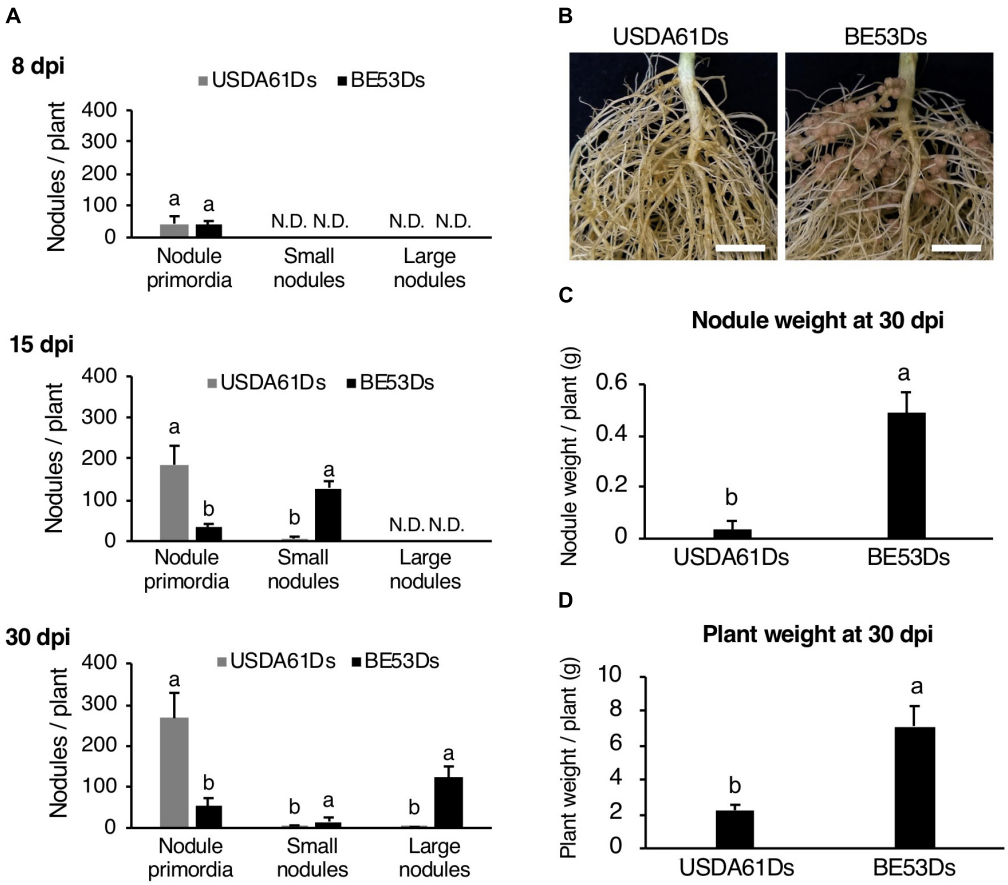

FIGURE 5 | Nodulation properties of *Vigna radiata* cv. KPS1 inoculated with the *B. elkanii* USDA61Ds and BE53Ds. **(A)** The number of nodule primordia and small and large nodules at 8, 15, and 30 dpi. N.D., not detected. **(B)** Roots of KSP1 plants at 30 dpi; scale bars: 1 cm. **(C)** Nodule weight and **(D)** plant weight of KPS1 plants at 30 dpi. The data shown are the means of at least five plants, and the error bars indicate standard deviations. Statistical analysis by Fisher's method was performed to compare the symbiotic phenotypes obtained with USDA61Ds and BE53Ds. Means followed by different letters are significantly different at the 5% level.

KPS1 (Nguyen et al., 2017). To confirm that the symbiotic phenotype was induced by inactivation of *innB* and not by an additional mutation, we complemented the BE53 mutant with the *innB* gene and its promoter region. The resulting complemented strain exhibited a symbiotic phenotype similar to wild-type USDA61 (**Supplementary Figure S4**). These results confirm that *innB* was responsible for the altered nodulation phenotype on KPS1.

To further characterize the negative impact of InnB on nodulation, we monitored the nodulation process of KPS1 inoculated with DsRed-tagged *B. elkanii* strains. Early in nodulation (8 dpi) wild-type and mutant induced a similar number of nodule primordia (**Figure 5A**). However, at later stages (15 and 30 dpi), plants developed a higher number of nodule primordia if infected with the wild-type as compared to the infection with the *innB* mutant (5- to 20-fold). In contrast, almost no nodules were formed with the wild-type strain but the *innB* mutant was a very efficient nodulator (**Figures 5A–C**). In line with that, nodule weight and plant weight were significantly increased with BE53Ds-inoculated plants (**Figure 5D**). Similar results for the time point 40 dpi were observed previously (Nguyen et al., 2017).

InnB Abolishes Infection and Nodule Organogenesis in *V. radiata*

To explore the effect of *innB* on infective properties of *B. elkanii*, we investigated the infection process in KPS1 plants using GUS-tagged strains of USDA61 and BE53. Examination of early infection events in KPS1 roots revealed that USDA61 and BE53 both infected KPS1 root hairs and formed nodule primordia. However, the number of infected nodule primordia and small nodules was significantly different between USDA61 and BE53 (**Figure 6**). At 8 dpi, BE53 efficiently infected KPS1 roots, thereby resulting in a higher number of infected nodule primordia than those of the wild-type. Most nodule primordia in KPS1 plants inoculated with USDA61 were uninfected (**Figure 6**). In contrast to the infection phenotypes observed at 8 dpi, USDA61 induced a higher number of infected nodule primordia at 15 dpi than did BE53G. Many efficiently infected small nodules instead were formed on roots of KPS1 inoculated with BE53 (**Figure 6**). The

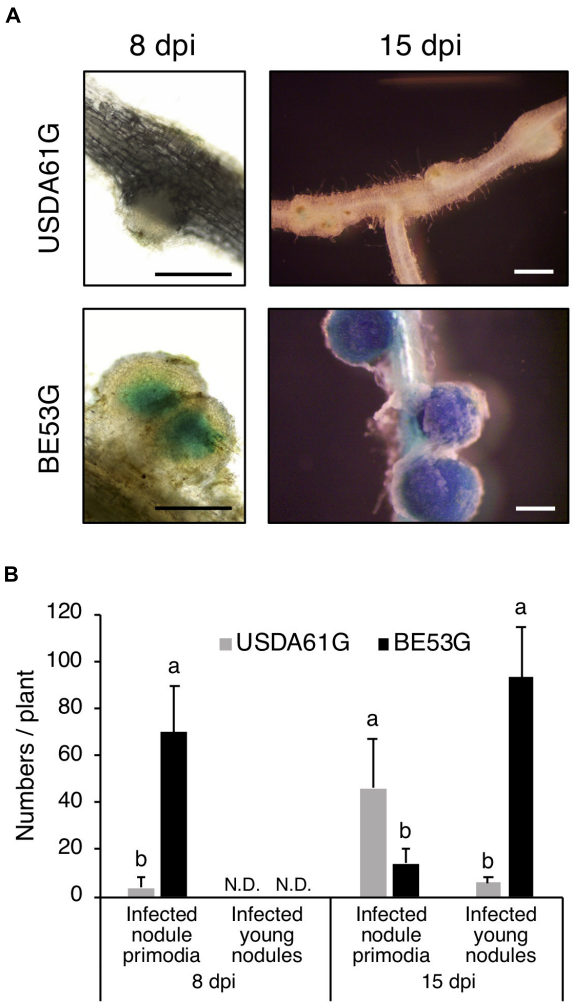

FIGURE 6 | Infection properties of *V. radiata* cv. KPS1 inoculated with *Bradyrhizobium elkaii* USDA61G and BE53G. **(A)** Infected nodule primordia and small nodules. Scale bars: 500 μm. **(B)** The number of infected nodule primordia and small nodules formed on KPS1 plants. The data shown are means of five plants, and the error bars indicate standard deviations. Means followed by different letters at the same timepoint (dpi) are significantly different at the 5% level.

small nodules formed by all plants inoculated with BE53 were deep blue, probably because of the high number of active rhizobia inside (**Figure 6**).

InnB Promotes Nodulation of *V. mungo*

To explore the importance of InnB in symbiosis with legumes, we conducted inoculation tests using several *Vigna* species. Among these species, *V. mungo* (L.) Hepper cv. PI173934 formed numerous nodules following inoculation with USDA61 (approximately 140 nodules per plant) (**Figure 7**). In contrast, BErhcJ and BE53 induced significantly lower numbers of nodules, and plant weights were decreased. These observations indicate that the T3SS promotes symbiosis with *V. mungo* and that InnB is one of the positive effectors for the symbiosis. Intriguingly, BE53 induced a significantly higher number of small nodules than BErhcJ, which suggests that USDA61 harbors an additional positive effector.

DISCUSSION

We previously identified five novel *B. elkanii* genes that are responsible for the incompatibility with *V. radiata* KPS1. One of the genes, *innB*, encodes a hypothetical protein that contains a *tts* box in its promoter region and thus seems to possess T3SS-related functions (Nguyen et al., 2017). As previously reported, the *innB* mutant BE53 can nodulate KPS1 but not *Rj4* soybean (Nguyen et al., 2017), which indicates that InnB causes a highly specific incompatibility with KPS1 but not with *Rj4* plants. In the present study, we analyzed the *innB* gene by examining gene expression, protein secretion and symbiotic phenotypes.

Homologs of the InnB protein were found in T3SS-harboring rhizobia, but not in other plant-associated bacteria. Other rhizobial T3-secreted proteins, such as NopC, NopI, NopL and NopP, have also been identified as *Rhizobium*-specific and have no homologs in plant or animal pathogens (Deakin and Broughton, 2009; Jiménez-Guerrero et al., 2015). These reports imply that InnB has a symbiosis-specific function. Notably, homologs in *B. japonicum* (strains USDA6 and Is-34) and *B. diazoefficiens* (strains USDA110 and USDA122) are highly similar to either the N-terminal or internal region of InnB (**Figure 1** and **Supplementary Figure S1**). Our preliminary experiment in agreement with Sugawara et al. (2018) showed that USDA110 was not incompatible with KPS1, thus suggesting that the homolog of USDA110 (BAC47263) lacks a functional domain for inducing incompatibility. In contrast, InnB homologs in other bradyrhizobia, such as *B. elkanii* strain USDA76 and *B. yuanmingense* strains CCBAU10071 and BR3267, showed a high degree of query coverage, suggesting that these proteins have common functions in symbiosis.

Similar to other *nop* genes, the transcription of *innB* was found to be regulated by flavonoids and the transcriptional regulator TtsI. In addition, the different transcriptional levels of *nodC* in the absence and presence of genistein in the wild-type and *ttsI* mutant suggest that *nodC* expression is slightly reduced in a TtsI mutant background (**Figure 2** and **Supplementary Figure S2**). The mechanism underlying the reduced *nodC* expression remains unclear. Notably, the transcriptional levels of *nopA* and *nodC* are lower than that of *innB*, suggesting that they might function differently in protein secretion and nodulation process (**Supplementary Figure S2**). Although transcription of *tts* genes were clearly inducible by genistein, the addition of genistein did not significantly change the extracellular protein patterns of *B. elkanii* strains (**Figure 3**). These results suggest that the T3SS is activated without genistein under the tested conditions. Therefore, unidentified regulators or inducers are likely be involved in the regulation of *tts* genes in *B. elkanii*.

An analysis of extracellular proteins confirmed that InnB is not essential for the secretion of other proteins. It has been shown that the mutations of genes encoding T3SS components, such as *nopA* and *nopB*, significantly affect the secretion of other secreted

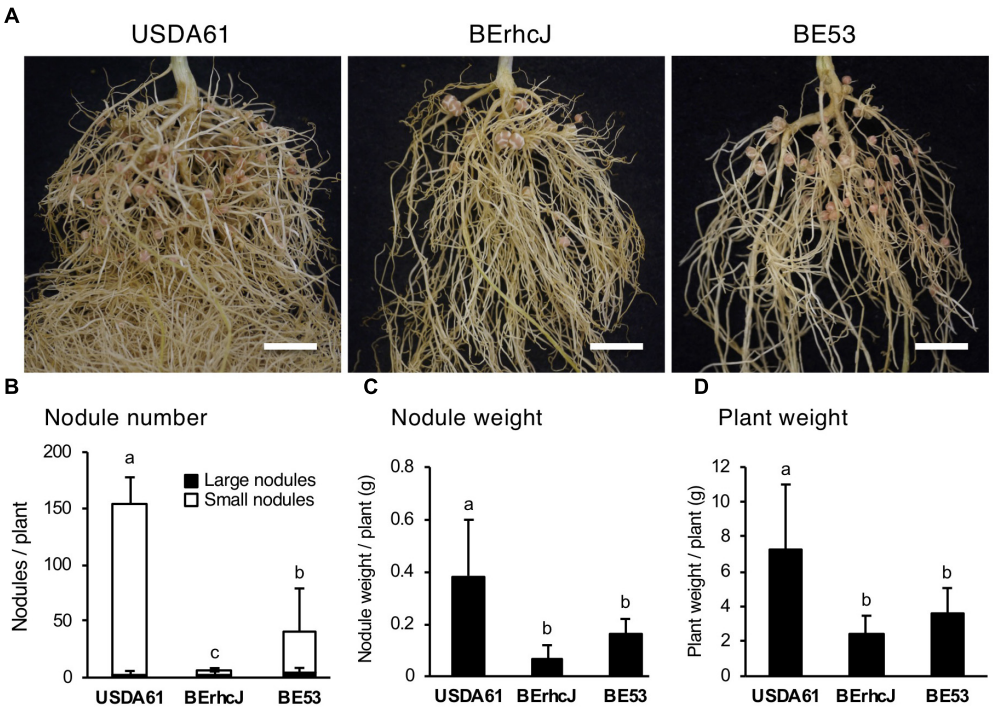

FIGURE 7 | Symbiotic properties of *Vigna mungo* cv. PI173934 (black gram) inoculated with *B. elkanii* strains. **(A)** Roots of black gram inoculated with *B. elkanii* strains; scale bars: 1 cm. Nodule number **(B)**, fresh nodule weight **(C)**, and fresh plant weight **(D)** of *V. mungo* at 35 dpi. White and black bars in **(B)** represent the number of small (<2 mm) and large (≥2 mm) nodules, respectively. The data shown are the means of at least 10 plants from two independent assays. The error bars indicate standard deviations. Means followed by different letters are significantly different at the 5% level.

proteins and nodule formation (Deakin et al., 2005). In our experiment, Nops, such as NopA, NopC and NopX, were visible in both BE53 and USD61 extracellular protein samples, but not in those of T3SS-deficient BErhcJ (**Figure 3**), thus indicating that InnB is a secreted protein and not a component of the secretion apparatus.

The InnB protein, which was predicted to have a molecular mass of approximately 83.11 kDa, was not clearly detected by SDS-PAGE (**Figure 3**). To further confirm the secretion of *innB*, we constructed a 3xFLAG-tagged *innB*. The generated construct was transferred to either USAD61 or a *ttsI* mutant, generating BEinnBF and BEttsIinnBF, respectively. However, we could not detect InnB fragment in the culture supernatant of both strains by western blotting (**Supplementary Figure S3B**). Notably, the InnB homolog in *B. diazoefficiens* USDA110 was also not detected in the extracellular proteins of USDA110 (Hempel et al., 2009). It is likely that the InnB protein was secreted at quite low levels or secreted InnB proteins undergo a certain modification or degradation.

The translocation of InnB into soybean nodule cells was verified by a Cya reporter assay (**Figure 4**). Translocation of rhizobial T3 effectors such as NGR234 NopP (Schechter et al., 2010), NopC (Jiménez-Guerrero et al., 2015), HH103 NopL (Jiménez-Guerrero et al., 2017), and USDA110 NopE (Wenzel et al., 2010) into host cells has been similarly confirmed by Cya assays. The InnB-induced cAMP accumulation observed in our study was much lower than that of other Nops. This result may reflect the lower secretion and translocation of InnB compared with other Nops.

In *V. radiata*, USDA61 induced numerous nodule primordia, but the presence of InnB halted the subsequent nodulation process. While BE53 induced a higher number of infected small nodules on KPS1 roots at 15 dpi, the number of nodule primordia formed by USDA61 increased continuously until 30 dpi (**Figures 5**, **6**). The failure of small nodule formation correlates well with an increase in nodule primordia formation (**Figure 5**). Taken together, KPS1 halted USDA61 infection and nodule organogenesis before small nodule formation due to the presence of InnB. Probably, the InnB secreted into host cells interacts specifically with *Vigna* resistance (*R*) genes and triggers immune responses (effector-triggered immunity), thus resulting in host defense responses and consequently halting infection and nodulation by USDA61.

Although nodulation on KPS1 by USDA61 was heavily restricted, a few nodules were occasionally observed on the roots (**Figure 5**). According to previous research, USDA61 can infect host legumes such as *Arachis hypogaea* (Ibáñez and Fabra, 2011) and *Aeschynomene* spp. (Bonaldi et al., 2011) via "crack entry" (intercellular infection). In soybean, infection via crack entry to form nodules is mediated by the T3SS of *B. elkanii* and may induce a defense response in *Rj4* plants (Okazaki et al., 2013; Yasuda et al., 2016). However, T3SS-mediated crack entry infection is rare and weak and only results in the formation of several small nodules or bumps (Yasuda et al., 2016). In contrast,

rhizobial infection through infection threads (ITs) can induce a stronger host defense that is completely able to block nodule formation (Yasuda et al., 2016). We observed that USDA61, but not the *innB*-deficient mutant, failed to induce root hair curling and only weakly infected KPS1 roots via ITs; nevertheless, a few large nodules occasionally formed at the base of lateral roots (**Supplementary Figure S5**). In addition, most USDA61-induced nodules were more poorly infected than those induced by BE53 (**Supplementary Figure S5**). These observations imply that the T3 effector-triggered host defense occasionally fails to completely block the nodule formation of USDA61-infected cells. In these cases, the USDA61 infection may occur via crack entry of the lateral roots of KPS1.

In *V. mungo*, BE53 induced less nodules than USDA61, indicating that the InnB plays a beneficial role in the symbiosis with this species. It was reported that the *V. mungo* plants were nodulated by *Bradyrhizobium* spp. (closely related with *B. yuanmingense*) but not by *B. japonicum* or *B. diazoefficiens* (Appunu et al., 2009). Notably, InnB homologs with a high coverage ratio were specifically found in *Bradyrhizobium* spp., but not in *B. japonicum* or *B. diazoefficiens* (**Figure 1**). These suggest that the symbionts of *V. mungo* specifically possess InnB for enhancing the interaction with this host plants. Intriguingly, the number of BE53-formed small nodules is higher than that formed by infection with BErhcJ, implying the presence of an additional positive effector. Further studies are required to elucidate the specific functions of the *Rhizobium*-specific T3 effector InnB and the additional effector in nodulation among different legumes.

In summary, we have presented evidence that the *innB* gene of *B. elkanii* encodes a novel T3 effector involved in the control of symbiosis with *Vigna* species. The conservation of InnB homologs among rhizobia suggests a symbiosis-specific function for *innB*, especially in interactions between bradyrhizobia and *Vigna* spp.

AUTHOR CONTRIBUTIONS

HN and SO designed the research and wrote the paper. HN performed the research and analyzed the data. SR, MY, and MG contributed new reagents and analytic tools.

FUNDING

This work was supported in part by JSPS KAKENHI (Grant Nos. JP15KK0276 and JP16H04889) and JSPS Bilateral Program (Joint Research Projects) (Grant No. 16932112).

ACKNOWLEDGMENTS

We thank K. Suzuki for her kind help.

SUPPLEMENTARY MATERIAL

The Supplementary Material for this article can be found online at: https://www.frontiersin.org/articles/10.3389/fmicb.2018.03155/full#supplementary-material

REFERENCES

Appunu, C., N'Zoue, A., Moulin, L., Depret, G., and Laguerre, G. (2009). *Vigna mungo*, *V. radiata* and *V. unguiculata* plants sampled in different agronomical–ecological–climatic regions of India are nodulated by *Bradyrhizobium yuanmingense*. *Syst. Appl. Microbiol.* 32, 460–470. doi: 10.1016/J.SYAPM.2009.05.005

Babst, M., Hennecke, H., and Fischer, H.-M. (1996). Two different mechanisms are involved in the heat-shock regulation of chaperonin gene expression in *Bradyrhizobium japonicum*. *Mol. Microbiol.* 19, 827–839. doi: 10.1046/j.1365-2958.1996.438968.x

Bonaldi, K., Gargani, D., Prin, Y., Fardoux, J., Gully, D., Nouwen, N., et al. (2011). Nodulation of *Aeschynomene afraspera* and A. indica by photosynthetic *Bradyrhizobium* sp. strain ORS285: the nod-dependent versus the nod-independent symbiotic interaction. *Mol. Plant Microbe. Interact.* 24, 1359–1371. doi: 10.1094/MPMI-04-11-0093

Broughton, W. J., Jabbouri, S., and Perret, X. (2000). Keys to symbiotic harmony. *J. Bacteriol.* 182, 5641–5652. doi: 10.1128/JB.182.20.5641-5652.2000

Cullimore, J. V., Ranjeva, R., and Bono, J.-J. (2001). Perception of lipo-chitooligosaccharidic Nod factors in legumes. *Trends Plant Sci.* 6, 24–30. doi: 10.1016/S1360-1385(00)01810-0

Deakin, W. J., and Broughton, W. J. (2009). Symbiotic use of pathogenic strategies: rhizobial protein secretion systems. *Nat. Rev. Microbiol.* 7, 312–320. doi: 10.1038/nrmicro2091

Deakin, W. J., Marie, C., Saad, M. M., Krishnan, H. B., and Broughton, W. J. (2005). NopA is associated with cell surface appendages produced by the type III secretion system of *Rhizobium* sp. strain NGR234. *Mol. Plant Microbe. Interact.* 18, 499–507. doi: 10.1094/MPMI-18-0499

Faruque, O. M., Miwa, H., Yasuda, M., Fujii, Y., Kaneko, T., Sato, S., et al. (2015). Identification of *Bradyrhizobium elkanii* genes involved in incompatibility with soybean plants carrying the Rj4 allele. *Appl. Environ. Microbiol.* 81, 6710–6717. doi: 10.1128/AEM.01942-15

Göttfert, M., Röthlisberger, S., Kündig, C., Beck, C., Marty, R., and Hennecke, H. (2001). Potential symbiosis-specific genes uncovered by sequencing a 410-kilobase DNA region of the *Bradyrhizobium japonicum* chromosome. *J. Bacteriol.* 183, 1405–1412. doi: 10.1128/JB.183.4.1405-1412.2001

Green, M. R., and Sambrook, J. (2012). *Molecular Cloning?: A Laboratory Manual*. Cold Spring Harbor, NY: Cold Spring Harbor Laboratory Press.

Guttman, D. S., Vinatzer, B. A., Sarkar, S. F., Ranall, M. V., Kettler, G., and Greenberg, J. T. (2002). A functional screen for the type III (Hrp) secretome of the plant pathogen *Pseudomonas syringae*. *Science* 295, 1722–1726. doi: 10.1126/science.295.5560.1722

Hayashi, M., Shiro, S., Kanamori, H., Mori-Hosokawa, S., Sasaki-Yamagata, H., Sayama, T., et al. (2014). A thaumatin-like protein, Rj4, controls nodule symbiotic specificity in soybean. *Plant Cell Physiol.* 55, 1679–1689. doi: 10.1093/pcp/pcu099

Hempel, J., Zehner, S., Göttfert, M., and Patschkowski, T. (2009). Analysis of the secretome of the soybean symbiont *Bradyrhizobium japonicum*. *J. Biotechnol.* 140, 51–58. doi: 10.1016/j.jbiotec.2008.11.002

Hueck, C. J. (1998). Type III protein secretion systems in bacterial pathogens of animals and plants. *Microbiol. Mol. Biol. Rev.* 62, 379–433.

Ibáñez, F., and Fabra, A. (2011). Rhizobial Nod factors are required for cortical cell division in the nodule morphogenetic programme of the *Aeschynomeneae* legume Arachis. *Plant Biol.* 13, 794–800. doi: 10.1111/j.1438-8677.2010.00439.x

Jiménez-Guerrero, I., Pérez-Montaño, F., Medina, C., Ollero, F. J., and López-Baena, F. J. (2015). NopC is a *Rhizobium*-specific type 3 secretion system effector secreted by *Sinorhizobium (Ensifer) fredii* HH103. *PLoS One* 10:e0142866. doi: 10.1371/journal.pone.0142866

Jiménez-Guerrero, I., Pérez-Montaño, F., Medina, C., Ollero, F. J., and López-Baena, F. J. (2017). The *Sinorhizobium (Ensifer) fredii* HH103 nodulation outer

protein NopI is a determinant for efficient nodulation of soybean and cowpea plants. *Appl. Environ. Microbiol.* 83, e02770-16. doi: 10.1128/AEM.02770-16

Krause, A., Doerfel, A., and Göttfert, M. (2002). Mutational and transcriptional analysis of the type III secretion system of *Bradyrhizobium japonicum*. *Mol. Plant Microbe. Interact.* 15, 1228–1235. doi: 10.1094/MPMI.2002.15.12.1228

Krishnan, H. B., Lorio, J., Kim, W. S., Jiang, G., Kim, K. Y., DeBoer, M., et al. (2003). Extracellular proteins involved in soybean cultivar-specific nodulation are associated with pilus-like surface appendages and exported by a type III protein secretion system in *Sinorhizobium fredii* USDA257. *Mol. Plant Microbe. Interact.* 16, 617–625. doi: 10.1094/MPMI.2003.16.7.617

Kumar, S., Stecher, G., and Tamura, K. (2016). MEGA7: molecular evolutionary genetics analysis version 7.0 for bigger datasets. *Mol. Biol. Evol.* 33, 1870–1874. doi: 10.1093/molbev/msw054

López-Baena, F. J., Vinardell, J. M., Pérez-Montaño, F., Crespo-Rivas, J. C., Bellogín, R. A., Espuny, M. D. R., et al. (2008). Regulation and symbiotic significance of nodulation outer proteins secretion in *Sinorhizobium fredii* HH103. *Microbiology* 154, 1825–1836. doi: 10.1099/mic.0.2007/016337-0

Madsen, L. H., Tirichine, L., Jurkiewicz, A., Sullivan, J. T., Heckmann, A. B., Bek, A. S., et al. (2010). The molecular network governing nodule organogenesis and infection in the model legume *Lotus japonicus*. *Nat. Commun.* 1, 1–12. doi: 10.1038/ncomms1009

Marie, C., Deakin, W. J., Ojanen-Reuhs, T., Diallo, E., Reuhs, B., Broughton, W. J., et al. (2004). TtsI, a key regulator of rhizobium species NGR234 is required for type III-dependent protein secretion and synthesis of rhamnose-rich polysaccharides. *Mol. Plant Microbe Interact.* 958, 958–966. doi: 10.1094/MPMI.2004.17.9.958

Marie, C., Deakin, W. J., Viprey, V., Kopciñska, J., Golinowski, W., Krishnan, H. B., et al. (2003). Characterization of Nops, nodulation outer proteins, secreted via the type III secretion system of NGR234. *Mol. Plant Microbe Interact.* 16, 743–751. doi: 10.1094/MPMI.2003.16.9.743

Miwa, H., and Okazaki, S. (2017). How effectors promote beneficial interactions. *Curr. Opin. Plant Biol.* 38, 148–154. doi: 10.1016/j.pbi.2017.05.011

Nguyen, H., Miwa, H., Kaneko, T., Sato, S., and Okazaki, S. (2017). Identification of *Bradyrhizobium elkanii* genes involved in incompatibility with *Vigna radiata*. *Genes* 8:374. doi: 10.3390/genes8120374

Okazaki, S., Hattori, Y., and Saeki, K. (2007). The *Mesorhizobium loti* purB gene is involved in infection thread formation and nodule development in *Lotus japonicus*. *J. Bacteriol.* 189, 8347–8352. doi: 10.1128/JB.00788-07

Okazaki, S., Kaneko, T., Sato, S., and Saeki, K. (2013). Hijacking of leguminous nodulation signaling by the rhizobial type III secretion system. *Proc. Natl. Acad. Sci. U.S.A.* 110, 17131–17136. doi: 10.1073/pnas.1302360110

Okazaki, S., Okabe, S., Higashi, M., Shimoda, Y., Sato, S., Tabata, S., et al. (2010). Identification and functional analysis of type III effector proteins in *Mesorhizobium loti*. *Mol. Plant Microbe Interact.* 23, 223–234. doi: 10.1094/MPMI-23-2-0223

Okazaki, S., Zehner, S., Hempel, J., Lang, K., and Göttfert, M. (2009). Genetic organization and functional analysis of the type III secretion system of *Bradyrhizobium elkanii*. *FEMS Microbiol. Lett.* 295, 88–95. doi: 10.1111/j.1574-6968.2009.01593.x

Oldroyd, G. E. D., Murray, J. D., Poole, P. S., and Downie, J. A. (2011). The rules of engagement in the legume-rhizobial symbiosis. *Annu. Rev. Genet.* 45, 119–144. doi: 10.1146/annurev-genet-110410-132549

Pérez-Montaño, F., Jiménez-Guerrero, I., Acosta-Jurado, S., Navarro-Gómez, P., Ollero, F. J., Ruiz-Sainz, J. E., et al. (2016). A transcriptomic analysis of the effect of genistein on *Sinorhizobium fredii* HH103 reveals novel rhizobial genes putatively involved in symbiosis. *Sci. Rep.* 6, 1–12. doi: 10.1038/srep31592

Perret, X., Staehelin, C., and Broughton, W. J. (2000). Molecular basis of symbiotic promiscuity. *Microbiol. Mol. Biol. Rev.* 64, 180–201. doi: 10.1128/MMBR.64.1.180-201.2000

Petnicki-Ocwieja, T., Schneider, D. J., Tam, V. C., Chancey, S. T., Shan, L., Jamir, Y., et al. (2002). Genomewide identification of proteins secreted by the Hrp type III protein secretion system of *Pseudomonas syringae* pv. tomato DC3000. *Proc. Natl. Acad. Sci. U.S.A.* 99, 7652–7657. doi: 10.1073/pnas.112183899

Radutoiu, S., Madsen, L. H., Madsen, E. B., Jurkiewicz, A., Fukai, E., Quistgaard, E. M. H., et al. (2007). LysM domains mediate lipochitin-oligosaccharide recognition and Nfr genes extend the symbiotic host range. *EMBO J.* 26, 3923–3935. doi: 10.1038/sj.emboj.7601826

Regensburger, B., and Hennecke, H. (1983). RNA polymerase from *Rhizobium japonicum*. *Arch. Microbiol.* 135, 103–109. doi: 10.1007/BF00408017

Sadowsky, M. J., Tully, R. E., Cregan, P. B., and Keyser, H. H. (1987). Genetic diversity in *Bradyrhizobium japonicum* serogroup 123 and its relation to genotype-specific nodulation of soybean. *Appl. Environ. Microbiol.* 53, 2624–2630.

Sánchez, C., Iannino, F., Deakin, W. J., Ugalde, R. A., and Lepek, V. C. (2009). Characterization of the *Mesorhizobium loti* MAFF303099 type-three protein secretion system. *Mol. Plant Microbe Interact.* 22, 519–528. doi: 10.1094/MPMI-22-5-0519

Schäfer, A., Tauch, A., Jäger, W., Kalinowski, J., Thierbach, G., and Pühler, A. (1994). Small mobilizable multi-purpose cloning vectors derived from the *Escherichia coli* plasmids pK18 and pK19: selection of defined deletions in the chromosome of *Corynebacterium glutamicum*. *Gene* 145, 69–73. doi: 10.1016/0378-1119(94)90324-7

Schechter, L. M., Guenther, J., Olcay, E. A., Jang, S., and Krishnan, H. B. (2010). Translocation of NopP by *Sinorhizobium fredii* USDA257 into *Vigna unguiculata* root nodules. *Appl. Environ. Microbiol.* 76, 3758–3761. doi: 10.1128/AEM.03122-09

Sory, M.-P., and Cornelis, G. R. (1994). Translocation of a hybrid YopE-adenylate cyclase from *Yersinia enterocolitica* into HeLa cells. *Mol. Microbiol.* 14, 583–594. doi: 10.1111/j.1365-2958.1994.tb02191.x

Staehelin, C., and Krishnan, H. B. (2015). Nodulation outer proteins: double-edged swords of symbiotic rhizobia. *Biochem. J.* 470, 263–274. doi: 10.1042/BJ20150518

Sugawara, M., Takahashi, S., Umehara, Y., Iwano, H., Tsurumaru, H., Odake, H., et al. (2018). Variation in bradyrhizobial NopP effector determines symbiotic incompatibility with Rj2-soybeans via effector-triggered immunity. *Nat. Commun.* 9:3139. doi: 10.1038/s41467-018-05663-x

Viprey, V., Del Greco, A., Golinowski, W., Broughton, W. J., and Perret, X. (1998). Symbiotic implications of type III protein secretion machinery in Rhizobium. *Mol. Microbiol.* 28, 1381–1389. doi: 10.1046/j.1365-2958.1998.00920.x

Wassem, R., Kobayashi, H., Kambara, K., Le Quéré, A., Walker, G. C., Broughton, W. J., et al. (2008). TtsI regulates symbiotic genes in Rhizobium species NGR234 by binding to tts boxes. *Mol. Microbiol.* 68, 736–748. doi: 10.1111/j.1365-2958.2008.06187.x

Wen, S., Chen, X., Xu, F., and Sun, H. (2016). Validation of reference genes for real-time quantitative PCR (qPCR) analysis of *Avibacterium paragallinarum*. *PLoS One* 11:e0167736. doi: 10.1371/journal.pone.0167736

Wenzel, M., Friedrich, L., Göttfert, M., and Zehner, S. (2010). The type III-secreted protein NopE1 affects symbiosis and exhibits a calcium-dependent autocleavage activity. *Mol. Plant Microbe Interact.* 23, 124–129. doi: 10.1094/MPMI-23-1-0124

Wilson, K. J., Sessitsch, A., Corbo, J. C., Giller, K. E., Akkermans, A. D. L., and Jefferson, R. A. (1995). β-Glucuronidase (GUS) transposons for ecological and genetic studies of rhizobia and other Gram-negative bacteria. *Microbiology* 141, 1691–1705. doi: 10.1099/13500872-141-7-1691

Yasuda, M., Miwa, H., Masuda, S., Takebayashi, Y., Sakakibara, H., and Okazaki, S. (2016). Effector-triggered immunity determines host genotype-specific incompatibility in legume-rhizobium symbiosis. *Plant Cell Physiol.* 57, 1791–1800. doi: 10.1093/pcp/pcw104

Conflict of Interest Statement: The authors declare that the research was conducted in the absence of any commercial or financial relationships that could be construed as a potential conflict of interest.

frontiers in Plant Science

REVIEW
published: 18 December 2018
doi: 10.3389/fpls.2018.01860

Interaction and Regulation of Carbon, Nitrogen, and Phosphorus Metabolisms in Root Nodules of Legumes

*Ailin Liu[1,2], Carolina A. Contador[1,2], Kejing Fan[1,2] and Hon-Ming Lam[1,2]**

[1] Centre for Soybean Research, State Key Laboratory of Agrobiotechnology, Shatin, Hong Kong, [2] School of Life Sciences, The Chinese University of Hong Kong, Shatin, Hong Kong

Members of the plant family Leguminosae (Fabaceae) are unique in that they have evolved a symbiotic relationship with rhizobia (a group of soil bacteria that can fix atmospheric nitrogen). Rhizobia infect and form root nodules on their specific host plants before differentiating into bacteroids, the symbiotic form of rhizobia. This complex relationship involves the supply of C_4-dicarboxylate and phosphate by the host plants to the microsymbionts that utilize them in the energy-intensive process of fixing atmospheric nitrogen into ammonium, which is in turn made available to the host plants as a source of nitrogen, a macronutrient for growth. Although nitrogen-fixing bacteroids are no longer growing, they are metabolically active. The symbiotic process is complex and tightly regulated by both the host plants and the bacteroids. The metabolic pathways of carbon, nitrogen, and phosphate are heavily regulated in the host plants, as they need to strike a fine balance between satisfying their own needs as well as those of the microsymbionts. A network of transporters for the various metabolites are responsible for the trafficking of these essential molecules between the two partners through the symbiosome membrane (plant-derived membrane surrounding the bacteroid), and these are in turn regulated by various transcription factors that control their expressions under different environmental conditions. Understanding this complex process of symbiotic nitrogen fixation is vital in promoting sustainable agriculture and enhancing soil fertility.

Keywords: rhizobia, bacteroids, nitrogen fixation, legumes, root nodule, phosphate homeostasis, metabolism, symbiosis

OPEN ACCESS

Edited by:
Benjamin Gourion, UMR2594 Plant Interactions Laboratory Microorganisms (LIPM), France

Reviewed by:
George Colin DiCenzo, Università degli Studi di Firenze, Italy
Michael Frederick Dunn, National Autonomous University of Mexico, Mexico

***Correspondence:**
Hon-Ming Lam
honming@cuhk.edu.hk

Specialty section:
This article was submitted to Plant Microbe Interactions, a section of the journal Frontiers in Plant Science

Received: *21 September 2018*
Accepted: *30 November 2018*
Published: *18 December 2018*

Citation:
Liu A, Contador CA, Fan K and Lam H-M (2018) Interaction and Regulation of Carbon, Nitrogen, and Phosphorus Metabolisms in Root Nodules of Legumes. Front. Plant Sci. 9:1860. doi: 10.3389/fpls.2018.01860

INTRODUCTION

Leguminosae (Fabaceae) is the third largest family of angiosperms with 750 genera and around 19,500 species (The Legume Phylogeny Working Group, 2013). Most legumes can establish a mutualistic association with alpha- and beta-proteobacteria to obtain biological nitrogen (reviewed by Andrews and Andrews, 2017; Sprent et al., 2017). Rhizobia are soil bacteria known for being

able to establish symbiosis with legume plants. Symbiotic nitrogen fixation (SNF) can be carried out once rhizobia are established inside the cells of root nodules formed from newly differentiated tissue in the roots of host plants. The host plant provides the microsymbiont with dicarboxylates together with other nutrients, in exchange for fixed nitrogen in the form of ammonium and amino acids (Udvardi and Day, 1997). Nitrogen-fixing legumes contribute to nitrogen enrichment of the soil and therefore are valuable in improving soil fertility. The legume–rhizobium association has an important impact on sustainable agriculture since it provides more than 65% of the biologically fixed nitrogen in agricultural systems (Herridge et al., 2008).

Studies on legume–rhizobium symbiosis have covered a large number of legume species, such as soybean (*Glycine max*), bird's foot trefoil (*Lotus japonicus*), alfalfa (*Medicago sativa*), barrelclover (*Medicago truncatula*), common bean (*Phaseolus vulgaris*), garden pea (*Pisum sativum*), common vetch (*Vicia sativa*), and narrowleaf lupin (*Lupinus angustifolius*) (Dupont et al., 2012). Although *M. sativa–Sinorhizobium meliloti* and *P. sativum–Rhizobium leguminosarum* associations are also well-studied symbiotic system (Kneen and LaRue, 1984; Jones et al., 2007), the genetic models of legume–rhizobium symbiosis are mainly focused on *L. japonicus–Mesorhizobium loti* and *M. truncatula–S. meliloti* associations, due to the small diploid genomes, high levels of genetic diversity, and well-established transformation systems of *L. japonicus* and *M. truncatula* (Oldroyd and Geurts, 2001; Oldroyd, 2005). *L. japonicus* possesses determinate root nodules, which are spherical with a well-defined, homogeneous central fixation zone composed of infected rhizobia-filled cells surrounded by uninfected cells (Schultze and Kondorosi, 1998). In contrast, *M. truncatula* forms indeterminate nodules which are cylindrical and consist of a gradient of developmental zones (Timmers et al., 1999).

Owing to their complex makeup, legume nodules have been extensively studied with respect to their metabolism and regulation. After the SNF process has been established in mature nodules, several biological processes occur simultaneously inside the nodules, including biological nitrogen fixation carried out by bacteroids, carbon–nitrogen metabolism, and exchange between host plants and bacteroids, and metabolite transport across cell membranes (Resendis-Antonio et al., 2011; Udvardi and Poole, 2013; Clarke et al., 2014). Root nodules mediate the influx of carbon sources and efflux of nitrogen compounds. The host plant supplies sucrose which will be converted to sources of energy and organic acids for fixation of atmospheric nitrogen, while the endosymbiont returns organic fixation products to the host (Day et al., 2001). Moreover, SNF in legume nodules exerts a high demand for phosphates (Gunawardena et al., 1992; Saad and Lam-Son, 2017). The phosphate concentration in nodules is threefold higher than in other organs or tissues (Sa and Israel, 1991). Under phosphate starvation, the phosphate acquisition rate increases in nodules to make them less vulnerable compared to other organs (Thuynsma et al., 2014; Saad and Lam-Son, 2017). Optimal plant phosphate requirement is about 0.05–0.30% of total dry weight, and inorganic phosphate is the main form absorbed by plants (Temple et al., 1998; Saad and Lam-Son, 2017).

Better understanding of the metabolic components participating in N_2 fixation and the key regulators that control the processes in legume nodules are a crucial step in seeking possible ways to enhance SNF and further increase legume productivity. In this review, we focus on the latest knowledge on root nodules including the nodule types (the section "Legume Nodule Types and Their Compatible Rhizobia"), the metabolic changes, transportation and regulation mechanisms in host plant (the section "Overview of Metabolism and Regulation in the Host Plant") and bacteroids (the section "Metabolism and Transport in Bacteroids").

LEGUME NODULE TYPES AND THEIR COMPATIBLE RHIZOBIA

About 90% of the species within the family Leguminosae (Fabaceae) can fix atmospheric nitrogen through a symbiotic association with soil bacteria known as rhizobia (Rascio and La Rocca, 2013; Andrews and Andrews, 2017). Rhizobia are diazotrophic Gram-negative bacteria able to form nitrogen-fixing nodules on the roots of legumes, where they differentiate into bacteroids (Rosenberg et al., 2014). Rhizobia present different specificities toward different host plant species based on the recognition of specific signal molecules (Nod factors) (Spaink, 2000; Poole et al., 2018). However, promiscuity has been observed in some cases. For example, *Sinorhizobium fredii* strain NGR234 is able to establish symbiosis with over 100 plant legumes such as cultivated soybean (*G. max*), wild soybean (*Glycine soja*), pigeon pea (*Cajanus cajan*), and cowpea (*Vigna unguiculata*) (reviewed in Brenner et al., 2009). Recently, analysis on legume–rhizobia symbioses was published where specificity (reviewed in Andrews and Andrews, 2017) and biogeography distribution (reviewed in Sprent et al., 2017) of nodulating legumes and their symbionts were discussed in detail.

Nodules are divided into two types: determinate and indeterminate. Determinate nodules are characteristic of soybean and common bean. Legumes such as alfalfa and garden pea present indeterminate nodules. Indeterminate nodules display five developmental zones: meristem (Zone I), infection and differentiation (Zone II), transition region between Zone II and Zone III in which bacteria are engulfed by plant cells (interzone II–III), nitrogen fixation (Zone III), and senescence (Zone IV) (Vasse et al., 1990). The meristem is active in indeterminate nodules and continues to grow, unlike in determinate nodules where meristem cells die once the nodules are mature. The meristem is the distal zone to the root and Zone IV is the proximal to the root attachment site. Zone-specific transcriptional and metabolic changes have been reported in the nodules formed between *M. truncatula* with *S. meliloti* and *S. medicae*, respectively (Roux et al., 2014; Ogden et al., 2017). A fifth zone (Zone V) has been described in alfalfa nodules (Timmers et al., 2000). This zone is proximal to the senescence zone and contains saprophytic intracellular rhizobia that do not undergo bacteroid differentiation. **Table 1** summarizes examples of legume–rhizobium associations and nodule types.

TABLE 1 | Rhizobia, host plant associations, and nodule types.

Nodule type	Rhizobia	Host plant
Determinate	*Mesorhizobium loti*	*Lotus japonicum*
	Rhizobium tropici	*Phaseolus vulgaris*
	Bradyrhizobium japonicum	*Glycine max*
		Vigna unguiculata
	Sinorhizobium fredii	*Glycine max*
		Vigna unguiculate
		Cajanus cajan
		Glycine soja
	Rhizobium leguminosarum bv. trifolii	*Phaseolus vulgaris*
		Trifolium repens
	Rhizobium etli	*Phaseolus vulgaris*
	Rhizobium leguminosarum bv. phaseoli	*Phaseolus vulgaris*
	Bradyrhizobium spp.	*Aeschynomene afraspera*
		Aeschynomene indica
Indeterminate	*Rhizobium leguminosarum bv. viciae*	*Pisum sativum*
		Vicia cracca
		Vicia hirsute
		Vicia faba
		Lens culinaris Medik
	Sinorhizobium meliloti	*Medicago sativa*
		Medicago truncatula
	Mesorhizobium loti	*Leucaena leucocephala*
	Mesorhizobium cicero	*Cicer arietinum*
	Mesorhizobium mediterranum	*Cicer arietinum*
	Cupriavidus taiwanensis	*Mimosa pudica*
		Mimosa diplotricha
		Mimosa priga
	Burkholderia spp.	*Mimosa pudica*
		Mimosa priga
Determinate and indeterminate	*Azorhizobium caulinodans*	*Sesbania rostrata*

OVERVIEW OF METABOLISM AND REGULATION IN THE HOST PLANT

Carbon Metabolism

Sucrose is the primary carbon resource for energy supply and carbon skeletons for SNF and is supplied to legume nodules by transportation from the shoots (Gordon et al., 1998). However, sucrose is not used directly as a substrate by isolated nitrogen-fixing bacteroids to support nitrogenase activity, as demonstrated in the cases of soybean (Stovall and Cole, 1978), garden pea (Glenn and Dilworth, 1981), lupin (Tomaszewska et al., 1991), and alfalfa (Miller et al., 1988). In nodules, sucrose can be processed by one of two enzymes, sucrose synthase (SS; EC 2.4.1.13) and alkaline invertase (AI; EC 3.2.1.26), as shown in **Figure 1**. SS performs a reversible UDP-dependent cleavage of sucrose into UDP-glucose (UDP-Glc) and fructose (Akazawa and Okamoto, 1980). SS activity is reduced in the SNF-defective mutant, *rug4*, of *P. sativum*, indicating that SS plays an important role in nodule functions (Gordon et al., 1998, 1999). Moreover, overexpressing the antisense of *MtSucS1* (encoding enzyme SS) in *M. truncatula* impaired the plant growth and nodulation in the *MtSucS1*-reduced nodules, and the contents of amino acids and their derivatives were also found to be reduced, which suggest SS is a crucial player in the establishment and maintenance of an efficient SNF process (Baier et al., 2007). Six SS isoforms have been identified, and the mutants of SS isoform *sus1-1* and *sus3-1* showed 38% and 67% reduction of SS activity, respectively, in nodules formed by inoculating *L. japonicus* with *M. loti* strain Tono, while the double mutant plants of *sus1-1/sus3-1* had significantly impaired growth and their nodule SS activities were reduced by 94% compared to the wild type under the same growth conditions. This further shows that SS is essential in nodulation maintenance (Horst et al., 2007). In addition, when exposed to drought stress, nitrogen fixation in nodules declined, and the activity of SS was severely inhibited in various species (*M. sativa*, *P. sativum*, and *P. vulgaris*), and led to the further limitation of carbon availability in bacteroids (Ramos et al., 1999; Gálvez et al., 2005; Naya et al., 2007).

The other sucrose-catabolizing enzyme, AI, is a hydrolase, first identified in soybean nodules, that irreversibly cleaves sucrose into fructose and glucose (Copeland and Morell, 1985). The isolation and purification of AI was also carried out from chickpea nodules (Asthir and Singh, 1997). In *L. japonicus*, the expression level of gene *LjInv1* encoding enzyme AI was twofold higher in mature nodules than in uninfected roots. Enzyme activity assays showed that LjInv1 contributed to the production of hexoses and other biosynthetic processes in developing nodules (Flemetakis et al., 2006). In *G. max* and *M. truncatula* root nodules, an alkaline/neutral *Inv* gene was found to have enhanced transcription levels in developing root nodules inferring an increased need for sucrose degradation (Flemetakis et al., 2006; Tesfaye et al., 2006). However, there is not much direct evidence to prove that AI is essential for the regulation of nodule metabolism.

The resulting UDP-Glc and free hexoses (glucose and fructose) are phosphorylated by hexokinase (EC 2.7.1.1) and enter glycolysis or oxidative pentose phosphate pathways. In nodules, the host plant provides carbon sources for bacteroid activities in the form of dicarboxylates, particularly malate and succinate (Day, 1991). Phosphoenolpyruvate carboxylase (PEPC; EC 4.1.1.31) and malate dehydrogenase (MDH; EC 1.1.1.82) convert the carbon flux from glycolysis to form malate (**Figure 1**). PEPC catalyzes the conversion of PEP into oxaloacetate (OAA). The active enzymes are less sensitive to malate, which act as a negative feedback control (Nimmo, 2000). The nodule PEPC was found to be activated with phosphorylation and its sensitivity was inhibited by L-malate *in vitro* and *in vivo* (Schuller and Werner, 1993; Zhang et al., 1995). In *L. japonicus*, abundant transcript of *LjPEPC1* was found in the vascular bundles of nodules and bacteroid-infected cells, while *LjPEPC2* was expressed in roots and shoots at low levels and postulated as the housekeeping isoform. Moreover, regulatory phosphorylation of PEPC is thought to be mainly controlled by the PEPC kinase (PEPC-PK) (Vidal and Chollet, 1997), and the expression of

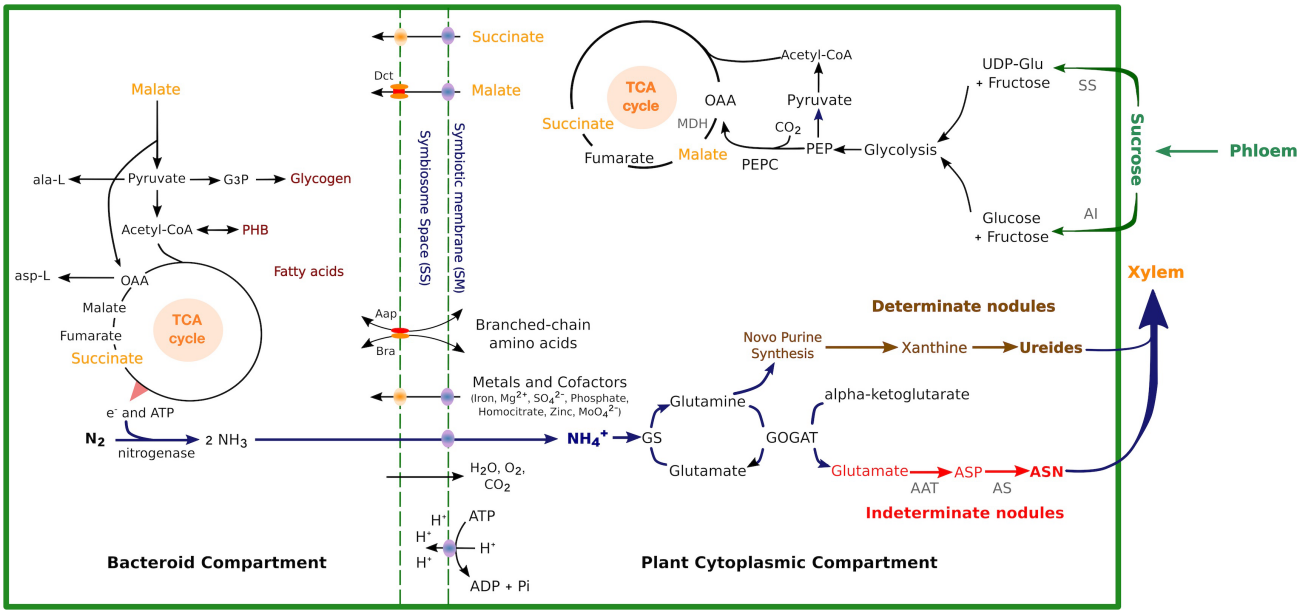

FIGURE 1 | Schematics of carbon and nitrogen metabolic pathways with key enzymes, metabolites, and transporters in determinate nodules and indeterminate nodules. Sucrose in the plant cytosol is split into glucose and fructose by AI or UDP-Glc and fructose via SS, which is then catabolized via glycolysis to PEP. Carbon from PEP and carbonic acid is diverted to OAA and then malate by PEPC and the neMDH, respectively. OAA may be further converted to succinate or fumarate. Carbon sources are transported across the peribacteroid and bacteroid membranes and enter the TCA cycle in the bacteroid to be metabolized. Transport of inorganic ions and cofactors required for SNF across the SM is indicated. The ammonia produced by the SNF is transported back to the plant and assimilated by GS and GOGAT into Gln and Glu (blue arrows). In indeterminate nodules, Glu and Gln are further converted to Asp and Asn by AAT and AS, respectively (red arrows). In determinate nodules, Gln enters purine synthesis pathway and is converted to ureides (brown arrows). AI, alkaline invertase; UDP-Glc, UDP-glucose; SS, sucrose synthase; PEP, phosphoenolpyruvate; OAA, oxaloacetate; PEPC, PEP-carboxylase; MDH, malate dehydrogenase; PHB, polyhydroxybutyrate; AAT, aspartate aminotransferase; AS, asparagine synthetase; ASP, aspartate; ASN, asparagine.

LjPEPC-PK shares a similar pattern with *LjPEPC1* in mature nodules (Nakagawa et al., 2003). The OAA is then converted to malate by MDH in a reversible reaction, and this can then be uptaken by bacteroids directly (**Figure 1**). In alfalfa, five species of cDNAs were found to encode MDH, but only one of them had a nodule-enhanced expression pattern (Miller et al., 1998). One nodule-enhanced MDH (neMDH) was found in garden pea (Fedorova M. et al., 1999). Two MDH isoforms were found in the *L. japonicus* nodule by transcriptome profiling, one of which is a cytosolic MDH (cMDH) and the other a neMDH (Takanashi et al., 2012). The activity of cMDH in *L. angustifolius* nodules was shown to increase under P-deficient conditions, supporting the involvement of cMDH in nodules (Le Roux et al., 2014).

Besides the enzymes described above, some other carbon metabolic enzymes also play a role in legume nodules. *MsSPSA*, encoding sucrose phosphate synthase (SPS; EC 2.3.1.14) in *M. sativa* L., is involved in the first step of sucrose synthesis, and the expression of *MsSPSA* showed a nodule-enhanced pattern. SPS showed higher activities in the nodules formed by wild-type *S. meliloti*, compared to nodules inoculated with a N-deficient Fix$^-$ strain (a Tn5 insertional mutation in *nifH*; Hirsch et al., 1983), suggesting an important role in maintaining a stable carbohydrate/energy supply for the actively nitrogen-fixing symbiont (Aleman et al., 2010).

Multiple environmental stresses result in the inhibition of carbon metabolism in host legumes, resulting in the suppression of SNF efficiency in nodules. Under salt stress, the concentration of sucrose was decreased, and major carbon metabolic enzymes such as SS and AI showed lower activity in both *M. truncatula* nodules (indeterminate nodules) and *L. japonicus* nodules (determinate nodules) (López et al., 2008). When garden pea plants were cultured under drought stress, the SS activity was down-regulated, indicating the normal carbon metabolic pathway was inhibited. The NADP-dependent isocitrate dehydrogenase (ICDH; EC1.1.1.42) was reported to balance C/N metabolic fluxes in leaves (Gallardo et al., 1995; Gálvez and Gadal, 1995). The enhancement of ICDH activity in nodules was probably the result of compensating for the C and N imbalance or supplying additional NADPH to neutralize the effects of the increased production of reactive oxygen species (ROS) as a consequence of drought stress (Gálvez et al., 2005).

Nitrogen Metabolism

Ammonia exported from the bacteroids diffuses into the cytosol of the infected host cells to be rapidly assimilated. Amino acids and/or ureides are then synthesized and exported from the legume nodules to the shoots (**Figure 1**). The determinate-nodule legumes primarily transport allantoin and allantoate (ureides) as fixed-N compounds, while the indeterminate nodules assimilate amides in the form of asparagine (Asn) and glutamine (Gln) (Sprent, 2009). The first step of ammonium assimilation is apparently the same in amide- and ureide-exporting legume

nodules (Todd et al., 2006). In both cases, nitrogen fixed in the bacteroids is exported into the host cell cytosol, where ammonia is converted to Gln and glutamate (Glu) by the enzymes Gln synthetase (GS; EC 6.3.1.2) and Glu synthase (NADH-GOGAT; EC 1.4.1.14). In indeterminate nodules, Glu and Gln are further converted to aspartate (Asp) and Asn by Asp aminotransferase (AAT EC 2.6.1.1) and Asn synthetase (AS; EC 6.3.5.4). While for determinate nodules, Gln further entry purine synthesis pathway and convert to ureides as final product exported in to host plant (**Figure 1**).

Glutamine synthetase, as the enzyme for the first step of ammonia assimilation in the infected root cells, is a key component of nitrogen metabolism in nodules. It catalyzes the ATP-dependent amination of Glu to Gln. GS possesses two major isoforms largely separated by their subcellular localization, plastidic GS2 and cytosolic GS1 (Temple et al., 1998; Lea and Miflin, 2003). In *M. truncatula* nodules, three *GS* genes have been identified: cytosolic *MtGS1a* and *MtGS1b*, and plastid *MtGS2*, where MtGS1a accounts for 90% of the GS activity in nodules (Carvalho et al., 1997, 2000). Impairment of GS activity using phosphinothricin resulted in the inhibition of nodule growth, and the promotion of nodule senescence. The reduced activity of GS also suppressed Asn biosynthesis, as demonstrated by the lower expression of *AS* transcripts and lower Asn content (Seabra et al., 2012). NADPH-GOGAT is another enzyme involved in the assimilation of NH_4^+, by transferring the amide group from Gln to α-ketoglutarate (**Figure 1**). In transgenic *M. sativa* expressing antisense *NADPH-GOGAT*, GOGAT activities were much reduced in the nodules. The transgenic *M. sativa* inoculated with *S. meliloti* exhibited moderate chlorosis, lower nodule weight, and reduction of N_2 fixation efficiency compared to the control (Schoenbeck et al., 2000).

In addition to primary nitrogen assimilation by converting ammonia into amino acids, ureide biosynthesis is also a common pathway among tropical legumes such as soybean, common bean, and cowpea, which generally form determinate nodules (Tajima, 2004). The allantoin and allantoate are the final nitrogen forms exported from soybean nodules to the shoots (McClure and Israel, 1979). Before ureide synthesis, ammonia enters a purine synthesis pathway, which is catalyzed by xanthine oxidase and xanthine dehydrogenase into urate, whose activities have been detected in both infected cells and uninfected cells in cowpea nodules. While uricase, which catalyzes the irreversible conversion of urate to allantoin, was detected in uninfected cells but not infected cells (Atkins et al., 1997). Moreover, the genes *GmALN3* and *GmALN4*, encoding the enzyme allantoinase (EC 3.5.2.5) that converts allantoin to allantoate, were expressed in soybean nodules (Duran and Todd, 2012). Gln may also be enzymatically transformed into xanthine through the *de novo* purine synthesis pathway (Werner and Witte, 2011; **Figure 1**).

Phosphate Metabolism

Phosphate is the second most limiting macronutrient element required for crop growth after nitrogen, and there is a particularly high demand for phosphates in the nodules of N_2-fixing legumes (Gunawardena et al., 1992; Vance et al., 2000). Phosphate, as an essential macronutrient, is incorporated into organic compounds such as nucleic acids (DNAs and RNAs), enzymes, ATP, sugar phosphates, phospholipids, and so on. Such organic phosphates are involved in many plant biochemical processes such as nutrient transport and photosynthesis. As a component of chromosomes, phosphates play an important role in cell division and organogenesis, and help to transfer the genetic information from one generation to the next (Ahemad and Oves, 2011). The soluble inorganic phosphate (Pi) is the most abundant metabolite in *Bradyrhizobium japonicum* cells. The Pi concentration in free-living *B. japonicum* cells is 8.1 μmol g^{-1} FW and 29.2 μmol g^{-1} FW in bacteroids. Massive amounts of Pi are transported into bacteroids through phosphate transporters and are highly involved in the metabolism of bacteroids. Indeed, SNF expends a great quantity of energy involving phosphorylated intermediates (Vauclare et al., 2013).

Legume Metabolic Changes Under Pi Deficiency

Deprivation of Pi can lead to an ATP shortage and a decrease in key metabolic enzymes (e.g., those involved in photosynthesis), and therefore is tightly correlated with plant growth (Czarnecki et al., 2013; Saad and Lam-Son, 2017). Although low Pi availability causes a decline in SNF, the responses to Pi deficiency vary among different legumes. There are two main strategies: one is to make changes to nitrogen and carbon metabolism, such as N acquisition and assimilation as well as carbon source adjustments, and the other is to enhance Pi uptake and recycling in nodules (Wang et al., 2010; Qin et al., 2012; Udvardi and Poole, 2013).

To investigate the metabolic changes in legume nodules under low-Pi stress, metabolic profiling has been done in common bean and chickpea (Hernandez et al., 2009; Zhang N. et al., 2012). Hernandez et al. (2009) performed a metabolic profiling using common bean plants inoculated with *Rhizobium tropici* CIA899 cultivated under Pi-deficient and Pi-sufficient conditions. The levels of 13 metabolites were significantly changed when comparing between the two conditions. Among these, amino acids and other nitrogen metabolites, such as urea, spermidine, and putrescine, were decreased in nodules under low-Pi conditions while most of the carbon metabolites including organic acids and polyhydroxy acids were increased (Hernandez et al., 2009). Similar changes were also found in chickpea inoculated with two different *Mesorhizobium* strains, *M. ciceri* CP-31 (*Mc*CP-31) and *M. mediterranum* SWRI9 (*Mm*SWRI9) (Nasr Esfahani et al., 2016). These two *Mesorhizobium* strains inoculated on chickpea showed a differential symbiotic performance under both control and low-Pi condition. *Mc*Cp-31-chickpea exhibited a higher symbiotic efficiency and higher Pi concentration than *Mm*SWRI9–chickpea under normal and low-Pi conditions. The differences in SNF efficiency between the two types of chickpea–*Mesorhizobium* associations were correlated with various changes in carbon and nitrogen metabolites. For instance, the activities of most carbon and nitrogen metabolic enzymes, such as AAT, GS, and MDH, were increased in *Mc*Cp-31–chickpea nodules, while the activities of these same enzymes were either the same or reduced in *Mm*SWRI9–chickpea nodules. These results provide evidence that host plants adjust their carbon and nitrogen metabolic

pathway to maintain the SNF efficiency under Pi deficiency condition (Nasr Esfahani et al., 2016).

According to previous studies, under low Pi availability, nodules would largely decrease the utilization of atmospheric nitrogen as the nitrogen source and utilize more soil nitrogen (such as NO_3^- and NH_4^+) instead, as shown in **Figure 2** (Valentine et al., 2017). The reason for such a shift is not only that NO_3^- itself is a strong inhibitor of nodulation and SNF, but also that the consumption of carbon as an energy source for nitrogen uptake from soil is less than that for SNF (Minchin and Witty, 2005). In *Virgilia divaricata*, the carbon cost related to SNF ranges from 3.3 to 6.6 gCg^{-1}-N (gram of carbon was used when fixed each gram of N_2), while the carbon cost of NO_3^- reduction is not more than 2.5 gCg^{-1}-N. Hence, the assimilation of nitrogen from the soil would save more organic carbon for plant growth (Minchin and Witty, 2005). In SNF nodules, the host plant provides photosynthetically fixed carbon to symbiosomes as the major energy source. In turn, bacteria in the nodule fix N_2 by the activities of nitrogenases and release NH_4^+ to the host cells. The carbon transported to symbiosomes is mainly in the form of TCA cycle dicarboxylates (such as malate) and is also used as the carbon skeletons for the syntheses of amino acids from N_2 (Rosendahl et al., 1990; Valentine et al., 2017; **Figure 2**). For example, in *L. angustifolius* cv. Wonga, there is an increased rate of malate synthesis via PEPC and MDH under long-term Pi deficiency. Although malate is the major energy source for symbiosomes, high malate accumulation could inhibit N_2 fixation and nitrogen assimilation (Le Roux et al., 2008).

Nitrogen Export From Nodules

As aforementioned, in exchange for the nutrient supply, ammonia and/or alanine and Asp are translocated into the legume cytosol from the symbiosome and then assimilated into ureides or amides. Under Pi deprivation, legumes prefer exporting more ureides, due to the lower carbon cost (**Figure 2**). This was demonstrated through an experimental determination

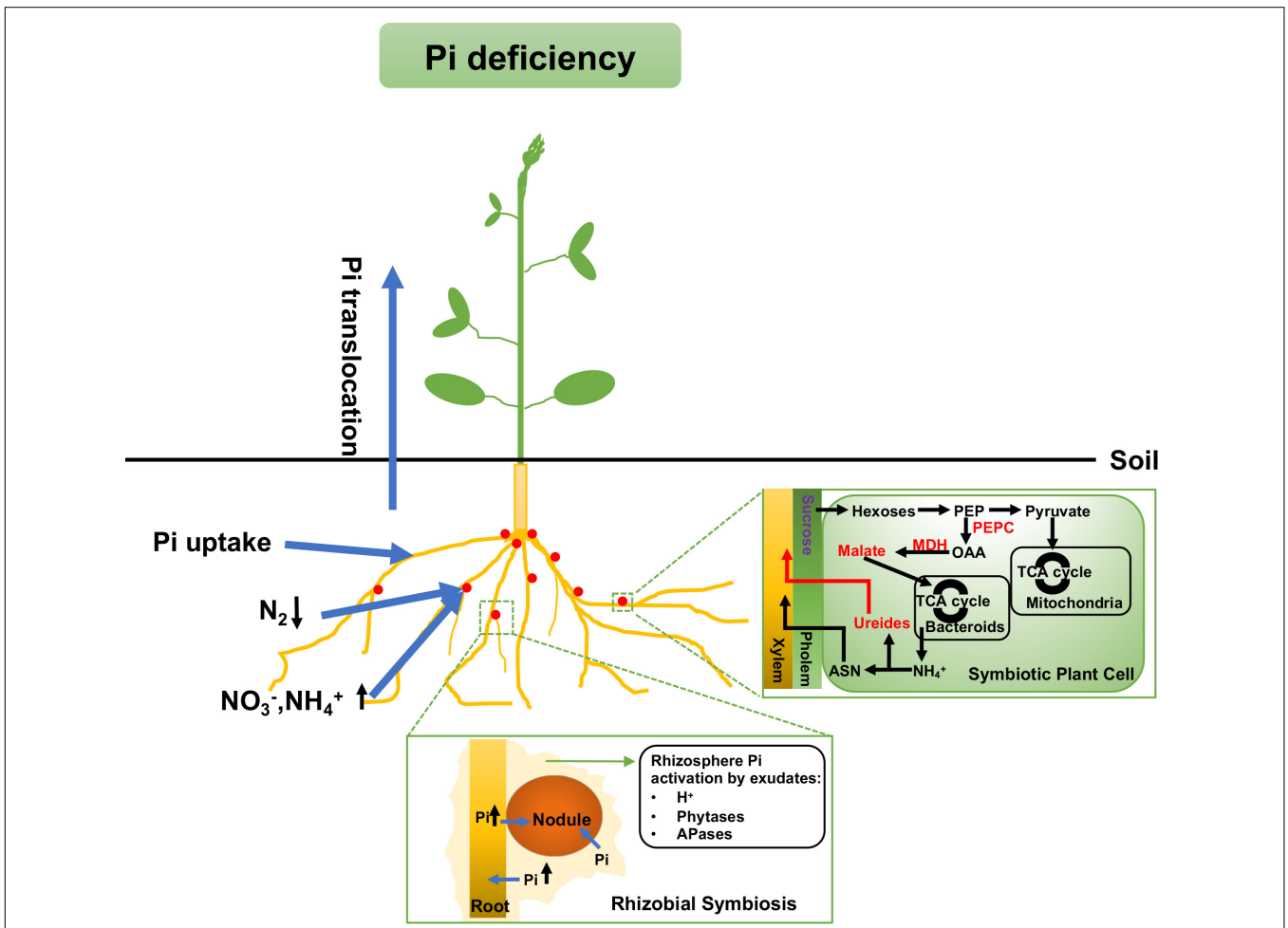

FIGURE 2 | Mechanisms for maintaining Pi homeostasis under Pi deficiency in legumes. Legumes use more soil N (such as NO_3^- and NH_4^+) as the main nitrogen source rather than through SNF. There is also a malate accumulation in both types of nodules and more ureides export in determine nodules under Pi deficiency. A red or purple label means the metabolite content or enzyme activity is up- or down-regulated, respectively. Arrows up (↑) and down (↓) mean the nutrient uptake is up- or down-regulated, respectively. SNF, symbiotic nitrogen fixation; PEP, phosphoenolpyruvate; PEPC, phosphoenolpyruvate carboxylase; OAA, oxaloacetate; MDH, malate dehydrogenase; ASN, asparagine.

of C and N budgets in the tropical legume cowpea and the temperate legume lupin. The results were 1.4 gCg^{-1} fixed N in cowpea which forms ureide-exporting nodules, and a minimum of 3.9 gCg^{-1} fixed N in lupin which forms amide-exporting nodules. The result indicates that the export of ureides is more economical in the use of carbon (Atkins, 1991). The shift to higher amounts of ureide export under Pi stress was also observed in soybean, where there was higher accumulation of ureides relative to amino acids in nodules (Le Roux et al., 2009). The switch to ureide exports may reduce the carbon cost under Pi stress, which has a positive effect on legume growth.

Pi Homeostasis in Legume Nodules

Under Pi stress, legumes exhibit very flexible mechanisms to maintain Pi homeostasis in nodules. On the one hand, legumes increase Pi acquisition from the external environment. On the other hand, plants adopt flexible Pi recycling and internal Pi conservation mechanisms to improve Pi remobilization (Nasr Esfahani et al., 2016; Saad and Lam-Son, 2017).

Pi acquisition from the external environment

Pi acquisition from the external environment by plants is affected by nitrogen metabolism. Pretreatment with NH_4^+ and NO_3^- can increase Pi uptake from soil in *Zea mays* roots (Smith and Jackson, 1987). Acquisition of NH_4^+ can lead to a release of proton (H^+) that decreases the pH in the rhizosphere, which in turn stimulates Pi solubility and uptake (Zhao et al., 2009). Legumes tend to take up NH_4^+ and NO_3^- from the soil through the roots in both Pi stress and Pi sufficient conditions (Dan and Brix, 2009). In turn, more acquisition of NH_4^+ can improve the availability of Pi in the external environment.

Plant acid phosphatases (APases) can hydrolyze organic phosphates to improve soil Pi availability in legumes (**Figure 2**). Under Pi stress, APases become catalytically better using the same amount of nodule crude extract, which is an efficient way to utilize organic phosphates (Araújo et al., 2008). In addition, phytases can hydrolyze phytate into myoinositol and Pi to improve the Pi level in the rhizosphere for uptake through the roots (Araújo et al., 2008). The expression and activities of phytases are also induced by Pi deprivation in *P. vulgaris* nodules. Two recombinant inbred lines (RILs) of *P. vulgaris*, RILs 115 (P-efficient) and 147 (P-inefficient), were inoculated with *R. tropici* CIAT 899 strain and planted in Pi-deficient conditions. Under low Pi condition, the accumulation of phytase transcripts was observed in the nodules of both lines, and it is more enhanced in Line RIL115 than in Line RIL147. The increase in phytase and phosphatase enzyme activities and higher SNF efficiency were found in RIL115 under Pi-deficient treatment, indicating a possible role of phytase activity in nodules to maintain SNF under Pi deficiency condition (Lazali et al., 2013).

The uptake of Pi is also under the regulation of high-affinity Pi transporters. Plants have two identified Pi uptake mechanisms: a high-affinity system that may be up-regulated under low Pi condition and a low-affinity system which is constitutively expressed (Hernandez et al., 2009; Nasr Esfahani et al., 2016). In this review, we focus on the high-affinity Pi transporters. Most high-affinity Pi transporters are induced by Pi starvation and expressed in the root hairs and root epidermis which are directly exposed to soil Pi (Liu et al., 2008). Among Pi transporters, the Pht1 family is the most intensively studied in plants (Gu et al., 2016). Pht1, localized in the plasma membrane, is directly related to Pi uptake from soil and Pi translocation in the plant. Some Pht1s are directly under the control of the central regulators of Pi starvation signaling, the phosphate starvation response (PHR) transcription factors (Rubio et al., 2001; reviewed in Gu et al., 2016). In *G. max*, 15 *Pht1* paralogs have been identified by bioinformatics and experimentation. The expressions of all 15 *GmPht1*s are up-regulated under low Pi condition compared to high Pi condition. By overexpressing each *GmPHT1* paralog in the yeast Pi-transporter mutant PAM2 (Δ*pho84* Δ*pho89*), *GmPht1;1*, *GmPht1;2*, *GmPht1;5*, *GmPht1;7*, and *GmPht1;10* are found to be high-affinity Pi transporters and the others are lower affinity Pi transporters (Fan et al., 2013). A Pi starvation-induced high-affinity Pi transporter, *GmPT5* (*Glyma10g04230*), was also identified, which was considered to play an important role in maintaining nodular Pi homeostasis. *GmPT5* is expressed in the junction area between roots and young nodules, and mainly functions in transporting Pi from roots to nodules. Higher expression of *GmPT5* leads to more Pi being transported from root to nodule, which is beneficial for maintaining SNF (Qin et al., 2012).

Internal phosphate recycling and phosphate conservation

Besides the uptake of Pi from the external environment, legume nodules also develop phosphate recycling and phosphate conservation mechanisms under Pi deficiency (**Figure 2**) (Saad and Lam-Son, 2017). A report showed that chickpea could re-allocate Pi from roots to nodules when facing Pi stress. A sharp reduction in Pi (by around 78%) in roots was detected in chickpea, which the researchers assumed that the missing Pi was transported into nodules in order to prevent the complete depletion of nodular Pi (Nasr Esfahani et al., 2016). Common bean was also reported to mobilize Pi from nucleic acids and phospholipids (Hernandez et al., 2009). Under low Pi conditions, *V. divaricata* exhibited a lower Pi uptake rate but higher levels of phosphohydrolase exudation. This suggests that *V. divaricata* may prefer to recycle internal nodular Pi pools and use alternate bypass routes to conserve Pi rather than directly uptaking Pi from soil (Vardien et al., 2016).

Regulation of Metabolism in Legume Nodules of Host Plants

Regulators of Carbon and Nitrogen Metabolism

It is an important challenge for legumes to maintain a balance between supplying the nodules with the amount of carbon required for nitrogen fixation while retaining sufficient carbon for growth, as well as keeping the nitrogen efflux from the nodules at an optimum level. The host plant regulates the symbiotic process by controlling nodule development and nodule numbers as well as by adjusting the nodule turnover and the level of nitrogen fixation (Ferguson et al., 2010; Sulieman and Schulze, 2010). The balance between plant nitrogen demand and nitrogen fixation rate is finely tuned to reach the nitrogen concentration that allows maximum plant growth. In common bean, nitrogen translocated

from senescing lower leaves to nodules resulted in lower nitrogen fixation rate (Fischinger et al., 2006). Autoregulation of nodulation (AON) is the main systemic negative feedback mechanism of host plants to negatively regulate SNF in nodules (Ferguson et al., 2010). AON has been identified using several legume mutants with the super nodulation phenotype, such as the *G. max* mutant *nts-1*, *M. truncatula* mutant *sunn*, and *L. japonicus* mutant *har1*, were found to lack in a leucine-rich repeat receptor-like protein kinase for AON in shoots (Krusell et al., 2002; Nishimura et al., 2002; Schnabel et al., 2005). CLAVATA3/embryo-surrounding region (CLE) peptides are a group of small (12–13 amino acids) secreted peptides derived from the C-terminal region of preproproteins. In *M. truncatula*, it has been suggested that *MtCLE12* or *MtCLE13* plays a role for CLE signaling in controlling nodule numbers. These peptides are generated in roots and transported to leaves via the xylem to trigger the AON response (Mortier et al., 2010). *LjCLE-RS1* and *LjCLE-RS2* were also found to be involved in regulating nodule formation in *L. japonicus* (Magori and Kawaguch, 2010).

Regulator for Pi Homeostasis

Legumes have evolved to adopt strategies to maintain the nodular Pi homeostasis (Sulieman and Tran, 2015). Multiple genes and proteins work as regulators (Rubio et al., 2001; Yao Z.F. et al., 2014; Sulieman and Tran, 2015). A MYB-CC-type transcription factor (*PHR1*), a small non-coding RNA (microRNA399), and proteins containing the SYG1/PHO81/XPR1 (SPX) domain all play important roles in Pi stability in nodules, and are considered to be vital regulators (Xue et al., 2017). DNA methylation may also be involved in the nodular Pi homeostasis regulation, but it still needs further research (Kim et al., 2015; Yong-Villalobos et al., 2015; Crampton et al., 2016).

In soybean, 35 GmPHR members have been identified. Among them, *GmPHR25* is induced by Pi starvation and it in turn increased the transcripts of 11 out of 14 high-affinity Pi transporters as well as those of 5 other Pi starvation-responsive genes (Xue et al., 2017). This evidence indicated that *GmPHR25* is a vital Pi homeostasis regulator in soybean (Xue et al., 2017). Besides small non-coding RNAs, long non-coding RNAs (lncRNAs) are also involved in Pi homeostasis. In the legume model plant, *M. truncatula*, three phosphate deficiency-induced LncRNAs (*PDILs*) have been characterized through their corresponding *Tnt1* mutants. *PDIL1* suppresses the degradation of *MtPHO2*, working as a positive Pi homeostasis regulator. However, *PDIL2* and *PDIL3* may directly inhibit Pi transporters, therefore working as negative regulators (Wang et al., 2017).

Proteins containing the *SPX* domain are considered to be vital regulators in the plant Pi signaling network (Yao Z.F. et al., 2014). In common bean, *PvSPX1–PvSPX3* are all induced by Pi starvation, but *PvSPX1* had higher sensitivity and faster response to Pi starvation than the other two *PvSPX*s. Ten Pi starvation-responsive genes are induced by overexpressing *PvSPX1*, even with an increase in Pi concentration at the same time. It was further shown that the overexpression of *PvPHR1* resulted in a decrease in *PvSPX1* transcripts. Therefore, *PvSPX1* is a positive regulator in maintaining Pi homeostasis and is itself regulated by *PvPHR1* (Yao Z.F. et al., 2014). But in soybean, *GmSPX1* is a negative regulator in the Pi signaling network, and may be involved in phosphate starvation by inhibiting the expression of *GmMYB48*, a phosphate starvation-induced gene (Zhang et al., 2016). *GmSPX3* is also induced by Pi starvation, and considered to be a positive regulator which induces seven Pi starvation-responsive genes in soybean hairy root (Yao Z. et al., 2014). Genes found to be associated with legume Pi homeostasis are listed in **Table 2**.

METABOLISM AND TRANSPORT IN BACTEROIDS

Nitrogen Assimilation

Nitrogenase Complex

Symbiotic nitrogen fixation by rhizobia in legume root nodules is carried out through the nitrogenase enzyme complex. Nitrogenase catalyzes the following reaction:

$$N_2 + 8e^- + 8H^+ + 16ATP \rightarrow 2NH_3 + H_2 + 16ADP + 16Pi.$$

This reaction describes the reduction of nitrogen to ammonia, and is associated with a high energetic cost (ATP). The enzymatic complex of nitrogenase consists of two enzymes: dinitrogenase reductase, a dimeric Fe-protein encoded by the *nifH* gene, and dinitrogenase, a tetrameric FeMo-protein encoded by the *nifDK* gene (Rascio and La Rocca, 2013; Rubio and Ludden, 2015). These enzymes are rapidly deactivated in the presence of atmospheric concentrations of oxygen (Dixon and Wheeler, 1986).

Regulation of Nitrogenase Activity

Nitrogenase activity is reduced at high oxygen concentrations. Nodules provide low oxygen environments for the N_2-fixing bacteroids, as observed in soybean nodules where the oxygen concentration is 56 nM (Kuzma et al., 1993) and even lower concentrations have been registrated (Appleby, 1984). Therefore, oxygen tension is a key regulator of genes required for N_2 fixation, nitrogenase synthesis (*nif* genes), and microoxic respiration (*fix* genes). The nitrogen fixation signaling pathway differs between rhizobium strains. In *S. meliloti*, the heme-containing FixL, a signal-transducing membrane protein, acts as the oxygen sensor for the system. In the absence of oxygen, FixL autophosphorylates and transfers the phosphate to FixJ (Gilles-Gonzalez et al., 1991; Lois et al., 1993). This transcriptional factor in turn regulates positively the expression of two regulatory genes, *nifA* and *fixK*. NifA is a transcriptional activator that controls the expressions of nitrogen fixation genes, *fixABCX*, *nifN*, *nifB*, and *nifHDK* (Gong et al., 2006). FixK upregulates the expression of *fixNOQP* and *fixT* (Batut et al., 1989; Foussard et al., 1997). FixT represses the expression of *nifA* (Foussard et al., 1997) and FixNOQP is a cytochrome terminal oxidase *cbb3* with a high affinity for oxygen that allows ATP production required for the nitrogen fixation process (Preisig et al., 1993). However, in *B. japonicum*, the FixLJ system is not required to induce the expression of *nifA* (Fischer and Hennecke, 1987), but instead it is RegSR that mediates positive control to transcription of *nifA* (Lindemann et al., 2007).

TABLE 2 | Genes involved in legume Pi homeostasis.

Gene	Species	Annotation	Response to Pi deficiency	Description	References
PvPHR1	*Phaseolus vulgaris*	MYB-CC TF	Induced	Overexpression of *PvPHR1* can activate a subset of Pi starvation-responsive genes and increase Pi concentration.	Valdés-López et al., 2008; Moris et al., 2004
GmPHR25	*Glycine max*	MYB-CC TF	Induced	Overexpression of GmPHR25 can activate 11 high-affinity Pi transporters and 5 Pi starvation-responsive genes and increase Pi concentration.	Xue et al., 2017
GmSPX1	*Glycine max*	SPX domain-containing protein	Induced	Induced by Pi starvation by interacting with *GmMYB48*; Overexpression of *GmSPX1* can decrease Pi concentration.	Zhang et al., 2016
GmSPX3	*Glycine max*	SPX domain-containing protein	Induced	Overexpression of *GmSPX3* can activate 7 Pi starvation-responsive genes and increase Pi concentration.	Yao Z. et al., 2014
PvSPX1	*Phaseolus vulgaris*	SPX domain-containing protein	Induced	Overexpression of *PvSPX1* can activate 10 Pi starvation-responsive genes and increase Pi concentration.	Yao Z.F. et al., 2014
PvPHO2	*Phaseolus vulgaris*	Ubiquitin E2 conjugase	Suppressed	Regulate Pi starvation responses	Valdés-López and Hernández, 2008
CaPHT1;4	*Cicer arietinum*	High-affinity Pi transporter	Induced	Involved in Pi acquisition and mobilization	Nasr Esfahani et al., 2016
GmPT5	*Glycine max*	High-affinity Pi transporter	Induced	Involved in Pi transportation from root to nodule	Qin et al., 2012
CaPHO1	*Cicer arietinum*	Phosphatase 1	Unchanged	Involved in Pi transporting into the xylem	Nasr Esfahani et al., 2016
LjPHO3	*Lotus japonicus*	Sucrose/H+ symporter	NA	Mediate Pi starvation responses	Qin et al., 2016
PvTIFY	*Phaseolus vulgaris*	JAZ TF	Induced	Involved in the regulation of Pi deficiency	Aparicio-Fabre et al., 2013
MtmiR399	*Medicago truncatula*	MicroRNA	Induced	Regulate *PHO2* and Pi transporter	Li et al., 2018
MtPDIL1	*Medicago truncatula*	LncRNA	Induced	Suppress degradation of *MtPHO2*	Wang et al., 2017
MtPDIL2	*Medicago truncatula*	LncRNA	Suppressed	Suppress Pi transporter	Wang et al., 2017
MtPDIL3	*Medicago truncatula*	LncRNA	Suppressed	Suppress Pi transporter	Wang et al., 2017

FixLJ cascade system varies in some bacteria. FnrN, belonging to the CRP-Fnr family of global transcriptional factors found in bacteria, acts as the oxygen sensor in *R. leguminosarum* bv. *viciae* VF39 and *Rhizobium etli* CNPAF512 (Patschkowski et al., 1996; Moris et al., 2004). Both organisms synthesize FnrN and FixK. In *R. leguminosarum*, FnrN is the main oxygen sensor responsible for the induction of *fixNOQP* and is in turn induced by the FixL protein (Boesten and Priefer, 2004). In contrast, the expression of *fnrN* is autoregulated in *R. etli* CNPAF512 (Moris et al., 2004). Other cases of rhizobia oxygen-response cascade have been previously described in detail (Terpolilli et al., 2012).

Dicarboxylate Metabolism

Most rhizobia are obligate aerobes. The C_4-dicarboxylic acids supplied by the host plant must be metabolized through the tricarboxylic acid (TCA) cycle in the bacteroid. Malate, the primary carbon source of bacteroids, is converted to pyruvate and CO_2 via the NAD^+-dependent malic enzyme (DME). Pyruvate is subsequently decarboxylated by pyruvate dehydrogenase to form acetyl-coenzyme A (acetyl-CoA) and enters the TCA cycle. DME is required to provide pyruvate to the TCA cycle in *S. meliloti* and *Azorhizobium caulinodans* (Zhang Y. et al., 2012). *S. meliloti* possesses two distinct malic enzymes, an $NAD(P)^+$-dependent enzyme (DME) (EC 1.1.1.39) and a strictly $NADP^+$-dependent enzyme (TME) (EC 1.1.1.40) (Driscoll and Finan, 1993, 1996; Voegele et al., 1999). In addition, acetyl-CoA can be produced alternatively by phosphoenolpyruvate carboxykinase (PCK) which catalyzes the decarboxylation of OAA to PEP. Symbiotic phenotypes of *pck* mutants vary depending on the host plant. *pckA* mutants of *R. leguminosarum* MNF3085 fix nitrogen at rates comparable to wild type, while *pckA* mutants of *S. meliloti* show a reduced N_2 fixation capacity (McKay et al., 1985; Finan et al., 1991). In *R. leguminosarum* and *S. fredii* strain NGR234, DME or a pathway involving PCK and pyruvate kinase (PYK) can synthesize the precursors required for SNF (Zhang Y. et al., 2012). Enzymes participating in the TCA cycle have been identified in *B. japonicum* strain USDA110 (Sarma and Emerich, 2006), *R. leguminosarum* (McKay et al., 1985), *S. meliloti* (Djordjevic, 2004), and *R. tropici* (Romanov et al., 1994). However, TCA cycle involvement probably varies among rhizobia. Evidence shows that *S. meliloti*, *R. tropici*, and *R. leguminosarum* utilize the full oxidative TCA cycle to provide

ATP, precursors of amino acid synthesis, as well as reducing equivalents for N_2 fixation. Enzymes of the TCA cycle appear to be essential for nitrogen fixation in *S. meliloti* since mutations in succinate dehydrogenase (*sdh*), malate dehydrogenase (*mdh*), isocitrase dehydrogenase (*icd*), 2-oxoglutarate dehydrogenase, aconitase (*acnA*), and citrate synthase (*gltA*) abolish N_2 fixation, despite that nodules were formed (Duncan and Fraenkel, 1979; McDermott and Kahn, 1992; Mortimer et al., 1999; Dymov et al., 2004; Koziol et al., 2009). In contrast, *B. japonicum* shows a higher metabolic plasticity. Mutations in fumarase (*fumC*), ICDH (*idhA*), alpha-ketoglutarate dehydrogenase (*agdA*), and acotinase (*acnA*) in *B. japonicum* USDA110 still show phenotypes capable of fixing nitrogen (Acuña et al., 1991; Thöny-Meyer and Künzler, 1996; Green and Emerich, 1997; Shah and Emerich, 2006). Transcriptome analyses of *R. etli* bacteroids have suggested that the TCA cycle is inactive in these bacteroids (Vercruysse et al., 2011), but additional experiments are required to explain how the bacteroids obtain the ATP necessary for nitrogen fixation in these cases. A comparative metabolic profiling study between free-living *R. leguminosarum* and pea bacteroids showed that the TCA cycle is not the only path to oxidize dicarboxylic acids derived from the host plant in the bacteroids (Terpolilli et al., 2016). Metabolic profiling and flux analysis revealed that pea bacteroids divert acetyl-CoA into TCA and the production of lipid or polyhydroxybutyrate (PHB). These findings suggest new pathways for electron allocation in nitrogen-fixing bacteroids where lipogenesis may be a requirement in legume nodules.

Carbon Storage

The legume–rhizobium symbiosis determines the accumulation of specific metabolites inside the microsymbiont. Excess carbon and reducing power provided by the host plant can be stored as polymers, glycogen, or lipids in bacteroids (**Figure 1**). PHB is accumulated in large cytoplasmic granules in the bacteroids that form determinate nodules (such as in common bean and soybean), but not in the indeterminate nodules of alfalfa, garden pea, and chickpea (**Table 1**; Tombolini and Nuti, 1989; Kim et al., 1996).

The PHB biosynthesis pathway consists of three steps. β-Ketothiolase (PhaA) catalyzes the first step in this pathway with the formation of acetoacetyl-CoA from acetyl-CoA. Acetoacetyl-CoA is then reduced to D-β-hydroxybutyryl-CoA by an NADH-dependent acetoacetyl-CoA (PhaB), and then PHB synthase (PhaC) catalyzes the final formation of PHB (Lodwig and Poole, 2003). In *S. meliloti* and *R. etli*, *phaA* and *phaB* form an operon, *phaAB*.

Fix^+ symbiotic phenotypes have been observed in *S. meliloti* when mutations were introduced to disable the synthesis of PHB or alter the ability to utilize PHB cycle intermediates to support growth (Povolo et al., 1994; Aneja and Charles, 1999; Cai et al., 2000). Effective nodules were also observed when *R. leguminosarum* mutant strains defective in the *phaC* gene were used to inoculate bean (determinate nodules) or pea (indeterminate nodules) (Lodwig et al., 2005). However, a reduced nitrogen fixation capability was observed when PHB synthesis was abolished in *A. caulinodans*. In *A. caulinodans*, impaired PHB synthetase activity results in the loss of nitrogen fixation capacity both *ex planta* and in symbiosis with the tropical legume *Sesbania rostrata* (Mandon et al., 1998). These evidences suggest that PHB may play certain roles in nitrogen fixation of some legume–rhizobium systems.

Polyhydroxybutyrate synthesis is regulated in *R. etli* and *S. meliloti* by the PHA (polyhydroxyalkanoate) regulator (PhaR), previously called AniA (Povolo and Casella, 2000; Encarnación et al., 2002). PhaR homologs in other bacterial species bind to their own promoters and to the promoter of *phaP* (Maehara et al., 2001). PhaP, a phasin, binds to the surface of PHB granules and can control the size of the PHB granules (Kuchta et al., 2007; Mezzina et al., 2014). In *Bradyrhizobium diazoefficiens*, the regulation of PHB synthesis is mediated through the interaction between PhaR and $FixK_2$, regulators associated with the synthesis of PHB and microoxic metabolism (Quelas et al., 2016).

Glycogen is co-produced with PHB in free-living rhizobia such as *R. leguminosarum* and *S. meliloti* under nutrient-limiting conditions (Povolo et al., 1994; Lodwig et al., 2005). The role of glycogen in SNF has been studied in some rhizobia. A glycogen synthase mutant (*glgA*) of *R. tropici* showed an enhanced symbiotic performance as measured by an increase in plant dry weight and nodule number, but the mechanisms behind this phenotype are uncertain (Marroquí et al., 2001). In garden pea bacteroids, a *glgA* mutant of *R. leguminosarum* did not alter nitrogen fixation rates, as indicated by the acetylene reduction assay for nitrogenase activity. Plants inoculated with a *phaC*/*glgA* double mutant resulted in similar phenotypes to wild-type-inoculated plants (Lodwig et al., 2005). In contrast, the *glgA* mutant of *S. meliloti* resulted in lower levels of N_2 fixation in both *M. truncatula* and *M. sativa* (Wang et al., 2007). Thus, the SNF capability of *S. meliloti* is affected by both PHB and glycogen availability.

In *Bradyrhizobium* sp. ORS278, studies have shown that mutations in genes involved in the Calvin–Benson–Bassham (CBB) cycle result in deficiency in nitrogen fixation. The CBB cycle consumes 3 mol of ATP and 2 mol of reducing equivalents per mol of carbon dioxide. The symbiotic phenotypes suggest that *Bradyrhizobium* sp. ORS278 uses the Calvin cycle as a reductant store to regulate carbon flux. Specifically, phosphoglycerate kinase (CbbK) and ribulose 1,5-biphosphate carboxylase (RuBisCO) large chain (CbbL1) have been identified as being involved in the symbiotic process (Bonaldi et al., 2010; Gourion et al., 2011). Thus, the relevance of different carbon storage compounds in the symbiotic process varies depending on the rhizobial strain.

Transport in Bacteroids

Symbiotic Membrane: A Regulatory Barrier

Mature bacteroids drive nitrogen fixation inside root nodules, releasing ammonia to the plant cell cytosol to be incorporated into nitrogenous compounds. Ammonia assimilation is severely

reduced in bacteroids due to a coordinated response where growth-associated pathways are switched off and biosynthesis of amino acids is downregulated but still present (Li et al., 2013). However, bacteroids require the supply of some plant-derived amino acids to support bacteroid development (Prell et al., 2009; Mulley et al., 2011; reviewed in Dunn, 2014). The supply of amino acids is plant-type specific (Randhawa and Hassani, 2002). For example, alfalfa is not able to provide sufficient histidine to the histidine auxotrophs of *S. meliloti* in nodules (Malek and Kowalski, 1977) unlike the cowpea host plant where similar mutants of rhizobial strain IRC256 are able to fix nitrogen (McLaughlin et al., 1987). The transport of nutrients is regulated by the symbiosome membrane (SM). SM is a plant-derived membrane that controls the metabolite exchanges in the legume–rhizobia symbiosis via specific transport systems and encloses a single bacteroid in indeterminate nodules or several bacteroids in determinate nodules (Clarke et al., 2014). Different transport mechanisms have been identified across the legume SM such as carbon, nitrogen, and cation transport systems, but most of them are not characterized (Day et al., 2001; Clarke et al., 2015). The main metabolite transport systems are schematically represented in **Figure 1**.

Dicarboxylate Transport

C_4-Dicarboxylates are the major metabolites that are transported across SM to generate ATP in the bacteroids. A dicarboxylate transporter for malate and succinate has been identified in the soybean SM (Udvardi et al., 1988). This transporter possesses a higher affinity for malate than for succinate. However, the gene encoding the transporter has not been identified in any legume. A dicarboxylate transporter has been characterized in the SM of a non-legume, *Alnus glutinosa* AgDCAT1 was shown to transport dicarboxylates (malate, succinate, fumarate, and OAA) when expressed in *Escherichia coli* (Jeong, 2004). AgDCAT1 belongs to the peptide transporter family (PTR) and proteins from this family are candidates for dicarboxylate transporters in legumes since experimental evidence shows that PTR-encoding genes are induced in legume nodules (Colebatch et al., 2004; Libault et al., 2010). Members of this family have been identified in the proteomic studies of the soybean SM, but their functions have not been characterized (Clarke et al., 2015). In rhizobia, a C_4-dicarboxylate transport system (Dct) has been identified and characterized. Dct consists of a permease encoded by *dctA* and a two-component sensor-regulator system (DctBD) encoded by *dctB* and *dctD*. DctBD responds to the presence of C_4-dicarboxylates and regulates *dctA* expression (reviewed in Yurgel and Kahn, 2004). *dctA* mutants of *Rhizobium trifolii* are unable to transport dicarboxylates and form ineffective nodules (Fix^-) in *Trifolium repens* and *Trifolium pratense*. The resulting infected plant cells accumulated large amounts of starch (Ronson et al., 1981).

Ammonia and Ammonium Transport

The ammonia produced by nitrogen fixation in bacteroids is probably protonated to ammonium after diffusing into the peribacteroid space (PBS) or symbiosome space (SS, the region between the SM and the bacteroid) (**Figure 1**). An H^+-ATPase pumps H^+ into the PBS, generating an acidic environment (Udvardi et al., 1991) and forming a membrane potential (Udvardi and Day, 1989). ATPase activity has been detected on the SM of soybean (Blumwald et al., 1985; Fedorova E. et al., 1999), lupin (Robertson et al., 1978; Domigan et al., 1988), and garden pea root nodules (Szafran and Haaker, 1995). Re-uptake of NH_4^+ by bacteroids is prevented by the repression of the bacteroid ammonium carrier, Amt, during the symbiotic state (Howitt et al., 1986). At present, two pathways have been proposed for the transport of fixed nitrogen into the host plant: a monovalent cation channel for NH_4^+ (Whitehead et al., 2008) and an aquaglyceroporin, nodulin 26 (Nod26), for NH_3 transport. Nod26 is a transmembrane protein able to transport H_2O, NH_3, and other solutes (Weaver et al., 1994; Rivers et al., 1997; Hwang et al., 2010). It was first identified in the soybean SM (Fortin et al., 1987) and constitutes the major protein component of the SM (Rivers et al., 1997).

Amino Acid Transport

Host plants supply amino acids to the microsymbionts during the differentiation of rhizobia to bacteroids and for nitrogen fixation (Mulley et al., 2011). Recent analyses of the soybean proteome have revealed a putative amino acid transporter (GmAPC1), a homolog to members of the amino acid-polyamine-organocation (APC) family of transport proteins (Clarke et al., 2015). Previous studies have shown that the soybean SM is permeable to alanine and Asp (Whitehead et al., 1998). An Asp transporter has been identified in SM vesicles from root nodules of garden pea (Rudbeck et al., 1999).

In addition, rhizobia also encode transport systems that regulate the exchange of amino acids between the bacteroids and the host cell (Udvardi and Poole, 2013). For instance, while the bacteroids formed by *R. leguminosarum* bv. *viciae* in the indeterminate pea nodules are auxotrophs for branched amino acids, branch-chain amino acid transporters, Aap (AapJQMP) and Bra (BraDEFGC) are developed in the bacteroids (Prell et al., 2009). This symbiotic phenotype is known as symbiotic auxotrophy (Dunn, 2014) and occurs in both determinate and indeterminate nodules (de las Nieves Peltzer et al., 2008; Prell et al., 2010; di Cenzo et al., 2015).

TABLE 3 | Available metabolic reconstructions of rhizobia.

Model	Organism	Scope	Reference
*i*OR363	*R. etli*	SNF[a]	Resendis-Antonio et al., 2007
*i*OR450	*R. etli*	SNF[a]	Resendis-Antonio et al., 2012
*i*HZ565	*S. meliloti*	SNF[a]	Zhao et al., 2012
*i*GD1575	*S. meliloti*	Whole cell	di Cenzo et al., 2016
*i*GD726	*S. meliloti*	Core metabolism	di Cenzo et al., 2018
*i*YY1101	*B. diazoefficiens*	Whole cell	Yang et al., 2017

[a]*SNF, symbiotic nitrogen fixation.*

Metabolic Modeling of SNF

Constraint-based modeling enables the determination of the metabolic capabilities of an organism (Feist et al., 2009; Oberhardt et al., 2009). These metabolic models have been used successfully to bridge the gap between current knowledge and metabolic phenotypes (Schellenberger et al., 2011). Metabolic reconstructions are based on physiological and biochemical information on primary and specialized metabolic pathways, genome information, and available -omics data. These models have allowed for the prediction of the metabolic behavior of microorganisms under different nutrient availabilities and simulated gene deletions or over-expressions (Contador et al., 2015; Razmilic et al., 2018). In an attempt to get new insights into the genetic interactions that orchestrate the complex metabolic interactions in nitrogen-fixing bacteria, metabolic models have been used to study the rhizobial metabolism. Genome-scale models have been combined with experimental data to identify essential genes and to simulate the metabolic behaviors of rhizobia under nitrogen fixation conditions in legume nodules. High-throughput experimental data aimed to identify key genes, proteins and metabolites have been used in these studies to validate the model predictions.

At present, few manually curated rhizobial reconstructions are available despite their important roles in sustainable agriculture. These reconstructions cover different metabolic tasks from only the symbiotic process that takes place in the rhizobium to the complete set of metabolic reactions of the bacteria cell. *i*OR363, a reconstruction for *R. etli* CFN42, was the first model available for any rhizobium (Resendis-Antonio et al., 2007). This model describes the SNF process inside the determinate nodules of *P. vulgaris* and includes the main reactions associated with the nitrogen fixation process and the metabolic pathways, such as PHB synthesis, that allow simulating the accumulation of this polymer during the symbiotic process (Resendis-Antonio et al., 2007). Also, a symbiotic reaction was defined to represent this specific legume–rhizobia symbiosis. The symbiotic reaction describes the exchange of nutrients between the host plant and the bacteroid to establish symbiotic relationships and to obtain or produce chemical compounds required by the process of nitrogen fixation. A symbiotic auxotrophy hypothesis and nitrogenase requirements were included in its definition. This model has been updated to include new data sets available of this system (Resendis-Antonio et al., 2011, 2012).

On the other hand, the metabolic reconstructions for *S. meliloti* have different scopes. *i*HZ565 was designed to represent the SNF of *S. meliloti* 1021 with host plants such as alfalfa (Zhao et al., 2012). The reconstruction process gave insight about the missing context-specific information and genome annotation errors. Additionally, a new symbiotic reaction was proposed to capture specific SNF mechanisms of *S. meliloti* in indeterminate nodules. The first representation of the whole metabolism of a rhizobium cell was built for *S. meliloti* (*i*GD1575) to enable the characterization of the metabolic capabilities of rhizobia in bulk soil, rhizosphere, and nodule (di Cenzo et al., 2016). *i*GD1575 encompasses 94% of the genes present in *i*HZ565. Recently, *i*GD1575 and gene essentiality experiments were used to build a model of the core metabolism of *S. meliloti* (di Cenzo et al., 2018). Pfau et al. (2018) have described the symbiotic relationship of *M. truncatula* with *S. meliloti* through constraint-based modeling (Pfau et al., 2018). Metabolic models were used to study the metabolic exchange between the host plant and the rhizobial symbiont. An *in silico* representation of the metabolic network of *B. diazoefficiens* USDA110 (*i*YY1101) has also been constructed (Yang et al., 2017). This reconstruction was used to build context-specific models to describe the metabolic differences observed between the free-living state of *B. diazoefficiens* USDA110 and symbiotic bacteroid. These models will provide a starting point for building metabolic reconstructions of closely related organisms such as other rhizobial strains and modeling frameworks to study these symbiotic interactions (Baumler et al., 2011; Monk et al., 2013; Ong et al., 2014). **Table 3** summarizes the available metabolic models of rhizobia.

CONCLUSION

The regulatory mechanisms regarding the formation and maintenance of root nodules for SNF are multi-faceted and association-specific, but they all involve the tight regulation of the flow of metabolites between the host plants and the bacteroids, as well as the different levels of controls over each step in the metabolic pathways through the metabolic enzymes involved and the transcription factors that regulate their expressions. Each host plant–rhizobium association has its own unique requirements and control mechanisms despite the overall common features. It is therefore critical that we have as much understanding as possible of the detailed mechanisms that make up this symbiotic relationship.

AUTHOR CONTRIBUTIONS

H-ML designed the conceptual framework of this paper and coordinated the writing. AL and KF wrote the part on metabolism and regulation of host plant. CC wrote the part on metabolism and regulation of bacteroids and metabolic models. AL, CC, and H-ML revised and polished the article.

FUNDING

This work was supported by the Hong Kong Research Grants Council General Research Fund (14108014) and Area of Excellence Scheme (AoE/M-403/16), CUHK VC Discretionary Fund VCF2014004, and the Lo Kwee-Seong Biomedical Research Fund to H-ML.

ACKNOWLEDGMENTS

Jee-Yan Chu copy-edited this manuscript.

REFERENCES

Acuña, G., Ebeling, S., and Hennecke, H. (1991). Cloning, sequencing, and mutational analysis of the *Bradyrhizobium japonicum* fumC-like gene: evidence for the existence of two different fumarases. *J. Gen. Microbiol.* 137, 991–1000. doi: 10.1099/00221287-137-4-991

Ahemad, M., and Oves, M. (2011). "Biological importance of phosphorus and phosphate solubilizing microbes," in *Characterization of Chromium (VI) Reducing, Plant Growth Promoting Rhizobacteria as a Potential Bio-Fertilizer in Cr (VI) Contaminated Soil View Project*, eds M. S. Khan, and A. Zaidi (Hauppauge, NY: Nova Science Publishers)

Akazawa, T., and Okamoto, K. (1980). "Biosynthesis and metabolism of sucrose," in *The Biochemistry of Plants: A Comprehensiue Treatise: Carbohydrates: Structure and Function*, ed. J. Preis (Amsterdam: Elsevier), 199–220.

Aleman, L., Ortega, J. L., Martinez-Grimes, M., Seger, M., Holguin, F. O., Uribe, D. J., et al. (2010). Nodule-enhanced expression of a sucrose phosphate synthase gene member (*MsSPSA*) has a role in carbon and nitrogen metabolism in the nodules of alfalfa (*Medicago sativa* L.). *Planta* 231, 233–244. doi: 10.1007/s00425-009-1043-y

Andrews, M., and Andrews, M. E. (2017). Specificity in legume-rhizobia symbioses. *Int. J. Mol. Sci.* 18:E705. doi: 10.3390/ijms18040705

Aneja, P., and Charles, T. C. (1999). Poly-3-hydroxybutyrate degradation in Rhizobium (*Sinorhizobium*) *meliloti*: isolation and characterization of a gene encoding 3-hydroxybutyrate dehydrogenase. *J. Bacteriol.* 181, 849–857.

Aparicio-Fabre, R., Guillén, G., Loredo, M., Arellano, J., Valdés-López, O., Ramírez, M., et al. (2013). Common bean (*Phaseolus vulgaris* L.) PvTIFY orchestrates global changes in transcript profile response to jasmonate and phosphorus deficiency. *BMC Plant Biol.* 13:26. doi: 10.1186/1471-2229-13-26

Appleby, C. A. (1984). Leghemoglobin and *rhizobium* respiration. *Annu. Rev. Plant Physiol.* 35, 443–478. doi: 10.1146/annurev.pp.35.060184.002303

Araújo, A. P., Plassard, C., and Drevon, J. J. (2008). Phosphatase and phytase activities in nodules of common bean genotypes at different levels of phosphorus supply. *Plant Soil* 312, 129–138. doi: 10.1007/s11104-008-9595-3

Asthir, B., and Singh, R. (1997). Purification and characterization of neutral invertase from chickpea nodules. *Indian J. Biochem. Biophys.* 34, 529–534.

Atkins, C. A. (1991). "Ammonia assimilation and export of nitrogen from the legume nodule," in *Biochemistry of Nitrogen Fixation*, eds M. J. Dilworth, and A. R. Glenn (Amsterdam: Elsevier Science), 293–319.

Atkins, C. A., Smith, P., and Storer, P. J. (1997). Reexamination of the intracellular localization of *de novo* purine synthesis in cowpea nodules. *Plant Physiol.* 113, 127–135. doi: 10.1104/pp.113.1.127

Baier, M. C., Barsch, A., Kuster, H., and Hohnjec, N. (2007). Antisense repression of the *Medicago truncatula* nodule-enhanced sucrose synthase leads to a handicapped nitrogen fixation mirrored by specific alterations in the symbiotic transcriptome and metabolome. *Plant Physiol.* 145, 1600–1618. doi: 10.1104/pp.107.106955

Batut, J., Daveran-Mingot, M. L., David, M., Jacobs, J., Garnerone, A. M., and Kahn, D. (1989). fixK, a gene homologous with fnr and crp from *Escherichia coli*, regulates nitrogen fixation genes both positively and negatively in *Rhizobium meliloti*. *EMBO J.* 8, 1279–1286. doi: 10.1002/J.1460-2075.1989.TB03502.X

Baumler, D. J., Peplinski, R. G., Reed, J. L., Glasner, J. D., and Perna, N. T. (2011). The evolution of metabolic networks of *E. coli*. *BMC Syst. Biol.* 5:182. doi: 10.1186/1752-0509-5-182

Blumwald, E., Fortin, M. G., Rea, P. A., Verma, D. P., and Poole, R. J. (1985). Presence of host-plasma membrane type H-ATPase in the membrane envelope enclosing the bacteroids in soybean root nodules. *Plant Physiol.* 78, 665–672. doi: 10.1104/pp.78.4.665

Boesten, B., and Priefer, U. B. (2004). The C-terminal receiver domain of the *Rhizobium leguminosarum* bv. viciae FixL protein is required for free-living microaerobic induction of the fnrN promoter. *Microbiology* 150, 3703–3713. doi: 10.1099/mic.0.27323-0

Bonaldi, K., Gourion, B., Fardoux, J., Hannibal, L., Cartieaux, F., Boursot, M., et al. (2010). Large-scale transposon mutagenesis of photosynthetic *Bradyrhizobium* Sp. Strain ORS278 reveals new genetic loci putatively important for Nod-independent symbiosis with *Aeschynomene indica*. *Mol. Plant Microbe Interact.* 23, 760–770. doi: 10.1094/MPMI-23-6-0760

Brenner, D. J., Krieg, N. R., and Staley, J. T. (eds) (2009). *Bergey's Manual of Systematic Bacteriology: The Proteobacteria*, 2nd Edn, Vol. 2. Berlin: Springer. doi: 10.1007/978-0-387-68489-5

Cai, G. Q., Driscoll, B. T., and Charles, T. C. (2000). Requirement for the enzymes acetoacetyl coenzyme A synthetase and poly-3-hydroxybutyrate (PHB) synthase for growth of *Sinorhizobium meliloti* on PHB cycle intermediates. *J. Bacteriol.* 182, 2113–2118. doi: 10.1128/JB.182.8.2113-2118.2000

Carvalho, H., Sunkel, C., Salema, R., and Cullimore, J. V. (1997). Heteromeric assembly of the cytosolic glutamine synthetase polypeptides of *Medicago truncatula*: complementation of a glnA *Escherichia coli* mutant with a plant domain-swapped enzyme. *Plant Mol. Biol.* 35, 623–632. doi: 10.1023/A:1005884304303

Carvalho, H. G., Lescure, N., de Billy, F., Chabaud, M., Lima, L. M., Salema, R., et al. (2000). Cellular expression and regulation of the Medicago truncatula cytosolic glutamine synthetase genes in root nodules. *Plant Mol. Biol.* 42, 741–756. doi: 10.1023/A:1006304003770

Clarke, V. C., Loughlin, P. C., Day, D. A., and Smith, P. M. C. (2014). Transport processes of the legume symbiosome membrane. *Front. Plant Sci.* 5:699. doi: 10.3389/fpls.2014.00699

Clarke, V. C., Loughlin, P. C., Gavrin, A., Chen, C., Brear, E. M., Day, D. A., et al. (2015). Proteomic analysis of the soybean symbiosome identifies new symbiotic proteins. *Mol. Cell. Proteomics* 14, 1301–1322. doi: 10.1074/mcp.M114.043166

Colebatch, G., Desbrosses, G., Ott, T., Krusell, L., Montanari, O., Kloska, S., et al. (2004). Global changes in transcription orchestrate metabolic differentiation during symbiotic nitrogen fixation in *Lotus japonicus*. *Plant J.* 39, 487–512. doi: 10.1111/j.1365-313X.2004.02150.x

Contador, C. A., Rodríguez, V., Andrews, B. A., and Asenjo, J. A. (2015). Genome-scale reconstruction of *Salinispora tropica* CNB-440 metabolism to study strain-specific adaptation. *Antonie Van Leeuwenhoek* 108, 1075–1090. doi: 10.1007/s10482-015-0561-9

Copeland, L., and Morell, M. (1985). Hexose kinases from the plant cytosolic fraction of soybean nodules. *Plant Physiol.* 79, 114–117. doi: 10.1104/pp.79.1.114

Crampton, M., Sripathi, V. R., Hossain, K., and Kalavbacharla, V. (2016). Analyses of methylomes derived from Meso-American common ean (*Phaseolus vulgaris* L.) using MeDIP-Seq and whole genome sodium bisulfite-sequencing. *Front. Plant Sci.* 7:447. doi: 10.3389/fpls.2016.00447

Czarnecki, O., Yang, J., Weston, D. J., Tuskan, G. A., and Chen, J. G. (2013). A dual role of strigolactones in phosphate acquisition and utilization in plants. *Int. J. Mol. Sci.* 14, 7681–7701. doi: 10.3390/ijms14047681

Dan, T. H., and Brix, H. (2009). Growth responses of the perennial legume *Sesbania sesban* to NH4 and NO3 nutrition and effects on root nodulation. *Aquat. Bot.* 91, 238–244. doi: 10.1016/j.aquabot.2009.07.004

Day, D. A. (1991). Carbon metabolism and compartmentation in nitrogen fixing legume nodules. *Plant Physiol. Biochem.* 29, 185–201.

Day, D. A., Kaiser, B. N., Thomson, R., Udvardi, M. K., Moreau, S., and Puppo, A. (2001). Nutrient transport across symbiotic membranes from legume nodules. *Aust. J. Plant Physiol.* 28, 667–674. doi: 10.1071/PP01028

de las Nieves Peltzer, M., Roques, N., Poinsot, V., Aguilar, O. M., Batut, J., and Capela, D. (2008). Auxotrophy accounts for nodulation defect of most *Sinorhizobium meliloti* mutants in the branched-chain amino acid biosynthesis pathway. *Mol. Plant Microbe Interact.* 21, 1232–1241. doi: 10.1094/MPMI-21-9-1232

di Cenzo, G. C., Checcucci, A., Bazzicalupo, M., Mengoni, A., Viti, C., Dziewit, L., et al. (2016). Metabolic modelling reveals the specialization of secondary replicons for niche adaptation in *Sinorhizobium meliloti*. *Nat. Commun.* 7:12219. doi: 10.1038/ncomms12219

di Cenzo, G. C., Zamani, M., Cowie, A., and Finan, T. M. (2015). Proline auxotrophy in *Sinorhizobium meliloti* results in a plant-specific symbiotic phenotype. *Microbiology* 161, 2341–2351. doi: 10.1099/mic.0.000182

diCenzo, G. C., Benedict, A. B., Fondi, M., Walker, G. C., Finan, T. M., Mengoni, A., et al. (2018). Robustness encoded across essential and accessory replicons of the ecologically versatile bacterium *Sinorhizobium meliloti*. *PLoS Genet.* 14:e1007357. doi: 10.1371/journal.pgen.1007357

Dixon, R., and Wheeler, C. (1986). *Nitrogen Fixation in Plants*. New York, NY: Chapman and Hall.

Djordjevic, M. A. (2004). *Sinorhizobium meliloti* metabolism in the root nodule: a proteomic perspective. *Proteomics* 4, 1859–1872. doi: 10.1002/pmic.200300802

Domigan, N. M., Farnden, K. J. F., Robertson, J. G., and Monk, B. C. (1988). Characterization of the peribacteroid membrane ATPase of lupin root nodules. *Arch. Biochem. Biophys*. 264, 564–573. doi: 10.1016/0003-9861(88)90322-0

Driscoll, B. T., and Finan, T. M. (1993). NAD(+)-dependent malic enzyme of *Rhizobium meliloti* is required for symbiotic nitrogen fixation. *Mol. Microbiol.* 7, 865–873. doi: 10.1111/j.1365-2958.1993.tb01177.x

Driscoll, B. T., and Finan, T. M. (1996). NADP+-dependent malic enzyme of *Rhizobium meliloti*. *J. Bacteriol.* 178, 2224–2231. doi: 10.1128/jb.178.8.2224-2231.1996

Duncan, M. J., and Fraenkel, D. G. (1979). Alpha-Ketoglutarate dehydrogenase mutant of *Rhizobium meliloti*. *J. Bacteriol.* 137, 415–419.

Dunn, M. F. (2014). Key roles of microsymbiont amino acid metabolism in rhizobia-legume interactions. *Crit. Rev. Microbiol.* 41, 411–451. doi: 10.3109/1040841X.2013.856854

Dupont, L., Alloing, G., Pierre, O., El, S., Hopkins, J., Hrouart, D., et al. (2012). *The Legume Root Nodule: From Symbiotic Nitrogen Fixation to Senescence*. London: INTECH Open Access Publisher. doi: 10.5772/34438

Duran, V. A., and Todd, C. D. (2012). Four allantoinase genes are expressed in nitrogen-fixing soybean. *Plant Physiol. Biochem.* 54, 149–155. doi: 10.1016/j.plaphy.2012.03.002

Dymov, S. I., Meek, D. J. J., Steven, B., and Driscoll, B. T. (2004). Insertion of transposon Tn5tac1 in the *Sinorhizobium meliloti* malate dehydrogenase (mdh) gene results in conditional polar effects on downstream TCA cycle genes. *Mol. Plant. Microbe. Interact.* 17, 1318–1327. doi: 10.1094/MPMI.2004.17.12.1318

Encarnación, S., Del Carmen Vargas, M., Dunn, M. F., Dávalos, A., Mendoza, G., Mora, Y., et al. (2002). Ania regulates reserve polymer accumulation and global protein expression in *Rhizobium etli*. *J. Bacteriol.* 184, 2287–2295. doi: 10.1128/JB.184.8.2287-2295.2002

Fan, C., Wang, X., Hu, R., Wang, Y., Xiao, C., Jiang, Y., et al. (2013). The pattern of phosphate transporter 1 genes evolutionary divergence in *Glycine max* L. *BMC Plant Biol.* 13:48. doi: 10.1186/1471-2229-13-48

Fedorova, E., Thomson, R., Whitehead, L. F., Maudoux, O., Udvardi, M. K., and Day, D. A. (1999). Localization of H+-ATPases in soybean root nodules. *Planta* 209, 25–32. doi: 10.1007/s004250050603

Fedorova, M., Tikhonovich, I. A., and Vance, C. P. (1999). Expression of C-assimilating enzymes in pea (*Pisum sativum* L.) root nodules. In situ localization in effective nodules. *Plant Cell Environ.* 22, 1249–1262. doi: 10.1046/j.1365-3040.1999.00490.x

Feist, A. M., Herrgård, M. J., Thiele, I., Reed, J. L., and Palsson, B. Ø (2009). Reconstruction of biochemical networks in microorganisms. *Nat. Rev. Microbiol.* 7, 129–143. doi: 10.1038/nrmicro1949

Ferguson, B. J., Indrasumunar, A., Hayashi, S., Lin, M. H., Lin, Y. H., Reid, D. E., et al. (2010). Molecular analysis of legume nodule development and autoregulation. *J. Integr. Plant Biol.* 52, 61–76. doi: 10.1111/j.1744-7909.2010.00899.x

Finan, T. M., McWhinnie, E., Driscoll, B., and Watson, R. (1991). Complex symbiotic phenotypes result from gluconeogenic mutations in *Rhizobium meliloti*. *Mol. Plant Microbe Interact.* 4, 386–392. doi: 10.1094/MPMI-4-386

Fischer, H.-M., and Hennecke, H. (1987). Direct response of *Bradyrrhizobium japonicum nifA*-mediated *nif* gene regulation to cellular oxygen status. *Mol. Gen. Genet.* 209, 621–626. doi: 10.1007/BF00331174

Fischinger, S. A., Drevon, J. J., Claassen, N., and Schulze, J. (2006). Nitrogen from senescing lower leaves of common bean is re-translocated to nodules and might be involved in a N-feedback regulation of nitrogen fixation. *J. Plant Physiol.* 163, 987–995. doi: 10.1016/j.jplph.2006.03.017

Flemetakis, E., Efrose, R. C., Ott, T., Stedel, C., Aivalakis, G., Udvardi, M. K., et al. (2006). Spatial and temporal organization of sucrose metabolism in *Lotus japonicus* nitrogen-fixing nodules suggests a role for the elusive alkaline/neutral invertase. *Plant Mol. Biol.* 62, 53–69. doi: 10.1007/s11103-006-9003-4

Fortin, M. G., Morrison, N. A., and Verma, D. P. S. (1987). Nodulin-26, a peribacteroid membrane nodulin is expressed independently of the development of the peribacteroid compartment. *Nucleic Acids Res.* 15, 813–824. doi: 10.1093/nar/15.2.813

Foussard, M., Garnerone, A.-M., Ni, F., Soupène, E., Boistard, P., and Batut, J. (1997). Negative autoregulation of the *Rhizobium meliloti fixK* gene is indirect and requires a newly identified regulator, FixT. *Mol. Microbiol.* 25, 27–37. doi: 10.1046/j.1365-2958.1997.4501814.x

Gallardo, F., Gálvez, S., Gadal, P., and Cánovas, F. M. (1995). Changes in NADP+-linked isocitrate dehydrogenase during tomato fruit ripening. *Planta* 196, 148–154. doi: 10.1007/BF00193228

Gálvez, L., González, E. M., and Arrese-Igor, C. (2005). Evidence for carbon flux shortage and strong carbon/nitrogen interactions in pea nodules at early stages of water stress. *J. Exp. Bot.* 56, 2551–2561. doi: 10.1093/jxb/eri249

Gálvez, S., and Gadal, P. (1995). On the function of the NADP-dependent isocitrate dehydrogenase isoenzymes in living organisms. *Plant Sci.* 105, 1–14. doi: 10.1016/0168-9452(94)04041-E

Gilles-Gonzalez, M. A., Ditta, G. S., and Helinski, D. R. (1991). A haemoprotein with kinase activity encoded by the oxygen sensor of *Rhizobium meliloti*. *Nature* 350, 170–172. doi: 10.1038/350170a0

Glenn, A., and Dilworth, M. (1981). Oxidation of substrates by isolated bacteroids and free-living cells of *Rhizobium leguminosarum* 384 1. *J. Gen. Microbiol.* 126, 243–247.

Gong, Z. Y., He, Z. S., Zhu, J. B., Yu, G. Q., and Zou, H. S. (2006). *Sinorhizobium meliloti nifA* mutant induces different gene expression profile from wild type in alfalfa nodules. *Cell Res.* 16, 818–829. doi: 10.1038/sj.cr.7310096

Gordon, A. J., Minchin, F. R., James, C. L., and Komina, O. (1999). Sucrose synthase in legume nodules is essential for nitrogen fixation. *Plant Physiol.* 120, 867–878. doi: 10.1104/pp.120.3.867

Gordon, A. J., Skot, L., Webb, K. J., Minchin, F. R., James, C. L., Wang, T. L., et al. (1998). "Down regulation of nodule sucrose synthase by mutation and antisense," in *Proceedings of the 11th International Congress on Biological Nitrogen Fixation for the 21st Century* (Paris: Institute Pasteur), 473–473. doi: 10.1007/978-94-011-5159-7_288

Gourion, B., Delmotte, N., Bonaldi, K., Nouwen, N., Vorholt, J. A., and Giraud, E. (2011). Bacterial RuBisCO is required for efficient *Bradyrhizobium/Aeschynomene* symbiosis. *PLoS One* 6:e21900. doi: 10.1371/journal.pone.0021900

Green, L. S., and Emerich, D. W. (1997). The formation of nitrogen fixing bacteroids is delayed but not abolished in soybean infected by an a-ketoglutarate dehydrogenase deficient mutant of *Bradyrhizobium japonicum*. *Plant Physiol.* 114, 1359–1368. doi: 10.1104/pp.114.4.1359

Gu, M., Chen, A., Sun, S., and Xu, G. (2016). Complex regulation of plant phosphate transporters and the gap between molecular mechanisms and practical application: What is missing? *Mol. Plant* 9, 396–416. doi: 10.1016/j.molp.2015.12.012

Gunawardena, S. F. B. N., Danso, S. K. A., and Zapata, F. (1992). Phosphorus requirements and nitrogen accumulation by three mungbean (*Vigna radiata* (L) Welzek) cultivars. *Plant Soil* 147, 267–274. doi: 10.1007/BF00029078

Hernandez, G., Valdes-Lopez, O., Ramirez, M., Goffard, N., Weiller, G., Aparicio-Fabre, R., et al. (2009). Global changes in the transcript and metabolic profiles during symbiotic nitrogen fixation in phosphorus-stressed common bean plants. *Plant Physiol.* 151, 1221–1238. doi: 10.1104/pp.109.143842

Herridge, D. F., Peoples, M. B., and Boddey, R. M. (2008). Global inputs of biological nitrogen fixation in agricultural systems. *Plant Soil* 311, 1–18. doi: 10.1007/s11104-008-9668-3

Hirsch, A. M., Bang, M., and Ausubel, F. M. (1983). Ultrastructural analysis of ineffective alfalfa nodules formed by nif:: Tn5 mutants of *Rhizobium meliloti*. *J. Bacteriol.* 155, 367–380.

Horst, I., Welham, T., Kelly, S., Kaneko, T., Sato, S., Tabata, S., et al. (2007). TILLING mutants of *Lotus japonicus* reveal that nitrogen assimilation and fixation can occur in the absence of nodule-enhanced sucrose synthase. *Plant Physiol.* 144, 806–820. doi: 10.1104/pp.107.097063

Howitt, S. M., Udvardi, M. K., Day, D. A., and Gresshoff, P. M. (1986). Ammonia transport in free-living and symbiotic *Rhizobium* sp. ANU289. *J. Gen. Microbiol.* 132, 257–261. doi: 10.1099/00221287-132-2-257

Hwang, J. H., Ellingson, S. R., and Roberts, D. M. (2010). Ammonia permeability of the soybean nodulin 26 channel. *FEBS Lett.* 584, 4339–4343. doi: 10.1016/j.febslet.2010.09.033

Jeong, J. (2004). A nodule-specific dicarboxylate transporter from Alder is a member of the peptide transporter family. *Plant Physiol.* 134, 969–978. doi: 10.1104/pp.103.032102

Jones, K. M., Kobayashi, H., Davies, B. W., Taga, M. E., and Walker, G. C. (2007). How rhizobial symbionts invade plants: the *Sinorhizobium-Medicago* model. *Nat. Rev. Microbiol.* 5, 619–633. doi: 10.1038/nrmicro1705

Kim, K., Do El Baidouri, M., Abernathy, B., Iwata-Otsubo, A., Chavarro, C., Gonzales, M., et al. (2015). A comparative epigenomic analysis of polyploidy-derived genes in soybean and common bean. *Plant Physiol.* 168, 1433–1447. doi: 10.1104/pp.15.00408

Kim, S. A., Copeland, L., and Copeland, L. E. S. (1996). Enzymes of poly-beta-hydroxybutyrate metabolism in soybean and chickpea bacteroids. *Appl. Environ. Microbiol.* 62, 4186–4190.

Kneen, B. E., and LaRue, T. A. (1984). Peas (*Pisum sativum* L.) with strain specificity for *Rhizobium leguminosarum*. *Heredity* 52, 383–389. doi: 10.1038/hdy.1984.46

Koziol, U., Hannibal, L., Rodríguez, M. C., Fabiano, E., Kahn, M. L., and Noya, F. (2009). Deletion of citrate synthase restores growth of *Sinorhizobium meliloti* 1021 aconitase mutants. *J. Bacteriol.* 191, 7581–7586. doi: 10.1128/JB.00777-09

Krusell, L., Madsen, L. H., Sato, S., Aubert, G., Genua, A., Szczyglowski, K., et al. (2002). Shoot control of root development and nodulation is mediated by a receptor-like kinase. *Nature* 420, 422–426. doi: 10.1038/nature01207

Kuchta, K., Chi, L., Fuchs, H., Pötter, M., and Steinbüchel, A. (2007). Studies on the influence of phasins on accumulation and degradation of PHB and nanostructure of PHB granules in *Raistonia eutropha* H16. *Biomacromolecules* 8, 657–662. doi: 10.1021/bm060912e

Kuzma, M. M., Hunt, S., and Layzell, D. B. (1993). Role of oxygen in the limitation and inhibition of nitrogenase activity and respiration rate in individual soybean nodules. *Plant Physiol.* 101, 161–169. doi: 10.1104/pp.101.1.161

Lazali, M., Zaman-Allah, M., Amenc, L., Ounane, G., Abadie, J., and Drevon, J.-J. (2013). A phytase gene is overexpressed in root nodules cortex of *Phaseolus vulgaris*-rhizobia symbiosis under phosphorus deficiency. *Planta* 238, 317–324. doi: 10.1007/s00425-013-1893-1

Le Roux, M., Phiri, E., Khan, W., Şakiroğlu, M., Valentine, A., and Khan, S. (2014). Expression of novel cytosolic malate dehydrogenases (cMDH) in *Lupinus angustifolius* nodules during phosphorus starvation. *J. Plant Physiol.* 171, 1609–1618. doi: 10.1016/j.jplph.2014.07.020

Le Roux, M. R., Khan, S., and Valentine, A. J. (2008). Organic acid accumulation may inhibit N2 fixation in phosphorus-stressed lupin nodules. *New Phytol.* 177, 956–964. doi: 10.1111/j.1469-8137.2007.02305.x

Le Roux, M. R., Khan, S., and Valentine, A. J. (2009). Nitrogen and carbon costs of soybean and lupin root systems during phosphate starvation. *Symbiosis* 48, 102–109. doi: 10.1007/BF03179989

Lea, P. J., and Miflin, B. J. (2003). Glutamate synthase and the synthesis of glutamate in plants. *Plant Physiol. Biochem.* 41, 555–564. doi: 10.1016/S0981-9428(03)00060-3

Li, Y., Tian, C. F., Chen, W. F., Wang, L., Sui, X. H., and Chen, W. X. (2013). High-resolution transcriptomic analyses of *Sinorhizobium* sp. NGR234 bacteroids in determinate nodules of *Vigna unguiculata* and indeterminate nodules of *Leucaena leucocephala*. *PLoS One* 8:e70531. doi: 10.1371/journal.pone.0070531

Li, Z., Xu, H., Li, Y., Wan, X., Ma, Z., Cao, J., et al. (2018). Analysis of physiological and miRNA responses to Pi deficiency in alfalfa (*Medicago sativa* L.). *Plant Mol. Biol.* 96, 473–492. doi: 10.1007/s11103-018-0711-3

Libault, M., Farmer, A., Brechenmacher, L., Drnevich, J., Langley, R. J., Bilgin, D. D., et al. (2010). Complete transcriptome of the soybean root hair cell, a single-cell model, and its alteration in response to *Bradyrhizobium japonicum* infection. *Plant Physiol.* 152, 541–552. doi: 10.1104/pp.109.148379

Lindemann, A., Moser, A., Pessi, G., Hauser, F., Friberg, M., Hennecke, H., et al. (2007). New target genes controlled by the *Bradyrhizobium japonicum* two-component regulatory system RegSR. *J. Bacteriol.* 189, 8928–8943. doi: 10.1128/JB.01088-07

Liu, J., Versaw, W. K., Pumplin, N., Gomez, S. K., Blaylock, L. A., and Harrison, M. J. (2008). Closely related members of the *Medicago truncatula PHT1* phosphate transporter gene family encode phosphate transporters with distinct biochemical activities. *J. Biol. Chem.* 283, 24673–24681. doi: 10.1074/jbc.M802695200

Lodwig, E., and Poole, P. (2003). Metabolism of *Rhizobium* bacteroids. *Crit. Rev. Plant Sci.* 22, 37–78. doi: 10.1080/713610850

Lodwig, E. M., Leonard, M., Marroqui, S., Wheeler, T. R., Findlay, K., Downie, J. A., et al. (2005). Role of polyhydroxybutyrate and glycogen as carbon storage compounds in pea and bean bacteroids. *Mol. Plant Microbe Interact.* 18, 67–74. doi: 10.1094/MPMI-18-0067

Lois, A. F., Weinstein, M., Ditta, G. S., and Helinski, D. R. (1993). Autophosphorylation and phosphatase activities of the oxygen-sensing protein *FixL* of *Rhizobium meliloti* are coordinately regulated by oxygen. *J. Biol. Chem.* 268, 4370–4375.

López, M., Herrera-Cervera, J. A., Iribarne, C., Tejera, N. A., and Lluch, C. (2008). Growth and nitrogen fixation in *Lotus japonicus* and *Medicago truncatula* under NaCl stress: nodule carbon metabolism. *J. Plant Physiol.* 165, 641–650. doi: 10.1016/j.jplph.2007.05.009

Maehara, A., Doi, Y., Nishiyama, T., Takagi, Y., Ueda, S., Nakano, H., et al. (2001). PhaR, a protein of unknown function conserved among short-chain-length polyhydroxyalkanoic acids producing bacteria, is a DNA-binding protein and represses *Paracoccus denitrificans phaP* expression in vitro. *FEMS Microbiol. Lett.* 200, 9–15. doi: 10.1016/S0378-1097(01)00182-3

Magori, S., and Kawaguch, M. (2010). Analysis of two potential long-distance signaling molecules, *LjCLE-RS1/2* and jasmonic acid, in a hypernodulating mutant too much love. *Plant Signal. Behav.* 5, 403–405. doi: 10.4161/psb.5.4.10801

Malek, W., and Kowalski, M. (1977). Auxotrophic mutations related to symbiotic properties if *Rhizobium meliloti* strain L5-30. *Acta Microbiol. Pol.* 26, 345–350.

Mandon, K., Michel-reydellet, N., Encarnacio, S., Kaminski, P. A., Leija, A., Cevallos, M. A., et al. (1998). Poly-β-hydroxybutyrate turnover in *Azorhizobium caulinodans* is required for growth and affects *nifA* expression. *J. Bacteriol.* 180, 5070–5076.

Marroquí, S., Zorreguieta, A., Santamaría, C., Temprano, F., Soberón, M., Megías, M., et al. (2001). Enhanced symbiotic performance by *Rhizobium tropici* glycogen synthase mutants. *J. Bacteriol.* 183, 854–864. doi: 10.1128/JB.183.3.854-864.2001

McClure, P. R., and Israel, D. W. (1979). Transport of nitrogen in the xylem of soybean plants. *Plant Physiol.* 64, 411–416. doi: 10.1104/pp.64.3.411

McDermott, T. R., and Kahn, M. L. (1992). Cloning and mutagenesis of the *Rhizobium meliloti* isocitrate dehydrogenase gene. *J. Bacteriol.* 174, 4790–4797. doi: 10.1128/jb.174.14.4790-4797.1992

McKay, I., Glenn, A., and Dilworth, M. (1985). Gluconeogenesis in Rhizobium leguminosarum MNF3841. *J. Gen. Microbiol.* 131, 2067–2073. doi: 10.1099/00221287-131-8-2067

McLaughlin, W., Singh, I., and Ahmad, M. (1987). Characterization of Tn5-induced symbiotically defective mutants of cowpea rhizobia. *Lett. FEMS Microbiol.* 41, 331–336. doi: 10.1111/j.1574-6968.1987.tb02222.x

Mezzina, M. P., Wetzler, D. E., Catone, M. V., Bucci, H., Di Paola, M., and Pettinari, M. J. (2014). A phasin with many faces: structural insights on PhaP from *Azotobacter* sp. FA8. *PLoS One* 9:e103012. doi: 10.1371/journal.pone.0103012

Miller, R. W., Mcrae, D. G., Ai-Jobore, A., and Berndt, W. B. (1988). Respiration supported nitrogenase activity of isolated *Rhizobium meliloti* bacteroids. *J. Cell. Biochem.* 38, 35–49. doi: 10.1002/jcb.240380105

Miller, S. S., Driscoll, B. T., Gregerson, R. G., Gantt, J. S., and Vance, C. P. (1998). Alfalfa malate dehydrogenase (MDH): molecular cloning and characterization of five different forms reveals a unique nodule-enhanced MDH. *Plant J.* 15, 173–184. doi: 10.1046/j.1365-313X.1998.00192.x

Minchin, F. R., and Witty, J. F. (2005). "Respiratory/carbon costs of symbiotic nitrogen fixation in legumes," in *Plant Respiration*, eds H. Lambers, and M. Ribas-Carbo (Dordrecht: Springer-Verlag), 195–205. doi: 10.1007/1-4020-3589-6_11

Monk, J. M., Charusanti, P., Aziz, R. K., Lerman, J. A., Premyodhin, N., Orth, J. D., et al. (2013). Genome-scale metabolic reconstructions of multiple *Escherichia coli* strains highlight strain-specific adaptations to nutritional environments. *Proc. Natl. Acad. Sci. U.S.A.* 110, 20338–20343. doi: 10.1073/pnas.1307797110

Moris, M., Dombrecht, B., Xi, C., Vanderleyden, J., and Michiels, J. (2004). Regulatory role of *Rhizobium etli* CNPAF512 fnrN during symbiosis. *Appl. Environ. Microbiol.* 70, 1287–1296. doi: 10.1128/AEM.70.3.1287-1296.2004

Mortier, V., Den Herder, G., Whitford, R., Van de Velde, W., Rombauts, S., D'haeseleer, K., et al. (2010). CLE peptides control *Medicago truncatula* nodulation locally and systemically. *Plant Physiol.* 153, 222–237. doi: 10.1104/pp.110.153718

Mortimer, M. W., McDermott, T. R., York, G. M., Walker, G. C., and Kahn, M. L. (1999). Citrate synthase mutants of *Sinorhizobium meliloti* are ineffective and have altered cell surface polysaccharides. *J. Bacteriol.* 181, 7608–7613.

Mulley, G., White, J. P., Karunakaran, R., Prell, J., Bourdes, A., Bunnewell, S., et al. (2011). Mutation of GOGAT prevents pea bacteroid formation and N2

fixation by globally downregulating transport of organic nitrogen sources. *Mol. Microbiol.* 80, 149–167. doi: 10.1111/j.1365-2958.2011.07565.x

Nakagawa, T., Izumi, T., Banba, M., Umehara, Y., Kouchi, H., Izui, K., et al. (2003). Characterization and expression analysis of genes encoding phosphoenolpyruvate carboxylase and phosphoenolpyruvate carboxylase kinase of *Lotus japonicus*, a model legume. *Mol. Plant. Microbe. Interact.* 16, 281–288. doi: 10.1094/MPMI.2003.16.4.281

Nasr Esfahani, M., Kusano, M., Nguyen, K. H., Watanabe, Y., Ha, C., Van Saito, K., et al. (2016). Adaptation of the symbiotic *Mesorhizobium*-chickpea relationship to phosphate deficiency relies on reprogramming of whole-plant metabolism. *Proc. Natl. Acad. Sci. U.S.A.* 113, E4610–E4619. doi: 10.1073/pnas.1609440113

Naya, L., Ladrera, R., Ramos, J., Gonzalez, E. M., Arrese-Igor, C., Minchin, F. R., et al. (2007). The response of carbon metabolism and antioxidant defenses of alfalfa nodules to drought stress and to the subsequent recovery of plants. *Plant Physiol.* 144, 1104–1114. doi: 10.1104/pp.107.099648

Nimmo, H. G. (2000). The regulation of phosphoenolpyruvate carboxylase in CAM plants. *Trends Plant Sci.* 5, 75–80. doi: 10.1016/S1360-1385(99)01543-5

Nishimura, R., Hayashit, M., Wu, G. J., Kouchi, H., Imaizumi-Anrakull, H., Murakami, Y., et al. (2002). HAR1 mediates systemic regulation of symbiotic organ development. *Nature* 420, 426–429. doi: 10.1038/nature01231

Oberhardt, M. A., Palsson, B. Ø, and Papin, J. A. (2009). Applications of genome-scale metabolic reconstructions. *Mol. Syst. Biol* 5:320. doi: 10.1038/msb.2009.77

Ogden, A. J., Gargouri, M., Park, J. J., Gang, D. R., and Kahn, M. L. (2017). Integrated analysis of zone-specific protein and metabolite profiles within nitrogen-fixing *Medicago truncatula-Sinorhizobium medicae* nodules. *PLoS One* 12:e0180894. doi: 10.1371/journal.pone.0180894

Oldroyd, G. E. D. (2005). Peace talks and trade deals. Keys to long-term harmony in legume-microbe symbioses. *Plant Physiol.* 137, 1205–1210. doi: 10.1104/pp.104.057661

Oldroyd, G. E. D., and Geurts, R. (2001). *Medicago truncatula*, going where no plant has gone before. *Trends Plant Sci.* 6, 552–554. doi: 10.1016/S1360-1385(01)02153-7

Ong, W., Vu, T. T., Lovendahl, K. N., Llull, J. M., Serres, M. H., Romine, M. F., et al. (2014). Comparisons of *Shewanella* strains based on genome annotations, modeling, and experiments. *BMC Syst. Biol.* 8:31. doi: 10.1186/1752-0509-8-31

Patschkowski, T., Schlüter, A., and Priefer, U. B. (1996). *Rhizobium leguminosarum* bv. viciae contains a second *fnr/fixK*-like gene and an unusual *fixL* homologue. *Microbiology* 21, 267–280.

Pfau, T., Christian, N., Masakapalli, S. K., Sweetlove, L. J., Poolman, M. G., and Ebenhöh, O. (2018). The intertwined metabolism during symbiotic nitrogen fixation elucidated by metabolic modelling. *Sci. Rep.* 8:12504. doi: 10.1038/s41598-018-30884-x

Poole, P., Ramachandran, V., and Terpolilli, J. (2018). Rhizobia: from saprophytes to endosymbionts. *Nat. Rev. Microbiol.* 16, 291–303. doi: 10.1038/nrmicro.2017.171

Povolo, S., and Casella, S. (2000). A critical role for aniA in energy-carbon flux and symbiotic nitrogen fixation in *Sinorhizobium meliloti*. *Arch. Microbiol.* 174, 42–49. doi: 10.1007/s002030000171

Povolo, S., Tombolini, R., Morea, A., Anderson, A. J., Casella, S., and Nuti, M. (1994). Isolation and characterization of mutants of *Rhizobium meliloti* unable to synthesize poly-beta-hydroxybutyrate. *Can. J. Microbiol.* 40, 823–829. doi: 10.1139/m94-131

Preisig, O., Anthamatten, D., and Hennecke, H. (1993). Genes for a microaerobically induced oxidase complex in *Bradyrhizobium japonicum* are essential for a nitrogen-fixing endosymbiosis. *Proc. Natl. Acad. Sci. U.S.A.* 90, 3309–3313. doi: 10.1073/pnas.90.8.3309

Prell, J., Bourdès, A., Kumar, S., Lodwig, E., Hosie, A., Kinghorn, S., et al. (2010). Role of symbiotic auxotrophy in the *Rhizobium*-legume symbioses. *PLoS One* 5:e13933. doi: 10.1371/journal.pone.0013933

Prell, J., White, J. P., Bourdes, A., Bunnewell, S., Bongaerts, R. J., and Poole, P. S. (2009). Legumes regulate bacteroid development and persistence by the supply of branched-chain amino acids. *Proc. Natl. Acad. Sci. U.S.A.* 106, 12477–12482. doi: 10.1073/pnas.0903653106

Qin, L., Zhao, J., Tian, J., Chen, L., Sun, Z., Guo, Y., et al. (2012). The High-affinity phosphate transporter GmPT5 regulates phosphate transport to nodules and nodulation in soybean. *Plant Physiol.* 159, 1634–1643. doi: 10.1104/pp.112.199786

Qin, S., Tang, Y., Chen, Y., Wu, P., Li, M., Wu, G., et al. (2016). Overexpression of the starch phosphorylase-like gene (*PHO3*) in *Lotus japonicus* has a profound effect on the growth of plants and reduction of transitory starch accumulation. *Front. Plant Sci.* 7:1315. doi: 10.3389/fpls.2016.01315

Quelas, J. I., Mesa, S., Mongiardini, E. J., Jendrossek, D., and Lodeiro, A. R. (2016). Regulation of polyhydroxybutyrate synthesis in the soil bacterium *Bradyrhizobium diazoefficiens*. *Appl. Environ. Microbiol.* 82, 4299–4308. doi: 10.1128/AEM.00757-16

Ramos, M. L. G., Gordon, A. J., Minchin, F. R., Sprent, J. I., and Parsons, R. (1999). Effect of water stress on nodule physiology and biochemistry of a drought tolerant cultivar of common bean (*Phaseolus vulgaris* L.). *Ann. Bot.* 83, 57–63. doi: 10.1006/anbo.1998.0792

Randhawa, G. S., and Hassani, R. (2002). Role of rhizobial biosynthetic pathways of amino acids, nucleotide bases and vitamins in symbiosis. *Indian J. Exp. Biol.* 40, 755–764.

Rascio, N., and La Rocca, N. (2013). *Biological Nitrogen Fixation: Reference Module in Earth Systems and Environmental Sciences*. Amsterdam: Elsevier Inc. doi: 10.1016/B978-0-12-409548-9.00685-0

Razmilic, V., Castro, J. F., Andrews, B., and Asenjo, J. A. (2018). Analysis of metabolic networks of *Streptomyces leeuwenhoekii* C34 by means of a genome scale model: prediction of modifications that enhance the production of specialized metabolites. *Biotechnol. Bioeng.* 115, 1815–1828. doi: 10.1002/bit.26598

Resendis-Antonio, O., Hernández, M., Mora, Y., and Encarnación, S. (2012). Functional modules, structural topology, and optimal activity in metabolic networks. *PLoS Comput. Biol.* 8:e1002720. doi: 10.1371/journal.pcbi.1002720

Resendis-Antonio, O., Hernández, M., Salazar, E., Contreras, S., Batallar, G. M., Mora, Y., et al. (2011). Systems biology of bacterial nitrogen fixation: high-throughput technology and its integrative description with constraint-based modeling. *BMC Syst. Biol.* 5:120. doi: 10.1186/1752-0509-5-120

Resendis-Antonio, O., Reed, J. L., Encarnación, S., Collado-Vides, J., and Palsson, B. (2007). Metabolic reconstruction and modeling of nitrogen fixation in *Rhizobium etli*. *PLoS Comput. Biol.* 3:e192. doi: 10.1371/journal.pcbi.0030192

Rivers, R. L., Dean, R. M., Chandy, G., Hall, J. E., Roberts, D. M., and Zeidel, M. L. (1997). Functional-analysis of nodulin-26, an aquaporin in soybean root-nodule symbiosomes. *J. Biol. Chem.* 272, 16256–16261. doi: 10.1074/jbc.272.26.16256

Robertson, J. G., Warburton, M. P., Lyttleton, P., Fordyce, A. M., and Bullivant, S. (1978). Membranes in lupin root nodules II. Preparation and properties of peribacteroid membranes and bacteroid envelope inner membranes from developing lupin nodules. *J. Cell. Sci.* 30, 151–174.

Romanov, V. I., Hernandezlucas, I., Martinezromero, E., Hernandez-Lucas, I., and Martinez-Romero, E. (1994). Carbon metabolism enzymes of *Rhizobium tropici* cultures and bacteroids. *Appl. Environ. Microbiol.* 60, 2339–2342.

Ronson, C. W., Lyttleton, P., and Robertson, J. G. (1981). C(4)-dicarboxylate transport mutants of *Rhizobium trifolii* form ineffective nodules on *Trifolium repens*. *Proc. Natl. Acad. Sci. U.S.A.* 78, 4284–4288. doi: 10.1073/pnas.78.7.4284

Rosenberg, E., DeLong, E. F., Lory, S., Stackebrandt, E., and Thompson, F. (2014). *The Prokaryotes*, 4th Edn. Berlin: Springer-Verlag. doi: 10.1007/978-3-642-30138-4

Rosendahl, L., Vance, C. P., and Pedersen, W. B. (1990). Products of dark CO2 fixation in pea root nodules support bacteroid metabolism. *Plant Physiol.* 93, 12–19. doi: 10.1104/pp.93.1.12

Roux, B., Rodde, N., Jardinaud, M. F., Timmers, T., Sauviac, L., Cottret, L., et al. (2014). An integrated analysis of plant and bacterial gene expression in symbiotic root nodules using laser-capture microdissection coupled to RNA sequencing. *Plant J.* 77, 817–837. doi: 10.1111/tpj.12442

Rubio, L. M., and Ludden, P. W. (2015). Biosynthesis of the iron-molybdenum cofactor of nitrogenase. *Annu. Rev. Microbiol.* 62, 93–111. doi: 10.1002/9781119053095.ch7

Rubio, V., Linhares, F., Solano, R., Martín, A. C., Iglesias, J., Leyva, A., et al. (2001). A conserved MYB transcription factor involved in phosphate starvation signaling both in vascular plants and in unicellular algae. *Genes Dev.* 15, 2122–2133. doi: 10.1101/gad.204401

Rudbeck, A., Mouritzen, P., and Rosendahl, L. (1999). Characterization of aspartate transport across the symbiosome membrane in pea root nodules. *J. Plant Physiol.* 155, 576–583. doi: 10.1016/S0176-1617(99)80057-1

Sa, T. M., and Israel, D. W. (1991). Energy status and functioning of phosphorus-deficient soybean nodules. *Plant Physiol.* 97, 928–935. doi: 10.1104/PP.97.3.928

Saad, S., and Lam-Son, P. T. (2017). *Legume Nitrogen Fixation in Soils with Low Phosphorus Availability*. Berlin: Springer International Publishing. doi: 10.1007/978-3-319-55729-8

Sarma, A. D., and Emerich, D. W. (2006). A comparative proteomic evaluation of culture grown vs nodule isolated *Bradyrhizobium japonicum*. *Proteomics* 6, 3008–3028. doi: 10.1002/pmic.200500783

Schellenberger, J., Que, R., Fleming, R. M. T., Thiele, I., Orth, J. D., Feist, A. M., et al. (2011). Quantitative prediction of cellular metabolism with constraint-based models: the COBRA Toolbox v2.0. *Nat. Protoc.* 6, 1290–1307. doi: 10.1038/nprot.2011.308

Schnabel, E., Journet, E. P., De Carvalho-Niebel, F., Duc, G., and Frugoli, J. (2005). The *Medicago truncatula SUNN* gene encodes a CLV1-like leucine-rich repeat receptor kinase that regulates nodule number and root length. *Plant Mol. Biol.* 58, 809–822. doi: 10.1007/s11103-005-8102-y

Schoenbeck, M. A., Temple, S. J., Trepp, G. B., Blumenthal, J. M., Samac, D. A., Gantt, J. S., et al. (2000). Decreased NADH glutamate synthase activity in nodules and flowers of alfalfa (*Medicago sativa* L.) transformed with an antisense glutamate synthase transgene. *J. Exp. Bot.* 51, 29–39. doi: 10.1093/jxb/51.342.29

Schuller, K. A., and Werner, D. (1993). Phosphorylation of soybean (*Glycine max* L.) nodule phosphoenolpyruvate carboxylase in vitro decreases sensitivity to inhibition by L-malate. *Plant Physiol.* 101, 1267–1273. doi: 10.1104/pp.101.4.1267

Schultze, M., and Kondorosi, A. (1998). Regulation of symbiotic root nodule development. *Annu. Rev. Genet.* 32, 33–57. doi: 10.1146/annurev.genet.32.1.33

Seabra, A. R., Pereira, P. A., Becker, J. D., and Carvalho, H. G. (2012). Inhibition of glutamine synthetase by phosphinothricin leads to transcriptome reprograming in root nodules of *Medicago truncatula*. *Mol. Plant Microbe Interact.* 25, 976–992. doi: 10.1094/MPMI-12-11-0322

Shah, R., and Emerich, D. W. (2006). Isocitrate dehydrogenase of *Bradyrhizobium japonicum* is not required for symbiotic nitrogen fixation with soybean. *J. Bacteriol.* 188, 7600–7608. doi: 10.1128/JB.00671-06

Smith, F. W., and Jackson, W. A. (1987). Nitrogen enhancement of phosphate transport in roots of *Zea mays* L.: i. Effects of ammonium and nitrate pretreatment. *Plant Physiol.* 84, 1314–1318. doi: 10.1104/pp.84.4.1314

Spaink, H. P. (2000). Root nodulation and infection factors produced by rhizobial bacteria. *Annu. Rev. Microbiol.* 54, 257–288. doi: 10.1146/annurev.micro.54.1.257

Sprent, J. I. (2009). *Legume Nodulation: A Global Perspective*. Hoboken, NJ: John Wiley & Sons. doi: 10.1002/9781444316384

Sprent, J. I., Ardley, J., and James, E. K. (2017). Biogeography of nodulated legumes and their nitrogen-fixing symbionts. *New Phytol.* 215, 40–56. doi: 10.1111/nph.14474

Stovall, I., and Cole, M. (1978). Organic acid metabolism by isolated *Rhizobium japonicum* bacteroids. *Plant Physiol.* 61, 787–790. doi: 10.1104/pp.61.5.787

Sulieman, S., and Schulze, J. (2010). The efficiency of nitrogen fixation of the model legume *Medicago truncatula* (Jemalong A17) is low compared to *Medicago sativa*. *J. Plant Physiol.* 167, 683–692. doi: 10.1016/j.jplph.2009.12.016

Sulieman, S., and Tran, L. S. P. (2015). Phosphorus homeostasis in legume nodules as an adaptive strategy to phosphorus deficiency. *Plant Sci.* 239, 36–43. doi: 10.1016/j.plantsci.2015.06.018

Szafran, M. M., and Haaker, H. (1995). Properties of the peribacteroid membrane ATPase of pea root modules and its effect on the nitrogenase activity. *Plant Physiol.* 108, 1227–1232. doi: 10.1104/PP.108.3.1227

Tajima, S. (2004). Ureide biosynthesis in legume nodules. *Front. Biosci.* 9, 1374–1381. doi: 10.2741/1345

Takanashi, K., Takahashi, H., Sakurai, N., Sugiyama, A., Suzuki, H., Shibata, D., et al. (2012). Tissue-specific transcriptome analysis in nodules of *Lotus japonicus*. *Mol. Plant. Microbe. Interact.* 25, 869–876. doi: 10.1094/MPMI-01-12-0011-R

Temple, S. J., Vance, C. P., and Gantt, J. S. (1998). Glutamate synthase and nitrogen assimilation. *Trends Plant Sci.* 3, 51–56. doi: 10.1016/S1360-1385(97)01159-X

Terpolilli, J. J., Hood, G. A., and Poole, P. S. (2012). What determines the efficiency of N2-fixing Rhizobium-legume symbioses? *Adv. Microb. Physiol.* 60, 325–389. doi: 10.1016/B978-0-12-398264-3.00005-X

Terpolilli, J. J., Masakapalli, S. K., Karunakaran, R., Webb, I. U. C., Green, R., Watmough, N. J., et al. (2016). Lipogenesis and redox balance in nitrogen-fixing pea bacteroids. *J. Bacteriol.* 198, 2864–2875. doi: 10.1128/JB.00451-16

Tesfaye, M., Samac, D. A., and Vance, C. P. (2006). Insights into symbiotic nitrogen fixation in *Medicago truncatula*. *Mol. Plant microbe Interact.* 19, 330–341. doi: 10.1094/MPMI-19-0330

The Legume Phylogeny Working Group (2013). Legume phylogeny and classification in the 21st century: progress, prospects and lessons for other species-rich clades Legume phylogeny and classification in the 21st century: progress, prospects and lessons for other species-rich clades. *Taxon* 62, 217–248. doi: 10.12705/622.8

Thöny-Meyer, L., and Künzler, P. (1996). The *Bradyrhizobium japonicum* aconitase gene (*acnA*) is important for free-living growth but not for an effective root nodule symbiosis. *J. Bacteriol.* 178, 6166–6172. doi: 10.1128/jb.178.21.6166-6172.1996

Thuynsma, R., Valentine, A., and Kleinert, A. (2014). Phosphorus deficiency affects the allocation of below-ground resources to combined cluster roots and nodules in *Lupinus albus*. *J. Plant Physiol.* 171, 285–291. doi: 10.1016/J.JPLPH.2013.09.001

Timmers, A. C. J., Auriac, M.-C., and Truchet, G. (1999). Refined analysis of early symbiotic steps of the rhizobium-Medicago interaction in relationship with microtubular cytoskeleton rearrangements. *Development* 126, 3617–3628.

Timmers, A. C. J., Soupene, E., Auriac, M.-C., de Billy, F., Vasse, J., Boistard, P., et al. (2000). Saprophytic intracellular rhizobia in alfalfa nodules. *Mol. Plant Microbe Interact.* 13, 1204–1213. doi: 10.1094/MPMI.2000.13.11.1204

Todd, C. D., Tipton, P. A., Blevins, D. G., Piedras, P., Pineda, M., and Polacco, J. C. (2006). Update on ureide degradation in legumes. *J. Exp. Bot.* 57, 5–12. doi: 10.1093/jxb/erj013

Tomaszewska, B., Jarmuszkiewicz, W., and Schrmm, R. W. (1991). The role of malate in the metabolism of mitochondria and symbiosomes from lupin root nodules. *Plant Physiol. Biochem.* 29, 489–496.

Tombolini, R., and Nuti, M. P. (1989). Poly (β-hydroyxalkanoate) biosynthesis and accumulation by different *Rhizobium* species. *FEMS Microbiol. Lett.* 60, 299–304.

Udvardi, M., Lister, D. L., and Day, D. A. (1991). ATPase activity and anion transport across the peribacteroid membrane of isolated soybean symbiosomes. *Microbiology* 156, 362–366.

Udvardi, M., and Poole, P. S. (2013). Transport and metabolism in legume-rhizobia symbioses. *Annu. Rev. Plant Biol.* 64, 781–805. doi: 10.1146/annurev-arplant-050312-120235

Udvardi, M. K., and Day, D. A. (1989). Electrogenic ATPase activity on the peribacteroid membrane of soybean (*Glycine max* L.) root nodules. *Plant Physiol.* 90, 982–987. doi: 10.1104/pp.90.3.982

Udvardi, M. K., and Day, D. A. (1997). Metabolite transport across symbiotic membranes of legume nodules. *Annu. Rev. Plant Physiol. Plant Mol. Biol.* 48, 493–523. doi: 10.1146/annurev.arplant.48.1.493

Udvardi, M. K., Price, G. D., Gresshoff, P. M., and Day, D. A. (1988). A dicarboxylate transporter on the peribacteroid membrane of soybean nodules. *FEBS Lett.* 231, 36–40. doi: 10.1016/0014-5793(88)80697-5

Valdés-López, O., Arenas-huertero, C., Ramírez, M., Girard, L., Sánchez, F., Vance, C. P., et al. (2008). Essential role of MYB transcription factor: *PvPHR1* and microRNA: PvmiR399 in phosphorus-deficiency signalling in common bean roots. *Plant Cell Environ.* 31, 1834–1843. doi: 10.1111/j.1365-3040.2008.01883.x

Valdés-López, O., and Hernández, G. (2008). Transcriptional regulation and signaling in phosphorus starvation: what about legumes? *J. Integr. Plant Biol.* 50, 1213–1222. doi: 10.1111/j.1744-7909.2008.00758.x

Valentine, A. J., Kleinert, A., and Benedito, V. A. (2017). Adaptive strategies for nitrogen metabolism in phosphate deficient legume nodules. *Plant Sci.* 256, 46–52. doi: 10.1016/j.plantsci.2016.12.010

Vance, C. P., Graham, P. H., and Allan, D. L. (2000). "Biological nitrogen fixation: phosphorus-a critical future need?," in *Nitrogen Fixation: From Molecules to Crop Productivity*, eds F. O. Pedrosa, M. Hungria, G. Yates, and W. E. Newton (Dordrecht: Kluwer Academic Publishers), 509–514. doi: 10.1007/0-306-47615-0_291

Vardien, W., Steenkamp, E. T., and Valentine, A. J. (2016). Legume nodules from nutrient-poor soils exhibit high plasticity of cellular phosphorus recycling and conservation during variable phosphorus supply. *J. Plant Physiol.* 191, 73–81. doi: 10.1016/j.jplph.2015.12.002

Vasse, J., de Billy, F., Camut, S., and Truchet, G. (1990). Correlation between ultrastructural differentiation of bacteroids and nitrogen fixation in alfalfa nodules. *J. Bacteriol.* 172, 4295–4306. doi: 10.1128/jb.172.8.4295-4306.1990

Vauclare, P., Bligny, R., Gout, E., and Widmer, F. (2013). An overview of the metabolic differences between *Bradyrhizobium japonicum* 110 bacteria and differentiated bacteroids from soybean (*Glycine max*) root nodules: an *in vitro* 13C- and 31P-nuclear magnetic resonanc. *FEMS Microbiol. Lett.* 343, 49–56. doi: 10.1111/1574-6968.12124

Vercruysse, M., Fauvart, M., Beullens, S., Braeken, K., Cloots, L., Engelen, K., et al. (2011). A comparative transcriptome analysis of *Rhizobium etli* bacteroids: specific gene expression during symbiotic nongrowth. *Mol. Plant Microbe Interact.* 24, 1553–1561. doi: 10.1094/MPMI-05-11-0140

Vidal, J., and Chollet, R. (1997). Regulatory phosphorylation of C4 PEP carboxylase. *Trends Plant Sci.* 2, 230–237. doi: 10.1016/S1360-1385(97)01046-7

Voegele, R. T., Mitsch, M. J., and Finan, T. M. (1999). Characterization of two members of a novel malic enzyme class. *Biochim. Biophys. Acta* 1432, 275–285. doi: 10.1016/S0167-4838(99)00112-0

Wang, C., Saldanha, M., Sheng, X., Shelswell, K. J., Walsh, K. T., Sobral, B. W. S., et al. (2007). Roles of poly-3-hydroxybutyrate (PHB) and glycogen in symbiosis of *Sinorhizobium meliloti* with *Medicago* sp. *Microbiology* 153, 388–398. doi: 10.1099/mic.0.29214-0

Wang, T., Zhao, M., Zhang, X., Liu, M., Yang, C., Chen, Y., et al. (2017). Novel phosphate deficiency-responsive long non-coding RNAs in the legume model plant Medicago truncatula. *J. Exp. Bot.* 68, 5937–5948. doi: 10.1093/jxb/erx384

Wang, X., Shen, J., and Liao, H. (2010). Acquisition or utilization, which is more critical for enhancing phosphorus efficiency in modern crops? *Plant Sci.* 179, 302–306. doi: 10.1016/j.plantsci.2010.06.007

Weaver, C. D., Shomer, N. H., Louis, C. F., and Roberts, D. M. (1994). Nodulin 26, a nodule-specific symbiosome membrane protein from soybean, is an ion channel. *J. Biol. Chem.* 269, 17858–17862.

Werner, A. K., and Witte, C. P. (2011). The biochemistry of nitrogen mobilization: purine ring catabolism. *Trends Plant Sci.* 16, 381–387. doi: 10.1016/j.tplants.2011.03.012

Whitehead, L. F., Day, D. A., and Tyerman, S. D. (2008). Divalent cation gating of an ammonium permeable channel in the symbiotic membrane from soybean nodules. *Plant J.* 16, 313–324. doi: 10.1046/j.1365-313X.1998.00298.x

Whitehead, L. F., Young, S., and Day, D. A. (1998). Aspartate and alanine movement across symbiotic membranes of soybean nodules. *Soil Biol. Biochem.* 30, 1583–1589. doi: 10.1016/S0038-0717(97)00229-0

Xue, Y., Bin Xiao, B. X., Zhu, S. N., Mo, X. H., Liang, C. Y., Tian, J., et al. (2017). *GmPHR25*, a *GmPHR* member up-regulated by phosphate starvation, controls phosphate homeostasis in soybean. *J. Exp. Bot.* 68, 4951–4967. doi: 10.1093/jxb/erx292

Yang, Y., Hu, X. P., and Ma, B. G. (2017). Construction and simulation of the *Bradyrhizobium diazoefficiens* USDA110 metabolic network: a comparison between free-living and symbiotic states. *Mol. Biosyst.* 13, 607–620. doi: 10.1039/C6MB00553E

Yao, Z., Tian, J., and Liao, H. (2014). Comparative characterization of *GmSPX* members reveals that *GmSPX3* is involved in phosphate homeostasis in soybean. *Ann. Bot.* 114, 477–488. doi: 10.1093/aob/mcu147

Yao, Z. F., Liang, C. Y., Zhang, Q., Chen, Z. J., Xiao, B. X., Tian, J., et al. (2014). *SPX1* is an important component in the phosphorus signalling network of common bean regulating root growth and phosphorus homeostasis. *J. Exp. Bot.* 65, 3299–3310. doi: 10.1093/jxb/eru183

Yong-Villalobos, L., González-Morales, S. I., Wrobel, K., Gutiérrez-Alanis, D., Cervantes-Peréz, S. A., Hayano-Kanashiro, C., et al. (2015). Methylome analysis reveals an important role for epigenetic changes in the regulation of the Arabidopsis response to phosphate starvation. *Proc. Natl. Acad. Sci. U.S.A.* 112, E7293–E7302. doi: 10.1073/pnas.1522301112

Yurgel, S. N., and Kahn, M. L. (2004). Dicarboxylate transport by rhizobia. *FEMS Microbiol. Rev.* 28, 489–501. doi: 10.1016/j.femsre.2004.04.002

Zhang, J., Zhou, X., Xu, Y., Yao, M., Xie, F., Gai, J., et al. (2016). Soybean SPX1 is an important component of the response to phosphate deficiency for phosphorus homeostasis. *Plant Sci.* 248, 82–91. doi: 10.1016/j.plantsci.2016.04.010

Zhang, N., Venkateshwaran, M., Boersma, M., Harms, A., Howes-Podoll, M., Den Os, D., et al. (2012). Metabolomic profiling reveals suppression of oxylipin biosynthesis during the early stages of legume-rhizobia symbiosis. *FEBS Lett.* 586, 3150–3158. doi: 10.1016/j.febslet.2012.06.046

Zhang, X. Q., Li, B., and Chollet, R. (1995). In vivo regulatory phosphorylation of soybean nodule phosphoenolpyruvate carboxylase. *Plant Physiol.* 108, 1561–1568. doi: 10.1104/pp.108.4.1561

Zhang, Y., Aono, T., Poole, P., and Finan, T. M. (2012). NAD(P)+-malic enzyme mutants of *Sinorhizobium* sp. strain ngr234, but not *Azorhizobium caulinodans* ors571, maintain symbiotic N2 fixation capabilities. *Appl. Environ. Microbiol.* 78, 2803–2812. doi: 10.1128/AEM.06412-11

Zhao, H., Li, M., Fang, K., Chen, W., and Wang, J. (2012). In silico insights into the symbiotic nitrogen fixation in *Sinorhizobium meliloti* via metabolic reconstruction. *PLoS One* 7:e31287. doi: 10.1371/journal.pone.0031287

Zhao, X. Q., Shen, R. F., and Sun, Q. B. (2009). Ammonium under solution culture alleviates aluminum toxicity in rice and reduces aluminum accumulation in roots compared with nitrate. *Plant Soil* 315, 107–121. doi: 10.1007/s11104-008-9736-8

Conflict of Interest Statement: The authors declare that the research was conducted in the absence of any commercial or financial relationships that could be construed as a potential conflict of interest.

frontiers in Microbiology

ORIGINAL RESEARCH
published: 21 December 2018
doi: 10.3389/fmicb.2018.03194

Water-Soluble Humic Materials Regulate Quorum Sensing in *Sinorhizobium meliloti* Through a Novel Repressor of *expR*

*Yuan-Yuan Xu[1], Jin-Shui Yang[1], Cong Liu[1], En-Tao Wang[2], Ruo-Nan Wang[1], Xiao-Qian Qiu[1], Bao-Zhen Li[1], Wen-Feng Chen[1] and Hong-Li Yuan[1]**

[1] State Key Laboratory of Agrobiotechnology and Key Laboratory of Soil Microbial, Ministry of Agriculture, College of Biological Sciences, China Agricultural University, Beijing, China, [2] Escuela Nacional de Ciencias Biológicas, Instituto Politécnico Nacional, Mexico City, Mexico

OPEN ACCESS

Edited by:
Hon-Ming Lam, The Chinese University of Hong Kong, China

Reviewed by:
Muthu Venkateshwaran, University of Wisconsin–Platteville, United States
Yangrong Cao, Huazhong Agricultural University, China

***Correspondence:**
Hong-Li Yuan
hlyuan@cau.edu.cn;
yuanaemoil@cau.edu.cn

Specialty section:
This article was submitted to Plant Microbe Interactions, a section of the journal Frontiers in Microbiology

Received: *03 September 2018*
Accepted: *10 December 2018*
Published: *21 December 2018*

Citation:
Xu Y-Y, Yang J-S, Liu C, Wang E-T, Wang R-N, Qiu X-Q, Li B-Z, Chen W-F and Yuan H-L (2018) Water-Soluble Humic Materials Regulate Quorum Sensing in Sinorhizobium meliloti Through a Novel Repressor of expR. Front. Microbiol. 9:3194. doi: 10.3389/fmicb.2018.03194

Quorum sensing (QS) plays an important role in the growth, nodulation, and nitrogen fixation of rhizobia. In this study, we show that water-soluble humic materials (WSHM) repress the expression of the QS related genes *sinI, sinR,* and *expR* in *Sinorhizobium meliloti.* This decreased the production of *N*-acetyl homoserine lactones (AHL) and exopolysaccharides (EPS), and ultimately increased *S. meliloti* cell density. We also identified a novel regulator, SMc03890 (renamed QsrR), which binds directly to the *expR* promoter. Deletion of *qsrR* increased *expR* expression. WSHM repressed the expression of *expR* by augmenting the interaction between QsrR and the *expR* promoter; this was determined by a bacterial-one-hybrid assay. These effects of WSHM on the QS system in *S. meliloti* may be the underlying mechanism by which WSHM increase the symbiotic nitrogen fixation of *Medicago sativa* inoculated with *S. meliloti*. This study provides the first evidence that humic acids regulate the QS of rhizobia and suggests that WSHM could be used as fertilizers to improve the efficiency of symbiotic nitrogen fixation.

Keywords: *Sinorhizobium meliloti*, quorum sensing, humic materials, ExpR regulator, bacterial communication

INTRODUCTION

Quorum sensing (QS) is a bacterial communication mechanism in which cell physiology and behavior are coordinated with population density (Bogino et al., 2015). In symbiotic nitrogen-fixing bacteria (rhizobia), QS plays a key role in their growth and the formation of symbiosis with their legume hosts (Bogino et al., 2015; Koul et al., 2016). In the QS system of *Sinorhizobium meliloti* 8530 (**Figure 1**), SinI is responsible for synthesis of the QS signaling molecules, *N*-acetyl homoserine lactones (AHL). The expression of *sinI* is induced by SinR; meanwhile, ExpR either mediates a positive regulatory feedback loop by inducing the expression of *sinI* or a negative feedback regulation by down-regulating the expression of *sinR*, depending on the AHL concentration (Charoenpanich et al., 2013; Calatrava-Morales et al., 2018). In addition to regulating the genes involved in nodulation and nitrogen fixation (Hoang et al., 2004), AHL-ExpR complex also up-regulate the expression of *exp* operon, which is involved in EPS II synthesis, and down-regulate genes related to bacterial motility, such as *visN, visR,* and *rem* (Gurich and Gonzalez, 2009; Mueller and González, 2010). The number of pink nodules induced by the *sinI* mutant decreased compared

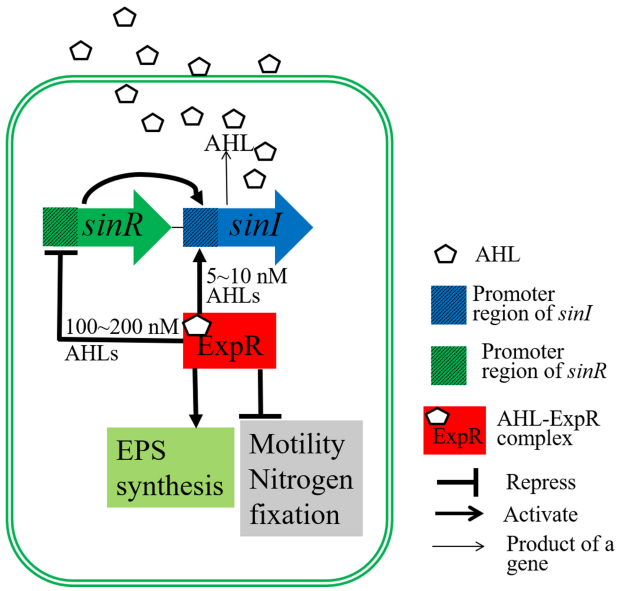

FIGURE 1 | Regulatory diagram of the *S. meliloti* quorum sensing system. The transcription of *sinI,* which encodes AHL synthase, is induced by SinR. *sinI* transcription can also be induced by the AHL-ExpR complex at low AHL concentrations (5∼10 nM). The AHL-ExpR complex represses *sinR* expression at high AHL concentrations (100∼200 nM). Furthermore, the AHL-ExpR complex induces the expression of genes related to EPS biosynthesis, and represses the expression of genes important for motility, nodulation, and nitrogen fixation.

with the WT strain due to the inability of the *sinI* mutant to repress the expression of motility genes at high cell densities (Gurich and Gonzalez, 2009). The *expR* mutant, *S. meliloti* 1021, grows more rapidly and has an increased nodule occupancy (10∼20% higher than the WT strain, *S. meliloti* 8530) (Charoenpanich et al., 2015).

Many compounds have been reported to interfere with the bacterial QS systems (Kalia, 2013; Gonzalez-Ortiz et al., 2014). For rhizobia, L-canavanine, which is extracted from alfalfa seed exudates, inhibits the expression of *S. meliloti expR* gene (Keshavan et al., 2005), while the flavonoids induce the expression of AHL synthesis genes in *Sinorhizobium fredii* SMH12 and in *Rhizobium etli* ISP42 (Pérez-Montaño et al., 2011). Generally, compounds that interfere with microbial QS systems are heterocyclic compounds containing groups such as furan, pyridine, butyrolactone, benzene ring, and quinoline (Gonzalez and Keshavan, 2006; Christensen et al., 2013). These compounds have chemical structures similar to those of humic materials (Gao T.G. et al., 2015); thus, it is possible that humic materials may also interfere with microbial QS systems.

Humic materials are supramolecules derived from the residues of degraded plant, animal and microbial cells (Hayes and Wilson, 1997), with structures of relatively small self-assembled molecules that are held together by multiple weak interactions, such as hydrogen and van der Waals bonds. Generally, humic materials include, but are not limited to, *n*-alkanoic acids, *n*-alkanols, hydrocarbons, hydroxyacids, aromatic compounds, polyhydroxylated compounds, steroids, terpenoids, and *N*-heterocyclic compounds (Nebbioso and Piccolo, 2012). Humic materials are the most biological active compounds in soil that could stimulate plant growth as phytohormones (Traversa et al., 2013; Savy et al., 2017), enhance ATPase activity, promote nutrient utilization of plant (Jannin et al., 2012; Canellas et al., 2015), and stimulate the growth of bacteria (Tikhonov et al., 2010). In a previous study, we revealed that the water-soluble humic materials (WSHM) that are produced by lignite biodegradation enhanced the growth, cell metabolism, and nutrient transport of *Bradyrhizobium liaoningense* CCBAU05525, as well as its nodulation with soybean (12∼26% increased yield in soybean grains) (Gao T.G. et al., 2015). Therefore, WSHM could be a potential fertilizer to improve the legume yield.

In the present study, we examined the effects of WSHM on the QS system and the symbiotic nitrogen fixation of *S. meliloti*, and revealed that WSHM enhance the growth and nitrogen fixation of *S. meliloti* by regulating the QS system. This is the first report showing the effects of WSHM on the QS system in *S. meliloti*. Finally, we identified QsrR as a novel repressor of *expR* in this bacterium.

MATERIALS AND METHODS

WSHM, Bacterial Strains, and Plasmids

Water-soluble humic materials were extracted from lignite collected from a Coal Mine in Inner Mongolia of China according to previously described methods (Dong et al., 2006; Jiang et al., 2013). Briefly, the lignite powder was inoculated with *Penicillium* sp. P6 and *Bacillus* sp. Y7 and incubated at 28°C for 2 weeks. Biodegraded lignite was diluted tenfold in deionized water, stirred, and centrifuged three times at 9000 × *g* for 15 min. The supernatant was filtered through Whatman No. 1 filter paper and the filtrated (WSHM) were dried at 40°C for about 72 h, weighed, and stored in a vacuum-dried chamber. In the WSHM, 68 aromatic, aliphatic, and nitrogen-based compounds were detected by tetramethyl ammonium hydroxide (TMAH)-py-GC/MS (Gao T.G. et al., 2015).

All the bacterial strains and plasmids used in this study are listed in **Supplementary Table S1**. Among them, *S. meliloti* 1021 is a native mutant in which the ORF of *expR* is interrupted by an insertion; while *S. meliloti* 8530 is a derivative of *S. meliloti* 1021 by excising this insertion spontaneously. Since most *S. meliloti* strains harbor a functional *expR* (Pellock et al., 2002), *S. meliloti* 8530 was considered as the wild type strain. *Agrobacterium tumefaciens* KYC55 (pJZ372, pJZ384, pJZ410) was used as a bioassay strain for ultrasensitive detection of AHL.

Growth Response of *S. meliloti* 8530 to WSHM

Sinorhizobium meliloti 8530 was preincubated in 50 mL of YM broth (Gao T.G. et al., 2015) for 4 days at 28°C with shaking (150 rpm). The culture was used to inoculate 50 mL of either YM broth (control) or YM broth with 500 mg L^{-1} WSHM at a final OD_{600} of 0.01. The cultures were incubated at 28°C with

shaking (150 rpm) for 5–6 days and samples were plated using serial dilutions every 12 h to evaluate the rhizobia cell density. This assay was performed thrice in triplicate.

Response of AHL Production to WSHM

Agrobacterium tumefaciens KYC55 (pJZ372, pJZ384, pJZ410) was incubated in AT medium [KH_2PO_4, 10.7 g; $MgSO_4 \cdot 7H_2O$, 160 mg; $CaCl_2$, 78 mg; $FeSO_4 \cdot 7H_2O$, 5 mg; $MnSO_4 \cdot H_2O$, 2.2 mg; $(NH_4)_2SO_4$, 2 g; glucose, 5 g; in 1 L of distilled water; pH adjusted to 7.3 with K_2HPO_4; tetracycline, spectinomycin, and gentamycin at final concentrations of 2, 100, and 100 μg/mL respectively] with shaking at 150 rpm for 2 days to yield up to 10^9 cells mL^{-1} (Zhu et al., 2003). The AHL production was detected as previously described (Zheng et al., 2006). Briefly, the cell-free supernatant of *S. meliloti* 1021 or 8530 culture (**Figure 2B**) was added to fresh AT broth at the ratio of 10% (v/v). The cell-free supernatant of *A. tumefaciens* strain R10 (pCF218) (Zhu et al., 2003) culture was used as positive control to assess the AHL sensitivity of *A. tumefaciens* KYC55 under these experimental conditions. The same volume of sterilized water (Control) or WSHM solution (500 mg L^{-1}) was added separately into AT broth as negative controls. All the AT media prepared for tests were inoculated with approximately 10^7 cells mL^{-1} of *A. tumefaciens* KYC55 and incubated with aeration (150 rpm) for 16–20 h at 28°C. The β-galactosidase activity in each culture was quantitatively analyzed to estimate the concentration of AHL (Zhu et al., 2003). β-galactosidase activity (Miller units) was calculated as $OD_{420} \times 10^3$/(time of reaction in minutes × volume of culture in milliliters × OD_{600}) (Pérez-Montaño et al., 2011). Assays were conducted in triplicate for three times.

Response of EPS Synthesis to WSHM Treatment

The effects of WSHM on EPS synthesis were analyzed for the wild type strain *S. meliloti* 8530, which can produce EPS I (succinoglycan), EPS II (galactoglucan), and linear mixed-linkage β-glucan (MLG) (Pérez-Mendoza et al., 2015), as well as for *S. meliloti* 1021, which could produce EPS I and extremely low level of EPS II (Pellock et al., 2002). Both strains were cultured in GMS medium (Staehelin et al., 2006) with and

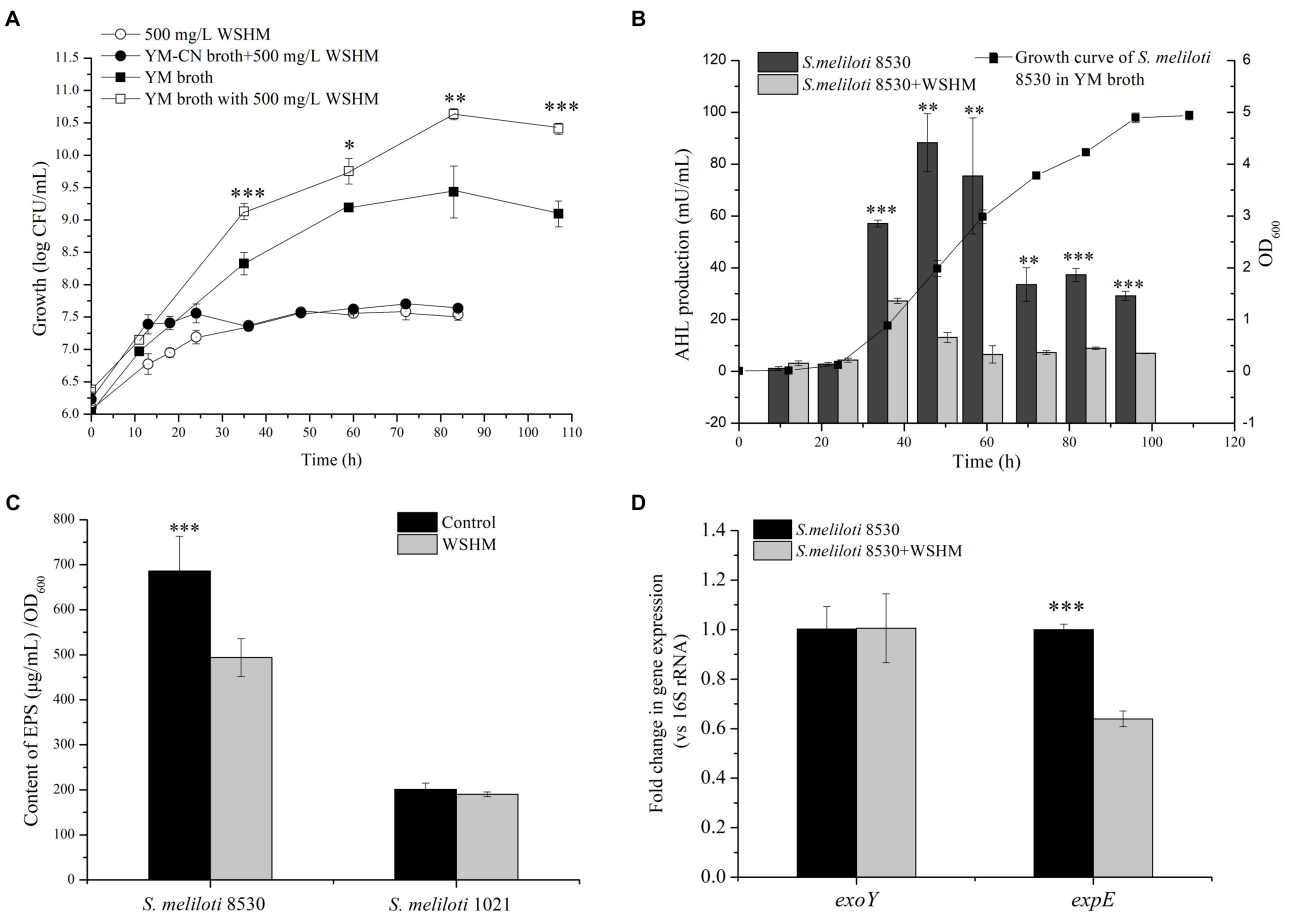

FIGURE 2 | Effects of WSHM on the growth **(A)**, AHL production **(B)**, exopolysaccharide production **(C)**, and *exoY* and *expE* gene expression **(D)** in *S. meliloti* 8530. All the data are expressed as average ± standard deviation (SD) ($n = 3$). Statistical significance was assessed by Student's *t*-tests (*$P < 0.05$; **$P < 0.01$; ***$P < 0.001$). For exopolysaccharides production **(C)**, *S. meliloti* 1021 (Δ*expR*) was also included. **(A)** YM-CN broth: the nitrogen (yeast extract) and carbon (mannitol) source in YM broth were removed.

without 500 mg L^{-1} of WSHM for 5 days. EPSs were collected as described by Staehelin et al. (2006) and quantified in triplicate by the anthrone-sulfuric acid method (Jones, 2012).

Expression of *exoY* and *expE* Genes in Response to WSHM

The effects of WSHM on the expression of *exoY* and *expE,* which are responsible for EPS I and EPS II synthesis, respectively (Mueller and González, 2010), were analyzed by reverse transcription quantitative real-time PCR (RT-qPCR). *S. meliloti* 8530 was cultured in YM broth (control) or YM broth supplied with 500 mg L^{-1} WSHM as mentioned above. Samples were collected at the end of exponential phrase (OD_{600} = 1.5–2.0). Total RNA was isolated using the RNA Pure Bacteria Kit (CWBIO, Beijing, China) according to the manufacturer's instructions. First strand cDNAs were synthesized using PrimeScript Reverse Transcriptase (RT) (TaKaRa Code: D2680S) according to the manufacturer's instructions. These cDNA samples were used for RT-qPCR with primers specific to *exoY* and *expE* genes (**Supplementary Table S2**). A 167 bp fragment of 16S rRNA gene was used as an internal control for normalization (Pérez-Montaño et al., 2014). Each 20 μL-reaction contained 10 μL of Power SYBR Green Master Mix (ABI, United States). The PCR program was: 95°C for 10 min, followed by; 40 cycles of 95°C for 15 s and 60°C for 1 min, followed by the melting curve. PCR was performed on an ABI 7500 Thermocycler and data were analyzed using the $2^{-\Delta\Delta Ct}$ method (Jannin et al., 2012). The experiment was performed for three times with four technical replicates.

Expression of QS Genes in Response to WSHM

The bacteria were cultured same as described above (see Expression of *exoY* and *expE* Genes in Response to WSHM). The expression of QS genes following WSHM treatment was analyzed by RT-qPCR as mentioned above with primers specific to *sinI, sinR,* and *expR* (**Supplementary Table S2**). The cDNA obtained from cultures of *S. meliloti* 8530, *S. meliloti* 1021 (Δ*expR*), *S. meliloti* MG170 (Δ*sinR*), and *S. meliloti* MG32 (Δ*sinI*) (**Supplementary Table S1**) with or without WSHM were used as templates, and the experiment was performed three times with four replicates.

Deletion of *qsrR* and Its Effect on *expR* Expression in Response to WSHM

Agrobacterium tumefaciens interacts with plant hosts similar to those of rhizobia. Thus, in order to analyze the repression mechanisms of WSHM on *expR* expression, the QS regulation system in *A. tumefaciens* (Gonzalez and Keshavan, 2006) was compared with that in *S. meliloti* 8530. AccR of *A. tumefaciens* can counteract *traR* repression by directly binding with opines produced by the plant host. Since protein SMc03890 in strain 8530, which was renamed as QsrR in this study, was very similar to AccR (with 31% similarity of amino acid sequence) and were both DeoR family transcriptional regulators, we hypothesized that QsrR could be capable of mediating the effects of WSHM on *expR* expression. To test this hypothesis, the *S. meliloti*Δ*qsrR* mutant strain was constructed via homologous recombination. Furthermore, by fusing the *expR* promoter region with the *lacZ* structural gene, the change in *expR* expression caused by the deletion of *qsrR* was determined by the activity of β-galactosidase. Refer to **Supplementary Methods** for detailed description of the process.

Previous reports have evidenced that the eukaryotic hosts are capable of interfering with bacterial QS by producing molecular signals, like flavonoid (Kalia, 2013; Nievas et al., 2017), and flavonoid homologs have been detected in WSHM (Gao T.G. et al., 2015). In order to analyze whether WSHM function as a plant signal (like opines) to represses QS in *S. meliloti*, *expR* gene expression levels in *S. meliloti* 8530 or *S. meliloti*Δ*qsrR* following treatment with either WSHM (500 mg L^{-1}) or alfalfa seed exudates (2%, v/v) were determined by measuring the activity of β-galactosidase (Chai et al., 2010). Alfalfa seed exudates were prepared according to Cai et al. (2009). Assays were conducted in triplicate and repeated three times.

QsrR Purification and Electrophoretic Mobility Shift Assays (EMSAs)

The full-length ORF of *qsrR* was amplified using the primers *qsrR*281 and *qsrR*282 (**Supplementary Table S2**) and cloned into pET28a. The recombinant plasmid pET28a-*qsrR* was transformed into *Escherichia coli* Rosetta (DE3) and cultured in LB medium with 0.4 mM isopropyl-β-D-thiogalactoside (IPTG) for induction at 37°C. The QsrR protein with a His tag (His_6-QsrR) was purified with Ni-loaded nitrilotriacetic acid (NTA) resin (GE Healthcare) from cultures of *E. coli* Rosetta (DE3) carrying the recombinant plasmid. Electrophoretic mobility shift assays (EMSAs) were used to detect the interaction between the QsrR protein and the *expR* promoter using a DIG Gel Shift Kit, 2nd Generation (Roche), according to the manufacturer's instructions. The promoter region of *expR* was amplified with primers *expR*11 and *expR*12 (**Supplementary Table S2**). Binding specificity was evaluated through addition of ∼100-fold excess of unlabeled *expR* promoter fragments, which competed with the labeled probe to bind with His_6-QsrR. A labeled non-specific DNA probe from *Streptomyces avermitilis* was used as negative control. EMSAs were repeated at least twice.

Bacterial One-Hybrid Assay

The experimental procedure was similar to that of Luo et al. (2014). Briefly, the gene *qsrR* was amplified with primers 03890BHf and 03890BHr (**Supplementary Table S2**), excised with Not I/Bgl II, and cloned into the bait plasmid pB1H1 to generate pB1H1-*qsrR*. Fragments R1 and R4 in the promoter region of *expR* were cloned into the prey plasmid pH3U3, respectively. pH3U3-R1 and pH3U3-R4 were not self-activating prey confirmed previously (see **Supplementary Methods** for detail). Then the plasmid pairs pB1H1-*qsrR*/pH3U3-R1 and pB1H1-*qsrR*/pH3U3-R4 were transformed into *E. coli* USO respectively. The growth of the transformants of *E. coli* USO, including USO: pB1H1-*zif268*/pH3U3-*zif268* as positive control

(+/+); USO: pB1H1/pH3U3 (−/−), USO: pB1H1/pH3U3-R1 and USO: pB1H1/pH3U3-R4 as negative controls (−/+); and two transformants with *qsrR,* USO: pB1H1-*qsrR*/pH3U3-R1 and USO: pB1H1-*qsrR*/pH3U3-R4 (+/+), were determined on NM medium without histidine and with varying concentrations of 3-AT. We expected the transformants with *qsrR* to survive on NM medium containing 3-AT, as long as QsrR interacts with the *expR* promoter region to recruit RNA polymerase and activate the transcription of the reporter gene *HIS3*. Higher levels of *HIS3* gene expression enable the bacteria grow on NM medium with higher concentrations of 3-AT. Assays were repeated three times.

Effects of WSHM on Plant Growth and Nodulation by *S. meliloti*

Sinorhizobium meliloti was cultured aerobically at 28°C in YM broth (Gao T.G. et al., 2015) for 2 days to OD_{600} = 1.0 (about 10^8 CFU mL^{-1}) and were used as inoculant. *Medicago sativa* seeds were surface-sterilized by 3% (v/v) NaClO for 3 min, germinated on 0.7% agar-water plates in the dark at 28°C for 24–48 h. The germinated seeds were planted in pots (three seeds per pot) filled with 300 cm^3 of vermiculite and moisturized with low-N nutrient solution (Vincent, 1970). Six treatments with seven replicates (i.e., pots) were included: no inoculation control with and without WSHM (500 mg L^{-1}); inoculation treatments of wild type strain (*S. meliloti* 8530, 1 mL) with and without WSHM; and inoculation treatments of Δ*qsrR* strain (1 mL) with and without WSHM (**Table 1**). Plants were grown in a greenhouse at 25 ± 2°C during the day and 17 ± 2°C at night with 60% relative humidity. Pots were rearranged daily to give a random distribution of growth conditions. After 45 days, all of the alfalfa plants were harvested and the number, fresh weight, and nitrogenase activity of the nodules, as well as the dry weight of the plants, were determined for each pot. The nitrogenase activity was analyzed by acetylene reduction assay, for which the whole roots with nodules in each pot (three plants) were put into a sealed bottle and incubated with acetylene (Suganuma et al., 1998), and the nitrogenase activity was calculated as μmol C_2H_4 /h · g of nodule. Then, the number and fresh weight of nodules in each pot were counted. The pooled data for each pot (three plants) were considered as one sample, and statistical analysis was conducted using Duncan test. Finally, several root nodules were sliced and treated for transmission electron microscopy (TEM) according to Bourassa et al. (2017) to evaluate the effects of WSHM treatment on the number and morphology of bacteroids in nodules induced by *S. meliloti* 8530.

RESULTS

The Growth of *S. meliloti* in Response to WSHM

As shown in **Figure 2A**, the cell density of *S. meliloti* 8530 was about 3.5 × 10^7 CFU/mL (83 h) in the WSHM solution or in YM-CN broth (without carbon/nitrogen source) supplied with WSHM. While it was 2.51 × 10^9 CFU/mL in YM broth and 3.98 × 10^{10} CFU/mL in YM broth supplied with WSHM, which corresponds to 14.8-fold increase in cell density by WSHM at the stationary phase (**Figure 2A**). We could calculate from these data that only 0.09% of the total cell number increased in YM broth supplied with WSHM could be attributed to the additional nutrient sources from WSHM. Therefore, this growth enhancement can be mainly attributed to the stimulation effect of WSHM.

Synthesis of AHL in Response to WSHM

In this analysis, the AHL detector strain, *A. tumefaciens* KYC55 did not respond to WSHM but did respond to the AHL produced by *A. tumefaciens* R10 (**Supplementary Figure S1**). Thus, *A. tumefaciens* KYC55 was used to investigate the effects of WSHM on AHL production in *S. meliloti*. AHL synthesis in *S. meliloti* 8530 started in the beginning of exponential phase and reached a peak during the middle of exponential phase (50 h); while the AHL synthesis during the whole potential phase was significantly decreased (60–93%) by WSHM (**Figure 2B**). WSHM treatment also reduced the production of AHL in *S. meliloti* 1021 by 57.9% (from 65 to 28 mU/mL, 50 h of incubation) (**Supplementary Figure S1**). Additionally, increased production of AHL by *A. tumefaciens* R10 in response to WSHM was observed (**Supplementary Figure S1**). These results suggest that WSHM could regulate the QS system in *S. meliloti*.

TABLE 1 | Effects of WSHM on nodulation of *M. sativa* inoculated with *S. meliloti* Δ*qsrR* or *S. meliloti* 8530 (WT) in the greenhouse*.

Treatment	Nodule			Plant dry weight (mg/pot)
	Number of nodules per pot#	Fresh weight of nodule (mg/pot)	Nitrogenase activity (μmol C_2H_4 /h · g)	
Control	0	0	0	46.4 ± 6.3a
WSHM	0	0	0	48.9 ± 10.1a
WT	21.75 ± 2.99ab	16.86 ± 3.35a	11.75 ± 2.56a	83.0 ± 7.0b
WT+WSHM	24.60 ± 2.30b	21.90 ± 5.03a	18.38 ± 5.64b	158.0 ± 26.0c
Δ*qsrR*	24.75 ± 7.14ab	20.24 ± 8.08a	19.92 ± 4.55b	87.0 ± 49.0b
Δ*qsrR*+WSHM	16.40 ± 3.51a	21.37 ± 7.28a	17.19 ± 3.84ab	98.0 ± 11.0b

*Values are expressed as average ± standard deviation (n = 7). Values in the same column that have different letters are statistically significant as assessed by Duncan test ($P < 0.05$). #Three plants were included in each pot.

EPS Synthesis and *exoY*/*expE* Expression of *S. meliloti* in Response to WSHM

Exopolysaccharides synthesis in *S. meliloti* 1021 was low (<200 μg ml^{-1}) and was not affected by WSHM (**Figure 2C**); while EPS synthesis in *S. meliloti* 8530 was high (680 μg ml^{-1}) without WSHM and was decreased by 30.87% (480 μg ml^{-1}) with WSHM treatment.

For *expE,* a gene involved in EPS II synthesis and regulated by AHL-ExpR, its expression was down-regulated significantly by treatment with WSHM (**Figure 2D**); meanwhile, the expression of *exoY*, a gene involved in EPS I synthesis, was not affected by WSHM in *S. meliloti* 8530. All of these results suggest that WSHM did not affect the synthesis of EPS I, but decreased the production of EPS II and MLG.

Impact of WSHM on the Expression of Genes Involved in QS

In this analysis, WSHM treatment significantly down-regulated the expression of *sinI, sinR,* and *expR* in *S. meliloti* 8530 (**Figure 3A**); while in the *expR* mutant strain, *S. meliloti* 1021, WSHM only down-regulated *sinR* expression and did not alternate *sinI* expression (**Figure 3B**). In addition, the expression levels of both *sinI* and *expR* were down-regulated by WSHM in the *sinR* mutant (MG170, **Figure 3C**). These results suggest that the repression of *sinI* in *S. meliloti* 8530 by WSHM is due to the repression of *expR* and is independent of *sinR*. In the *sinI* mutant (MG32), the expression levels of the *sinR* and *expR* genes were down-regulated by WSHM (**Figure 3D**); suggesting that the effects of WSHM on *sinR* and *expR* expression are independent of *sinI*. Furthermore, the *sinR* expression was down-regulated by WSHM in both *S. meliloti* 8530 and *S. meliloti* 1021 (Δ*expR*), suggesting that the repression of *sinR* expression by WSHM is independent of ExpR.

Effects of WSHM on the Expression of *expR* in *S. meliloti* Δ*qsrR*

The expression level of the *expR* gene in *S. meliloti*Δ*qsrR* (SMc03890 deletion, see Section "Deletion of *qsrR* and Its Effect on *expR* Expression in Response to WSHM" for detail) was significantly higher than that in the WT (**Figure 4**), suggesting that QsrR represses *expR* transcription. Thus, the SMc03890 gene was renamed *qsrR,* for "quorum sensing regulator *expR* repressor." As expected, the *expR* gene was down-regulated

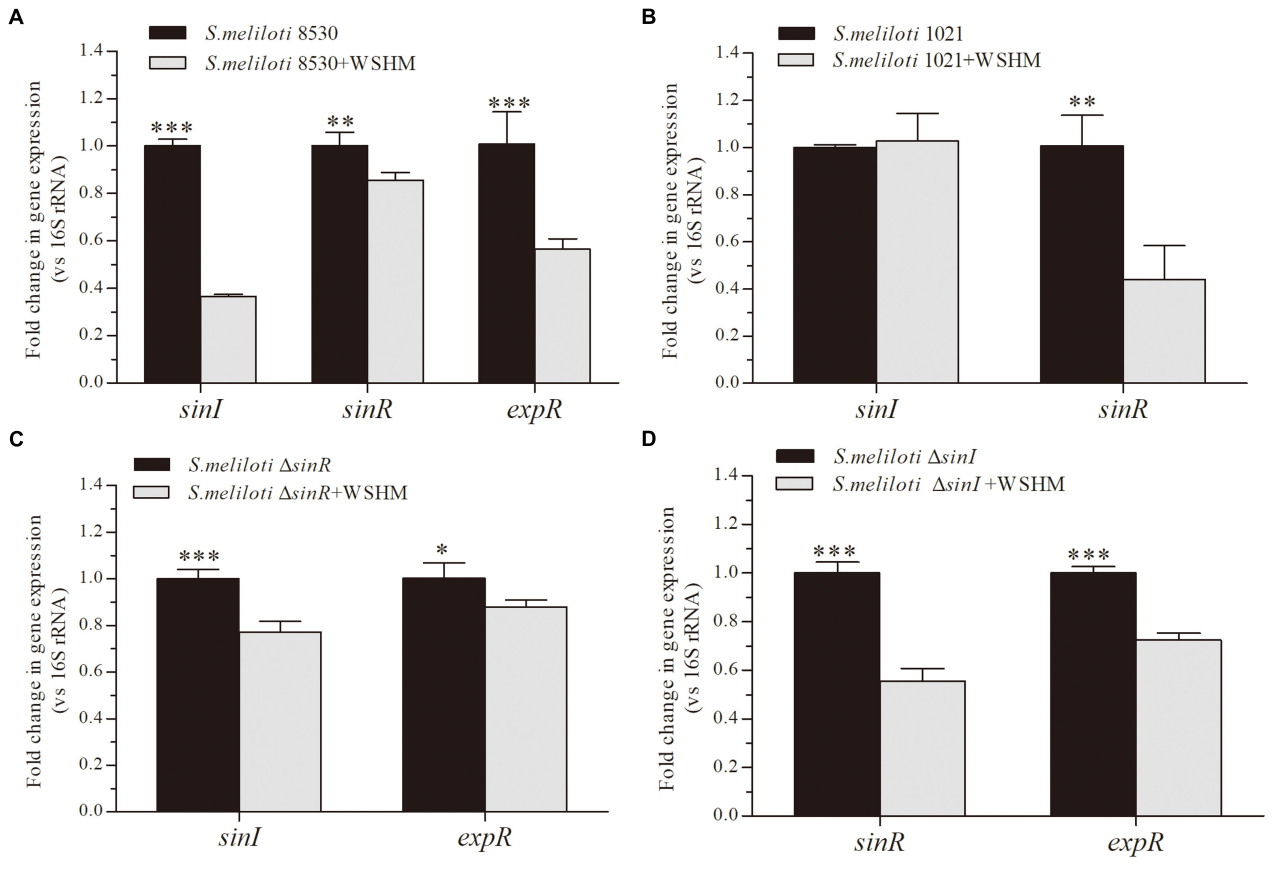

FIGURE 3 | Effects of WSHM on the expression of genes involved in the QS system in *S. meliloti* 8530 **(A)**, *S. meliloti* 1021 **(B)**, *S. meliloti* Δ*sinR* **(C)**, and *S. meliloti* Δ*sinI* **(D)**. Data are expressed as average ± SD (n = 3). Statistical significance was determined using Student's t-tests (*P < 0.05; **P < 0.01; ***P < 0.001).

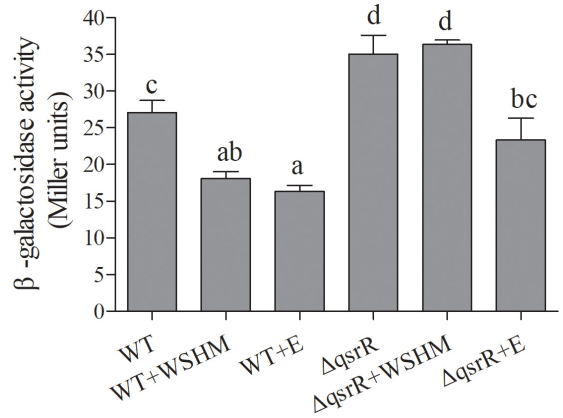

FIGURE 4 | Expression of P_{expR}-*lacZ* in *S. meliloti* 8530 (WT) and *S. meliloti* Δ*qsrR* mutant treated with either 500 mg L^{-1} WSHM or 2% alfalfa seed exudates (E), respectively. Alfalfa seed exudates were used to assess whether WSHM could repress *expR* expression in a manner similar with plant signal. Data are expressed as average ± SEM for three replicates. Different letters indicate statistical significance as assessed by Duncan tests ($P < 0.05$).

significantly in response to WSHM in *S. meliloti* 8530, but not in *S. meliloti* Δ*qsrR,* suggesting that QsrR is responsible for repressing *expR* expression in response to WSHM. Meanwhile, alfalfa seed exudates significantly repressed *expR* expression in both *S. meliloti* 8530 and *S. meliloti* Δ*qsrR* (**Figure 4**), suggesting that the repression of *expR* expression by seed exudates is independent of QsrR.

Potentiated Interaction Between QsrR and *expR* Promoter by WSHM

In order to test whether QsrR regulate the expression of *expR* directly or indirectly, EMSA were performed. As shown in **Figure 5**, a retarded DNA was observed when His_6-QsrR (3.3 μM) was added to the assay mixture, indicating that QsrR was able to bind directly with the promoter region of *expR* gene. There was no retardation in the binding specificity assay or the negative control. These findings indicate that the transcription of *expR* is directly regulated by QsrR. In the EMSA test that determined the effect of WSHM on the interaction between QsrR and *expR* promoter, no band was detected when WSHM was added into the reaction system (data not shown). This might result from the possibility that WSHM interfered with the experimental process of EMSA, such as electrophoresis or binding of DNA with nylon membrane. Therefore, the role of WSHM in regulating *expR* expression via QsrR was further investigated by a bacterial one-hybrid assay (see **Supplementary Methods** and **Supplementary Figure S3** for detail). The negative control strains *E. coli* USO (pB1H1/pH3U3-R1) and USO (pB1H1/pH3U3-R4) did not express *qsrR* and grew poorly; meanwhile, the positive strains USO (pB1H1-*qsrR*/pH3U3-R1) and USO (pB1H1-*qsrR*/pH3U3-R4) expressed *qsrR* and grew much better than the negative controls on selective medium (NM+3-AT) (**Figure 6C**). The positive strains were able to grow on medium with 2 mM of 3-AT that confirmed the ability of QsrR to bind with the promoter region of the *expR* gene. The binding region of QsrR is closer to the start of SMc03900 gene rather than that of *expR* (region R4, **Figure 6B**). In addition, the growth of the positive strains was significantly enhanced when WSHM were added to the selective medium; tolerance to 3-AT also increased from 2 to 5 mM. Meanwhile, growth of the negative control strains (USO: pB1H1/pH3U3-R1 and USO: pB1H1/pH3U3-R4) was not enhanced by WSHM on NM medium containing either 3 or 5 mM of 3-AT, further confirming that WSHM do not serve as a source of nutrients for these strains. These results suggest that QsrR can bind with the promoter region of *expR* gene, while WSHM can significantly potentiate this interaction.

Effects of WSHM on *M. sativa* Growth and Nodulation With *S. meliloti* 8530

Water-soluble humic materials treatment increased plant dry weight by 5.4% compared to the control (**Table 1**). The nitrogenase activity and plant dry weight of *M. sativa* inoculated with *S. meliloti* 8530 and 500 mg L^{-1} of WSHM were significantly increased by 56.4 and 90.36%, respectively, compared with plants inoculated only with *S. meliloti* 8530, while no statistically significant difference was detected in nodule number and nodule fresh weight (13.1 and 29.9%) between these two treatments. No significant difference was observed in nitrogenase activity, plant dry weight, nodule number, or nodule fresh weight between the *M. sativa* inoculated with *S. meliloti* Δ*qsrR* +/− WSHM. Besides, the nitrogenase activity of plants inoculated with *S. meliloti* Δ*qsrR* alone was significantly increased by 69.53% compared with plants inoculated with *S. meliloti* 8530.

Transmission electron microscopy was performed to tested whether the increased nitrogenase activity of *M. sativa* inoculated with *S. meliloti* 8530 by WSHM was due to increased bacteroid density in nodules. The TEM images revealed that the number and morphology of bacteroids in alfalfa nodules induced by *S. meliloti* 8530 were not impacted by WSHM treatment (**Supplementary Figure S4**). Thus, WSHM may have affected the nitrogenase activity of the root nodules by other mechanisms, such as regulating the expression of nitrogen fixation genes or improving the energy supply to the bacteroids.

DISCUSSION

Quorum sensing regulates metabolically costly cooperative behaviors of bacteria depending on the environmental and physiological characteristics, such as production of exopolysaccharides, motility, and life-style switches related to symbiosis with eukaryotic hosts (Hense and Schuster, 2015; Calatrava-Morales et al., 2018). Many plant-associated bacteria communicate with the plant host through QS (González and Venturi, 2013; Schikora et al., 2016). The ExpR/Sin system is the sole QS system in *S. meliloti* 8530 (Krol and Becker, 2014) (**Figure 1**) that is involved in the regulation of metabolic and symbiotic procedures (Hoang et al., 2004; Gurich and Gonzalez, 2009). Our study regarding the effects of WSHM on the ExpR/Sin system in *S. meliloti* 8530 yielded several important findings.

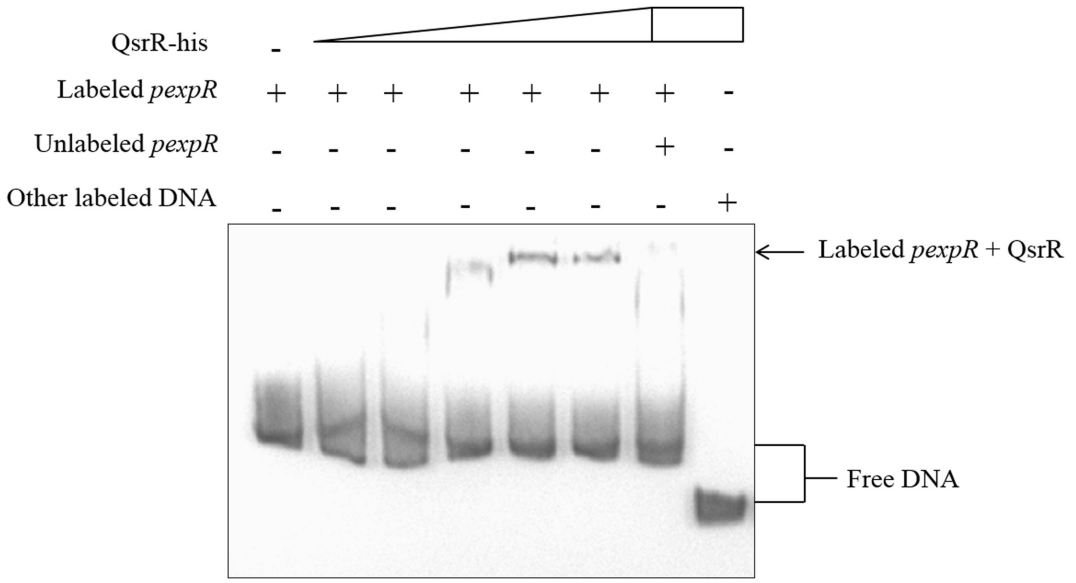

FIGURE 5 | Electrophoretic mobility shift assays confirmed direct binding of QsrR to the *expR* promoter (*pexpR*). *pexpR* is a 286 bp DNA fragment from the translational start codon of gene *expR*. Each lane contained 0.005 nM of labeled *pexpR*. The labeled *pexpR* and a ∼100-fold excess of the unlabeled *pexpR* were used in competitive assays. Labeled non-specific DNA from *Streptomyces avermitilis* was used as negative control. The amount of His_6-QsrR added in each lane were 0 μM, 0.92 Mm, 1.65 μM, 2.38 μM, 3.3 μM, 4.77 μM, 4.77 μM, and 4.77 μM, respectively.

SMc03890, renamed as *qsrR*, was shown to code a protein that directly represses *expR* gene transcription (**Figures 4–6**). As a versatile LuxR homolog regulator, ExpR directly or indirectly regulates the expression of at least 570 genes and plays a central role in the QS network in *S. meliloti* (Hoang et al., 2004; Gurich and Gonzalez, 2009; Charoenpanich et al., 2013). Thus, *qsrR* might have an essential function in different processes of *S. meliloti*. Previously, few studies on the regulation of the *expR* gene have been performed. One previous study showed that L-canavanine can repress *expR* expression as an arginine analog (Keshavan et al., 2005); meanwhile, Gao M. et al. (2015) reported that the RNA-binding protein Hfq regulates *expR* post-transcriptionally at higher population densities. Our study described QsrR as a novel repressor for *expR* transcription (**Figure 4**) and revealed the physical interaction between QsrR and the *expR* promoter by EMSA (**Figure 5**) and one-hybrid assays (**Figure 6C**). In addition, the increased nitrogenase activity in the nodules formed by *S. meliloti*Δ*qsrR* compared with those formed by *S. meliloti* 8530 (**Table 1**) suggests that QsrR may also regulate the expression of other genes, including those involved in nitrogen fixation. The function of QsrR is worthy of further research due to the versatile role of ExpR in regulating the metabolism and nodulation of *S. meliloti*. For example, the specificity of DNA sequences that can bind with QsrR might be further studied in order to reveal details in the interaction between QsrR and *expR* promoter.

The regulation of QS system in *S. meliloti* by WSHM via repressing *expR* expression (**Figures 2–4**) was evidenced for the first time, although different biological effects of humic materials on plants (Jannin et al., 2012; Traversa et al., 2013; Canellas et al., 2015; Savy et al., 2017) and bacteria (Tikhonov et al., 2010) have been demonstrated. The results from **Figures 4–6** demonstrated that QsrR may mediate the repression of *expR* expression by WSHM. It is possible that WSHM also repress *sinR* expression via additional mechanisms since QsrR cannot bind with the promoter region of *sinR* (**Supplementary Figure S2**). Moreover, our results suggest that WSHM function in a manner comparable to alfalfa seed exudates and may act as plant signal to repress *expR* gene expression in *S. meliloti* (**Figure 4**). Previous reports have demonstrated that plants are able to produce compounds that mimic or inhibit bacterial QS processes to promote their development of beneficial traits (Gao et al., 2003; Schikora et al., 2016; Nievas et al., 2017). WSHM might help plants to regulate bacterial QS and improve the symbiotic relationship between the host plant and bacteria. Compounds such as furan, pyrrole, benzpyrole, benzene rings, and esters have been identified in WSHM (Gao T.G. et al., 2015) and they may interfere with microbial QS systems (Gonzalez and Keshavan, 2006; Christensen et al., 2013). However, further investigation is needed to identify the compounds responsible for *S. meliloti* QS regulation in WSHM or alfalfa seed exudates.

In addition, the results suggest that the inactivation of rhizobia ExpR/Sin genes in nodules might be due to regulation by the plant host. Even though the QS system in *S. meliloti* has been reported to control cell functions essential for successful plant invasion, the ExpR/Sin genes were inactive in nodules due to an unknown mechanism (Gurich and Gonzalez, 2009). Alfalfa seed exudates and WSHM repressed the expression of *expR* in *S. meliloti* (**Figure 4**), suggesting that the inactivity of ExpR/Sin genes in nodules is a response of rhizobia to the host signal molecules. The repression of *expR* by host signal might due to the presence of L-canavanine in alfalfa seed exudates and L-canavanine could

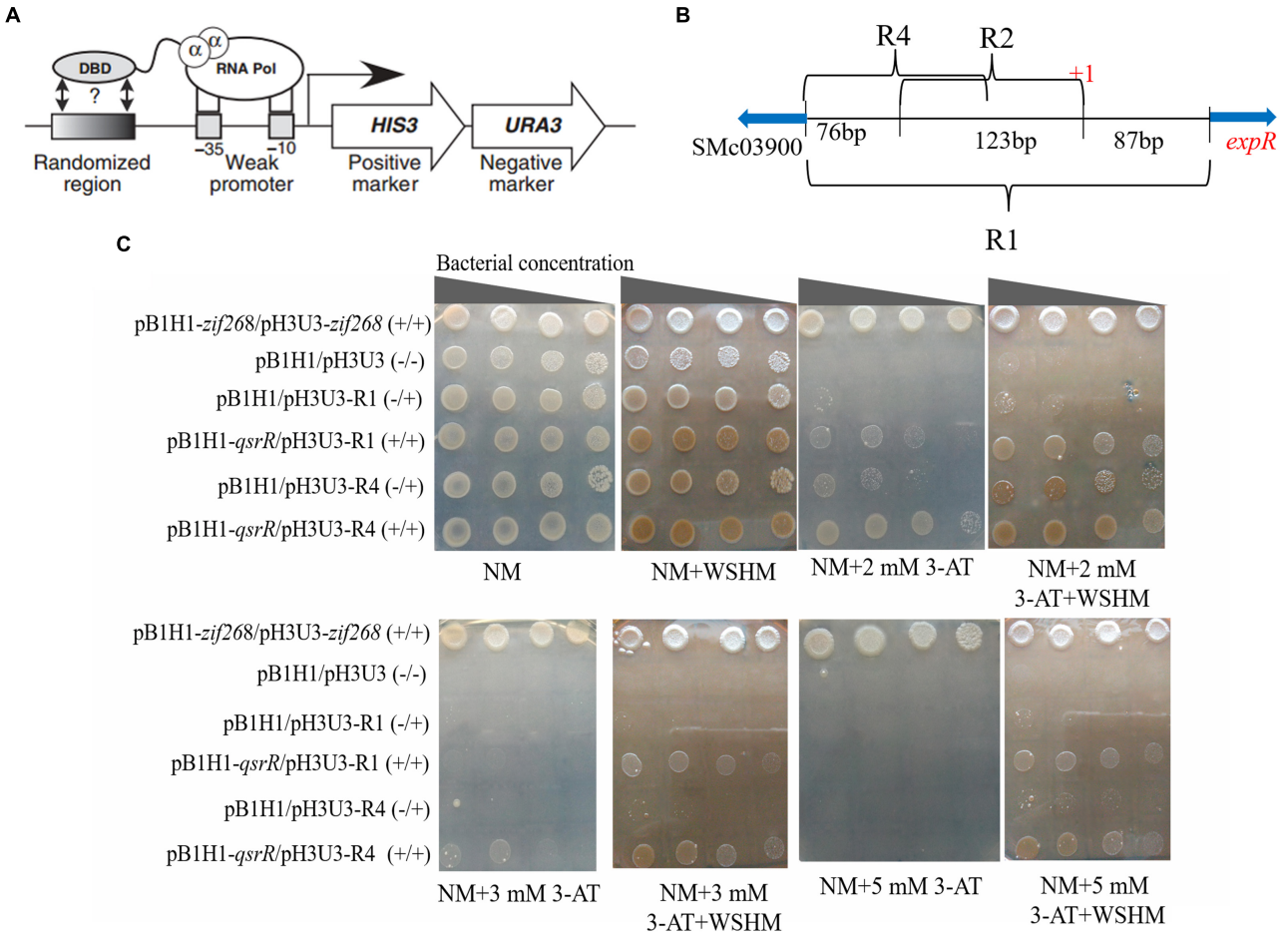

FIGURE 6 | Bacterial-one-hybrid assays showing interaction between *expR* promoter (R1, R4) and QsrR which was potentiated by WSHM. **(A)** Schematic diagram of bacterial one-hybrid system. The HIS3/URA3 cistron is in the pH3U3 prey vector. The target DNA sequences were ligated to pH3U3. The binding of DNA-binding domain (DBD, ligated to pB1H1) with the target DNA sequence enables the transcription of *HIS3* and *URA3*. The expression of *HIS3* enabled *E. coli* USO grow on NM selective medium containing the desired concentration of 3-amino-triazole (3-AT), a competitive inhibitor of HIS3. The expression of *URA3* prevented *E. coli* USO growth on medium containing 5- fluoroorotic acid (5-FOA). This figure was adopted from Meng et al. (2005). **(B)** Schematic diagram of the promoter region of gene *expR* which was cloned into pH3U3. "+1" in red was marked as the transcription start site of *expR* which was located in 87 bp upstream of ATG of *expR* (Charoenpanich et al., 2013). Regions R1, R2, and R4 were ligated to pH3U3 prey vector to detect the binding region of QsrR. Region R1 is the entire intergenic region between *expR* and SMc03900. Region R2 is the middle region of R1 which lost the 87bp right flank and the 76bp left flank of R1. Region R4 is the left flank of R1 (142 bp). The blue arrows indicate transcriptional direction of *expR* and SMc03900. Region R2 was excluded from further analyses because of the high level self-activation of (*E. coli* USO: pB1H1/pH3U3-R2) (see Materials and Methods for details). **(C)** The interaction of QsrR and *pexpR* was assayed by the growth of bacteria on selective medium (NM lacking histidine) supplemented with 2, 3, or 5 mM of 3-AT. The genetic information of test strains is labeled on the left. "+/–" indicated that *qsrR* gene was cloned into pB1H1 (+) or the plasmid was left empty (–), and similar information for pH3U3. Images were assembled and the marked lines were eliminated without modifying the observed data in Adobe Photoshop CS5.

cause misfolding of the ExpR protein (Keshavan et al., 2005), while ExpR has been reported to possess the potential for self-regulation (Charoenpanich et al., 2013).

Water-soluble humic materials can stimulate *S. meliloti* growth by repressing QS. Although WSHM contain 52.18% C and 3.72% N (Gao et al., 2012) and humic acids could act as C or N source for bacteria growth (Tikhonov et al., 2010; Gao T.G. et al., 2015), only 0.09% of the increased biomass in WSHM treatment could be contributed to the C/N supply by WSHM in YM broth (**Figure 2A**). Thus, we conclude that WSHM increase *S. meliloti* 8530 growth mainly due to the regulatory effects on cell metabolism. The repression of the QS system in *S. meliloti* 8530 by WSHM could stimulate growth (**Figures 2**, **3**), which supported the observation that QS restrains growth in *S. meliloti, M. huakuii, R. leguminosarum,* and *Rhizobium* sp. NGR234 (Wilkinson et al., 2002; He et al., 2003; Gao et al., 2006; Charoenpanich et al., 2015).

Water-soluble humic materials could regulate EPS synthesis, mainly decrease EPS II and MLG production, but do not affect EPS I production (**Figures 2C,D**). Amongst the three kinds of EPS produced by *S. meliloti* 8530 (Pérez-Mendoza et al., 2015), EPS I is the most efficient compound at initiating and maintaining infection threads (Jones, 2012). The probability of causing aberrant infection threads by EPS II, which is less

efficient than EPS I at inducing infection thread formation, is 8–10 times higher than that of EPS I (Pellock et al., 2000). Furthermore, EPS synthesis in rhizobia is energy consuming; thus, EPS II is not required if EPS I is present (Zhan et al., 1989; Mithöfer, 2002). Even though MLG is involved in the attachment of *S. meliloti* to alfalfa roots, there was no significant difference in nodulation occupancy between a wild-type and a MLG synthesis deficient mutant (Pérez-Mendoza et al., 2015). Therefore, EPS II and MLG are not likely to be essential for efficient nodulation between *S. meliloti* and alfalfa. This notion is supported by the fact that the nodule occupancy of *S. meliloti* 1021 (Δ*expR*) was 10–20% higher than that of *S. meliloti* 8530 (Charoenpanich et al., 2015). Thus, shutting down EPS II and MLG production with WSHM may promote symbiotic nitrogen fixation between *S. meliloti* and *M. sativa.* It is noteworthy that the ExpR/Sin QS system can regulate EPS II and MLG production (Mueller and González, 2010; Pérez-Mendoza et al., 2015), while EPS I biosynthesis becomes independent of QS in the absence of ExpR, and mutations to *expR* did not alter the amounts of EPS I produced (Glenn et al., 2007). This may be because MucR increases the production of EPS I independently of QS (Mueller and González, 2010). Thus, WSHM may regulate EPS production in *S. meliloti* 8530 through their regulation of the QS system.

Water-soluble humic materials improved symbiotic nitrogen fixation between *M. sativa* and *S. meliloti* (**Table 1**). Since WSHM did not affect the density of bacteroids in nodules (**Supplementary Figure S4**), the increase in nitrogenase activity of *M. sativa* following treatment with WSHM (**Table 1**) may be due to the enhanced expression of *nifA* gene via repressing *expR* expression. It has been reported that AHL-ExpR repress the expression of genes related to nitrogen fixation, such as *fixTQK,* which induce the expression of *nifA* (Hoang et al., 2004; Charoenpanich et al., 2013). In addition, the failed of significant increase in nodule number and nodule fresh weight of *M. sativa* by WSHM may result from the fact that nodule number and nodule weight are controlled by the plant host to ensure optimal growth (Mortier et al., 2012; Zipfel and Oldroyd, 2017). The promotion of nitrogen fixation between *S. meliloti* and *M. sativa* by WSHM offers an economical and efficient route for improving biological nitrogen fixation in agriculture. In a field experiment, WSHM treatment (500 mg/mL) on seeds (375 g WSHM per ha) increased alfalfa yield by 29% per year (unpublished data).

CONCLUSION

We identified QsrR as a direct repressor of *expR* (a gene central to the QS system in *S. meliloti* 8530) transcription. WSHM were proposed to repress *expR* expression by modulating the interaction between QsrR and the *expR* promoter, and ultimately decrease AHL, EPS II and MLG production. Consequently, WSHM increased the growth of *S. meliloti,* as well as symbiotic nitrogen fixation with *M. sativa*. In addition, both *expR* and *sinR* were down-regulated by WSHM with independent mechanisms. We hypothesize that QsrR may mediate the repression of *expR* expression by WSHM; however, the mechanism by which WSHM down regulate *sinR* expression requires further investigation.

AUTHOR CONTRIBUTIONS

Y-YX, J-SY, CL, and H-LY conceived and designed the study. Y-YX, R-NW, and X-QQ performed the experiments. Y-YX and E-TW wrote the manuscript. Y-YX, and B-ZL participated in the preparation of water-soluble humic materials. H-LY and W-FC helped to design the experiments and drafted the manuscript.

FUNDING

This work was supported by the National Natural Science Foundation of China (Grant No. 31770541), the Special Fund for Agro-scientific Research in the Public Interest (Grant No. 201403048-2) and by the fund for Shanxi "1331 Project" Collaborative Innovation Center.

ACKNOWLEDGMENTS

We thank Mengsheng Gao for providing *S. meliloti*Δ*sinI* and Δ*sinR* mutant strains, Li Luo for providing strain *S. meliloti* 8530, Scot A. Wolfe and Zhi Chen for providing bacterial-one-hybrid system, and Jun Zhu for providing *Agrobacterium tumefaciens* KYC55 (pJZ372, pJZ384, and pJZ410) and R10 (pCF218). We would also like to thank Lijie Sun for the very helpful discussions.

SUPPLEMENTARY MATERIAL

The Supplementary Material for this article can be found online at: https://www.frontiersin.org/articles/10.3389/fmicb.2018.03194/full#supplementary-material

REFERENCES

Bogino, P. C., Nievas, F. L., and Giordano, W. (2015). A review: quorum sensing in *Bradyrhizobium*. *Appl. Soil Ecol.* 94, 49–58. doi: 10.1016/j.apsoil.2015.04.016

Bourassa, D. V., Kannenberg, E. L., Sherrier, D. J., Buhr, R. J., and Carlson, R. W. (2017). The lipopolysaccharide lipid a long-chain fatty acid is important for *Rhizobium leguminosarum* growth and stress adaptation in free-living and nodule environments. *Mol. Plant Microbe Interact.* 30, 161–175. doi: 10.1094/MPMI-11-16-0230-R

Cai, T., Cai, W., Zhang, J., Zheng, H., Tsou, A. M., Xiao, L., et al. (2009). Host legume-exuded antimetabolites optimize the symbiotic rhizosphere. *Mol. Microbiol.* 73, 507–517. doi: 10.3390/genes9050263

Calatrava-Morales, N., McIntosh, M., and Soto, M. J. (2018). Regulation mediated by N-Acyl Homoserine Lactone quorum sensing signals in the *Rhizobium*-Legume symbiosis. *Genes* 9, 263. doi: 10.1111/j.1365-2958.2009.06790.x

Canellas, L. P., Olivares, F. L., Aguiar, N. O., Jones, D. L., Nebbioso, A., Mazzei, P., et al. (2015). Humic and fulvic acids as biostimulants in horticulture. *Sci. Hortic.* 196, 15–27. doi: 10.1016/j.scienta.2015.09.013

Chai, Y., Norman, T., Kolter, R., and Losick, R. (2010). An epigenetic switch governing daughter cell separation in *Bacillus subtilis*. *Gene Dev.* 24, 754–765. doi: 10.1101/gad.1915010

Charoenpanich, P., Meyer, S., Becker, A., and McIntosh, M. (2013). Temporal expression program of quorum sensing-based transcription regulation in *Sinorhizobium meliloti*. *J. Bacteriol.* 195, 3224–3236. doi: 10.1128/JB.00234-13

Charoenpanich, P., Soto, M. J., Becker, A., and McIntosh, M. (2015). Quorum sensing restrains growth and is rapidly inactivated during domestication of *Sinorhizobium meliloti*. *Environ. Microbiol. Rep.* 7, 373–382. doi: 10.1111/1758-2229.12262

Christensen, Q. H., Grove, T. L., Booker, S. J., and Greenberg, E. P. (2013). A high-throughput screen for quorum-sensing inhibitors that target acyl-homoserine lactone synthases. *Proc. Natl. Acad. Sci. U.S.A.* 110, 13815–13820. doi: 10.1073/pnas.1313098110

Dong, L., Yuan, Q., and Yuan, H. (2006). Changes of chemical properties of humic acids from crude and fungal transformed lignite. *Fuel* 85, 2402–2407. doi: 10.1016/j.fuel.2006.05.027

Gao, M., Tang, M., Guerich, L., Salas-Gonzalez, I., and Teplitski, M. (2015). Modulation of *Sinorhizobium meliloti* quorum sensing by Hfq-mediated post-transcriptional regulation of ExpR. *Environ. Microbiol. Rep.* 7, 148–154. doi: 10.1111/1758-2229.12235

Gao, M., Teplitski, M., Robinson, J. B., and Bauer, W. D. (2003). Production of substances by *Medicago truncatula* that Affect Bacterial Quorum Sensing. *Mol. Plant Microbe Interact.* 16, 827–834. doi: 10.1094/MPMI.2003.16.9.827

Gao, T. G., Jiang, F., Yang, J. S., Li, B. Z., and Yuan, H. L. (2012). Biodegradation of Leonardite by an alkali-producing bacterial community and characterization of the degraded products. *Appl. Microbiol. Biotechnol.* 93, 2581–2590. doi: 10.1007/s00253-011-3669-5

Gao, T. G., Xu, Y. Y., Jiang, F., Li, B. Z., Yang, J. S., Wang, E. T., et al. (2015). Nodulation characterization and proteomic profiling of *Bradyrhizobium liaoningense* CCBAU05525 in response to water-soluble humic materials. *Sci. Rep.* 5:10836. doi: 10.1038/srep10836

Gao, Y., Zhong, Z., Sun, K., Wang, H., and Zhu, J. (2006). The quorum-sensing system in a plant bacterium *Mesorhizobium huakuii* affects growth rate and symbiotic nodulation. *Plant Soil* 286, 53–60. doi: 10.1007/s11104-006-9025-3

Glenn, S. A., Gurich, N., Feeney, M. A., and Gonzalez, J. E. (2007). The ExpR/Sin quorum-sensing system controls succinoglycan production in *Sinorhizobium meliloti*. *J. Bacteriol.* 189, 7077–7088. doi: 10.1128/JB.00906-07

Gonzalez, J. E., and Keshavan, N. D. (2006). Messing with bacterial quorum sensing. *Microbiol. Mol. Biol. Rev.* 70, 859–875. doi: 10.1128/MMBR.00002-06

González, J. F., and Venturi, V. (2013). A novel widespread interkingdom signaling circuit. *Trends Plant Sci.* 18, 167–174. doi: 10.1016/j.tplants.2012.09.007

Gonzalez-Ortiz, G., Quarles Van, Ufford, H. C., Halkes, S. B., Cerda-Cuellar, M., Beukelman, C. J., et al. (2014). New properties of wheat bran: anti-biofilm activity and interference with bacteria quorum-sensing systems. *Environ. Microbiol.* 16, 1346–1353. doi: 10.1111/1462-2920.12441

Gurich, N., and Gonzalez, J. E. (2009). Role of quorum sensing in *Sinorhizobium meliloti*-Alfalfa Symbiosis. *J. Bacteriol.* 191, 4372–4382. doi: 10.1128/JB.00376-09

Hayes, M. H. B., and Wilson, W. S. (eds). (1997). *Humic Substances, Peats and Sludges: Health and Environmental Aspects*. Amsterdam: Elsevier.

He, X., Chang, W., Pierce, D. L., Seib, L. O., Wagner, J., and Fuqua, C. (2003). Quorum sensing in *Rhizobium* sp. Strain NGR234 regulates conjugal transfer (tra) gene expression and influences growth rate. *J. Bacteriol.* 185, 809–822. doi: 10.1128/JB.185.3.809-822.2003

Hense, B. A., and Schuster, M. (2015). Core principles of bacterial autoinducer systems. *Microbiol. Mol. Biol. Rev.* 79, 153–169. doi: 10.1128/MMBR.00024-14

Hoang, H. H., Becker, A., and Gonzalez, J. E. (2004). The LuxR homolog ExpR, in combination with the Sin quorum sensing system, plays a central role in *Sinorhizobium meliloti* gene expression. *J. Bacteriol.* 186, 5460–5472. doi: 10.1128/JB.186.16.5460-5472.2004

Jannin, L., Arkoun, M., Ourry, A., Laîné, P., Goux, D., Garnica, M., et al. (2012). Microarray analysis of humic acid effects on *Brassica napus* growth: involvement of N. C and S metabolisms. *Plant Soil* 359, 297–319. doi: 10.1007/s11104-012-1191-x

Jiang, F., Li, Z., Lv, Z., Gao, T., Yang, J., Qin, Z., et al. (2013). The biosolubilization of lignite by *Bacillus* sp. Y7 and characterization of the soluble products. Fuel 103, 639–645. doi: 10.1016/j.fuel.2012.08.030

Jones, K. M. (2012). Increased production of the exopolysaccharide succinoglycan enhances *Sinorhizobium meliloti* 1021 symbiosis with the host plant *Medicago truncatula*. *J. Bacteriol.* 194, 4322–4331. doi: 10.1128/JB.00751-12

Kalia, V. C. (2013). Quorum sensing inhibitors: an overview. *Biotechnol. Adv.* 31, 224–245. doi: 10.1016/j.biotechadv.2012.10.004

Keshavan, N. D., Chowdhary, P. K., Haines, D. C., and Gonzalez, J. E. (2005). L-Canavanine made by *Medicago sativa* interferes with quorum sensing in *Sinorhizobium meliloti*. *J. Bacteriol.* 187, 8427–8436. doi: 10.1128/JB.187.24.8427-8436.2005

Koul, S., Prakash, J., Mishra, A., and Kalia, V. C. (2016). Potential Emergence of Multi-quorum Sensing Inhibitor Resistant (MQSIR) Bacteria. *Indian J. Microbiol.* 56, 1–18. doi: 10.1007/s12088-015-0558-0

Krol, E., and Becker, A. (2014). Rhizobial homologs of the fatty acid transporter FadL facilitate perception of long-chain acyl-homoserine lactone signals. *Proc. Natl. Acad. Sci. U.S.A.* 111, 10702–10707. doi: 10.1073/pnas.1404929111

Luo, S., Sun, D., Zhu, J., Chen, Z., Wen, Y., and Li, J. (2014). An extracytoplasmic function sigma factor, σ25, differentially regulates avermectin and oligomycin biosynthesis in *Streptomyces avermitilis*. *Appl. Microbiol. Biotechnol.* 98, 7097–7112. doi: 10.1007/s00253-014-5759-7

Meng, X., Brodsky, M. H., and Wolfe, S. A. (2005). A bacterial one-hybrid system for determining the DNA-binding specificity of transcription factors. *Nat. Biotechnol.* 23, 988–994. doi: 10.1038/nbt1120

Mithöfer, A. (2002). Suppression of plant defence in rhizobia– legume symbiosis. *Trends Plant Sci.* 7, 440–444. doi: 10.1016/S1360-1385(02)02336-1

Mortier, V., Holsters, M., and Goormachtig, S. (2012). Never too many? *How legumes control nodule numbers. Plant Cell Environ.* 35, 245–258. doi: 10.1111/j.1365-3040.2011.02406.x

Mueller, K., and González, J. E. (2010). Complex regulation of symbiotic functions is coordinated by MucR and quorum sensing in *Sinorhizobium meliloti*. *J. Bacteriol.* 193, 485–496. doi: 10.1128/JB.01129-10

Nebbioso, A., and Piccolo, A. (2012). Advances in humeomics: enhanced structural identification of humic molecules after size fractionation of a soil humic acid. *Anal. Chim. Acta* 720, 77–90. doi: 10.1016/j.aca.2012.01.027

Nievas, F., Vilchez, L., Giordano, W., and Bogino, P. (2017). *Arachis hypogaea* L. produces mimic and inhibitory quorum sensing like molecules. *Antonie van Leeuwenhoek* 110, 891–902. doi: 10.1007/s10482-017-0862-2

Pellock, B. J., Cheng, H.-P., and Walker, G. C. (2000). Alfalfa root nodule invasion efficiency is dependent on *Sinorhizobium meliloti* polysaccharides. *J. Bacteriol.* 182, 4310–4318. doi: 10.1128/JB.182.15.4310-4318.2000

Pellock, B. J., Teplitski, M., Boinay, R. P., Bauer, W. D., and Walker, G. C. (2002). A LuxR homolog controls production of symbiotically active extracellular polysaccharide II by Sinorhizobium meliloti. *J. Bacteriol.* 184, 5067–5076. doi: 10.1128/JB.184.18.5067-5076.2002

Pérez-Montaño, F., Guasch-Vidal, B., González-Barroso, S., López-Baena, F. J., Cubo, T., Ollero, F. J., et al. (2011). Nodulation-gene-inducing flavonoids increase overall production of autoinducers and expression of N-acyl homoserine lactone synthesis genes in rhizobia. *Res. Microbiol.* 162, 715–723. doi: 10.1016/j.resmic.2011.05.002

Pérez-Montaño, F., Jimenez-Guerrero, I., Del Cerro, P., Baena-Ropero, I., Lopez-Baena, F. J., Ollero, F. J., et al. (2014). The symbiotic biofilm of *Sinorhizobium fredii* SMH12, ncessary for successful colonization and symbiosis of Glycine max cv Osumi, is regulated by quorum sensing systems and inducing flavonoids via NodD1. *PLoS One* 9:e105901. doi: 10.1371/journal.pone.0105901

Pérez-Mendoza, D., Rodríguez-Carvajal, M. Á., Romero-Jiménez, L., Farias, G. d. A., Lloret, J., Gallegos, M. T., et al. (2015). Novel mixed-linkage β-glucan activated by c-di-GMP in *Sinorhizobium meliloti*. *Proc. Natl. Acad. Sci. U.S.A.* 112, E757–E765. doi: 10.1073/pnas.1421748112

Savy, D., Canellas, L., Vinci, G., Cozzolino, V., and Piccolo, A. (2017). Humic-Like water-soluble lignins from giant reed (*Arundo donax* L.) display hormone-like activity on plant growth. *J. Plant Growth Regul.* 36, 995–1001. doi: 10.1007/s00344-017-9696-4

Schikora, A., Schenk, S. T., and Hartmann, A. (2016). Beneficial effects of bacteria-plant communication based on quorum sensing molecules of the N-acyl homoserine lactone group. *Plant Mol. Biol.* 90, 605–612. doi: 10.1007/s11103-016-0457-8

Staehelin, C., Forsberg, L. S., D'Haeze, W., Gao, M. Y., Carlson, R. W., Xie, Z. P., et al. (2006). Exo-oligosaccharides of *Rhizobium* sp. Strain NGR234 are required for symbiosis with various legumes. *J. Bacteriol.* 188, 6168–6178. doi: 10.1128/JB.00365-06

Suganuma, N., Sonoda, N., Nakane, C., Hayashi, K., Hayashi, T., Tamaoki, M., et al. (1998). Bacteroids isolated from ineffective nodules of *Pisum sativum* mutant E135 (*syml3*) lack nitrogenase activity but contain the two protein components of nitrogenase. *Plant Cell Physiol.* 39, 1093–1098. doi: 10.1093/oxfordjournals.pcp.a029307

Tikhonov, V., Yakushev, A., Zavgorodnyaya, Y. A., Byzov, B., and Demin, V. (2010). Effects of humic acids on the growth of bacteria. *Eurasian Soil Sci.* 43, 305–313. doi: 10.1134/S1064229310030087

Traversa, A., Loffredo, E., Gattullo, C. E., Palazzo, A. J., Bashore, T. L., and Senesi, N. (2013). Comparative evaluation of compost humic acids and their effects on the germination of switchgrass (*Panicum vigatum* L.). *J. Soils Sediments* 14, 432–440. doi: 10.1007/s11368-013-0653-y

Vincent, J. M. (1970). *A Manual for the Practical Study of Root Nodule Bacteria*. Oxford: Blackwell.

Wilkinson, A., Danino, V., Wisniewski-Dye, F., Lithgow, J. K., and Downie, J. A. (2002). N-Acyl-homoserine lactone inhibition of rhizobial growth is mediated by two quorum-sensing genes that regulate plasmid transfer. *J. Bacteriol.* 184, 4510–4519. doi: 10.1128/JB.184.16.4510-4519.2002

Zhan, H., Levery, S. B., Lee, C. C., and Leigh, J. A. (1989). A second exopolysaccharide of *Rhizobium meliloti* strain SU47 that can function in root nodule invasion. *Proc. Natl. Acad. Sci. U.S.A.* 86, 3055–3059. doi: 10.1073/pnas.86.9.3055

Zheng, H., Zhong, Z., Lai, X., Chen, W. X., Li, S., and Zhu, J. (2006). A LuxR/LuxI-type quorum-sensing system in a plant bacterium, *Mesorhizobium tianshanense*, controls symbiotic nodulation. *J. Bacteriol.* 188, 1943–1949. doi: 10.1128/JB.188.5.1943-1949.2006

Zhu, J., Chai, Y., Zhong, Z., Li, S., and Winans, S. C. (2003). *Agrobacterium* bioassay strain for ultrasensitive detection of *N*-acylhomoserine lactone-type quorum-sensing molecules: detection of autoinducers in *Mesorhizobium huakuii*. *Appl. Environ. Microbiol.* 69, 6949–6953. doi: 10.1128/AEM.69.11.6949-6953.2003

Zipfel, C., and Oldroyd, G. E. (2017). Plant signalling in symbiosis and immunity. *Nature* 543, 328–336. doi: 10.1038/nature22009

Conflict of Interest Statement: The authors declare that the research was conducted in the absence of any commercial or financial relationships that could be construed as a potential conflict of interest.

frontiers in Plant Science

ORIGINAL RESEARCH
published: 16 January 2019
doi: 10.3389/fpls.2018.01992

SNARE Proteins LjVAMP72a and LjVAMP72b Are Required for Root Symbiosis and Root Hair Formation in *Lotus japonicus*

Aoi Sogawa[1†], Akihiro Yamazaki[2†], Hiroki Yamasaki[1], Misa Komi[1], Tomomi Manabe[1], Shigeyuki Tajima[1], Makoto Hayashi[2] and Mika Nomura[1]*

[1] Faculty of Agriculture, Kagawa University, Kagawa, Japan, [2] RIKEN Center for Sustainable Resource Science, Yokohama, Japan

SNARE (soluble N-ethyl maleimide sensitive factor attachment protein receptor) proteins mediate membrane trafficking in eukaryotic cells. Both LjVAMP72a and LjVAMP72b are members of R-SNARE and belong to a symbiotic subgroup of VAMP72 in *Lotus japonicus*. Their sequences are closely related and both were induced in the root upon rhizobial inoculation. The expression level of *LjVAMP72a* in the nodules was higher than in the leaves or roots; however, *LjVMAP72b* was expressed constitutively in the leaves, roots, and nodules. Immunoblot analysis showed that not only LjVAMP72a but also LjVAMP72b were accumulated in a symbiosome-enriched fraction, suggesting its localization in the symbiosome membrane during nodulation. Since there was 89% similarity between LjVAMP72a and LjVAMP72b, knockdown mutant by RNAi suppressed both genes. The suppression of both genes impaired root nodule symbiosis (RNS). The number of bacteroids and the nitrogen fixation activity were severely curtailed in the nodules formed on knockdown roots (*RNAi-LjVAMP72a/72b*). Arbuscular mycorrhization (AM) was also attenuated in knockdown roots, indicating that *LjVAMP72a* and *LjVAMP72b* were required to establish not only RNS but also AM. In addition, transgenic hairy roots of *RNAi-LjVAMP72a/72b* suppressed the elongation of root hairs without infections by rhizobia or arbuscular mycorrhizal fungi. Amino acid alignment showed the symbiotic subclade of VAMP72s containing *LjVAMP72a* and *LjVAMP72b* were a conserved six amino acid region (HHQAQD) within the SNARE motif. Taken together, our data suggested that LjVAMP72a and LjVAMP72b positively controlled both symbioses and root hair formation by affecting the secretory pathway.

Keywords: ***Lotus japonicus*, nitrogen fixation, root hair, SNARE, symbiosis, VAMP72**

OPEN ACCESS

Edited by:
Kiwamu Minamisawa, Tohoku University, Japan

Reviewed by:
Norio Suganuma, Aichi University of Education, Japan
Fan Chen, Institute of Genetics and Developmental Biology (CAS), China

***Correspondence:**
Mika Nomura
nomura@ag.kagawa-u.ac.jp

[†] These authors have contributed equally to this work

Specialty section:
This article was submitted to Plant Microbe Interactions, a section of the journal Frontiers in Plant Science

Received: *13 September 2018*
Accepted: *20 December 2018*
Published: *16 January 2019*

Citation:
Sogawa A, Yamazaki A, Yamasaki H, Komi M, Manabe T, Tajima S, Hayashi M and Nomura M (2019) SNARE Proteins LjVAMP72a and LjVAMP72b Are Required for Root Symbiosis and Root Hair Formation in Lotus japonicus. Front. Plant Sci. 9:1992. doi: 10.3389/fpls.2018.01992

INTRODUCTION

Legume-rhizobia interaction has developed from complex signal exchange. Upon sensing host plant-derived flavonoids, rhizobia produce and secrete lipochito-oligosaccharides called nodulation factors (nod factors), which are then recognized by the host and trigger multiple events leading to establishing root nodule symbiosis (RNS) (Dénarié et al., 1996; Oldroyd, 2013). During nodulation, bacterial infection and nodule organogenesis take place in epidermal and cortical cells, respectively (Suzaki and Kawaguchi, 2014). Nod factors trigger deformation and curling of root hairs. Rhizobia then penetrate into root hairs via infection threads (Kouchi et al., 2010;

Oldroyd, 2013). Simultaneously, cell division occurs in the cortical layer to form nodule primordia (Oldroyd, 2013). When infection threads reach the nodule primordia, rhizobia are released from the infection threads to nodule primordia by an endocytosis-like process, in which rhizobial cells are surrounded by host-derived membranes [symbiosome membrane (SM)] called a "symbiosome" (Newcomb, 1976; Verma et al., 1978). In addition to RNS, legumes establish an endosymbiotic association with arbuscular mycorrhizal fungi (AMF). AMF secrete sulfated and non-sulfated lipochito-oligosaccharide signals (Myc-LCOs), which function as signals for allowing AMF to enter host roots (Maillet et al., 2011). AMF penetrate the root epidermis by forming hyphopodia on the root surface and extend their internal hyphae toward the inner cortex, where they form arbuscules that are surrounded by a plant plasma membrane called a periarbuscular membrane (PAM). These dynamic changes to form a SM and PAM are closely associated by membrane trafficking of endoplasmic reticulum (ER) and/or Golgi apparatus and their transport vesicles (Robertson et al., 1978; Newcomb and McIntyre, 1981; Roth and Stacy, 1989; Genre et al., 2012).

SNARE (soluble NSF attachment protein receptor) proteins are known to mediate the transport vesicle, and its molecules have a highly conserved coiled-coil domain known as a SNARE motif (Harbury, 1998; Jahn et al., 2003). The SNARE-mediated membrane trafficking forms SNARE complexes with R-SNARE on the vesicle and two or three Q-SNAREs on the target membrane. During the past decade, it has been clear that SNARE proteins play roles in general homeostatic and housekeeping functions within the cell. In *Arabidopsis*, two plasma membrane-localized Qa-SNAREs, SYP123 and SYP132, mediate membrane trafficking for root hair formation (Ichikawa et al., 2014). Recently, a symbiotic Qa-SNARE protein, SYP132A, has been shown to be generated by alternative termination of transcription and is essential for the formation of both SM and PAM in *Medicago truncatula* (Huisman et al., 2016; Pan et al., 2016). R-SNAREs located on the transport vesicles are classified into three groups: Sec22, YKT6, and VAMP7 (McNew et al., 1997; Galli et al., 1998; Gonzalez et al., 2001). VAMP7 consists of two major subgroups in plants: VAMP71 and VAMP72 (Sanderfoot, 2007). VAMP71 is known to have a similar function to mammalian VAMP7s; however, another group, VAMP72, appears to be specific to green plants (Sanderfoot, 2007). The *Arabidopsis* VAMP72 proteins except AtVAMP727 are localized in the plasma membrane (Marmagne et al., 2004; Uemura et al., 2004). To determine the specific function for symbiosis, it is better to focus on *VAMP72* in legume plants. In *M. truncatula*, VAMP721d and VAMP721e are required for both RNS and arbuscular mycorrhization (AM) (Ivanov et al., 2012). For *Lotus japonicus*, there are reports on SNARE-mediated membrane trafficking in nodules. The sed5-like *LjSYP132-1*, Qa-SNARE, contributes to nodule formation and plant growth development (Mai et al., 2006). *SYP71*, Qc-SNARE, plays a role in symbiotic nitrogen fixation (Hakoyama et al., 2012). However, there is no report on R-SNARE. In this study, we focused on an R-SNARE, *VAMP72*, in the formation of symbiotic interfaces. Our data revealed that *LjVAMP72a* and *LjVAMP72b* were required for both RNS and AM as well as for root hair development.

MATERIALS AND METHODS

Plant and Microbial Materials

Seeds of *L. japonicus* B129 Gifu (Handberg and Stougaard, 1992) were surface sterilized with 3% sodium hypochlorite and then germinated. Six-day-old seedlings were transplanted onto sterile vermiculite with a half concentration of B&D medium (Broughton and Dilworth, 1971), followed by inoculation with *Mesorhizobium loti* strain MAFF303099 at 7 days after transplanting. Plants were grown in a growth chamber at 24°C under a 16 h light/b h dark condition.

RNA Extraction and Real-Time PCR Analysis

Total RNA was isolated from various organs of *L. japonicus* using the RNeasy Plant Mini Kit according to the manufacturer's instructions (Qiagen, Tokyo, Japan). The cDNA was synthesized using PrimeScript RT Master Mix (Takara, Shiga, Japan). Quantitative RT-PCR reactions were performed in triplicate on cDNA (equivalent to about 100 ng of RNA) using the SYPR premix Ex Taq (Takara), and real time detection was performed on a Thermal Cycler Dice Real Time System II (Takara) with the primer set shown in **Supplementary Table S1**. Ubiquitin was used as an internal standard. All data were normalized because the expression levels of ubiquitin are equal in each sample. All experiments were performed with more than three biological replications.

Orthology Prediction and Phylogeny Reconstruction

Putative orthologs of *MtVAMP72d* were searched for in a database consisting of genomes and transcriptomes (i.e., all available CDSs) of 70 green plant species (Sato et al., 2008; Carleton College, and The Science Education Resource Center, 2010; Goodstein et al., 2012; Dash et al., 2016) (see **Supplementary Table S1** for the complete list). OrthoReD (Battenberg et al., 2017) was used to predict the orthologs of MtVAMP72d with its amino acid sequence as a query against the database without setting any outgroups. Based on the phylogenetic tree reconstructed by OrthoReD, a clade of putative orthologs of MtVAMP72d in several species (*A. thaliana*, *Glycine max*, *L. japonicus*, *M. truncatula*, *Solanum lycopersicum*, *Populus trichocarpa*, and *Vitis vinifera* following Ivanov et al., 2012) was determined manually. Gene names corresponding to Gene ID used in this study were listed in **Supplementary Table S2**.

The phylogeny of these putative orthologs was reconstructed. Amino acid sequences of these putative orthologs were aligned using MAFFT v7.407 (Katoh and Standley, 2013). Based on the multiple sequence alignment, the most likely phylogeny was reconstructed using RAxML v8.2.12 (Stamatakis, 2006). The best of four parallel runs was chosen as the most likely tree to avoid having the tree lodged onto a local optimum. Rapid bootstrapping of 100 replicates was also carried out using RAxML v8.2.12.

DNA Sequencing

Isolated cDNA and PCR amplified products were sequenced according to the manufacturer's instructions for the DNA sequencer (Model 3700; Applied Biosystems, CA, United States). The CDS of *LjVAMP72b* was speculated by genome sequence (Sato et al., 2008) and nodule cDNA was amplified with following primers; FW, 5′-ATGGGTCAGAACCAGAGATC-3′; RV, 5′-CCTTTCCTCGCATAATCACAA-3′ using Tks Gflex DNA polymerase (Takara, Japan). The resulting PCR product was sequenced from both strands.

Construction of *LjVAMP72a prom::GUS*, *RNAi-LjVAMP72a/72b*, and *LjVAMP72a-GFP*

To construct the *LjVAMP72a* promoter fused to the *GUS* gene, the *GUS-NOS* gene was first cloned into the *Xba*I/*Sal*I sites of p*C1300GFP*, kindly provided by Dr. H. Kouchi (National Institute of Agricultural Sciences, Tsukuba), producing the *GUS-NOS in pC1300 GFP*. The 5′-flanking regions [−1,817 to before ATG of the translation-initiation site in the *LjVAMP72a* gene (genome clone; CM0066)] was then cloned into the *GUS-NOS in pC1300GFP*, following the production of *LjVAMP72a prom::GUS*.

To construct *RNAi-LjVAMP72a/72b*, the cDNA of *LjVAMP72a* was amplified using PCR from an EST clone MR100a03 (accession No. BP083622) with the following primers: RNAi-f, 5′-ATG GAT CCC TCG AGA ATG GCT ACA CAT ATT-3′ and RNAi-r, 5′-ATA TCG ATG GTA CCT TTT GGG AAT CCA CGA-3′. The amplified cDNA fragments for the RNAi construct was subcloned into the appropriate cloning sites of *pC1300GFP*. The procedure for constructing it has been described previously (Shimomura et al., 2006). Since the amplified cDNA has high similarity between *LjVAMP72a* and *LjVAMP72b*, the knockdown mutant suppressed both genes. Therefore the mutant was named as *RNAi-LjVAMP72a/72b*.

To construct *LjVAMP72a-GFP*, used by *Arabidopsis* suspension cells, *LjVAMP72a* cDNA was fused to the *sGFP* under the control of CaMV35S-sGFP (S65T)-NOS3′ (Niwa et al., 1999), provided by Dr. Y. Niwa, University of Shizuoka.

Hairy Root Transformation

Hairy root transformation of *L. japonicus* Gifu using *Agrobacterium rhizogenes* LBA1334 was performed according to a procedure described previously (Kumagai and Kouchi, 2003). Transgenic hairy roots with GFP fluorescence were selected and transferred to vermiculite pots with a half concentration of B&D medium. Plants were grown in a growth cabinet at 24°C (16 h light/b h dark). After 1 week, the plants were transferred to pots and then inoculated with *M. loti* MAFF303099 and continued to grow in the same medium.

Histochemical GUS Staining

Hairy roots transformed with the *LjVAMP72a prom::GUS* construct were stained for 2 h at 37°C as described previously (Mai et al., 2006). GUS-stained nodules were observed using a DM6 upright microscope (Leica, Germany) with a differential interference contrast mode. Mycorrhized roots were embedded in 5% agarose, sliced in b0 μm sections using a Zero 1 super microslicer (D.S.K., Japan), and observed using the DM6 (Leica).

Transient Expression of the GFP-Fused Protein, LjVAMP72a-GFP, in *Arabidopsis* Suspension Cells

LjVAMP72a cDNA was fused to the *sGFP* of a CaMV35S-sGFP (S65T)-NOS3′ vector, producing the *LjVAMP72a-GFP*. RFP-tagged *Arabidopsis AtSYP722*, *AtSYP722-RFP*, was kindly provided by Dr. T. Ueda, University of Tokyo. The transient expression of LjVAMP72a-GFP and AtSYP722-RFP in *Arabidopsis* suspension culture cells was performed following a previous report (Ueda et al., 2001).

Detection of LjVAMP72a and LjVAMP72b Proteins

Plant tissue (0.1 g) was harvested after 35 days infection and homogenized with a mortar and pestle in extraction buffer containing 250 mM Tris-HCl (pH 7.5), 700 mM sucrose,

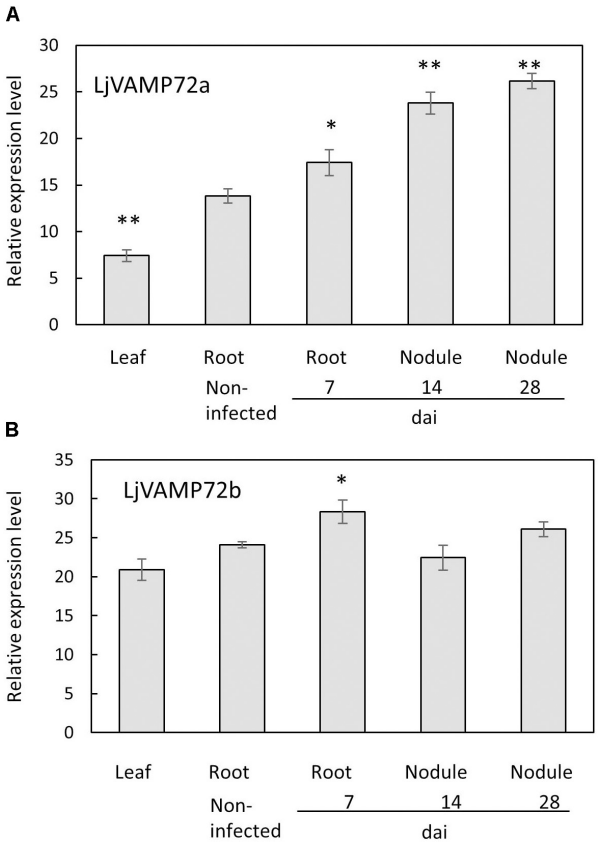

FIGURE 1 | (A,B) Expression of *LjVAMP72a* and *LjVAMP72b* mRNA after inoculation with *M. loti*. The ubiquitin was used as an internal control. dai: days after inoculation. Experiments were performed with more than three biological replications. Statistically significant differences compared with non-infected roots were indicated by asterisks (*$p < 0.05$, **$p < 0.001$).

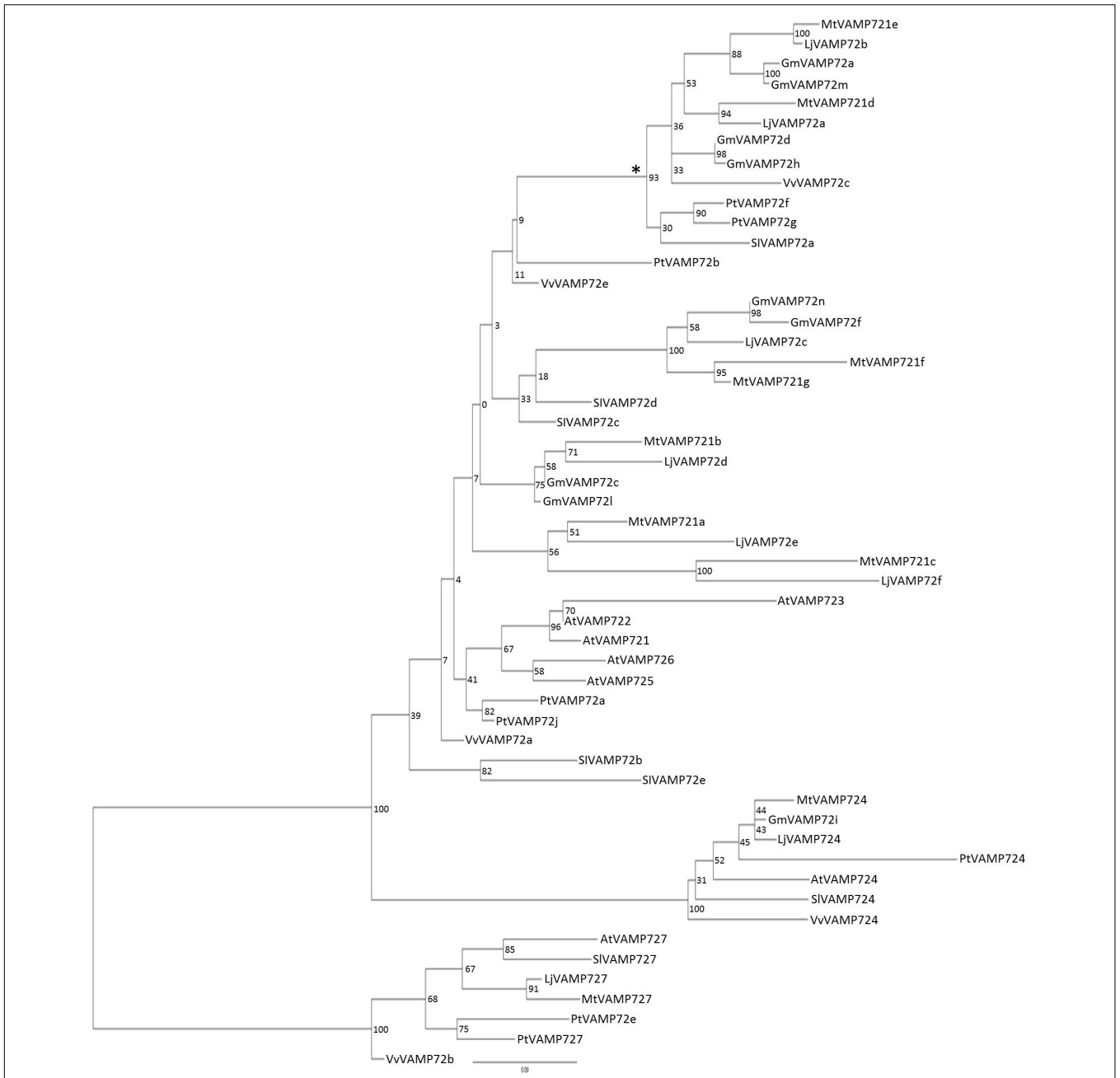

FIGURE 2 | Phylogenetic tree of VAMP72s. Phylogenetic tree of VAMP72s among *L. japonicus* (LjVAMP72s), *Medicago truncatula* (MtVAMP72s), *G. max* (GmVAMP72s), *Phaseolus vulgaris* (PvVAMP72s), *Vitis vinifera* (VvVAMP72s), *Populus trichocarpa* (PtVAMP72s), *Solanum lycopersicum* (SlVAMP72s), and *Arabidopsis thaliana* (AtVAMP72s). Gene ID corresponding to gene name was listed in **Supplementary Table S2**. The symbiotic subgroup was indicated with an asterisk. AtVAMP727 was used as an outgroup.

100 mM KCl, 2% (w/v) insoluble polyvinylpolypyrrolidone, 2% 2-mercaptoethanol, and 2% SDS. After total maceration, water-saturated phenol was added and then centrifuged at 3,000 × *g* for 20 min. The phenol fraction was isolated and five volumes of methanol plus 100 mM ammonium acetate including 10 mM 2-mercaptoethanol were added. After incubation at −80°C for 2 h, the solution was centrifuged at 15,000 × *g* for 5 min, and the pellets were resuspended with sample buffer [50 mM Tris-HCl (pH 6b), 100 mM DTT, 2% SDS, and 10% glycerol]. SDS-polyacrylamide gel electrophoresis (SDS-PAGE) was performed according to the procedure of Nomura et al. (2006). Immunoblot analysis was performed with rabbit antisera raised against a protein of (ENIEKVLDRGEKIE) antibody as the primary antibody and detected using ECL and a western blotting detection system (GE Healthcare, United Kingdom). Since the produced antibody can detect both proteins, the

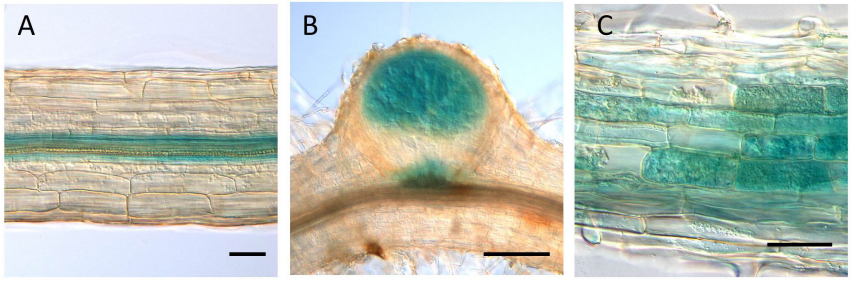

FIGURE 3 | *LjVAMP72a* promoter activity during symbioses. The promoter activity of LjVAMP72a was visualized by staining the β-glucuronidase activity in transgenic hairy roots under three different conditions: **(A)** non-inoculated, **(B)** inoculated with *M. loti* MAFF303099, and **(C)** inoculated with *R. irregularis*. Pictures were taken at 14 and 48 days after inoculation for **(B,C)**, respectively. Scale bars represent 100 μm for **(A,C)** and 200 μm for **(B)**.

resulting antibody was named anti-LjVAMP72a/72b antibody. The protein concentration was determined using the Lowry method (Lowry et al., 1951). Lb antibody raised against rabbit was kindly provided by Prof. N. Suganuma, Aichi University of Education, Japan.

Isolation of Symbiosome Fraction From the Nodules

Fresh nodules (10–15 g) at 4 weeks post infection were used to isolate the symbiosome fraction. The symbiosome fraction was isolated from Percoll discontinuous gradients (Day et al., 1989).

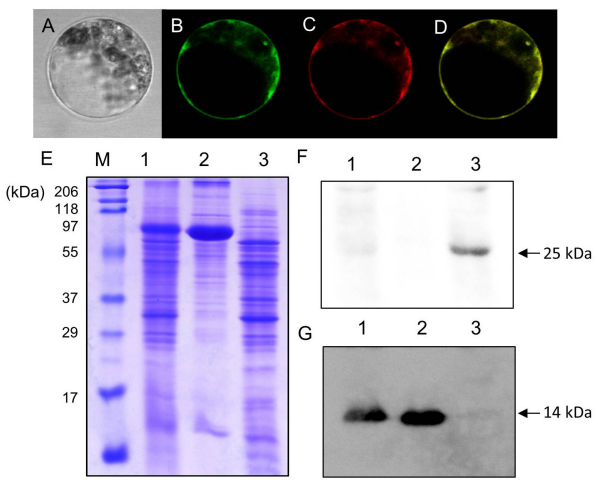

FIGURE 4 | Cellular localization of LjVAMP72a and LjVAMP72b. **(A–D)** Transient expression of LjVAMP72a in *Arabidopsis* suspension cells. The GFP-tagged LjVAMP72a **(B)** and RFP-tagged *Arabidopsis* AtSYP722 **(C)** were transiently expressed in the protoplasts of *Arabidopsis* cells. Bright field **(A)** and fluorescence images were captured from the same cells expressing each GFP-tagged LjVAMP72a **(B)** or RFP-tagged AtSYP722 **(C)**. **(D)** is a merging of **(B,C)**. **(E)** Fractionated extracts from nodules were separated by SDS-PAGE and stained with CBB. **(F,G)** Immunoblot analysis using anti-LjVAMP72a/72b antibody **(F)** or anti-Lb antibody **(G)**. Lane 1: crude extract from nodules, lane 2: supernatant of the crude extract, lane 3: symbiosome-enriched fraction of a Percoll-mediated equilibrium density-gradient centrifugation. Arrowheads indicate LjVAMP72a/72b **(F)** and Lb **(G)**, respectively.

In brief, nodule homogenate was centrifuged at 1,000 rpm for 15 min, and the pellet was then suspended with washing medium and further centrifuged at 2,000 rpm for 10 min. The resulting pellet was used for Percoll discontinuous gradients (80, 60, and 45%), and loose pellets were collected from the bottom of the 80% layer and the 60/80% interface as a symbiosome fraction. The isolated symbiosome fraction was suspended in washing medium and used for immunoblot analysis. After centrifugation at 1,000 and 2,000 rpm, both supernatants were used as a soluble fraction.

Assay for Acetylene Reduction

For acetylene reduction activity, transgenic hairy root nodules were selected under fluorescence microscopy because the GFP gene was inserted in the construct vectors. The activity of GFP-positive nodules was measured using gas chromatography (Shimadzu GC-8A; Kyoto, Japan) as previously described (Suganuma et al., 1998). Experiments were performed with more than three biological replications.

Root Hair Phenotype in *RNAi-LjVAMP72a/72b* Knockdown Roots

Hairy roots of *L. japonicus* expressing the *LjVAMP72a* and *LjVAMP72b* knockdown construct (*RNAi-LjVAMP72a/72b*) were observed using the DM6 (Leica). Pictures were tiled using Microsoft Image Composite Editor (Microsoft, United States). The length of the root hairs was measured from a position 1 mm from the root tip. The length of 50 root hairs per transgenic plant was measured using Image J. Experiments were performed with more than three biological replications.

Mycorrhization Assay

Lotus japonicus expressing the *RNAi-LjVAMP72a/72b* construct or *GFP* only (empty vector) in the hairy roots were planted in plastic pots filled with sterile vermiculites in ½ Hoagland culture medium and inoculated with *Rhizophagus irregularis* (Premier Tech, Rivière-du-Loup, Canada) at 100 spores/plant. At 6 weeks after inoculation, the roots were stained with 0.05% trypan blue, and AM events were numbered and calculated using the line intersect method (McGonigle et al., 1990). Pictures of AMF-inoculated roots were taken using the DM6 (Leica) after staining.

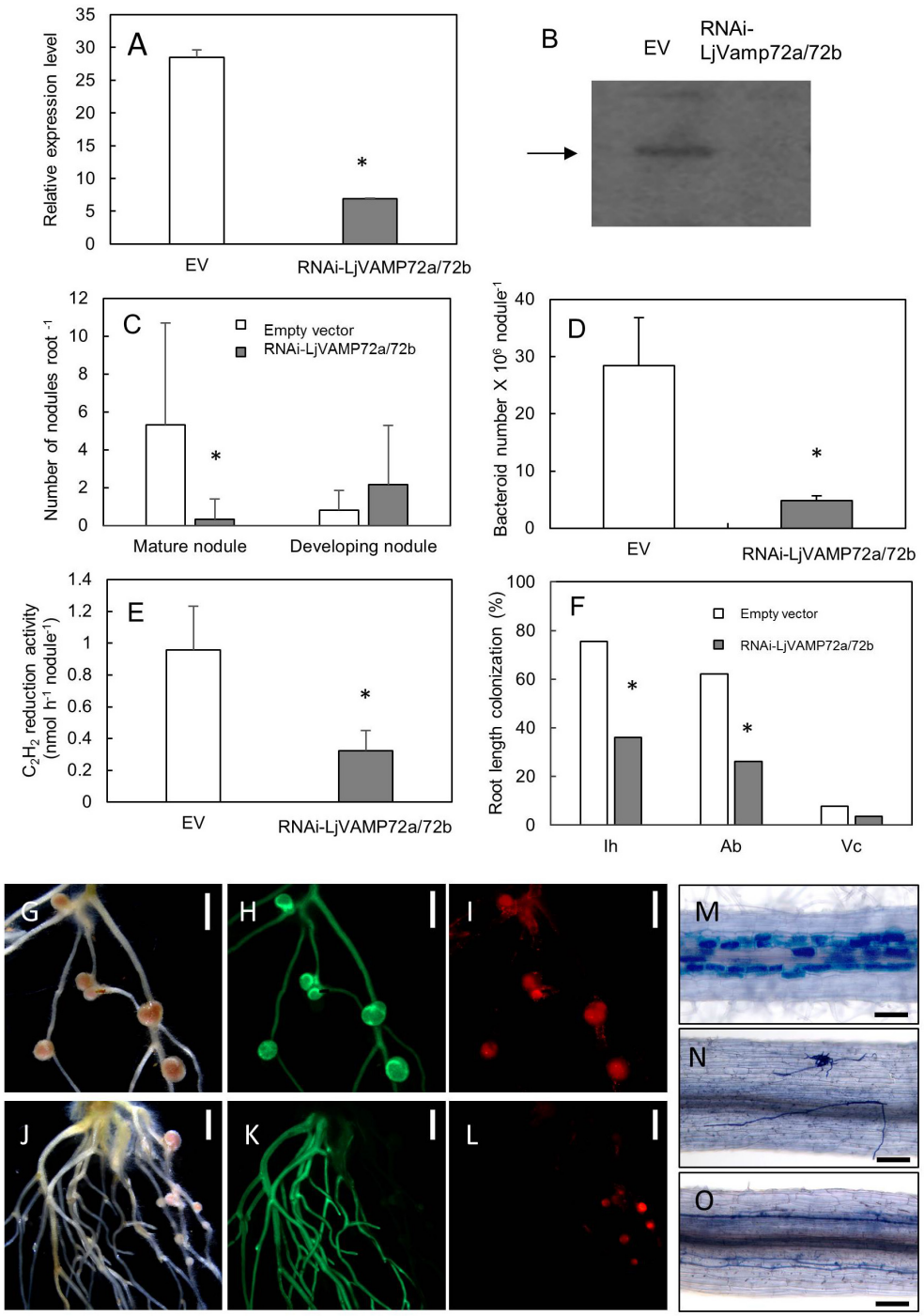

FIGURE 5 | LjVAMP72a and LjVAMP72b were required for RNS and AM. RNA interference of *LjVAMP72a/72b* was confirmed using qRT-PCR **(A)** and western blot using an anti-LjVAMP72a/72b antibody **(B)**. Arrowhead indicates LjVAMP72a. LjVAMP72a/72b knockdown attenuated the number of mature nodules **(C)**, the number of bacteroids **(D)**, acetylene reduction activity **(E)**, and arbuscular mycorrhization **(F)**. Photos of nodulation and arbuscular mycorrhization **(G–O)**. Pictures of *M. loti* DsRed13-inoculated hairy roots transformed with an empty vector **(G–I)** or RNAi-LjVAMP72a/72b **(J–L)** at 28 days after inoculation were taken with a bright field **(G,J)**, GFP fluorescence **(H,K)**, and DsRed fluorescence **(I,L)**. Transgenic hairy roots transformed with an empty vector **(M)** or with RNAi-LjVAMP72a/72b **(N,O)** were inoculated with *R. irregularis* and were stained with toluidine blue at 42 days after inoculation. The square boxes of white and gray in **(C,F)** indicate transgenic hairy roots transformed empty vector and RNAi-LjVAMP72a/72b, respectively. EV, empty vector; Ih, internal hyphae; Ab, arbuscule; Vc, vesicle. Scale bars represent 2 mm for **(G–L)** and 100 μm for **(M–O)**. All experiments were performed with more than three biological replications. Statistically significant differences compared with EV are indicated by asterisks ($p < 0.01$).

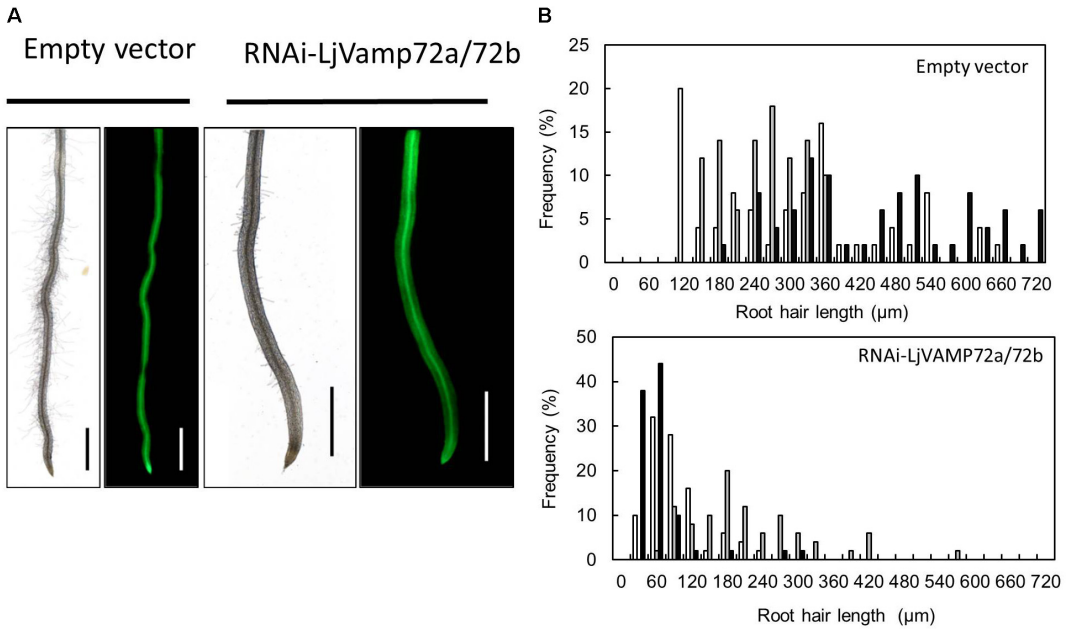

FIGURE 6 | *LjVAMP72a* and *LjVAMP72b* functioned in the development of root hairs. **(A)** Transgenic hairy roots expressing either an empty vector or RNAi-LjVAMP72a/72b were subjected to microscopic observation for bright field (left) and GFP fluorescence (right). Scale bars represent 1 mm. **(B)** Histogram of root hair length in each transgenic hairy root. Upper and lower panels show transgenic lines transformed with empty vector and RNAi-LjVAMP72a/72b, respectively. Different colors indicate independent transgenic hairy roots.

Analysis of Nodulation and Bacteroid Number in Transgenic Hairy Roots

Hairy roots were inoculated with *M. loti* strain MAFF303099 expressing a red fluorescent protein from *Discosoma* sp. (DsRed) (Maekawa et al., 2009) and used in our nodulation test. Transgenic hairy roots were selected by GFP fluorescence and observed under a fluorescence microscope (Olympus SZX9). After infection of DsRed-labeled *M. loti*, bacteroid was isolated from the nodule and the number of bacteroid in each transgenic nodule was counted using fluorescent microscope BX51 (Olympus).

RESULTS

LjVAMP72a and *LjVAMP72b* Were Induced Upon Rhizobial Inoculation

The genome database of *L. japonicus*[1] possesses several VAMP72 proteins from LjVAMP72a to LjVAMP72f, LjVAMP724 and LjVAMP727. We found that one of the LjVAMP72s, *LjVAMP72a* in *L. japonicus*, was expressed in the nodules, induced upon rhizobial inoculation, and peaked at 14 days after inoculation (**Figure 1**). In addition, the genome database contains another *LjVAMP72*, *LjVAMP72b*, which has high homology to *LjVAMP72a*. There was 89% similarity between LjVAMP72a and LjVAMP72b. The expression of the *LjVAMP72a* genes was induced in the infected roots and nodules; however, *LjVAMP72b* was expressed constitutively in the leaves, roots, and nodules (**Figure 1**).

The phylogenic analysis (**Figure 2**) showed that both LjVAMP72a and LjVAMP72b belong to the "symbiotic" subgroup and were orthologous to MtVAMP721d and MtVAMP721e, respectively, which have been reported to function in symbioses (Ivanov et al., 2012).

The GUS expression by the *LjVAMP72a* promoter was detected at the vascular bundle in non-infected roots (**Figure 3A**). The expression was strongly induced in nodule primordia upon rhizobial inoculation besides its basal expression at the vascular bundles of the roots (**Figure 3B**). The GUS induction at the vascular bundle of infected roots was detected with longer staining (data not shown). The higher GUS expression by the *LjVAMP72a* promoter in the nodules than that in the roots was identical to that expression level of the *LjVAMP72a* in nodules was higher than that in roots at 28 days after infection (**Figure 1**). AM also positively affected *LjVAMP72a* promoter activity. During AM, *LjVAMP72a* was induced in cells where arbuscules formed (**Figure 3C**). These data suggested that the *LjVAMP72a* plays a role in both symbioses, RNS and AM. Because the genome sequence of *LjVAMP72b* was not completed, we have not constructed the *LjVAMP72b* promoter fused to the GUS gene.

Localization of LjVAMP72a and LjVAMP72b in RNS

Uemura et al. (2004) identified AtVAMP722 SNARE localized in the plasma membrane in *Arabidopsis* suspension cells. **Figure 4** shows LjVAMP72a co-localization with AtVAMP722 in

[1]http://www.kazusa.or.jp/lotus/

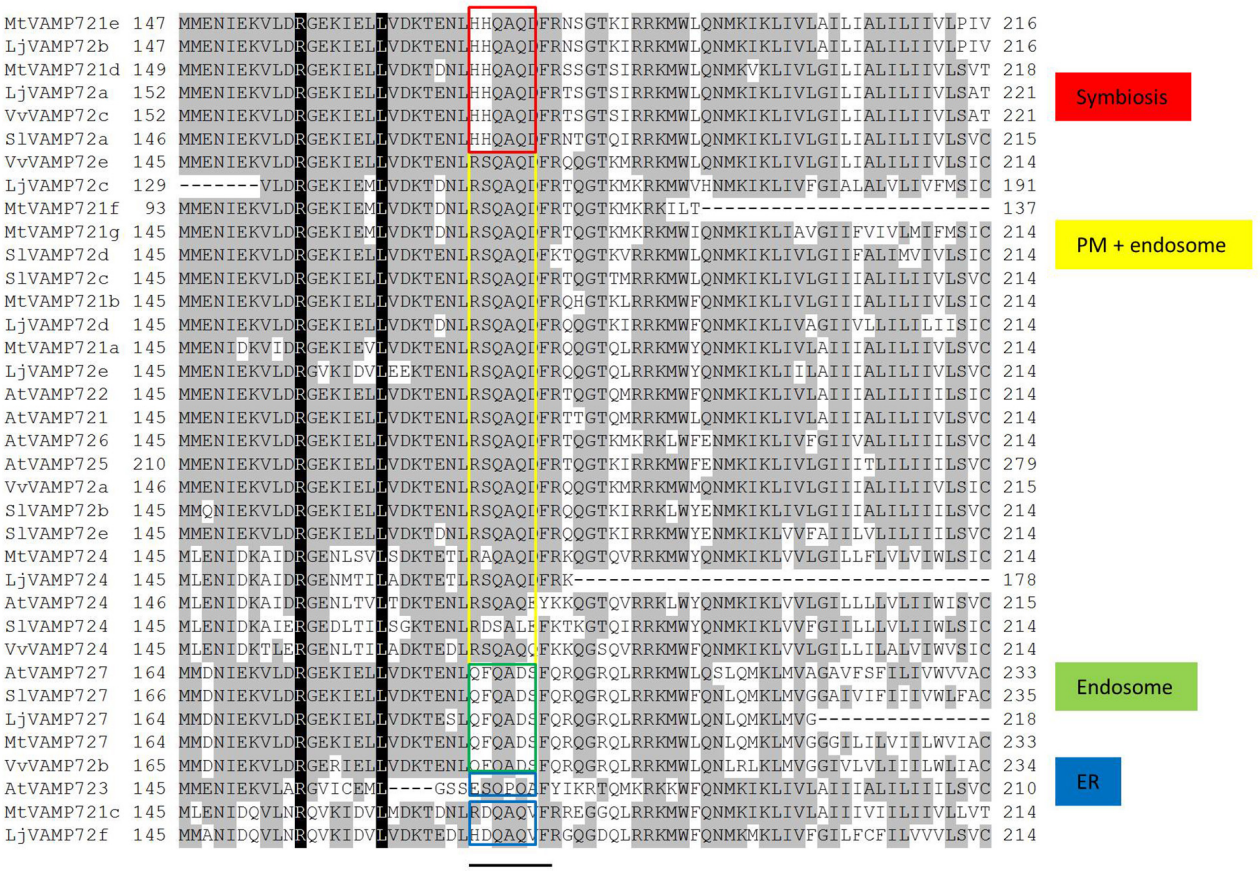

FIGURE 7 | Sequence alignment of the VAMP72 group in plants. Conserved residues are shaded in black. A bar under the alignment represents the regions of possible localization signals (Uemura et al., 2004). Red boxes are conserved in the symbiotic VAMP72 subgroup.

suspension culture cells of *A. thaliana*, indicating its localization in plasma membrane (**Figures 4A–D**). We have produced a peptide antibody that can detect both LjVAMP72a and LjVAMP72b. After isolating the symbiosome-enriched fraction, immunoblot analysis was performed (**Figure 4**). Since the deduced molecular weight of LjVAMP72a and LjVAMP72b was similar (ca. 25 kDa), one band was detected at the deduced molecular size in the symbiosome-enriched fraction (**Figure 4F**, Lane 3). The LjVAMP72a and LjVAMP72b were not fractionated in the soluble fractions in which leghaemoglobin was detected (**Figure 4G**, Lanes 1 and 2). SM contains some of components present in the plasma membrane and the results showing its localization in the plasma membrane were obtained in *Arabidopsis* suspension cells. Taken together, these data indicated that LjVAMP72a and LjVAMP72b localized in the SM.

LjVAMP72a and LjVAMP72b Functioned in Symbioses

We made the transgenic hairy roots of knockdown *LjVAMP72a* genes. RNA interference of LjVAMP72a was confirmed using qRT-PCR (**Figure 5A**). Immunoblot analysis showed that no band could be detected in a knockdown mutant, suggesting that both LjVAMP72a and LjVAMP72b were suppressed in the knockdown mutant (**Figure 5B**). Therefore, the knockdown mutant was named as *RNAi-LjVAMP72a/72b*.

The number of mature nodules was significantly lower in the *RNAi-LjVAMP72a/72b* roots compared with that in the roots transformed with an empty vector (**Figures 5C,G–L**). On the other hand, the number of developing nodules of *RNAi-LjVAMP72a/72b* increased, and the number of bacteroids and acetylene reduction activity were severely attenuated in the *RNAi-LjVAMP72a/72b* roots (**Figures 5D,E**).

LjVAMP72a and *LjVAMP72b* also positively affected AM (**Figures 5F,M–O**). Frequencies of the internal hyphae invasion, arbuscular and vesicle formation were significantly impaired in the *RNAi-LjVAMP72a/72b* knockdown roots (**Figure 5F**). **Figure 5N** shows the external hyphae did not invade the roots. Some of the infected roots only exhibited internal hyphae with almost no arbuscule when *LjVAMP72a/72b* was knocked-down (**Figure 5O**), whereas the empty vector control barely affected arbuscule formation (**Figure 5M**). These data speculate the symbiotic membranes would be developed by the vesicle trafficking through the LjVAMP72a and LjVAMP72b, resulting that the *RNAi-LjVAMP72a/72b* knockdown attenuated symbioses. These results were in line

with a previous report in which the VAMP721d and VAMP721e double knockdown attenuated the number of nodules in *M. truncatula* (Ivanov et al., 2012).

LjVAMP72a and *LjVAMP72b* Positively Controls the Elongation of Root Hairs

Suppression of *LjVAMP72a* and *LjVAMP72b* mRNAs also affected the elongation of root hairs. *RNAi-LjVAMP72a/72b* knockdown roots exhibited significantly fewer root hairs or almost root hair-less phenotypes (**Figure 6**), suggesting that LjVAMP72a and LjVAMP72b functioned not only in symbioses but also in the development of root hairs.

Amino Acid Sequence Alignment Conserved for the Symbiosis

SNARE proteins have a highly conserved coined-coil domain, called a SNARE motif (Harbury, 1998). Uemura et al. (2004) found a six amino acid region that could be classified by its subcellular localization within the SNARE motif. **Figure 7** shows the sequence alignment of the VAMP72 groups. The aligned sequences were selected from legume plants, non-legume plants including *A. thaliana*. The alignment shows that the six amino acid regions (RSQAQD and QFQADS) of VAMP72s in *L. japonicus* were identical to the AtVAMP72s that localize in plasma membrane and endosome, respectively. These common six amino acid regions were detected in other species: *M. truncatula*, *A. thaliana*, *S. lycopersicum*, and *Vitis vulgaris*. A different six amino acid region (HHQAQD) was conserved in the "symbiotic" VAMP72 subgroup, including LjVAMP72a and LjVAMP72b (**Figure 7**).

DISCUSSION

For membrane trafficking, VAMP72 of R-SNARE is specific to green plants (Sanderfoot, 2007). Based on genome sequence information (Sato et al., 2008), rhizobia-induced *LjVAMP72a* and *LjVAMP72b* are classified in the symbiotic VAMP72 subgroup.

The producing knockdown mutant (*RNAi-LjVAMP72a/72b*) was suppressed both expressions (**Figure 5B**). In addition, RNS and AM were severely reduced on the *LjVAMP72a/72b* knockdown roots (**Figure 5**) and LjVAMP72a and LjVAMP72b were enriched in the symbiosome-containing fraction (**Figure 4F**), so LjVAMP72a and LjVAMP72b might be involved in the formation of a SM as reported in *M. truncatula* (Ivanov et al., 2012).

Both *LjVAMP72a* and *LjVAMP72b* were expressed in the nodules. The only difference was that the expression level of *LjVAMP72a* in the nodules was higher than that in the leaves or roots; however, *LjVAMP72b* was expressed constitutively in the leaves, roots, and nodules (**Figure 1**). A slight induction of *LjVAMP72b* appeared in the infected roots at 7 days compared with the non-infected roots. The data suggest that the expression ratio of *LjVAMP72a* and *LjVAMP72b* plays a role in forming the infection thread and the following SM. More data is needed to determine the different functions of the two.

Uemura et al. (2004) speculated that the six amino acid region within the SNARE motif differs depending on the subcellular localization in *Arabidopsis* VAMP72 proteins. From the genome data base, there were eight VAMP 72 genes in *L. japonicus* (**Figure 2**). In the alignment analysis (**Figure 7**), we could speculate the membrane localization of these Vamp72s from six amino acid region within the SNARE motif. Moreover, we found the symbiotic subgroup containing LjVAMP72a and LjVAMP72b conserved a different six amino acid region (HHQAQD). The symbiotic subgroup includes to non-legume genes, such as SlVAMP72a and VvVAMP72c (**Figure 2**, Ivanov et al., 2012) in *S. lycopersicum* and *V. vulgaris*, respectively, indicating that the *VAMP72s* with the six amino acid region (HHQAQD) is conserved among the R-SNARE for the localization of AM. The development of SM by LjVAMP72a and LjVAMP72b would be recruited during the evolution. The localization of another VAMP72s in *L. japonicus* (**Figure 7**) could be speculated from the six amino acid region that of AtVAMP72s localizing in the plasma membrane or endosome, except LjVAMP72f. The LjVAMP72f has a higher similarity to MtVAMP72c; however, there was no conserved amino acid in AtVAM72s of *A. thaliana*. Future studies may give more insight into the localization of LjVAMP72f.

We also found that LjVAMP72a/72b knockdown roots exhibited impaired root hair elongation (**Figure 6**), which was not reported in *M. truncatula* (Ivanov et al., 2012). Root hairs normally emerge at the apical end of root epidermal cells, implying that these cells are polarized because of vesicle targeting (Enami et al., 2009). In *Arabidopsis*, VAMP721/722/724 localizes in root hairs, and these AtVAMP72s form SNARE complexes with Q-SNARE, SYP123, and SYP132 (Ichikawa et al., 2014). LjVAMP72a and LjVAMP72b belonging to VAMP721 would have dual functions of root hair development and symbiotic membrane formation. Therefore, the Q-SNAREs responsible for root hair development and symbiotic membrane formation need to be confirmed. Taken together, our data suggested that the LjVAMP72a and LjVAMP72b played a role in RNS and AM as well as root hair development. Dual physiological activity of LjVAMP72a and LjVAMP72b likely involves a change in the vesicle cargo during the transition from plant growth to the symbiosis stage.

AUTHOR CONTRIBUTIONS

AS and AY performed most of the experiments and contributed equally. MH and MN designed the experiments. HY, MK, TM, and ST participated in some part of the study.

FUNDING

This work was supported by a Grant-in-Aid (Grant No. 25450084, MN) and by the Special Coordination Funds for Promoting Science and Technology from the Ministry of Education, Culture, Sports, Science and Technology of Japan.

ACKNOWLEDGMENTS

We thank Dr. Keisuke Yokota, National Institute of Agrobiological Sciences, Tsukuba, Japan and Dr. Shusei Sato, Tohoku University, Japan for their technical support.

SUPPLEMENTARY MATERIAL

The Supplementary Material for this article can be found online at: https://www.frontiersin.org/articles/10.3389/fpls.2018.01992/full#supplementary-material

REFERENCES

Battenberg, K., Lee, E. K., Chiu, J. C., Berry, A. M., and Potter, D. (2017). OrthoReD: A rapid and accurate orthology prediction tool with low computational requirement. *BMC Bioinformatics* 18:310. doi: 10.1186/s12859-017-1726-5

Broughton, W. J., and Dilworth, M. J. (1971). Control of leghaemoglobin synthesis in snake beans. *Biochem. J.* 125, 1075–1080. doi: 10.1042/bj1251075

Carleton College, and The Science Education Resource Center (2010). *Genome Explorer*. Available at: https://serc.carleton.edu/exploring_genomics/index.html

Dash, S., Cannon, E. K. S., Kalberer, S. R., Farmer, A. D., and Cannon, S. B. (2016). "PeanutBase and other bioinformatic resources for peanut (Chapterb)," in *Peanuts Genetics, Processing, and Utilization*, eds H. T. Stalker and R. F. Wilson (New York, NY: Elsevier), 241–252.

Day, D., Price, G., and Udvardi, M. (1989). Membrane interface of the *Bradyrhizobium japonicum–Glycine max* symbiosis: peribacteroid units from soyabean nodules. *Aust. J. Plant Physiol.* 16:69. doi: 10.1071/PP9890069

Dénarié, J., Debellé, F., and Promé, J.-C. (1996). Rhizobium Lipo-chitooligosaccharide nodulation factors: signaling molecules mediating recognition and morphogenesis. *Annu. Rev. Biochem.* 65, 503–535. doi: 10.1146/annurev.bi.65.070196.002443

Enami, K., Ichikawa, M., Uemura, T., Kutsuna, N., Hasezawa, S., Nakagawa, T., et al. (2009). Differential expression control and polarized distribution of plasma membrane-resident SYP1 SNAREs in *Arabidopsis thaliana*. *Plant Cell Physiol.* 50, 280–289. doi: 10.1093/pcp/pcn197

Galli, T., Zahraoui, A., Vaidyanathan, V. V., Raposo, G., Tian, J. M., Karin, M., et al. (1998). A novel tetanus neurotoxin-insensitive vesicle-associated membrane protein in SNARE complexes of the apical plasma membrane of epithelial cells. *Mol. Biol. Cell* 9, 1437–1448. doi: 10.1091/mbc.9.6.1437

Genre, A., Ivanov, S., Fendrych, M., Faccio, A., Zarsky, V., Bisseling, T., et al. (2012). Multiple exocytotic markers accumulate at the sites of perifungal membrane biogenesis in arbuscular mycorrhizas. *Plant Cell Physiol.* 53, 244–255. doi: 10.1093/pcp/pcr170

Gonzalez, L. C. Jr., Weis, W. I., and Scheller, R. H. (2001). A novel SNARE N-terminal domain revealed by the crystal structure of Sec22b. *J. Biol. Chem.* 276, 24203–24211. doi: 10.1074/jbc.M101584200

Goodstein, D. M., Shu, S., Howson, R., Neupane, R., Hayes, R. D., Fazo, J., et al. (2012). Phytozome: a comparative platform for green plant genomics. *Nucleic Acids Res.* 40, D1178–D1186. doi: 10.1093/nar/gkr944

Hakoyama, T., Oi, R., Hazuma, K., Suga, E., Adachi, Y., Kobayashi, M., et al. (2012). The SNARE protein SYP71 expressed in vascular tissues is involved in symbiotic nitrogen fixation in *Lotus japonicus* nodules. *Plant Physiol.* 160, 897–905. doi: 10.1104/pp.112.200782

Handberg, K., and Stougaard, J. (1992). *Lotus japonicus*, an autogamous, diploid legume species for classical and molecular genetics. *Plant J.* 2, 487–496. doi: 10.1111/j.1365-313X.1992.00487.x

Harbury, P. A. B. (1998). Springs and zippers: coiled coils in SNARE-mediated membrane fusion. *Structure* 6, 1487-1491. doi: 10.1016/S0969-2126(98)00147-6

Huisman, R., Hontelez, J., Mysore, K. S., Wen, J., Bisseling, T., and Limpens, E. (2016). A symbiosis-dedicated SYNTAXIN OF PLANTS 13II isoform controls the formation of a stable host-microbe interface in symbiosis. *New Phytol.* 211, 1338–1351. doi: 10.1111/nph.13973

Ichikawa, M., Hirano, T., Enami, K., Fuselier, T., Kato, N., Kwon, C., et al. (2014). Syntaxin of plant proteins SYP123 and SYP132 mediate root hair tip growth in *Arabidopsis thaliana*. *Plant Cell Physiol.* 55, 790–800. doi: 10.1093/pcp/pcu048

Ivanov, S., Fedorova, E. E., Limpensa, E., Mita, S. D., Genre, A., Bonfante, P., et al. (2012). Rhizobium–legume symbiosis shares an exocytotic pathway required for arbuscule formation. *Proc. Natl. Acad. Sci. U.S.A.* 109, 8316–8321. doi: 10.1073/pnas.1200407109

Jahn, R., Lang, T., and Sudhof, T. C. (2003). Membrane fusion. *Cell* 112, 519–533. doi: 10.1016/S0092b674(03)00112-0

Katoh, K., and Standley, D. M. (2013). MAFFT multiple sequence alignment software version 7: improvements in performance and usability. *Mol. Biol. Evol.* 30, 772–780. doi: 10.1093/molbev/mst010

Kouchi, H., Imaizumi-Anraku, H., Hayashi, M., Hakoyama, T., Nakagawa, T., Umehara, Y., et al. (2010). How many peas in a pod? Legume genes responsible for mutualistic symbioses underground. *Plant Cell Physiol.* 51, 1381–1397. doi: 10.1093/pcp/pcq107

Kumagai, H., and Kouchi, H. (2003). Gene silencing by expression of hairpin RNA in *Lotus japonicus* roots and root nodules. *Mol. Plant Microbe Interact.* 16, 663–668. doi: 10.1094/MPMI.2003.16b.663

Lowry, O. H., Rosebrough, N. J., Farr, A. L., and Randall, R. J. (1951). Protein measurement with the Folin phenol reagent. *J. Biol. Chem.* 193, 265–275.

Maekawa, T., Maekawa-Yoshikawa, M., Takeda, N., Imaizumi-Anraku, H., Murooka, Y., and Hayashi, M. (2009). Gibberellin controls the nodulation signaling pathway in *Lotus japonicus*. *Plant J.* 58, 183–194. doi: 10.1111/j.1365-313X.2008.03774.x

Mai, H. T., Nomura, M., Takegawa, K., Asamizu, E., Sato, S., Kato, T., et al. (2006). Identification of a Sed5-like SNARE gene LjSYP32-1 that contributes to nodule tissue formation of *Lotus japonicus*. *Plant Cell Physiol.* 47, 829–838. doi: 10.1093/pcp/pcj054

Maillet, F., Poinsot, V., André, O., Puech-Pagès, V., Haouy, A., Gueunier, M., et al. (2011). Fungal lipochitooligosaccharide symbiotic signals in arbuscular mycorrhiza. *Nature* 469, 58–63. doi: 10.1038/nature09622

Marmagne, A., Rouet, M.-A., Ferro, M., Rolland, N., Alcon, C., Joyard, J., et al. (2004). Identification of new intrinsic proteins in *Arabidopsis* plasma membrane proteome. *Mol. Cell Proteomics* 3, 675–691. doi: 10.1074/mcp.M400001-MCP200

McGonigle, T. P., Miller, M. H., Evans, D. G., Fairchild, G. L., and Swan, J. A. (1990). A new method which gives an objective measure of colonization of roots by vesicular—arbuscular mycorrhizal fungi. *New Phytol.* 115, 495–501. doi: 10.1111/j.1469b137.1990.tb00476.x

McNew, J. A., Søgaard, M., Lampen, N. M., Machida, S., Ye, R. R., Lacomis, L., et al. (1997). Ykt6p, a prenylated SNARE essential for endoplasmic reticulum-Golgi transport. *J. Biol. Chem.* 272, 17776–17783. doi: 10.1074/jbc.272.28.17776

Newcomb, W. (1976). A correlated light and electron microscopy study of symbiotic growth and differentiation in *Pisum sativum* root nodules. *Can. J. Bot.* 54, 2163–2186. doi: 10.1139/b76-233

Newcomb, W., and McIntyre, L. (1981). Development of root nodules of mung bean (*Vigna radiata*): a reinvestigation of endocytosis. *Can. J. Bot.* 59, 2478–2499. doi: 10.1139/b81-299

Niwa, Y., Hirano, T., Yoshimoto, K., Shimizu, M., and Kobayashi, H. (1999). Non-invasive quantitative detection and applications of non-toxic, S65T-type green fluorescent protein in living plants. *Plant J.* 18, 455–463. doi: 10.1046/j.1365-313X.1999.00464.x

Nomura, M., Mai, H. T., Fujii, M., Hata, S., Izui, K., and Tajima, S. (2006). Phosphoenolpyruvate carboxylase plays a crucial role in limiting nitrogen fixation in lotus japonicus nodules. *Plant Cell Physiol.* 47, 613–621. doi: 10.1093/pcp/pcj028

Oldroyd, G. E. D. (2013). Speak, friend, and enter: signalling systems that promote beneficial symbiotic associations in plants. *Nat. Rev. Microbiol.* 11, 252–263. doi: 10.1038/nrmicro2990

Pan, H., Oztas, O., Zhang, X., Wu, X., Stonoha, C., Wang, E., et al. (2016). A symbiotic SNARE protein generated by alternative termination of transcription. *Nat. Plants* 2:15197. doi: 10.1038/nplants.2015.197

Robertson, J. G., Lyttleton, P., Bullivant, S., and Grayston, G. F. (1978). Membranes in lupin root nodules. I. the role of Golgi bodies in the biogenesis of infection threads and peribacteroid membranes. *J. Cell Sci.* 30, 129–149.

Roth, L. E., and Stacy, G. (1989). Cytoplasmic membrane systems involved in bacterium release into soybean nodule cells as studied with two *Bradyrhizobium japonicum* mutant strains. *Eur. J. Cell. Biol.* 49, 24–32.

Sanderfoot, A. (2007). Increases in the number of SNARE genes parallels the rise of multicellularity among the green plants. *Plant Physiol.* 144, 6–17. doi: 10.1104/pp.106.092973

Sato, S., Nakamura, Y., Kaneko, T., Asamizu, E., Kato, T., Nakao, M., et al. (2008). Genome structure of the legume, *Lotus japonicus*. *DNA Res.* 15, 227–239. doi: 10.1093/dnares/dsn008

Shimomura, K., Nomura, M., Tajima, S., and Kouchi, H. (2006). LjnsRING, a novel RING finger protein, is required for symbiotic interactions between *Mesorhizobium loti* and *Lotus japonicus*. *Plant Cell Physiol.* 47, 1572–1581. doi: 10.1093/pcp/pcl022

Stamatakis, A. (2006). RAxML-VI-HPC: maximum likelihood-based phylogenetic analyses with thousands of taxa and mixed models. *Bioinformatics* 22, 2688–2690. doi: 10.1093/bioinformatics/btl446

Suganuma, N., Sonoda, N., Nakane, C., Hayashi, K., Hayashi, T., Tamaoki, M., et al. (1998). Bacteroids isolated from infective nodules of *Pisum sativum* mutant E135 (*sym13*) lack nitrogenase activity but contain the two protein components of nitrogenase. *Plant Cell Physiol.* 39, 1093–1098. doi: 10.1093/oxfordjournals.pcp.a029307

Suzaki, T., and Kawaguchi, M. (2014). Root nodulation: a developmental program involving cell fate conversion triggered by symbiotic bacterial infection. *Curr. Opin. Plant Biol.* 21, 16–22. doi: 10.1016/j.pbi.2014.06.002

Ueda, T., Yamaguchi, M., Uchimiya, H., and Nakano, A. (2001). Ara6, a plant-unique novel type Rab-GTPase, functions in the endocytic pathway of *Arabidopsis thaliana*. *EMBO J.* 20, 4730–4741. doi: 10.1093/emboj/20.17.4730

Uemura, T., Ueda, T., Ohniwa, R. L., Nakano, A., Takeyasu, K., and Sato, M. H. (2004). Systematic analysis of SNARE molecules in *Arabidopsis*: dissection of the post-Golgi network in plant cells. *Cell Struct. Funct.* 29, 49–65. doi: 10.1247/csf.29.49

Verma, D. P., Kazazian, V., Zogbi, V., and Bal, A. K. (1978). Isolation and characterization of the membrane envelope enclosing the bacteroids in soybean root nodules. *J. Cell Biol.* 78, 919–936. doi: 10.1083/jcb.78.3.919

Conflict of Interest Statement: The authors declare that the research was conducted in the absence of any commercial or financial relationships that could be construed as a potential conflict of interest.

frontiers in Plant Science

ORIGINAL RESEARCH
published: 01 February 2019
doi: 10.3389/fpls.2019.00075

Genetic Analysis and Mapping of QTLs for Soybean Biological Nitrogen Fixation Traits Under Varied Field Conditions

*Qing Yang†, Yongqing Yang†, Ruineng Xu, Huiyong Lv and Hong Liao**

Root Biology Center, College of Resources and Environment, Fujian Agriculture and Forestry University, Fuzhou, China

OPEN ACCESS

Edited by:
Hon-Ming Lam, The Chinese University of Hong Kong, China

Reviewed by:
Brett James Ferguson, The University of Queensland, Australia
Oswaldo Valdes-Lopez, National Autonomous University of Mexico, Mexico
Yinglong Chen, University of Western Australia, Australia

***Correspondence:**
Hong Liao
hliao@fafu.edu.cn;
hliao@scau.edu.cn

†These authors have contributed equally to this work

Specialty section:
This article was submitted to Plant Microbe Interactions, a section of the journal Frontiers in Plant Science

Received: *16 August 2018*
Accepted: *17 January 2019*
Published: *01 February 2019*

Citation:
Yang Q, Yang Y, Xu R, Lv H and Liao H (2019) Genetic Analysis and Mapping of QTLs for Soybean Biological Nitrogen Fixation Traits Under Varied Field Conditions. Front. Plant Sci. 10:75. doi: 10.3389/fpls.2019.00075

Soybean is an important economic and green manure crop that is widely used in intercropping and rotation systems due to its high biological nitrogen fixation (BNF) capacity and the resulting reduction in N fertilization. However, the genetic mechanisms underlying soybean BNF are largely unknown. Here, two soybean parent genotypes contrasting in BNF traits and 168 $F_{9:11}$ recombinant inbred lines (RILs) were evaluated under four conditions in the field. The parent FC1 always produced more big nodules, yet fewer nodules in total than the parent FC2 in the field. Furthermore, nodulation in FC1 was more responsive to environmental changes than that in FC2. Broad-sense heritability (h^2_b) for all BNF traits varied from 0.48 to 0.87, which suggests that variation in the observed BNF traits was primarily determined by genotype. Moreover, two new QTLs for BNF traits, *qBNF-16* and *qBNF-17*, were identified in this study. The *qBNF-16* locus was detected under all of the four tested conditions, where it explained 15.9–59.0% of phenotypic variation with LOD values of 6.31–32.5. Meanwhile *qBNF-17* explained 12.6–18.6% of observed variation with LOD values of 4.93–7.51. Genotype group analysis indicated that the FC1 genotype of *qBNF-16* primarily affected nodule size (NS), while the FC2 genotype of *qBNF-16* promoted nodule number (NN). On the other hand, the FC1 genotype of *qBNF-17* influenced NN and the FC2 genotype of *qBNF-17* impacted NS. The results on the whole suggest that these two QTLs might be valuable markers for breeding elite soybean varieties with high BNF capacities.

Keywords: QTLs (quantitative trait loci), BNF capacities, RILs (recombinant inbred lines), nodule number and nodule dry weight, nodule size, field conditions tests

INTRODUCTION

As an important economic crop, soybean is a main source of edible oil and protein for human around the world due to the high oil (20–25%) and high protein (42–45%) contents in the seeds (Aziz et al., 2016). At the same time, the high capacity of biological nitrogen fixation (BNF) found in leguminous crops, including soybean, makes this a key source of green manure in agro-ecosystems (Kumudini et al., 2008; Chen and Liao, 2017; Yang et al., 2017).

Nitrogen (N) is one of the most limiting factors in crop production. In order to obtain high yields, farmers tend to supply excessive amounts of N fertilizers, which not only increases input costs, but also causes potentially adverse effects on the environment, including air and water

pollution (Santos et al., 2013; Li et al., 2016). Although N is abundant in the atmosphere, plants are unable to acquire it directly on their own, because it predominantly exists in the inert form of N_2. BNF is a process in which plant unavailable atmospheric N_2 is converted into readily available ammonia (NH_3) in nodules formed through symbiotic associations between plants and microbes (Fox et al., 2016; Yang et al., 2017).

Chemical synthesis provides 118 million metric tons of fertilizer N each year (Joseph et al., 2016). In comparison, it is estimated that symbiosis between nitrogen-fixing rhizobia and plants provides 50–70 million tons of N for agricultural systems each year (Herridge et al., 2008). As one of the most important legume crops, soybean fixes 16.4 million tons of N annually, which represents 77% of the total N fixed by legume crops (Herridge et al., 2008). In modern agricultural systems, soybean is typically considered to have the most potential for sustaining green agricultural systems. For example, in Brazil, over 70% of the N required for soybean growth is derived primarily from BNF (Peoples et al., 2009). Therefore, breeding elite soybean cultivars with high BNF capacities and high yields could be an efficient way to maintain agriculture sustainability.

Soybean BNF capacity is influenced by many environmental factors. Among them, rhizobial strains play critically roles in the nitrogen fixation capacity of soybean nodules (Denison and Kiers, 2004), and which could be classed into three genotype/phenotypes: mutualistic rhizobia, parasitic rhizobia and non-symbiotic. To facilitate agriculture sustainability, mutualistic rhizobia are preferred to become parasitic and non-symbiotic rhizobia, because that parasitic and non-symbiotic rhizobia fix little nitrogen or even unable to infect legumes at all (Denison and Kiers, 2004). For example, Yang et al. (2017) found that upon inoculation with effective rhizobial strains, nodule numbers and dry weights of a RIL population did not significantly vary compared to inoculation with less effective strains, yet shoot dry weight increased by 18.25% on average. Other research has revealed that inoculation with effective rhizobium strains in soybean not only enhances nodule fresh weight, but also increases N and P contents, as well as, yield in the field (Qin et al., 2012). These results imply that rhizobial inoculation increases soybean BNF capacity mainly due to the effects of particular rhizobial species and strains. Beyond rhizobial species, BNF capacity has also been associated with soil characteristics, such as high soil nitrate levels, which tend to reduce nitrogen fixation capacity (Nohara et al., 2005; Yang et al., 2009), and low available phosphorus, which not only limits legume growth, but also inhibits BNF capacity (Adelson et al., 2000; Ward, 2011). Furthermore, water stress also appears to affect BNF capacity (Nascimento et al., 2016; Jemo et al., 2017). In short, BNF is a complex process that is affected by host and symbiotic genotypes, along with the context of environmental conditions in which the symbiosis occurs.

High BNF efficiency mainly depends on the phenotypes expressed in symbiosis between host plants and rhizobia (Nicolás et al., 2006), including the readily observable traits of nodule number (NN), nodule weight (NW), and nodule size (NS). In a relatively stable field environment, the heritability of nodulation traits may exceed 0.8 (Yang et al., 2017), suggesting that nodulation traits are mainly controlled by genetic loci. To date, a number of QTLs for nodulation traits have been identified at different stages of soybean development in pots or in field. These QTLs are distributed on several linkage groups (LGs), including D1b, A1, C2, O, B1, H, B2, E, J, and I (Tanya et al., 2005; Nicolás et al., 2006; Santos et al., 2013; Yang et al., 2017). Some QTLs, such as *qBNF-C2*, *qBNF-O* and *qBNF-B1*, are co-located with yield trait loci (Yang et al., 2017), implying that BNF capacity might affect soybean yield. Therefore, breeding new soybean varieties that produce higher yields through optimization of BNF capacity promises to be a feasible and economic strategy. Unfortunately, possibly due to technical limitations and labor costs, most of the QTLs for BNF traits obtained from field observations are preliminary and minor, so they are not likely to be useful as markers in soybean breeding programs. As a result, progress in studying BNF associated QTL markers in field experiments has lagged behind marker studies for other soybean traits.

Despite the volume of research devoted to mining QTLs for soybean BNF capacity in the field, fine mapping of QTLs regulating nodulation traits in soybean still remain largely unknown. In the present study, two soybean genotypes contrasting in nodulation traits and 168 $F_{9:11}$ recombinant inbred lines (RILs) bred from their progeny were grown in the field to evaluate the effects of N level and rhizobial inoculation on nodulation and BNF traits, as well as, to identify associated QTLs.

MATERIALS AND METHODS

Plant Materials and Field Trials

In this study, a soybean population consisting of 168 $F_{9:11}$ RILs was derived from a cross between two accessions contrasting in BNF capacity, FC1 (a cultivar accession with high BNF capacity) and FC2 (a semi-wild landrace with low BNF capacity), using the single seed descent (SSD) method. This population was further used to construct a genetic linkage map to detect QTLs associated with BNF traits, as well as, to evaluate effects of N level and rhizobial inoculation on BNF traits. A field trial under four environmental conditions was carried out at the Zhaoxian experimental farm (E114.48°, N37.50°) of the Institute of Genetics and Developmental Biology, Chinese Academy of Sciences. The four environmental conditions included with (+R) or without rhizobial inoculation (-R) at two field sites contrasting in long-term nitrogen fertilization (HN: high N; LN: low N). Three highly effective rhizobium strains, BXYD3, BXBL9, and BDYD1, which were previously identified belonging to *Bradyrhizobium elkanii* based on morphological and 16s ribosomal DNA sequence analysis (Cheng et al., 2009), were used as mixture inoculants in this study. The rhizobial inoculation treatment was applied to seeds as described by Qin et al. (2012). Briefly, soybean seeds were uniformly mixed with rhizobium inoculants before planting. The soil at the experiment site is a *Fluventic Ustochrept* soil. Basic characteristics of the top 20 cm of soil in the HN and LN field are shown in **Table 1**. The previous crop was wheat, which was fertilized with 202.5 kg·ha^{-1} of $(NH_4)_2HPO_4$ and 187.5 kg·ha^{-1} of urea as base fertilizer, and 75 kg·ha^{-1} of urea as additional fertilizer during the elongation

TABLE 1 | Basic characteristics of the field soils where the tested soybean lines were grown.

Field	pH	Nitrate N (mg·kg^{-1})	Available P (mg·kg^{-1})	Available K (mg·kg^{-1})	Organic matter (g·kg^{-1})
HN	8.12 ± 0.10	90.25 ± 9.51	16.17 ± 2.96	89.53 ± 12.53	1.93 ± 0.20
LN	8.04 ± 0.08	58.17 ± 7.10	14.70 ± 2.24	87.75 ± 8.50	1.97 ± 0.27

stage in the HN field. No fertilizer was applied during soybean growth. Field management (i.e., pest control and irrigation, etc.) followed local farmer practices. Parental genotypes and RILs were planted in a split plot design with plots arranged in randomized complete blocks within each block of split plots. There were two plots for each RILs in each treatment, and in total, were 1,360 plots in the field. Thirty seeds were sown per plot in three 3 m rows spaced 0.5 m apart.

Plant Sampling and Measurements

At the R4 stage, three representative plants from each plot were harvested, and in total, six plants were harvested for each line in each treatment. Plant roots were manually extracted from the soil to ensure the integrity of the root systems. All nodules were removed and cleared carefully from roots prior to drying in a 37°C oven. Three nodulation traits, namely NN, NW, and NS, were investigated for subsequent analysis. NS was calculated by the quotient of total NW and NN. NN and NW were derived from individual plant. The plants were dried at 60°C, and then measured dry weight and total N content (TNC) using a continuous flow analyzer as described by Bao (2000). The TNC was used to represent the BNF capacity.

Genotyping by High-Throughput Sequencing

Genomic DNA of the two parents were extracted using commercial extraction kit, DNeasy Plant Mini Kit (QIAGEN, Germany), following the manufacturer protocol. Library construction and sequencing were performed on the Illumina sequencing platform. Briefly, genomic DNA was fragmented to 100–300 bp size and two replicate genomic DNA re-sequencing libraries (100–300 bp insert) were prepared for two entire lanes sequencing on Hiseq X10 PE150 sequencing system. Genotyping by sequencing (GBS) libraries were constructed using the EcoRI and NIaIII enzymes modified from the Elshire's protocol (Elshire et al., 2011). The simple description as follows: after genomic DNA extracting, 100 ng of DNA for each plant were used for digesting reaction with EcorI and NIaIII (New England Biolabs, Ipswich, MA, United States) in 96-well plates. Then, the reactions were mixed with about 25 pmol of unique A1 and A2 adapters per well. The libraries in 96-well plates were then pooled, further DNA fragments size 400–600 bp were isolated on a 1% agarose gel and purified using a PCR purification kit (NEB), and then amplified for 12 cycles using Phusion DNA polymerase (NEB). Finally, the pooled libraries were adjusted to 10 nmol and sequenced with PE125 on the HiSeq4000 (Illumina, San Diego, CA, United States). Both genomic DNA re-sequencing and GBS were performed by Genedenovo Biotechnology Co., Ltd. (Guangzhou, China).

SNP Identification and Bin Map Construction

For SNPs calling, the Burrows-Wheeler Aligner (BWA) was used to align the clean reads from each plant against the reference genome *Glycine max* Wm82.a2.v1 with the settings 'mem 4 -k 32 -M' (Li and Durbin, 2009). Genotypes of all samples were determined by using the GATK's Unified Genotyper. SNPs were filtered using GATK's Variant Filtration with follow parameters (-Window 4, -filter "QD < 2.0 ||FS > 60.0|| MQ < 40.0," -G_filter "GQ < 20") and SNPs with segregation distortion or sequencing errors were eliminated. The physical positions of each SNP were further determined by using the software tool ANNOVAR (Wang et al., 2010). Polymorphic parental markers were recorded as male genotype "a" and female genotype "b," other segregation patterns were recorded as missing data "−." However, the reading depth of SNP variants outside the range of 5–1,500 would be also considered as missing data. After that, Chi-square (χ^2) tests were conducted for all SNPs to detect segregation distortion. The sliding window (1 kb) approach was used to evaluate groups of consecutive SNPs for utility in genotyping and avoidance of false positive population based SNPs. Qualified bins of SNP markers were then used to construct genetic linkage maps using Join Map 4.1. The regression algorithm and Kosambi mapping function were used in marker distance calculation. The LOD value was set according to the chromosome numbers. A Perl SVG module was used to draw the linkage map. Bin markers were named as Ch"x"."y" according to results of SNP calling, "x" and "y" represent "chromosome number" and "physical position," respectively.

QTL Detection

Multiple-QTL model (MQM) implemented in MapQTL6.0 (Van Ooijen, 2009) was used to detect QTLs for nodulation and BNF capacity traits. The critical logarithm of odds (LOD) threshold was set to 4.5 for declaring the significance of a QTL in a particular genomic region. A total of 1,000 permutations with *P*-values <0.05 was used to verify LOD scores. QTLs for which the LOD score simultaneously exceeded 4.5 and the genome wide LOD, were considered as high confidence QTLs in MQM mapping.

Statistical Analysis

Data for the three BNF traits were used for variance and QTL analysis. Analysis of variance (ANOVA) was implemented in the QTL ICIMapping V4.1 software (Meng et al., 2015). Parental genotypes were also planted with six replications, which were analyzed separately from the RILs. Broad sense heritability (h^2_b) was estimated for each trait according to: $h^2_b = VG/(VG + VE)$, with VG as the variance between RILs and VE as the variance

within RILs. The Student's *t*-test was used to test the significance of the effects of N level and rhizobial inoculation on each trait in RILs. Multi-factor and multivariate analysis of variance (ANOVA) was also performed using SPSS 19 (Colin and Paul, 2012).

RESULTS

Phenotype Evaluation of Two Parents

The two parental genotypes, FC1 and FC2, contrasted in root growth and nodulation in the field under natural conditions. ANOVA revealed significant genotypic variation between parental genotypes for NN ($P < 0.001$) and NS ($P < 0.01$), as well as, a significant interaction between rhizobium inoculation and genotype on NW ($P < 0.05$) (**Table 2**). Compared with FC2, FC1 had a shallower root architecture denoted by more roots in the top soil, and more big nodules than FC2 in the field (**Figures 1A–C**). However, FC2 formed more nodules than FC1 in each environment, as indicated by 83.90–1473.09% differences in NN under the four tested environments (**Figure 1D**). Interestingly, NW of FC2 was only higher than that of FC1 in plots without rhizobial inoculation (-R), but not in HN+R or LN+R (**Figure 1E**). Nodules on FC1 roots were much bigger than on FC2 roots in all treatments except HN-R, with NS being 450.11%, 260.89%, and 382.50% bigger for FC1 compared to FC2 in HN+R, LN-R, and LN+R, respectively (**Figure 1F**), indicating that FC1 was more conducive to nodule development in response to rhizobial inoculation.

In addition, N level significantly influenced nodulation on FC1 but not FC2. NN increasing by 535.71% or 41.94%, NW increasing by 323.70% or 235.96%, and NS increasing by 12.90% and 181.63% in response to rhizobium inoculation in LN and HN treatments, respectively (**Figures 1D–F**). These results strongly suggest that nodulation traits are much more sensitive to environment changes for FC1 than for FC2, which might be controlled by genetic loci.

Phenotypic Variation Among Recombinant Inbred Lines (RILs)

As shown in **Table 3**, significant phenotypic variation existed for all three nodulation traits within the 168 $F_{9:11}$ soybean RILs under different environments. As expected, among the RILs, high N supply significantly suppressed nodule formation and development as indicated by declines of 33.31% and 30.91% in NN, 63.72% and 63.72% in NW, and 29.87% and 51.98% in NS, with or without rhizobial inoculation, respectively (**Figures 2A–C**). Furthermore, TNC increased in response to rhizobial inoculation at both N levels, with a greater impact in LN than in HN (**Figure 2D**), suggesting that BNF capacity is inhibited by high N supply in the RIL population.

The mean value for each trait among all RILs was between the mean values of the two parents, while the maximum and minimum values were beyond the extremes of the two parents. Distributions for the nodulation traits under all conditions were approximately normal according to Kurtosis and Skewness values calculated over six replicates. Broad-sense heritability (h^2_b) for all the traits under the tested environments varied from 0.48 to 0.87, with generally higher values being observed in LN than in HN plots (**Table 3**). Overall, the results herein suggested that variations in nodulation traits mainly depended on genotype.

Construction of Genetic Linkage Map

After strict screening, 168 strains of the RIL population were accepted and genotyped using a sliding-window method (Chang and Lee, 2004). Bin markers for each chromosome were screened, and a total of 3,319 recombinant bin markers were identified (**Table 4**). A genetic map was constructed by mapping these 3,319 bin markers onto the 20 soybean chromosomes (**Supplementary Figure S1**). The complete genetic distance of the linkage map was 2,537.6 cM. The average distance between two adjacent markers was 0.76 cM. Among the 20 soybean chromosomes, chromosome 7 had the highest number of bin markers at 194, which cover a genetic length of 157.9 cM. Chromosome 10 held the fewest markers, 100, over a distance of 101.0 cM. The *W* gene located on chromosome 13 has been identified in previous work as responsible for flower color (Takahashi et al., 2010). In order to examine the fidelity of the genetic map constructed herein, this flower color gene was mapped relative to the bin markers used in the current study. As expected, the gene encoding flower color was mapped as the *W* gene located on chromosome 13 at bin marker Chr13.17168452, with a high LOD value of 74.56 (**Supplementary Figure S1**). This clearly demonstrated that the linkage map constructed in this study is a high quality map that can be used in further studies.

QTL Identification for Nodulation Traits

A total of 12 significant QTLs explaining 12.6–59% of the phenotypic variation observed among the 168 $F_{9:11}$ soybean RILs were identified for nodulation traits in the field under four environment conditions (**Table 5**). The LOD values of these QTL varied from 4.93 to 32.52. However, 10 of the QTLs were closely mapped on Chromosome 16, and the other two QTLs were mapped on Chromosome 17 at two very closely linked locations. These results indicating that all of the significant QTLs might be controlled by two genetic loci, which were, therefore, named as *qBNF-16* and *qBNF-17*. Among them, *qBNF-16* is a stable and major QTL, which was detected under all four of the environment conditions, and explained 40.9%–59% and 15.9%–45.4% of the variation in NS and NN, respectively. The additive effects of *qBNF-16* for NS and NN were derived from FC1 and FC2, respectively. In contrast, *qBNF-17* was only detected in LN-R, and it explained 18.6% and 12.6% of the variation in NN and NW, respectively. The additive effects of *qBNF-17* for NN and NW were derived from FC1 and FC2, respectively. As for interactions between traits, the results in this study indicated that NN is negatively correlated with NS.

Effects of Genotype on Nodulation Traits Under Varied Environmental Conditions

Biological nitrogen fixation capacity can be represented by plant total nitrogen content (TNC) (Li et al., 2016). In order to evaluate the effects of *qBNF-16* and *qBNF-17* on nodulation traits, the

TABLE 2 | ANOVA for variation in biological nitrogen fixation traits between two parental genotypes.

Traits	R	N	G	R × N	R × G	N*G	R × N × G
NN	0.54	0.53	5.03E-06*	0.36	0.13	0.13	0.87
NW	0.22	0.26	0.94	0.21	0.02*	0.12	0.52
NS	0.17	0.88	0.01*	0.71	0.13	0.99	0.6

R, rhizobium inoculation; N, nitrogen level; G, genotype; R × N, interaction effects of rhizobium inoculation and nitrogen level; R × G, interaction effects of rhizobium inoculation and genotype; N × G, interaction effects of nitrogen level and genotype; R × N × G, interaction effects of rhizobium inoculation, nitrogen level and genotype. Asterisks indicated significant differences through ANOVA at the 5% (*) level.

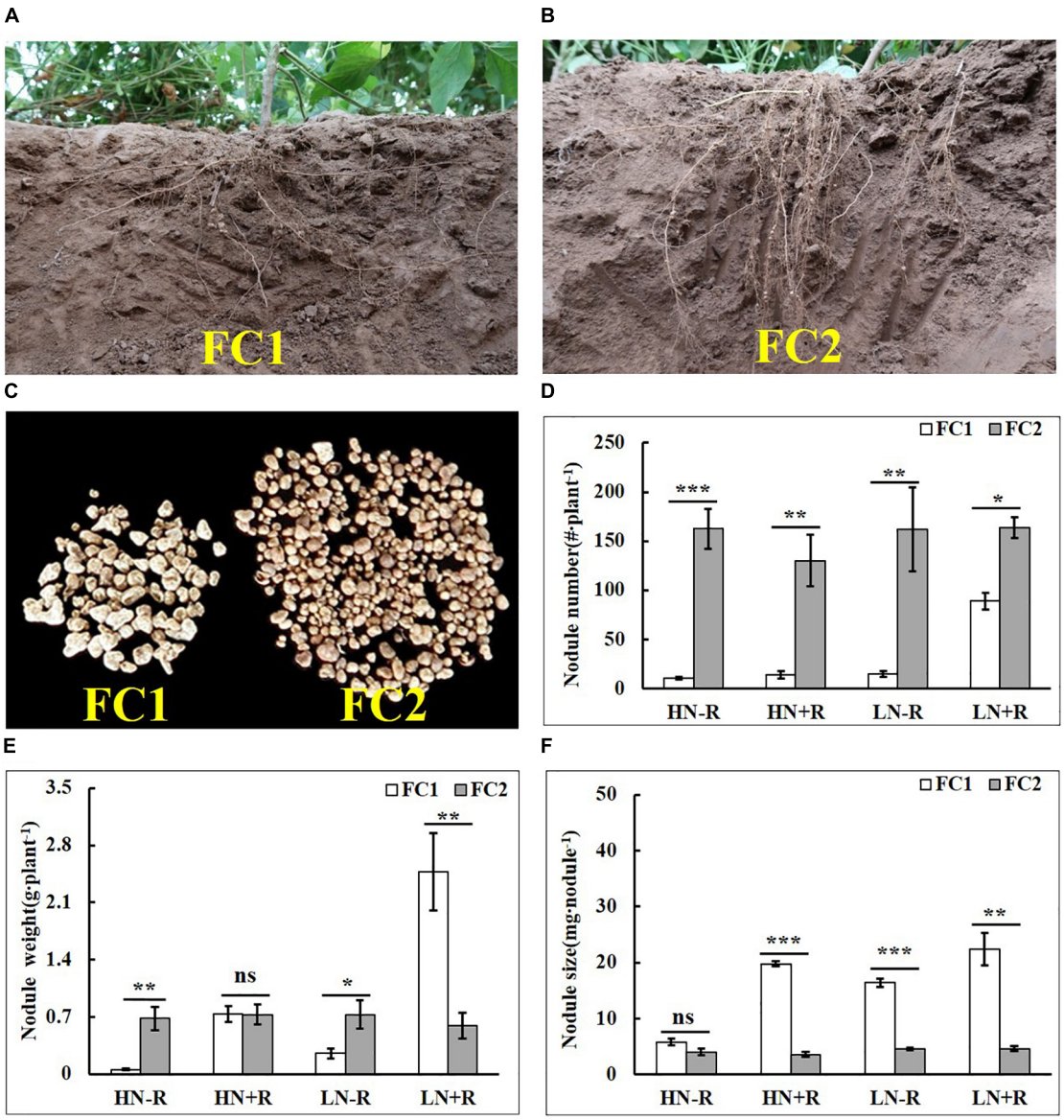

FIGURE 1 | Root and nodule characteristics for FC1 and FC2 soybean parental lines in the field under four environment conditions. **(A,B)** Root and nodule characteristics of FC1 and FC2. **(C)** Nodule size and number for FC1 and FC2 under natural conditions. **(D–F)** Nodule number, nodule weight, and nodule size on roots of FC1 and FC2 under four environments. Bars represented means ± SE from six replications. Asterisks indicated significant differences between FC1 and FC2 in the Student *t*-test at 5% (*), 1% (**) and 1‰ (***) levels, while "ns" represented no significant difference. "HN" and "LN" denoted high and low nitrogen, "+R" and "-R" denoted the inoculation or non-inoculation of rhizobium.

TABLE 3 | Phenotypic variation and genetic analysis of biological nitrogen fixation traits using 168 $F_{9:11}$ soybean RILs under different field conditions.

Trait	Environment	Parents		RILs						
		FC1	FC2	Mean ± SD	Min	Max	CV%	h^2_b	Skew	Kurt
NN (#·plant^{-1})	HN-R	10.33 ± 3.01	162.5 ± 49.49	119.45 ± 129.22	1	985	108.18	0.76	0.76	−0.05
	HN+R	14 ± 9.64	130.2 ± 65.08	131.10 ± 116.15	1	938	88.60	0.48	0.88	0.26
	LN-R	14.67 ± 6.66	162 ± 103.68	156.36 ± 164.38	1	1047	105.13	0.83	1.02	0.31
	LN+R	89 ± 21	163.67 ± 26.86	174.78 ± 130.44	4	835	74.63	0.63	0.65	−0.33
NW (g·plant^{-1})	HN-R	0.06 ± 0.02	0.68 ± 0.35	0.43 ± 0.40	0	2.51	91.96	0.62	1.01	1.03
	HN+R	0.74 ± 0.24	0.73 ± 0.31	0.66 ± 0.57	0	5.78	85.96	0.69	0.78	0.15
	LN-R	0.25 ± 0.15	0.73 ± 0.42	0.72 ± 0.50	0	3.56	70.08	0.67	0.49	0.12
	LN+R	2.48 ± 1.16	0.6 ± 0.39	1.06 ± 0.70	0	4.16	66.54	0.70	1.12	1.45
NS (mg·nodule^{-1})	HN-R	5.83 ± 1.57	4.01 ± 1.4	6.36 ± 6.30	0.16	53.8	99.03	0.70	1.57	2.99
	HN+R	36.77 ± 29.41	3.6 ± 1.17	7.12 ± 7.13	0.2	87.38	100.2	0.75	1.38	1.37
	LN-R	16.42 ± 1.77	4.55 ± 0.63	9.93 ± 9.77	0.26	81.21	98.34	0.87	1.64	2.98
	LN+R	22.35 ± 7.1	4.63 ± 1.19	8.81 ± 7.86	0	73.15	89.19	0.86	1.36	1.81

RILs, recombinant inbred lines; NN (nodule number, #·plant^{-1}); NW (nodule weight, g·plant^{-1}); NS (nodule size, mg· nodule^{-1}); HN (high nitrogen condition); LN (low nitrogen condition); −R (without rhizobium inoculation); +R (with rhizobium inoculation); Min and Max, the minimum and maximum values of NN, NW, and NS; CV%, coefficient of variation; h^2_b, broad-sense heritability; Skew and Kurt, Skewness and Kurtosis.

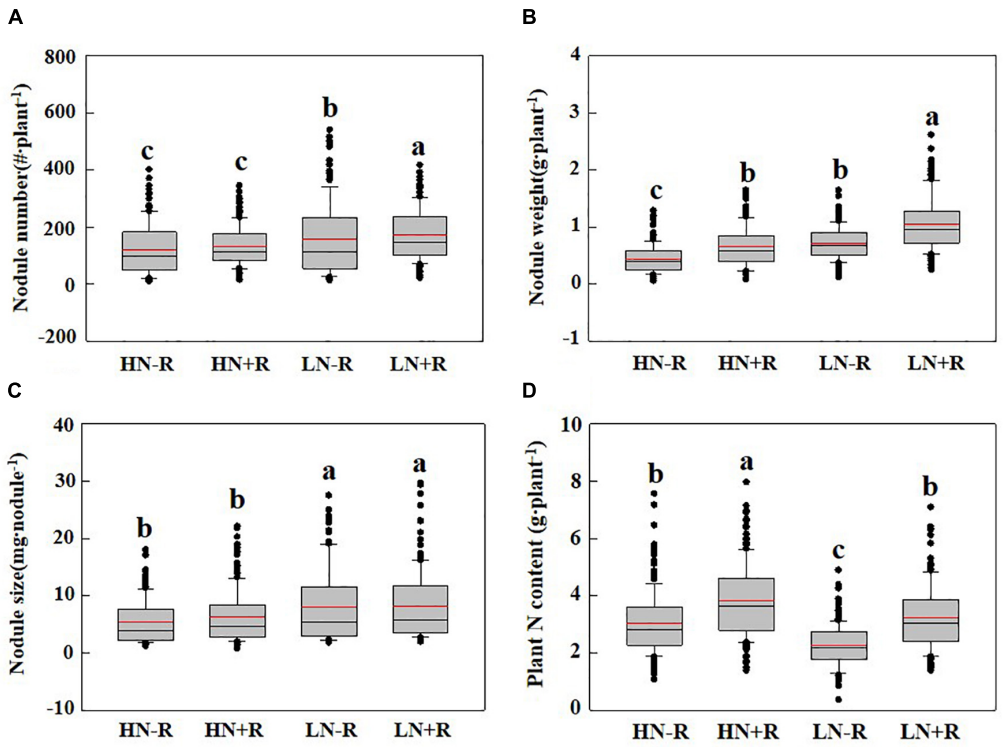

FIGURE 2 | Biological nitrogen fixation (BNF) traits as affected by N level and rhizobium in RILs. **(A)** Nodule number; **(B)** nodule weight; **(C)** nodule size; and **(D)** plant nitrogen content. The black and red lines, lower and upper edges, and bars above or below the boxes represented median and mean values, 25th, 75th, 5th, and 95th percentiles of all data, respectively. Different letter(s) over error bars indicated significance differences between HN-R, HN+R, LN-R, and LN+R conditions through the Student *t*-test at the 1% level.

168 $F_{9:11}$ lines were classed into two distinct genotypic groups based on bin markers Chr16.37147484 and Chr17.12638388. Then, comparative analysis of nodulation traits and TNC were conducted among different environments between these two groups.

The genotype of *qBNF-16* significantly affected NN and NS, but not NW and TNC (**Figure 3**). The FC1 group had fewer, yet larger nodules than the FC2 group (**Figures 3A,C**). This suggested that the FC1 genotype of *qBNF-16* supported nodule development, while the FC2 genotype of *qBNF-16* promoted

TABLE 4 | Summary of bin marker characteristics of recombinant inbred line (RIL) population.

Chr	Genetic distance/cM	Physical length	Number of bin markers	Average coverage distance/cM
Chr01	123.1	56510449	169	0.73
Chr02	131.0	47706575	165	0.79
Chr03	140.0	45730193	169	0.83
Chr04	158.1	51405255	188	0.84
Chr05	97.5	41919006	140	0.70
Chr06	152.2	50892625	177	0.86
Chr07	157.9	43534570	194	0.81
Chr08	186.5	47709553	174	1.07
Chr09	155.5	50173153	131	1.19
Chr10	101.0	51542279	100	1.01
Chr11	168.5	34671664	110	1.53
Chr12	119.4	40030102	178	0.67
Chr13	121.8	45514498	175	0.70
Chr14	83.7	47841279	171	0.49
Chr15	75.0	51710377	191	0.39
Chr16	76.1	37192783	178	0.43
Chr17	137.0	41348852	178	0.77
Chr18	103.2	57961359	182	0.57
Chr19	82.3	50522110	175	0.47
Chr20	167.7	47868276	174	0.96
Total	2537.6	941784958	3319	0.76

nodule formation. Furthermore, the FC1 genotype of *qBNF-16* was responsive to rhizobial inoculation, as indicated by increases of NN of 93.20% and 55.34%, NW of 126.97% and 87.08%, and TNC of 25.18% and 56.56% upon rhizobial inoculation in HN and LN plots, respectively. Meanwhile, NS was only affected by N level. The FC2 genotype of *qBNF-16* was also influenced by N level, as showed by decreases in NN of 42.04% or 24.07%, and in NW of 64.69% or 51.69% in HN plots with or without rhizobial inoculation, respectively.

The genotype of *qBNF-17* also only significantly affected NN and NS, but had opposite effects compared to *qBNF-16* (**Figure 4**) impacts. The FC2 group had fewer, but bigger nodules than the FC1 group (**Figures 4A,C**), suggesting that the FC2 genotype of *qBNF-17* participated in nodule development, while the FC1 genotype of *qBNF-17* advanced nodule formation. Both N level and rhizobial inoculation significantly impacted NW and TNC for both FC1 and FC2 genotypes of *qBNF-17*, while only N level affected NS, and rhizobial inoculation only influenced NN for the FC2 genotype at the *qBNF-17* locus in LN plots.

DISCUSSION

By 2050, agricultural production might need to be increased by 70% in order to satisfy the needs of a growing population (Joseph et al., 2016). In order to achieve higher yields, farmers tend to supply excessive amounts of fertilizers, which often leads to environmental problems (Li et al., 2016). Legumes, particularly soybean, not only could provide oil and protein for humans, but also can improve soil quality and reduce the need for N fertilizers. This benefit of growing legumes is due to the unique capability among this family to participate in BNF, which converts atmospheric nitrogen (N_2) into ammonia with the assistance of rhizobia in symbiotically derived organs known as nodules (Udvardi and Poole, 2013). Identification and fine mapping QTLs for BNF capacity hold the promise of facilitating the development of soybean cultivars with higher yield potentials and superior BNF capacities that will improve our ability to meet food and environment demands.

Soybean yield has been demonstrated being largely dependent on root architecture (RA) and BNF capacity (Li et al., 2016; Chen and Liao, 2017; Yang et al., 2017), and the effects of RA and BNF capacity on yield are also associated with each other. For example, RA of legume roots is not only involved in elaboration of root system through lateral root formation, but also in nodule formation with rhizobia from soils (Yendrek et al., 2010).

TABLE 5 | Putative QTLs detected for biological nitrogen fixation traits using 168 $F_{9:11}$ soybean RILs in the field.

Integrated QTL[a]	Environment[b]	Separate QTL	Chr	Marker or interval[c]	Position (cM)	LOD	Add[d]	PVE (%)[e]
qBNF-16	HN-R	*qNN-HN-R*	Gm16	Chr16.37147484	17.63	22.12	65.49	45.4
		qNS-HN-R	Gm16	Chr16.37147484	17.63	25.25	−4.78	50.0
	HN+R	*qNN- HN+R*	Gm16	Chr16.37559118	18.55	6.31	29.19	15.9
		qNW-HN+R	Gm16	Chr16.36986426	16.09	7.60	−0.17	18.8
		qNS-HN+R	Gm16	Chr16.37147484	17.63	19.18	−3.31	40.9
	LN-R	*qNN-LN-R*	Gm16	Chr16.37156866	17.87	15.63	69.79	28.4
		qNS-LN-R	Gm16	Chr16.37147484	17.63	30.50	−6.01	56.7
	LN+R	*qNN-LN+R*	Gm16	Chr16.37147484	17.63	14.91	55.68	33.6
		qNW-LN+R	Gm16	Chr16.36986426	16.09	10.12	−0.25	24.2
		qNS-LN+R	Gm16	Chr16.37147484	17.63	32.52	−5.08	59.0
qBNF-17	LN-R	*qNN-LN-R*	Gm17	Chr17.12638388	61.78	7.51	−55.58	18.6
		qNW-LN-R	Gm17	Chr17.12728155- Chr17.13805621	60.24	4.93	0.40	12.6

[a]BNF, biological N_2 fixation. [b]LN and HN mean low and high N fertilizer field, respectively, and "−R" and "+R" mean without and with rhizobial inoculation, respectively. [c]Marker or interval, markers or support intervals on the linkage map in which the LOD is the largest. [d]Add value >0 and <0 stand for increasing effects of the QTLs derived from FC2 and FC1, respectively. [e]PVE (%), percentage of phenotypic variance explained by the QTL.

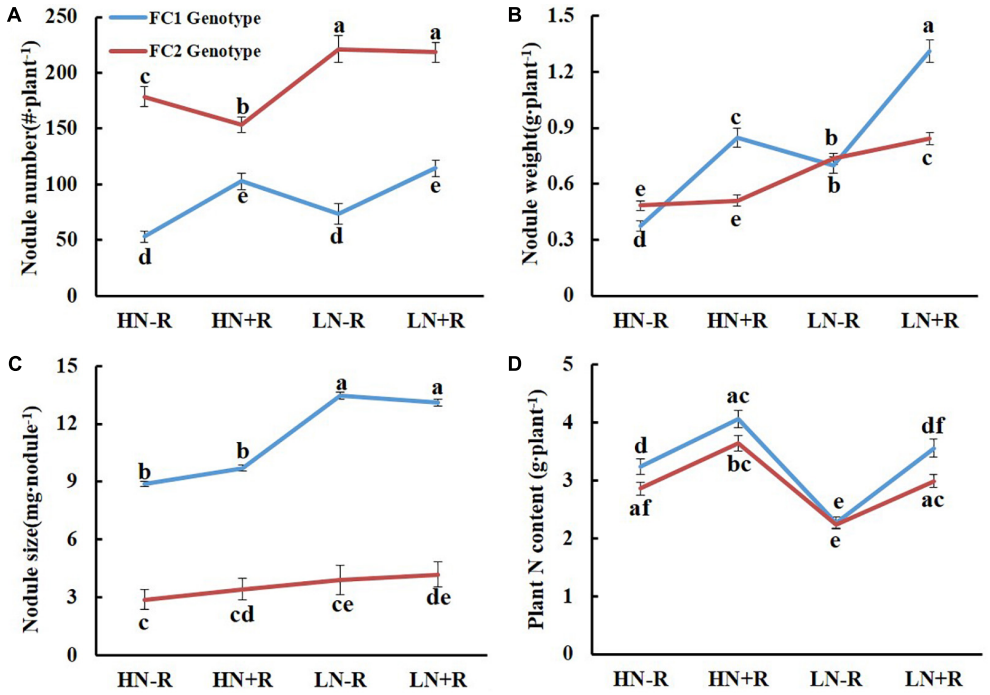

FIGURE 3 | Effects of qBNF-16 genotypes on BNF traits. **(A)** Nodule number; **(B)** nodule weight; **(C)** nodule size; and **(D)** whole plant nitrogen content. Based on SNP marker Chr16.37147484, the RIL population was divided into FC1 and FC2 genotype groups which consisted of 72 and 92 lines, respectively. The blue and red line represented mean ± SE values for the FC1 and FC2 genotype groups. Different letter(s) over the standard error bar indicated significant differences of mean values at the 5% level.

However, information of the relationships between RA and BNF remains limited. Our recent research suggested that the soybean plants with shallow RA had more and heavier nodules, as well as higher SDW. Meanwhile, soybean roots became shallower after inoculating with rhizobia, showing strong synergistic interactions between RA and BNF (Yang et al., 2017). In this study, the two soybean accession FC1 and FC2 contrasting in RA were evaluated in varied field conditions. Interestingly, we found that the parental genotype FC1 with shallow RA preferred to form fewer but bigger nodules compared with the parental genotype FC2 with deep RA, implying that more complicate relationships between RA and BNF exited and need to be further evaluated.

Since effective rhizobial strains play critical roles in facilitating soybean production with high nitrogen fixation capacity, lots of commercial rhizobial strains have been isolated and applied in the field (Menna et al., 2006; Thuita et al., 2012; Sivparsad et al., 2015). However, none of the commercial rhizobial strains could meet the needs for all crop species and/or all cultivars in the same species in the field (Thomas-Oates et al., 2003). In this study, FC2 had a higher nodulation ability with numerous small nodules than FC1, which was possibly caused by non-selectivity compatibility of FC2 to most indigenous rhizobia, and this non-selectivity compatibility greatly related to plant species (i.e., genotype). On the other hand, phenotypes of both FC1 and FC2 were the results of synergetic interactions between indigenous rhizobia (most likely including parasitic rhizobia), inoculants, genotype and other environmental factors. However, the BNF capacity of small nodules (diameter <2 mm) was significantly lower than that of big nodules (diameter >2 mm) (Li et al., 2018). Contrastingly, FC1 seemed to have a higher compatibility with the inoculated rhizobial strains than indigenous soil rhizobia as indicated by great increases of NN and NW after rhizobium inoculation, especially at low N level (**Figure 1**). Since highly effective and affinitive rhizobial species are necessary for high BNF capacities to produce high yields in soybean (Peoples et al., 2009; Qin et al., 2012; Yang et al., 2017), TNC was measured for the RIL population to evaluate the effect of a highly effective and affinitive rhizobial species on soybean BNF capacity in the field. As expected, inoculation with highly effective and affinitive rhizobia led to 44.5% and 25.1% increase of TNC of RILs in low and high N conditions, respectively (**Figure 2**). Furthermore, the mean value of TNC in RILs did not significantly vary between HN-R and LN+R treatments, suggesting that rhizobium inoculation is an alternative way to meet N demand for soybean growth.

Nodulation traits that heavily influence BNF capacity are affected by many environment factors, such as nutrient availability, soil characteristics, abiotic stress, and soil tillage systems (Soedarjo et al., 2003; Adak and Kibritci, 2016; Chetan et al., 2016; Kunert et al., 2016). In soybean, although symbiotic N_2 fixation can provide the nitrogen needed for plant growth, symbiotically fixed N is not always sufficient for producing high yields (Kunert et al., 2016). High N fertilizer application on the other hand has a negative impact on nodulation

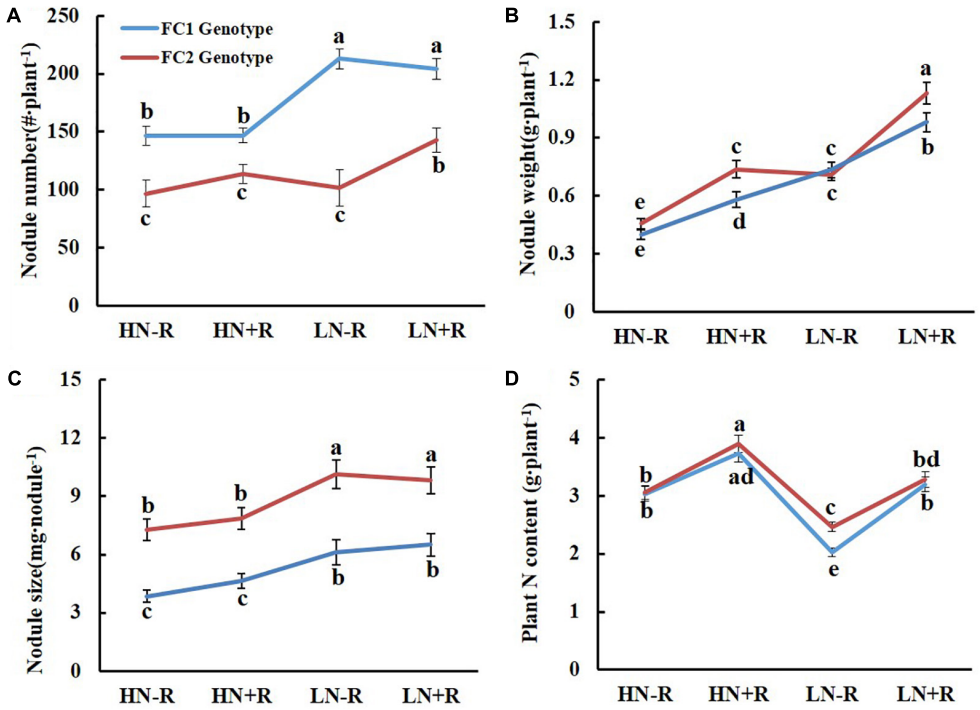

FIGURE 4 | Effect of qBNF-17 genotypes on nodulation traits. **(A)** Nodule number; **(B)** nodule weight; **(C)** nodule size; and **(D)** whole plant nitrogen content. Based on SNP marker Chr17.12638388, the RIL population was divided into FC1 and FC2 genotype groups which consisted of 83 and 81 lines, respectively. The blue and red line represented mean ± SE values for the FC1 and FC2 genotype groups. Different letter(s) over the standard error bar indicated significant differences of mean values at the 5% level.

(Ferguson et al., 2010). In this study, BNF traits was studied in a field with low N and high N plots in which variation in nodule formation could proceed with or without rhizobial inoculation. As expected, the mean values of three BNF traits (i.e., NN, NW and NS) were significantly higher by 32.2–62.3% in low N plots than in high N plots, indicating that BNF capacities are higher when N is limited (**Table 3**). This is consistent with previous reports that high N status has a negative impact on nodulation traits (Ferguson et al., 2010; Abera and Tadele, 2016; Adak and Kibritci, 2016; Hu et al., 2016; Xia et al., 2017).

Genetics are the internal elements that might affect soybean BNF capacity along with environmental elements. Therefore, identification and mapping of QTLs for BNF traits holds promise for breeding efforts seeking to develop soybean varieties with high BNF capacities, which will allow growers to reduce N fertilization and maintain beneficial eco-systems. To successfully reach these goals, a high h^2_b is necessary for identified solid QTLs. In this study, the h^2_b for NW and NS are stable under different environments, with values ranging from 0.62 to 0.70 and 0.70 to 0.87, respectively. For NN, rhizobial inoculation significantly decreased values of h^2_b to 0.48 and 0.63 in HN and LN field plots (**Table 3**), respectively, while other h^2_b values for nodulation traits remain above 0.75 without rhizobial inoculation under both LN and HN field conditions. This high level of heritability is consistent with previous reports (Souza et al., 2000; Santos et al., 2013; Yang et al., 2017). This strongly indicates that genetics is the main force affecting nodulation trait variation in the field, and, furthermore, the RIL population developed in this work is suitable for QTL identification.

Nodulation traits are difficult to quantify and study in field conditions. Although more than 20 QTLs for BNF traits have been identified in previous studies[1], most of them were not adequately tested in field conditions, or there is a lack of adequate repetition required for obtaining precise QTL effect estimates. In addition, a high resolution genetic map is also necessary for precise QTL identification. Unfortunately, none of previous QTLs reports built on SSR based genetic maps exhibit adequate precision, possibly due to technical limitations. Therefore, it is not surprising that among previously identified QTLs for nodulation traits, relatively low LOD values ranging from 1.28 to 8.77 were detected, and none of them could explain more than 40% of variation (López-Bucio et al., 2003; Tanya et al., 2005; Nicolás et al., 2006; Santos et al., 2013; Yang et al., 2017). In this study, QTLs were precisely identified by using six representative plants for phenotypic observations, while a high resolution genetic map was constructed to detect QTLs under multiple environments. As a result of this effort, a QTL, *qBNF-16*, explaining as much as 59% of genetic variation, and with LOD values of up to 32.52 was identified and mapped. Most importantly, *qBNF-16* is a stable QTL that was detected under all four tested environments. Therefore, *qBNF-16* can be considered

[1]https://www.soybase.org/

as a valuable locus which might be useful for breeding high BNF capacity soybean varieties.

Integration of QTLs for BNF traits in a previous reported reveals that a total of 18 QTLs affect BNF traits under field conditions (see footnote 1). These QTLs are distributed on linkage groups D1a(2), C1(1), A1(1), C2(4), A2(1), K(1), B1(1), E(2), L(2), and I(3). None of these QTLs co-locate or are closely linked with QTLs identified in our study, suggesting that *qBNF-16* and *qBNF-17* are two new QTLs. Taken together, in this study, two new QTLs for soybean nodulation and BNF capacity traits in the field conditions were identified and tested under different environments. The results indicate that these QTLs can be used as molecular markers for breeding elite soybean varieties with high BNF capacities.

DATA AVAILABILITY STATEMENT

Any related SNPs data can be available on request by contacting the corresponding author directly.

AUTHOR CONTRIBUTIONS

HLi designed the experiments and critically revised the manuscript. QY and YY analyzed the data and wrote the manuscript. QY, YY, RX, and HLv carried out the experiments.

FUNDING

This work was jointly supported by China National Key Program for Research and Development (2016YFD0100700), the Strategic Priority Research Program of the Chinese Academy of Sciences (XDB15030202), and National Natural Science Foundation of China (31601814).

ACKNOWLEDGMENTS

We would like to acknowledge staff members of the Institute of Genetics and Developmental Biology, Chinese Academy of Sciences, especially Yiping Tong for providing HN and LN level experimental farm sites, and Weiqi Zhu for field management, the graduate students of the Root Biology Center, Fujian Agriculture and Forestry University for soybean harvesting, and Dr. Thomas Walk of Golden Fidelity LLC for critical reviewing.

SUPPLEMENTARY MATERIAL

The Supplementary Material for this article can be found online at: https://www.frontiersin.org/articles/10.3389/fpls.2019.00075/full#supplementary-material

REFERENCES

Abera, H., and Tadele, B. (2016). Effect of *Rhizobium* inoculation and nitrogen fertilization on nodulation and yield response of common bean (*Phaseolus vulgaries* L.) at Boloso Sore, Southern Ethiopia. *Int. Jagric Biol.* 6, 2224–2225.

Adak, M. S., and Kibritci, M. (2016). Effect of nitrogen and phosphorus levels on nodulationand yield components in faba bean (*Vicia faba* L.). *Legume Res.* 39, 991–994. doi: 10.18805/lr.v0iOF.3773

Adelson, P. A., Marcelo, G. T., and Dejair, L. D. A. (2000). Growth and yield of common bean cultivars at two soil phosphorus levels under biological nitrogen fixation. *Pesqui Agropecu Bras.* 35, 809–817. doi: 10.1590/S0100-204X2000000400019

Aziz, A., Ahiabor, B., Opoku, A., and Abaidoo, R. (2016). Contributions of *Rhizobium* inoculants and phosphorus fertilizer to biological nitrogen fixation, growth and grain yield of three soybean varieties on a Fluvic Luvisol. *Exp. Agric.* 10, 1–11. doi: 10.9734/ajea/2016/20072

Bao, S. D. (2000). *Soil and Agricultural Chemistry Analysis*. Beijing: China Agricultural Press.

Chang, J. H., and Lee, W. S. (2004). A sliding window method for finding recently frequent itemsets over online data streams. *J. Inf. Sci. Eng.* 20, 753–762.

Chen, L. Y., and Liao, H. (2017). Engineering crop nutrient efficiency for sustainable agriculture. *J. Integr. Plant Biol.* 59, 710–735. doi: 10.1111/jipb.12559

Cheng, F., Cao, G., Wang, X., Zhao, J., Yan, X., and Liao, H. (2009). Isolation and application of effective nitrogen fixation rhizobial strains on low-phosphorus acid soils in South China. *Sci. Bull.* 54, 412–420. doi: 10.1007/s11434-008-0521-0

Chetan, C., Rusu, T., Chetan, F., and Simon, A. (2016). Influence of soil tillage systems and weed control treatments on root nodules, production and qualitative indicators of soybean. *Procedia Technol.* 22, 457–464. doi: 10.1016/j.protcy.2016.01.088

Colin, D. G., and Paul, R. K. (2012). IBM SPSS statistics 19 made simple. *J. R. Stat. Soc.* 4:1183.

Denison, R. F., and Kiers, E. T. (2004). Lifestyle alternatives for rhizobia: mutualism, parasitism, and forgoing symbiosis. *FEMS Microbiol. Lett.* 237, 187–193. doi: 10.1016/j.femsle.2004.07.013

Elshire, R. J., Glaubitz, J. C., Sun, Q., Poland, J. A., Kawamoto, K., Buckler, E. S., et al. (2011). A robust, simple genotyping-by-sequencing (GBS) approach for high diversity species. *PLoS One* 6:e19379. doi: 10.1371/journal.pone.0019379

Ferguson, B. J., Indrasumunar, A., Hayashi, S., Lin, M. H., Lin, Y. H., Reid, D. E., et al. (2010). Molecular analysis of legume nodule development and autoregulation. *J. Integr. Plant Biol.* 52, 61–76. doi: 10.1111/j.1744-7909.2010.00899.x

Fox, A. R., Soto, G., Valverde, C., Russo, D., Lagares, A., Zorreguieta, A., et al. (2016). Major cereal crops benefit from biological nitrogen fixation when inoculated with the nitrogen-fixing bacterium *Pseudomonas* protegens Pf-5 X940. *Environ. Microbiol.* 18, 3522–3534. doi: 10.1111/1462-2920.13376

Herridge, D. F., Peoples, M. B., and Boddey, R. M. (2008). Global inputs of biological nitrogen fixation in agricultural systems. *Plant Soil* 311, 1–18. doi: 10.1007/s11104-008-9668-3

Hu, F., Zhao, C., Feng, F., Chai, Q., Mu, Y., and Zhang, Y. (2016). Improving N management through intercropping alleviates the inhibitory effect of mineral N on nodulation in pea. *Plant Soil* 412, 235–251. doi: 10.1007/s11104-016-30632

Jemo, M., Sulieman, S., Bekkaoui, F., Olomide, O. A. K., Hashem, A., Abd Allah, E. F., et al. (2017). Comparative analysis of the combined effects of different water and phosphate levels on growth and biological nitrogen fixation of nine cowpea varieties. *Front. Plant Sci.* 8:2111. doi: 10.3389/fpls.2017.02111

Joseph, M. J., Soon, G. L., and Ashley, M. S. (2016). The next green movement: plant biology for the environment and sustainability. *Science* 353, 1241–1244. doi: 10.1126/science.aag1698

Kumudini, S., Omielan, J., and Hume, D. J. (2008). Soybean genetic improvement in yield and the effect of late-season shading and nitrogen source and supply. *Agron. J.* 100, 278–290. doi: 10.2134/agronj2006.0201

Kunert, K. J., Vorster, B. J., Fenta, B. A., Kibido, T., Dionisio, G., and Foyer, C. H. (2016). Drought stress responses in soybean roots and nodules. *Front. Plant Sci.* 7:1015. doi: 10.3389/fpls.2016.01015

Li, H., and Durbin, R. (2009). Fast and accurate short read alignment with Burrows–Wheeler transform. *Bioinformatics* 25, 1754–1760. doi: 10.1093/bioinformatics/btp324

Li, X., Zeng, R., and Liao, H. (2016). Improving crop nutrient efficiency through root architecture modifications. *J. Integr. Plant Biol.* 58, 193–202. doi: 10.1111/jipb.12434

Li, X., Zheng, J., Yang, Y., and Liao, H. (2018). *Increasing nodule size1* expression is required for normal rhizobial symbiosis and nodule development. *Plant Physiol.* 178, 1233–1248. doi: 10.1104/pp.18.01018

López-Bucio, J., Cruz-Ramìrez, A., and Herrera-Estrella, L. (2003). The role of nutrient availability in regulating root architecture. *Curr. Opin. Plant Biol.* 6, 280–287. doi: 10.1016/s1369-5266(03)000359

Meng, L., Li, H., Zhang, L., and Wang, J. (2015). QTL IciMapping: integrated software for genetic linkage map construction and quantitative trait locus mapping in biparental populations. *Crop J.* 3, 269–283. doi: 10.1016/j.cj.2015.01.001

Menna, P., Hungria, M., Barcellos, F. G., Bangel, E. V., Hess, P. N., and Martinez-Romero, E. (2006). Molecular phylogeny based on the 16S rRNA gene of elite rhizobial strains used in Brazilian commercial inoculants. *Syst. Appl. Microbiol.* 29, 315–332. doi: 10.1016/j.syapm.2005.12.002

Nascimento, V. C. D., Prete, C. E. C., and Nogueira, M. A. (2016). Biological nitrogen fixation in soybean under water restriction and exposed to 1-methylcyclopropene. *Pesq. Agropec. Bras.* 51, 818–823. doi: 10.1590/s0100-204x2016000700004

Nicolás, M. F., Hungria, M., and Arias, C. A. A. (2006). Identification of quantitative trait loci controlling nodulation and shoot mass in progenies from two Brazilian soybean cultivars. *Field Crop Res.* 95, 355–366. doi: 10.1016/j.fcr.2005.04.012

Nohara, T., Nakayama, N., Takahashi, M., Maruyama, S., Shimada, S., and Arihara, J. (2005). Cultivar differences in dependence on nitrogen fixation of soybeans in the field with a high soil nitrate level determinated by the relative ureide abundance method. *Proc. Crop Sci. Soc. Jpn.* 74, 316–324. doi: 10.1626/jcs.74.316

Peoples, M. B., Brockwell, J., Herridge, D. F., Rochester, I. J., Alves, B. J. R., and Urquiaga, S. (2009). The contributions of nitrogen-fixing crop legumes to the productivity of agricultural systems. *Symbiosis* 48, 1–17. doi: 10.1007/BF03179980

Qin, L., Zhao, J., Tian, J., Chen, L., Sun, Z., Guo, Y., et al. (2012). The high-affinity phosphate transporter GmPT5 regulates phosphate transport to nodules and nodulation in soybean. *Plant Physiol.* 159, 1634–1643. doi: 10.1104/pp.112.199786

Santos, M. A., Geraldi, I. O., Garcia, A. A. F., Bortolatto, N., Schiavon, A., and Hungria, M. (2013). Mapping of QTLs associated with biological nitrogen fixation traits in soybean. *Hereditas* 150, 17–25. doi: 10.1111/j.1601-5223.2013.02275.x

Sivparsad, B. J., Chiuraise, N., and Laing, M. D. (2015). Comparative evaluation of commercial rhizobial inoculants of soybean. *South Afr. J. Plant Soil* 33, 157–160. doi: 10.1080/02571862.2015.1092177

Soedarjo, M., Saleh, N., Adisarwanto, T., and Ishiki, K. (2003). Characterization and effectiveness of rhizobia isolated from nodules of soybean grown on al-rich acid soils. *Jpn. J. Trop. Agric.* 47, 63–64.

Souza, A. A., Boscariol, R. L., Moon, D. H., Camargo, L. E. A., and Tsai, S. M. (2000). Effects of *Phaseolus vulgaris* QTL in controlling host-bacteria interactions under two levels of nitrogen fertilization. *Genet. Mol. Biol.* 23, 155–161. doi: 10.1590/S1415-47572000000100029

Takahashi, R., Dubouzet, J. G., Matsumura, H., Yasuda, K., and Iwashina, T. (2010). A new allele of flower color gene *W1* encoding flavonoid 3′5′-hydroxylase is responsible for light purple flowers in wild soybean *Glycine soja*. *BMC Plant Biol.* 10:155. doi: 10.1186/1471-2229-10-155

Tanya, P., Srinives, P., Toojinda, T., Vanavichit, A., and Lee, S. H. (2005). Identification of SSR markers associated with N2-fixation components in soybean [*Glycine max* (L.) Merr.]. *Korean J. Genet.* 27, 351–359.

Thomas-Oates, J., Bereszczak, J., Edwards, E., Gill, A., Noreen, S., Zhou, J. C., et al. (2003). A catalogue of molecular, physiological and symbiotic properties of soybean-nodulating rhizobial strains from different soybean cropping areas of China. *Syst. Appl. Microbiol.* 26, 453–465. doi: 10.1078/072320203322497491

Thuita, M., Pypers, P., Herrmann, L., Okalebo, R. J., Othieno, C., Muema, E., et al. (2012). Commercial rhizobial inoculants significantly enhance growth and nitrogen fixation of a promiscuous soybean variety in Kenyan soils. *Biol. Fertil. Soils* 48, 87–96. doi: 10.1007/s00374-011-0611-z

Udvardi, M., and Poole, P. S. (2013). Transport and metabolism in legume-rhizobia symbioses. *Annu. Rev. Plant Biol.* 64, 781–805. doi: 10.1146/annurev-arplant-050312-120235

Van Ooijen, J. W. (2009). *MapQTL 6, Software for the Mapping of Quantitative Trait Loci in Experimental Populations of Diploid Species*. Wageningen: Kyazma B.V.

Wang, K., Li, M., and Hakonarson, H. (2010). ANNOVAR: functional annotation of genetic variants from high-throughput sequencing data. *Nucleic Acids Res.* 38:e164. doi: 10.1093/nar/gkq603

Ward, A. (2011). *Phosphorus Limitation of Soybean and Alfalfa Biological Nitrogen Fixation on Organic Dairy Farms*. M.Sc. thesis, NSAC, Bible Hill.

Xia, X., Ma, C., Dong, S., Xu, Y., and Gong, Z. (2017). Effects of nitrogen concentrations on nodulation and nitrogenase activity in dual root systems of soybean plants. *J. Soil Sci. Plant Nutr.* 63, 1–13. doi: 10.1080/00380768.2017.1370960

Yang, Y., Zhao, Q., Li, X., Ai, W., Liu, D., Qi, W., et al. (2017). Characterization of genetic basis on synergistic interactions between root architecture and biological nitrogen fixation in soybean. *Front. Plant Sci.* 8:1466. doi: 10.3389/fpls.2017.01466

Yang, Z. W., Shen, Y. Y., Xie, T. L., and Tan, G. Y. (2009). Biological nitrogen fixation efficiency in soybean under different levels of nitrogen supply. *Acta Bot. Boreali Occident Sin.* 29, 574–579.

Yendrek, C. R., Lee, Y.-C., Morris, V., Liang, Y., Pislariu, C. I., Burkart, G., et al. (2010). A putative transporter is essential for integrating nutrient and hormone signaling with lateral root growth and nodule development in *Medicago truncatula*. *Plant J.* 62, 100–112. doi: 10.1111/j.1365-313X.2010.04134.x

Conflict of Interest Statement: The authors declare that the research was conducted in the absence of any commercial or financial relationships that could be construed as a potential conflict of interest.

frontiers in Plant Science

ORIGINAL RESEARCH
published: 15 February 2019
doi: 10.3389/fpls.2019.00141

Redox Systemic Signaling and Induced Tolerance Responses During Soybean–*Bradyrhizobium japonicum* Interaction: Involvement of Nod Factor Receptor and Autoregulation of Nodulation

*Tadeo F. Fernandez-Göbel[1], Rocío Deanna[2], Nacira B. Muñoz[1,3], Germán Robert[1,3], Sebastian Asurmendi[4] and Ramiro Lascano[1,3]**

[1] *Instituto de Fisiología y Recursos Genéticos Vegetales, Centro de Investigaciones Agropecuarias, Instituto Nacional de Tecnología Agropecuaria, Córdoba, Argentina,* [2] *Departamento de Ciencias Farmacéuticas, Facultad de Ciencias Químicas, Instituto Multidisciplinario de Biología Vegetal, Universidad Nacional de Córdoba, Consejo Nacional de Investigaciones Científicas y Técnicas, Córdoba, Argentina,* [3] *Cátedra de Fisiología Vegetal, Facultad de Ciencias Exactas, Físicas y Naturales, Universidad Nacional de Córdoba, Córdoba, Argentina,* [4] *Instituto de Biotecnología, Centro de Investigaciones en Ciencias Veterinarias y Agronómicas, Instituto Nacional de Tecnología Agropecuaria, Buenos Aires, Argentina*

OPEN ACCESS

Edited by:
Jeremy Astier, INRA UMR1347 Agroécologie, France

Reviewed by:
Pascal Ratet, Institut des Sciences des Plantes de Paris Saclay (IPS2), France
Marc Libault, The University of Oklahoma, United States

***Correspondence:**
Ramiro Lascano
hrlascano@hotmail.com;
lascano.ramiro@conicet.gov.ar

Specialty section:
This article was submitted to Plant Microbe Interactions, a section of the journal Frontiers in Plant Science

Received: *17 September 2018*
Accepted: *28 January 2019*
Published: *15 February 2019*

Citation:
Fernandez-Göbel TF, Deanna R, Muñoz NB, Robert G, Asurmendi S and Lascano R (2019) Redox Systemic Signaling and Induced Tolerance Responses During Soybean–Bradyrhizobium japonicum Interaction: Involvement of Nod Factor Receptor and Autoregulation of Nodulation. Front. Plant Sci. 10:141. doi: 10.3389/fpls.2019.00141

The symbiotic relationship between legumes and nitrogen-fixing rhizobia induces local and systemic responses, which ultimately lead to nodule formation. The autoregulation of nodulation (AON) is a systemic mechanism related to innate immunity that controls nodule development and involves different components ranging from hormones, peptides, receptors to small RNAs. Here, we characterized a rapid systemic redox changes induced during soybean–*Bradyrhizobium japonicum* symbiotic interaction. A transient peak of reactive oxygen species (ROS) generation was found in soybean leaves after 30 min of root inoculation with *B. japonicum*. The ROS response was accompanied by changes in the redox state of glutathione and by activation of antioxidant enzymes. Moreover, the ROS peak and antioxidant enzyme activation were abolished in leaves by the addition, in either root or leaf, of DPI, an NADPH oxidase inhibitor. Likewise, these systemic redox changes primed the plant increasing its tolerance to photooxidative stress. With the use of non-nodulating *nfr5*-mutant and hyper-nodulating *nark*-mutant soybean plants, we subsequently studied the systemic redox changes. The *nfr5*-mutant lacked the systemic redox changes after inoculation, whereas the *nark*-mutant showed a similar redox systemic signaling than the *wild type* plants. However, neither *nfr5*- nor *nark*-mutant exhibited tolerance to photooxidative stress condition. Altogether, these results demonstrated that (i) the early redox systemic signaling during symbiotic interaction depends on a Nod factor receptor, and that (ii) the induced tolerance response depends on the AON mechanisms.

Keywords: systemic changes, redox signaling, rhizobia, soybean symbiosis, ISR/PGPR-like response, autoregulation of nodulation

INTRODUCTION

The symbiotic interaction between legume plants and nitrogen-fixing soil bacteria has great importance at a basic, ecological and economic level and, the legume–rhizobium symbiosis interaction is the most important in terms of the biological nitrogen fixation (Graham and Vance, 2003). Moreover, the legume–rhizobium interaction could also induce PGPR like-responses, improving host plant growth and tolerance/resistance to abiotic/biotic stress conditions. In this sense, it has been postulated that the enhanced tolerance/resistance in inoculated plants is achieved by an ISR modulated by JA and ET (Pieterse et al., 2014).

Rhizobia have acquired the ability to evade the initial microbe-associated molecular pattern (MAMP) triggered immunity (Boller and Felix, 2009) by modulating the host immune response to avoid being recognized as a pathogen (Zamioudis and Pieterse, 2012). In this regard, many biochemical, molecular and hormonal changes occur at local and systemic levels during the legume–rhizobium interaction so that rhizobia coordinate the organogenesis of the nodule with infection (Nadzieja et al., 2018).

The species-specific interaction between rhizobia and their host plant is determined by nodulation (Nod) factors from rhizobia and the structure of the Nod-factor receptor (NFR) in the host. Nod factors are formed by a chitin backbone with an N-linked fatty acid moiety attached to the non-reducing terminal sugar and other modifications (Oldroyd and Downie, 2008; Oldroyd et al., 2011).

Nitrogen availability and Nod factors are major local regulators. On the other hand, an innate immunity-related mechanism, called AON, is the systemic control of the nodulation process and involves long-distance root–shoot–root signaling (Caetano-Anolles and Gresshoff, 1991; Ferguson et al., 2010, 2018). During AON, rhizobia trigger the synthesis of CLE peptides in the root (GmRIC1 and GmRIC2 in soybean) that move via xylem to the shoot, where they bind to a LRR receptor kinase, the nodulation autoregulation receptor kinase (NARK). This binding triggers the production of a SDI, which moves back to the roots and inhibits nodule formation (Searle et al., 2003; Okamoto et al., 2009, 2013; Ferguson et al., 2010, 2018; Indrasumunar et al., 2011; Reid et al., 2013). Although the chemical nature of SDI is not completely known, some evidence postulates CKs as putative SDI (Chen et al., 2014; Sasaki et al., 2014; Mens et al., 2018).

Abbreviations: ABA, abscisic acid; AON, autoregulation of nodulation; APX, ascorbate peroxidase; CAT, catalase; CKs, cytokinins; DPI, diphenyleneiodonium; ET, ethylene; GmNARK, *Glycine max* nodulation autoregulation receptor kinase; GR, glutathione reductase; hpi, hours post inoculation; HAR1, hypernodulation aberrant root formation 1; IPT, isopentenyl transferase; ISR, induced systemic resistance; JA, jasmonic acid; LCO, lipo-chitooligosaccharide; LRR, leucine-rich repeat; MAMPs, microorganism associated molecular patterns; MDA, malondialdehyde; NF, Nod factors; NFR5, Nod factor receptor 5; NIC, nitrate-induced CLE peptides; PAL, phenylalanine ammonia-lyase; PGPR, plant growth-promoting rhizobacteria; PQ, paraquat; RBOH, respiratory burst oxidase homolog; RIC, rhizobia-induced CLE peptides; ROS, reactive oxygen species; SA, salicylic acid; SAA, systemic acquired acclimation; SAR, systemic acquired resistance; SDI, shoot-derived inhibitor; SOD, superoxide dismutase.

Reactive oxygen species were initially characterized as toxic by-products of aerobic metabolism. Nowadays, however, ROS are also considered signaling molecules involved in several signaling pathways in organisms from bacteria to mammal. Thus, the concept of oxidative stress moves toward oxidative or redox signaling. This dual role of ROS depends on its tight generation/scavenging ratio in different subcellular location. The ROS scavenging capacity of plants is supported by the well-known antioxidant system, which is composed by soluble antioxidants like ascorbate and glutathione as well as by enzymes like SODs, CATs, APXs, and GRs. This system forms a hub that acts as a cellular redox state buffering mechanism that regulates the cellular redox homeostasis. Changes of the cellular redox state provide important information and act on the sensing, signaling and response to internal or external stimuli (Asada, 1999; Foyer and Noctor, 2009).

The RBOH proteins or NADPH oxidase complex in plants are major sources of apoplastic ROS and key players in the oxidative or redox signaling. RBOH mediates cell-to-cell communication and long-distance signaling in response to different stress conditions. The long-distance or systemic signaling mediated by ROS travels at a rate similar to an electric signal, and is independent of ET, JA, or SA signaling. The systemic redox signaling participates in the regulation of systemic acclimatory mechanism to stress conditions (Miller et al., 2009). ROS and nitric oxide are involved in the systemic defense signals, either against pathogens or abiotic stress, as evidenced by their synthesis upon these stresses, and can be propagated over long distances through the phloem (Gaupels et al., 2017).

Local redox changes in root hairs and roots induced during different stages of the symbiotic interaction have also a key role in nodulation regulation (Peleg-Grossman et al., 2007; Cárdenas et al., 2008; Muñoz et al., 2012, 2014b; Robert et al., 2014, 2018; Arthikala et al., 2017).

In this study, we analyzed the systemic redox changes during the *Glycine max–Bradyrhizobium japonicum* interaction and their implications on ISR/PGPR-like response. In addition, we investigated the involvement of Nod factors perception and AON mechanisms in the ISR/PGPR-like response by performing experiments with non-nodulating *nfr5*- and hyper-nodulating *nark*-soybean mutants. Thus, the feature of AON as an autoimmunity mechanism as well as the involvement of the anti-senescence hormone CKs in the systemic control of nodule development led us to hypothesize that AON mechanisms are underlying the ISR/PGPR-like response induced during legume–rhizobia symbiotic interaction.

MATERIALS AND METHODS

Plant and Bacterial Growth Conditions

Glycine max (L.) Merr. *cv.* Bragg *wild type (wt)*, *nts1007* (hyper nodulating *nark*-mutant) and *nod139* (non-nodulating *nfr5*-mutant) (Carroll et al., 1985, 1986) were used in this work. Seeds were surface-disinfected for 10 min in sodium hypochlorite 5% (v/v) and washed successively with distilled water. The seeds were germinated on filter paper moistened with distilled water in a

chamber at 28°C in the dark for 3 days. Then, seedlings were placed in aerated plastic trays with B&D solution (Broughton and Dilworth, 1971) supplemented with 0.625 mM KNO_3 and 0.313 mM $Ca(NO_3)_2$ (1,25 mM of total nitrogen concentration). The B&D solution was replaced every 7 days. Soybean plants were grown in a growth chamber under 16 h photoperiod (250 μmol m^{-2} s^{-1}) at 26 ± 2°C.

Bradyrhizobium japonicum USDA 138 strain was cultured in yeast extract mannitol (YEM) medium (Vincent, 1971) at 28°C with constant agitation (180 rpm) for 5 days. For the treatments, the bacteria were washed and resuspended in sterile water (OD_{600} = 0.8).

Treatments Conditions

The root of 12-days-old soybean plants were inoculated with 2.5 mL of washed *B. japonicum* USDA 138 strain (OD_{600} = 0.8) per liter of hydroponic medium. The first trifoliate leaf was collected at different times post-inoculation and immediately frozen or used for measurement.

For the DPI treatments, an NADPH-oxidase inhibitor (50 μM), was added 30 min before inoculating *B. japonicum* to either the root or leaf according to the experiment. The inhibitor was added to the hydroponic medium for the root application or sprinkled locally in the first trifoliate leaf. DPI application does not affect the normal growth of *B. japonicum* (Muñoz et al., 2012).

For the photooxidative stress treatment, the first trifoliate leaf of 12-days-old inoculated and non-inoculated (control) plants were treated with 1,1′-dimethyl-4, 4′-bipyridinium dichloride (PQ). PQ is a viologen that acts at the photosystem I level by intercepting the electrons that are going from ferredoxin to NADP+, thus enhancing chloroplastic ROS generation and inhibiting ascorbate regeneration (Asada, 1999). The leaves were splashed uniformly with 20 μM of PQ and 0.01% Tween 20 at 24 and 48 hpi and physiological parameters were measured after 24 h of PQ treatments. PQ was replaced by water in control treatments.

Purified Nod factors and chitosan treatments were performed in the same way than *B. japonicum* inoculation, in the hydroponic medium. Chitosan is a fungal elicitor.

Apoplastic Superoxide Radical (O_2^-) and Hydrogen Peroxide (H_2O_2) Production in Leaves

Superoxide levels were determined histochemically with nitro-blue tetrazolium (NBT) staining, which reacts with superoxide radicals to produce a blue formazan precipitate. Leaves were incubated in 0.01% (w/v) NBT solution in 25 mM K-Hepes buffer (pH 7.6) in the darkness at 28°C for 2 h. Color images were transformed in invert 8-bit images and gray value intensity of the blue stain was quantified using the ImageJ software (Schneider et al., 2012).

H_2O_2 generation was histochemically determined with 3,3′-diaminobenzidine (DAB) staining. The leaves were incubated in 0.02% (w/v) DAB solution in 50 mM Tris acetate buffer (pH 5) and incubated in the darkness at 28°C for 2 h. Color images were transformed into invert 8-bit images and gray value intensity of the DAB stain was quantified using Optimas 6 (Optimas Corporation, Bothell, WA, United States). Total optical density (OD) was calculated as log inverse gray value of pixels within an area boundary relative to the analyzed area.

Hydrogen peroxide was also estimated in leaf extracts as previously described by Guilbault et al. (1968). A blank with CAT was included for each sample. Frozen leaf samples were ground to a fine powder with liquid nitrogen and homogenized 1/10 (w/v) in 50 mM potassium phosphate buffer (pH 7.5), containing 1 mM EDTA and 1% polyvinylpolypyrrolidone (PVPP). Homogenates were centrifuged at 16,000 × *g* at 4°C for 25 min and the supernatant was used to determine protein and hydrogen peroxide concentrations.

Glutathione and Ascorbate Content

The glutathione and ascorbate content in soybean leaves were determined as previously described by our group (Rodríguez et al., 2010). Leaf samples were homogenized (100 mg of fresh weight material) in 1 mL of cold 3% trichloroacetic acid (TCA) and 100 mg PVPP. The homogenate was centrifuged at 10,000 × *g* at 4°C for 15 min and the supernatant was collected to for analyze of glutathione and ascorbate content.

Antioxidant Enzymatic Activities

Superoxide dismutase activity was determined spectrophotometrically at 560 nm, as previously described by Casano et al. (1997). GR activity was assayed following the decrease at A340 nm because of NADPH oxidation, according to Schaedle and Bassham (1977). CAT activity was determined by measuring the decrease at 240 nm because of H_2O_2 degradation (Gallego et al., 1996). APX activity was measured according to Nakano and Asada (1981) by measuring the H_2O_2-dependent oxidation of ascorbate at 290 nm (the extract medium for this enzyme contained 5 mM ascorbate).

Total Protein Content

Soluble proteins were estimated according to Bradford (1976). Bovine serum albumin was used as a standard for calibration.

Chlorophyll Content

The Chlorophyll content of the first trifoliate leaf was estimated using a handheld SPAD CL01 meter (Hansatech Instruments, Pentney King's Lynn, United Kingdom). The results are expressed as unitless parameter (SPAD units, 0 to 100), which is proportional to leaf chlorophyll.

Chlorophyll Fluorescence and Photosynthesis

Quantum efficiency of PSII photochemistry under ambient light conditions (250 μmol photon m^{-2} s^{-1}, 25 ± 2°C) (ΦPSII) was measured using a pulse amplitude modulated fluorometer (FMS2, Hansatech Instruments, Pentney King's Lynn, United Kingdom). F_v/F_m ratio was calculated using $(F_m - F_0)/F_m$, where F_m is maximal fluorescence yield of the dark-adapted state and F_0 is minimum fluorescence yield (Maxwell and Johnson, 2000).

Photosynthesis was determined using a portable infrared gas analyzer (Li-COR-6400, United States). Leaf chamber setting parameters were: LED light source of 800 μmol. m^{-2} s^{-1}, leaf temperature 25–26°C, CO_2 concentration of 400 μmol. mol^{-1} and 500 flow.

Performance Index

The performance index, is an indicator of leaf vitality, the measurements were performed with the Pocket PEA chlorophyll fluorimeter (Hansatech Instruments, Pentney King's Lynn, United Kingdom).

Total Antioxidant Capacity (FRAP), Malondialdehyde Content (MDA), Chlorophylls, and Sugars

The samples were homogenized using a mortar and pestle under liquid nitrogen and adding 80% EtOH. Then, centrifugation was carried out at 12,000 × *g*, 4°C during 10 min. This extracts were used to measure FRAP, lipid peroxidation (MDA content), chlorophylls and sugars.

For FRAP determination, 5 μL of supernatant was diluted 20 times with 80% EtOH and mixed with 100 μL reaction buffer (5 mL of acetate buffer 0.3 M pH 3.6; 0.5 mL of TPTZ 10 mM (2,4, 6 Tris (2 pyridyl) s-triazine) diluted in 40 mM HCl and 0.5 mL of $FeCl_3$ 200 mM). This mixture was left to stand for 20 min at room temperature to react and the reaction was subsequently measured at 593 nm. TROLOX was used as a standard to calculate FRAP capacity of the samples (Benzie and Strain, 1996).

Malondialdehyde levels were quantified according to Heath and Packer (1968). Briefly, 200 μL of each sample was mixed with 200 μL of 20% TCA + 0.5% TBA, incubated at 80°C for 20 min and immediately cooled in ice. The mix was centrifuged at 13,000 × *g* for 10 min and the absorbance of the supernatant was read at 532 nm and 600 nm.

Chlorophylls were calculated by spectrofluorometry at 654 nm in a reaction with 50 μL of extract and 450 μL of EtOH.

Sugars were determine in a reaction of 5 μL of each extract with 45 μL of EtOH and 150 μL of antrone that was incubated 20 min at 4°C, 30 min at 80°C and 20 min at 25°C. The reactions were subsequently measured at 620 nm. Glucose was used to calibrate a standard curve.

Phenylalanine Ammonia-Lyase Activity (PAL)

The PAL activity was measure according to Beaudoin-Eagan and Thorpe (1985). The enzyme activity was expressed in nmol of *trans*-cinnamic acid.mg $protein^{-1}.min^{-1}$, where 1 U is defined as 1 nmol *trans*-cinnamic acid.mg $protein^{-1}.min^{-1}$. 300 mg of leaf samples were homogenized in 3 mL of Tris-HCl buffer 50 mM pH 8.5 with 2-mercaptoethanol 14.4 mM and 100 mg PVPP, and centrifuged at 6,000 × *g* for 10 min at 4°C. The supernatant were passed through a column of celite and centrifuged at 10,000 × *g* for 15 min at 4°C. Total protein concentration was determined using the Bradford (1976) assay.

Hormone Identification and Quantification by Liquid Chromatography Electrospray Ionization Tandem Mass Spectrometry (LC-ESI/MS-MS)

Phytohormones were extracted from 200 g of dry weight leaf as previously described (Durgbanshi et al., 2005) with some modifications. Plant material was homogenized in an ultraturrax T25 basic homogenizer (IKA, Staufen; Germany) with 5 mL deionized water. D2-SA and D6-JA (Leibniz- Institute of Plant Biochemistry; Halle, Germany) were used as internal standards. A total of 50 ng of each standard was added to the samples. The samples were centrifuged at 1,540 × *g* for 15 min and the supernatant was adjusted to pH 2.8 with 15% (v/v) acetic acid and extracted twice with diethyl ether. The organic fraction was evaporated under vacuum. Dried extracts were dissolved in 1 mL methanol and filtered on a vacuum manifold at a flow rate below 1 $mL.min^{-1}$. The eluate was evaporated at 35°C under vacuum in SpeedVac SC110 (Savant Instruments; New York, NY, United States). Four biological replicates were used for the assays.

Hormones were separated from samples using reversed-phase high-performance liquid chromatography (HPLC). An Alliance 2695 separation module (Waters; Milford, MA, United States) equipped with a Resteck Ultra C18 column (100 × 2.1 mm, 3 μm) was used to maintain performance of the analytical column. Fractions were separated using a gradient of increasing methanol concentration, constant glacial acetic acid concentration (0.2% in water), and an initial flow rate of 0.2 mL min^{-1}. The gradient was increased linearly from 40% methanol/60% water-acetic acid at 25 min to 80% methanol/20% water-acetic acid. After 1 min, the initial conditions were restored, and the system was allowed to equilibrate for 7 min. Hormones were identified and quantified using a quadruple tandem mass spectrometer (Quattro Ultima, Micromass; Manchester, United Kingdom) fitted with an electrospray ion (ESI) source, in multiple reactions monitoring mode (MRM). This assay was performed using precursor ions and their transitions (m/z) to SA (m/z 137/93), D2-SA (m/z 141/97) and JA (m/z 209/59), D6-JA (m/z 215/59) with retention times of 4.35 and 14.30 min, respectively. Collision energies used were 20 eV for both and the cone voltage was 35 V. The analyses were accomplished using MassLynk version 4.1 (Micromass).

Ethylene Content by Gas Chromatography

Prior to *B. japonicum* inoculation, 12-days-old plants were transferred to 580 cm^3 glass jars containing 100 mL of B&D solution. Three plants per bottle were placed and inoculated with *B. japonicum*. The containers were sealed to prevent the loss of gaseous hormone. Subsequently, samples were taken through syringes of 10 mL 30 min post inoculation, and subsequently conserved in sealed 10 cm^3 vial tubes at 4°C until quantification.

Ethylene content was determined by gas chromatography according to adaptations of the methodology described by Hardy et al. (1968). Briefly, 1 mL of air sample was injected and quantification was carried out for 2 min in a Hewlett Packard

Series II 5890 gas chromatograph by determining the ET peak between the retention times of 1.4 and 1.55 min.

Statistical Analysis

Three independent experiments with their corresponding number of replicates for each case were performed in different dates. All data are presented as the mean ± standard error (SE). Comparisons between different treatments were analyzed by ANOVA and Tukey tests using InfoStatTM Software (Di Rienzo et al., 2016). The results were considered significant when $p < 0.05$.

A multivariate statistical analysis was performed using a principal component analysis (PCA) (Johnson and Wichern, 2006) to explore associations between genotypes/treatments and the set of physiological variables.

RESULTS

NADPH Oxidase-Dependent Systemic Redox Changes Are Induced in Soybean Leaves After Root Inoculation With *Bradyrhizobium japonicum*

As mentioned above, the establishment of the symbiotic relationship between legumes and rhizobia depends on both local and systemic complex signaling pathways (Ferguson et al., 2018). In this regard, although the participation of local ROS signaling in roots after symbiont perception has been widely studied (Cárdenas et al., 2008; Muñoz et al., 2012, 2014a; Damiani et al., 2016), much less is known about the ROS systemic production during the legume–rhizobium interaction. We evaluated histochemically the systemic ROS (O_2^- and H_2O_2) generation in leaves after 30, 60, 120 and 240 min of root inoculation with *B. japonicum* (**Figures 1A,B**). The pictures of the stained leaves were transformed in numeric values using image processing software as described in "Materials and Methods." Besides, the content of H_2O_2 in leaves was also quantified by spectrofluorometer (**Figure 1C**). Interestingly, the H_2O_2 and O_2^- generation were differentially modulated in leaves after root inoculation (**Figure 1**). The inoculated plants displayed H_2O_2 generation from 30 to 120 min after root inoculation and the levels were higher than those of the control plants (**Figures 1A,C**). However, these levels decreased after 240 min post inoculation even below the levels of H_2O_2 observed in the control plants (**Figure 1A**).

In the case of O_2^-, a transient peak of O_2^- generation was induced at 30 min post inoculation, whereas no differences were observed in the later times with respect to the non-inoculated control plants (**Figure 1B**). Moreover, this systemic and transient response was specific for *B. japonicum*. Indeed, the addition of purified Nod factors to the roots induced a transient systemic ROS induction, whereas treatments with chitosan, a fungal elicitor, induced a sustained systemic ROS induction (**Supplementary Figure S1**).

In order to further characterize the cellular redox state changes in leaves after root inoculation, the content of ascorbic acid, glutathione, MDA and the activities of SOD, GR, CAT, and APX were measured (**Figures 2**, **3**).

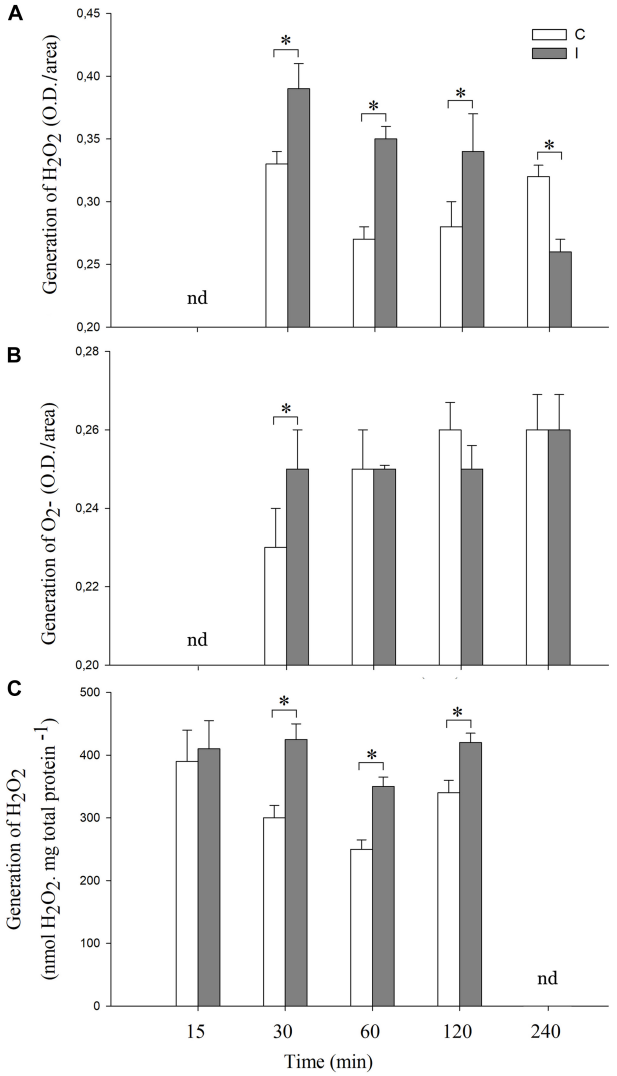

FIGURE 1 | Systemic ROS generation is induced after root inoculation with *B. japonicum*. Leaves of non-inoculated (control, C) and inoculated (I) plants were sampled at different times after root inoculation (nd represent times not determined), and incubated with **(A)** 3,3′-diaminobenzidine (DAB) or **(B)** NBT for H_2O_2 and O_2^- staining, respectively. The pictures of the stained leaves were transformed into 8-bit images and the gray value intensity (O.D.) was quantified by image processing software. Results are the means of three independent experiments (four leaves per treatment). Data are means ± SE. Asterisks indicate significant difference between control and inoculated treatments ($p < 0.05$, Tukey test). **(C)** H_2O_2 quantification by spectrofluorometer. The results are the means of three independent experiments (six leaves per treatment). Data are means ± SE. Asterisks indicate significant difference between control and inoculated treatments ($p < 0.05$, Tukey test).

The total ascorbic acid content increased in leaves only at 30 min post inoculation compared to leaves of non-inoculated plants (**Figure 2A**). No significant differences were observed in the ascorbic acid redox state (reduced/total ratio) at any

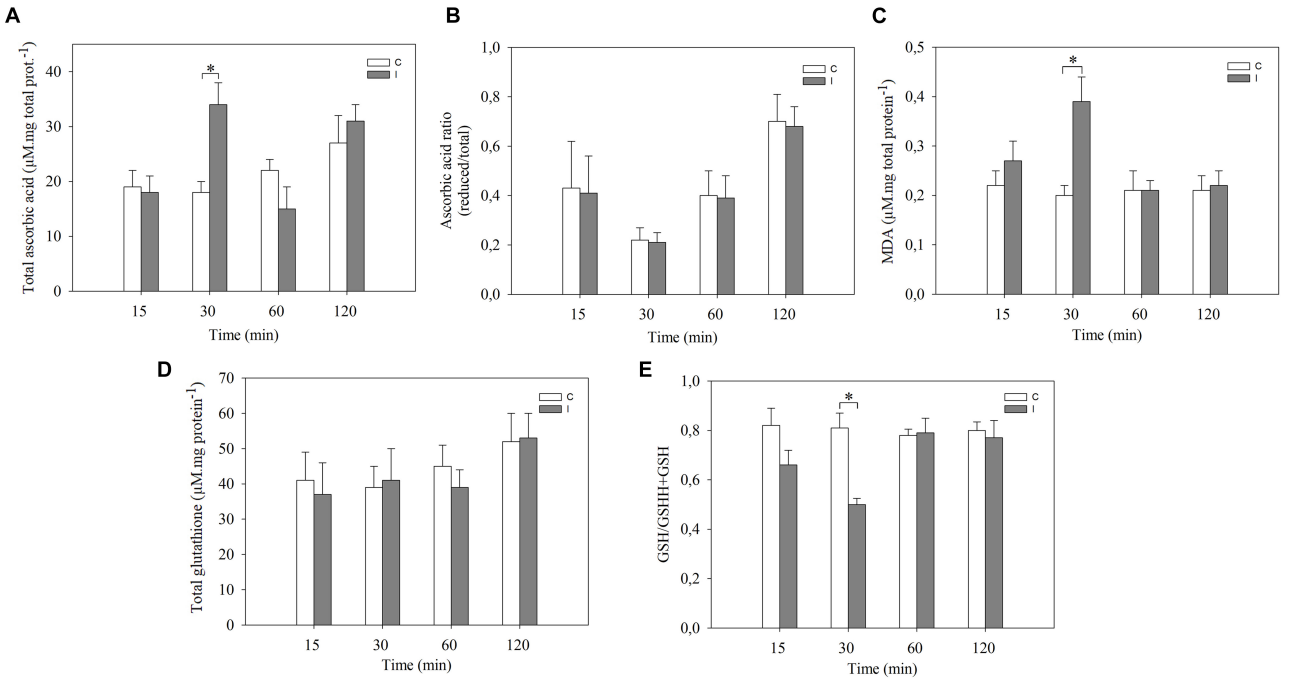

FIGURE 2 | Systemic redox changes are observed after root inoculation with *B. japonicum*. Leaves of non-inoculated (control, C) and inoculated (I) plants were sampled at different times after root inoculation and **(A)** total ascorbic acid, and **(D)** glutathione levels were measured. The reduced/total ratio of **(B)** ascorbic acid, and **(E)** glutathione was calculated. MDA content **(C)** was quantified. Data are means ± SE of three independent experiments. Asterisks indicate significant difference between control and inoculated treatments ($p < 0.05$, Tukey test).

of the evaluated times (**Figure 2B**). On the other hand, total glutathione content in leaves remained unaltered with the inoculation. The glutathione redox state (reduced/total ratio), however, decreased at 30 min in leaves of inoculated plants compared with control plants (**Figures 2D,E**). Likewise, the content of MDA, which is an intermediary metabolite of lipid peroxidation used as an oxidative stress marker, significantly increased in leaves of inoculated plants after 30 min of root inoculation thereby correlating with ROS induction (**Figure 2C**).

NADPH oxidase complex plays important roles in local signaling during symbiotic interaction (Peleg-Grossman et al., 2007; Cárdenas et al., 2008; Montiel et al., 2012; Muñoz et al., 2012; Robert et al., 2018) as well as in systemic signaling triggered by wounding, heat, cold, high-intensity light, and salinity stress (Miller et al., 2009). To investigate the participation of this complex during the systemic ROS induction in leaves after root inoculation, we pretreated the roots or leaves with 50 µM DPI, a well-known inhibitor of flavoprotein enzymes that is extensively used as an NADPH oxidase inhibitor (**Figure 3**). Interestingly, the induced systemic ROS generation observed in leaves of inoculated plants was completely abolished when DPI was applied in leaf, and a partial inhibited when DPI was applied in root (**Figure 3A**). Moreover, this inhibitor completely abolished the induction of SOD, GR, and CAT activities observed in leaves 30 min post inoculation (**Figures 3B–D**). Nevertheless, no significant differences were observed in the APX activity (**Figure 3E**).

In addition, JA, SA, and ET levels remained apparently unaltered in leaves 30 min after root inoculation with *B. japonicum* (**Figure 4**).

NFR5-Dependent Systemic ROS Induction After Root Inoculation

To further study the systemic redox changes induced during the soybean–*B. japonicum* interaction, we analyzed ROS generation in leaves of non-nodulating *nfr5*-mutant and hyper-nodulating *nark*-mutant soybean plants after 30 min of root inoculation (**Figure 5**). The leaves of *nark*-mutants showed a systemic ROS induction in response to *B. japonicum* inoculation similarly to that of the *wt* soybean plants (**Figure 5**). However, neither the systemic generation of H_2O_2 nor O_2^- were induced in leaves of *nfr5*-mutant soybean plants 30 min post inoculation (**Figure 5**).

From Root to Shoot: Root Inoculation Induced Systemic Tolerance to Photooxidative Stress

The legume–rhizobium symbiotic interaction can mediate an increased tolerance to abiotic stresses in host plants by an ISR modulated by JA and ET (Dimkpa et al., 2009; Pieterse et al., 2014). Furthermore, genetic and cell biological evidences revealed the role of ROS as a second messenger during the plant responses to the environment (Miller et al., 2007, 2008; Melchiorre et al., 2009). In this regard, the NADPH oxidase complex not only initiates ROS production but also amplifies

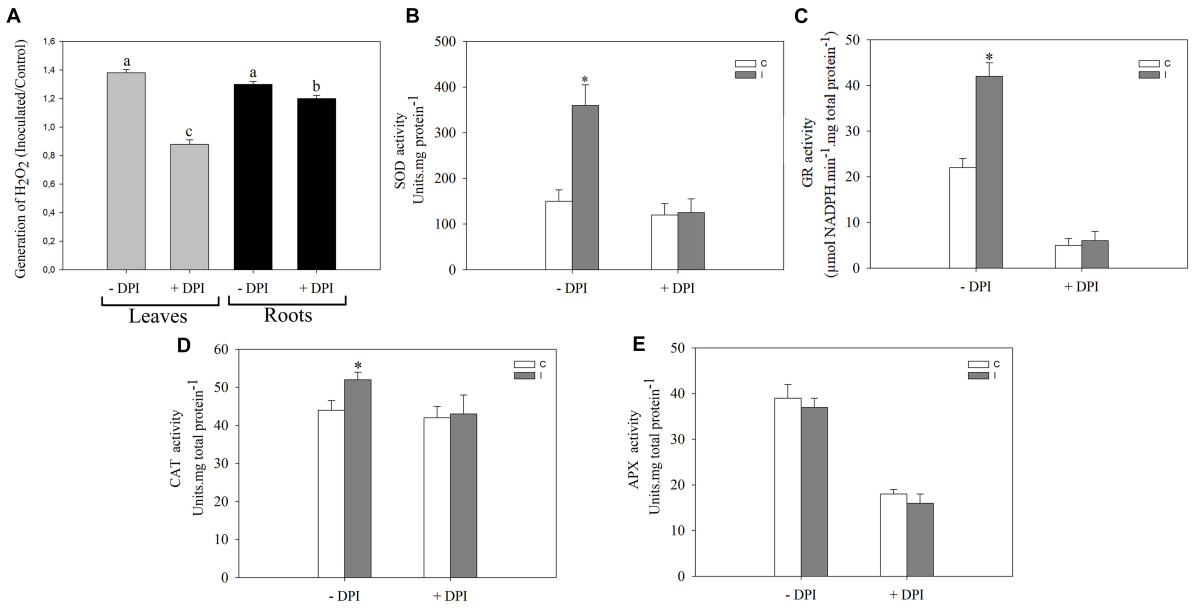

FIGURE 3 | NADPH oxidase complex modulates the systemic redox changes after root inoculation with *B. japonicum*. Leaves or roots of 12-days-old soybean plants were pretreated 30 min with 50 µM DPI (+DPI) or DMSO (–DPI), and then roots were inoculated with *B. japonicum*. After 30 min of root inoculation, leaves of non-inoculated (control, C) and inoculated (I) plants were sampled and incubated with **(A)** 3,3′-diaminobenzidine (DAB) for H_2O_2 quantification. The results are expressed relative to non-inoculated plants (assigned a value of 1). DAB precipitated in leaves was measured and transformed into optical density (OD) by the image processing software Optimas®. The results are the means of three independent experiments (four leaves per treatment). Different letters indicate significant differences between the treatments ($p < 0.05$, Tukey test). SOD **(B)**, GR **(C)**, CAT **(D)** and APX **(E)** activities were measured 30 min post inoculation in leaves of plants whose roots were pretreated with DPI (+DPI) or DMSO (–DPI). Data are means ± SE of three independent experiments. Asterisks indicate significant difference between control and inoculated treatments ($p < 0.05$, Tukey test).

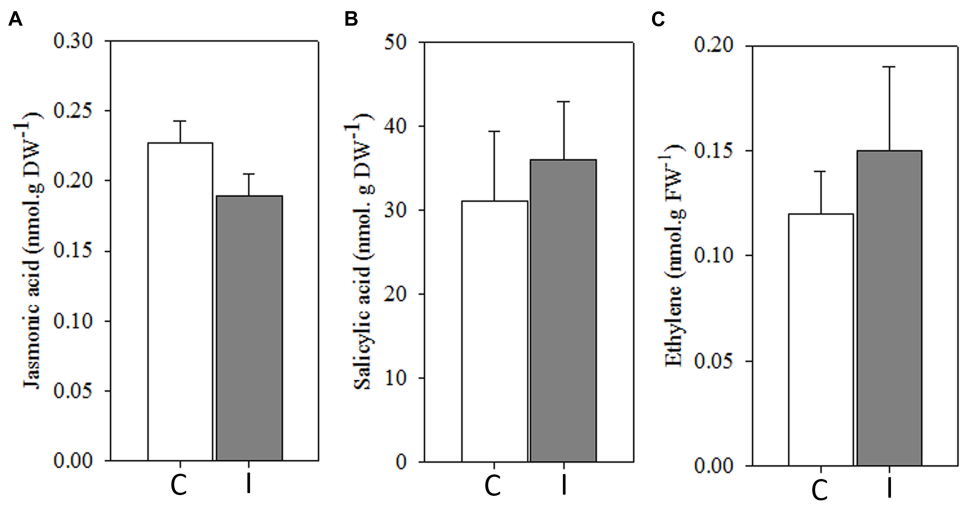

FIGURE 4 | Systemic ROS generation precedes to systemic hormonal changes after root inoculation with *B. japonicum*. Jasmonic acid **(A)**, salicylic acid **(B)**, and ethylene **(C)** were quantified 30 min after root inoculation from leaves of non-inoculated (control, C) and inoculated (I) plants. Data are the means of four leaves ± SE for jasmonic acid and salicylic acid, and seven leaves for ethylene of three independent experiments. No significant differences were observed between control and inoculated plants ($p < 0.05$, Tukey test).

them (Foreman et al., 2003; Torres and Dangl, 2005; Miller et al., 2009; Robert et al., 2009).

Stress conditions, in general, are associated with increases in the ROS production, mainly in the chloroplasts, which ultimately leads to photooxidative stress. In order to evaluate the systemic beneficial effects of the symbiotic interaction, the tolerance of non-inoculated and inoculated plants to PQ treatments, an herbicide that increase the chloroplasts ROS production

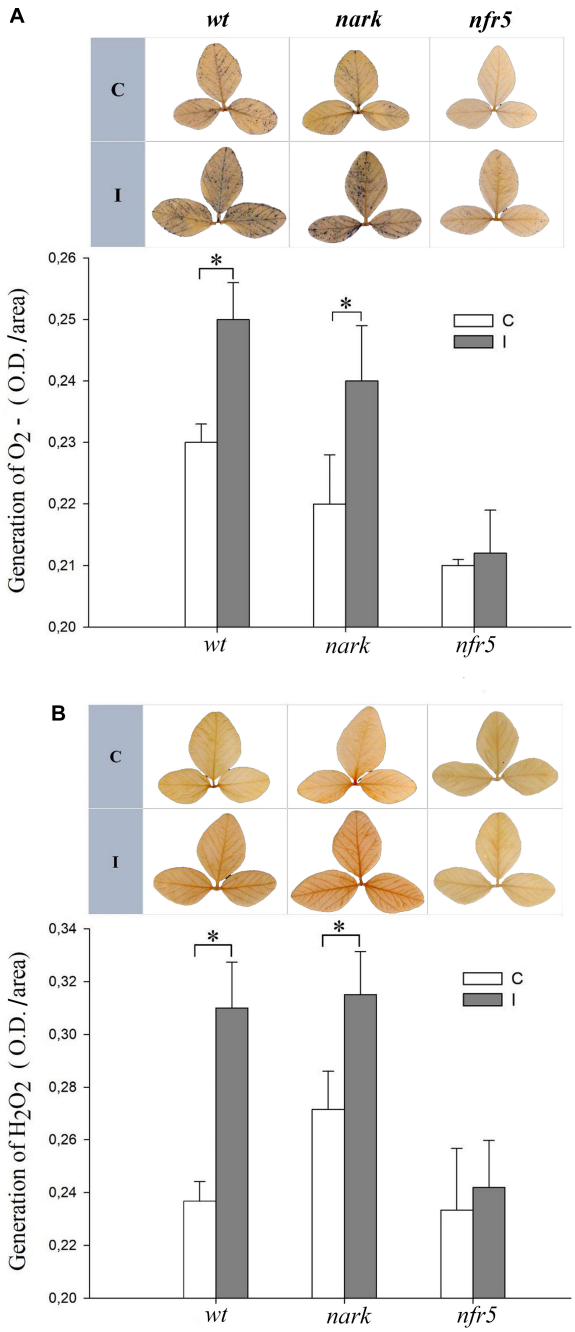

FIGURE 5 | The systemic ROS induction after *B. japonicum* inoculation depends on NFR5 signaling pathways. Roots of 12-days-old *nfr5* and *nark*-soybean mutant plants or *wt* plants were inoculated with *B. japonicum* (I), and the first trifoliate leaf was sampled after 30 min and incubated with **(A)** nitroblue tetrazolium (NBT) or **(B)** 3,3′-diaminobenzidine (DAB) for O_2^- and H_2O_2 staining, respectively. Non-inoculated plants were used as control (C). Upper panels, NBT and DAB stained leaves; lower panels, NBT and DAB quantification. The pictures of the stained leaves were transformed into 8-bit images and the gray value intensity (O.D.) was quantified with image processing software. The results are the means of three independent experiments (four leaves per treatment). Data are means ± SE. Asterisks indicate significant differences between control and inoculated plants ($p < 0.05$, Tukey test).

(Lascano et al., 2003, 2012; Melchiorre et al., 2009; Robert et al., 2009), were evaluated. The first trifoliate leaf of non-inoculated and inoculated plants was treated with PQ at 24 and 48 h post inoculation. The selected physiological parameters related to photosynthesis to be assessed after 24 h of PQ application were SPAD, PSII, and F_v/F_m (**Supplementary Figure S2**). Under control conditions (without PQ), no significant differences were observed between non-inoculated and inoculated plants (**Supplementary Figure S3**). Likewise, no significant differences were observed between non-inoculated and inoculated plants treated with PQ at 24 h after root inoculation (**Figure 6**). However, the leaves of inoculated plants were more tolerant than leaves of non-inoculated plants when PQ was applied after 48 h of root inoculation (**Figure 6**).

ISR/PGPR-Like Response: Participation of Nod-Factors and AON-Signaling Pathways?

To evaluate the involvement of Nod-factors and AON signaling in an ISR/PGPR-like response induced during soybean–*B. japonicum* interaction, *nrf5*- and *nark*-mutant soybean plants were used. Leaves of mutant and *wt* plants were treated with PQ 48 h after root inoculation, and then diverse physiological–biochemical parameters were assessed (**Figure 7**). The performance index is an integrative and sensitive parameter that gives quantitative information on the plant performance reflecting the functionality of both photosystems I and II (Strasser et al., 2000). After PQ treatments, leaves of *wt* inoculated plants showed an increase in the performance index in comparison to leaves of non-inoculated *wt* plants (**Figure 7A**). However, the leaves of inoculated and non-inoculated *nfr5*-mutant plants showed no significant differences after this treatment (**Figure 7A**). Curiously, the *nark*-mutant plants showed a lower tolerance upon inoculation (**Figure 7A**). Furthermore, the photosynthesis rates were significantly lower in *wt* non-inoculated with respect to *wt* inoculated plants, whereas no effect of inoculation was observed in leaves of *nfr5*- and *nark*-soybean mutants (**Figure 7B**). In a PCA performed to identify associations between physiological–biochemical parameters and the different plant genotypes under photooxidative stress treatments, the first two principal components (PC 1 and PC 2) of the analysis explained 85.1% of total variability in the data (**Figure 7C**). In a PCA, the cosine of the angle between two parameter vectors approximates the association among the parameters, with acute and obtuse angles indicating positive and negative correlations, respectively, and right angles denoting no correlation between parameters. The PC1 of the biplot indicated that SPAD, performance index, F_v/F_m, photosynthesis, stomatic conductance and FRAP were positively associated and these vectors were oriented toward *wt*-inoculated plants (**Figure 7C**). Interestingly, control and inoculated *nfr5*- and *nark*-mutant genotypes were located closed to non-inoculated *wt* plants (**Figure 7C**).

Phenylalanine ammonia lyase activity, a key enzyme of the phenylpropanoid pathway and another ISR marker, was evaluated. The analysis of PAL activity revealed that this activity

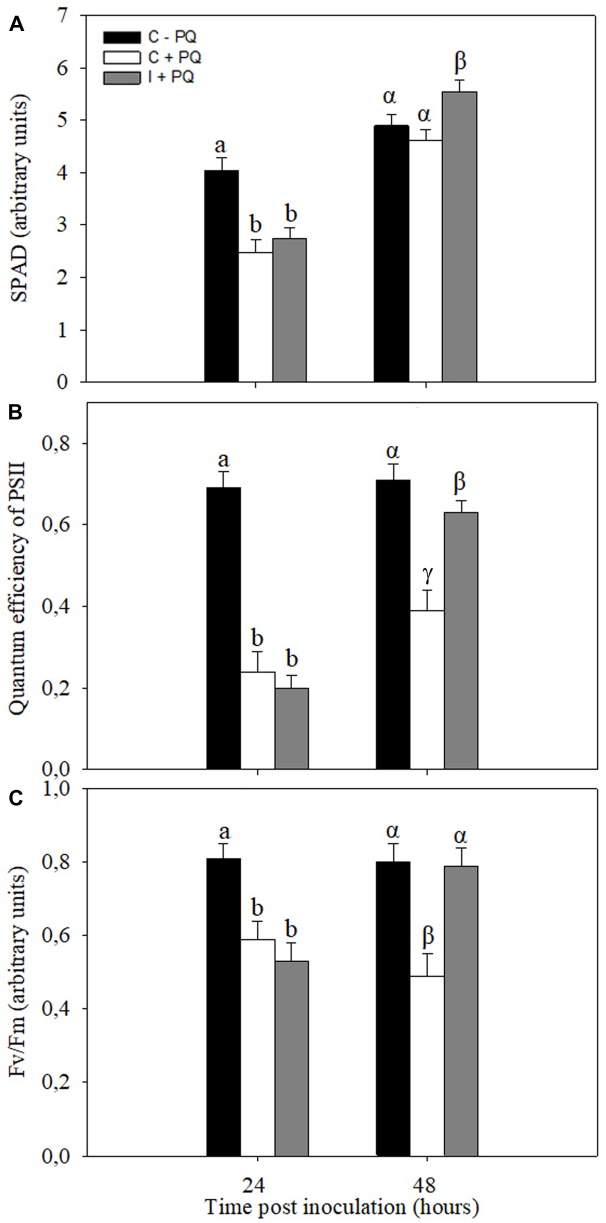

FIGURE 6 | Root inoculation induced photooxidative stress tolerance in leaves. Paraquat (PQ; 20 μM) was sprayed in the first trifoliate leaf of inoculated plants after 24 and 48 h of root inoculation with *B. japonicum* (I +PQ). Non-inoculated plants were used as a control (C +PQ) and without PQ (C –PQ). The chlorophyll content (SPAD) **(A)**, quantum efficiently of the PSII (ΦPSII) **(B)**, and maximum quantum efficiency of Photosystem II (F_v/F_m) **(C)** were analyzed 24 h after PQ treatment. The results are the means of three independent experiments (nine leaves per treatment). Data are means ± SE. Different Latin and Greek letters indicate significant differences between treatments after 24 and 48 h post inoculation, respectively ($p < 0.05$, Tukey test).

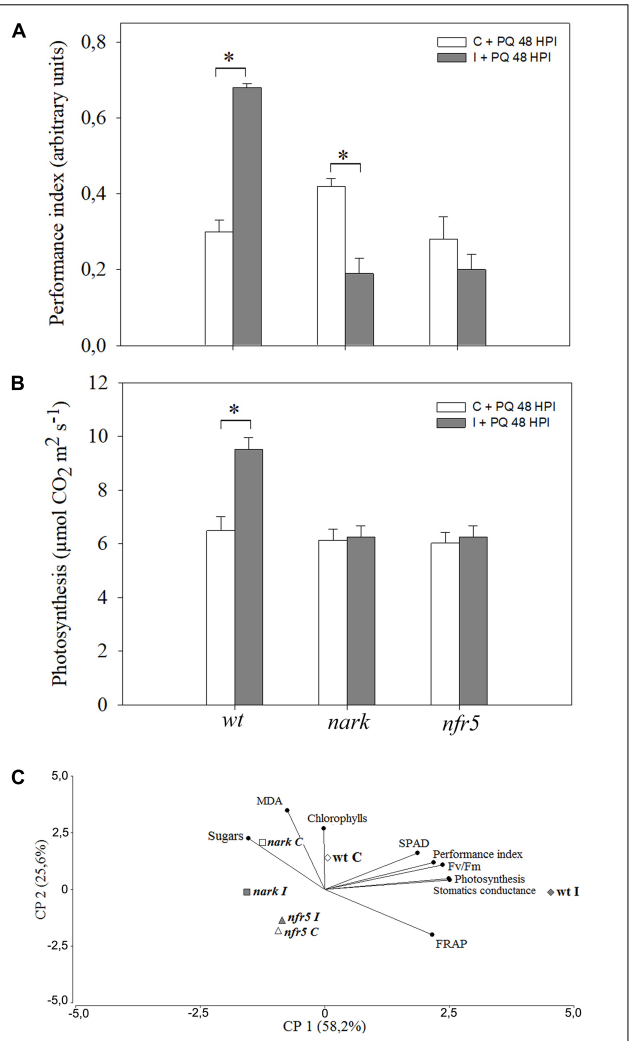

FIGURE 7 | The induced-photooxidative stress tolerance in leaves after *B. japonicum* inoculation depends on Nod factors- and AON-signaling pathways. The first trifoliate leaf of 12-days-old *nfr5*- and *nark*-mutant soybean plants and *wild type* (*wt*) plants were sprayed with 20 μM paraquat (PQ) after 48 h of root inoculation with *B. japonicum* (I). Non-inoculated plants were used as a control (C). The chlorophyll content, SPAD, maximum quantum efficiency of Photosystem II (F_v/F_m), sugars and MDA content, photosynthesis, stomatic conductance, performance index and the ferric reducing ability of plasma (FRAP) were analyzed 24 h after PQ treatment. **(A)** Performance index (PI) was set as an indicator of the overall fitness of the photosynthetic apparatus. **(B)** Net photosynthesis. Data are means ± SE of nine leaves of three independent experiments. Asterisks indicate significant differences between control and inoculated plants ($p < 0.05$, Tukey test). **(C)** Biplot from the first and second principal components (PC1 and PC2) of principal components analysis (PCA) showing relationships between inoculated *wt* plants and SPAD; Performance Index; F_v/F_m; Photosynthesis; Stomatic conductance and FRAP.

was induced in leaves of *wt* inoculated plants as compared to *wt* non-inoculated, while no significant differences were observed between non-inoculated and inoculated *nfr5*- and *nark*-mutant plants (**Figure 8**).

Likewise, to analyze the participation of hormones related to ISR or AON, we assessed the levels of JA and SA in leaves after 72 h of root inoculation (**Supplementary Figure S4**). The content of these hormones was similar among treatments and genotypes (**Supplementary Figure S4**).

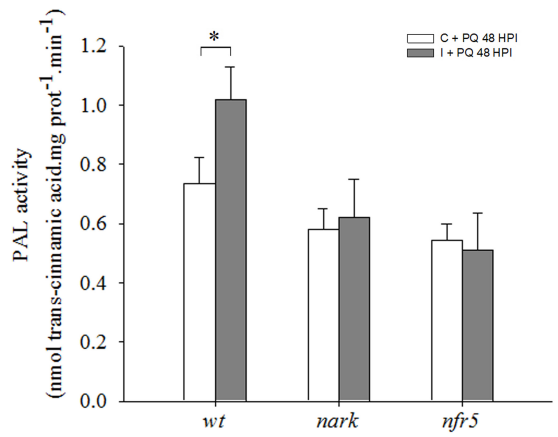

FIGURE 8 | Phenylalanine ammonia-lyase (PAL) is induced under photooxidative stress conditions in *wild type* (*wt*) inoculated plants. The first trifoliate leaf of 12-days-old *nfr5*- and *nark*-mutant soybean plants and *wt* plants was sprayed with 20 μM paraquat (PQ) after 48 h of root inoculation with *B. japonicum* (I), non-inoculated plants were used as a control (C). PAL activity was measured in the first trifoliate leaves after 24 h of PQ treatment. Data are means ± SE of three leaves of three independent experiments. Asterisks indicate significant differences between comparisons ($p < 0.05$, Tukey test).

DISCUSSION

The relationships between plants and microorganisms are active, co-evolutionary processes that can result in incompatible or compatible interactions. The great majority of microorganisms are not able to invade and establish compatible interaction with plants, whereas a few species have developed strategies to establish a compatible interaction ranging from mutualistic (symbiotic) to pathogenic interactions. Plants recognize different signal molecules from microorganisms, like MAMPs and other pathogenic and symbiotic signals that modulate the immune system of plants (Limpens et al., 2015; Couto and Zipfel, 2016). The ligand molecules, receptors and the downstream signaling pathways involved in plant–microorganism interaction have been deeply characterized in the last 10 years (Zipfel and Oldroyd, 2017). In this sense, the species-specific legume rhizobium symbiotic interactions and race-specific plant pathogen interactions share many similarities (Cao et al., 2017). MAMPs and symbiotic signals are recognized by cell-surface receptor kinases, which are composed by an extracellular domain involved in ligand perception, a transmembrane domain, and an intracellular kinase domain (Gourion et al., 2015; Miwa and Okazaki, 2017; Masson-Boivin and Sachs, 2018).

Legume rhizobium symbiotic interactions are orchestrated by a fine-tuning molecular dialog. Initially, the recognition of both Nod factors and MAMPs involves different cellular events, including increases of ROS production and cytosolic calcium concentration. Previously, we characterized the local redox changes and calcium involvement in root hairs during soybean–*B. japonicum* symbiotic interaction under control, abiotic and biotic stress conditions. A specific symbiotic calcium-dependent ROS signature occurred during the early events of soybean–*B. japonicum* symbiosis, which was completely different to ROS signature induced by pathogen elicitors or by abiotic stressful condition during the symbiotic interaction (Muñoz et al., 2012). Under moderate short-term salt stress (50 mM NaCl) treatment, *B. japonicum* could be sensed as a pathogen and its sensing may induce root hair cell death by a hypersensitive-like response and therefore may inhibit the nodulation process (Muñoz et al., 2012; Robert et al., 2014, 2018). Interestingly, the addition of calcium partially rescued the root hair death and inhibition of nodulation (Muñoz et al., 2014a). These results are in line with recent study that showed close similarities between symbiotic an immune pathway (Zipfel and Oldroyd, 2017).

In addition to generating local responses in roots, plant microorganism interactions also induce systemic responses that prepare the whole plant to upcoming challenges. SAR and ISR are the most studied systemic responses triggered by pathogen or beneficial microorganism, respectively. These systemic responses are mainly modulated by SA, for SAR, and JA and ET, for ISR. On the other hand, SAA is a systemic response triggered by abiotic stress conditions that provoke excess excitation energy, where chloroplastic and apoplastic ROS production play a key role.

Even when some evidence demonstrates the role of ROS as systemic signals (Miller et al., 2009; Gilroy et al., 2014), this aspect has not been investigated in legume–rhizobium interaction. The initial aim of the present work was to characterize the systemic redox changes induced during the soybean–*B. japonicum* symbiotic interaction and to assess their relationship with ISR/PGPR-like response. Our results showed that soybean–*B. japonicum* interaction induces a rapid redox systemic changes given by a transient peak of ROS at 30 min post inoculation (**Figure 1**). Furthermore, this interaction produces changes in the total content of ascorbate, glutathione redox state as well as higher MDA content (**Figure 2**), and higher antioxidant enzymes activity (**Figure 3**). Ascorbate-glutathione-NADPH and the interconnected antioxidant enzymes of the Asada–Halliwell cycle are key components of the redox hub that controls the cellular redox state. Perturbations of this redox buffering mechanism trigger redox signaling pathways, where even the oxidative damage could be also part of the oxidative or redox signaling, explaining the dual role of ROS as toxic and signal molecules. Ascorbate and glutathione are the major soluble antioxidants. The redox potential among NADPH, glutathione and ascorbate, where glutathione has middle values between NADPH and ascorbate could explain why we found changes in the redox state only in glutathione pool. Moreover, many evidences indicate that conditions with enhanced ROS production has less impact on the ascorbate redox state pool than on glutathione pool, generating altered cellular redox state characterized by a highly reduced state of the ascorbate pool and partially oxidized state of the glutathione pool. Changes in the glutathione redox state have been previously characterized in oxidative signaling processes (Kranner et al., 2006; Foyer and Noctor, 2011). The cellular redox state, mainly determined by the ratio between generation and scavenging capacity of ROS in different subcellular compartments, is an integral source of information for the plant cell that modulates

growth, development and different responses to environmental conditions (Foyer and Noctor, 2011). Recently, systemically auto propagating waves of ROS, calcium and electric signals has been integrated in a model for rapid systemic cell-to-cell communication in plants that is involved in the acclimation to abiotic stress condition (Choi et al., 2017). In this regard, the NADPH oxidase complex (RBOH respiratory burst homolog protein) plays a key role within this model. The RBOH proteins are localized on the plasma membrane and generate superoxide radical in the apoplast, which quickly dismutates to hydrogen peroxide spontaneously or by SOD activity.

Our results also showed that the inhibitor of NADPH oxidase complex, DPI, abolished the systemic redox changes induced during the soybean–*B. japonicum* symbiotic interaction, indicating the involvement of this complex in the systemic redox signaling (**Figure 3**).

As it was mentioned above, ROS and redox changes could act as priming molecules and thus improve the responses to different stress conditions. In line with this, inoculated soybean plants were more tolerant to a photooxidative stress condition induced by PQ treatments. This finding indicates that *B. japonicum* inoculation could prime soybean plants by inducing ISR/PGPR-like response through redox changes (**Figures 5–7**, **9**).

To further investigate the specificity of the systemic response and its role in the ISR/PGPR-like response, we performed treatments with purified Nod-factors from *B. japonicum* as well as using Nod factor receptor plant mutants (**Figures 5**, **7** and **Supplementary Figure S1**). Similarly to *B. japonicum* inoculation, Nod factors treatment induced transient peak of ROS. Moreover, the systemic response was completely different when plant roots were treated with two derivatives of chitin oligosaccharides, Nod factors or chitosan, a potent pathogen elicitor (**Supplementary Figure S1**).

The Nod factor receptors have been characterized in different legumes. They are composed by pairs of LysM-receptor kinases and therefore share many similarities to chitin receptors. Soybean contains two genes GmNFR5α and GmNFR5β among others within its genome but only GmNFR5α is functional in *Glycine max*. Chemically induced non-nodulating nod139 mutant (Carroll et al., 1986) present a single nucleotide substitutions (non-sense) within the coding region of the GmNFR5α and this results in the elimination of most of the kinase domain (Indrasumunar et al., 2010). The *B. japonicum* inoculation of *nfr5*-mutant (nod139) lacked the systemic ROS changes and was non-tolerant to photooxidative stress conditions through ISR/PGPR-like response (**Figures 5**, **7**, **9**).

In this study, we also analyzed the participation of AON in the systemic redox changes and ISR/PGPR-like response induced by *B. japonicum* inoculation. For this purpose, we used mutant plants that lost the GmNARK function (nts1007 with a mutation of V370D) and that exhibit supernodulation phenotypes (Searle et al., 2003; Lin et al., 2010). GmNARK

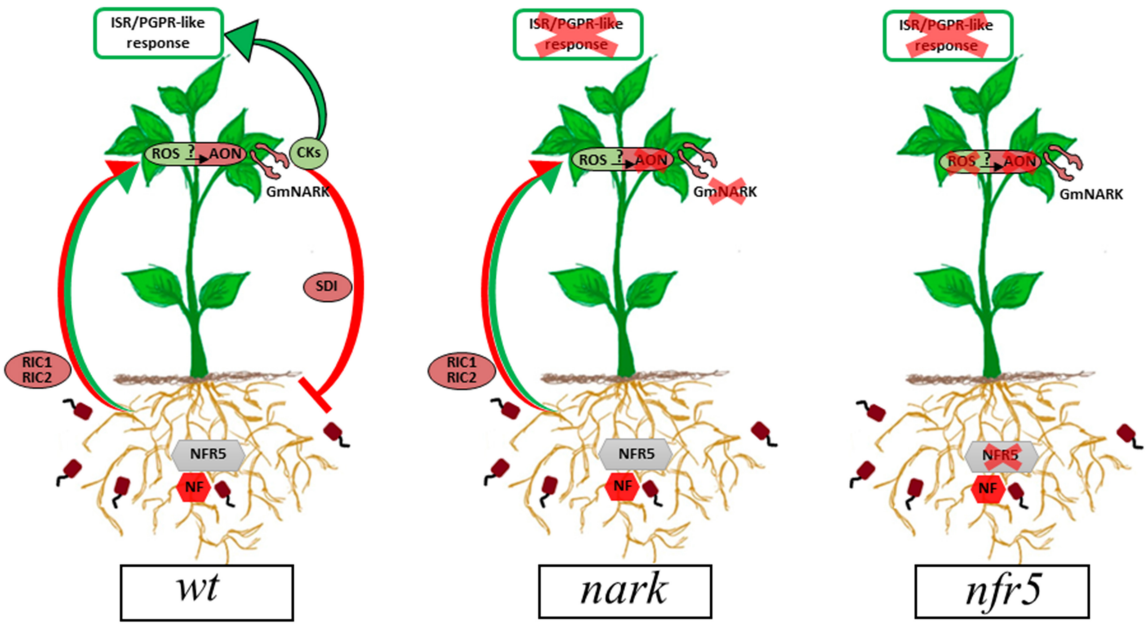

FIGURE 9 | Proposed model for the ISR/PGPR-like response induced during *B. japonicum*–soybean interaction. Red arrows and circles indicate the already described signaling pathway involved in AON. Green arrows and circles indicate the proposed signaling pathways arising from this research. In *wt* plants, rhizobia-induced CLE peptides (RIC1 and RIC2) are produced in root after NFR5-dependent symbiont perception. Then, CLE peptides are transported via xylem to shoot, where they bind to GmNARK triggering the production of the SDI, which moves back to the roots and inhibits nodule formation (red arrows and circles). A potential role for the systemic ROS production in the AON mechanism as well as in the ISR/PGPR-like response is proposed. In this sense, cytokinins play a dual role, participating in the mechanism involved in AON and in the ISR/PGPR-like response (green arrows and circles). AON, autoregulation of nodulation; CKs, cytokinins; GmNARK, *Glycine max* nodulation autoregulation receptor kinase; ISR, induced systemic resistance; NF, Nod factors; NFR5, Nod factor receptor 5; PGPR, plant growth-promoting rhizobacteria; ROS, reactive oxygen species; RIC, rhizobia-induced CLE peptides; SDI, shoot-derived inhibitor.

is an LRR receptor kinase homolog to *Arabidopsis thaliana* CLAVATA1, but without conserved function of inflorescence meristem regulation. GmNARK is expressed in the root and shoot and its main function is in local and systemic regulation of nodulation. Locally, root GmNARK plays a key role in the nitrate inhibition of nodulation mediated by NIC (Lim et al., 2011; Reid et al., 2011a, 2013; Mirzaei et al., 2017; Ferguson et al., 2018). Systemically, leaf GmNARK participates in the AON by perceiving CLE peptides from rhizobium inoculated roots (RIC1 and RIC2) and inducing the synthesis of SDI, which is transported by phloem to the root where it provokes the inhibition of nodulation (Searle et al., 2003; Lim et al., 2011; Reid et al., 2011b; Ferguson et al., 2018). The *nark*-mutant showed the same systemic redox changes than the *wt* plants (**Figure 5**); however, this mutant failed to induce the ISR/PGPR-like response with tolerance to photooxidative stress condition (**Figures 7**, **9**). Likewise, the phenylalanine ammonia-lyase (PAL) activity, which catalyzes the conversion of L-phenylalanine to *trans*-cinnamic acid, showed a significant increase only in the inoculated *wt* plants, whereas this activity remained unaltered in both mutants upon the inoculation (**Figure 8**). These results indicate that both Nod factors perception and AON signaling are necessary for the activation of PAL, the key enzyme in the phenylpropanoid pathway and a marker of ISR and primed plants (Conrath, 2011).

Transcriptomic analysis using this mutants showed that GmNARK regulates the expression of JA pathway genes and participates in plant defense responses (Kinkema and Gresshoff, 2008). The promoter region of GmNARK gene contains multiple *cis*-elements involved in plant responses to hormones and biotic stresses. Likewise, GmNARK expression is induced by ABA and NaCl and its overexpression increases the sensitivity to salt and ABA treatment, thus indicating the involvement of this receptor also in the responses to abiotic stresses (Cheng et al., 2018). Pieterse et al. (2014) have well established the importance of SA, JA/ET as key signals in the regulation of the plant systemic immune responses SAR and ISR. In the present work, these hormones neither showed any difference in *wt* soybean at 30 min post inoculation (**Figure 4**), where the ROS peak was detected, nor at 72 h post inoculation in *wt, nark* and *nfr5* (**Supplementary Figure S4**), where the ISR/PGPR-like response is established.

The molecular identity of SDI is still unknown. In *Lotus japonicum* the CLE-RS1/2-HAR1 interaction triggered the production of CKs in shoot, which have been postulated as SDI. CKs production in the shoot of *Lotus* is mediated by the activation of isopentenyl transferase 3 (LjIPT3) in a HAR1 dependent pathway (Sasaki et al., 2014). Likewise, CKs have been largely characterized as positive regulator of nodulation at root level (Murray et al., 2007). This dual role could depend on the site of synthesis, the concentration and the type of CKs as well as the receptor involved in the process. Moreover, the CKs that promote nodulation are independent of AON signaling. However, the anti-senescence and stress tolerance functions of CKs induced during legume–rhizobium symbiotic interaction have not been studied yet. In this context, we propose that ISR/PGPR-like response induced during legume–rhizobium symbiotic interaction may be related to the AON-related CKs (**Figure 9**).

After root inoculation, and in opposition to what was observed in *Lotus*, recent data showed an GmNARK-independent induction of GmIPT5, an ortholog of LjIPT3 in soybean shoots (Mens et al., 2018). This finding suggests differences between soybean and *Lotus* pathway or an uncertainty of the IPT-AON association.

Altogether, our results showed that the NADPH-dependent transient systemic redox changes induced after root inoculation with *B. japonicum* in soybean rely upon Nod factor signaling and that these changes are involved in the priming and induction of the ISR/PGPR-like response (**Figure 9**). In this sense, CKs play a dual role, participating in the mechanism involved in AON and ISR/PGPR-like response (**Figure 9**). Finally, the involvement of the AON mechanisms in the ISR/PGPR-like response also suggests that systemic redox changes induced during soybean–*B. japonicum* interaction are early components of the AON pathway. Nevertheless, future studies should be addressed to confirm this hypothesis.

AUTHOR CONTRIBUTIONS

RL, SA, and NM designed the experiments. TF-G and RD conducted the experiments. TF-G analyzed the data. TF-G, GR, and RL co-wrote the manuscript.

FUNDING

This work was supported by grants from the Agencia de Promoción Científica y Tecnológica, Argentina (PICT-2008-0067), Instituto Nacional de Tecnología Agropecuaria (INTA-PNBIO-1131022), and Secretaria de Ciencia y Tecnología (SECYT) Universidad Nacional de Córdoba.

ACKNOWLEDGMENTS

Thanks to the Consejo Nacional de Investigaciones Científicas y Técnicas de la República Argentina (CONICET) and Instituto Nacional de Tecnología Agropecuaria (INTA). TF-G is a Ph.D. student from CONICET and RL and SA are researchers from CONICET. Thanks to Julia Verónica Sabio y Garcia for the help with the English of the manuscript.

SUPPLEMENTARY MATERIAL

The Supplementary Material for this article can be found online at: https://www.frontiersin.org/articles/10.3389/fpls.2019.00141/full#supplementary-material

FIGURE S1 | Systemic H_2O_2 generation in leaves after root treatments with *B. japonicum*, purified Nod factors and chitosan. H_2O_2 was quantified by spectrofluorometer. The results are the means of three independent experiments (six leaves per treatment). Data are means ± SE. Asterisks indicate significant difference between non-inoculated and inoculated plants ($p < 0.05$, Tukey test).

FIGURE S2 | Diagram of the experimental system for paraquat (PQ) treatment. 12-days-old soybean plants were inoculated with *B. japonicum*, and PQ treatments were performed in leaves at 24 and 48 h post inoculation (hpi). The physiological parameters were measured 24 h after PQ treatment.

FIGURE S3 | Relatives values (inoculated/control) of SPAD, PSII and F_v/F_m in plants at 24 and 48 h without paraquat (PQ) treatments; the parameters were measured at 48 and 72 h post inoculation, respectively. The results are the means of three independent experiments (nine leaves per treatment). Data are means ± SE. No significant differences were observed between non-inoculated and inoculated plants ($p < 0.05$, Tukey test).

FIGURE S4 | Jasmonic acid **(A)** and salicylic acid **(B)** contents in leaves of non-inoculated and inoculated plants at 72 h post inoculation (hpi). The results are the means of four replicates ± SE ($p < 0.05$, Tukey test). No significant differences were observed between non-inoculated and inoculated plants.

REFERENCES

Arthikala, M.-K., Montiel, J., Sánchez-López, R., Nava, N., Cárdenas, L., and Quinto, C. (2017). Respiratory burst oxidase homolog gene a is crucial for rhizobium infection and nodule maturation and function in common bean. *Front. Plant Sci.* 8:2003. doi: 10.3389/fpls.2017.02003

Asada, K. (1999). The water-water cycle in chloroplasts: scavenging of active oxygens and dissipation of excess photons. *Ann. Rev. Plant Physiol. Plant Mol. Biol.* 50, 601–639. doi: 10.1146/annurev.arplant.50.1.601

Beaudoin-Eagan, L. D., and Thorpe, T. A. (1985). Tyrosine and phenylalanine ammonia lyase activities during shoot initiation in tobacco callus cultures. *Plant physiol.* 78, 438–441. doi: 10.1104/pp.78.3.438

Benzie, I. F. F., and Strain, J. J. (1996). The ferric reducing ability of plasma (FRAP) as a measure of "antioxidant power": the frap assay. *Anal. Biochem.* 239, 70–76. doi: 10.1006/abio.1996.0292

Boller, T., and Felix, G. (2009). A renaissance of elicitors: perception of microbe-associated molecular patterns and danger signals by pattern-recognition receptors. *Ann. Rev. Plant Biol.* 60, 379–406. doi: 10.1146/annurev.arplant.57.032905.105346

Bradford, M. M. (1976). A rapid and sensitive method for the quantitation of microgram quantities of protein utilizing the principle of protein-dye binding. *Anal. Biochem.* 72, 248–254. doi: 10.1016/0003-2697(76)90527-3

Broughton, W. J., and Dilworth, M. J. (1971). Control of leghaemoglobin synthesis in snake beans. *Biochem. J.* 125, 1075–1080. doi: 10.1042/bj1251075

Caetano-Anolles, G., and Gresshoff, P. M. (1991). Plant genetic control of nodulation. *Ann. Rev. Microbiol.* 45, 345–382. doi: 10.1146/annurev.mi.45.100191.002021

Cao, Y., Halane, M. K., Gassmann, W., and Stacey, G. (2017). The role of plant innate immunity in the legume-rhizobium symbiosis. *Ann. Rev. Plant Biol.* 68, 535–561. doi: 10.1146/annurev-arplant-042916-041030

Cárdenas, L., Martínez, A., Sánchez, F., and Quinto, C. (2008). Fast, transient and specific intracellular ROS changes in living root hair cells responding to Nod factors (NFs). *Plant J.* 56, 802–813. doi: 10.1111/j.1365-313X.2008.03644.x

Carroll, B. J., Mcneil, D. L., and Gresshoff, P. M. (1986). Mutagenesis of soybean (*Glycine max* (L.) Merr.) and the isolation of non-nodulation mutants. *Plant Sci.* 47, 109–114. doi: 10.1016/0168-9452(86)90057-9

Carroll, B. J., McNeil, D. L., and Gresshofft, P. M. (1985). Isolation and properties of soybean [*Glycine max* (L.) Merr.] mutants that nodulate in the presence of high nitrate concentrations. *PNAS* 82, 4162–4166. doi: 10.1073/pnas.82.12.4162

Casano, L. M., Gómez, L. D., Lascano, H. R., González, C. A., and Trippi, V. S. (1997). Inactivation and degradation of CuZn-SOD by active oxygen species in wheat chloroplasts exposed to photooxidative stress. *Plant Cell Physiol.* 38, 433–440. doi: 10.1093/oxfordjournals.pcp.a029186

Chen, Y., Chen, W., Li, X., Jiang, H., Wu, P., Xia, K., et al. (2014). Knockdown of LjIPT3 influences nodule development in lotus japonicus. *Plant Cell Physiol.* 55, 183–193. doi: 10.1093/pcp/pct171

Cheng, C., Li, C., Wang, D., Zhai, L., and Cai, Z. (2018). The soybean gmNARK affects ABA and salt responses in transgenic *Arabidopsis thaliana*. *Front. Plant Sci.* 9:514. doi: 10.3389/fpls.2018.00514

Choi, W. G., Miller, G., Wallace, I., Harper, J., Mittler, R., and Gilroy, S. (2017). Orchestrating rapid long-distance signaling in plants with Ca2+, ROS and electrical signals. *Plant J.* 90, 698–707. doi: 10.1111/tpj.13492

Conrath, U. (2011). Molecular aspects of defence priming. *Trends Plant Sci.* 16, 524–531. doi: 10.1016/j.tplants.2011.06.004

Couto, D., and Zipfel, C. (2016). Regulation of pattern recognition receptor signalling in plants. *Nat. Rev. Immunol.* 16, 537–552. doi: 10.1038/nri.2016.77

Damiani, I., Pauly, N., Puppo, A., Brouquisse, R., and Boscari, A. (2016). Reactive oxygen species and nitric oxide control early steps of the legume – rhizobium symbiotic interaction. *Front. Plant Sci.* 7:454. doi: 10.3389/fpls.2016.00454

Di Rienzo, J. E., Casanoves, F., Balzarini, M. G., González, L., Tablada, M., and Robledo, C. W. (2016). *InfoStat: Statistical Software*. Córdoba: Grupo InfoStat, FCA, Universidad Nacional de Córdoba.

Dimkpa, C., Weinand, T., and Asch, F. (2009). Plant-rhizobacteria interactions alleviate abiotic stress conditions. *Plant Cell Environ.* 32, 1682–1694. doi: 10.1111/j.1365-3040.2009.02028.x

Durgbanshi, A., Arbona, V., Pozo, O., Miersch, O., Sancho, J. V., and Gómez-Cadenas, A. (2005). Simultaneous determination of multiple phytohormones in plant extracts by liquid chromatography-electrospray tandem mass spectrometry. *J. Agric. Food Chem.* 53, 8437–8442. doi: 10.1021/jf050884b

Ferguson, B. J., Indrasumunar, A., Hayashi, S., Lin, M., Lin, Y., Reid, D. E., et al. (2010). Molecular analysis of legume nodule development and autoregulation. *J. Interact. Plant Biol.* 52, 61–76. doi: 10.1111/j.1744-7909.2010.00899.x

Ferguson, B. J., Mens, C., Hastwell, A. H., Zhang, M. B., Su, H., Jones, C. H., et al. (2018). Legume nodulation: the host controls the party. *Plant Cell Environ.* 42, 41–51. doi: 10.1111/pce.13348

Foreman, J., Demidchik, V., Bothwell, J. H. F., Mylona, P., Miedema, H., Torres, M. A., et al. (2003). Reactive oxygen species produced by NADPH oxidase regulate plant cell growth. *Nature* 422, 442–446. doi: 10.1038/nature01485

Foyer, C. H., and Noctor, G. (2009). Redox regulation in photosynthetic organisms. *Antioxid. Redox Signal.* 11, 861–905. doi: 10.1089/ars.2008.2177

Foyer, C. H., and Noctor, G. (2011). Ascorbate and glutathione: the heart of the redox hub. *Plant Physiol.* 155, 2–18. doi: 10.1104/pp.110.167569

Gallego, S. M., Benavides, M. P., and Tomaro, M. L. (1996). Effect of heavy metal ion excess on sunflower leaves: evidence for involvement of oxidative stress. *Plant Sci.* 121, 151–159. doi: 10.1016/S0168-9452(96)04528-1

Gaupels, F., Durner, J., and Kogel, K. (2017). Production, amplification and systemic propagation of redox messengers in plants? The phloem can do it all! *New Phytol.* 214, 554–560. doi: 10.1111/nph.14399

Gilroy, S., Suzuki, N., Miller, G., Choi, W. G., Toyota, M., Devireddy, A. R., et al. (2014). A tidal wave of signals: calcium and ROS at the forefront of rapid systemic signaling. *Trends Plant Sci.* 19, 623–630. doi: 10.1016/j.tplants.2014.06.013

Gourion, B., Berrabah, F., Ratet, P., and Stacey, G. (2015). Rhizobium – legume symbioses: the crucial role of plant immunity. *Trends Plant Sci.* 20, 186–194. doi: 10.1016/j.tplants.2014.11.008

Graham, P. H., and Vance, C. P. (2003). Update on legume utilization legumes: importance and constraints to greater use. *Plant Physiol.* 131, 872–877. doi: 10.1104/pp.017004

Guilbault, G. G., Brignac, P. J., and Juneau, M. (1968). New substrates for the fluorometric determination of oxidative enzymes. *Anal. Chem.* 40, 1256–1263. doi: 10.1021/ac60264a027

Hardy, R. W. F., Holsten, R. D., Jackson, E. K., and Burns, R. C. (1968). The acetylene - ethylene assay for N2 fixation: laboratory and field evaluation. *Plant Physiol.* 43, 1185–1207. doi: 10.1104/pp.43.8.1185

Heath, R. L., and Packer, L. (1968). Photoperoxidation in isolated chloroplasts. *Arch. Biochem. Biophys.* 125, 189–198. doi: 10.1016/0003-9861(68)90654-1

Indrasumunar, A., Kereszt, A., Searle, I., Miyagi, M., Li, D., Nguyen, C. D. T., et al. (2010). Inactivation of duplicated nod factor receptor 5 (NFR5) genes in recessive loss-of-function non-nodulation mutants of allotetraploid soybean (*Glycine max* L. Merr.). *Plant Cell Physiol.* 51, 201–214. doi: 10.1093/pcp/pcp178

Indrasumunar, A., Searle, I., Lin, M., Kereszt, A., Men, A., Carroll, B. J., et al. (2011). Nodulation factor receptor kinase 1 a controls nodule organ number in soybean

(*Glycine max* L. Merr). *Plant J.* 65, 39–50. doi: 10.1111/j.1365-313X.2010.04398.x

Johnson, R. A., and Wichern, D. W. (2006). Multivariate analysis. *Encycl. Stat. Sci.* 2011, 8279–8282. doi: 10.1109/IEMBS.2011.6092041

Kinkema, M., and Gresshoff, P. M. (2008). Investigation of downstream signals of the soybean autoregulation of nodulation receptor kinase GmNARK. *Mol. Plant Microbe Interact.* 21, 1337–1348. doi: 10.1094/MPMI-21-10-1337

Kranner, I., Birtić, S., Anderson, K. M., and Pritchard, H. W. (2006). Glutathione half-cell reduction potential: a universal stress marker and modulator of programmed cell death? *Free Radic. Biol. Med.* 40, 2155–2165. doi: 10.1016/j.freeradbiomed.2006.02.013

Lascano, H. R., Melchiorre, M. N., Luna, C. M., and Trippi, V. S. (2003). Effect of photooxidative stress induced by paraquat in two wheat cultivars with differential tolerance to water stress. *Plant Sci.* 164, 841–848. doi: 10.1016/S0168-9452(03)00073-6

Lascano, R., Muñoz, N., Robert, G., Rodriguez, M., Melchiorre, M., Trippi, V., et al. (2012). "Paraquat: an oxidative stress inducer," in *Herbicides - Properties, Synthesis and Control of Weeds*, ed. M. N. Hasaneen (London: InTech).

Lim, C. W., Lee, Y. W., and Hwang, C. H. (2011). Soybean nodule-enhanced CLE peptides in roots act as signals in gmnark-mediated nodulation suppression. *Plant Cell Physiol.* 52, 1613–1627. doi: 10.1093/pcp/pcr091

Limpens, E., van Zeijl, A., and Geurts, R. (2015). Lipochitooligosaccharides modulate plant host immunity to enable endosymbioses. *Ann. Rev. Phytopathol.* 53, 311–334. doi: 10.1146/annurev-phyto-080614-120149

Lin, Y., Ferguson, B. J., Kereszt, A., and Gresshoff, P. M. (2010). Suppression of hypernodulation in soybean by a leaf- extracted, NARK- and Nod factor-dependent, low molecular mass fraction. *New Phytol.* 185, 1074–1086. doi: 10.1111/j.1469-8137.2009.03163.x

Masson-Boivin, C., and Sachs, J. L. (2018). Symbiotic nitrogen fixation by rhizobia — the roots of a success story. *Curr. Opin. Plant Biol.* 44, 7–15. doi: 10.1016/j.pbi.2017.12.001

Maxwell, K., and Johnson, G. N. (2000). Chlorophyll fluorescence—a practical guide. *J. Exp. Bot.* 51, 659–668. doi: 10.1093/jxb/51.345.659

Melchiorre, M., Robert, G., Trippi, V., Racca, R., and Lascano, H. R. (2009). Superoxide dismutase and glutathione reductase overexpression in wheat protoplast: photooxidative stress tolerance and changes in cellular redox state. *Plant Growth Regul.* 57, 57–68. doi: 10.1007/s10725-008-9322-3

Mens, C., Li, D., Haaima, L. E., Gresshoff, P. M., and Ferguson, B. J. (2018). Local and systemic effect of cytokinins on soybean nodulation and regulation of their isopentenyl transferase (IPT) biosynthesis genes following rhizobia inoculation. *Front. Plant Sci.* 9:1150. doi: 10.3389/fpls.2018.01150

Miller, G., Schlauch, K., Tam, R., Cortes, D., Torres, M. A., Shulaev, V., et al. (2009). The plant NADPH oxidase RBOHD mediates rapid systemic signaling in response to diverse stimuli. *Sci. Signal.* 2:ra45. doi: 10.1126/scisignal.2000448

Miller, G., Shulaev, V., and Mittler, R. (2008). Reactive oxygen signaling and abiotic stress. *Physiol. Plant.* 133, 481–489. doi: 10.1111/j.1399-3054.2008.01090.x

Miller, G., Suzuki, N., Rizhsky, L., Hegie, A., Koussevitzky, S., and Mittler, R. (2007). Double mutants deficient in cytosolic and thylakoid ascorbate peroxidase reveal a complex mode of interaction between reactive oxygen species, plant development, and response to abiotic stresses. *Plant Physiol.* 144, 1777–1785. doi: 10.1104/pp.107.101436

Mirzaei, S., Batley, J., El-Mellouki, T., Liu, S., Meksem, K., Ferguson, B. J., et al. (2017). Neodiversification of homeologous CLAVATA1-like receptor kinase genes in soybean leads to distinct developmental outcomes. *Sci. Rep.* 7:8878. doi: 10.1038/s41598-017-08252-y

Miwa, H., and Okazaki, S. (2017). How effectors promote beneficial interactions. *Curr. Opin. Plant Biol.* 38, 148–154. doi: 10.1016/j.pbi.2017.05.011

Montiel, J., Nava, N., Cárdenas, L., Sánchez-López, R., Arthikala, M.-K., Santana, O., et al. (2012). A Phaseolus vulgaris NADPH oxidase gene is required for root infection by rhizobia. *Plant Cell Physiol.* 53, 1751–1767. doi: 10.1093/pcp/pcs120

Muñoz, N., Robert, G., Melchiorre, M., Racca, R., and Lascano, R. (2012). Saline and osmotic stress differentially affects apoplastic and intracellular reactive oxygen species production, curling and death of root hair during *Glycine max* L.– *Bradyrhizobium japonicum* interaction. *Environ. Exp. Bot.* 78, 76–83. doi: 10.1016/j.envexpbot.2011.12.008

Muñoz, N., Rodriguez, M., Robert, G., and Lascano, R. (2014a). Negative short-term salt effects on the soybean-*Bradyrhizobium japonicum* interaction and partial reversion by calcium addition. *Funct. Plant Biol.* 41, 96–105. doi: 10.1071/FP13085

Muñoz, N., Soria-díaz, M. E., Manyani, H., Sánchez-matamoros, R. C., Gil Serrano, A., Megías, M., et al. (2014b). Structure and biological activities of lipochitooligosaccharide nodulation signals produced by *Bradyrhizobium japonicum* USDA 138 under saline and osmotic stress. *Biol. Fertil. Soils* 50, 207–215. doi: 10.1007/s00374-013-0843-1

Murray, J., Karas, B., Sato, S., Tabata, S., Amyot, L., and Szczyglowski, K. (2007). A cytokinin perception mutant colonized by rhizobium in the absence of nodule organogenesis. *Science* 315, 101–104. doi: 10.1126/science.1132514

Nadzieja, M., Kelly, S., Stougaard, J., and Reid, D. (2018). Epidermal auxin biosynthesis facilitates rhizobial infection in *Lotus japonicus*. *Plant J.* 95, 101–111. doi: 10.1111/tpj.13934

Nakano, Y., and Asada, K. (1981). Hydrogen peroxide is scavenged by ascorbate-specific peroxidase in spinach chloroplasts. *Plant Cell Physiol.* 22, 867–880. doi: 10.1093/oxfordjournals.pcp.a076232

Okamoto, S., Ohnishi, E., Sato, S., Takahashi, H., Nakazono, M., Tabata, S., et al. (2009). Nod factor/nitrate-induced CLE genes that drive HAR1-mediated systemic regulation of nodulation. *Plant Cell Physiol.* 50, 67–77. doi: 10.1093/pcp/pcn194

Okamoto, S., Shinohara, H., Mori, T., Matsubayashi, Y., and Kawaguchi, M. (2013). Root-derived CLE glycopeptides control nodulation by direct binding to HAR1 receptor kinase. *Nat. Commun.* 4:2191. doi: 10.1038/ncomms3191

Oldroyd, G. E. D., and Downie, J. A. (2008). Coordinating nodule morphogenesis with rhizobial infection in legumes. *Anual Rev. Plant Biol.* 59, 519–546. doi: 10.1146/annurev.arplant.59.032607.092839

Oldroyd, G. E. D., Murray, J. D., Poole, P. S., and Downie, J. A. (2011). The rules of engagement in the legume-rhizobial symbiosis. *Anual Rev. Genet.* 45, 119–144. doi: 10.1146/annurev-genet-110410-132549

Peleg-Grossman, S., Volpin, H., and Levine, A. (2007). Root hair curling and rhizobium infection in *Medicago truncatula* are mediated by phosphatidylinositide-regulated endocytosis and reactive oxygen species. *J. Exp. Bot.* 58, 1637–1649. doi: 10.1093/jxb/erm013

Pieterse, C. M. J., Zamioudis, C., Berendsen, R. L., Weller, D. M., Van Wees, S. C. M., and Bakker, P. A. H. M. (2014). Induced systemic resistance by beneficial microbes. *Ann. Rev. Phytopathol.* 52, 347–375. doi: 10.1146/annurev-phyto-082712-102340

Reid, D. E., Ferguson, B. J., and Gresshoff, P. M. (2011a). Inoculation- and nitrate-induced CLE peptides of soybean control NARK-dependent nodule formation. *Mol. Plant Microb. Interact.* 24, 606–618. doi: 10.1094/MPMI-09-10-0207

Reid, D. E., Ferguson, B. J., Hayashi, S., Lin, Y., and Gresshoff, P. M. (2011b). Molecular mechanisms controlling legume autoregulation of nodulation. *Ann. Bot.* 108, 789–795. doi: 10.1093/aob/mcr205

Reid, D. E., Li, D., Ferguson, B. J., and Gresshoff, P. M. (2013). Structure – function analysis of the Gm RIC1 signal peptide and CLE domain required for nodulation control in soybean. *J. Exp. Bot.* 64, 1575–1585. doi: 10.1093/jxb/ert008

Robert, G., Melchiorre, M., Racca, R., Trippi, V., and Lascano, H. R. (2009). Apoplastic superoxide level in wheat protoplast under photooxidative stress is regulated by chloroplast redox signals: effects on the antioxidant system. *Plant Sci.* 177, 168–174. doi: 10.1016/j.plantsci.2009.05.001

Robert, G., Muñoz, N., Alvarado-Affantranger, X., Saavedra, L., Davidenco, V., Rodríguez-Kessler, M., et al. (2018). Phosphatidylinositol 3-kinase function at very early symbiont perception: a local nodulation control under stress conditions? *J. Exp. Bot.* 69, 2037–2048. doi: 10.1093/jxb/ery030

Robert, G., Muñoz, N., Melchiorre, M., Sanchez, F., and Lascano, R. (2014). Expression of animal anti-apoptotic gene Ced-9 enhances tolerance during *Glycine max* L.– *Bradyrhizobium japonicum* interaction under saline stress but reduces nodule formation. *PLoS One* 9:e101747. doi: 10.1371/journal.pone.0101747

Rodríguez, M., Taleisnik, E., Lenardon, S., and Lascano, R. (2010). Are Sunflower chlorotic mottle virus infection symptoms modulated by early increases in leaf sugar concentration? *J. Plant Physiol.* 167, 1137–1144. doi: 10.1016/j.jplph.2010.03.004

Sasaki, T., Suzaki, T., Soyano, T., Kojima, M., Sakakibara, H., and Kawaguchi, M. (2014). Shoot-derived cytokinins systemically regulate root nodulation. *Nat. Commun.* 5:4983. doi: 10.1038/ncomms5983

Schaedle, M., and Bassham, J. (1977). Chloroplast glutathione reductase. *Plant Physiol.* 59, 1011–1012. doi: 10.1104/pp.59.5.1011

Schneider, C. A., Rasband, W. S., and Eliceiri, K. W. (2012). NIH Image to imageJ: 25 years of image analysis. *Nat. Methods* 9, 671–675. doi: 10.1038/nmeth.2089

Searle, I. R., Men, A. E., Laniya, T. S., Buzas, D. M., Iturbe-Ormaetxe, I., Carroll, B. J., et al. (2003). Long-distance signaling in nodulation directed by a clavata1-like receptor kinase. *Science* 299, 109–112. doi: 10.1126/science.1077937

Strasser, R. J., Srivastava, A., and Tsimilli-Michael, M. (2000). "The fluorescence transient as a tool to characterize and screen photosynthetic samples," *Probing Photosynthesis: Mechanism, Regulation and Adaptation*, eds P. Mohanty, U. Yunus, and M. Pathre (London: Taylor and Francis), 443–480.

Torres, M. A., and Dangl, J. L. (2005). Functions of the respiratory burst oxidase in biotic interactions, abiotic stress and development. *Curr. Opin. Plant Biol.* 8, 397–403. doi: 10.1016/j.pbi.2005.05.014

Vincent, J. M. (1971). *A Manual for the Practical Study of Root-nodule Bacteria*. Oxford: Blackwell Scientifoc Publications.

Zamioudis, C., and Pieterse, C. M. J. (2012). Modulation of host immunity by beneficial microbes. *MPMI* 25, 139–150. doi: 10.1094/MPMI-06-11-0179

Zipfel, C., and Oldroyd, G. E. D. (2017). Plant signalling in symbiosis and immunity. *Nature* 543, 328–336. doi: 10.1038/nature22009

Conflict of Interest Statement: The authors declare that the research was conducted in the absence of any commercial or financial relationships that could be construed as a potential conflict of interest.

frontiers in Plant Science

ORIGINAL RESEARCH
published: 19 February 2019
doi: 10.3389/fpls.2019.00131

Effects of Different Chemical Forms of Nitrogen on the Quick and Reversible Inhibition of Soybean Nodule Growth and Nitrogen Fixation Activity

Natsumi Yamashita[1†], Sayuri Tanabata[2†], Norikuni Ohtake[1], Kuni Sueyoshi[1], Takashi Sato[3], Kyoko Higuchi[4], Akihiro Saito[4] and Takuji Ohyama[1,4]*

[1] Faculty of Agriculture, Niigata University, Niigata, Japan, [2] College of Agriculture, Ibaraki University, Mito, Japan, [3] Faculty of Bioresource Sciences, Akita Prefectural University, Akita, Japan, [4] Faculty of Applied Biosciences, Tokyo University of Agriculture, Tokyo, Japan

OPEN ACCESS

Edited by:
Kiwamu Minamisawa, Tohoku University, Japan

Reviewed by:
Shigeyuki Tajima, Kagawa University, Japan
Brett James Ferguson, The University of Queensland, Australia

***Correspondence:**
Takuji Ohyama
ohyama@niigata-u.ac.jp; to206474@nodai.ac.jp

[†]These authors have contributed equally to this work as the first authors

Specialty section:
This article was submitted to Plant Microbe Interactions, a section of the journal Frontiers in Plant Science

Received: *16 August 2018*
Accepted: *25 January 2019*
Published: *19 February 2019*

Citation:
Yamashita N, Tanabata S, Ohtake N, Sueyoshi K, Sato T, Higuchi K, Saito A and Ohyama T (2019) Effects of Different Chemical Forms of Nitrogen on the Quick and Reversible Inhibition of Soybean Nodule Growth and Nitrogen Fixation Activity. Front. Plant Sci. 10:131. doi: 10.3389/fpls.2019.00131

It has been reported that supply of nitrate to culture solution rapidly and reversibly inhibits nodule growth and nitrogen fixation activity of soybean. In this study, the effects of ammonium, urea, or glutamine on nodule growth and nitrogen fixation activity are compared with that for nitrate. Soybean plants were cultivated with a nitrogen-free nutrient solution, then 1 mM-N of nitrate, ammonium, glutamine, or urea were supplied from 12 DAP until 17 DAP. Repression of nodule growth and nitrogen fixation activity at 17 DAP were observed by ammonium, urea, and glutamine like nitrate, although the inhibitory effects were milder than nitrate. The removal of nitrogen from the culture solutions after nitrogen treatments resulted in a recovery of the nodule growth. It was found that the glutamine treatment followed by N-free cultivation gave highest nitrogen fixation activity about two times of the control. Tracer experiments with ^{15}N and ^{13}C were performed to evaluate the translocation of N and C to the different tissues. Culture solutions containing a ^{15}N-labeled nitrogen source were supplied from 21 DAP, and the whole shoots were exposed to $^{13}CO_2$ for 60 min on 23 DAP, and plants were harvested on 24 DAP. The percentage distribution of ^{15}N in nodules was highest for ammonium (1.4%) followed by glutamine (0.78%), urea (0.32%) and nitrate (0.25%). The percentage distribution of ^{13}C in the nodules was highest for the control (11.5%) followed by urea (5.8%), glutamine (2.6%), ammonium (2.3%), and nitrate (2.3%). The inhibitory effects of nitrogen compounds appeared to be related to a decrease in photoassimilate partitioning in the nodules, rather than ^{15}N transport into the nodules. The free amino acid concentrations after nitrogen treatments were increased in the nodules and leaves by nitrate, in the roots by ammonium, in the stems by urea, and the roots, stems, and leaves by glutamine treatment. The concentrations of asparagine, aspartate, and

glutamine were increased after nitrogen treatments. By the long-term supply of nitrogen for 2-weeks, nitrate significantly increased the lateral roots and leaf growth. The long-term supply of urea and glutamine also promoted the lateral roots and leaf growth, but ammonium suppressed them.

Keywords: ammonium, glutamine, nodule growth, nitrate, nitrogen fixation activity, soybean, urea, ^{15}N and ^{13}C tracer experiment

INTRODUCTION

Soybean plants can use both the nitrogen (N) fixed by root nodules and the N absorbed from the roots. However, it is well known that the development of root nodules and N_2 fixation activity are repressed when the nodulated roots are exposed to high concentrations of combined form of nitrogen, especially nitrate, a major chemical form of inorganic nitrogen in upland fields (Gibson and Harper, 1985; Imsande, 1986; Streeter, 1988; Ohyama et al., 2012). It was suggested that multiple effects of nitrate inhibition occur, such as the decreases in nodule number, nodule mass, and N_2 fixation activity, as well as the acceleration of nodule senescence or disintegration, so nitrate inhibition cannot be explained in a simple way (Harper, 1987; Streeter, 1988). In addition, the effects of nitrate on nodule growth are influenced by nitrate concentration, placement in the medium, and treatment period (Yashima et al., 2003, 2005) as well as legume species (Harper and Gibson, 1984; Davidson and Robson, 1986).

Many hypotheses have been proposed regarding the causes of nitrate inhibition of nodulation and nitrogen fixation, such as carbohydrate-deprivation in nodules, feedback inhibition by a product of nitrate metabolism such as Asn or ureides (allantoic acid and allantoin) (Serraj et al., 1999, Vadez et al., 2000), and decreased oxygen diffusion into the nodules which restricts the respiration of bacteroides (Schuller et al., 1988; Vessey et al., 1988; Gogorcena et al., 1997; Gordon et al., 2002).

Direct (local) supply of nitrate to the nodulated part of the roots and indirect (systemic) supply from the distal part of the roots have elicited different responses of nodule growth and nitrogen fixation activity (Yashima et al., 2003, 2005). Further, direct effect of 5 mM nitrate on growth and nitrogen fixation activity of the nodules was quick and reversible in hydroponically cultured soybean seedlings (Fujikake et al., 2002, 2003). The diameter of the individual nodule was measured by a slide caliper under the controlled environmental conditions from 10 to 24 DAP. The diameter of a root nodule attached to the primary root increased from 1 to 6 mm for 2 weeks in N-free culture conditions. The increase in diameter of the nodule was almost completely stopped after 1 day of supplying 5 mM nitrate. However, nodule growth quickly returned to the normal growth rate following the withdrawal of nitrate from the solution.

The effects of nitrate on soybean nodule growth have been monitored at 1-h intervals, and the growth of nodules was measured with newly developed computer software (Saito et al., 2014; Tanabata et al., 2014). Nodule growth began to be suppressed quickly at several hours after the addition of 5 mM of nitrate compared with control plants. Similar repressive effects were observed on the growth rate of the primary roots. Conversely, the growth rate of soybean lateral roots was promoted by the addition of 5 mM of nitrate (Saito et al., 2014).

Plant leaves have been exposed to ^{11}C or ^{14}C-labeled carbon dioxide to investigate the effect of 5 mM nitrate on photosynthate translocation and distribution to nodules and roots (Fujikake et al., 2003). The supply of 5 mM nitrate stimulated the translocation rate and the distribution of labeled-C in the nitrate-fed part of the roots. However, the ^{14}C partitioning to nodules markedly decreased. These results indicated that a decrease in photoassimilate supply to the nodules might be involved primarily in the quick and reversible nitrate inhibition of soybean nodule growth. A question remains, however, as to whether a quick and reversible effect of nitrate inhibition on nodule growth and nitrogen fixation is specific for nitrate, or might a similar effect occur for application of the other nitrogen sources such as ammonium sulfate, urea, or Gln. In addition, the inhibitory effect of the nitrogen compound might be caused directly by the accumulation of nitrogen compounds in nodules or via changes in photoassimilate partitioning in nodules as in the case of nitrate inhibition.

Amino acids are the key metabolites in nitrogen (N) metabolism of higher plants (Ohyama et al., 2017). First, the inorganic N such as ammonium absorbed in the roots or produced from nitrate reduction, nitrogen fixation in root nodules and photorespiration in leaves, are initially assimilated into Gln and glutamate (Glu) by GS/GOGAT pathway. Second, amino acids are the essential components of proteins. Third, amino acids are used for a long distance transport of nitrogen among organs (roots, nodules, stems, leaves, pod, seeds, apical buds) through xylem or phloem. Forth, non-protein amino acids may play a role in protecting plants from feeding damages by animals, insects or infection by fungi.

The nitrogen assimilation in soybean nodules, the time course experiment with $^{15}N_2$ feedings in the nodulated intact soybean plants with specific inhibitors revealed that the ammonia produced by nitrogen fixation in bacteroid is rapidly released to the cytosol of the infected cells and is initially assimilated into amide group of Gln by the enzyme GS, then the Gln and 2-OG produce two moles of Glu by the enzyme glutamate synthase (GOGAT) (Ohyama and Kumazawa, 1978, 1980a). Some part of

Abbreviations: Ala, alanine; ARA, acetylene reduction activity; Arg, arginine; AS, asparagine synthetase; Asn, asparagine; Asp, aspartic acid; Cys, cysteine; DAP, days after planting; GABA, 4-aminobutanoic acid; Gln, glutamine; Glu, glutamic acid; Gly, glycine; GOGAT, glutamine 2-oxoglutarate aminotransferase (glutamate synthase); GS, glutamine synthetase; His, histidine; Ile, isoleucine; Leu, leucine; Lys, lysine; Met, methionine; NR, nitrate reductase; NiR, nitrite reductase; Phe, phenylalanine; Pro, proline; Ser, serine; Trp, tryptophan; Tyr, tyrosine; Val, valine.

Gln is used for purine base synthesis and uric acid is transported from the infected cells to the adjacent uninfected cells in the central symbiotic region of nodule. Uric acid is catabolized into allantoin and allantoic acid in the uninfected cells, then transported to the shoot through xylem vessels in the roots and stems. A small portion of fixed N was assimilated into Ala and Glu in the bacteroides, but it was not metabolized by GS/GOGAT pathway (Ohyama and Kumazawa, 1980b). It is established that the ureides are the principal N transport compounds from soybean nodules, but Asn is also transported from nodules. Huber and Streeter (1984) reported that Gln-dependent AS catalyses the amidation of aspartate to Asn in the cytosol fraction of infected zone of soybean nodules. Minamisawa et al. (1986) estimated the Asn and ureide pools in soybean nodules after $^{15}N_2$ exposure to the nodulated roots for 5.5 h, and revealed that fixed N in the transport form of Asn-N was about 1/5 of ureide-N.

In the present research, nodulated soybean seedlings were supplied with sodium nitrate, ammonium sulfate, urea, or Gln for 5 days from 12 to 17 DAP, and the effects of nitrogen supply on nodule growth and nitrogen fixation activity as measured by ARA were determined on 17 DAP. Control plants were grown with an N-free culture solution throughout the experimental period. In a further study, plants were grown continuously in an N-free solution for 7 days from 17 to 24 DAP after 5 days of nitrogen treatments. In this series of experiments, nodule growth was measured every day, and the effect of the different nitrogen compounds on nodule volume was evaluated.

In a second experiment, a ^{13}C and ^{15}N double tracer experiment was conducted. Culture solutions containing 1 mM-N of ^{15}N-labeled $Na^{15}NO_3$, $(^{15}NH_4)_2SO_4$, ^{15}N-urea, or ^{15}N-Gln were supplied for 3 days from 21 to 24 DAP. The whole shoot of the ^{15}N-supplied plant was enclosed in a plastic bag on 23 DAP, and the leaves in the plastic bag were exposed to $^{13}CO_2$. At 26 h after $^{13}CO_2$ exposure, plants were harvested on 24 DAP. Control plants were grown in a N-free culture solution throughout the experiment period. The plants were freeze-dried and then separated into nodules, roots, stems, and leaves. The tissue samples corresponding to each part were ground into a fine powder and the ^{15}N and ^{13}C enrichment in these parts were determined. The free amino acids in the nodules, roots, stems, and leaves of the plants treated with ^{15}N and ^{13}C were extracted with 80% ethanol before analysis using a Waters Aquity UPLC system.

In a final experiment, a long-term effect on the root architectures and whole plant growth with supplying N compounds for 2 weeks were observed The 20-day-old soybean plants were treated with the culture solutions containing 1 mM $NaNO_3$, 0.5 mM $(NH_4)_2SO_4$, 0.5 mM urea or 0.5 mM Gln for 2 weeks. Three lateral roots were marked with the color strings, and the main root length, marked lateral roots length and nodule diameter were measured at 1 and 2 weeks during treatments. After treatments, the plants were separated into roots and shoots, and the root length and leaf area were analyzed by the plant image analyzer. Plants were dried in a ventilation oven and dry weight of each tissue was measured.

MATERIALS AND METHODS

Plant Material and Growth Conditions

Soybean [*Glycine max* (L.) Merr. cv. Williams] seeds were inoculated with a suspension of *Bradyrhizobium diazoefficiens* (strain USDA 110) and sown in vermiculite. After 5 DAP, each seedling was transplanted to a glass bottle with 800 mL of N-free nutrient solution (Fujikake et al., 2002). The culture solution was continuously aerated by an air-pump and changed three times a week. Plants were cultivated in a climate chamber (28/18°C day/night temperature, 55% relative humidity, 228 μmol m^{-2} s^{-1} PPFD, 16/8 h day/night photoperiod).

The Effects of the Application of Nitrogen Compounds on Nodule Growth

Culture solutions containing 1 mM nitrogen source [1 mM $NaNO_3$, 0.5 mM $(NH_4)_2SO_4$, 0.5 mM urea or 0.5 mM Gln] were supplied for 5 days from 12 to 17 DAP (Experiment 1). The solution was renewed every day. Control plants were grown with an N-free culture solution throughout the experimental period. The ARA was measured on 17 DAP, then the dry weight of each tissue was determined.

In the second experiment (Experiment 2), the plants were cultivated with the various nitrogen compounds (same as in the Experiment 1) and then were continually grown with a N-free solution from 17 to 24 DAP. Control plants were grown with an N-free culture solution from 12 to 24 DAP. The diameter (d) of the horizontal axis of five selected nodules attached to the main root per single plant was measured by a slide caliper every day, then the effects of nitrogen compounds on nodule growth were evaluated from the changes in nodule volume. The volume of each nodule was calculated by the formula for the volume of a sphere $4\pi r^3/3$, where r is the radius of a nodule (r = d/2). Then the ARA was measured on 24 DAP, and the dry weight of each tissue was determined. The experiment was replicated four individual plants. Statistical analysis was performed using Tukey's test.

Acetylene Reduction Activity

The nodulated root of each plant in Experiments 1 and 2 was separated from the shoot and immediately incubated with 10% (V/V) acetylene in a 600 ml glass bottle at 25°C for 20 min, then the ethylene produced by nitrogenase was monitored by a gas chromatography equipped with FID (Gas Chromatograph 163, Hitachi, Tokyo, Japan) fitted with a Porapack N column (GL Science, Tokyo, Japan). We could not detect the wound-induced ethylene production without acetylene in this system.

^{13}C and ^{15}N Double Tracer Experiment

Soybean plants were cultivated in a solution culture with an N-free solution until 21 DAP, and different forms of nitrogen compounds were supplied for 3 days when the inhibitory effect on nodule growth became apparent in Experiment 2 (Experiment 3). Culture solution containing ^{15}N-labeled 1 mM nitrogen sources (1 mM $Na^{15}NO_3$; 6.82 atom%, 0.5 mM $(^{15}NH_4)_2SO_4$; 7.07 atom%, 0.5 mM ^{15}N-urea; 5.08 atom%, or 0.5 mM amide, amino ^{15}N-Gln; 8.67 atom%), were supplied from 21 to 24 DAP.

The solutions were renewed every day. On 23 DAP, the whole shoot of a plant was enclosed in a plastic bag (Gas volume about 2 L, 270 × 200 mm). Two mL of $^{13}CO_2$ (99.0 atom%) was injected into each plastic bag and the CO_2 concentration in the bag was monitored by an infrared CO_2 analyzer (Testo535, Testo Co. Ltd., Yokohama, Japan) (**Supplementary Figure S1**). At 30 min after the first injection, the $^{13}CO_2$ was almost depleted, thus a further 2 mL of $^{13}CO_2$ was injected. Plants were exposed to the $^{13}CO_2$ for 60 min in total, then the plastic bag was removed. At 26 h after $^{13}CO_2$ exposure, plants were harvested on 24 DAP. Control plants were grown with an N-free culture solution throughout the experimental period. The plants were immediately frozen with liquid nitrogen and dried in a freeze-drier. The plants were separated into leaves, stems, roots, and nodules. The samples of each part were ground into a fine powder by a vibratory mill. The ^{15}N and ^{13}C enrichment in tissue parts were determined using an Elemental analyzer (EA1110, Thermo Electron) -IRMS coupled system (DELTA Plus Advantage, Thermo Electron,Boston, MA, United States).

Analysis of Free Amino Acids

The free amino acids in the nodules, roots, stems and leaves of the plants treated with ^{15}N and ^{13}C (Experiment 3) were extracted with 80% (V/V) ethanol, then derivatized with AQC (6-aminoquinolyl-*N*-hydroxysuccinimidyl-carbamate) reagent, and analyzed by a Waters Aquity UPLC system equipped with a Waters AccQ Tag Ultra column (Waters, Milford, MA, United States) (Nagumo et al., 2009).

Long-Term Effects of Various N Compounds on Root Architecture and Plant Growth

Twenty-day-old soybean plants were treated with the culture solutions containing 1 mM $NaNO_3$, 0.5 mM $(NH_4)_2SO_4$, 0.5 mM urea or 0.5 mM Gln for 2 weeks (Experiment 4). Culture solutions were renewed every 2 days. The root structure and shoot phenotypes were monitored after 2-weeks treatments. Three lateral roots were marked with the color strings tied above a nodule, and the main root length, marked lateral root length and diameter of nodules attached to the lateral roots were measured at 1 and 2 weeks during treatments. The chlorophyll concentration (SPAD values) after 2-week treatments were determined for second, third, and fourth leaves by Chlorophyll meter SPAD-502 (Konica Minolta Sensing, Inc., Japan). The plants were separated into roots and shoots, and the root length and leaf area were analyzed by the plant image analyzer (WinRHIZO, STD 4800, Regent Instruments Inc., Canada). Plant samples were dried in a ventilation oven and dry weight of each tissue was measured.

RESULTS

Effects of Various Nitrogen Compounds on Plant Growth and Acetylene Reduction Activity

Figure 1 shows the dry weight for each plant tissue on 17 DAP after various nitrogen treatments for 5 days (Experiment 1). The total plant dry weight was 559 mg (control), 570 mg (nitrate), 610 mg (ammonium), 599 mg (urea), and 651 mg (Gln). The dry weights of roots (**Figure 1B**), stems (**Figure 1C**), and leaves (**Figure 1D**) of plants with N compounds were similar or slightly higher than those of the control plants. In the case of the dry weights of nodules, the values were repressed by the supply of 1 mM-N for 5 days compared with control plants (**Figure 1A**). The dry weight values for nodules were 28.5 mg (control), 12.7 mg (nitrate), 21.4 mg (ammonium), 21.6 mg (urea), and 18.4 mg (Gln). Based on Tukey's test, the nodule dry weight for the control plant was significantly different ($P < 0.05$) compared to all the nitrogen treated plants. The addition of the nitrogen compounds resulted in reductions of nodule dry weight of 45% (nitrate), 75% (ammonium), 76% (urea), and 65%, (Gln) relative to the control plants, respectively. The repressive effect of nitrogen compounds was the strongest for nitrate, while weaker repression occurred for additions of ammonium, urea, and Gln. The numbers of nodules per plant, 48.5 (control), 43.8 (nitrate), 45.8 (ammonium), 43.8 (urea), and 39.5 (Gln), were not significantly different among the four different nitrogen treatments (**Supplementary Figure S2**).

Figure 2 shows the ARA per a single plant and the specific ARA per nodule dry weight. The average ARA per plant was 0.90 μmol ethylene formed per h (control), 0.39 μmol (nitrate), 0.53 μmol (ammonium), 0.50 μmol (urea), and 0.53 μmol (Gln) (**Figure 2A**). The addition of nitrogen compounds resulted in a reduction in the ARA of 43% (nitrate), 59% (ammonium), 56% (urea), and 59% (Gln) relative to control plants, respectively. Based on Tukey's test, the ARA for the control plant was significantly different compared to that for nitrate treatment. The specific ARAs per g dry weight of nodules were 31.1 μmol ethylene formed per h per g dry weight (control), 30.1 μmol (nitrate), 24.3 μmol (ammonium), 23.9 μmol (urea), and 28.5 μmol (Gln) (**Figure 2B**). The addition of nitrogen compounds resulted in a reduction of the specific ARA to 97% (nitrate), 78% (ammonium), 77% (urea), and 92%, (Gln) relative to the control plants, respectively. The specific ARAs were not significantly different for the different nitrogen treatments according to Tukey's test. These findings suggested that the repression of the total ARA by the different N treatments was mainly due to a decrease in nodule weight rather than a specific ARA effect.

The Effects of Application of Various Chemical Forms of Nitrogen From 12 to 17 DAP Followed by Cultivation With an N-Free Solution

In a second experiment, plants were cultivated with various forms of nitrogen compounds from 12 to 17 DAP and then cultivation was continued with an N-free solution from 17 to 24 DAP in all treatments. **Figure 3** shows the changes in nodule volume from 12 to 24 DAP. The control soybean nodules grew steadily from 12 to 24 DAP in an N-free nutrient solution. When 1 mM nitrate was supplied at 12 DAP, the nodule growth was quickly repressed from the next day after nitrate addition, and stopped completely after the second day on 14 DAP. The addition of ammonium also quickly repressed the nodule growth from the first day and the

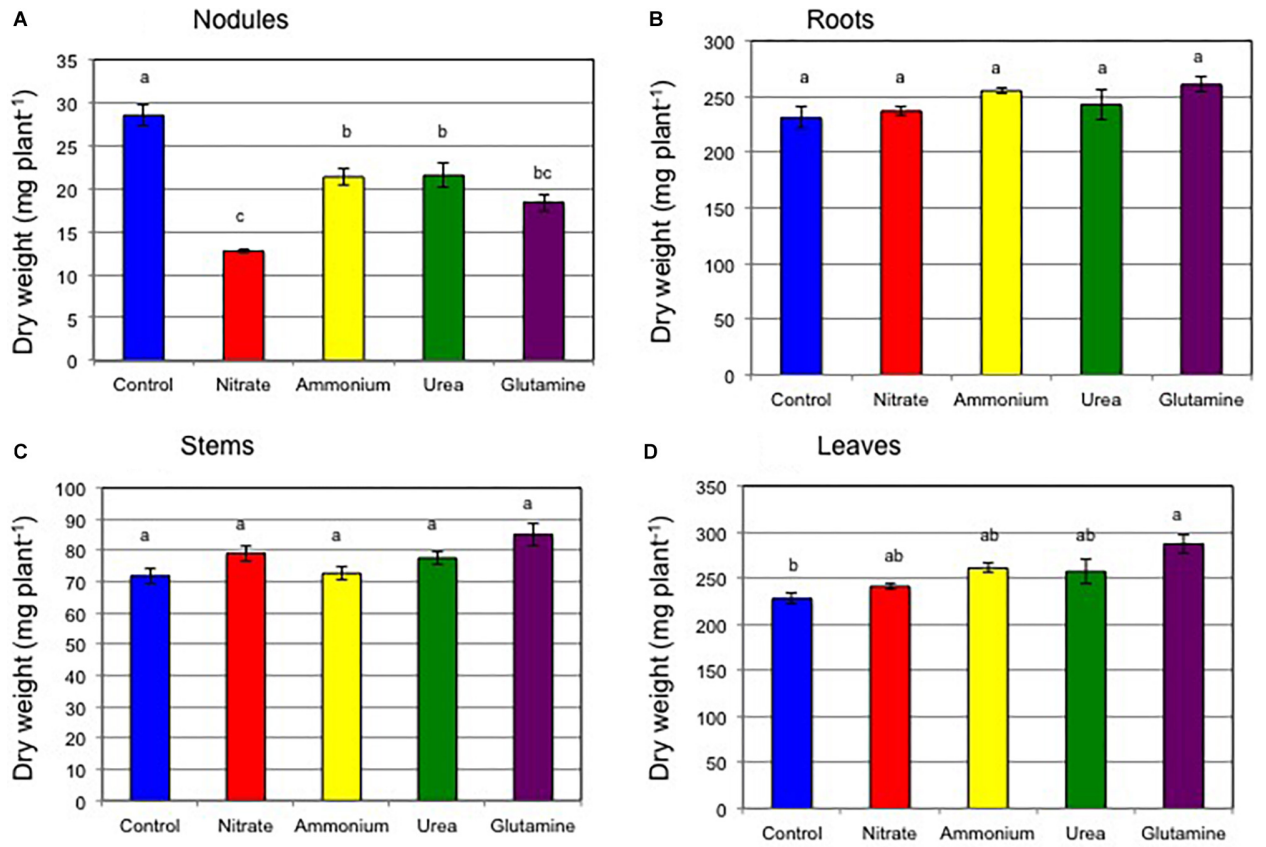

FIGURE 1 | Comparison of the dry weight of each plant tissue at 17 DAP supplied with control (N-free), nitrate, ammonium, urea, or glutamine from 12 to 17 DAP (Experiment 1). **(A)** Nodules. **(B)** Roots. **(C)** Stems. **(D)** Leaves. Averages and standard errors are shown (n = 4). Different letters above the column indicate significant differences at <0.05 by Tukey's test.

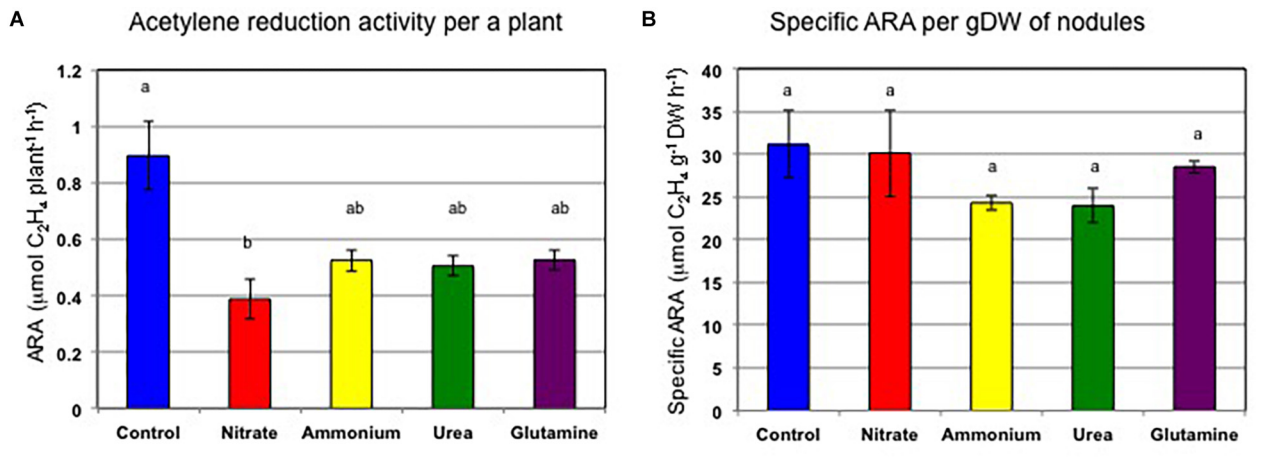

FIGURE 2 | Acetylene reduction activity per single plant, and specific acetylene reduction activity per nodule g dry weight on 17 DAP supplied with control (N-free), nitrate, ammonium, urea, or glutamine from 12 to 17 DAP for 5 days (Experiment 1). **(A)** ARA per single plant. **(B)** Specific ARA per g dry weight of nodules. Averages and standard errors are shown (n = 4). Different letters above the column indicate significant differences at <0.05 by Tukey's test.

increase in the nodule volume was less than half of that in the control on the third day on 15 DAP. The addition of urea and Gln resulted in similar growth patterns. The nodule growth was slightly repressed after 14 DAP, but the repression was weaker compared with that for the nitrate and ammonium treatments. After replacing the N-based culture solutions with the N-free

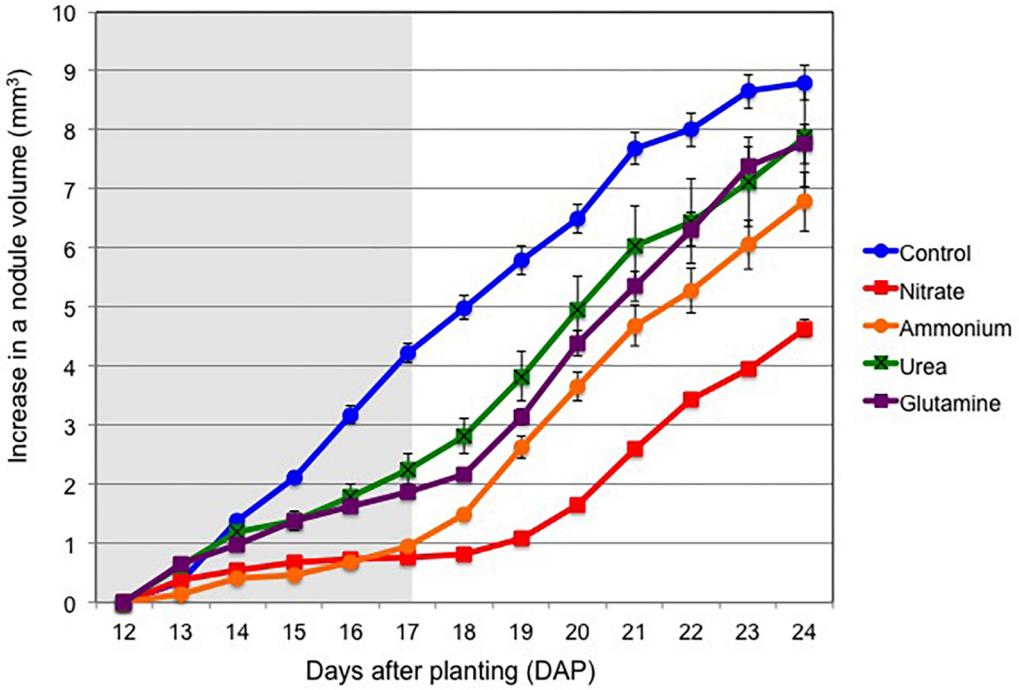

FIGURE 3 | Changes in nodule volume from 12 to 24 DAP for treatments with control (N-free), nitrate, ammonium, urea, or glutamine from 12 to 17 DAP, thereafter cultivated with a N-free culture solution (Experiment 2). Shaded background indicates N treatment period, and white background indicates cultivation with N-free medium. Average and standard error are shown (n = 5).

solution on 17 DAP, the nodule growths for all treatments showed quick recoveries, although there was a longer time-lag of about 2 days after the addition of nitrate.

Figure 4 shows the dry weight of each plant tissue on 24 DAP after various nitrogen treatments for 5 days from 12 to 17 DAP and with continued growth in the N-free medium from 17 to 24 DAP (Experiment 2). The total plant dry weights were 904 mg (control), 1,150 mg (nitrate), 1,200 mg (ammonium), 1,195 mg (urea), and 1,290 mg (Gln). The dry weights of roots, stems, and leaves of plants receiving the various N treatments were slightly higher than those of the control plants. Compared with nodule dry weight just after N treatment on 17 DAP (**Figure 1A**), the dry weights of nodules of the plants with N were recovered compared with control plants on 24 DAP after continued growth in the N-free medium for 7 days (**Figure 4A**). The dry weights of the nodules were 64.8 mg (control), 44.8 mg (nitrate), 64.5 mg (ammonium), 70.3 mg (urea), and 68.8 mg (Gln); the nodule dry weights were not significantly different among all treatments according to Tukey's test. The addition of nitrogen compounds from 12 to 17 DAP tended to increase the dry weights of roots (**Figure 4B**), stems (**Figure 4C**), and leaves (**Figure 4D**) at 24 DAP.

Figure 5 shows the ARA per single plant and the specific ARA per g nodule dry weight on 24 DAP. The average ARAs per single plant were 5.4 μmol (control), 3.4 μmol (nitrate), 4.0 μmol (ammonium), 5.6 μmol (urea), and 9.2 μmol (Gln) ethylene formed per h per g nodule dry weight (**Figure 5A**). The ARA levels recovered to levels near that of the control for cultivation with the N-free solution after the addition of the nitrogen compounds. Unexpectedly, the addition of Gln from 12 to 17 DAP increased significantly the ARA (172%) on 24 DAP compared to the treatment for the control. The specific ARA were 81.6 μmol (control), 75.4 μmol (nitrate), 65.5 μmol (ammonium), 82.8 μmol (urea), and 133.5 μmol (Gln) ethylene formed per h per g dry weight of nodules (**Figure 5B**), and the specific ARAs were significantly different for treatment by Gln compared to the other nitrogen compounds according to Tukey's test.

^{15}N and ^{13}C Double Tracer Experiment

Supplementary Table S1 shows the dry weight of each tissue of soybean plants for ^{15}N and ^{13}C double tracer experiment. The nodule dry weights of the plants with various N compounds were relatively low compared with that of the control plants although statistically not significant according to Tukey's test. **Figure 6** shows the nitrogen concentrations in each tissue of the soybean plant at 24 DAP after cultivation with various N compounds for 3 days from 21 to 24 DAP. The nitrogen concentrations in nodules were similar about 53–56 mgN g^{-1} dry weight for the various treatments including that for the control plants (**Figure 6A**). In contrast, the nitrogen concentrations of roots (**Figure 6B**), stems (**Figure 6C**), and leaves (**Figure 6D**) were significantly higher in the plants supplied with N compounds. The nitrogen levels in the roots treated with Gln had the highest concentrations at 31 mgN g^{-1} dry weight, the levels being significantly higher than that for the other treatments.

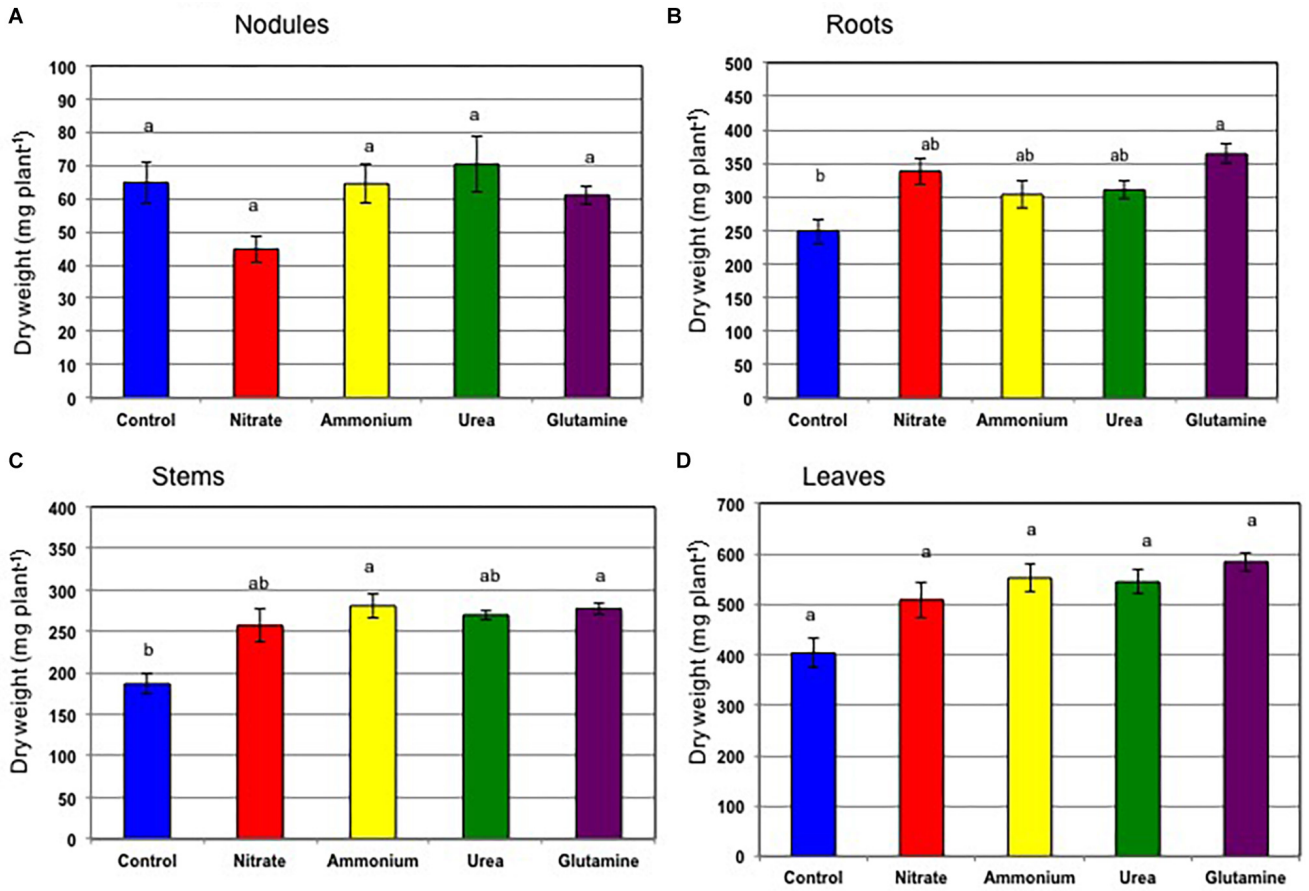

FIGURE 4 | Comparison of the dry weight of each plant tissue on 24 DAP for treatment with control (N-free), nitrate, ammonium, urea, or glutamine from 12 to 17 DAP, thereafter cultivated with a N-free culture solution (Experiment 2). **(A)** Nodules. **(B)** Roots. **(C)** Stems. **(D)** Leaves. Averages and standard errors are shown (n = 4). Different letters above the column indicate significant differences at <0.05 by Tukey's test.

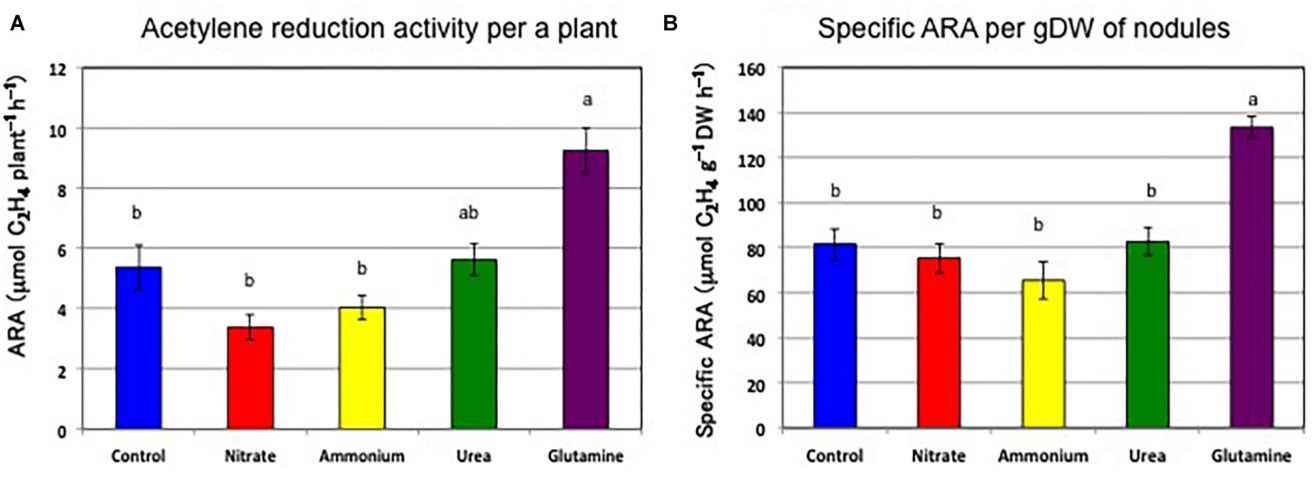

FIGURE 5 | Acetylene reduction activity per single plant and specific acetylene reduction activity per nodule g dry weight on 24 DAP for treatments with control (N-free), nitrate, ammonium, urea, or glutamine for 5 days from 12 to 17 DAP with continuation of growth from 17 to 24 DAP with N-free medium (Experiment 2). **(A)** ARA per single plant. **(B)** Specific ARA per g dry weight of nodules. Averages and standard errors are shown (n = 4). Different letters above the column indicate significant differences at <0.05 by Tukey's test.

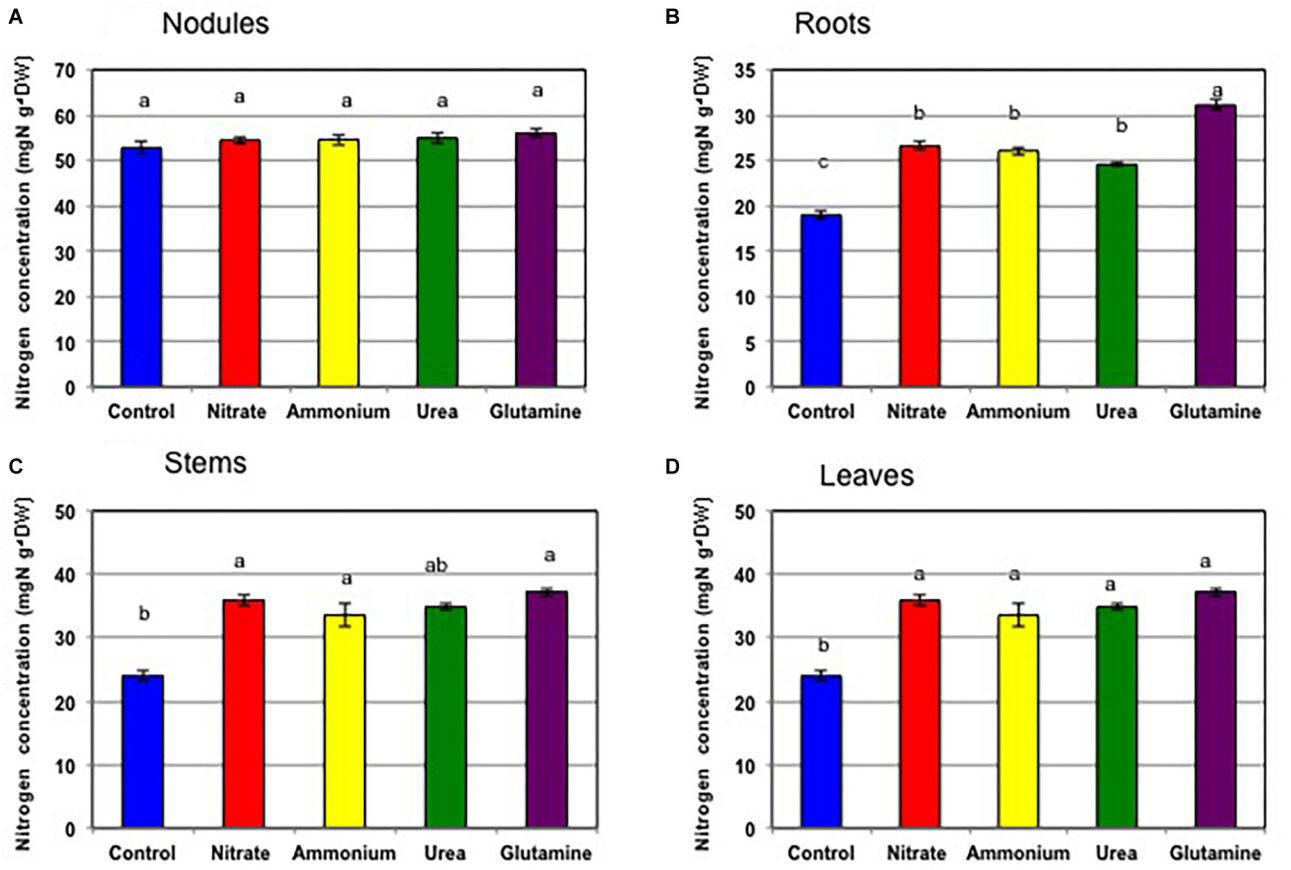

FIGURE 6 | Nitrogen concentration in tissues of soybean plants treated with control (N-free), nitrate, ammonium, urea, or glutamine for 3 days from 21 to 24 DAP (Experiment 2). **(A)** Nodules. **(B)** Roots. **(C)** Stems. **(D)** Leaves. Averages and standard errors are shown (n = 4). Different letters above the column indicate significant differences at <0.05 by Tukey's test.

Figure 7 shows the amounts of N in each tissue derived from the ^{15}N-labeled sources supplied for 3 days from 21 to 24 DAP. The culture solutions containing 11.3 mg of labeled N, were changed every day, so a total of 33.6 mg of ^{15}N-labeled N was supplied during the period of the labeling experiment. The total amounts of N derived from the ^{15}N-labeled source were 0 mg (control), 9.75 mg (nitrate), 8.71 mg (ammonium), 7.04 mg (urea), and 9.67 mg (Gln), respectively. These results indicated that urea and Gln as well as nitrate and ammonium were absorbed efficiently from the roots, although urea absorption tended to be lower than that of the other compounds; this finding, however, was not statistically significant. The ^{15}N-labeled N was not depleted from the culture solution, because the daily supply of labeled N was 11.3 mg, which was higher than the total amount of ^{15}N absorbed by a plant in the 3 days. The amounts of N derived from ^{15}N in the nodules (**Figure 7A**) were 0 mg (control), 0.14 mg (nitrate), 0.26 mg (ammonium), 0.14 mg (urea), and 0.29 mg (Gln). The amounts of N from Gln and ammonium were significantly higher than those from nitrate and urea. The amounts of N derived from ^{15}N in the roots (**Figure 7B**) were 0 mg (control), 3.08 mg (nitrate), 2.78 mg (ammonium), 2.87 mg (urea), and 4.61 mg (Gln). The amount of N from Gln was significantly higher than that from nitrate, ammonium, or urea. The amount of N from ^{15}N in the stems tended to be high in the stem treated with ammonium (**Figure 7C**), and that was high in the leaves treated with nitrate (**Figure 7D**).

The percentage distribution of ^{15}N (**Supplementary Table S2**) in the shoots (stems + leaves) was highest for nitrate (67%), and ammonium (65%) treatments followed by urea (57%) and then Gln (49%). The percentage distribution of ^{15}N in the leaves was highest for nitrate treatment (57%), followed by ammonium treatment (49%), urea (45%) and then Gln (41%). In contrast, the percentage distribution of ^{15}N in the stems was highest for ammonium treatment (16%), followed by urea (12%), nitrate (10%) and Gln (9%). The percentage distribution of ^{15}N in the roots was highest for Gln treatment (48%), followed by urea (41%), and ammonium (32%) and then nitrate (32%). The percentage distribution of ^{15}N in the nodules was higher for Gln (3.0%) and ammonium (2.9%) relative to that for nitrate (1.5%) and urea (1.9%).

The total contents of C derived from ^{13}C-labeled CO_2 were 993 μg (control), 925 μg (nitrate), 991 μg (ammonium), 993 μg (urea), and 1021 μg (Gln). About 2000 μg of ^{13}C was exposed to each plant in the form of $^{13}CO_2$, so about one half of the supplied

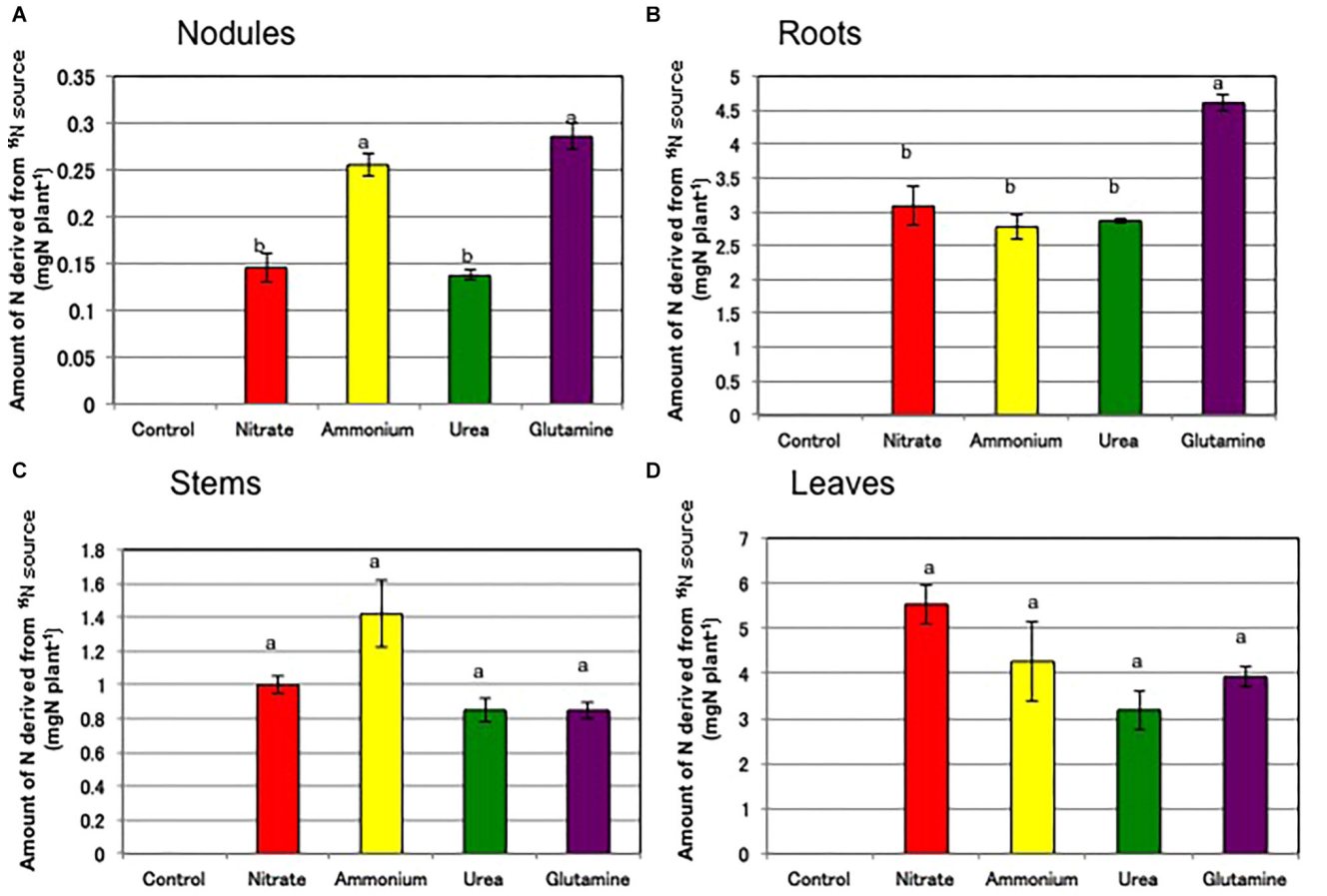

FIGURE 7 | Amounts of N derived from ^{15}N-labeled source in each tissue of soybean plants on 24 DAP supplied for 3 days from 21 to 24 DAP (Experiment 3). **(A)** Nodules. **(B)** Roots. **(C)** Stems. **(D)** Leaves. Averages and standard errors are shown (n = 4). Different letters above the column indicate significant differences among each treatment at <0.05 by Tukey's test.

^{13}C remained in the plant at 1 day after $^{13}CO_2$ exposure. The other half may not be fixed during incubation period, and be lost by respiration of the plants during 26 h after $^{13}CO_2$ exposure. **Figure 8** shows the amounts of C derived from ^{13}C-labeled CO_2 in the tissues of the soybean plants supplied for 1 h at 23 DAP. The amounts of C from ^{13}C in the nodules (**Figure 8A**) were 85 μg (control), 27 μg (nitrate), 34 μg (ammonium), 54 μg (urea), and 34 μg (Gln). The addition of nitrogen compounds resulted in the reductions in the amounts of C derived from ^{13}C, the relative reductions to the control (100%) being 32% (nitrate), 40% (ammonium), 64% (urea), and 40% (Gln), respectively. The amounts of C from ^{13}C in the nodules were significantly different for the control and the other treatments except for urea. The amounts of C from ^{13}C were not significantly different in the roots (**Figure 8B**) and the leaves (**Figure 8D**) for the different nitrogen treatments. The amount of C derived from ^{13}C was significantly high in the stems treated with ammonium compared with nitrate, urea, and Gln (**Figure 8C**).

Supplementary Table S3 shows the percentage distribution of ^{13}C for the various N treatments. The percentage distribution of ^{13}C in the nodules was highest for the control treatment (11.5%) followed by urea (5.8%), Gln (2.6%), ammonium (2.3%), and nitrate (2.3%). The amounts of ^{13}C in the nodules (**Figure 8A**) and the percentage distributions of ^{13}C in the nodules were in accordance with the decrease in nodule growth (**Figures 1**, **3**) and the ARAs (**Figure 2**). The percentage distribution of ^{13}C in the roots was the lowest for the ammonium treatment (19.7%), but this treatment also resulted in the highest percentage distribution of ^{13}C in the stem (30.6%). The percentage distribution of ^{13}C in the leaves was highest for nitrate treatment (56.7%) followed by urea (50.1%) and Gln (50.1%), ammonium (47.4%), the lowest value being in the in control (35.4%).

Free Amino Acid Concentration in Soybean Tissue

Figure 9 shows the free amino acid concentrations in the nodules (**Figure 9A**), roots (**Figure 9B**), stems (**Figure 9C**), and leaves (**Figure 9D**) at 24 DAP after 3 days of nitrogen supply. For the nodules (**Figure 9A**), the total amino acid N concentration was lowest in the control (410 μgN g^{-1} dry weight), and highest for nitrate supplementation (2,820 μgN g^{-1} dry weight), with

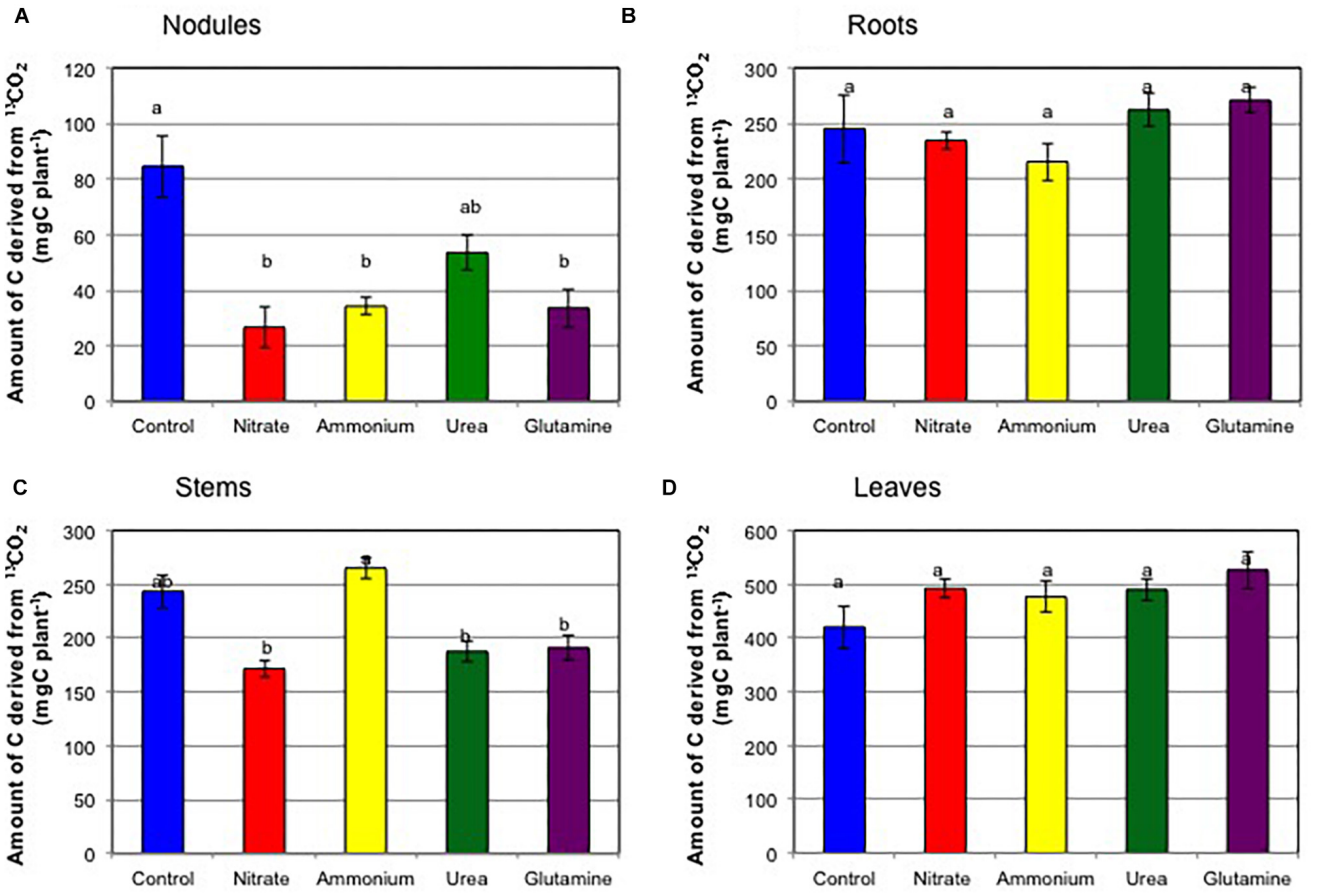

FIGURE 8 | Amounts of C derived from ^{13}C-labeled CO_2 in each tissue of soybean plants on 24 DAP supplied for 1 h at 23 DAP (Experiment 3). **(A)** Nodules. **(B)** Roots. **(C)** Stems. **(D)** Leaves. Averages and standard errors are shown (n = 4). Different letters above the column indicate significant differences among each treatment at <0.05 by Tukey's test.

intermediate values being obtained for ammonium (1,300 μgN g^{-1} dry weight), urea (1,020 μgN g^{-1} dry weight) and Gln (1,240 μgN g^{-1} dry weight) treatments. In the control nodules Asp, Asn, Ala, Ser, Glu, and Gln were the major free amino acids. In the nodules obtained for nitrate supplementation, there were about a sevenfold increase in total free amino acid concentration relative to that for the control nodules, and Asp, Glu, Asn, Ala, and GABA were the major amino acids. In the nodules supplemented with ammonium, urea, and Gln the increase was about three times that for the control nodules, and Asp, Asn, Glu, Gln, GABA, and Ser were the major amino acids for these treatments, the relative composition of the amino acid N being not markedly different among the treatments. The Gln concentration in the nodules treated with Gln did not increase excessively.

The total free amino acid N concentrations in the roots (**Figure 9B**) were lowest for the control roots (273 μgN g^{-1} dry weight), and highest in the roots treated with ammonium (1,840 μgN g^{-1} dry weight), followed by Gln (1,260 μgN g^{-1} dry weight), urea (890 μgN g^{-1} dry weight), and nitrate (310 μgN g^{-1} dry weight). In the control roots, Asp, Glu, Asn, Ser, Ala, and Gln were major free amino acids. The Supply of nitrogen compounds increased Asn and Asp irrespective of the chemical form of nitrogen supplied. The supply of Gln and ammonium also increased the Gln concentration, although the level was much less than that of Asn.

The total free amino acid N concentrations in the stems (**Figure 9C**) were the lowest for the control stems (244 μgN g^{-1} dry weight), and highest in the stems treated with urea (2,610 μgN g^{-1} dry weight), followed by Gln (1,840 μgN g^{-1} dry weight), ammonium (1,490 μgN g^{-1} dry weight) and nitrate (580 μgN g^{-1} dry weight). In the control stems, Asp, GABA, and Cys were the major free amino acids. In general, irrespective of the chemical form of nitrogen, the supply of nitrogen compounds increased the concentration of Asn and Asp, the same as that found for the roots. The supply of Gln increased the Gln concentration in the stems.

The total free amino acid N concentrations in the leaves (**Figure 9D**) were lowest in the control leaves (293 μgN g^{-1} dry weight), and highest in the leaves treated with nitrate (950 μgN g^{-1} dry weight), followed by urea (820 μgN g^{-1} dry weight), ammonium (750 μgN g^{-1} dry weight), and Gln (630 μgN g^{-1} dry weight). In the control leaves, GABA, Asp,

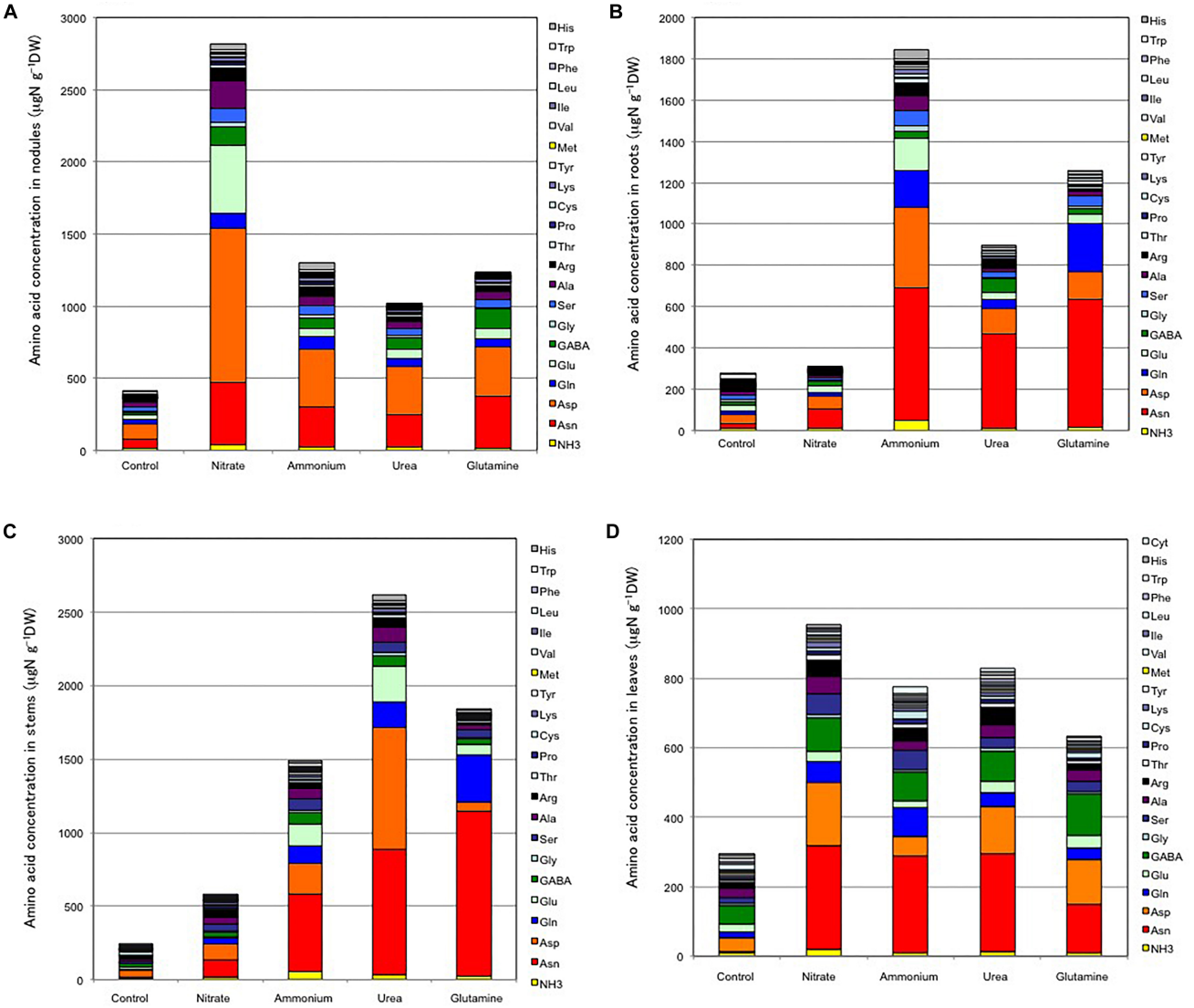

FIGURE 9 | Free amino acid concentrations in each tissue of soybean plants on 24 DAP supplied with various N compounds from 21 to 24 DAP (Experiment 3). **(A)** Nodules. **(B)** Roots. **(C)** Stems. **(D)** Leaves. Averages are shown (n = 4).

Ala, Arg, and Gln were the major free amino acids. The supply of nitrogen compounds increased Asn, Asp, GABA, Gln and Ser, irrespective of the chemical form of the supplied nitrogen. The supply of Gln did not increase the Gln concentration in the leaves.

The concentrations (**Supplementary Table S4**) and the relative concentrations (**Supplementary Table S5**) of free amino acids in each tissue for the various nitrogen treatments relative to those in the control plants were calculated. The relative concentrations of free ammonium were relatively high in the stems treated with ammonium (×8.6), urea (×5.5) and Gln (×4.2), and in the roots treated with ammonium (×4.9). Among the free amino acids, the relative concentrations of Asn were very high in roots (×4–25), stems (×9–80), leaves (×21–45), and nodules (×3.4–6.6). The relative concentrations of Asp were high especially in the nodules treated with nitrate (×10), in the roots treated with ammonium (×9.5), and in the stems treated with urea (×20). The relative concentrations of Gln were high especially in the stems (×24) and roots (×14) treated with Gln. The relative concentrations of Glu were high in the nodules treated with nitrate (×13), in the stems treated with urea (×25), ammonium (×15) and Gln (×8). The relative concentrations of GABA were high in the nodules for treatments with all nitrogen compounds and values were less the roots, stems, and leaves. The relative concentrations of Cys were markedly enhanced in the nodules and leaves but repressed in the stems. The relative concentrations of His were increased in the nodules, roots, and stems but decreased in the leaves. The relative concentrations of Trp in most tissue parts decreased as a result of the nitrogen treatments. The same was true in the case of Leu, Met, and Tyr in the leaves, Cys in the stems, and Met in the roots.

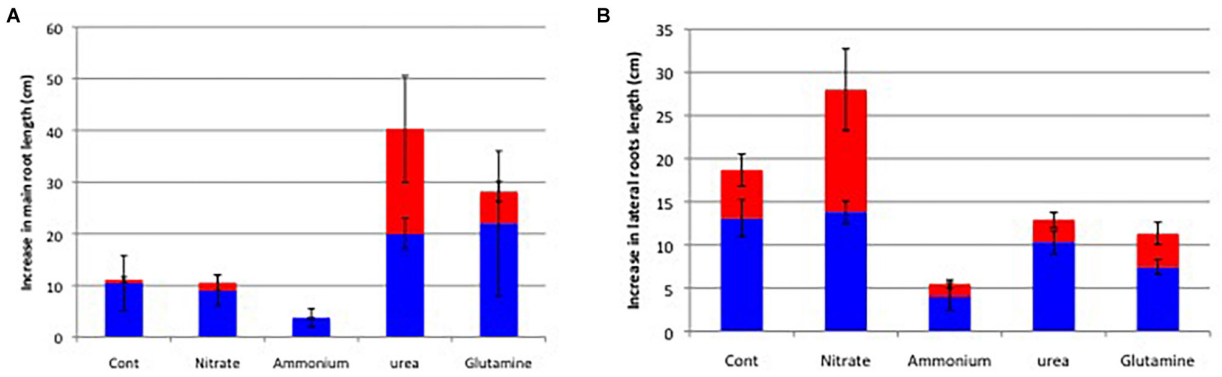

FIGURE 10 | Increase in main roots **(A)** and the selected lateral roots **(B)** after the first week from 20 to 27 DAP (Blue bar), and the second week from 27 to 34 DAP (Red bar) of the treatments with various forms of N compounds (Experiment 4).

Long-Term Effects of Various N Compounds From 20 to 34 DAP on Root Architecture and Plant Growth

Figure 10 shows the increase in the main root length (**Figure 10A**) and marked three lateral root length (**Figure 10B**) on 34 DAP after various nitrogen treatments for 14 days from 20 to 34 DAP (Experiment 3). The main root length increased about 10 cm for the first week period of control and nitrate treatments from 20 to 27 DAP, but those for the second week period from 27 to 34 DAP was almost completely stopped. The application of ammonium most severely inhibited the main root growth for the first and second weeks. Contrary, the application of urea and Gln continued to increase the main root length for the first and second period of treatments. The average length of marked three lateral roots was about 13 cm and 6 cm during the first and second weeks in control treatment. Those in nitrate treatment were 14 cm and 14 cm during the first and second weeks and longest among treatments. Those in ammonium treatment were 4 cm and 1 cm during the first and second weeks, and most strongly inhibited among treatments. The marked lateral root length in the urea and Gln treatments was slightly lower than control treatment either in the first and second weeks.

Figure 11 shows the total root length analyzed by WinRHIZO (**Figure 11A**) and the dry weight of the roots (**Figure 11B**). Both figures show the significant increase in the total root length and root dry weight in nitrate treatment compared with control treatment. The ratio of the total root length (nitrate/control) is x2.4-fold and much higher than the ratio of the dry weight (x1.6) indicate that fine roots growth was promoted by nitrate treatment. On the other hand, the total root length and root dry weight were lower in the ammonium treatment compared with the control treatment. The total root length and dry weight in urea and Gln treatments were slightly higher than the control roots. **Supplementary Figure S1** shows the photos of the root system with various N treatments after 1 week treatment on 27 DAP. The nitrate promoted the fine lateral root growth, while ammonium depressed new root growth compared with the control plant. The roots with urea and Gln treatments show the increased root growth between control and nitrate treatments.

After 2 weeks N treatments on 34 DAP, the nodule dry weight was highest in control, followed by urea, Gln, nitrate and ammonium treatment (**Supplementary Figure S4A**). On the other hand, the repression of three selected nodule growth were the highest in ammonium and nitrate, followed by urea and Gln (**Supplementary Figure S4B**). Nodule numbers are around 40 to 65, and not significantly different among treatments.

Two weeks of the long-term nitrogen treatments affected the whole plant growth (**Supplementary Figure S5**). After 2 weeks N treatments on 34 DAP, the average total plant dry weight was 2,008 mg (control), 3,114 mg (nitrate), 1,755 mg (ammonium), 2,569 mg (urea), and 2,612 mg (Gln). Nitrate treatment showed the highest growth promotion of leaves, stems, petioles, and buds but not for nodules. Urea and Gln treatments moderately increased the plant growth compared with the control, but ammonium repressed the growth of each organ. **Supplementary Figure S6** shows the photos of shoot organs among treatments, and **Supplementary Figure S7** shows the total leaf area analyzed by WinRHIZO. These figures clearly show that nitrate promoted the leaf growth as well as root growth. Urea and Gln treatment showed moderate promotion of leaf growth compared with the control plants. The ammonium treatment repressed the leaf growth as well as the root growth. **Supplementary Figure S8** shows the SPAD value of the second, third, and fourth leaves with various N treatments. The SPAD values with Gln were the highest followed by those with urea, nitrate, control, and ammonium. The 2 weeks nitrogen treatment markedly affected the bud development, and the average number of the lateral buds was 1 in control, 3.7 in nitrate, 0 in ammonium, 2 in urea, and 5 in Gln (**Supplementary Figure S6**).

DISCUSSION

Effects of Various Nitrogen Compounds on Nodule Growth and Acetylene Reduction Activity

From the daily changes of nodule volume from 12 to 17 DAP with following supplementation (1 mM-N nitrate, ammonium,

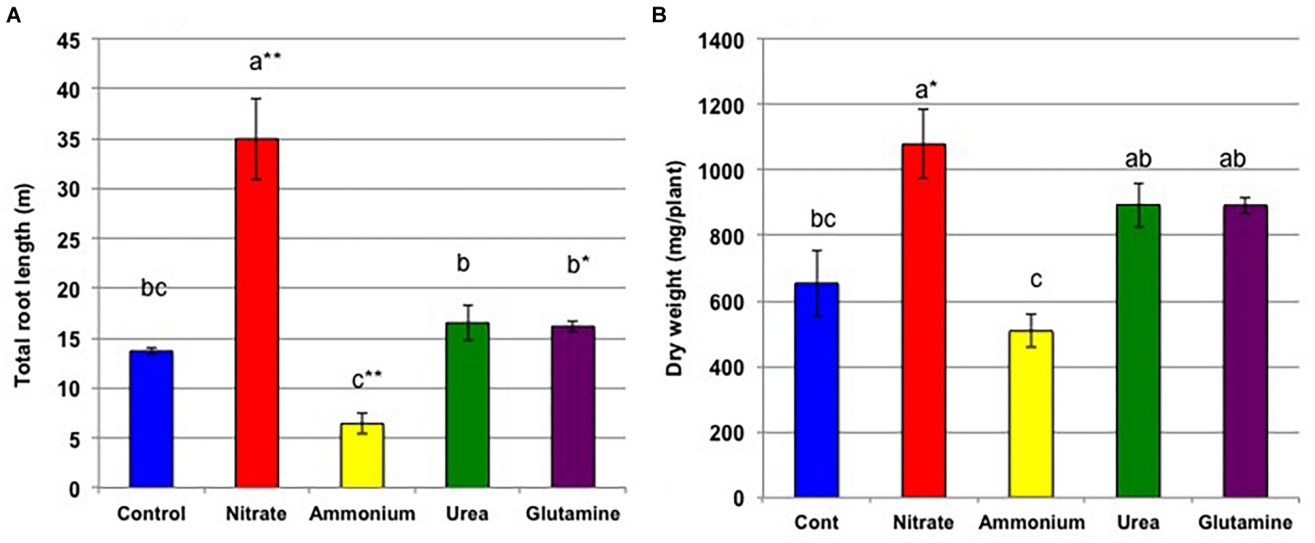

FIGURE 11 | Total root length **(A)** and the dry weight of roots **(B)** on 34 DAP after 2 weeks of the treatments with various forms of N compounds (Experiment 4). Averages and standard errors are shown (n = 3). Different letters above the column indicate significant differences among each treatment at <0.05 by Tukey's test.

urea, and Gln), and the continuation of cultivation with the N-free culture solution from 17 to 24 DAP (**Figure 3**), quick and reversible inhibitory effects on nodule growth were evident for ammonium, urea, and Gln supplementation. The inhibitory effects of ammonium were as high as that for nitrate during the period from 12 to 17 DAP, whereas the inhibitory effects for urea and Gln were less compared to that for ammonium and nitrate treatments. After a change of the culture solution to an N-free solution, recovery of nodule growth was observed from the next day in the case of urea, Gln, and ammonium in contrast to that for nitrate treatment where there was a 2 days time-lag. In this experiment a 1 mM-N supplementation was used, but the inhibitory effect of nitrate on nodule growth was similar to a previous experiment using 5 mM nitrate (Fujikake et al., 2002, 2003).

The effect of the nitrogen compounds on the nodule dry weight (**Figure 1A**) and the ARA per a single plant (**Figure 2A**) at 17 DAP after the N treatments resulted in significant repression in growth compared to that for the control. The specific ARAs were not inhibited compared with the control after 5 days of supplementation with the various forms of N (**Figure 2B**) indicate that decline in total ARA is mainly due to reduced nodule dry weight. After 7 days of N-free cultivation (17–24 DAP), the nodule dry weights of the plants for ammonium, urea, and Gln supplementation recovered to the same levels as that for the control nodules (**Figure 4A**), although that for the nitrate-treated plants tended to be low. The ARAs per single plant at 24 DAP after 7 days of N-free cultivation did recover (**Figure 5A**), although nitrate supplementation resulted in the lowest ARA. It was surprising that the Gln treatment gave the highest ARA at 24 DAP, about two times higher than that of the control plants. The specific ARA per nodule dry weight for Gln supplementation was also significantly higher for the other treatments including that for the control nodules (**Figure 5B**). The reason for the promotion of specific ARAs by Gln at the physiological level is unknown.

Absorption and Transport of Various Chemical Forms of N in Soybean Plants

The total N derived from the ^{15}N-labeled sources were 9.75 mg (nitrate), 8.71 mg (ammonium), 7.04 mg (urea), and 9.67 mg (Gln), respectively. The percentage distribution of ^{15}N in the shoots (leaves + stems) was high for nitrate (67%) and ammonium (65%) treatments compared with urea (57%) and Gln (49%) (**Supplementary Table S2**). These results indicated that all N compounds including urea and Gln were actively absorbed in soybean roots and transported to the shoots in 3 days, although translocation of the absorbed N to the shoots was relatively slower for urea and Gln compared to that for nitrate and ammonium. In addition, the percentage distribution of ^{15}N in the nodules for nitrate (1.5%), ammonium (2.9%), Gln (3.0%) and urea (1.9%) treatments was relatively low among the tissues and appeared not to be directly related to the inhibitory effect on nodule growth and the ARA.

In an independent study (Ohyama, 1983), the transport of fixed $^{15}N_2$ in the nodules and absorbed $^{15}NO_3^-$ in the roots were compared at the pod filling stage. About 36% of the fixed N was found to remain in the nodules, and the rest was distributed in the roots (9%), stems (17%), leaves (18%), pods (10%) and seeds (10%) after just 10 h of $^{15}N_2$ treatment. In contrast, 36% of the absorbed $^{15}NO_3^-$ remained in the roots, and the rest was contained in the nodules (0.4%), stems (17%), leaves (36%), pods (5%) and seeds (5%) after 10 h of supplementation by $^{15}NO_3^-$. These results suggested that the transport rates from source organs, either the nodules or the roots, were similar, but fixed-N was more rapidly transported to the pods and seeds; also the absorbed nitrate was highly distributed in the leaves.

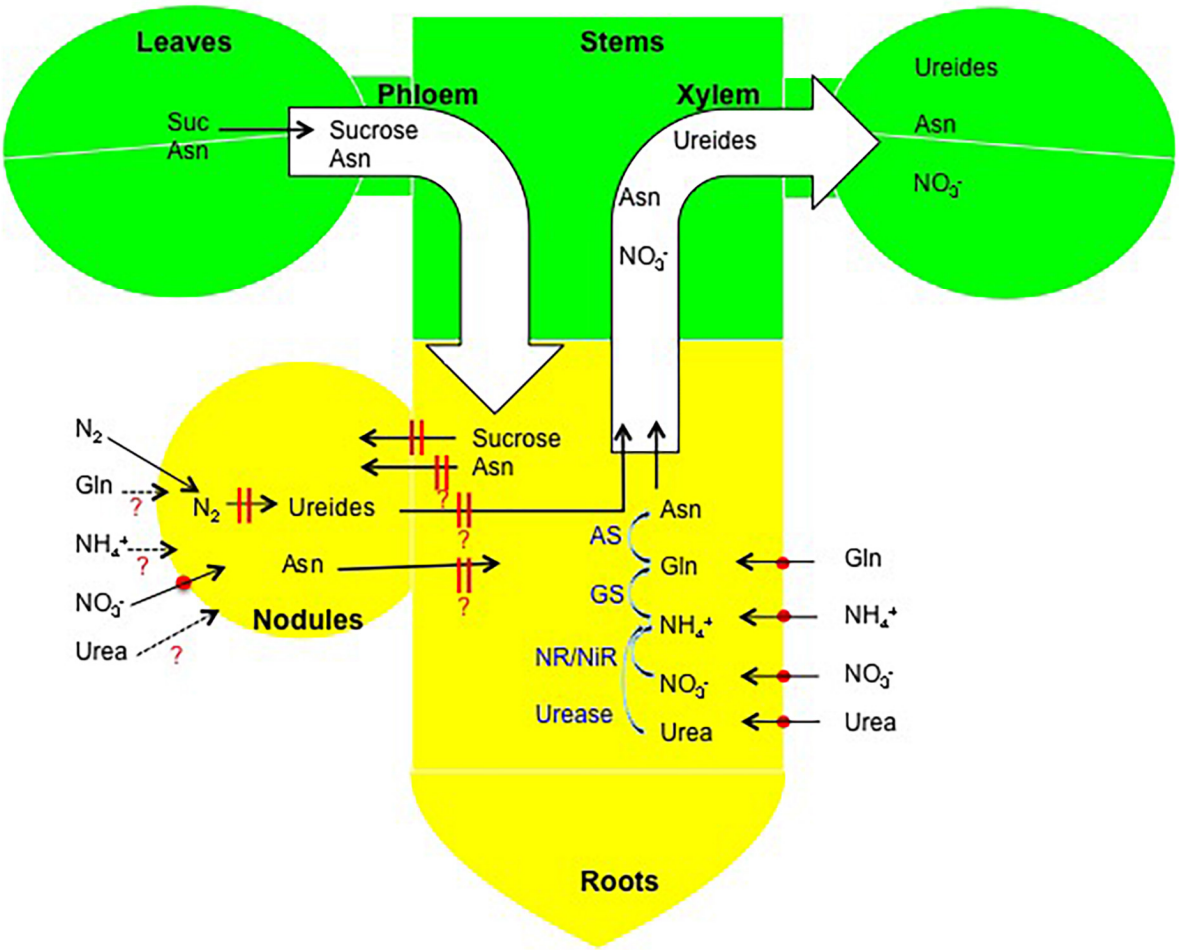

FIGURE 12 | Outline of the absorption, metabolism, and transport of various forms of N in soybean plants.

The nodulated soybean plants were treated with a culture solution containing $^{15}NO_3^-$, $^{15}NO_2^-$, or $^{15}NH_4^+$, and the absorption and transport of N were investigated (Ohyama et al., 1989b). After 24 h of ^{15}N-supply, the amount and distribution of ^{15}N among the roots, nodules, stems, and leaves were very similar between $^{15}NO_3^-$ and $^{15}NH_4^+$, although the absorption and transport to the shoot from $^{15}NO_2^-$ was much lower than that from $^{15}NO_3^-$ and $^{15}NH_4^+$ and most of the ^{15}N from the $^{15}NO_2^-$ remained in the roots.

In the present experiment (**Figure 7**), the absorption and distribution of ^{15}N among the tissues were relatively similar for $^{15}NO_3^-$ and $^{15}NH_4^+$. Absorption of urea tended to be lower than for the other compounds but urea and Gln were transported to the stems and leaves. The principal N compounds transported via the xylem from the nodules are ureides (allantoin and allantoic acid), which account for 80–90% of the total N in the xylem sap collected from nodulated soybean cultivated under N-free conditions. However, the xylem sap collected from non-nodulated soybean contains mainly amino acids and nitrate with a small portion of ureides (10–20%) (Ohyama et al., 2012). Asn is the principal amino acid in xylem sap collected from field grown soybean plants (Ohtake et al., 1995; Sato et al., 1998). Vitor et al. (2018) reported that Asp was the prominent amino acid component of phloem sap, followed by Glu, Asn, and Ser either in the nodulated or non-nodulated soybean cultured with nitrate or ammonium. The absorbed N supplied by $^{15}NO_3^-$ was very rapidly transported through the xylem (Ohyama et al., 1989a), and the absorption and transport of $^{13}NO_3^-$ were not affected by nodulation in the roots observed by a positron emitting tracer imaging system (Sato et al., 1999).

Nitrogen Metabolism

The total free amino acid concentration increased in all plant tissues for the various nitrogen treatments (**Figure 9**). The most prominent increases in tissue concentrations, irrespective of N-forms, were Asn and Asp. In Gln treatment, the free Asn concentration was higher than that of Gln, suggesting that the absorbed Gln in the roots was readily converted to Asn and transported in the forms of Asn and Asp. Most of the ammonium in the culture solution may have been assimilated in the roots by the GS/GOGAT (glutamine synthetase/glutamate synthase) pathway to Gln, then Asn was formed from Gln and Asp by the

enzyme AS. A part of nitrate absorbed in the roots is initially reduced by NR and NiR to ammonium and then assimilated into Gln via the GS/GOGAT pathway. The remaining nitrate may have been translocated to the leaves and reduced and assimilated there. Absorbed urea may have been hydrolyzed to ammonium and carbon dioxide by urease, with ammonium then being assimilated via the GS/GOGAT pathway. The absorbed Gln in the roots may have been assimilated into Asn by AS.

Absorption and Metabolism of Urea

Urea may be absorbed either directly from roots, or after urea degradation by soil microbes. It has been recognized that urea is a plant metabolite derived either from root uptake or from catabolism of Arg by arginase (Witte, 2011). In soybean plants, it is reported that urea may be produced during ureide degradation (Tod and Polacco, 2004). The present experiments use hydroponics without soil micro-organisms, therefore, urea might be directly absorbed by the roots, although plants have not been aseptically cultivated. Plants possess a high affinity secondary active urea transporters (DUR3) and passive transporters (MIPs). Urease is a unique nickel enzyme and it hydrolyzes urea to ammonia and carbamate, and the carbamate rapidly decays to ammonia and carbon dioxide non-enzymatically. Soybean has two ureases, a highly expressed embryo-specific urease encoded by the *Eu1* gene (Meyer-Bothling et al., 1987; Witte, 2011), and a ubiquitous urease found in all tissues encoded by *Eu4* (Torisky et al., 1994; Witte, 2011).

Absorption and Metabolism of Glutamine

Amino acids can be absorbed and utilized in *Arabidopsis*, and the supply of L-Gln and L-Asn promotes plant growth (Forsum et al., 2008). Hirner et al. (2006) reported that *Arabidopsis* LHT1 is a high-affinity broad specificity plasma membrane-bound transporter for cellular amino acid uptake in both roots and leaves. The H^+-independent Gln transport in the root tips of *Arabidopsis* has also been reported (Yang et al., 2010).

Involvement of Carbon Supplementation in the Inhibition of Nodule Growth and Nitrogen Fixation Activity by Nitrogen Compounds

The percentage distribution of ^{13}C in nodules was highest in control treatment (11.5%), which was higher than that of urea (5.8%), Gln (2.6%), ammonium (2.3%), and nitrate (2.3%) (**Supplementary Table S3**). The decrease in photosynthetic carbon supply seems to cause the repression of nodule growth (**Figure 3**) and a decrease in the ARA (**Figure 2**), irrespective of N forms. In previous experiments, where soybean shoots were exposed to ^{14}C-labeled CO_2 for 2h, the addition of 5 mM of nitrate to the culture solution stimulated the translocation of labeled-C to the roots from 5.2 to 9.1% of total photoassimilate and decreased the partitioning of C to the nodules from 9.1 to 4.3% just after $^{14}CO_2$ exposure (Fujikake et al., 2003). These findings indicated that a decreased supply of photoassimilate to nodules might be involved in the quick but reversible nitrate inhibition of nodule growth and its nitrogen fixation activity. In addition, the inhibitory effect of nitrate was alleviated by the addition of sucrose to the medium. These results indicated that the decrease in photoassimilate supply to nodules may be involved in the quick and reversible nitrate inhibition of soybean growth. The decrease in photoassimilate partitioning to the nodule may be caused by the increased photoassimilate consumption in the roots to absorb and assimilate N sources for providing energy and carbon skeletons of amino acids. In addition, N sources might affect root growth rate and the architecture (Kiba and Krapp, 2016).

In the continuous long-term N treatments for 2 weeks from 20 to 34 DAP, we observe the difference of root architecture by N sources, especially nitrate significantly promoted the lateral root growth, with moderate promotion by urea and Gln but repressed the root growth by ammonium (**Figures 10**, **11**). The promotion of lateral root growth by nitrate, urea, and Gln was in accordance with increase in leaf growth (**Supplementary Figures S3**, **S4**) and increase in chlorophyll contents (**Supplementary Figure S6**). The depressive effects by ammonium on root and leaf was not observed in Experiment 1 (**Figure 1**) and Experiment 2 (**Figure 4**). The repression by ammonium in Experiment 4 may be long-term ammonium supply gave ammonium toxicity on the roots, or the decrease in the pH in solution might affect the roots. In Experiment 1 and 2 the culture solution was changed every day, but in Experiment 4 the culture solution was changed every 2 days.

Very recently, transcriptome and metabolome analyses have revealed that nitrate supply promoted nitrogen and carbon metabolism in soybean roots, but tends to repress nitrogen and carbon metabolism in the nodules (Ishikawa et al., 2018). A microarray-based transcriptome analysis was carried out on soybean roots and nodules after 24 h of 5 mM nitrate treatment. Nitrate treatment enhanced substantially the gene expression of nitrate transport and the nitrogen assimilation pathways in the roots, but much less so in the case of nodules. Gene expression related to glycolysis and the TCA cycle in the roots were also increased but those in the nodules were repressed after 24 h of nitrate treatment. Metabolome analysis of roots and nodules were in accordance with transcriptome analysis, and both analyses support the hypothesis that nitrate supply promotes carbon use in the roots and as a result decreases carbon transport to the nodules.

Models of Absorption, Metabolism, and Transport of Various N Forms in a Nodulated Soybean Plant

Figure 12 gives an outline of the flow of fixed-N in the nodules and the N-compounds supplied to the culture solution. Ammonium (NH_4^+), nitrate (NO_3^-), urea, and Gln are absorbed by ammonium transporter, nitrate transporter, urea transporter, and amino acid transporter in the cell membrane of the epidermal or cortical cells of the roots. A high accumulation of NH_4^+ is known to be toxic to plants, so most of NH_4^+ absorbed in the roots should be assimilated rapidly to Gln by GS. The Gln is converted to Asn and Asp in the roots, then transported to the shoots via the xylem. The absorbed Gln from solution can be assimilated in the same way as NH_4^+. A portion of NO_3^-

absorbed in the roots is reduced by NR to NO_2^- and the NO_2^- is reduced to NH_4^+ by NiR in the roots, then assimilated the same as for NH_4^+. The other part of NO_3^- is transported to the shoot via the xylem and reduced and assimilated in the leaves. The absorbed urea in the roots may be hydrolyzed to NH_4^+ in the roots, but some urea may be transported to the shoots and metabolized in the stems and leaves. It was shown that NO_3^- is absorbed from the nodule surface (Mizukoshi et al., 1995), possibly by the NO_3^- transporter, because nitrate transporter genes were promoted after 24 h of NO_3^- treatment (Ishikawa et al., 2018). It is not known whether NH_4^+, urea, and Gln are absorbed from nodule surface.

The decrease in nitrogen fixation activity may be caused by reduced photoassimilate supply, the same as for nodule growth inhibition. However, another possibility, Asn accumulation in nodules by nitrate in this study (**Figure 9A**) and the results by metabolome (Ishikawa et al., 2018) may be related to the a decrease in nitrogen fixation activity possibly through decreased oxygen permeability of the nodule cortex (Serraj et al., 1999) or other reasons. Further research is required to obtain a comprehensive understanding of the complex mechanisms and regulation by nitrogen and carbon for nodule growth and nitrogen fixation.

Concerning to the lateral root growth, Lavenus et al. (2013) reviewed that phytohormone auxin act as a common integrator to many endogenous and environmental signals regulating lateral root formation in model plant *Arabidopsis thaliana*. The changes in root and shoot growth by various N sources may be regulated by phytohormones such as auxin, cytokinin, ethylene, abscisic acid, gibellerines, brassinolide, etc., but the evidence had been not obtained for the relationship between N compounds and hormones in soybean related to lateral root growth and nodule growth as well.

CONCLUSION

A rapid and reversible repression of nodule growth and nitrogen fixation activity was observed by ammonium, urea, or Gln supply to the culture solution similar to that for nitrate, although the effect was milder for urea and Gln supply compared for nitrate and ammonium treatments. Nitrogen from ammonium, urea, and Gln was actively absorbed by the soybean roots and more than half of the absorbed N was transported to the shoot during the 3 days of application period. The application of the different chemical forms of N increased the free amino acids contents in each tissue, and Asn and Asp were the dominant amino acids. The distribution of labeled-C and not labeled N in the nodules correlated with the repression of nodule growth, nitrogen fixation activity, and nodule growth. It was found that the Gln treatment followed by N-free cultivation gave the highest nitrogen fixation activity, about two times higher than that of the control plants. The long-term supply of various N forms for 2 weeks, nitrate significantly increased plant growth, especially lateral root growth and leaf growth. The long-term supply of urea and Gln also promoted the lateral roots and leaf growth, but ammonium suppressed plant growth including root growth and leaf growth.

AUTHOR CONTRIBUTIONS

TO conceived the research, designed the experiments, analyzed the data, and wrote the manuscript. NY and ST carried out all the experiments and analysis. NO, KS, TS, KH, and AS gave valuable suggestions during the experiments and writing of the manuscript.

FUNDING

This research was supported by Grant-in-Aid for Scientific Research (B) No. 18380049 from Japan Society for the Promotion of Science.

SUPPLEMENTARY MATERIAL

The Supplementary Material for this article can be found online at: https://www.frontiersin.org/articles/10.3389/fpls.2019.00131/full#supplementary-material

FIGURE S1 | $^{13}CO_2$ injection into a plastic bag covering the plant shoot (Experiment 3) **(A)**. CO_2 concentration was monitored by infrared CO_2 analyzer **(B)**.

FIGURE S2 | Nodule number per single plant at 17 DAP supplied with various nitrogen compounds from 12 to 17 DAP (Experiment 1). Averages and standard errors are shown (n = 4). Different letters above the column indicate significant differences at <0.05 by Tukey's test.

FIGURE S3 | Photos of root systems with various N treatments for 1 week (Experiment 4). White square is 3 cm × 3 cm.

FIGURE S4 | Dry weight of nodules **(A)** after 2 weeks of N treatments, and the increase in the volume of three selected nodules in the first and the second week **(B)** (Experiment 4). Averages and standard errors are shown (n = 3). Different letters above the column indicate significant differences at <0.05 by Tukey's test.

FIGURE S5 | Dry weight of each organs after 2 weeks of various N treatments (Experiment 4).

FIGURE S6 | Photos of shoot organs with various N treatments for 2 week. White square is 3 cm × 3 cm (Experiment 4).

FIGURE S7 | Total leaf area per a plant after 2 weeks of various N treatments (Experiment 4). Averages and standard errors are shown (n = 3). Different letters above the column indicate significant differences at <0.05 by Tukey's test. *Indicate significantly differences between control at <0.05 by Student's T-test.

FIGURE S8 | SPAD value of the second, third, and fourth trifoliolate leaves after 2 weeks of various N treatments (Experiment 4). Averages and standard errors are shown (n = 3). Different letters above the column indicate significant differences at <0.05 by Tukey's test.

TABLE S1 | Dry weight of each tissue of soybean plants (Experiment 3).

TABLE S2 | Percentage distribution of ^{15}N labeled source among each tissue of soybean plants (Experiment 3).

TABLE S3 | Percentage distribution of ^{13}C among each tissue of soybean plants (Experiment 3).

TABLE S4 | Nitrogen concentration of free amino acids in each tissue of soybean plants treated with N compounds for 3 days (Experiment 3).

TABLE S5 | Relative concentration of free amino acids in each tissue of soybean plants treated with N compounds relative to control plants (Experiment 3).

REFERENCES

Davidson, I. A., and Robson, M. J. (1986). Effect of contrasting patterns of nitrate application on the nitrate uptake, N2-fixation, nodulation and growth of white clover. *Ann. Bot.* 57, 331–338. doi: 10.1093/oxfordjournals.aob.a087114

Forsum, O., Svennerstam, H., Ganeteg, U., and Nasholm, T. (2008). Capacities and constraints of amino acid utilization in *Arabidopsis*. *New Phytol.* 179, 1058–1069. doi: 10.1111/j.1469-8137.2008.02546.x

Fujikake, H., Yamazaki, A., Ohtake, N., Sueyoshi, K., Matsuhashi, S., Ito, T., et al. (2003). Quick and reversible inhibition of soybean root nodule growth by nitrate involves a decrease in sucrose supply to nodules. *J. Exp. Bot.* 54, 1379–1388. doi: 10.1093/jxb/erg147

Fujikake, H., Yashima, H., Sato, T., Ohtake, N., Sueyoshi, K., and Ohyama, T. (2002). Rapid and reversible nitrate inhibition of nodule growth and N2 fixation activity in soybean (*Glycine max* (L.) *Merr.*). *Soil Sci. Plant Nutr.* 48, 211–217. doi: 10.1080/00380768.2002.10409193

Gibson, A. H., and Harper, J. E. (1985). Nitrate effect on nodulation of soybean by *Bradyrhizobium japonicum*. *Crop Sci.* 25, 497–501. doi: 10.2135/cropsci1985.0011183X002500030015x

Gogorcena, Y., Gordon, A. J., Escuredo, P. R., Minchin, F. R., Witty, J. F., Moran, J. F., et al. (1997). N2 fixation, carbon metabolism, and oxidative damage in nodules of dark-stressed common bean plants. *Plant Physiol.* 113, 1193–1201. doi: 10.1104/pp.113.4.1193

Gordon, A. J., Skøt, L., James, C. L., and Minchin, F. R. (2002). Short-term metabolic response of soybean root nodules to nitrate. *J. Exp. Bot.* 53, 423–428. doi: 10.1093/jexbot/53.368.423

Harper, J. E. (1987). "Nitrogen metabolism," in *Soybeans: Improvement, Production, and Uses*, 2nd Edn, ed. J. R. Wilcox (Madison, WI: ASA), 497–533.

Harper, J. E., and Gibson, A. H. (1984). Differential nodulation tolerance to nitrate among legume species. *Crop Sci.* 24, 797–801. doi: 10.2135/cropsci1984.0011183X002400040040x

Hirner, A., Ladwig, F., Stransky, H., Okumoto, S., Keinath, M., Harms, A., et al. (2006). Arabidopsis LHT1 is a high-affinity transporter for cellular amino acid uptake in both root epidermis and leaf mesophyll. *Plant Cell* 18, 1931–1946. doi: 10.1105/tpc.106.041012

Huber, T. A., and Streeter, J. G. (1984). Asparagine biosynthesis in soybean nodules. *Plant Physiol.* 74, 605–610. doi: 10.1104/pp.74.3.605

Imsande, J. (1986). Inhibition of nodule development in soybean by nitrate or reduced nitrogen. *J. Exp. Bot.* 37, 348–355. doi: 10.1093/jxb/37.3.348

Ishikawa, S., Ono, Y., Ohtake, N., Sueyoshi, K., Tanabata, S., and Ohyama, T. (2018). Transcriptome and metabolome analysis reveal that nitrate strongly promotes nitrogen and carbon metabolism in soybean roots, but tends to repress it in nodules. *Plants* 7:32. doi: 10.3390/plants7020032

Kiba, T., and Krapp, A. (2016). Plant nitrogen acquisition under low availability: regulation of uptake and root architecture. *Plant Cell Physiol.* 57, 707–714. doi: 10.1093/pcp/pcw052

Lavenus, J., Goh, T., Roberts, I., Guyomarc'h, S., Lucas, M., De Smet, I., et al. (2013). Lateral root development in *Arabidopsis*: fifty shades of auxin. *Trends Plant Sci.* 18, 450–458. doi: 10.1016/j.tplants.2013.04.006

Meyer-Bothling, L. E., Polacco, J. C., and Cianzio, S. R. (1987). Pleiotropic soybean mutants defective in both urease isozymes. *Mol. Gen. Genet.* 209, 432–438. doi: 10.1007/BF00331146

Minamisawa, K., Arima, Y., and Kumazawa, K. (1986). Characteristics of asparagine pool in soybean nodules in comparison with ureide pool. *Soil Sci. Plant Nutr.* 32, 1–14. doi: 10.1080/00380768.1986.10557476

Mizukoshi, K., Nishiwaki, T., Ohtake, N., Minagawa, R., Ikarashi, T., and Ohyama, T. (1995). Nitrate transport pathway into soybean nodules traced by tungstate and 15NO3-. *Soil Sci. Plant Nutr.* 41, 75–88. doi: 10.1080/00380768.1995.10419560

Nagumo, Y., Tanaka, K., Tewari, K., Thiraporn, K., Tsuchida, T., Honma, T., et al. (2009). Rapid quantification of Cyanamide by ultra-high-pressure liquid chromatography in fertilizer, soil or plant samples. *J. Chromatogr. A* 1216, 5614–5618. doi: 10.1016/j.chroma.2009.05.067

Ohtake, N., Nishiwaki, T., Mizukoshi, K., Minagawa, R., Takahashi, T., Chinushi, T., et al. (1995). Amino acid composition in xylem sap of soybean related to the evaluation of N2 fixation by the relative ureide method. *Soil Sci. Plant Nutr.* 41, 95–102. doi: 10.1080/00380768.1995.10419562

Ohyama, T. (1983). Comparative studies on the distribution of nitrogen in soybean plants supplied with N2 and NO3- at the pod filling stage. *Soil Sci. Plant Nutr.* 29, 133–145. doi: 10.1080/00380768.1983.10432415

Ohyama, T., Fujikake, H., Yashima, H., Tanabata, S., Ishikawa, S., Sato, T., et al. (2012). *Effect of Nitrate on Nodulation and Nitrogen Fixation of Soybean*. Available at: http://cdn.intechweb.org/pdfs/22777.pdf

Ohyama, T., and Kumazawa, K. (1978). Incorporation of 15N into various nitrogenous compounds in intact soybean nodules after exposure to 15N2 gas. *Soil Sci. Plant Nutr.* 24, 525–533. doi: 10.1080/00380768.1978.10433132

Ohyama, T., and Kumazawa, K. (1980a). Nitrogen assimilation in soybean nodules I. The role of GS/GOGAT system in the assimilation of ammonia produced by N2 fixation. *Soil Sci. Plant Nutr.* 26, 109–115. doi: 10.1080/00380768.1980.10433217

Ohyama, T., and Kumazawa, K. (1980b). Nitrogen assimilation in soybean nodules II. 15N2 assimilation in bacteroid and cytosol fractions of soybean nodules. *Soil Sci. Plant Nutr.* 26, 205–213. doi: 10.1080/00380768.1980.10431204

Ohyama, T., Ohtake, N., Sueyoshi, K., Ono, Y., Tsutsumi, K., Ueno, M., et al. (2017). *Amino acid Metabolism and Transport in Soybean Plants*. Available at: https://www.intechopen.com/books/amino-acid-new-insights-and-roles-in-plant-and-animal/amino-acid-metabolism-and-transport-in-soybean-plants

Ohyama, T., Kato, N., and Saito, K. (1989a). Nitrogen transport in xylem of soybean plants supplied with 15NO3-. *Soil Sci. Plant Nutr.* 35, 131–137. doi: 10.1080/00380768.1989.10434744

Ohyama, T., Saito, K., and Kato, N. (1989b). Assimilation and transport of nitrate, nitrite, and ammonia absorbed by nodulated soybean plants. *Soil Sci. Plant Nutr.* 35, 9–20. doi: 10.1080/00380768.1989.10434732

Saito, A., Tanabata, S., Tanabata, T., Tajima, S., Ueno, M., Ishikawa, S., et al. (2014). Effect of nitrate on nodule and root growth of soybean (*Glycine max* (L.) *Merr.*). *Int. J. Mol. Sci.* 15, 4464–4480. doi: 10.3390/ijms15034464

Sato, T., Ohtake, N., Ohyama, T., Ishioka, N. S., Watanabe, S., Osa, A., et al. (1999). Analysis of nitrate absorption and transport in non-nodulated and nodulated soybean plants with 13NO3- and 15NO3-. *Radioisotopes* 48, 450–458. doi: 10.3769/radioisotopes.48.450

Sato, T., Yashima, H., Ohtake, N., Sueyoshi, K., Akao, S., Harper, J. E., et al. (1998). Determination of leghemoglobin components and xylem sap composition by capillary electrophoresis in hypernodulation soybean mutants cultivated in the field. *Soil Sci. Plant Nutr.* 44, 635–645. doi: 10.1080/00380768.1998.10414487

Schuller, K. A., Minchin, F. R., and Gresshoff, P. M. (1988). Nitrogenase activity and oxygen diffusion in nodules of soybean cv. Bragg and a supernodulating mutant: effects of nitrate. *J. Exp. Bot.* 39, 865–877. doi: 10.1093/jxb/39.7.865

Serraj, R., Vadez, V., Denison, R. F., and Sinclair, T. R. (1999). Involvment of ureides in nitrogen fixation inhibition in soybean. *Plant Physiol.* 119, 289–296. doi: 10.1104/pp.119.1.289

Streeter, J. G. (1988). Inhibition of legume nodule formation and N2 fixation by nitrate. *CRC Crit. Rev. Plant Sci.* 7, 1–23. doi: 10.1080/07352688809382257

Tanabata, S., Tanabata, T., Saito, A., Tajima, S., Watanabe, S., Ishikawa, K., et al. (2014). Computational image analysis method for measuring size of nodule growth in soybean. *JPN. J. Soil Sci. Plant Nutr.* 85, 43–47.

Tod, C. D., and Polacco, J. C. (2004). Soybean cultivars 'Williams 82' and 'Maple Arrow' produce both urea and ammonia during ureide degradation. *J. Exp. Bot.* 55, 867–877. doi: 10.1093/jxb/erh100

Torisky, R. S., Griffin, J. D., Yenofsky, R. L., and Polacco, J. C. (1994). A single gene (*Eu4*) encodes the tissue-ubiquitous urease of soybean. *Mol. Gen. Ganet.* 242, 404–414. doi: 10.1007/BF00281790

Vadez, V., Sinclair, T. R., and Serraj, R. (2000). Asparagine and ureide accumulation in nodules and shoots as feedback inhibitors of N2 fixation in soybean. *Physiol. Plant* 110, 215–223. doi: 10.1034/j.1399-3054.2000.110211.x

Vessey, J. K., Walsh, K. B., and Layzell, D. B. (1988). Can a limitation in phloem supply to nodules account for the inhibitory effect of nitrate on nitrogenase activity in soybean? *Physiol. Plant.* 74, 137–146. doi: 10.1111/j.1399-3054.1988.tb04954.x

Vitor, S. C., do Amarante, L., and Sodek, L. (2018). Are phloem-derived amino acids the origin of the elevated malate concentration in the xylem sap following mineral N starvation in soybean? *Planta* doi: 10.1007/s00425-018-2914-x [Epub ahead of print].

Witte, C. P. (2011). Urea metabolism in plants. *Plant Sci.* 180, 431–438. doi: 10.1016/j.plantsci.2010.11.010

Yang, H., Bogner, M., Stierhof, Y.-D., and Ludewig, U. (2010). H+-Independent glutamine transport in plant root tips. *PLoS One* 5:e8917. doi: 10.1371/journal.pone.0008917

Yashima, H., Fujikake, H., Sato, T., Ohtake, N., Sueyoshi, K., and Ohyama, T. (2003). Systemic and local effects of long-term application of nitrate on nodule growth and N2 fixation in soybean (*Glycine max* [L.] *Merr.*). *Soil Sci. Plant Nutr.* 49, 825–834. doi: 10.1080/00380768.2003.10410344

Yashima, H., Fujikake, H., Yamazaki, A., Ito, S., Sato, T., Tewari, K., et al. (2005). Long-term effect of nitrate application from lower part of roots on nodulation and N2 fixation in upper part of roots of soybean (*Glycine max* (L.) *Merr.*) *in two-layered pot experiment*. *Soil Sci. Plant Nutr.* 51, 981–990. doi: 10.1111/j.1747-0765.2005.tb00137.x

Conflict of Interest Statement: The authors declare that the research was conducted in the absence of any commercial or financial relationships that could be construed as a potential conflict of interest.

The handling editor and reviewer BF declared their involvement as co-editors in the Research Topic, and confirm the absence of any other collaboration.

frontiers in Plant Science

ORIGINAL RESEARCH
published: 28 February 2019
doi: 10.3389/fpls.2019.00221

The PvNF-YA1 and PvNF-YB7 Subunits of the Heterotrimeric NF-Y Transcription Factor Influence Strain Preference in the *Phaseolus vulgaris–Rhizobium etli* Symbiosis

*Carolina Rípodas, Melisse Castaingts, Joaquín Clúa, Julieta Villafañe, Flavio Antonio Blanco† and María Eugenia Zanetti**

Instituto de Biotecnología y Biología Molecular, Facultad de Ciencias Exactas, Universidad Nacional de La Plata, La Plata – Centro Científico y Tecnológico La Plata, Consejo Nacional de Investigaciones Científicas y Técnicas, La Plata, Argentina

OPEN ACCESS

Edited by:
Kiwamu Minamisawa, Tohoku University, Japan

Reviewed by:
Oswaldo Valdes-Lopez, National Autonomous University of Mexico, Mexico
Federico Damian Ariel, Instituto de Agrobiotecnología del Litoral (IAL), Argentina

***Correspondence:**
María Eugenia Zanetti
ezanetti@biol.unlp.edu.ar
orcid.org/0000/0001-9565-1743

†*orcid.org/0000-0002-8380-8472*

Specialty section:
This article was submitted to Plant Microbe Interactions, a section of the journal Frontiers in Plant Science

Received: *04 September 2018*
Accepted: *08 February 2019*
Published: *28 February 2019*

Citation:
Rípodas C, Castaingts M, Clúa J, Villafañe J, Blanco FA and Zanetti ME (2019) The PvNF-YA1 and PvNF-YB7 Subunits of the Heterotrimeric NF-Y Transcription Factor Influence Strain Preference in the Phaseolus vulgaris–Rhizobium etli Symbiosis. Front. Plant Sci. 10:221. doi: 10.3389/fpls.2019.00221

Transcription factors of the Nuclear Factor Y (NF-Y) family play essential functions in plant development and plasticity, including the formation of lateral root organs such as lateral root and symbiotic nodules. NF-Ys mediate transcriptional responses by acting as heterotrimers composed of three subunits, NF-YA, NF-YB, and NF-YC, which in plants are encoded by relatively large gene families. We have previously shown that, in the *Phaseolus vulgaris* × *Rhizobium etli* interaction, the PvNF-YC1 subunit is involved not only in the formation of symbiotic nodules, but also in the preference exhibited by the plant for rhizobial strains that are more efficient and competitive in nodule formation. PvNF-YC1 forms a heterotrimer with the PvNF-YA1 and PvNF-YB7 subunits. Here, we used promoter:reporter fusions to show that both *PvNF-YA1* and *PvNF-YB7* are expressed in symbiotic nodules. In addition, we report that knock-down of *PvNF-YA1* and its close paralog *PvNF-YA9* abolished nodule formation by either high or low efficient strains and arrested rhizobial infection. On the other hand, knock-down of *PvNF-YB7* only affected the symbiotic outcome of the high efficient interaction, suggesting that other symbiotic NF-YB subunits might be involved in the more general mechanisms of nodule formation. More important, we present functional evidence supporting that both PvNF-YA1 and PvNF-YB7 are part of the mechanisms that allow *P. vulgaris* plants to discriminate and select those bacterial strains that perform better in nodule formation, most likely by acting in the same heterotrimeric complex that PvNF-YC1.

Keywords: nodulation, nitrogen fixation, Nuclear Factor Y, rhizobia, transcription factors

INTRODUCTION

Nitrogen (N) is an essential macronutrient for plant growth and development since it is part of many biological molecules such as nucleic acids, proteins, vitamins, and chlorophyll (Wang et al., 2012); however, its availability is frequently limited in soils of both natural and agronomical ecosystems. Most legume species overcome N limitation by establishing a symbiosis with N-fixing bacteria from different genera known as rhizobia. This interaction results in the formation of a new postembryonic root organ, the nodule, where bacteria allocate and convert atmospheric N to reduced forms that will be incorporated into the plant metabolism.

The root nodule symbiosis (RNS) can be divided into three stages. In the pre-symbiotic stage, the two organisms recognize each other through an exchange of diffusible molecules. Under N limiting conditions, roots of legumes exudate flavonoids/isoflavonoids that are perceived by rhizobia (Weston and Mathesius, 2013), which activate the synthesis and secretion of key molecules called Nod factors (NFs; Denarie et al., 1996). NFs are perceived by the host plant inducing the first morphological response, the curling of the root hair around the bacterial microcolony, which results in the formation of an infection pocket (Lerouge et al., 1990). The second stage is the infection, which consists in the penetration of bacteria into host tissues through a tubular structure referred to as the infection thread (IT). Concomitantly with this infection process, cell divisions are initiated in the root cortex of the host to form the nodular primordium. The third and last stage consists in the development of the nodule and the release of bacteria from the ITs into the host cells to form organelle-like structures called symbiosomes (Popp and Ott, 2011), where biological N fixation will take place.

Morphological and developmental responses observed during RNS are initiated by the binding of NFs to LysM domain-containing receptors located at the plant plasma membrane, which results in the hierarchical activation of a set of transcriptions factors (TFs). Specific members of the Nuclear Factor Y (NF-Y) gene family of TFs have been implicated at different stages of the RNS, from epidermal infection to nodule development. NF-Ys are evolutionary conserved heterotrimeric TFs composed of three subunits (NF-YA, NF-YB, and NF-YC). Genes encoding NF-Y subunits have diversified in the plant lineage forming relatively large gene families with specific functions (Petroni et al., 2012; Laloum et al., 2013). *In Medicago truncatula*, two NF-YA subunits, *MtNF-YA1* and *MtNF-YA2*, play important roles not only at early stages of rhizobial infection, but also at later stages of the RNS mediating both nodule organogenesis and the persistence of nodule meristems (Combier et al., 2006, 2008; Laloum et al., 2014; Laporte et al., 2014). On the other hand, *M. truncatula MtNF-YC1* and *MtNF-YC2* genes are required for nodule organogenesis, but not for intracellular infection by rhizobia (Baudin et al., 2015). Two NF-Y subunits of *Lotus japonicus*, *LjNF-YA1* and *LjNF-YB1*, were identified as direct transcriptional targets of the master symbiotic regulator Nodule Inception (NIN). Knock-down of *LjNF-YA1* by RNA interference (RNAi) arrested cell divisions associated with nodule formation, but did not affect epidermal infection. On the other hand, overexpression of *LjNF-YA1* stimulates cell proliferation, a phenotype that was enhanced by co-expression of *LjNF-YB1* (Soyano et al., 2013). In common bean (*Phaseolus vulgaris*), *PvNF-YC1* was identified as a key TF required for both nodule organogenesis and infection by *Rhizobium etli*, the predominant species present in common bean nodules (Zanetti et al., 2010).

Phaseolus vulgaris originated in Mesoamerica and further expanded to South America, resulting into two gene pools at distinct centers of genetic diversification (CGDs): the Mesoamerican and the Southern Andes CGDs (Bitocchi et al., 2012). These gene pools have undergone parallel and independent domestication at each CGD, thus the characteristics of each gene pool are evident in both wild and domesticated accessions (Bitocchi et al., 2013). The abundance of *R. etli* strains in each CGD has been correlated with a polymorphism of the *nodC* gene of *R. etli*, which encodes an *N*-acetylglucosamine transferase involved in the first steps of NF synthesis. Strains bearing the *nodC*-α allele (hereafter *nodC*-α strains) are predominant in Mesoamerican soils, whereas those carrying the *nodC*-δ allele are highly represented in the Andean region (Aguilar et al., 2004). Wild and domesticated beans from each CGD are more efficiently nodulated by those strains that are more abundant in the soils of the cognate geographical region (Peltzer Meschini et al., 2008). More interesting, nodules of Mesoamerican beans co-inoculated with an equicellular mixture of both rhizobial strains were predominantly occupied by *nodC*-α strains (Aguilar et al., 2004), leading to the suggestion that Mesoamerican beans have developed molecular mechanisms that allow them to discriminate and select those strains that have coevolved in the same CGD. A key component of this mechanism is the above-mentioned *PvNF-YC1* subunit of the NF-Y family of TFs (Zanetti et al., 2010). Overexpression of *PvNF-YC1* in Mesoamerican beans was sufficient not only to improve the symbiotic outcome (i.e., nodule number and shoot dry weight) of the less efficient strains carrying the *nodC*-δ allele, but also to alter nodule occupancy by *nodC*-α and *nodC*-δ strains, exposing that competitions in the rhizosphere can be controlled by the plant (Zanetti et al., 2010). Since NF-Ys act as heterotrimers to promote transcriptional activation/repression, we sought to identify and characterize the NF-YA and NF-YB subunits that form the symbiotic functional heterocomplex. Given the symbiotic specific expression pattern exhibited by *PvNF-YA1*, *PvNF-YA9*, and *PvNF-YB7* genes (Ripodas et al., 2015) and the physical interaction of PvNF-YC1 with PvNF-YA1 and PvNF-YB7 subunits (Baudin et al., 2015), we selected these members to conduct a functional characterization of their role in the RNS and in the strain preference observed in Mesoamerican beans. Here, we describe that simultaneous silencing of *PvNF-YA1* and its closest homolog, *PvNF-YA9*, impaired nodule organogenesis triggered by either *nodC*-α or *nodC*-δ strains and reduced bacterial infection. Interestingly, overexpression of PvNF-YA1, but not PvNF-YA9, was sufficient to alter nodule occupancy in roots co-inoculated with *nodC*-α and *nodC*-δ strains. On the other hand, knock-down of *PvFN-YB7* affected the number of nodules developed by a *nodC*-α, but not a *nodC*-δ strain, and altered nodule occupancy. All together, the results presented here highlight the functional implication of the heterotrimer formed by PvNF-YA1, PvNF-YB7 and PvNF-YC1 not only in the establishment of the RNS, but also in the mechanisms that determine strain specificity within the *P. vulgaris* × *R. etli* interaction.

MATERIALS AND METHODS

Biological Material and Generation of Composite Plants by *Agrobacterium rhizogenes* Transformation

Plant growth and transformation were performed essentially as previously described (Blanco et al., 2009; Zanetti et al., 2010).

Briefly, *P. vulgaris* seeds were surface sterilized and germinated on 10% (w/v) agar-H_2O for 2 days. Seedling were transferred to pots containing vermiculite and watered with Fahraeus media supplemented with 8 Mm KNO_3. Five days after transplantation, *P. vulgaris* plants were inoculated in the stem with a saturated suspension of *Agrobacterium rhizogenes* strain K599 using a syringe. Approximately 10 days after transformation, when hairy roots have emerged from the inoculation sites, the main root system was removed by cutting the stem 1 cm below the site of inoculation. Composite plants consisting on a wild type aerial part and transgenic hairy roots were transferred to acrylic boxes containing agar-Fahraeus covered with paper. Alternatively, for co-inoculation experiments, composite plants were transferred to pots containing vermiculite and watered with Fahraeus media. *R. etli* strains SC15 (*nodC*-α) and 55N1 (*nodC*-δ) were previously reported (Aguilar et al., 2004). The *R. etli* strain CFNx5 (*nodC*-α) expressing the DsRed protein was previously generated and described (Battaglia et al., 2014).

Vector Construction

To generate localization and/or overexpression constructs, the open reading frame of PvNF-YA1 was amplified by PCR using primers PvNF-YA1 OE F, PvNF-YA1 OE R (**Supplementary Table S1**), and cloned into the pENTR/D-TOPO vector (Invitrogen), creating pENTR-NF-YA1. For overexpression, the pENTR-NF-YA1 was recombined into the destination vector p35S:HF-GATA (Mustroph et al., 2009). Later on, the FLAG-PvNF-YA1 fragment was amplified by PCR using specific primers and cloned into the pENTR/D-TOPO to create pENTR-FLAG-NF-YA1, which was subsequently recombined into the final destination vector pK7WG2D, which carries EgfpER as a screenable marker for early visualization and selection of the transgenic roots (Karimi et al., 2002). For subcellular localization, a translational fusion of PvNF-YA1 to the C-terminal end of GFP was generated by recombination of the pENTR-NF-YA1 with pMDC43 (Curtis and Grossniklaus, 2003). For the overexpression of PvNF-YA9, the ORF of this transcript was synthetized by Life Technologies to be used as level-0 module in GoldenGate cloning[1]. Assembled level-1 modules expressing the fusion FLAG-PvNF-YA9 under the control of the constitutive promoter CaMV35S and a pAtUbi:GFP fusion as a transgenic root selection marker were finally cloned in a level-2 binary vector backbone EC50505[1]. For histochemical assays to measure glucuronidase activity, a 1.5 kb fragment of the promoter sequences of *PvNF-YA1* and *PvNF-YB7* was amplified with specific primers from common bean genomic DNA, cloned in the pENTR/D-TOPO vector, and finally introduced by recombination into the destination vector pKGWFS7, driving the expression of the fusion GFP-GUS. For silencing of *PvNF-YA1/A9* by RNAi, a 217 bp fragment corresponding to the 3′ UTR of *PvNF-YA1* was amplified by PCR, using PvNF-YA1/A9 RNAi F and PvNF-YA1/A9 RNAi R primers (**Supplementary Table S1**) and *P. vulgaris* cDNA as a template. Similarly, a fragment corresponding to the 3′ UTR was amplified using gene specific primers for knock-down of *PvNF-YB7* (**Supplementary Table S1**). Each PCR product was cloned into the entry vector pENTR/D-TOPO and recombined into the destination vector pK7GWIWG2D (II) (Karimi et al., 2002) to finally produce *PvNF-YA1/A9* RNAi and *PvNF-YB7* RNAi constructs, respectively. All binary vectors were introduced into *Agrobacterium tumefaciens* GV3101 and/or *A. rhizogenes* K599 by electroporation and then used for agroinfiltration of *Nicotiana benthamiana* leaves or for the generation of transgenic hairy roots in *P. vulgaris*.

β-Glucuronidase Activity

Activity of the enzyme β-glucuronidase was determined in *P. vulgaris* roots and nodules formed at 7 and 14 dpi with strain CFNX5, a *R. etli nodC*-α strain that expresses the fluorescent protein Ds-Red. Roots were cut into 2 cm sections and then infiltrated with a solution of the dye reactive: 100 mM TRIS-HCl pH 7, 2 mM X-Gluc (5-bromo-4-cloro-3-indolil-β-D-glucoronic acid, 0.01% v/v Triton X-100, 50 mM NaCl, 2.0 mM potassium ferrocyanide). Tissue was incubated at 37°C for 1–10 h until color development. After incubation, roots were observed by bright field microscopy to visualize GUS staining in whole roots or, in some cases, selected roots and nodules were embedded in 4% (w/v) agarose and cut to thin sections (55 μm) using a Leica VT1000 S Vibrating blade microtome. Tissue sections were analyzed by bright field microscopy in an inverted microscope (OLYMPUS IX51).

Phenotypic Analysis

Composite plants were generated and inoculated as described (Peltzer Meschini et al., 2008; Blanco et al., 2009). Primary and lateral root length and density were measured as previously reported (Battaglia et al., 2014). Nodule quantification and dry weight determination were performed as previously described (Zanetti et al., 2010). Non-transgenic (not fluorescent roots) were excised from the root system before phenotypic analysis before inoculation with rhizobia, thus only nodules formed in transgenic roots were taken into account. IT quantification and classification was performed essentially as previously described by Battaglia et al. (2014). Briefly, composite plants were inoculated with a *R. etli* strain CFNx5 that constitutively expresses the fluorescent protein Ds-Red. ITs were visualized and quantified under UV light. For co-inoculation experiments, composite plants were transferred to pots containing vermiculite. Five days after transplantation, roots were inoculated with 10 ml of a mixture of *R. etli* strains SC15 and 55N1 (ratio 1:1) as previously described (Zanetti et al., 2010). Four weeks after co-inoculation, more than 100 nodules from 10 independent plants for each construct were excised, crushed, and plated in Congo Red-YEM agar plates. The color of the bacteria grown on this media was recorded. Bacterial DNA was extracted, subjected to PCR amplification of the *nodC* gene, and digested with *Hinf*I to determine the restriction profile of the *nod*C gene as reported (Aguilar et al.,

[1]https://www.ensa.ac.uk/

2004). All experiments were conducted in three independent biological replicates.

Subcellular Localization Assays

The PvNF-YA1-GFP construct was introduced in *A. tumefaciens* GV3101 and *A. rhizogenes* K599 by electroporation. *A. tumefaciens* carrying PvNF-YA1 was co-infiltrated into *N. benthamiana* leaves with the viral silencing inhibitor protein P19 (Voinnet et al., 2003) as described (Battaglia et al., 2014). The subcellular localization in common beans roots was done by generation of *P. vulgaris* composite plants expressing the PvNF-YA1-GFP fusion (Zanetti et al., 2010).

RNA Extraction and Quantitative RT-PCR

RNA extraction, cDNA synthesis, and RT-qPCR assays in common bean were performed as previously reported (Ripodas et al., 2013). Transcript levels for each of the target genes were normalized to the endogenous elongation factor 1 α (*EF1α*) transcript levels. Primer sequences for quantitative RT-PCR analyses are shown in **Supplementary Table S1**. Data shown are mean values obtained in three or four independent biological experiments with two or three technical repeats.

Microscopy and Imaging

Bright-field and epifluorescence imaging of ITs formation were performed as described (Battaglia et al., 2014). Confocal microscopy of *P. vulgaris* roots, *N. benthamiana* leaves, and ITs observation were made with a Leica confocal microscope (SP5) using 20X and 40X objectives. Samples were excited with argon laser and emission spectra used to detect the fluorescence were: GFP (498–550 nm) and DsRed (578–626 nm).

Western Blots

Proteins from transgenic root tissue of individual composite plants were extracted, separated into 12% SDS-PAGE, and subjected to immunoblot analysis using anti-FLAG antibody (1:500; Sigma–Aldrich) as previously described (Zanetti et al., 2010).

RESULTS

PvNF-YA1 Is a Nuclear Localized TF Expressed in the Central Tissue of *P. vulgaris* Nodules

The current model for assembling of the heterotrimeric NF-Y complex proposes that the NF-YB interacts with NF-YC in the cytoplasm and the heterodimer translocates to the nucleus where it joins the NF-YA subunit. Consistent with this model, nuclear subcellular localization was described for several NF-YA proteins in different metazoan and plants species (Liu and Howell, 2010; Hackenberg et al., 2012; Baudin et al., 2015). In this study, nuclear subcellular localization of PvNF-YA1 was verified by expression of a translational fusion of PvNF-YA1 to the green fluorescent protein (GFP) into *N. benthamiana* leaf epidermal cells (**Figure 1A**). The GFP-PvNF-YA1 fusion protein was also detected in the nucleus of *P. vulgaris* root cells generated by *A. rhizogenes*–mediated transformation (**Figure 1B**), including epidermal root hairs (**Figures 1C,D**). As expected, free GFP was dispersed between the nucleus and the cytoplasm (**Figure 1E**).

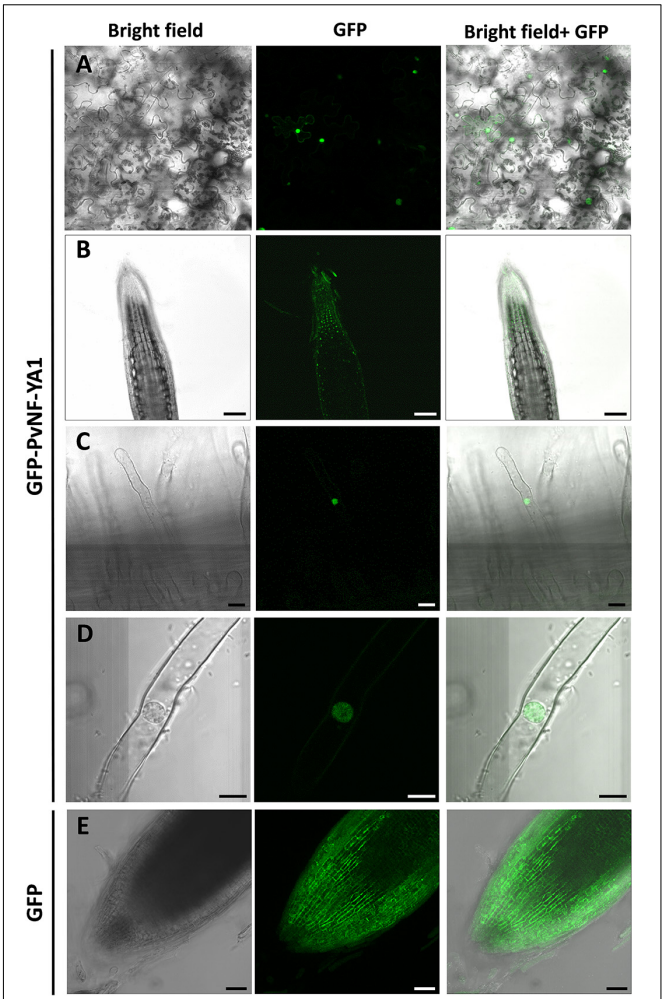

FIGURE 1 | Subcellular localization of PvNF-YA1 in *N. benthamiana* leaves and *P. vulgaris* roots. **(A)** Subcellular localization of the translational fusion GFP-NF-YA1 in epidermal cells of leaves of *N. benthamiana*. Images obtained under white (bright field) and UV light (GFP) by confocal microscopy, as well as the merged image (bright field + GFP), are shown. Scale bar: 50 μm. *P. vulgaris* roots expressing the GFP-NF-YA1 fusion **(B–D)** or free GFP **(E)** were observed by confocal microscopy. Images show the tip of a lateral roots **(B,E)** or root hairs **(C,D)**. Bright field, GFP channel, and merged (bright field + GFP) images are shown. The integration in *Z*-axis of 15 confocal sections is shown in **E**. Scale bars: 100 **(B)**, 25 **(C)**, 8 **(D)**, and 50 μm **(E)**.

Previous expression analysis of NF-YA family members reveled that *PvNF-YA1* transcripts accumulate at higher levels in nodules of 14 days post-inoculation than in roots or young nodules of 7 dpi (Ripodas et al., 2015). Here, we used a promoter:reporter fusion to investigate the activity of the *PvNF-YA1* promoter in different tissues of roots and nodules. A construct comprising approximately 2 kb upstream of the

translational initiation codon of *PvNF-YA1* fused to the open reading frame of *GUS* reporter gene was introduced into *P. vulgaris* roots by *A. rhizogenes*-mediated transformation. Histological staining of non-inoculated *ProPvNF-YA1*:*GUS* hairy roots revealed GUS activity in the vascular tissue of primary roots, but not in lateral root primordia (**Figure 2A**). GUS staining was also observed in lateral root meristem (**Figure 2B**), as well as in the vascular tissue of non-inoculated lateral roots (**Figures 2C,E**). Upon inoculation with a *R. etli* strain SC15 (carrying the *nodC*-α allele), a strong and a more intense GUS staining was detected on curled root hairs and epidermal cells surrounding the infection foci of the rhizobia susceptible zone, which contains elongating root hairs, but not in fully elongated root hairs (**Figures 2D,F**). At later time points, GUS staining was detected in the dividing cells of nodule primordia (**Figure 2G**) as well as in the central tissue of nodules formed by a *R. etli* strain carrying the *nodC*-α allele (**Figure 2H**).

Taken all together, the results presented in this section indicate that PvNF-YA1 is located in the nuclei of vascular tissues of primary and lateral roots, but also of rapidly dividing tissues such as lateral root meristems or nodule primordia. Importantly, *PvNF-YA1* is responsive to rhizobia, being active at early stages of the RNS (root hair curling), as well as at later stages in N-fixing nodules.

PvNF-YA1 and PvNF-YA9 Are Symbiotic Subunits Required for Nodule Formation and Bacterial Infection

We have previously shown that both *PvNF-YA1* and *PvNF-YA9* mRNA levels increased in roots at early stages of the symbiotic interaction (i.e., 24 hpi) with *R. etli*. However, *PvNF-YA1* transcript levels increased specifically upon inoculation with the more efficient *nodC*-α strain SC15, whereas *PvNF-YA9* mRNAs accumulated at higher levels in response to both *nodC*-α and *nocC*-δ strains as compared with non-inoculated roots (Ripodas et al., 2015). Additionally, Laloum et al. (2014) showed that the orthologs of *PvNF-YA1* and *PvNF-YA9* in *M. truncatula*, *MtNF-YA2* and *MtNF-YA1*, respectively, have partially redundant functions during RNS (Laloum et al., 2014). Thus, we questioned whether these two symbiotic NF-YA members play functions during the *P. vulgaris* × *R. etli* interaction. Anticipating that PvNF-YA1 and PvNF-YA9 might display redundant functions, an RNAi construct based on a sequence of the 3′ untranslated region (UTR) of *PvNF-YA1* mRNA that is highly similar to the 3′UTR of the PvNF-YA9 mRNA (**Supplementary Figure S1**) was designed to obtain *P. vulgaris* hairy roots with simultaneous reduction in *PvNF-YA1* and *PvNF-YA9* transcript levels. Transgenic roots were distinguished by visualization of the fluorescence emitted by the GFP protein, which is expressed under the control of the *rolD* promoter present in the T-DNA of the vector used for RNAi (see section "Materials and Methods"). Non-fluorescent roots were removed before collection of the tissue. RT-qPCR experiments verified that hairy roots from three independent *PvNF-YA1/9* RNAi plants exhibit reduced PvNF-YA1 and PvNF-YA9 mRNA levels (∼80%), as compared with control roots transformed with a *GUS* RNAi construct (**Figure 3A**). The fragment used for RNAi includes the *PvNF-YA1* binding sites for the microRNA miR169, a post-transcriptional mechanism that regulates most NF-YA family members (Combier et al.,

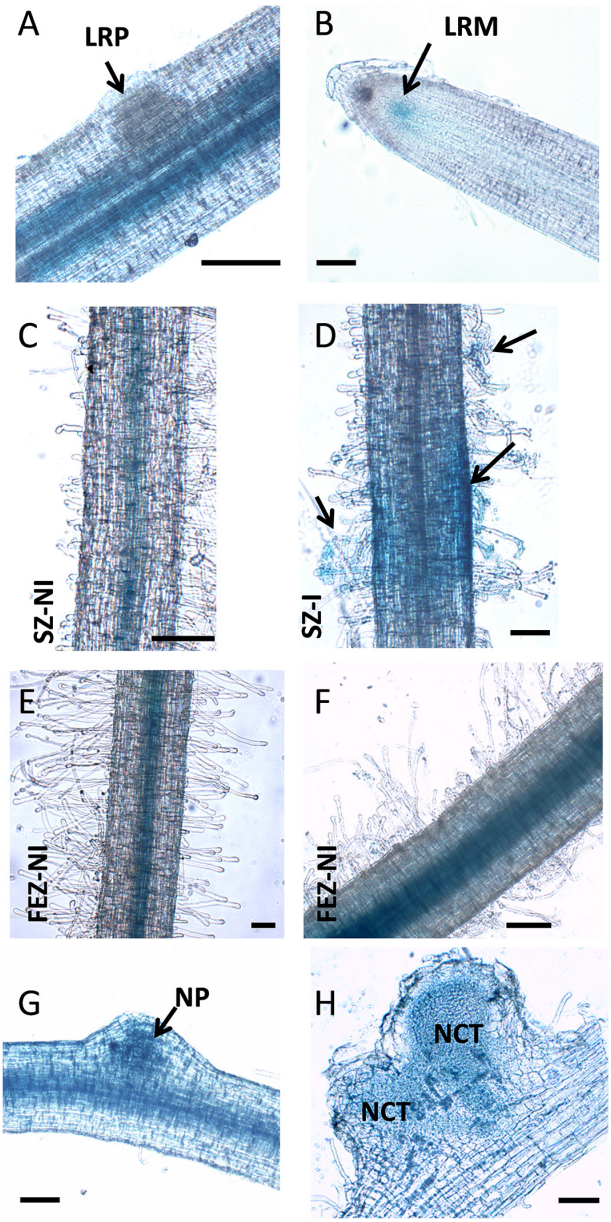

FIGURE 2 | *PvNF-YA1* promoter is active in roots and symbiotic nodules of *P. vulgaris*. Histochemical GUS staining of roots and nodule transformed with the *ProPvNF-YA1:GFPGUS* construct. **(A)** Non-inoculated (NI) primary root which containing a lateral root primordia (LRP). **(B)** Lateral root meristematic (LRM) zone of a NI lateral root. **(C)** Susceptible zone (SZ) of a NI lateral root. **(D)** SZ of lateral root inoculated (I) with *R. etli* strain SC15. Arrows point to infection sites. **(E)** Zone of fully elongated root hairs (FEZ) on a NI lateral root. **(F)** FEZ of a lateral root inoculated with *R. etli* strain SC15. **(G)** Nodule primordia (NP) or **(H)** nodules developed by *R. etli* strain SC15 at 6 or 14 dpi. NCT: nodule central tissue. Pictures are representative of images observed in more than three independent experiments. Bars: 200 μm.

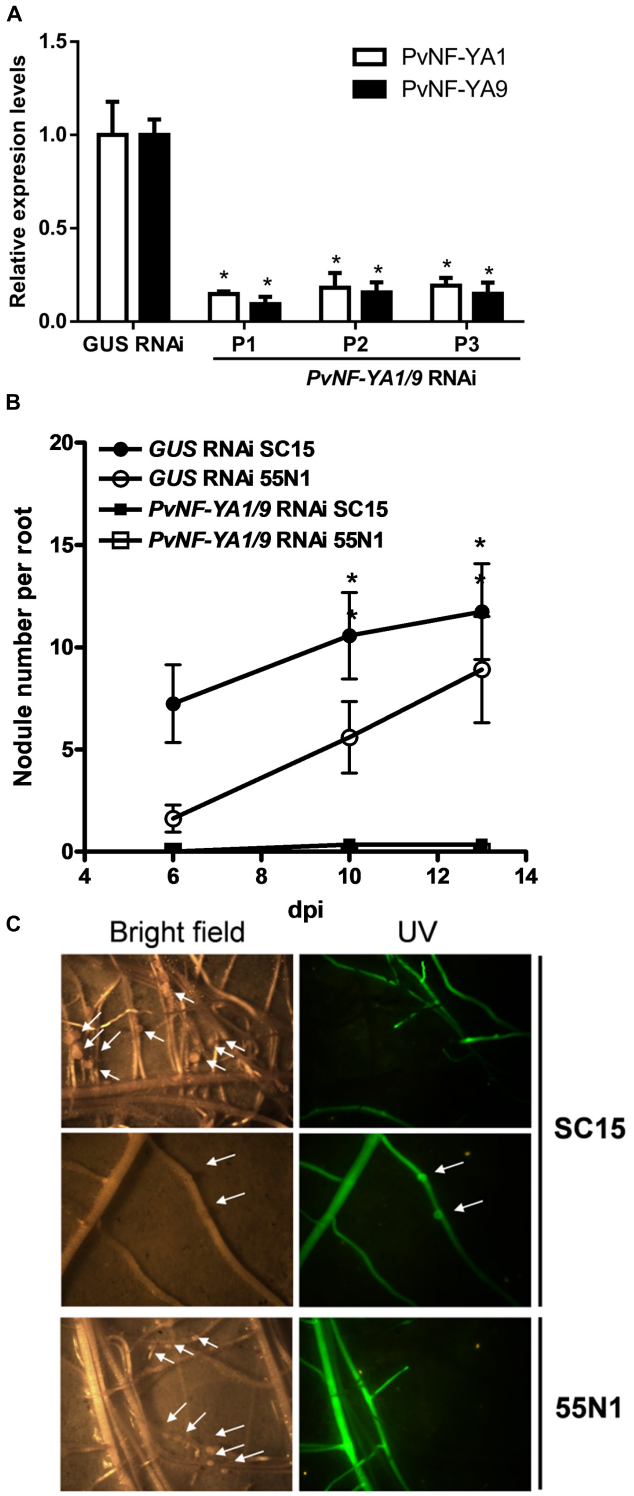

FIGURE 3 | Knock-down of *PvNF-YA1/9* abolished nodule formation in *P. vulgaris*. **(A)** RT-qPCR analysis of the mRNA levels of *PvNF-YA1* (white bars) and *PvNF-YA9* (black bars) in *GUS* RNAi transgenic roots (control) and root systems collected from three independent *PvNF-YA1/9* RNAi plants (P1, P2, and P3). Expression data were normalized to *PveEF1α* gene and are presented relative to the control roots. The error bars represent the SD of

(Continued)

FIGURE 3 | Continued

three technical replicates. Asterisks indicate statistical significant differences in a *t*-test with $p < 0.05$ comparing the values of each gene in each *PvNF-YA1/9* RNAi plant with the control *GUS* RNAi. **(B)** Number of nodules formed per root in *GUS* RNAi (control) and *PvNF-YA1/9* RNAi composite plants inoculated with the strains of *R. etli* SC15 and 55N1. Non-transgenic roots were removed before inoculation, thus only nodules formed in transgenic fluorescent hairy roots were registered. The error bars represent the SEM. Data are the average of three independent biological replicates with more than 60 transgenic roots for each condition. Asterisks indicate statistical significant differences in a *t*-test with $p < 0.05$ comparing. **(C)** Images illustrating the absence of nodules in fluorescent roots of plants transformed with the *PvNF-YA1/9* RNAi construct and their presence in the non-fluorescent roots that were not excised from the root system. The arrows mark the presence of two nodule primordia or bumps. Pictures were taken at 10 dpi with strains SC15 (upper panels) or 55N1 (lower panels).

TABLE 1 | Phenotypic analysis of root architecture in *GUS* RNAi and *PvNF-YA1/9* RNAi roots.

	Primary root length[a] (cm)	Lateral root length[b] (cm)	Lateral root density[c] (n/cm)
GUS RNAi	9.95 ± 0.40	2.20 ± 0.20	3.0 ± 0.20
PvNF-YA1/9 RNAi	9.15 ± 0.87	2.10 ± 0.15	2.46 ± 0.22

[a]Number of primary roots analyzed > 50. [b]Number of lateral roots analyzed > 100. [c]Density is expressed as the number of lateral roots per cm of primary root. Number of primary roots analyzed > 30. Values between GUS RNAi and PvNF-YA1/9 RNAi roots were not significantly different in an unpaired t-test with P < 0.05.

2006; Ripodas et al., 2015). Notably, expression of this RNAi construct did not affect the expression of other members of NF-YA family (**Supplementary Figure S2**). Specific members of *L. japonicus* and Arabidopsis NF-YA families (e.g., *LjNF-YA1*, *AtNF-YA2*, and *AtNF-YA10*) have been implicated in root development (Soyano et al., 2013; Sorin et al., 2014), thus we performed a phenotypic analysis of the root system. Knock-down of *PvNF-YA1/A9* RNAi did not alter the length of primary and lateral roots or the density of lateral roots (**Table 1**). Under symbiotic conditions, GFP-expressing transgenic *PvNF-YA1/9* RNAi roots barely developed nodules either after inoculation with *nodC*-α (SC15) or *nodC*-δ (55N1) strains (**Figures 3B,C**). Only two bumps were detected in over 100 *PvNF-YA1/9* RNAi roots examined in three independent experiments (**Figure 2C**). On the other hand, *GUS* RNAi roots or non-transgenic roots (non-fluorescent roots) that were not removed from the roots systems of *PvNF-YA1/9* RNAi composite plants, developed a higher number of nodules when inoculated with the more efficient strain of *R. etli* SC15 as compared with the less efficient strain 55N1 (**Figures 3B,C** first and third panels), as previously described (Blanco et al., 2009; Zanetti et al., 2010). These results indicate that *PvNF-YA1* and *PvNF-YA9* play key functions in nodule formation.

The availability of rhizobia strains expressing fluorescent markers allowed us to evaluate the number of infection events formed, as well as their progression toward cortical cells by fluorescence microscopy. Simultaneous knock-down of *PvNF-YA1/A9* in *P. vulgaris* roots provoked an important reduction in the density of ITs as compared with control roots transformed with the *GUS* RNAi

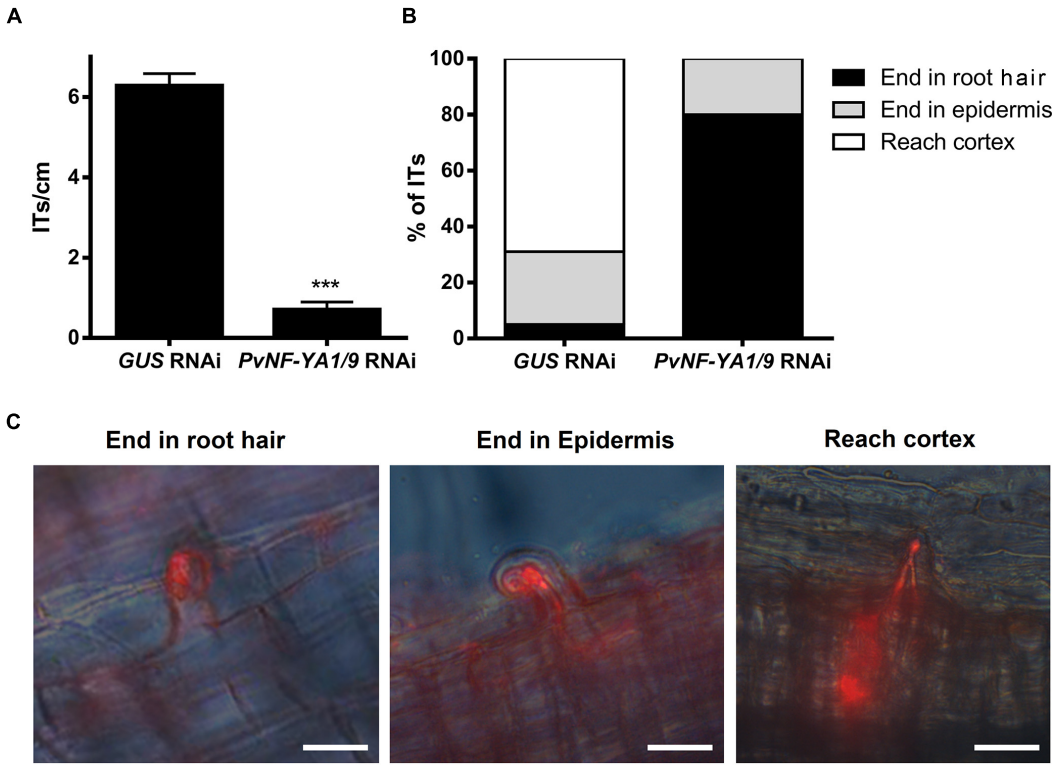

FIGURE 4 | Knock-down of *PvNF-YA1/A9* impaired the initiation and progression of infection events. **(A)** Number of ITs formed per centimeter of root in *GUS* RNAi and *PvNF-YA1/9* RNAi composite plants. ITs were quantified at 5 dpi with a *R. etli* strain CFNx5 (*nodC*-α) expressing the DsRed protein. Root segments from the susceptible zone were excised and visualized under fluorescent microscope. The number of roots segments analyzed was at least 50. Asterisks denote statistical significant differences in a *t*-test with $p < 0.001$. Data are the average of three independent biological replicates. **(B)** ITs formed were classified as events that reached the cortex (white bars), the epidermis (gray bars) or aborted in the root hair (black bars) and expressed as a percentage of the total of infection events. The number of ITs that abort in the root hairs or in the epidermis were significantly higher in the *PvNF-YA1/9* RNAi plants than in the *GUS* RNAi in a *t*-test with $p < 0.05$, whereas no events were recorded that reach the cortex in *PvNF-YA1/9* RNAi plants. Data are the average of three independent biological replicates. More than 50 root segments were analyzed in each biological replicate. **(C)** Images illustrating the classification shown in **B** as ITs that aborted in the root hair, in the epidermal cells, or that reached the cortical cells of *GUS* RNAi roots.

construct (**Figure 4A**). In addition, whereas in control plants 70% of ITs progressed and reached the cortical cell layer, nearly 80% of ITs formed in *PvNF-YA1/9* RNAi roots aborted in the root hair, 20% of them ended at the base of the epidermal cells, but none progressed to the cortex (**Figures 4B,C**). These results suggested these two members of the NF-YA family of *P. vulgaris* would be required for both the initiation and progression of rhizobial infection events.

Knock-Down of *PvNF-YA1/A9* Impairs Induction of Early Nodulins and Cell Cycle Genes

Considering the symbiotic phenotype observed in *PvNF-YA1/9* RNAi roots and the well-known function of NF-Y heterotrimers as transcriptional modulators, we investigated whether knock-down of *PvNF-YA1/9* affected the rhizobial-induced accumulation of nodulation marker transcripts. We selected *ERN1* (*ERF Required for Nodulation 1*), a mRNA encoding a transcription factor of the ERF (Ethylene Response Factor) family required for nodulation and rhizobial infection (Middleton et al., 2007) and *ENOD40* (*Early Nodulin 40*), a highly structured RNA required for cortical cell divisions that will form nodule primordia (Crespi et al., 1994). Previously, we have shown that these transcripts accumulated in *P. vulgaris* roots upon infection with *R. etli* strain SC15 and 55N1 (Zanetti et al., 2010; Mazziotta et al., 2013). RNA-sequencing data confirmed that these two nodulation marker transcripts accumulated to higher levels in wild type roots upon inoculation with either strain SC15 or 55N1 (**Supplementary Figure S3**; Dalla Via et al., 2015). Consistently with this observation, RT-qPCR experiments conducted in this study showed that both *ERN1* and *ENOD40* transcript levels increased more than 20 folds in control (*GUS* RNAi) hairy roots at 24 hpi as compared with non-inoculated *GUS* RNAi roots. However, *PvNF-YA1/9* RNAi roots failed to increase *ERN1* transcripts, and showed only a moderate increase (five folds) in *ENOD40* transcript levels in response to rhizobial infection (**Figure 5A** and **Supplementary Figure S4**). These results suggest that *PvNF-YA1/9* subunits might regulate

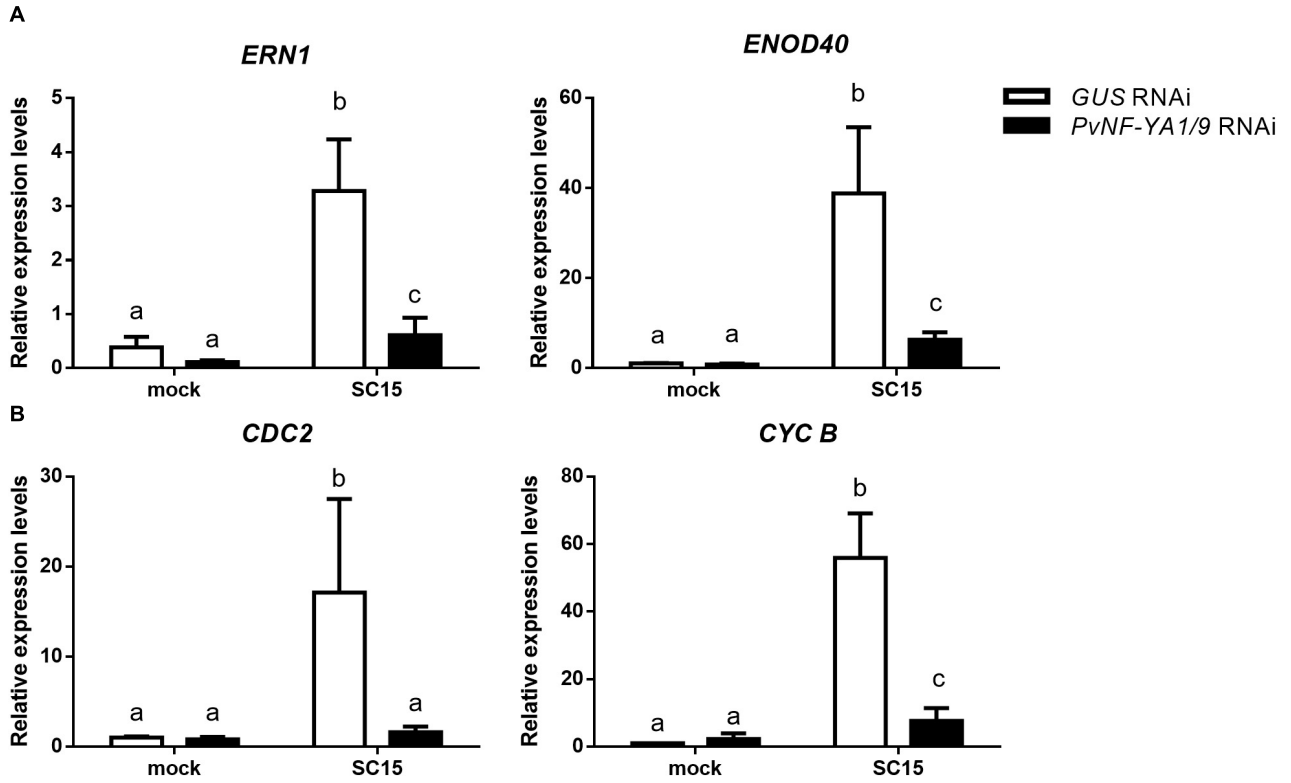

FIGURE 5 | Rhizobial induction of early nodulins and cell cycle genes is compromised by silencing of *PvNF-YA1/A9*. Roots expressing *GUS* (white bars) or *PvNF-YA1/9* RNAi (black bars) constructs were inoculated with the *R. etli* strain SC15 or mock inoculated with the media used to growth the rhizobia (mock). At 24 hpi, transcript levels of **(A)** nodulin and **(B)** cell cycle genes were determined by RT-qPCR. Values were normalized to *PvEF1α* and presented relative to the values of the mock-inoculated *GUS* RNAi roots. Error bars represent the SEM and different letters indicate that values are significantly different in a *t*-test with $p < 0.05$. Data are the average of three independent biological replicates, each performed with at least five independent plants.

directly or indirectly the expression of early nodulation genes in response to rhizobia.

In the context of nodulation, it has been shown that genes involved in cell cycle progression are activated at early time points after inoculation with rhizobia (Soyano et al., 2013; Breakspear et al., 2014). Transcripts of two cell cycle genes, *cyclin B* (*CYCB*) and *CDC2*, accumulated to higher levels in *P. vulgaris* roots in response to strain SC15, but not in response to strain 55N1 (Zanetti et al., 2010; **Supplementary Figure S3**). Moreover, we have shown that *PvNF-YC1* is required for accumulation of *CYCB* and *CDC2* mRNAs during the symbiosis of *P. vulgaris* with *R. etli* (Zanetti et al., 2010). Thus, we assessed whether silencing of *PvNF-YA1/A9* affected rhizobial-induced transcript accumulation of these cell cycle genes. As shown in **Figure 5B**, *PvNF-YA1/9* RNAi roots failed to accumulated higher transcript levels of *CDC2* and *CYCB* upon rhizobial infection in contrast with that observed in *GUS* RNAi roots. These results were consistently observed in three independent biological replicates (**Supplementary Figure S4**), suggesting a possible role of these NF-YA members in the re-activation of mitotic divisions of those cells committed for symbiosis, which is required for initiation of nodule organogenesis.

Overexpression of *PvNF-YA1*, but Not *PvNF-YA9*, Enhances the Symbiotic Outcome of a Less Efficient and Competitive Rhizobial Strain

The function of *PvNF-YA1* and *PvNF-YA9* in the establishment of the interaction between *P. vulgaris* and different rhizobia strains was investigated using transgenic roots that express a FLAG-tagged version of these subunits under the control of the nearly constitutive promoter Cauliflower Mosaic Virus 35S (CaMV35S), designated as FLAG-PvNF-YA1 and FLAG-PvNF-YA9. Roots transformed with the FLAG-PvNF-YA1 construct exhibited 2–10 fold times higher levels of *PvNF-YA1* mRNAs than control roots transformed with the empty vector (EV) as revealed by RT-qPCR in three different composite plant (**Figure 6A**). Western blot experiments using anti-FLAG antibodies verified the accumulation of the FLAG-PvNF-YA1 proteins and showed a relatively good correlation with *PvNF-YA1* transcript levels in the three independent composite plants analyzed here (**Figure 6B**). Phenotypic analysis of FLAG-NF-YA1 composite plants reveals that overexpression of *PvNF-YA1* had no effect on the length of the main and lateral roots (**Table 2**). FLAG-PvNF-YA1 roots showed a slight increase in the number of lateral roots developed by cm of root (density of lateral roots) compared to control

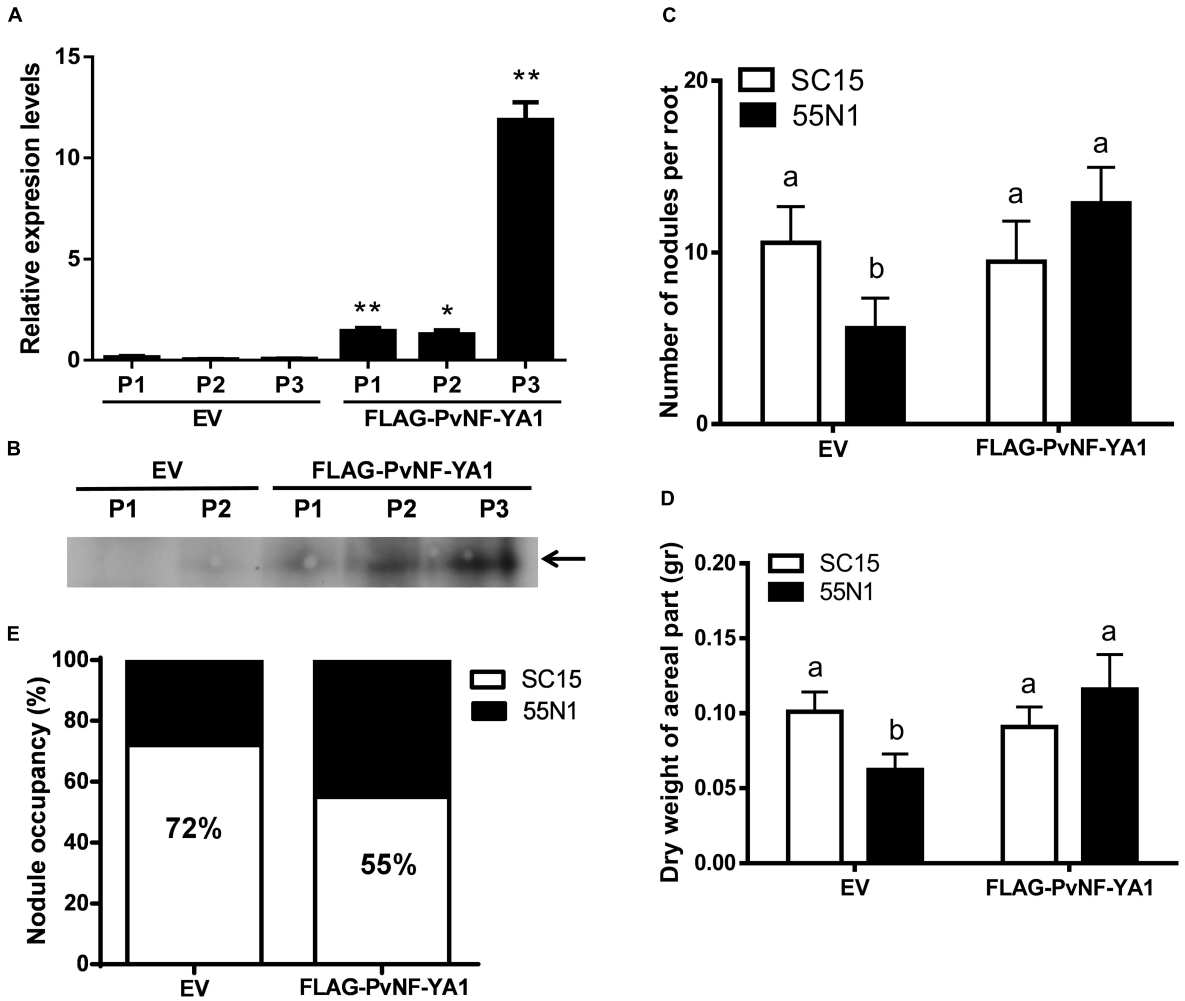

FIGURE 6 | Overexpression of PvNF-YA1 enhances nodulation of the less efficient *R. etli* strain 55N1 and alters nodule occupancy in *P. vulgaris*. **(A)** *PvNF-YA1* mRNA levels measured by RT-qPCR in control plants [empty vector (EV)] or independent roots of FLAG-PvNF-YA1. Error bars represent the SD of two technical replicates. Expression data were normalized to *PveEF1α* and presented as relative to EV. P1, P2, and P3 indicate the plant number. Asterisks indicate statistical significant differences in a *t*-test with $P < 0.05$. **(B)** Western blot analysis with α-FLAG antibody on root extracts from EV and FLAG-PvNF-YA1 plants. The band observed in the last three lines corresponds to the FLAG-PvNF-YA1 fusion of 38 kDa (arrow). P1, P2, and P3 correspond to the pool of transgenic roots of three different plants. **(C)** Number of nodules per root developed in control roots (EV) or FLAG-PvNF-YA1 at 10 dpi with strains of *R. etli* SC15 (white bars) or 55N1 (black bars). The error bars represent the SEM of the number of nodules formed per root present in more than 50 independent transgenic roots. Different letters indicate significantly different values in a *t*-test with $p < 0.05$. Data are the average of three independent biological experiments. **(D)** Dry weight of the aerial tissue of EV or FLAG-PvNF-YA1 composite plants at 21 dpi with strains of *R. etli* SC15 or 55N1. Error bars represent the SEM of at least 20 independent plants. Different letters indicate significantly different values in a *t*-test with $p < 0.05$. Data are the average of three independent biological experiments. **(E)** Percentage of nodule occupancy by strains SC15 (white) and 55N1 (black) in co-inoculation experiments. Nodule occupancy was determined at 21 dpi by examination of *nodC* polymorphic profiles of bacteria isolated from more than 100 individual nodules collected from a minimum of 10 co-inoculated plants for each construction. The results are the average of three independent biological experiments.

plants transformed with the EV; however, this difference was not statistically significant (**Table 2**).

To evaluate whether overexpression of *PvNF-YA1* affects the symbiotic outcome of *P. vulgaris* with different *R. etli* strains, FLAG-PvNF-YA1 and EV roots were inoculated with either the *nodC*-α strain SC15 or the *nodC*-δ strain 55N1 of *R. etli*. Overexpression of NF-YA1 did not produce a significant difference in the number of nodules per root formed by strain SC15 or in the dry weight of the aerial part (**Figures 6C,D**, white bars). However, upon inoculation with strain 55N1, FLAG-PvNF-YA1 roots formed a significantly greater number of nodules per root than control EV roots (**Figure 6C**, black bars). This increase in the number of nodules was correlated with an increase in the dry weight of the aerial part of the plant, which could be associated with increased efficiency of N fixation in the FLAG-PvNF-YA1 plants inoculated with 55N1 (**Figure 6D**, black bars). Notoriously, both parameters—nodule number and dry weight—of FLAG-PvNF-YA1 plants inoculated with 55N1 reached values comparable to those measured when plants were challenged with SC15. All these results show the same

TABLE 2 | Phenotypic analysis of root architecture in EV and FLAG-PvNF-YA1 roots.

	Primary root length[a] (cm)	Lateral root length[b] (cm)	Lateral root density[c] (n/cm)
EV	11.21 ± 0.45	1.18 ± 0.09	4.7 ± 0.5
FLAG-PvNF-YA1	10.15 ± 0.71	1.24 ± 0.12	5.8 ± 0.8

[a]Number of primary roots analyzed > 50. [b]Number of lateral roots analyzed > 50. [c]Density is expressed as the number of lateral roots per cm of primary root. Number of primary roots analyzed > 25. Values between EV and FLAG-PvNF-YA1 roots were not significantly different in an unpaired t-test with P < 0.05.

trend previously reported in plants overexpressing PvNF-YC1 (Zanetti et al., 2010). On the other hand, constitutive expression of FLAG-PvNF-YA9 in *P. vulgaris* roots did not affect the number of nodules formed by neither SC15 nor 55N1 strains of *R. etli* (**Supplementary Figures S5A,B**).

Previous studies have shown that Mesoamerican accession of *P. vulgaris* are preferentially nodulated by strains of rhizobia carrying the *nodC*-α allele when co-inoculated with strains with de *nodC*-δ allele (Aguilar et al., 2004). Moreover, overexpression of the PvNF-YC1 subunit was sufficient to alter nodule occupancy by these strains (Zanetti et al., 2010). Based on these previous observations and having found that the overexpression of *PvNF-YA1* affects the interaction with the less efficient and competitive strain 55N1, we proceeded to assess the role of PvNF-YA1 and PvNF-YA9 in the strain preference observed in Mesoamerican beans. Roots of composite plants were co-inoculated with an equicellular mixture of *R. etli* strains SC15 and 55N1. Nodules were collected at 21 dpi and the identity of the strain contained within individual nodules was evaluated by analyzing the phenotype of the strains growing in Congo red-YEM (Yeast Extract Mannitol) agar plates or the genotype by detection of the polymorphism of the *nodC* gene as previously described (Zanetti et al., 2010; **Supplementary Figure S6**). In control roots, 72% of the nodules were occupied by strain SC15 and only 28% by strain 55N1. Interestingly, FLAG-PvNF-YA1 roots showed an increase of 17% in the nodule occupancy by the strain 55N1 as compared to the control plants (**Figure 6E**), indicating that constitutive and ectopic expression of PvNF-YA1 is sufficient to alter nodule occupancy in Mesoamerican beans. On the contrary, overexpression of FLAG-PvNF-YA9 did not alter nodule occupancy by SC15 and 55N1 strains (**Supplementary Figure S5C**). Thus, these results suggest that PvNF-YA1, but not PvNF-YA9, might play functions in the strain preference observed in Mesoamerican beans by the strains carrying the *nodC*-α allele.

PvNF-YB7 Is Expressed in the Nodule Central Tissue and Required for the Selection of the Highly Efficient Nodulation Strain of *R. etli*

As already mentioned, the PvNF-YB7 subunit forms a heterotrimer *in planta* with PvNF-YA1 and PvNF-YC1 subunits, and *PvNF-YB7* mRNAs accumulate at higher levels in symbiotic nodules upon inoculation with *R. etli*. Thus, we focused our analysis in this specific member of the PvNF-YB family. A spatial expression analysis using a promoter:GUS construct was performed in transgenic hairy roots of *P. vulgaris*. Roots

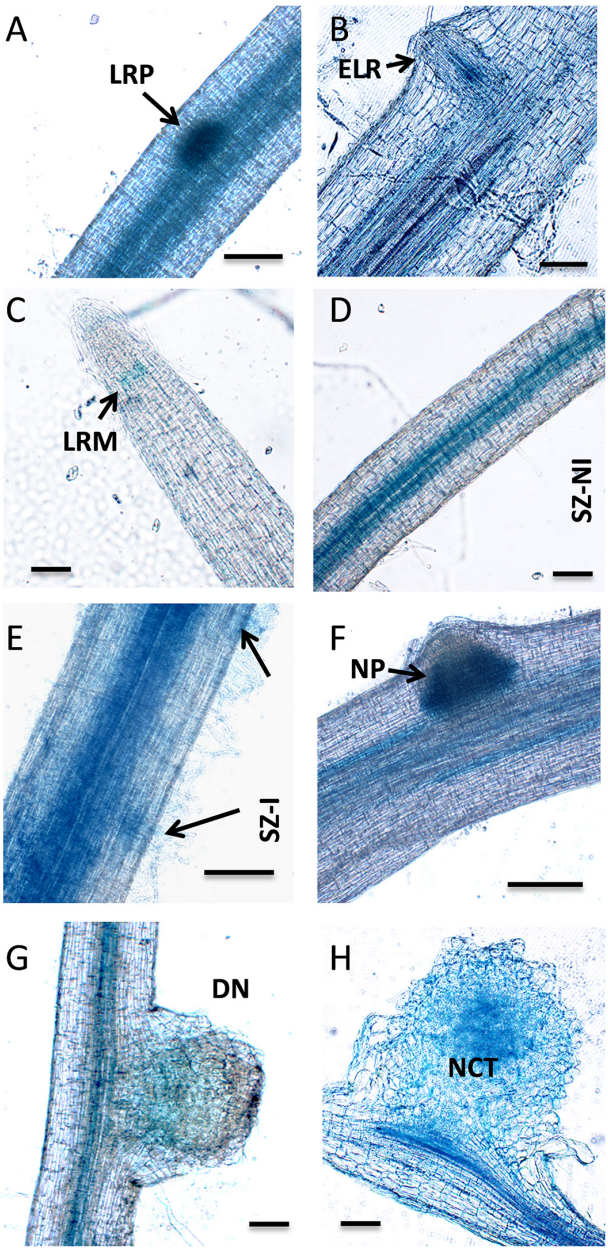

FIGURE 7 | Tissue-specific expression analysis of *PvNF-YB7* in roots and nodules of *P. vulgaris*. Histochemical GUS staining of roots and nodules transformed with the *ProPvNF-YB7:GUS* construct. **(A)** Non-inoculated (NI) primary root which containing a lateral root primordia (LRP). **(B)** Thin section of a primary root containing an emerged lateral root (ELR). **(C)** Lateral root meristem (LRM) of a NI lateral root. **(D)** Susceptible zone (SZ) of a NI lateral root. **(E)** SZ of lateral root inoculated (I) with *R. etli* strain SC15. Arrows point to infection sites. **(F)** Nodule primordia (NP) of 6 dpi, **(G)** developing nodule (DN) of 14 dpi, and **(H)** mature nodule of 21 dpi formed by strain SC15. NCT: nodule central tissue. Pictures are representative of images observed in more than three independent experiments. Bars: 200 μm.

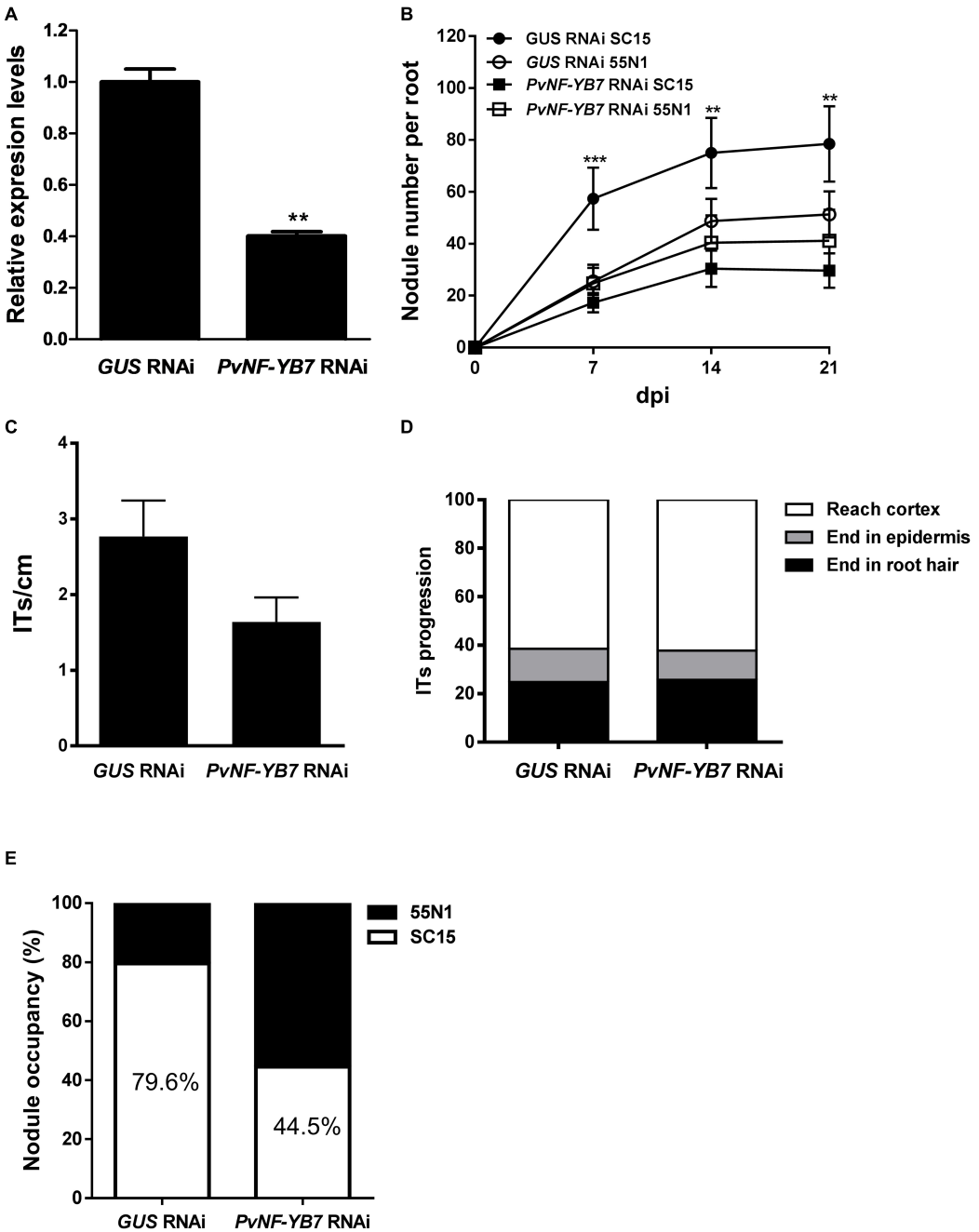

FIGURE 8 | Knock-down of *PvNF-YB7* reduces nodule formation and occupancy by the high efficient *R. etli* strain SC15. **(A)** RT-qPCR analysis of the mRNA levels of *PvNF-YB7* in *GUS* RNAi transgenic roots (control) and in roots from three independent *PvNF-YB7* RNAi plants. Expression data were normalized to *PveEF1*α gene and are presented relative to the control roots. Results are the average of two or three technical replicates. The error bars represent the SD. Asterisks indicate statistical significant differences in a *t*-test with $p < 0.01$. The results are representative of three independent biological experiments. **(B)** Number of nodules per root formed in *GUS* (control) and *PvNF-YB7* RNAi composite plants inoculated with the strains of *R. etli* SC15 and 55N1. The error bars represent the SEM. Data are the average of three independent biological replicates ($n > 50$ for each condition). Two or three asterisks indicate statistical significant differences in a *t*-test with $p < 0.01$ or $p < 0.001$. **(C)** Number of ITs formed per centimeter of root in *GUS* and *PvNF-YB7* RNAi composite plants. ITs were quantified at 5 dpi with a *R. etli* strain CFNx5 (*nodC*-α) expressing the DsRed protein. Data are the average of three independent biological replicates each with more than 50 roots segments from the susceptible zone. No statistical significant differences were found in a *t*-test with $p < 0.05$. Data are the average of three independent biological replicates. **(D)** ITs were classified as events that reached the cortex (white bars), the epidermis (gray bars), or aborted in the root hair (black bars) and expressed as a percentage of the total infection events. Data are the average of three independent biological replicates each with more than 50 independent roots segments. **(E)** Percentage of nodule occupancy by strains SC15 (white) and 55N1 (black) in co-inoculation experiments in *GUS* and *PvNF-YB7* RNAi roots. Nodule occupancy was determined at 21 dpi by examination of *nodC* polymorphic profiles of bacteria isolated from more than 100 individual nodules obtained from at least 10 composite plants. Results are the average of three independent biological replicates.

transformed with the *PromPvNF-YB7:GUS* construct exhibited GUS staining in the vascular tissue of the elongation zone of primary roots, as well as in the lateral root primordia (**Figure 7A**). GUS staining was also detected in the vasculature of emerged lateral roots (**Figure 7B**). In already developed lateral roots, expression of *PvNF-YB7* was observed in a small number of cells of the lateral root meristem as well as in the vasculature of the susceptible zone (**Figures 7C,D**). Under symbiotic conditions, GUS staining was observed in the curled root hairs of the susceptible zone (**Figure 7E**), in the dividing tissue of nodule primordia (**Figure 7F**), as well as in the base of developing nodule (**Figure 7G**) and in the central tissue of nodules developed by the *R. etli nodC*-α strain SC15 (**Figure 7H**). These results indicate that the *PvNF-YB7* promoter is active during nodule formation and support the notion that this subunit plays a relevant function in the establishment of symbiotic nodules. Then, we investigated the functional relevance of *PvNF-YB7* in the establishment of an efficient symbiotic interaction and in the strain preference in Mesomearican beans using RNAi-mediated gene silencing. Expression of an RNAi construct specifically designed to silence *PvNF-YB7* in *P. vulgaris* roots resulted in a significant reduction (>40%) of *PvNF-YB7* mRNA levels (**Figure 8A**). Interestingly, *PvNF-YB7* RNAi roots inoculated with the *nodC*-α strain SC15 developed nearly half of the nodules formed in control *GUS* RNAi roots; however, when inoculated with strain 55N1, *PvNF-YB7* RNAi and *GUS* RNAi roots developed a similar number of nodules (**Figure 8B**), indicating that PvNF-YB7 subunit might be one of the molecular components of *P. vulgaris* that are required for the establishment of an interaction with high efficient strains of *R. etli*. Rhizobial infection was slightly, but not significantly reduced by knock-down of *PvNF-YB7* as determined by the frequency of ITs formed by an RFP labeled *R. etli* strain carrying the *nodC*-α alelle (**Figure 8C**). In addition, progression of the infection events was not altered by the reduction in *PvNF-YB7* levels (**Figure 8D**), suggesting that this member of the NF-YB family is not strictly required for the initiation and elongation of ITs. Since silencing of *PvNF-YB7* affected nodule formation with SC15 but not with 55N1, we questioned whether this silencing could affect the strain selectivity observed in Mesoamerican beans. Notably, upon co-inoculation with a mixture of strains SC15 and 55N1, the occupancy of the nodules by strain SC15 was reduced in more than 35% in *PvNF-YB7* RNAi roots as compared with *GUS* RNAi roots (**Figure 8E**). All together, the results presented here support a role for *PvNF-YB7* in nodule organogenesis triggered specifically by the high efficient strain SC15.

DISCUSSION

Nuclear Factor Y TFs act as heterotrimers to activate or repress expression of their target genes. Since the individual subunits of the complex are encoded by relatively large gene families in plant genomes, it is crucial to elucidate the composition of the heterotrimers that would be acting in specific tissues or during the activation of morphogenetic programs, such as rhizobial infection and nodule organogenesis, which will largely rely on the tissue-specific expression pattern of individual members of these gene families. Our previous studies have shown that *PvNF-YA1*, *PvNF-YA9*, *PvNF-YB7* and *PvNF-YC1* are expressed in nodules (Ripodas et al., 2015). Here, the use of promoter:GFP-GUS constructs revealed that the promoters of both *PvNF-YA1* and *Pv-NF-YB7* are active in infected root hairs, as well as in the central tissue of N-fixing nodules developed by the strain of *R. etli* carrying the *nodC*-α allele. The expression pattern of these two subunits is reminiscent of that described for *LjNF-YA1* and *LjNF-YB1* in the legume *L. japonicus,* in which *LjNF-YA1* plays a crucial role in nodule formation (Soyano et al., 2013). In addition, it is consistent with that reported for MtNF-YA1 promoter at early stages of symbiosis between *M. truncatula* and *Sinorhizobium meliloti*, in which expression was detected in infected root hairs of the susceptible zone and in the central region of developing nodules (Laporte et al., 2014). The expression pattern of *PvNF-YA1* and *PvNF-YB7* partially overlap in roots under non-symbiotic conditions. Expression of *PvNF-YB7*, but not PvNF-YA1, was detected in lateral root primordia, suggesting that they might be acting in different heterotrimeric NF-Y complex at initial steps of lateral root formation, prior emergence. In already emerged lateral roots, expression of *PvNF-YA1* and *PvNF-YB7* overlap in vascular and meristematic tissue, suggesting that both subunits might be part of a heterotrimer involved in post-emergence lateral root growth. This speculation is consistent with the role assigned for LjNF-YA1 and LjNF-YB1 subunits in lateral root growth (Soyano et al., 2013). Since PvNF-YA1 and PvNF-YB7, together with PvNF-YC1, have been shown to be part of the same hetertorimeric complex *in planta* and their expression overlap in developing nodules formed by the more efficient strain of *R. etli*, it is possible to speculate that these two subunits might act in concert to promote nodule formation and/or development during the high efficient interaction established between Mesoamerican beans and strains of *R. etli* carrying the *nodC*-α allele. This speculation is supported by the phenotype observed in plants with altered levels of these NF-Y subunits. The results presented here revealed that both *PvNF-YA1/A9* and *PvNF-YB7* RNAi roots showed a significant reduction in the number of nodules formed by the strain SC15. A previous study indicated that silencing of *PvNF-YC1* also prevented nodule formation by this *R. etli* strain (Zanetti et al., 2010), indicating that the three subunits might act in concert in nodule formation and development triggered by the more efficient strain SC15. On the other hand, when plants were inoculated with the less efficient strain 55N1, nodule formation was also diminished in *PvNF-YA1/9* RNAi and *PvNF-YC1* RNAi roots, but not in *PvNF-YB7* RNAi roots. These results indicate that other NF-YB subunits, e.g., PvNF-YB10 or PvNF-YB12, which are also expressed in nodules (Ripodas et al., 2015), might fulfill this function when plants are challenged by a strain that is less efficient in nodule formation, presumably by heterotrimerization with PvNF-YC1 and PvNF-YA1 or PvNF-YA9. This was not unexpected since expression of a RNAi designed to specifically silence *MtNF-YB16* or a less specific RNAi that simultaneous knock-down four NF-YB gene family members (*MtNF-YB16/B18/B6/B11*) in *M. truncatula* did not revealed any noticeable symbiotic phenotype upon

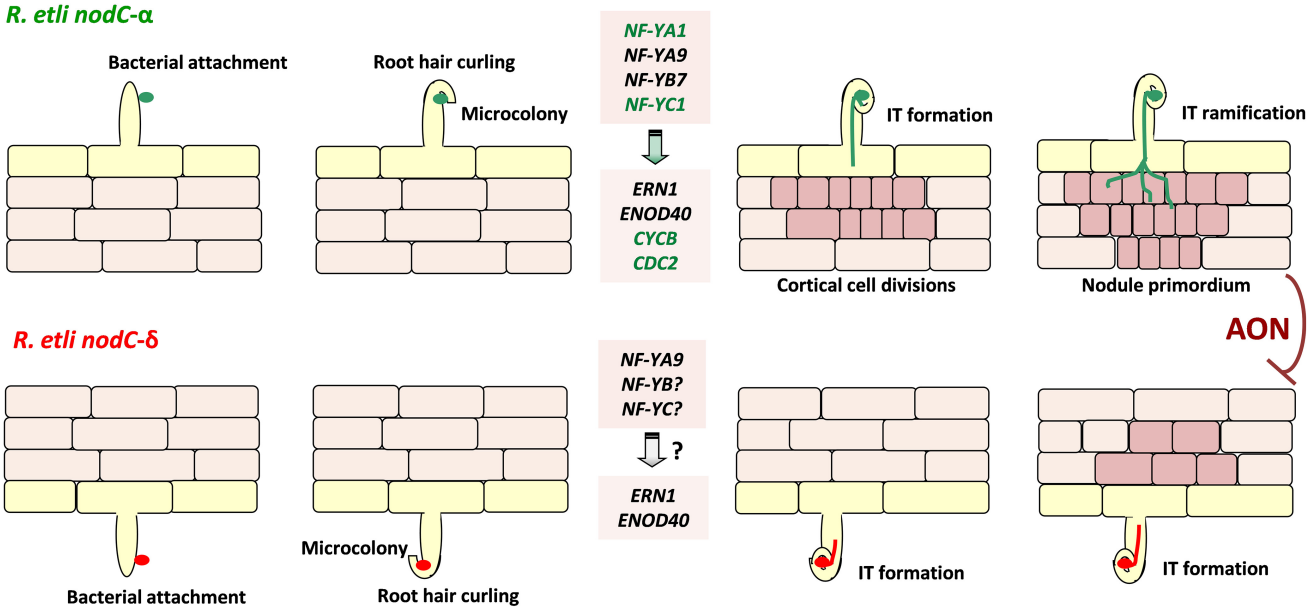

FIGURE 9 | Model illustrating the proposed function of the PvNF-YA1/-YB7/-YC1 heterotrimer in the strain preference observed in the *P. vulgaris* × *R. etli* interaction. Perception of *R. etli* strains *nodC*-α (represented in green, upper panels) by Mesoamerican *P. vulgaris* plants results in the root hair curling that entrap bacteria to form a microcolony. This perception also rapidly (within 24 hpi) and locally induces expression of genes encoding the PvNF-YA1 (and PvNF-YA9) and PvNF-YC1 subunits, which form a hetrotrimeric transcription factor with PvNF-YB7. Heterotrimer formation activates the expression of nodulation (*ERN1* and *ENOD40*) and the cell cycle (*CYCB* and *CDC2*) genes, promoting infection thread (IT) formation and cortical cell divisions. The IT progresses, ramifies, and reaches the nodule primordium to produce a functional nodule occupied by the *nodC*-α strain. On the other hand, perception of *nodC*-δ strains (represented in red, lower panels) leads to root hair curling, microcolony formation, and induction of *PvNF-YA9*, *ERN1*, and *ENOD40* in a similar way that *nodC*-α strains. However, induction of *PvNF-YA1* and *PvNF-YC1*, as well as *CYCB* and *CDC2*, is not observed at 24 hpi, delaying cortical cell divisions and the progression of ITs that contain the *nodC*-δ strain. As a consequence of these local responses, when both strains are present (e.g., in coinoculation experiments or in the field when both bacteria are present in the soil with even abundance) nodules are mainly occupied by the *nodC*-α strains. Since nodulation is systemically repressed by a systemic mechanisms referred as autoregulation of nodulation (AON), new nodule formation triggered by the *nodC*-δ strain is arrested once the appropriate number of nodules is reached. In this model, genes specifically induced at 24 hpi with the *nodC*-α strain are colored in green. PvNF-YA9 and other NF-YB and NF-YC subunits, as well as ERN1 and ENOD40, are activated also by the *nodC*-δ strain.

inoculation with *S. meliloti* (Baudin et al., 2015). In addition, two independent studies based on yeast-two hybrid assays performed with Arabidopsis NF-Y subunits revealed that NF-YB subunits tend to be more promiscuous in heterotrimer formation than NF-YA and NF-YC subunits (Calvenzani et al., 2012; Hackenberg et al., 2012). The fact that *PvNF-YB7* RNAi plants form nodules with both *R. etli* strains points toward a low degree of specificity in the NF-YB association for nodule formation, as previously proposed for the *M. truncatula* × *S. meliloti* interaction (Baudin et al., 2015). However, the observation that *PvNF-YB7* seems to be required for a high efficient nodule formation leads to speculate that the symbiotic outcome, at least in the case of *P. vulgaris* × *R. etli* interaction, might depend on strict NF-Y heterotrimer formation.

An interesting finding of this study is the observation that overexpression of PvNF-YA1, but not of PvNF-YA9, increased the efficiency of nodule formation when plants were inoculated with the less efficient strain 55N1; moreover, it was sufficient to increase the proportion of nodules occupied by 55N1 when co-inoculated with the higher competitive strain SC15. It must also be noted that *PvNF-YA1* proved to be responsive only to strain SC15, whereas *PvNF-YA9* expression is activated by both strains (Ripodas et al., 2015). Thus, PvNF-YA9 appears to be part of the more general pathway triggered by high or low efficient strains, which might explain why overexpression of this subunit did not altered nodule number or their occupancy. On the other hand, PvNF-YA1 seems to be part of the signaling pathway activated only by the high efficient strain SC15. The phenotype observed in PvNF-YA1 overexpressing roots is reminiscent of that previously described in plants overexpressing PvNF-YC1 (Zanetti et al., 2010). Considering the fact that PvNF-YA1 and PvNF-YC1 are able to interact in the same NF-Y trimeric complex (Baudin et al., 2015), we suggest that increased levels of both PvNF-YA1 and PvNF-YC1 could help to improve the symbiotic capacity of less efficient rhizobia. Moreover, these two NF-Y subunits are part of a symbiotic heterotrimeric TF that might work in the activation of the genetic program that allows Mesoamerican plants to discriminate between strains that are more or less efficient in nodule formation. A striking result regarding nodule occupancy by SC15 and 55N1 strains was obtained in *PvNF-YB7* RNAi plants. In these plants, nodules occupied by SC15 decreased by about 35% compared to controls. This might be most likely a consequence of the reduced capacity of these plants to form nodules upon inoculation with strain SC15.

Thus, we concluded that *PvNF-YB7* is required for high efficient nodule organogenesis in Mesoamerican *P. vulgaris* roots. This observation also reinforces the hypothesis that this specific NF-YB subunit might be an additional component of the genetic programs that determine the selectivity displayed by *P. vulgaris* plants for those strains that perform better in nodule formation. Based on this and previous studies (Zanetti et al., 2010; Ripodas et al., 2015), we propose a model that attempt to explain how PvNF-YA1, PVNF-YB7, and PvNF-YC1 function to control the strain preference observed in Mesoamerican accessions of *P. vulgaris* (**Figure 9**). In this model, specific activation of PvNF-YA1 and PvNF-YC1 in response to *nodC*-α strains, such as SC15, lead to a rapid activation of the morphological responses, such as cortical cell divisions (possibly due the specific and rapid activation of cell cycle genes) and progression of IT toward nodule primordia. These responses result in the formation of nodules occupied by *nodC*-α strains. On the other hand, *nodC*-δ strains fail to rapidly induce *PvNF-YA1* and *PvNF-YC1*, thus these morphological responses occurred slower in the presence of strains such as 55N1; as a consequence, nodules formed by these strains will be delayed. During symbiosis, existing N-fixing nodules inhibit the formation of new nodules by a mechanism referred to as autoregulation of nodulation (AON), which involves long distance signaling from root to shoot and back again (Ferguson et al., 2014). Within this context, the earliest formation of nodules occupied by a *nodC*-α strain will inhibit the formation of new nodules that might be colonized by a *nodC*-δ strain, explaining why in co-inoculation experiments or in the field, the majority of the nodules formed in Measomerican beans are occupied by *nodC*-α strains.

Infection events and their progression to the cortical cells were drastically reduced by introduction of the *PvNF-YA1/9* RNAi construct in *P. vulgaris* roots. Moreover, no ITs reaching the cortex were detected in *PvNF-YA1/9* RNAi roots, at least at the time points analyzed here, indicating that they might have aborted either in the root hair or the epidermis. Thus, these two NF-YA subunits play not only an important role in nodule organogenesis and development, but also in the epidermal and/or cortical responses that lead to a successful infection of the nodule. This phenotype resembles that previously reported by Laloum et al. (2014) in *M. truncatula* plants with reduced levels of *MtNF-YA1* and *MtNF-YA2* (the orthologs of *PvNF-YA9* and *PvNF-YA1*, respectively), where both frequency and progression of ITs were impaired. This phenotype is more pronounced than that observed in *M. truncatula* that are null mutants for the *MtNF-YA1* allele, which exhibited an increased number of ITs, but the morphology of ITs was abnormal and IT growth was arrested (Laporte et al., 2014). In contrast, *L. japonicus* plants with reduced levels of a single NF-YA subunit, LjNF-YA1 (the ortholog of PvNF-YA9 and MtNF-YA1 of *P. vulgaris* and *M. truncatula*, respectively), produced a normal amount of ITs without evidenced of IT arresting (Soyano et al., 2013), suggesting some functional redundancy with other NF-YA subunits in this legume species. Based on our results and those described by others, it is possible to conclude that two symbiotic NF-YA subunits play partially redundant and essential functions in the sophisticated intracellular infection by rhizobia observed in many legume species. On the other hand, expression of the *PvNF-YB7* RNAi construct did not produce any strong phenotype in the infection by rhizobia; except by a mild, but not significant reduction in the frequency of ITs. This indicates that other NF-YB subunits of *P. vulgaris* might exert redundant functions in the genetic program that leads to this intracellular mechanism of infection.

Nuclear Factor Y subunits have been involved in the control of cell division activities during the development of lateral root organs, either lateral roots or symbiotic nodules (Zanetti et al., 2010; Soyano et al., 2013; Sorin et al., 2014). Here, we found that lateral root growth or density was not significantly affected by knock-down of *PvNF-YA1* and *PvNF-YA9*, indicating that these subunits do not seem to be required or play redundant functions with other NF-YA members during the activation of cell divisions related to the initiation or growth of lateral roots. However, rhizobial induction of cell cycle genes such as *CDC2* and *CYCB* was almost completely abolished in *PvNF-YA1/9* RNAi roots, which is well correlated with the absence of nodule formation observed in these roots. In addition, induction of *ENOD40*, which is also required for cortical cell division activity during formation of nodule primordia, is reduced in *PvNF-YA1/9* RNAi roots. These results indicate that PvNF-YA1 and PvNF-YA9 participate not only in the transcriptional activation of early markers of infection such as *ERN1*, a direct target of the symbiotic NF-Y complex (Laloum et al., 2014; Baudin et al., 2015), but also in the control of cell division activities during nodule formation. A previous study revealed that the PvNF-YC1 subunit is also involved in the control of *CDC2* and *CYCB* during nodule formation (Zanetti et al., 2010). Future experiments will help to elucidate whether these and other cell cycle related genes are direct transcriptional targets of the symbiotic complex formed by the PvNF-YA1/9, PvNF-YB7 and PvNF-YC1 in *P. vulgaris* during the interaction with high or low efficient strains of *R. etli*.

AUTHOR CONTRIBUTIONS

MZ, FB, and CR conceived the research and designed the experiments. CR, MC, and JC performed the experiments with help from JV. MZ, CR, and JC analyzed the experimental results. CR and MZ wrote the manuscript. All the authors discussed the results and approved the final manuscript.

FUNDING

This research was supported by grants from Agencia Nacional de Promoción Científica y Tecnológica (ANPCyT) PICT2013-0384, PICT2014-0321, and PICT 2016-0582.

SUPPLEMENTARY MATERIAL

The Supplementary Material for this article can be found online at: https://www.frontiersin.org/articles/10.3389/fpls.2019.00221/full#supplementary-material

REFERENCES

Aguilar, O. M., Riva, O., and Peltzer, E. (2004). Analysis of *Rhizobium etli* and of its symbiosis with wild *Phaseolus vulgaris* supports coevolution in centers of host diversification. *Proc. Natl. Acad. Sci. U.S.A.* 101, 13548–13553. doi: 10.1073/pnas.0405321101

Battaglia, M., Rípodas, C., Clúa, J., Baudin, M., Aguilar, O. M., Niebel, A., et al. (2014). A nuclear factor Y interacting protein of the GRAS family is required for nodule organogenesis, infection thread progression, and lateral root growth. *Plant Physiol.* 164, 1430–1442. doi: 10.1104/pp.113.230896

Baudin, M., Laloum, T., Lepage, A., Rípodas, C., Ariel, F., Frances, L., et al. (2015). A phylogenetically conserved group of nuclear factor-Y transcription factors interact to control nodulation in legumes. *Plant Physiol.* 169, 2761–2773. doi: 10.1104/pp.15.01144

Bitocchi, E., Bellucci, E., Giardini, A., Rau, D., Rodriguez, M., Biagetti, E., et al. (2013). Molecular analysis of the parallel domestication of the common bean (*Phaseolus vulgaris*) in Mesoamerica and the Andes. *New Phytol.* 197, 300–313. doi: 10.1111/j.1469-8137.2012.04377.x

Bitocchi, E., Nanni, L., Bellucci, E., Rossi, M., Giardini, A., Zeuli, P. S., et al. (2012). Mesoamerican origin of the common bean (*Phaseolus vulgaris* L.) is revealed by sequence data. *Proc. Natl. Acad. Sci. U.S.A.* 109, E788–E796. doi: 10.1073/pnas.1108973109

Blanco, F. A., Meschini, E. P., Zanetti, M. E., and Aguilar, O. M. (2009). A small GTPase of the Rab family is required for root hair formation and preinfection stages of the common bean-Rhizobium symbiotic association. *Plant Cell* 21, 2797–2810. doi: 10.1105/tpc.108.063420

Breakspear, A., Liu, C., Roy, S., Stacey, N., Rogers, C., Trick, M., et al. (2014). The root hair "infectome" of *Medicago truncatula* uncovers changes in cell cycle genes and reveals a requirement for Auxin signaling in rhizobial infection. *Plant Cell* 26, 4680–4701. doi: 10.1105/tpc.114.133496

Calvenzani, V., Testoni, B., Gusmaroli, G., Lorenzo, M., Gnesutta, N., Petroni, K., et al. (2012). Interactions and CCAAT-binding of *Arabidopsis thaliana* NF-Y subunits. *PLoS One* 7:e42902. doi: 10.1371/journal.pone.0042902

Combier, J. P., de Billy, F., Gamas, P., Niebel, A., and Rivas, S. (2008). Trans-regulation of the expression of the transcription factor MtHAP2-1 by a uORF controls root nodule development. *Genes Dev.* 22, 1549–1559. doi: 10.1101/gad.461808

Combier, J. P., Frugier, F., de Billy, F., Boualem, A., El-Yahyaoui, F., Moreau, S., et al. (2006). MtHAP2-1 is a key transcriptional regulator of symbiotic nodule development regulated by microRNA169 in *Medicago truncatula*. *Genes Dev.* 20, 3084–3088. doi: 10.1101/gad.402806

Crespi, M. D., Jurkevitch, E., Poiret, M., d'Aubenton-Carafa, Y., Petrovics, G., Kondorosi, E., et al. (1994). enod40, a gene expressed during nodule organogenesis, codes for a non-translatable RNA involved in plant growth. *EMBO J.* 13, 5099–5112. doi: 10.1002/j.1460-2075.1994.tb06839.x

Curtis, M. D., and Grossniklaus, U. (2003). A gateway cloning vector set for high-throughput functional analysis of genes in planta. *Plant Physiol.* 133, 462–469. doi: 10.1104/pp.103.027979

Dalla Via, V., Narduzzi, C., Aguilar, O. M., Zanetti, M. E., and Blanco, F. A. (2015). Changes in the common bean transcriptome in response to secreted and surface signal molecules of *Rhizobium etli*. *Plant Physiol.* 169, 1356–1370. doi: 10.1104/pp.15.00508

Denarie, J., Debelle, F., and Prome, J. C. (1996). Rhizobium lipo-chitooligosaccharide nodulation factors: signaling molecules mediating recognition and morphogenesis. *Annu. Rev. Biochem.* 65, 503–535. doi: 10.1146/annurev.bi.65.070196.002443

Ferguson, B. J., Li, D., Hastwell, A. H., Reid, D. E., Li, Y., Jackson, S. A., et al. (2014). The soybean (*Glycine max*) nodulation-suppressive CLE peptide, GmRIC1, functions interspecifically in common white bean (*Phaseolus vulgaris*), but not in a supernodulating line mutated in the receptor PvNARK. *Plant Biotechnol. J.* 12, 1085–1097. doi: 10.1111/pbi.12216

Hackenberg, D., Wu, Y., Voigt, A., Adams, R., Schramm, P., and Grimm, B. (2012). Studies on differential nuclear translocation mechanism and assembly of the three subunits of the *Arabidopsis thaliana* transcription factor NF-Y. *Mol. Plant* 5, 876–888. doi: 10.1093/mp/ssr107

Karimi, M., Inze, D., and Depicker, A. (2002). GATEWAY vectors for Agrobacterium-mediated plant transformation. *Trends Plant Sci.* 7, 193–195. doi: 10.1016/S1360-1385(02)02251-3

Laloum, T., Baudin, M., Frances, L., Lepage, A., Billault-Penneteau, B., Cerri, M. R., et al. (2014). Two CCAAT-box-binding transcription factors redundantly regulate early steps of the legume-rhizobia endosymbiosis. *Plant J.* 79, 757–768. doi: 10.1111/tpj.12587

Laloum, T., De Mita, S., Gamas, P., Baudin, M., and Niebel, A. (2013). CCAAT-box binding transcription factors in plants: Y so many? *Trends Plant Sci.* 18, 157–166. doi: 10.1016/j.tplants.2012.07.004

Laporte, P., Lepage, A., Fournier, J., Catrice, O., Moreau, S., Jardinaud, M. F., et al. (2014). The CCAAT box-binding transcription factor NF-YA1 controls rhizobial infection. *J. Exp. Bot.* 65, 481–494. doi: 10.1093/jxb/ert392

Lerouge, P., Roche, P., Faucher, C., Maillet, F., Truchet, G., Promé, J. C., et al. (1990). Symbiotic host-specificity of Rhizobium meliloti is determined by a sulphated and acylated glucosamine oligosaccharide signal. *Nature* 344, 781–784. doi: 10.1038/344781a0

Liu, J. X., and Howell, S. H. (2010). bZIP28 and NF-Y transcription factors are activated by ER stress and assemble into a transcriptional complex to regulate stress response genes in Arabidopsis. *Plant Cell* 22, 782–796. doi: 10.1105/tpc.109.072173

Mazziotta, L., Reyonoso, M. A., Aguilar, O. M., Blanco, F. A., and Zanetti, M. E. (2013). Transcriptional and functional variation of NF-YC1 in genetically diverse accessions of *Phaseolus vulgaris* during the symbiotic association with *Rhizobium etli*. *Plant Biol.* 15, 808–818. doi: 10.1111/j.1438-8677.2012.00683.x

Meschini, E. P., Blanco, F. A., Zanetti, M. E., Beker, M. P., Küster, H., Pühler, A., et al. (2008). Host genes involved in nodulation preference in common bean (*Phaseolus vulgaris*)-*Rhizobium etli* symbiosis revealed by suppressive subtractive hybridization. *Mol. Plant Microbe Interact.* 21, 459–468. doi: 10.1094/MPMI-21-4-0459

Middleton, P. H., Jakab, J., Penmetsa, R. V., Starker, C. G., Doll, J., Kaló, P., et al. (2007). An ERF transcription factor in *Medicago truncatula* that is essential for Nod factor signal transduction. *Plant Cell* 19, 1221–1234. doi: 10.1105/tpc.106.048264

Mustroph, A., Zanetti, M. E., Jang, C. J., Holtan, H. E., Repetti, P. P., Galbraith, D. W., et al. (2009). Profiling translatomes of discrete cell populations resolves altered cellular priorities during hypoxia in Arabidopsis. *Proc. Natl. Acad. Sci. U.S.A.* 106, 18843–18848. doi: 10.1073/pnas.0906131106

Petroni, K., Kumimoto, R. W., Gnesutta, N., Calvenzani, V., Fornari, M., Tonelli, C., et al. (2012). The promiscuous life of plant NUCLEAR FACTOR Y transcription factors. *Plant Cell* 24, 4777–4792. doi: 10.1105/tpc.112.105734

Popp, C., and Ott, T. (2011). Regulation of signal transduction and bacterial infection during root nodule symbiosis. *Curr. Opin. Plant Biol.* 14, 458–467. doi: 10.1016/j.pbi.2011.03.016

Ripodas, C., Castaingts, M., Clua, J., Blanco, F., and Zanetti, M. E. (2015). Annotation, phylogeny and expression analysis of the nuclear factor Y gene families in common bean (*Phaseolus vulgaris*). *Front. Plant Sci.* 5:761. doi: 10.3389/fpls.2014.00761

Ripodas, C., Via, V. D., Aguilar, O. M., Zanetti, M. E., and Blanco, F. A. (2013). Knock-down of a member of the isoflavone reductase gene family impairs plant growth and nodulation in *Phaseolus vulgaris*. *Plant Physiol. Biochem.* 68, 81–89. doi: 10.1016/j.plaphy.2013.04.003

Sorin, C., Declerck, M., Christ, A., Blein, T., Ma, L., Lelandais-Brière, C., et al. (2014). A miR169 isoform regulates specific NF-YA targets and root architecture in Arabidopsis. *New Phytol.* 202, 1197–1211. doi: 10.1111/nph.12735

Soyano, T., Kouchi, H., Hirota, A., and Hayashi, M. (2013). Nodule inception directly targets NF-Y subunit genes to regulate essential processes of root nodule development in *Lotus japonicus*. *PLoS Genet.* 9:e1003352. doi: 10.1371/journal.pgen.1003352

Voinnet, O., Rivas, S., Mestre, P., and Baulcombe, D. (2003). An enhanced transient expression system in plants based on suppression of gene silencing by the p19 protein of tomato bushy stunt virus. *Plant J. Mar.* 33, 949–956. doi: 10.1046/j.1365-313X.2003.01676.x

Wang, D., Maughan, M. W., Sun, J., Feng, X., Miguez, F., Lee, D., et al. (2012). Impact of nitrogen allocation on growth and photosynthesis of miscanthus

(*Miscanthus* × *giganteus*). *Glob. Change Biol. Bioenergy* 4, 688–697. doi: 10.1111/j.1757-1707.2012.01167.x

Weston, L. A., and Mathesius, U. (2013) Flavonoids: their structure, biosynthesis and role in the rhizosphere, including allelopathy. *J. Chem. Ecol.* 39, 283–297. doi: 10.1007/s10886-013-0248-5

Zanetti, M. E., Blanco, F. A., Beker, M. P., Battaglia, M., and Aguilar, O. M. (2010). A C subunit of the plant nuclear factor NF-Y required for rhizobial infection and nodule development affects partner selection in the common bean-*Rhizobium etli* symbiosis. *Plant Cell* 22, 4142–4157. doi: 10.1105/tpc.110.079137

Conflict of Interest Statement: The authors declare that the research was conducted in the absence of any commercial or financial relationships that could be construed as a potential conflict of interest.

frontiers in Microbiology

ORIGINAL RESEARCH
published: 12 March 2019
doi: 10.3389/fmicb.2019.00407

Identification of Nitrogen-Fixing *Bradyrhizobium* Associated With Roots of Field-Grown Sorghum by Metagenome and Proteome Analyses

*Shintaro Hara[1], Takashi Morikawa[1], Sawa Wasai[1], Yasuhiro Kasahara[2], Taichi Koshiba[3], Kiyoshi Yamazaki[4], Toru Fujiwara[4], Tsuyoshi Tokunaga[3] and Kiwamu Minamisawa[1]**

[1] Graduate School of Life Sciences, Tohoku University, Sendai, Japan, [2] Institute of Low Temperature Science, Hokkaido University, Sapporo, Japan, [3] Earthnote Co., Ltd., Okinawa, Japan, [4] Graduate School of Agricultural and Life Sciences, The University of Tokyo, Tokyo, Japan

OPEN ACCESS

Edited by:
Benjamin Gourion, Laboratoire des Interactions Plantes-Microorganismes (LIPM), France

Reviewed by:
Angela Sessitsch, Austrian Institute of Technology (AIT), Austria
Claudia Knief, Universität Bonn, Germany

***Correspondence:**
Kiwamu Minamisawa
kiwamu@ige.tohoku.ac.jp

Specialty section:
This article was submitted to Plant Microbe Interactions, a section of the journal Frontiers in Microbiology

Received: 15 September 2018
Accepted: 15 February 2019
Published: 12 March 2019

Citation:
Hara S, Morikawa T, Wasai S, Kasahara Y, Koshiba T, Yamazaki K, Fujiwara T, Tokunaga T and Minamisawa K (2019) Identification of Nitrogen-Fixing Bradyrhizobium Associated With Roots of Field-Grown Sorghum by Metagenome and Proteome Analyses. Front. Microbiol. 10:407. doi: 10.3389/fmicb.2019.00407

Sorghum (*Sorghum bicolor*) is cultivated worldwide for food, bioethanol, and fodder production. Although nitrogen fixation in sorghum has been studied since the 1970s, N_2-fixing bacteria have not been widely examined in field-grown sorghum plants because the identification of functional diazotrophs depends on the culture method used. The aim of this study was to identify functional N_2-fixing bacteria associated with field-grown sorghum by using "omics" approaches. Four lines of sorghum (KM1, KM2, KM4, and KM5) were grown in a field in Fukushima, Japan. The nitrogen-fixing activities of the roots, leaves, and stems were evaluated by acetylene reduction and $^{15}N_2$-feeding assays. The highest nitrogen-fixing activities were detected in the roots of lines KM1 and KM2 at the late growth stage. Bacterial cells extracted from KM1 and KM2 roots were analyzed by metagenome, proteome, and isolation approaches and their DNA was isolated and sequenced. Nitrogenase structural gene sequences in the metagenome sequences were retrieved using two nitrogenase databases. Most sequences were assigned to *nifHDK* of *Bradyrhizobium* species, including non-nodulating *Bradyrhizobium* sp. S23321 and photosynthetic *B. oligotrophicum* S58^T. Amplicon sequence and metagenome analysis revealed a relatively higher abundance (2.9–3.6%) of *Bradyrhizobium* in the roots. Proteome analysis indicated that three NifHDK proteins of *Bradyrhizobium* species were consistently detected across sample replicates. By using oligotrophic media, we purified eight bradyrhizobial isolates. Among them, two bradyrhizobial isolates possessed 16S rRNA and *nif* genes similar to those in S23321 and S58^T which were predicted as functional diazotrophs by omics approaches. Both free-living cells of the isolates expressed N_2-fixing activity in a semi-solid medium according to an acetylene reduction assay. These results suggest that major functional N_2-fixing bacteria in sorghum roots are unique bradyrhizobia that

resemble photosynthetic *B. oligotrophicum* S58^T and non-nodulating *Bradyrhizobium* sp. S23321. Based on our findings, we discuss the N_2-fixing activity level of sorghum plants, phylogenetic and genomic comparison with diazotrophic bacteria in other crops, and *Bradyrhizobium* diversity in N_2 fixation and nodulation.

Keywords: *Bradyrhizobium*, nitrogen fixation, sorghum, metagenome, proteome

INTRODUCTION

Biological N_2 fixation in non-leguminous plants is required to improve agricultural sustainability by decreasing the global use of synthetic nitrogen fertilizers (Steffen et al., 2015; Yoneyama et al., 2017; Rosenblueth et al., 2018). Diazotrophic endophytes can provide fixed nitrogen to non-leguminous crops (Boddey et al., 2001; Yoneyama et al., 2017). ^{15}N-labeling significantly contributed to N_2 fixation in sugarcane (Yoneyama et al., 1997; Boddey et al., 2001). *Gluconacetobacter* and *Herbaspirillum* were isolated from sugarcane stems as candidate endophytic N_2-fixing bacteria (Cavalcante and Dobereiner, 1988; James, 2000). Recent metatranscriptome analyses targeting *nifH* (encoding dinitrogenase reductase) suggested that *Bradyrhizobium* members play a role in N_2 fixation in sugarcane (Thaweenut et al., 2011; Fischer et al., 2012; Rosenblueth et al., 2018). Abundant expression of *Bradyrhizobium* and *Azorhizobium nifH* was also detected in sweet potato stems and tubers (Terakado-Tonooka et al., 2008).

Sorghum [*Sorghum bicolor* (L.) Moench] is a C_4 plant. Sorghum has little breeding history compared to sugarcane and maize but has the potential for broad agro-ecological adaptation (Khawaja et al., 2014). Sorghum provides grain for use in food and feed, sugary juice for producing syrup or bioethanol and is an excellent fodder (Khawaja et al., 2014). Omics studies of sorghum-associated microbes (Naylor et al., 2017; Xu et al., 2018) showed that drought increased the abundance and activity of monoderm bacteria including *Actinobacteria* in field-grown sorghum and verified that these bacteria contribute to the drought-resistance of sorghum plants. Thus, sorghum root-associated microbiomes play an important role in determining plant fitness.

For nitrogen fixation in sorghum plants, Pedersen et al. (1978) first detected the N_2-fixing activities of washed root segments and soil cores of grain sorghum in NE, United States, in an acetylene reduction assay. Wani et al. (1984) observed the acetylene-reducing activity (ARA) of intact sorghum plants grown in pots. These studies suggested that sorghum-associated bacteria play a role in N_2 fixation. Coelho et al. (2008) reported several diazotrophic bacteria (*Paenibacillus*, *Azohydromonas*, *Ideonella*, *Rhizobium*, and *Bradyrhizobium*) in the rhizosphere soils of field-grown sorghum in Brazil based on *nifH* PCR of soil DNA extracts. However, N_2-fixing bacteria associated with sorghum plant tissues have not been fully explored.

Recent "omics" approaches have been used to identify and isolate functional diazotrophs in sugarcane (Thaweenut et al., 2011; Fischer et al., 2012), sweet potato (Terakado-Tonooka et al., 2008; Terakado-Tonooka et al., 2013), and paddy rice (Bao et al., 2014, 2016). Particularly, the combination of metagenome and metaproteome analyses based on extracted bacterial cells (EBCs) isolated from plant tissues (Ikeda et al., 2009) revealed type II methanotrophs in paddy rice roots as functional N_2-fixing bacteria (Bao et al., 2014; Minamisawa et al., 2016). We adopted a similar strategy to identify diazotrophs responsible for N_2 fixation in field-grown sorghum plants. We identified tissues showing significant N_2-fixing activity by ARA and $^{15}N_2$ fixation, identified functional diazotrophs by proteome analysis of nitrogenase proteins based on metagenomic data, and isolated bacteria with nitrogenase proteins and phylogenetic markers predicted from the omics results (**Figure 1**). Our results strongly suggest that bradyrhizobia fixed N_2 in the roots of filed-grown sorghum plants at late growth stages. Because the N_2-fixing bradyrhizobia in sorghum roots are phylogenetically close to an aquatic legume, *Aeschynomene* (Okubo et al., 2012a), we describe their functional roles.

MATERIALS AND METHODS

Plant Materials and Field Conditions

We used four lines (KM1, KM2, KM4, and KM5) of sorghum developed by Earthnote Co., Ltd. (Okinawa, Japan). KM1 is a late-ripening line with vigorous leaf growth. KM2 is an early-ripening line with lodging resistance and salt tolerance. KM4 and KM5 were pre-selected because of their high (KM4) and low (KM5) N_2-fixing activities as estimated by the ^{15}N dilution method (Lee et al., unpublished).

Seeds were sown in 200-cell plug trays on May 10, 2016. The seedlings were transplanted into a field owned by Earthnote (Fukushima, Japan; 37°30′46.43″140°34′13.7″) on June 6, 2016. The soil had the following chemical properties: pH (H_2O), 5.9; total C, 13.9 g kg^{-1} dry soil; total N, 0.8 g kg^{-1} dry soil; available phosphorus, 560.4 mg P kg^{-1} dry soil (Truog method). Before transplanting the seedlings, the field was treated with 85 kg N as urea, 84 kg N as controlled-release coated-urea fertilizer (LP100, JCAM Agri. Co., Ltd., Tokyo, Japan), which releases 80% of its total N over 100 days, and 85 kg K_2O as potassium sulfate per hectare. This is the standard fertilization regime used for sorghum cropping under the local conditions. Each line was planted in three plots, with 50 plants per plot (0.075 m between plants, 1.00 m between rows).

Outlines of Polyphasic Approach and Experimental Design

Figure 1 shows the outlines of our polyphasic approach based on nitrogen-fixing activity and omics analyses. Because the experimental designs were complicated for respective

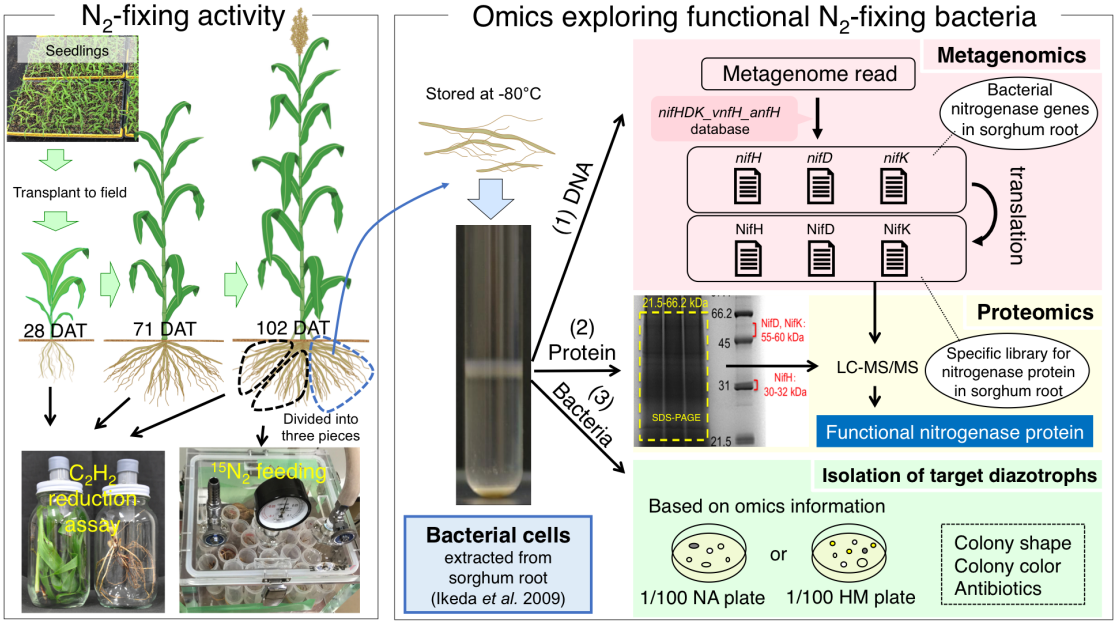

FIGURE 1 | Outline of "omics" strategy used to explore and identify functional N_2-fixing bacteria associated with sorghum plants. N_2-fixing activities were monitored in tissues of sorghum at different growth stages by acetylene reduction assay and were directly confirmed in an $^{15}N_2$ feeding experiment. Bacteria were extracted from sorghum root tissues with higher N_2-fixing activities, and their metagenomes (1) and proteomes (2) were analyzed. Functional N_2-fixing bacteria were isolated from the extracted bacteria (3). DAT = days after transplant.

analyses, we show the detailed sampling strategies used in the polyphasic approach along with the sorghum growth stages in **Supplementary Figures S1, S2**.

At least three plants were sampled individually from three different field plots or from the seedling trays for transplanting. When the sorghum seedlings were transplanted into the field, six seedlings were randomly selected from the plug trays [0 days after transplanting (DAT)], which were subjected to the acetylene reduction assay (**Supplementary Figure S1A**) as described below. At 28 DAT and 71 DAT, field-grown sorghum plants were harvested from three plots individually, and each plant tissue including the leaves, stems, and roots were subjected to the acetylene reduction assay (**Supplementary Figure S1B**). At 102 DAT, three plants were harvested from three plots individually, and the roots were washed with tap water, weighted, and further subdivided into three parts for the acetylene reduction assay, $^{15}N_2$-feeding analysis, and omics/isolation analysis (metagenome, proteome, bacterial isolation) (**Supplementary Figure S2** and **Figure 1**). Thus, the acetylene reduction assay, $^{15}N_2$-feeding experiment, and omics analyses (metagenome and proteome) were performed based on three biological replicates.

Acetylene Reduction Assay of Field-Grown Sorghum

Nitrogen-fixing activity was examined by the acetylene reduction assay (Schollhorn and Burris, 1967) at four growth stages: 0, 27, 71, and 102 DAT. Sorghum plants were maintained in the vegetative stage until 71 DAT, while the plants generally moved to the reproductive stage with ears at 102 DAT (**Figure 1**). One or two healthy plants were randomly sampled (**Supplementary Figures S1, S2**). The tissues to be used for ARA were determined according to the growth stage of the plant (**Figure 1**): 0 DAT, whole seedling; 28 DAT, shoot and root; 71 DAT, leaf, stem, and root; and 102 DAT, root. At 0 and 28 DAT, two plants were harvested, one of which was used for acetylene reduction with acetylene, while the others were used for control analysis without acetylene (**Supplementary Figure S1**). At 71 and 102 DAT, one plant was divided equally into two pieces of similar weight and structure; one piece was used to analyze acetylene reduction with acetylene and the other was used for control analysis without acetylene (**Supplementary Figures S1, S2**).

At 0 DAT, seedling roots were washed in tap water to remove adhering soil and placed in a 100-mL vial with a butyl rubber septum (SVG-100, Nichiden-Rika Glass Co., Ltd., Kobe, Japan) (**Figure 1**). At 27, 71, and 102 DAT, each tissue was placed in a 900-mL glass jar with a modified lid fitted with a butyl rubber W-plug (W-24T, Taiyo Kogyo, Tokyo, Japan) (**Figure 1**).

Acetylene gas (99.9999% vol/vol purity; Toho Acetylene Co., Tokyo, Japan) was injected to provide a concentration of 10% (vol/vol), and the vial or jar was incubated for 1 day at ambient temperature. We drew 20 mL of headspace gas in a sampling syringe and stored it in a vacuumed gas vial (SVG-5; Nichiden-Rika Glass Co.) until analysis. Gas samples (0.5 mL) were analyzed to determine their ethylene concentrations with a Shimadzu GC-18A gas chromatograph equipped with a flame ionization detector and Porapak R column as described previously (Elbeltagy et al., 2001).

$^{15}N_2$ Feeding of Field-Grown Sorghum

At 102 DAT, the divided roots from the same plant used for ARA were introduced into a gas chamber with a sampling port (**Figure 1** and **Supplementary Figure S2**). The gas phase in the chamber was replaced with 32% (v/v) $^{15}N_2$ (99.4 atom % ^{15}N; Shoko, Tokyo, Japan)/20% O_2/48% Ar. The negative control included air gas containing atmospheric N_2 [natural abundance of ^{15}N (0.366 atom %)]. After static incubation in the chamber at 25°C for 23 h in the dark, the root samples were dried at 80°C for 3 days and then powdered in a Multi-Beads Shocker (Yasui Kikai, Osaka, Japan). To determine the level of $^{15}N_2$ fixation in the roots, we analyzed ^{15}N and total N contents of the powdered root tissues with an elemental analyzer/isotope ratio mass spectrometer (Flash EA1112-Delta V Advantage ConFlo IV System; Thermo Fisher Scientific, Waltham, MA, United States).

Bacterial Cell Extraction and Metagenome Analysis

Root tissues of the same plant used for the ARA and $^{15}N_2$-feeding experiments were stored at −80°C for metagenome analysis (**Figure 1** and **Supplementary Figure S2**). EBCs, including both endophytes and epiphytes, were directly prepared from ∼100 g of root tissues as previously reported (Ikeda et al., 2009). The extraction of EBC allowed for the elimination of plant organelles and plant genomic DNA. Metagenomic DNA was prepared from the bacterial cells using an IsoPlant II kit (Nippon Gene, Tokyo, Japan) with bead beating treatment. In the first step, 0.5 g of bacterial cells were disrupted by bead beating in a Lysing Matrix B tube (MP Biomedicals, Santa Ana, CA, United States) with Solution I (Extraction Buffer) from the IsoPlant II kit. Bead beating was performed using a FastPrep FP100A (MP Biomedicals) at 5.5 m s^{-1} for 30 s. Other steps were conducted according to the manufacturer's instructions, and the DNA preparation was stored at −20°C until use.

DNA libraries were prepared using the Illumina TruSeq DNA library preparation kit v. 2 (Illumina, San Diego, CA, United States). The size and quality of the libraries were assessed using a BioAnalyzer High Sensitivity Chip, and the average fragment size was around 700 base pairs (bp). Next, 250-bp paired-end libraries were sequenced on an Illumina MiSeq sequencer. The quality of the sequence data was checked by using the FastQC v. 0.10.1 software[1]. Reads were trimmed using Prinseq-lite 0.20.4 (Schmieder and Edwards, 2011) with the following settings: -trim_left 20 -trim_right 5 -trim_qual_right 30 -min_qual_mean 20 -min_len 70.

Extraction of Structural Genes of Nitrogenase

To extract *nifH*, we first assigned the metagenomic reads in each sample according to the results of BLAST analysis against the *nifH* database (Gaby and Buckley, 2014) with a threshold identity of 90%. The *nifH* database developed by Gaby and Buckley (2014) contains 32,954 nitrogenase reductase genes sequences including *anfH*, an alternative nitrogenase that is a paralog of *nifH*, and *vnfH*, a V–Fe alternative nitrogenase. Next, we used candidate reads in BLAST searches against the NCBI NR database with an *E*-value threshold of 10^{-10} and removed false *nifH* reads by manual inspection of the BLAST results. *nifH* genes were taxonomically assigned based on the best BLAST hit and counted. The retrieved reads were translated into amino acid sequences and incorporated into our database for proteome analysis with taxonomic information. If a best-hit was part of a genome sequence, *nifD* and *nifK* were picked up and used for database construction as described below.

To extract *nifD* and *nifK*, we modified the *nifD* and *nifK* database of Gaby and Buckley (2014), which contains only 268 and 315 sequences, respectively. To enrich the *nifDK* database, sequences were collected from (i) NCBI databases matched with respective keywords ("nitrogenase molybdenum-iron," "*nifD*," or "*nifK*") and (ii) *nifD* and *nifK* encoded on genome sequences of *nifH* best-hits. The metagenomic reads in each sample were assigned according to the BLAST analysis against the *nifD* and *nifK* database with a threshold identity of 80% in-house. Next, the candidate reads of *nifD* and *nifK* from the metagenomic data were subjected to BLAST searches against the NCBI NR public database with an *E*-value threshold of 10^{-10}, and false *nifD* or *nifK* reads were removed by manual inspection of the BLAST results. The resulting DNA sequences of *nifD* and *nifK* were taxonomically assigned based on the best BLAST hit, translated into amino acid sequences, and incorporated in our nitrogenase database for proteome analysis with taxonomic information.

Community Analyses of Sorghum Root Microbes

Amplicon sequencing of 16S rRNA and metagenomics analysis targeting 31 AMPHORA genes (Wu and Eisen, 2008), which are housekeeping genes that are mostly present in single copies, were performed to analyze the bacterial community associated with the sorghum roots.

A partial bacterial 16S rRNA gene fragment was amplified by two-step PCR. First, a partial sequence of the V4 variable region was amplified with simultaneous addition of sequencing priming sites. The target region was amplified using primers 515F (5′-ACACTCTTTCCCTACACGACGCTCTTCCGATCTGTGCCAGCMGCCGCGGTAA-3′) and 806R (5′-GTGACTGGAGTTCAGACGTGTGCTCTTCCGATCTGGACTACHVGGGTWTCTAAT-3′) (Caporaso et al., 2011). In the second round of PCR, the first-round PCR products were amplified using the above sequencing priming sites as PCR priming sites by adding dual-index tag sequences and flow cell binding sites of the Illumina adapter. The primer sequences were 5′-AATGATACGGCGACCACCGAGATCTACAC–Index2–ACACTCTTTCCCTACACGACGC-3′ (forward) and 5′-CAAGCAGAAGACGGCATACGAGAT–Index1–GTGACTGGAGTTCAGACGTGTG-3′ (reverse). Each 20-μL PCR mixture contained 0.2 μL TaKaRa ExTaq HS DNA polymerase (TaKaRa Bio, Shiga, Japan), 2.0 μL of buffer (10 × Ex buffer), 1.6 μL of 2.5 mM dNTP mix, 1.0 μL of each forward and reverse primer (10 μM), and 1 μL of template DNA. First-round PCR conditions were as follows: 94°C for 2 min, followed by 25 cycles of 94°C for 30 s, 50°C

[1]http://www.bioinformatics.babraham.ac.uk/projects/fastqc/

for 30 s, and 72°C for 30 s. The PCR products were purified using an Agencourt AMPure XP purification system (Beckman Coulter, Brea, CA, United States) following the manufacturer's instructions. Second-round PCR conditions were as follows: 94°C for 2 min; 12 cycles of 94°C for 30 s, 60°C for 30 s, and 72°C for 30 s; and a final 72°C for 5 min. The purified tag-indexed PCR products were quantified by using a Qubit 2.0 Fluorometer and dsDNA HS Assay Kit (Life Technologies, Carlsbad, CA, United States). Samples were then pooled in equal amounts and sequenced by using a 250-bp paired-end sequencing protocol with the MiSeq Sequencing Reagent Kit v. 2 (Illumina) at Bioengineering Lab Co., Ltd., (Kanagawa, Japan). Sequence reads of all samples were processed using QIIME2 (Caporaso et al., 2010). In summary, assembly of pair-end reads was performed with default settings and then primer removal, quality control, and chimeric sequence trimming were performed using dada2 (Callahan et al., 2016). Taxonomic classification was assigned using a SILVA 16S rRNA reference alignment [Release 132 (Quast et al., 2013)]. Each sample contained 0.3–1.7% of plant organelle reads. Therefore, all sequences classified as chloroplast or mitochondria were removed.

A universal marker set of 31 protein-encoding phylogenetic marker genes was extracted from the metagenome data of KM1 and KM2 using AMPHORA2 with default settings (Wu and Scott, 2012).

Proteome Analysis

Proteins were extracted from the EBCs from the roots, and ∼50 μg of sample was separated by 12.5% sodium dodecyl sulfate-polyacrylamide gel electrophoresis (SDS–PAGE) and stained with Coomassie blue. Gel strips containing proteins ranging from 21.5 to 66.2 kDa (NifHDK protein sizes) were excised (**Figure 1**). Proteome analysis was performed as described previously (Kasahara et al., 2012; Bao et al., 2014). Briefly, the gel lanes were cut into strips of approximately 1 mm, and the gel strips were digested with trypsin. Nano-liquid chromatography (LC)–electrospray ionization–tandem mass spectrometry (MS/MS) analysis of the peptide mixtures was performed with an LTQ ion-trap MS (Thermo Fisher Scientific) coupled with a multidimensional high-performance LC (HPLC) Paradigm MS2 chromatograph (AMR, Inc., Tokyo, Japan) and nanospray electrospray ionization device (Michrom Bioresources, Inc., Auburn, CA, United States). The MS/MS data were searched against the protein database constructed in this study using Mascot program ver. 2.4 (Matrix Science, London, United Kingdom).

Isolation of Bradyrhizobia From Sorghum Roots

The bacterial cells extracted from the roots of lines KM1 and KM2 were pre-incubated at 28°C for 6 h in HM salt medium (Cole and Elkan, 1973) supplemented with 0.1% (w/v) arabinose and 0.025% (w/v) yeast extract to activate the bacterial cells for subsequent plating. These samples were serially diluted with sterilized water and plated on two types of agar plates, 1/100-strength nutrient medium (BD Biosciences, Franklin Lakes, NJ, United States) containing 1.5% agar and 10 mg L^{-1} polymixin B or 1/100-strength HM salt medium containing 1.5% agar and 10 mg L^{-1} polymixin B. This isolation strategy was used because *Bradyrhizobium* species are oligotrophic slow-growing bacteria (Okubo et al., 2012b, 2013) and resistant to polymyxin B (Hirayama et al., 2011; Piromyou et al., 2015a). After 10 days of cultivation at 28°C, slow-growing white colonies were picked up and re-streaked on the same types of agar plates for the first cultivation without polymixin B. This step was repeated one more time. Cell lysates of the resulting isolates were used to amplify the 16S rRNA gene by PCR as described previously (Itakura et al., 2009).

Phylogenetic Analyses of Bradyrhizobial Isolates

The 16S rRNA gene regions were amplified with Blend Taq polymerase (Toyobo, Osaka, Japan) and sequenced by direct PCR using universal forward (27f) and reverse (1492r) primers (Lane, 1991). The PCR conditions were as follows: preheating at 94°C for 2 min; 30 cycles of denaturation at 94°C for 30 s, annealing at 55°C for 30 s, and extension at 72°C for 90 s; extension at 72°C for 60 s; a final extension at 72°C for 5 min, and cooling at 12°C. For direct PCR sequence analysis with the 27f primer, an ABI Prism 3130xl genetic analyzer was used with a BigDye Terminator v. 3.1 Cycle Sequencing Ready-Reaction Kit (Applied Biosystems, Foster City, CA, United States). Phylogenetic trees of the gene sequences were constructed in MEGA v. 7.0 software (Tamura et al., 2011) by using the neighbor-joining method (Saitou and Nei, 1987).

Mapping of Shotgun Sequences

Genomic DNA of bradyrhizobial isolates TM122 or TM124 was extracted with an Illustra Bacteria GenomicPrep Mini Spin Kit (GE Healthcare, Little Chalfont, United Kingdom). DNA libraries were prepared with a Nextera DNA Sample Preparation Kit and sequenced on an MiSeq system using a MiSeq Reagent Nano Kit v. 2 (500 cycles) (both Illumina). Raw reads were trimmed in CLC Genomics Workbench v. 7.5.1 software (CLC Bio, Aarhus, Denmark) with the following parameters: ambiguous limit, 2; quality limit, 0.05; number of 5′ terminal nucleotides, 20; number of 3′ terminal nucleotides, 5; minimum number of nucleotides in reads, 70.

Shotgun sequence reads of the isolates were mapped to a reference genome of *B. diazoefficiens* USDA110^T (Kaneko et al., 2002). Mapping was performed in CLC Genomics Workbench software with the following parameters: mismatch cost, 2; insertion cost, 3; deletion cost, 3; length fraction, 0.9; similarity fraction, 0.9. The shotgun sequences of TM122 and TM124 were assembled in CLC Genomics Workbench software with default parameters. The contigs containing *nif* genes were annotated by using the Microbial Genome Annotation Pipeline (MiGAP[2]).

Acetylene Reduction Assay of Isolates

Bradyrhizobium sp. TM122, and TM124 were pre-cultured in HM medium (Cole and Elkan, 1973) with shaking at 28°C. Five

[2]http://www.migap.org/

milliliters of the exponential growing culture were collected by centrifugation (13,000 × *g*, 3 min, 4°C) and washed twice with sterilized water. The cell density was adjusted to 10^7 cells/mL, and 1 mL of the cell suspension was inoculated into 7 mL of Rennie semi-solid medium (5 g of sucrose, 5 g of mannitol, 0.5 mL of sodium lactate, 0.8 g of K_2HPO_4, 0.2 g of KH_2PO_4, 0.1 g of NaCl, 28 mg of $Na_2FeEDTA$, 25 mg of $Na_2MoO \cdot 4H_2O$, 100 mg of yeast extract, 0.2 g of $MgSO_4 \cdot 7H_2O$, 0.06 g of $CaCl_2$, 5 μg of biotin, 10 μg of *para*-aminobenzoic acid, and 0.2 g of noble agar per L) (Rennie, 1981) in a 28-mL test tube, which was capped with a butyl rubber W-plug. After the test tubes were incubated at 28°C for 3 days, 10% (v/v) of the gas phase was replaced with acetylene (99.9999% vol/vol purity; Toho Acetylene Co., Tokyo, Japan). The samples were re-incubated at 28°C without shaking for 3 days. The gas phase (0.5 mL) was sampled to determine the concentration of ethylene by a gas chromatograph as described above.

Acetylene Reduction Assay of Sorghum Seedling Inoculated With Isolates

Sorghum seeds of KM2 were shaken in 0.5% NaOCl solution for 1 min and then washed five times with sterile distilled water. Two sterilized seeds were planted in a Leonard's jar containing sterilized vermiculite (Inaba et al., 2012) and plant nutrient solution (Mae and Ohira, 1981) with 0.05 mM of NH_4NO_3 under aseptic conditions (**Supplementary Figure S3**). A cell suspension of TM122 or TM124 was added to the sorghum seeds at a concentration of 10^7 cells per seed.

The plants were grown in a growth cabinet (LH300; NK System Co., Ltd., Osaka, Japan) that provided 65 mol photons m^{-2} s^{-1} of photosynthetically active radiation (400–700 nm) under a daily cycle of 16 h of light and 8 h of dark at 25°C. After 7 days, the seedlings were thinned out to one plant. At 28 days after inoculation, the roots were carefully harvested and then transferred into a 100-mL vial with a butyl rubber septum (SVG-100, Nichiden-Rika Glass Co., Ltd.). Acetylene (10 mL) was introduced into the bottles, which were incubated for 24 h at 25°C in the dark.

Accession Numbers

DNA sequences obtained by the metagenomic analysis and 16S rRNA gene amplicon, TM122 genome, and TM124 genome were deposited under the accession numbers DRA006465, DRA006466, DRA006492, and DRA006493 in the DDBJ Sequence Read Archive, respectively. The sequences of 16S rRNA genes of bacterial isolates were deposited in DDBJ/EMBL/GenBank under the accession numbers LC367220–LC367221 and LC433572–LC433596, respectively.

RESULTS

Acetylene Reduction Assay of Field-Grown Sorghum

N_2-fixing activities were monitored at different growth stages for four sorghum lines (KM1, KM2, KM4, and KM5) by an acetylene reduction assay in closed bottles (**Figure 1** and **Supplementary Figures S1, S2**). Because sorghum tissues emit ethylene as a plant hormone, we calculated the ARA of bacterial nitrogenase as the difference in the rate of ethylene production in the presence and absence of acetylene (**Supplementary Table S1**).

We detected no ARA in the seedlings at 0 DAT or in the shoots and roots at 28 DAT (**Table 1**). However, we detected significant ARA values (KM1, 36.1 nmol $plant^{-1}$ h^{-1}, KM2, 52.6 nmol $plant^{-1}$ h^{-1}) at 71 DAT in the washed roots (**Table 1**). At 102 DAT, the roots of all lines showed significantly higher ARA values than at 71 DAT. Particularly, the roots of KM1 showed the highest ARA (585.8 nmol $plant^{-1}$ h^{-1}), followed by line KM2 (332.5 nmol $plant^{-1}$ h^{-1}). The ARA of KM5 roots (6.7 nmol $plant^{-1}$ h^{-1}) was significantly lower than that of KM1 (**Table 1**), indicating that root ARA depends on the sorghum genotype.

$^{15}N_2$-Feeding Experiment of Field-Grown Sorghum

The above results suggest that N_2 fixation in the roots is high in late growth stages of some sorghum lines. To confirm N_2 fixation more directly, we conducted $^{15}N_2$-feeding experiments using the roots at 102 DAT (**Figure 1** and **Supplementary Figure S2**). When the roots were exposed to $^{15}N_2$ for 23 h, ^{15}N was apparently incorporated into the root tissues inhabited by bacteria including diazotrophs, indicating that the bacteria fixed N_2 (**Table 2**). We calculated the $^{15}N_2$-fixing activity from the ^{15}N concentration (atom% excess) and total N amount (biomass × N content) (**Table 2**). Although the four lines showed $^{15}N_2$-fixation, the highest activity was detected in the roots of KM1 (102.8 μg N $plant^{-1}$ day^{-1}), which was significantly higher than the values in the other lines (**Table 2**). KM2 showed the second highest activity (40.7 μg N $plant^{-1}$ day^{-1}).

Comparison Between ARA and $^{15}N_2$-Feeding Experiments

ARA values were converted to gram N basis to compare the results of the ARA and $^{15}N_2$-feeding experiments (**Table 3**). N_2 fixation values in KM1 roots reached a maximum at 102 DAT and were nearly identical between the ARA and $^{15}N_2$-feeding methods (98.4–102.8 μg N $plant^{-1}$ day^{-1}; **Table 3**). N_2 fixation values in KM2 and KM4 roots were lower in the $^{15}N_2$ feeding method than in ARA measurement. KM5 roots consistently showed the lowest values (∼1 μg N $plant^{-1}$ day^{-1}) in both methods. Thus, we focused on the root microbiomes of KM1 and KM2 at 102 DAT for subsequent metagenome, proteome, and isolation analyses (**Figure 1**) because their N_2-fixing activities were the highest (**Table 2**).

Metagenome Analysis

We extracted bacterial cells from the roots of KM1 and KM2 with three biological replicates at 102 DAT. The metagenomes of the six DNA samples were sequenced by MiSeq. The metagenomic data comprised 4.3–5.4 × 10^6 reads and 196–208-bp average lengths per DNA sample (**Supplementary Table S2**).

By using a *nif* database (see section "Materials and Methods"), we retrieved genes encoding nitrogenase reductase (NifH) and

TABLE 1 | Acetylene-reducing activity (ARA) of four sorghum lines (KM1, KM2, KM4, and KM5) at each growth stage[a].

DAT	Tissue	Acetylene-reducing activity (ARA) (nmol C_2H_4 plant^{-1} h^{-1})							
		KM1		KM2		KM4		KM5	
0	Seedling	0.0 ± 0.0	C	0.1 ± 0.1	C	0.5 ± 0.4	C	−0.1 ± 0.0	C
28	Shoot	0.1 ± 0.3	C	−0.9 ± 0.2	C	0.1 ± 0.6	C	0.3 ± 0.6	C
28	Root	−0.1 ± 0.0	C	0.2 ± 0.1	C	0.0 ± 0.2	C	0.1 ± 0.0	C
71	Leaf	0.4 ± 0.4	C	1.6 ± 0.4	C†	0.2 ± 0.0	C	0.2 ± 0.1	C
71	Stem	1.4 ± 0.6	C	0.4 ± 0.5	C	0.7 ± 0.4	C	0.1 ± 0.5	C
71	Root	36.1 ± 10.9	C†	52.6 ± 15.6	C†	25.1 ± 9.2	C	1.7 ± 0.7	C
102	Root	585.8 ± 100.0	A‡	332.5 ± 21.8	B‡	292.1 ± 73.3	B†	6.7 ± 1.5	C†

[a]*Data are mean ± SEM (n = 3). Daggers indicate significant increase in ethylene production in the presence of acetylene (positive acetylene-reducing activity) compared to natural ethylene production in plant tissues in the absence of acetylene (Welch's t-test, †P < 0.05; ‡P < 0.01;* ***Supplementary Table S1****). DAT = days after transplanting. Means with the same letter were not significantly different by Tukey's HSD test (P < 0.05).*

TABLE 2 | Incorporation of ^{15}N from $^{15}N_2$ into sorghum roots at 102 days after transplant[a].

Sorghum line and gas phase	^{15}N concentration			Root biomass		Root N content	N_2 fixation	
	‰	Atom%	Atom% excess (a)	Root dry wt (g) plant^{-1} (b)		% of total dry wt (c)	μg-N plant^{-1} day^{-1} (d)	
KM1								
$^{15}N_2$	57.0 ± 14.0	0.387 ± 0.005	0.021 ± 0.005	88.7 ± 17.9	A	0.54 ± 0.06	102.8 ± 25.6	A
None	3.6 ± 1.4	0.368 ± 0.000						
KM2								
$^{15}N_2$	50.3 ± 23.0	0.385 ± 0.008	0.019 ± 0.008	46.5 ± 16.3	AB	0.57 ± 0.04	40.7 ± 9.0	B
None	1.3 ± 0.9	0.367 ± 0.000						
KM4								
$^{15}N_2$	41.7 ± 6.7	0.382 ± 0.002	0.016 ± 0.002	24.4 ± 3.6	B	0.68 ± 0.08	26.1 ± 3.2	B
None	1.5 ± 0.1	0.367 ± 0.000						
KM5								
$^{15}N_2$	34.4 ± 12.1	0.379 ± 0.004	0.013 ± 0.004	1.6 ± 0.3	B	0.61 ± 0.02	1.3 ± 0.5	B
None	1.2 ± 1.3	0.367 ± 0.000						

[a]*Data are mean ± SEM (n = 3). DAT = days after transplant. N_2 fixation was based on differences in ^{15}N concentrations between root systems with and without $^{15}N_2$ (None) (see text). Means with the same letter were not significantly different by Tukey's HSD test (P < 0.05). N_2 fixation rate (d) was respectively calculated for three datasets of each sorghum line according to the following formula: d (μg-N plant^{-1} day^{-1}) = (b × c × 10^{-2}) × 10^6 × a (atom%)/99.4 (atom%) × 24 h/23 h.*

TABLE 3 | Comparison of acetylene-reducing activity and $^{15}N_2$ feeding methods of evaluating N_2-fixing activity in roots of four sorghum lines at 102 days after transplant[a].

Sorghum line	N_2 fixation from acetylene-reducing activity (ARA)			N_2 fixation from $^{15}N_2$ feeding	^{15}N/ARA ratio
	nmol C_2H_4 plant^{-1} h^{-1}	nmol N_2 plant^{-1} day^{-1}	μg N plant^{-1} day^{-1}	μg N plant^{-1} day^{-1}	
KM1	585.8 ± 100.0	3515 ± 600	98.4 ± 16.8	102.8 ± 25.6	1.18 ± 0.41
KM2	332.5 ± 21.8	1995 ± 131	55.9 ± 3.7	40.7 ± 9.0	0.73 ± 0.16
KM4	292.1 ± 73.3	1753 ± 440	49.1 ± 12.3	26.1 ± 3.2	0.59 ± 0.11
KM5	6.7 ± 1.5	40 ± 9	1.1 ± 0.3	1.3 ± 0.5	1.21 ± 0.41

[a]*Average values of acetylene-reducing activity and $^{15}N_2$ feeding with SEM (n = 3) are derived from* ***Tables 1****,* ***2****, respectively. For calculations of nmol N_2 fixation from ARA, the molar conversion factor of 4 from ARA to N_2 fixation was based on equations 1 and 2 below. ^{15}N/ARA ratio indicates the ratio of N_2 fixation estimated by ARA and $^{15}N_2$ feeding experiments. $N_2 + 8H^+ + 8e^- + 16Mg\text{-}ATP \rightarrow 2NH_3 + H_2 + 16Mg\text{-}ADP + 16\ Pi$ (Eq. 1 for physiological reaction of nitrogenase). $4C_2H_2 + 8H^+ + 8e^- + 16Mg\text{-}ATP \rightarrow 4C_2H_4 + 16Mg\text{-}ADP + 16\ Pi$ (Eq. 2 for acetylene reduction by nitrogenase).*

dinitrogenase (NifDK) from the six datasets. Most nitrogenase genes were proteobacterial *nifHDK* genes (**Supplementary Table S3** for KM1, **Supplementary Table S4** for KM2) and did not include *vnfH*, *anfH*, or archaeal nitrogenase genes. At the genus level, *Bradyrhizobium nifHDK* genes were most abundant (**Figure 2A**, 55–86% in each nitrogenase gene of KM1 and KM2), and three *nif* structural genes (*nifHDK*) of *Bradyrhizobium* were consistently detected among the six datasets including sorghum lines KM1 and KM2 (**Figure 2A** and **Supplementary Table S5**). In contrast, *nifHDK* genes of other genera showed relatively low abundance (**Figure 2A**, 1–7% in each nitrogenase gene of KM1 and KM2), with

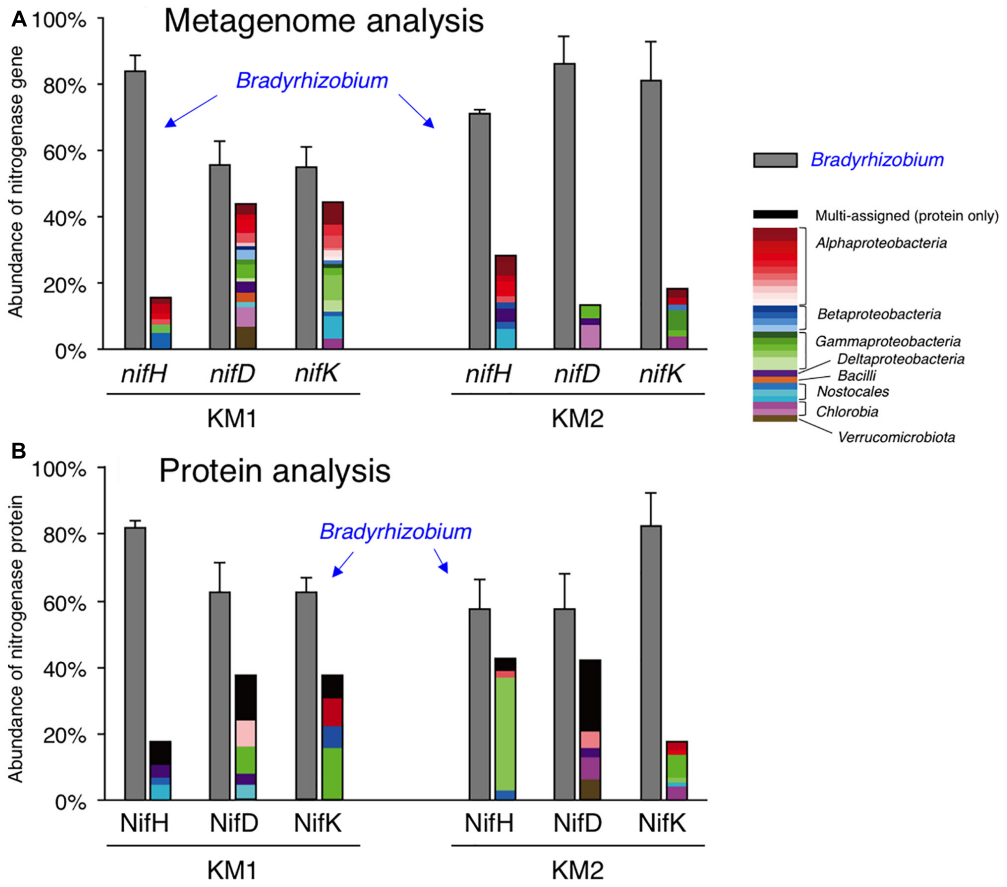

FIGURE 2 | Relative abundance of *nifHDK* reads **(A)** and NifHDK peptides **(B)** of respective bacterial genera. Data represent the average of three biological replications. The color of bars indicates assigned taxonomy. Gray indicates *Bradyrhizobium*. Black in panel B indicates multi-assigned peptides. Bar indicates standard error of three biological replicates.

parts of three *nif* structural genes (**Supplementary Table S5**). For example, *nif* structural genes from *Azorhizobium* were exclusively found in *nifDK* genes from the sorghum line KM1 (**Supplementary Table S5**).

BLAST analysis indicated that most bradyrhizobial *nifHDK* genes belonged to the non-nodulating *Bradyrhizobium* sp. S23321 (AP012279) (Okubo et al., 2012a) and photosynthetic *B. oligotrophicum* S58^T (AP012603) (Okubo et al., 2013) (**Supplementary Tables S6, S7**). Among the *Bradyrhizobium nifHDK* reads, S23321 *nifH* genes accounted for 40% of the *nifH* reads from KM1 reads and 45% of the *nifH* reads from KM2 reads. S58^T *nifH* genes accounted for 17% and 21%, respectively (**Supplementary Tables S6, S7**). Abundant *nifDK* reads were also observed in S23321 (31–37%) and S58 (11–29%) among *Bradyrhizobium nifDK* reads of sorghum lines KM1 and KM2 (**Supplementary Tables S6, S7**). These results suggest that *Bradyrhizobium*-homologous *nifHDK* genes are abundant in the KM1 and KM2 root microbiomes. The expression of nitrogenase genes is regulated by oxygen and nitrogen, as microbial N_2 fixation requires a large amount of energy (Yoneyama et al., 2017; Rosenblueth et al., 2018). Thus, we examined which *nifHDK* genes were expressed in the plant environments by determining their resulting protein levels.

Proteome Analysis

We analyzed the proteomes of EBCs from the roots of KM1 and KM2 at 102 DAT (**Figure 1**). The proteins were separated by SDS–PAGE, and we excised gel strips with protein sizes ranging from 21.5 to 66.2 kDa because the estimated sizes of NifH as well as NifD and NifK (Boyd and Peters, 2013; Gaby and Buckley, 2014) were 30–32 and 55–60 kDa, respectively (**Figure 1**). First, we constructed a database of NifHDK peptides based on the DNA sequences of *nifHDK* genes from our metagenome data (Data Set 1). Next, amino acid sequences of the peptide generated by proteome analysis (Data Set 2) were assigned based on 100% identity (Data Set 2) in the NifHDK database (Data Set 1). The results were summarized at the genus level (**Figure 2B** and **Table 4**), which revealed that the NifHDK peptides were from 15 genera and 1 family of *Alpha-*, *Beta-*, *Gamma-*, and *Delta-proteobacteria* and cyanobacteria in the root microbiomes. Among them, *Bradyrhizobium* NifHDK peptides were simultaneously detected in all three sampling replicates with an apparently higher abundance than those of

TABLE 4 | Total number of NifHDK peptides in root microbiomes of sorghum lines KM1 and KM2[a].

Class	Genus	KM1			KM2		
		NifH	NifD	NifK	NifH	NifD	NifK
Alphaproteobacteria	*Bradyrhizobium*	32**	17**	13**	23**	21**	27**
Alphaproteobacteria	*Hartmannibacter*			2*			2
Alphaproteobacteria	*Methylobacterium*						1
Alphaproteobacteria	*Rhizobium*	2			1		
Alphaproteobacteria	*Rhodospirillum*		2*			2*	
Betaproteobacteria	*Pseudodesulfovibrio*			1			
Gammaproteobacteria	*Klebsiella*		2*	4*			4*
Gammaproteobacteria	*Kosakonia*			1	15**	1	
Deltaproteobacteria	*Desulfovibrio*		1			1	
Nostocales	*Anabaena*	1			1		
Nostocales	*Calothrix*		1				
Nostocales	*Nostoc*	2					1
Chlorobia	*Chlorobaculum*					1	2*
Verrucomicrobia	*Opitutaceae*					3	
Others		2	4	1		3	
	Total	39	27	21	40	31	38

[a]*Data obtained from three biological replications. Asterisks indicate that each nitrogenase protein was detected in **three and *two replicates. The original data with three replications of sorghum plants are shown in* ***Supplementary Table S8****.*

other genera (**Table 4** and **Supplementary Table S8**). At the strain level, the bradyrhizobial NifHDK peptides (**Table 4**) were heavily assigned to NifHDK of *Bradyrhizobium* sp. S23321 and *B. oligotrophicum* S58 in sorghum lines KM1 and KM2, although the NifD peptide of *B. oligotrophicum* S58 was not detected in sorghum line KM2 (**Supplementary Table S9**). In contrast, NifH peptides of *Kosakonia* of *Gammaproteobacteria* were abundantly detected in KM2, whereas the corresponding NifDK peptides were not abundant (**Table 4** and **Supplementary Table S8**). Three peptides (NifHDK) were not simultaneously detected in non-bradyrhizobia (**Table 4**).

Therefore, our culture-independent results indicate that *Bradyrhizobium* species fixed N_2 at the late growth stage of sorghum lines KM1 and KM2 under field conditions. Particularly, close relatives of *Bradyrhizobium* sp. S23321 and *B. oligotrophicum* S58 are likely crucial candidates as functional diazotrophs in field-grown sorghum roots according to our proteome results.

Microbial Community of Sorghum Root

We sequenced amplicons of 16S rRNA genes to evaluate the relative abundance of *Bradyrhizobium* members in the root microbiomes of the four sorghum lines at 102 DAT. Taxonomic classification represented Amplicon Sequence Variants (ASVs) generated by dada2 (Callahan et al., 2016) in QIIME2 (Caporaso et al., 2010). The relative abundances of *Bradyrhizobium* (ASV 0004) in KM1 and KM2 root microbiomes were 2.9 and 3.0%, respectively (**Figure 3**). Phylogenetic analysis of our metagenomic data using 31 AMPHORA genes also showed a similar relative abundance of *Bradyrhizobium* of KM1 and KM2 (3.6%) (**Supplementary Figure S4**). These results suggest that *Bradyrhizobium* species are consistent members of the root microbiomes of sorghum lines KM1 and KM2.

Isolation of Bradyrhizobia From Sorghum Roots

Because horizontal transfer of *nif* genes among several linages of bacteria (Boyd and Peters, 2013), and even within *Bradyrhizobium* (Okubo et al., 2016), has been suggested, *Bradyrhizobium* may not always harbor bradyrhizobial *nif* genes. Therefore, we isolated bradyrhizobia from the sorghum roots on two types of oligotrophic media (1/100-strength nutrient agar medium or 1/100-strength HM agar medium) containing polymixin B. Twenty-eight slow-growing white colonies were isolated, eight of which were identified as *Bradyrhizobium* based on 16S rRNA gene sequencing (**Supplementary Table S10**). The other 20 isolates belonged to *Ancylobacter*, *Boseae*, *Sphingobium*, *Mesorhizobium*, *Deinococcus*, *Mycobacterium*, and *Terrabacter*.

Phylogenetic analysis based on 16S rRNA gene sequences indicated that bradyrhizobial isolates TM122 and TM124 were very close to photosynthetic *B. oligotrophicum* $S58^T$ (Okubo et al., 2013) and non-nodulating *Bradyrhizobium* sp. S23321 (Okubo et al., 2012a), respectively (**Figure 4**). The isolate TM220 apparently belonged to *B. diazoefficiens*, while the other bradyrhizobial isolates (TM102, TM228, TM233, TM239, and TM221) were close to *B. japonicum*. Both species are typical soybean endosymbionts (Kaneko et al., 2002, 2011). Metagenome and subsequent proteome analyses suggested that potential candidates of functional diazotrophs in the field-grown sorghum roots were close relatives of *Bradyrhizobium* sp. S23321 and *B. oligotrophicum* S58 (**Supplementary Tables S6, S7, S9**). Thus, we used the isolates TM122 and TM124 for subsequent genome analysis and N_2 fixation experiments.

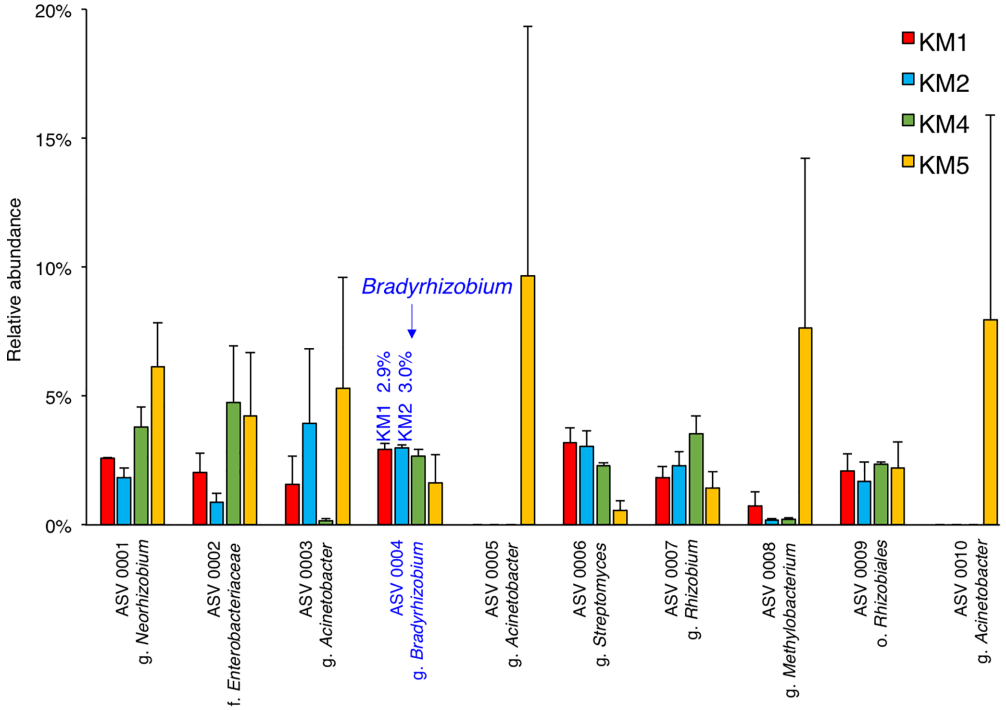

FIGURE 3 | Relative abundance of ten most abundant ASV (amplicon sequence variants) in sorghum lines KM1, KM2, KM4, and KM5 by amplicon analysis of 16S rRNA genes. The ASVs were identified at the lowest possible classification, where o. is order, f. is family and g. is genus. Bar indicates standard error of three biological replicates.

Draft Genome Analyses of Bradyrhizobial Isolates

Mapping of the MiSeq reads of TM122 and TM124 to the soybean-nodulating *B. diazoefficiens* USDA110^T genome showed that their genomes lacked symbiosis island structures of soybean bradyrhizobia that include *nod* genes (**Figure 5A**). A BLAST search confirmed that the genomes of both strains lacked the common nodulation genes (*nodDYABC*) required for legume nodulation (Andrews and Andrews, 2017). After assembling the MiSeq reads of TM122 and TM124, we retrieved the sequence contigs containing *nif* genes. The organization of *nif* genes in each genome resembled those of *B. oligotrophicum* S58^T and *Bradyrhizobium* sp. S23321, but differed from those of nodulating *B. diazoefficiens* USDA110^T, which contains symbiosis islands (Kaneko et al., 2002; Kaneko et al., 2011; Okubo et al., 2016).

Acetylene Reduction Assay of Two Bradyrhizobial Isolates

The potential for N_2 fixation by the two bradyrhizobial isolates was evaluated in free-living and plant-associated states (**Table 5**). Free-living cells of TM122 and TM124 in semi-solid medium produced ethylene over time in the presence of acetylene (**Supplementary Figure S5**) and showed significant ARA in the semi-solid medium (**Table 5**). This result indicates that both isolates can fix N_2 in a free-living state.

Thereafter, seeds from the sorghum line KM2 were inoculated with isolates TM122 or TM124 and aseptically grown for 28 days after inoculation (**Supplementary Figure S3**). We detected weak but significant ARA (22.6–31.4 pmol plant^{-1} h^{-1}) in the roots inoculated with TM122 compared to that in uninoculated roots. In contrast, TM124-inoculated roots showed no ARA under the two different treatments of N supply under our experimental conditions (**Table 5** and **Supplementary Figure S3**), which may have been because of weak colonization or low nitrogenase expression in the sorghum seedlings following TM124 inoculation.

DISCUSSION

Our omics results revealed that functional N_2-fixing bradyrhizobia associated with the roots of field-grown sorghum plants have significant N_2-fixing activities in late growth stages. Experimentally, in addition to the *nifH* gene encoding nitrogenase reductase (NifH), the usage of *nifDK* genes encoding NifDK facilitated the reliable identification of functional diazotrophs in sorghum roots (**Figure 2**), as the *nifH* gene is often diversely multiplicated (**Figure 5B**; Okubo et al., 2016). Here, we discuss the results in terms of the level of nitrogen fixation, phylogenetic comparison with diazotrophs in other crops, and *Bradyrhizobium* diversity in N_2 fixation and nodulation.

The N_2-fixing activities of the field-grown sorghum roots (102 DAT) were determined by both the ARA and $^{15}N_2$-feeding methods (**Tables 1**, **2**). The N_2-fixing activities of the roots were

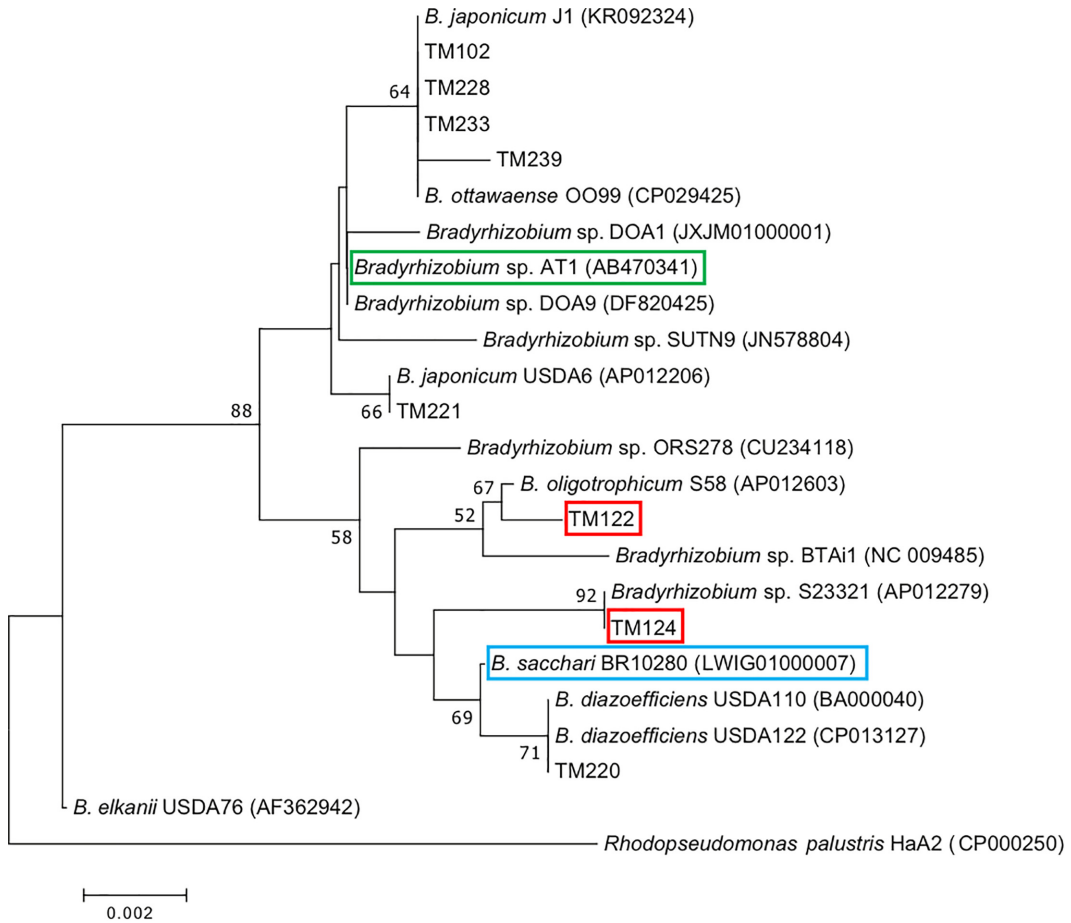

FIGURE 4 | Phylogenetic tree of 16S rRNA genes of bradyrhizobial isolates from sorghum roots (prefix TM) constructed by the neighbor-joining method. Numbers at the nodes are percentages of 1000 bootstrap replications supporting the partition. Red boxes indicate functional diazotrophs suggested by our omics analysis derived from sorghum roots (TM122, TM124), while blue and green boxes indicate diazotrophic bradyrhizobia from sugarcane (BR10280) and sweet potato (AT1), respectively.

consistent between the methods (**Table 3**), indicating that the values obtained for the N_2-fixing activities are reliable. Wani et al. (1984) evaluated the ARA of intact sorghum plants grown in sand, soil, and farmyard manure. Although the ARA depended on the manure content, temperature, and sorghum cultivar, the average ARA values of 15 cultivars was 625 nmol C_2H_4 plant^{-1} h^{-1} at 30–35°C during the day. This is similar to the value of 585.8 nmol C_2H_4 plant^{-1} h^{-1} in the KM1 roots (**Table 1**), although the experiments were performed in very different environments (**Supplementary Table S11**).

Active expression of the dinitrogenase reductase-encoded gene (*nifH*) was abundant in sugarcane stems, sweet potato stems, and pineapple leaves, which are rich in sugars and organic acids (Yoneyama et al., 2017). The leaves and stems of field-grown sorghum showed no ARA at 28 and 71 DAT except for a low ARA value for the sorghum line KM2 (**Table 1** and **Supplementary Table S1**). In contrast, considerably higher ARA values were detected in sorghum lines KM1, KM2, and KM4 at 71 DAT (**Table 1**). These results suggest that the functional N_2-fixing bacteria exclusively reside in the roots of field-grown sorghum.

Bradyrhizobium are versatile bacteria inhabiting soils and plants (Zhalnina et al., 2013; VanInsberghe et al., 2015; Jones et al., 2016; Szoboszlay et al., 2017). Genomic and ecological studies have focused on soybean bradyrhizobia (*B. diazoefficiens* and *B. japonicum*) because of their prominent roles in nodule formation and their agricultural significance (Masuda et al., 2016; Shiro et al., 2016; Saeki et al., 2017; Siqueira et al., 2017). However, photosynthetic diazotrophs often nodulate an aquatic legume, *Aeschynomene*, but sometimes lack *nod* genes (Giraud et al., 2007; Okubo et al., 2012a; Okazaki et al., 2016), and, thus, appear to function as an intermediate between free-living diazotrophs and classical nodulating diazotrophs (Okubo et al., 2013). Our results suggest that sorghum roots harbor functional N_2-fixing bradyrhizobia that are similar to photosynthetic *B. oligotrophicum* S58^T and *Bradyrhizobium* sp. S23321.

Recent metatranscriptome analyses targeting *nifH* genes suggested that *Bradyrhizobium* species play a role in sugarcane-associated N_2 fixation (Thaweenut et al., 2011; Fischer et al., 2012). Representative isolates, including BR10280^T, from surface-sterilized sugarcane tissues (Rouws et al., 2014) were

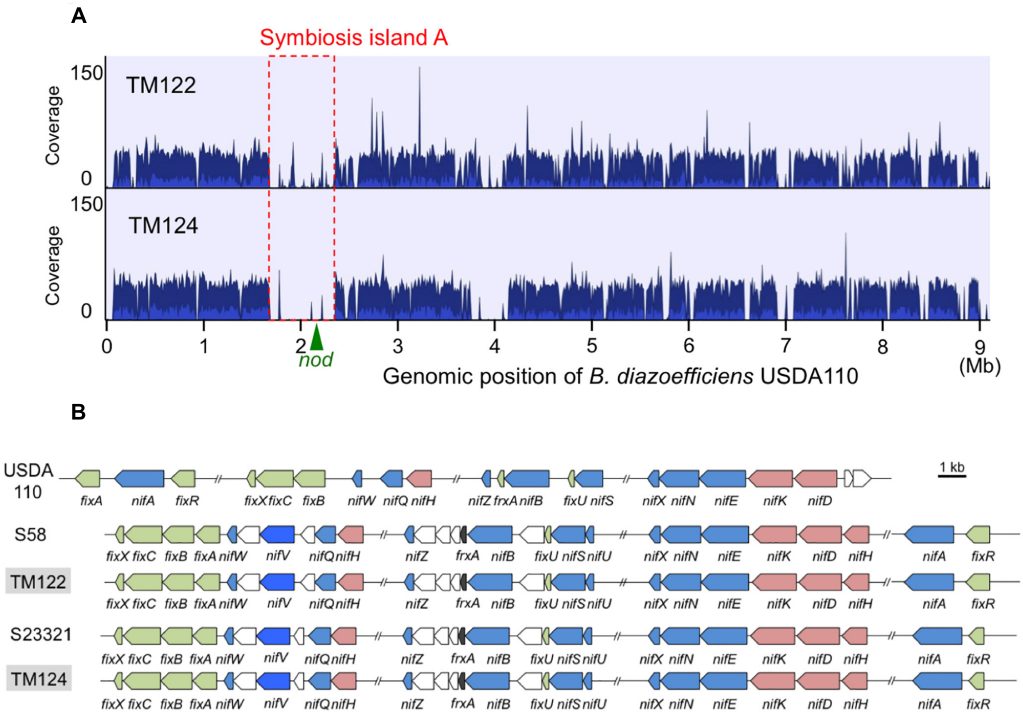

FIGURE 5 | Genomic comparison between sorghum root isolates of TM122 and TM124 and phylogenetically close bradyrhizobia. **(A)** Mapping of MiSeq reads of TM122 (1,191,548 reads of 213 bp in average length) and TM124 (1,190,703 reads of 208 bp in average length) on *B. diazoefficiens* USDA110^T genome with symbiosis island (Kaneko et al., 2002). The coverage within symbiosis island (red dotted lines) including *nod* genes (Kaneko et al., 2002, 2011) were apparently lower than those of other genomic regions. Cluster of *nif* genes of USDA110^T is located on symbiosis island (Kaneko et al., 2002). **(B)** The organization of *nif* genes of TM122 and TM124 (light gray) compared to those of *B. diazoefficiens* USDA110^T, *B. oligotrophicum* S58, and *Bradyrhizobium* sp. S23321. Colored pentagons indicate (pink) structural *nifHDK*, (blue) other *nif*, and (green) *fix* genes.

recently classified as *B. sacchari* (de Matos et al., 2017). The phylogenetic position of *B. sacchari* BR10280^T is close to that of *B. diazoefficiens* USDA110^T, a typical soybean-nodulating bacterium (**Figure 4**). *Bradyrhizobium* sp. AT1 (Terakado-Tonooka et al., 2013; Okubo et al., 2016) from sweet potato is close to the soybean-nodulating *B. japonicum* USDA6^T (**Figure 4**). Although the phylogenetic positions of eight sorghum isolates were widely distributed within *Bradyrhizobium* (**Figure 4**), our omics data suggest that the candidates responsible for *in planta* N_2 fixation are close relatives of *B. oligotrophicum* S58^T and *Bradyrhizobium* sp. S23321 such as TM122 and TM124. Recently, diverse non-diazotrophic bradyrhizobia were endophytically colonized in *Arabidopsis thaliana* roots (Schneijderberg et al., 2018). Therefore, functional diversity may be important for symbiosis and N_2 fixation.

TABLE 5 | Acetylene-reducing activity (ARA) of free-living cells of *Bradyrhizobium* sp. TM122 and TM124 in semi-solid medium and sorghum seedlings inoculated with TM122 and TM124.

Inoculation	Semi-solid medium (pmol tube^{-1} h^{-1})	Sorghum seedling (pmol plant^{-1} h^{-1})	
		Limited N	Continuous N
TM122	64.7 ± 7.8**	22.6 ± 4.7*	31.4 ± 7.5*
TM124	7810 ± 520***	7.71 ± 1.48	13.8 ± 0.8
Uninoculated	1.4 ± 0.1	8.26 ± 0.96	10.1 ± 1.7

*Data show average ± standard error of three replicates. Asterisk indicates significant difference compared with uninoculated treatment (Welch's t-test, *P < 0.05; **P < 0.01, and ***P < 0.01). After ammonium nitrate (0.05 mM) was supplied to all sorghum pots by 7 days after inoculation, the N supply was ceased (Limited N) or continued (Continuous N).*

Two bradyrhizobial isolates from the sorghum roots based on our omics data showed potential for N_2 fixation (ARA), at least in sorghum seedlings inoculated with TM122 (28 days after sowing) and in the free-living state for TM122 and TM124 (**Table 5**). Under field conditions, no ARA was detected in the sorghum roots at 28 DAT (53 days after sowing), but the highest ARA values were observed at 102 DAT (**Table 1**). There are two possibilities for explaining this growth-stage dependent phenomenon. First, N fertilization depletion may explain the highest nitrogenase activity at 102 DAT under field conditions. Second, physiological factors in plant-microbe interactions were likely involved. N_2 fixation also occurs at a high rate in the late growth stages of field-grown maize, although diazotrophic bacteria were not identified (van Deynze et al., 2018). Thus, the expression of bradyrhizobial nitrogenase may require specific environments that provide appropriate carbon source supply, chemical signals, and low oxygen concentration (Terakado-Tonooka et al., 2008; Rouws et al., 2014; Yoneyama et al., 2017)

along with plant stage and microbial community development in the roots. Recently, root mucilage of land maize was found to be a suitable microenvironment for N_2 fixation and subsequent plant assimilation of fixed nitrogen (van Deynze et al., 2018).

Bradyrhizobium cells often endophytically colonize plant roots (Chaintreuil et al., 2000; Okubo et al., 2012a, 2013; Piromyou et al., 2015b). *Bradyrhizobium* sp. SUT-PR9 deeply invaded the central tissues of rice roots (Piromyou et al., 2015a,b). Cells of *B. oligotrophicum* S58^T and *Bradyrhizobium* sp. ORS278 inhabited the surface tissues (epidermal and surface cortex cells) of cultivated and wild rice plants (Chaintreuil et al., 2000; Okubo et al., 2012b, 2013). Thus, bradyrhizobia may endophytically colonize sorghum root tissues. Microscopy studies should be conducted to localize bradyrhizobia in sorghum roots.

Interactions between diazotrophs and host plant genotypes have remained unclear in the use of N_2-fixing bacteria in crops (Okubo et al., 2013; Yoneyama et al., 2017). Further analyses targeting bradyrhizobia and sorghum genotypes may contribute to the understanding of the interactions between N_2-fixing bradyrhizobia and sorghum plants for sustainable agriculture.

CONCLUSION

The highest nitrogen-fixing activities were detected in the roots of sorghum lines KM1 and KM2 in the late growth stage (102 DAT). Nitrogenase structural genes (*nifH*, *nifD*, and *nifK*) in the metagenome sequences were assigned to *Bradyrhizobium* species by metagenome analysis. Proteome analysis indicated that three NifHDK proteins of *Bradyrhizobium* species were consistently detected across sample replicates. Most of these proteins were assigned to photosynthetic *B. oligotrophicum* S58^T and non-nodulating *Bradyrhizobium* sp. S23321. The polyphasic approach suggested that major functional N_2-fixing bacteria in the sorghum roots are unique bradyrhizobia that resemble non-nodulating *Bradyrhizobium* sp. S23321 and photosynthetic *B. oligotrophicum* S58^T.

AUTHOR CONTRIBUTIONS

SH, TK, KY, TF, TT, and KM designed the research. SH, TM, SW, and YK analyzed the data. SH and TM analyzed the DNA sequences of PCR products and metagenome. YK performed the proteome analysis. TK, SH, and SW characterized isolated diazotrophs. SH and KM wrote the article.

FUNDING

This work was supported by a Grant-in-Aid for Scientific Research (A) (26252065) and (B) (18H02112) from the Ministry of Education, Culture, Sports, Science and Technology of Japan, and by a grant from Earthnote Co., Ltd.

ACKNOWLEDGMENTS

We thank Mihoko Tokunaga, Maho Tokunaga, Hisayasu Tokunaga, Umeko Sakuma, and Junichi Yoneda (Earthnote) for their support in cultivation, sampling, acetylene reduction, and for providing information on sorghum.

SUPPLEMENTARY MATERIAL

The Supplementary Material for this article can be found online at: https://www.frontiersin.org/articles/10.3389/fmicb.2019.00407/full#supplementary-material

REFERENCES

Andrews, M., and Andrews, M. E. (2017). Specificity in legume-rhizobia symbioses. *Int. J. Mol. Sci.* 18:E705. doi: 10.3390/ijms18040705

Bao, Z., Okubo, T., Kubota, K., Kasahara, Y., Tsurumaru, H., Anda, M., et al. (2014). Metaproteomic identification of diazotrophic methanotrophs and their localization in root tissues of field-grown rice plants. *Appl. Environ. Microbiol.* 80, 5043–5052. doi: 10.1128/AEM.00969-14

Bao, Z., Shinoda, R., and Minamisawa, K. (2016). Draft genome sequence of *Methylosinus* sp. Strain 3S-1, an isolate from rice root in a low-N paddy field. *Genome Announc.* 4:e00932–16. doi: 10.1128/genomeA.00932-16

Boddey, R. M., Polidoro, J. C., Resende, A. S., Alves, B. J. R., and Urquiaga, S. (2001). Use of the 15N natural abundance technique for the quantification of the contribution of N2 fixation to sugar cane and other grasses. *Aust. J. Plant Physiol.* 28, 889–895. doi: 10.1071/PP01058

Boyd, E. S., and Peters, J. W. (2013). New insights into the evolutionary history of biological nitrogen fixation. *Front. Microbiol.* 4:201. doi: 10.3389/fmicb.2013.00201

Callahan, B. J., McMurdie, P. J., Rosen, M. J., Han, A. W., Johnson, A. J., and Holmes, S. P. (2016). DADA2: high-resolution sample inference from illumina amplicon data. *Nat. Methods* 13, 581–583. doi: 10.1038/nmeth.3869

Caporaso, J. G., Kuczynski, J., Stombaugh, J., Bittinger, K., Bushman, F. D., Costello, E. K., et al. (2010). QIIME allows analysis of high-throughput community sequencing data. *Nat. Methods* 7, 335–336. doi: 10.3389/fmicb.2013.00201

Caporaso, J. G., Lauber, C. L., Walters, W. A., Berg-Lyons, D., Lozupone, C. A., Turnbaugh, P. J., et al. (2011). Global patterns of 16S rRNA diversity at a depth of millions of sequences per sample. *Proc. Natl. Acad. Sci. U.S.A.* 108, 4516–4522. doi: 10.1073/pnas.1000080107

Cavalcante, V. A., and Dobereiner, J. (1988). A new acid-tolerant nitrogen-fixing bacterium associated with sugarcane. *Plant Soil* 108, 23–31. doi: 10.1007/BF02370096

Chaintreuil, C., Giraud, E., Prin, Y., Lorquin, J., Bâ, A., Gillis, M., et al. (2000). Photosynthetic bradyrhizobia are natural endophytes of the African wild rice *Oryza breviligulata*. *Appl. Environ. Microbiol.* 66, 5437–5447. doi: 10.1007/BF02370096

Coelho, M. R., de Vos, M., Carneiro, N. P., Marriel, I. E., Paiva, E., and Seldin, L. (2008). Diversity of nifH gene pools in the rhizosphere of two cultivars of sorghum (*Sorghum bicolor*) treated with contrasting levels of nitrogen fertilizer. *FEMS Microbiol. Lett.* 279, 15–22. doi: 10.1111/j.1574-6968.2007.00975.x

Cole, M. A., and Elkan, G. H. (1973). Transmissible resistance to penicillin G, neomycin, and chloramphenicol in *Rhizobium japonicum*. *Antimicrob. Agents Chemother.* 4, 248–253. doi: 10.1128/AAC.4.3.248

de Matos, G., Zilli, J., de Araújo, J., Parma, M., Melo, I., Radl, V., et al. (2017). Bradyrhizobium sacchari sp. nov., a legume nodulating bacterium isolated from sugarcane roots. *Arch. Microbiol.* 199, 1251–1258. doi: 10.1007/s00203-017-1398-6

Elbeltagy, A., Nishioka, K., Sato, T., Suzuki, H., Ye, B., Hamada, T., et al. (2001). Endophytic colonization and in planta nitogen fixation by a *Herbaspirillum* sp. isolated from wild rice spcies. *Appl. Environ. Microbiol.* 67, 5285–5293. doi: 10.1128/AEM.67.11.5285-5293.2001

Fischer, D., Pfitzner, B., Schmid, M., Simões-Araújo, J. L., Reis, V. M., Pereira, W., et al. (2012). Molecular characterisation of the diazotrophic bacterial community in uninoculated and inoculated field-grown sugarcane (*Saccharum* sp.). *Plant Soil* 356, 83–99. doi: 10.1007/s11104-011-0812-0

Gaby, J. C., and Buckley, D. H. (2014). A comprehensive aligned nifH gene database: a multipurpose tool for studies of nitrogen-fixing bacteria. *Database* 2014:bau001. doi: 10.1093/database/bau001

Giraud, E., Moulin, L., Vallenet, D., Barbe, V., Cytryn, E., Avarre, J. C., et al. (2007). Legumes symbioses: absence of Nod genes in photosynthetic bradyrhizobia. *Science* 316, 1307–1312. doi: 10.1126/science.1139548

Hirayama, J., Eda, S., Mitsui, H., and Minamisawa, K. (2011). Nitrate-dependent N2O emission from intact soybean nodules via denitrification by *Bradyrhizobium japonicum* bacteroids. *Appl. Environ. Microbiol.* 77, 8787–8790. doi: 10.1128/AEM.06262-11

Ikeda, S., Kaneko, T., Okubo, T., Rallos, L. E., Eda, S., Mitsui, H., et al. (2009). Development of a bacterial cell enrichment method and its application to the community analysis in soybean stems. *Microb. Ecol.* 58, 703–714. doi: 10.1007/s00248-009-9566-0

Inaba, S., Ikenishi, F., Itakura, M., Kikuchi, M., Eda, S., Chiba, N., et al. (2012). N2O emission from degraded soybean nodules depends on denitrification by *Bradyrhizobium japonicum* and other microbes in the rhizosphere. *Microbes Environ.* 27, 470–476. doi: 10.1264/jsme2.ME12100

Itakura, M., Saeki, K., Omori, H., Yokoyama, T., Kaneko, T., Tabata, S., et al. (2009). Genomic comparison of *Bradyrhizobium japonicum* strains with different symbiotic nitrogen-fixing capabilities and other Bradyrhizobiaceae members. *ISME J.* 3, 326–339. doi: 10.1038/ismej.2008.88

James, E. K. (2000). Nitrogen fixation in endophytic and associative symbiosis. *Field Crops Res.* 65, 197–209. doi: 10.1016/S0378-4290(99)00087-8

Jones, F. P., Clark, I. M., King, R., Shaw, L. J., Woodward, M. J., and Hirsch, P. R. (2016). Novel European free-living, non-diazotrophic *Bradyrhizobium* isolates from contrasting soils that lack nodulation and nitrogen fixation genes - a genome comparison. *Sci. Rep.* 6:25858. doi: 10.1038/srep25858

Kaneko, T., Maita, H., Hirakawa, H., Uchiike, N., Minamisawa, K., Watanabe, A., et al. (2011). Complete genome sequence of the soybean symbiont *Bradyrhizobium japonicum* strain USDA6T. *Genes* 2, 763–787. doi: 10.3390/genes2040763

Kaneko, T., Nakamura, Y., Sato, S., Minamisawa, K., Uchiumi, T., Sasamoto, S., et al. (2002). Complete genomic sequence of nitrogen-fixing symbiotic bacterium *Bradyrhizobium japonicum* USDA110. *DNA Res.* 9, 189–197. doi: 10.1093/dnares/9.6.189

Kasahara, Y., Morimo, H., Kuwan, M., and Kadoya, R. (2012). Genome-wide analytical approaches using semi-quantitative expression proteomics for aromatic hydrocarbon metabolism in *Pseudomonas putida* F1. *J. Microbiol. Meth.* 91, 434–442. doi: 10.1016/j.mimet.2012.09.017

Khawaja, C., Janssen, R., Rutz, D., Luquet, D., Trouche, G., Reddy, B. V. S., et al. (2014). *Energy Sorghum: An alternative Energy crop A Handbook*. Available at: http://oar.icrisat.org/9049/

Lane, D. J. (1991). "16S/23S rRNA sequencing," in *Nucleic Acid Techniques in Bacterial Systematics*, eds E. Stackebrandt and M. Goodfellow (Chichester: John Wiley and Sons), 115–175.

Mae, T., and Ohira, K. (1981). The remobilization of nitrogen related to leaf growth and senescence in rice plants (*Oryza sativa* L.). *Plant Cell Physiol.* 22, 1067–1074. doi: 10.1093/oxfordjournals.pcp.a076248

Masuda, S., Saito, M., Sugawara, C., Itakura, M., Eda, S., and Minamisawa, K. (2016). Identification of the hydrogen uptake gene cluster for chemolithoautotrophic growth and symbiosis hydrogen uptake in *Bradyrhizobium diazoefficiens*. *Microbes Environ.* 31, 76–78. doi: 10.1264/jsme2.ME15182

Minamisawa, K., Imaizumi-Anraku, H., Bao, Z., Shinoda, R., Okubo, T., and Ikeda, S. (2016). Are symbiotic methanotrophs key microbes for N acquisition in paddy rice root? *Microbes Environ.* 31, 4–10. doi: 10.1264/jsme2.ME15180

Naylor, D., DeGraaf, S., Purdom, E., and Coleman-Derr, D. (2017). Drought and host selection influence bacterial community dynamics in the grass root microbiome. *ISME J.* 11, 2691–2704. doi: 10.1038/ismej.2017.118

Okazaki, S., Tittabutr, P., Teulet, A., Thouin, J., Fardoux, J., Chaintreuil, C., et al. (2016). Rhizobium-legume symbiosis in the absence of Nod factors: two possible scenarios with or without the T3SS. *ISME J.* 10, 64–74. doi: 10.1038/ismej.2015.103

Okubo, T., Fukushima, S., Itakura, M., Oshima, K., Longtonglang, A., Teaumroong, N., et al. (2013). Genome analysis suggests that the soil oligotrophic bacterium *Agromonas oligotrophica* (*Bradyrhizobium oligotrophicum*) is a nitrogen-fixing symbiont of *Aeschynomene indica*. *Appl. Environ. Microbiol.* 79, 2542–2551. doi: 10.1128/AEM.00009-13

Okubo, T., Fukushima, S., and Minamisawa, K. (2012a). Evolution of *Bradyrhizobium-Aeschynomene* mutualism: living testimony of the ancient world or highly evolved state? *Plant Cell Physiol.* 53, 2000–2007. doi: 10.1093/pcp/pcs150

Okubo, T., Tsukui, T., Maita, H., Okamoto, S., Oshima, K., Fujisawa, T., et al. (2012b). Complete genome sequence of *Bradyrhizobium* sp. S23321: insights into symbiosis evolution in soil oligotrophs. *Microbes Environ.* 27, 306–315. doi: 10.1264/jsme2.ME11321

Okubo, T., Piromyou, P., Tittabutr, P., Teaumroong, N., and Minamisawa, K. (2016). Origin and evolution of nitrogen fixation genes on symbiosis islands and plasmid in *Bradyrhizobium*. *Microbes Environ.* 31, 260–267. doi: 10.1264/jsme2.ME15159

Pedersen, W. L., Chakrabarty, K. R. V., Klucas, R. V., and Vidaver, A. K. (1978). Nitrogen fixation (acetylene reduction) associated with roots of winter wheat and sorghum in Nebraska. *Appl. Environ. Microbiol.* 35, 129–135.

Piromyou, P., Greetatorn, T., Teamtisong, K., Okubo, T., Shinoda, R., Nuntakij, A., et al. (2015a). Preferential association of endophytic bradyrhizobia with different rice cultivars and its implications for rice endophyte evolution. *Appl. Environ. Microbiol.* 81, 3049–3061. doi: 10.1128/AEM.04253-14

Piromyou, P., Songwattana, P., Greetatorn, T., Okubo, T., Kakizaki, K. C., Prakamhang, J., et al. (2015b). The Type III secretion system (T3SS) is a determinant for rice-endophyte colonization by non-photosynthetic *Bradyrhizobium*. *Microbes Environ.* 30, 291–300. doi: 10.1264/jsme2.ME15080

Quast, C., Pruesse, E., Yilmaz, P., Gerken, J., Schweer, T., Yarza, P., et al. (2013). The SILVA ribosomal RNA gene database project: improved data processing and web-based tools. *Nucleic Acids Res.* 41, D590–D596. doi: 10.1093/nar/gks1219

Rennie, R. J. (1981). A single medium for the isolation of acetylene-reducing (dinitrogen-fixing) bacteria from soils. *Can. J. Microbiol.* 27, 8–14. doi: 10.1139/m81-002

Rosenblueth, M., Ormeño-Orrillo, E., López-López, A., Rogel, M. A., Reyes-Hernández, B. J., Martínez-Romero, J. C., et al. (2018). Nitrogen fixation in cereals. *Front. Microbiol.* 9:1794. doi: 10.3389/fmicb.2018.01794

Rouws, L. F. M., Leite, J., de Matos, G. F., Zilli, J. E., Coelho, M. R. R., Xavier, G. R., et al. (2014). Endophytic *Bradyrhizobium* spp. isolates from sugarcane obtained through different culture strategies. *Environ. Microbiol. Rep.* 6, 354–363. doi: 10.1111/1758-2229.12122

Saeki, Y., Nakamura, M., Mason, M. L. T., Yano, T., Shiro, S., Sameshima-Saito, R., et al. (2017). Effect of flooding and the nosZ gene in bradyrhizobia on bradyrhizobial community structure in the soil. *Microbes Environ.* 32, 154–163. doi: 10.1264/jsme2.ME16132

Saitou, N., and Nei, M. (1987). The neighbor-joining method: a new method for reconstructing phylogenetic trees. *Mol. Biol. Evol.* 4, 406–425. doi: 10.1093/oxfordjournals.molbev.a040454

Schmieder, R., and Edwards, R. (2011). Quality control and preprocessing of metagenomic datasets. *Bioinformatics* 27, 863–864. doi: 10.1093/bioinformatics/btr026

Schneijderberg, M., Schmitz, L., Cheng, X., Polman, S., Franken, C., Geurts, R., et al. (2018). A genetically and functionally diverse group of non-diazotrophic *Bradyrhizobium* spp. Colonizes the root endophytic compartment of *Arabidopsis thaliana*. *BMC Plant Biol.* 18:61. doi: 10.1186/s12870-018-1272-y

Schollhorn, R., and Burris, R. H. (1967). Acetylene as a competitive inhibitor of N2 fixation. *Proc. Natl. Acad. Sci. U.S.A.* 58, 213–216. doi: 10.1073/pnas.58.1.213

Shiro, S., Kuranaga, C., Yamamoto, A., Sameshima-Saito, R., and Saeki, Y. (2016). Temperature-dependent expression of nodC and community structure of

soybean-nodulating bradyrhizobia. *Microbes Environ.* 31, 27–32. doi: 10.1264/jsme2.ME15114

Siqueira, A. F., Minamisawa, K., and Sánchez, C. (2017). Anaerobic reduction of nitrate to nitrous oxide is lower in *Bradyrhizobium japonicum* than in *Bradyrhizobium diazoefficiens*. *Microbes Environ.* 32, 398–401. doi: 10.1264/jsme2.ME17081

Steffen, W., Richardson, K., Rockström, J., Cornell, S. E., Fetzer, I., Bennett, E. M., et al. (2015). Planetary boundaries: guiding human development on a changing planet. *Science* 347:1259855. doi: 10.1126/science.1259855

Szoboszlay, M., Dohrmann, A. B., Poeplau, C., Don, A., and Tebbe, C. C. (2017). Impact of land-use change and soil organic carbon quality on microbial diversity in soils across Europe. *FEMS Microbiol. Ecol.* 93:fix146 doi: 10.1093/femsec/fix146

Tamura, K., Peterson, D., Peterson, N., Stecher, G., Nei, M., and Kumar, S. (2011). MEGA5: molecular evolutionary genetics analysis using maximum likelihood, evolutionary distance, and maximum parsimony methods. *Mol. Biol. Evol.* 28, 2731–2739. doi: 10.1093/molbev/msr121

Terakado-Tonooka, J., Fujihara, S., and Ohwaki, Y. (2013). Possible contribution of *Bradyrhizobium* on nitrogen fixation in sweet potatoes. *Plant Soil* 367, 639–650. doi: 10.1007/s11104-012-1495-x

Terakado-Tonooka, J., Owaki, Y., Yamakawa, H., Tanaka, F., Yoneyama, T., and Fujihara, S. (2008). Expressed nifH genes of endophytic bacteria detected in field-grown sweet potatoes (*Ipomoea batatas* L.). *Microbes Environ.* 23, 89–93. doi: 10.1264/jsme2.23.89

Thaweenut, N., Hachisuka, Y., Ando, S., Yanagisawa, S., and Yoneyama, T. (2011). Two seasons' study on nifH gene expression and nitrogen fixation by diazotrophic endophytes in sugarcane (*Saccharum* spp. *hybrids)*: expression of nifH genes similar to those of rhizobia. *Plant Soil* 338, 435–449. doi: 10.1007/s11104-010-0557-1

van Deynze, A., Zamora, P., Delaux, P. M., Heitmann, C., Jayaraman, D., Rajasekar, S., et al. (2018). Nitrogen fixation in a landrace of maize is supported by a mucilage-associated diazotrophic microbiota. *PLoS Biol.* 16:e2006352. doi: 10.1371/journal.pbio.2006352

VanInsberghe, D., Maas, K. R., Cardenas, E., Strachan, C. R., Hallam, S. J., and Mohn, W. W. (2015). Non-symbiotic *Bradyrhizobium* ecotypes dominate North American forest soils. *ISME J.* 9, 2435–2441. doi: 10.1038/ismej.2015.54

Wani, S. P., Upadhyaya, M. N., and Dart, P. J. (1984). An intact plant assay for estimating nitrogense activity (C2H2 reduction) of sorghum and millet plants grown in pots. *Plant Soil* 82, 15–29. doi: 10.1007/BF02220766

Wu, M., and Eisen, J. A. (2008). A simple, fast, and accurate method of phylogenomic inference. *Genome Biol.* 9:R151. doi: 10.1186/gb-2008-9-10-r151

Wu, M., and Scott, A. J. (2012). Phylogenomic analysis of bacterial and archaeal sequences with AMPHORA2. *Bioinformatics* 28, 1033–1034. doi: 10.1093/bioinformatics/bts079

Xu, L., Naylor, D., Dong, Z., Simmons, T., Pierroz, G., Hixson, K., et al. (2018). Drought delays development of the sorghum root microbiome and enriches for monoderm bacteria. *Proc. Natl. Acad. Sci. U.S.A.* 115, E4284–E4293. doi: 10.1073/pnas.1717308115

Yoneyama, T., Muraoka, T., Kim, T. H., Dacanay, E. V., and Nakanishi, Y. (1997). The natural 15N abundance of sugarcane and neighboring plants in Brazil, the Philippines and Miyako (Japan). *Plant Soil* 189, 239–244. doi: 10.1023/A:1004288008199

Yoneyama, T., Terakado-Tonooka, J., and Minamisawa, K. (2017). Exploration of bacterial N2-fixation systems in association with soil-grown sugarcane, sweet potato, and paddy rice: a review and synthesis. *Soil Sci. Plant Nutri.* 63, 578–590. doi: 10.1080/00380768.2017.1407625

Zhalnina, K., de Quadros, P. D., Gano, K. A., Davis-Richardson, A., Fagen, J. R., Brown, C. T., et al. (2013). Ca. Nitrososphaera and Bradyrhizobium are inversely correlated and related to agricultural practices in long-term field experiments. *Front. Microbiol.* 4:104. doi: 10.3389/fmicb.2013.00104

Conflict of Interest Statement: The authors declare that the research was conducted in the absence of any commercial or financial relationships that could be construed as a potential conflict of interest.

Advantages of publishing in Frontiers

OPEN ACCESS
Articles are free to read for greatest visibility and readership

FAST PUBLICATION
Around 90 days from submission to decision

HIGH QUALITY PEER-REVIEW
Rigorous, collaborative, and constructive peer-review

TRANSPARENT PEER-REVIEW
Editors and reviewers acknowledged by name on published articles

Frontiers
Avenue du Tribunal-Fédéral 34
1005 Lausanne | Switzerland

Visit us: www.frontiersin.org
Contact us: info@frontiersin.org | +41 21 510 17 00

REPRODUCIBILITY OF RESEARCH
Support open data and methods to enhance research reproducibility

DIGITAL PUBLISHING
Articles designed for optimal readership across devices

FOLLOW US
@frontiersin

IMPACT METRICS
Advanced article metrics track visibility across digital media

EXTENSIVE PROMOTION
Marketing and promotion of impactful research

LOOP RESEARCH NETWORK
Our network increases your article's readership